GEOLOGICAL SURVEY OF CANADA

OPEN FILE 2408

Geological, geotechnical and geophysical studies along an onshore-offshore transect of the Beaufort Shelf

edited by

S.R. Dallimore

1991

Energy, Mines and Resources Canada
Énergie, Mines et Ressources Canada

Canada

GEOLOGICAL SURVEY OF CANADA

OPEN FILE 2408

Geological, geotechnical and geophysical studies along an onshore-offshore transect of the Beaufort Shelf

edited by

S.R. Dallimore

Contributing authors:

V.S. Allen, J.G. Bisson, S.M. Blasco, S.M. Birk, R.A. Burns, H.A. Christian, R.E. Cranston, S.R. Dallimore, L.D. Dyke, D. Gillespie, R.L. Good, J.A. Hanright, J.A. Hunter, K.A. Jenner, P.J. Kurfurst, J. Landva, J.F. Lewis, L. Maurice, F.M. Nixon, D.G. Paré, D.E. Patterson, J. Shimeld, A.E. Taylor, J.-S. Vincent, D.J. Woeller, A. Wilkinson

TABLE OF CONTENTS

ACKNOWLEDGEMENTS

Much of the work reported on in this volume would not have been possible without the assistance and support of many individuals and several institutions. During the planning stages and preparations for field work, Messrs. J. A. Heginbottom, C. Graham and J. Weaver, members of the PERD Committee 6.1.2, provided continual support and advice. Spring field studies were made possible only with the valued assistance of the staff of the Polar Continental Shelf Project who ably served to provide logistical support from their base in Tuktoyaktuk. Laboratory studies conducted in Inuvik relied on the use of the fine facilities available at the Inuvik Research Centre and the assistance of Messrs. G. White and L. Kutny.

The support of Gulf Canada Resources, through C. Graham, is acknowledged for arranging use of the mud chilling system utilized for the deep boreholes, for use of their charter helicopter, and for access to unpublished data which was critical for project planning. Data from the Isserk well was obtained with the assistance of Gulf Canada Resources and Esso Resources.

Special appreciation is extended to P.R. Hill of Hill Geoscience Research for supervising core logging during field operations, and to R.A. Harmes and G. Sonnichsen for providing technical assistance during field and logging phases of the program. The authors of this volume would also like to acknowledge the dedication and hard work of the staff of the numerous technical consultants and students who helped to plan the project and worked long hours in the field and the laboratory. Thanks are also due to J.A. Hanright, S.E. Pullan and K.A. Jenner, who assisted in technical editing of the manuscript.

Finally, the authors are grateful to Dr. B.R. Pelletier for carefully reviewing and editing the manuscript, and for his support in guiding the project through to completion.

CHAPTER 1

PROJECT OVERVIEW

1.1 INTRODUCTION

S.R. Dallimore

In the spring and summer of 1990, the Geological Survey of Canada conducted a field program to investigate the geology and geotechnical conditions of the Beaufort Sea Shelf and coastal areas in the vicinity of northern Richards Island to the east of Mackenzie delta. The field activities and subsequent laboratory studies conducted as part of this work were extensive and diverse. This Open File Report presents preliminary data and scientific results from these studies with only generalized interpretation and discussion. The technical review process has been limited and readers planning to utilize these data for further analyses are encouraged to contact the editor or individual authors of the relevant sections to review details of the project and receive data updates, should they be available.

The structure of this report reflects the nature of the field studies. Chapters II to V deal with the results of the so-called 'Onshore-Offshore Transect', while Chapter VI discusses shallow boreholes drilled in coastal areas of North Head on Richards Island. The goals and objectives of these two activities, while complimentary, were quite distinct with different funding sources and different participants.

Onshore-offshore Transect

The onshore-offshore transect project was designed from the outset to be a multi-disciplinary study aimed at quantifying the basic geotechnical conditions of the upper 100m of the Beaufort Sea Shelf sediments. The focus for the work was the nearshore area (usually in less than 10 m of water depth), characterized by a general lack of geoscience information sufficient to link geological and geotechnical conditions between land areas and offshore areas. The main components of the transect project are illustrated on the organizational chart presented as Figure 1.1.1. which shows that the greatest effort of this project was placed on the geotechnical borehole program. Surface geophysics and coastal mapping studies provided critical supplementary data to extend the borehole information and tie the borehole geological units with those exposed in coastal sections.

Boreholes completed as part of the onshore-offshore transect are 90BH1, 90BH1A, 90BH2, 90BH3, 90BH4, and 90BH5. Summary borehole logs are provided in Appendix A.

Figure 1.1.1 Flow chart showing organization of onshore-offshore transect project

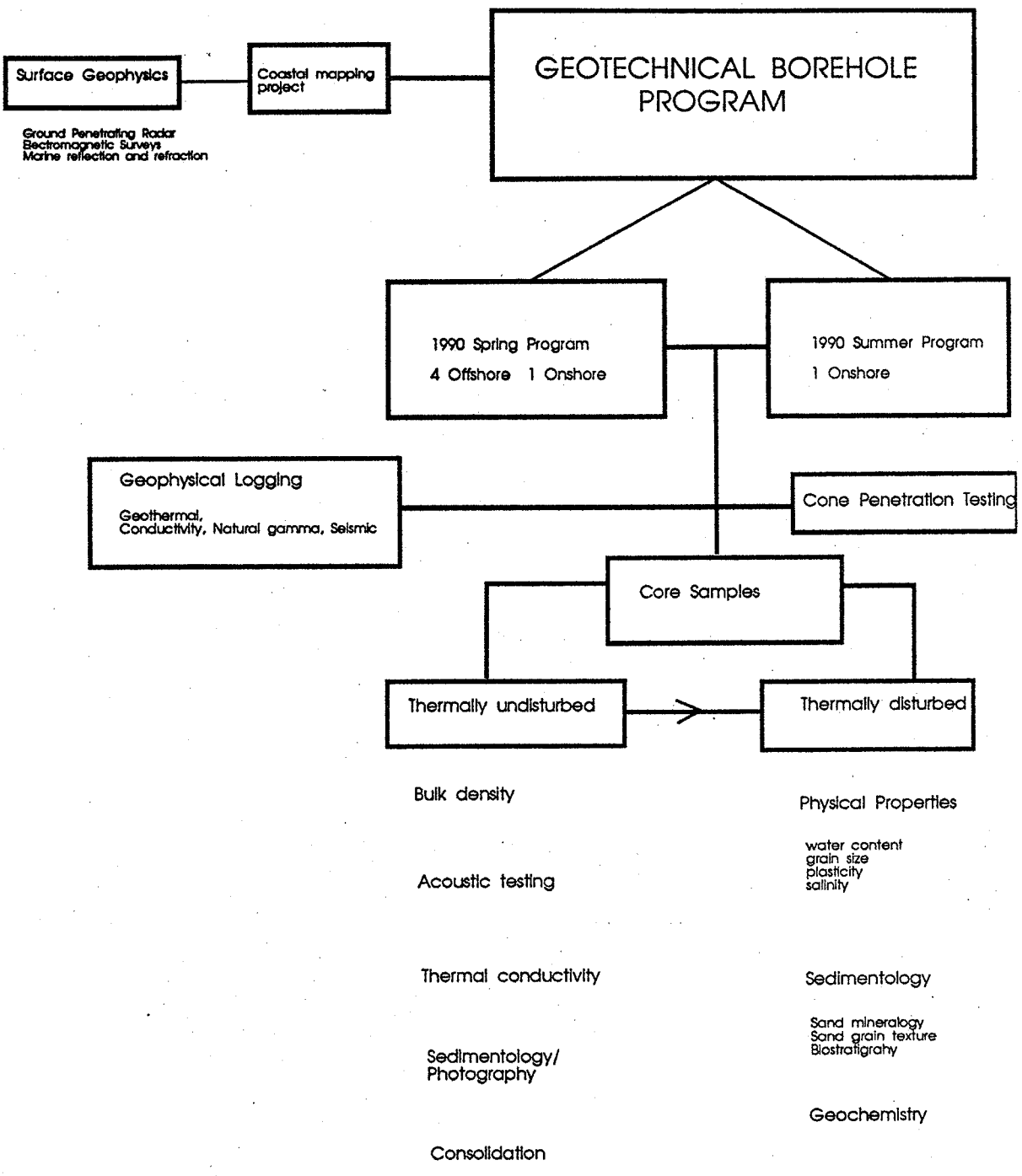

North Head Coastal Boreholes

The shallow boreholes completed in coastal areas in the vicinity of North Head were completed as a supplementary study to the spring onshore-offshore transect activities. The purpose of this work was to study the geological processes related to permafrost conditions in the coastal setting. A particular emphasis was placed on investigating the consequences of incorporating lacustrine basins in the nearshore zone as a result of coastal retreat.

Shallow boreholes are numbered 90BH6, 90BH7, and 90BH8. Summary logs of these boreholes are shown in Appendix A.

Funding

Funding for the onshore-offshore transect was secured from two separate sources. The Panel for Energy Research and Development (Committee 6.1.2) supported research related to geotechnical and permafrost concerns and the Northern Oil and Gas Action Program supported research related to the correlation of the geology between the onshore and offshore.

Funding for the North Head coastal boreholes was provided by the Northern Oil and Gas Action Program.

1.2 BOREHOLE POSITIONING

J.A. Hunter, R.A. Burns and R.L. Good

The borehole and cone penetrometer sites were positioned using a Trimble Navigation Ltd. GPS Pathfinder portable positioning system, which was leased from Surnav Corporation of Ottawa.

The Global Positioning System uses signals from a network of satellites operated by the U.S. Department of Defence. The Pathfinder can obtain position fixes at a rate of one per second with an accuracy of 25 m (circular error probable). The U.S. Department of Defence reserves the right to initiate selective availability at any time, which will purposely degrade the accuracy to 125 m C.E.P.

Since the GPS satellite network was not complete in March/April 1990 (only 12 of the total complement of 21 satellites were available), accurate fixes could only be made at certain times of the day. Figure 1.2.1 shows the availability of satellites with acceptable signal strengths and angle above the horizon ($>5^{\circ}$) for the field area on April 1, 1990. Four satellites are required for a 3-dimensional fix, whereas only three are required for a 2-dimensional (sea-surface) fix. Insufficient satellite availability, or "down-times", occurred between 03:00 and 03:30 (MST) and between 13:00 and 14:40 MST on April 1, 1990. The "down-times" shifted in time by 2 hours from March 15 to April 15.

The borehole and cone penetrometer sites were positioned between 09:00 and 13:00 MST from March 17 to 27. A series of line-up stakes were planted, 100 m apart, from the shoreline through all locations (a distance of approximately 21 km), to facilitate road-building. During the surveying period, each borehole location was positioned several times and, in general, positioning error was less than 20 m.

After April 1 the borehole locations were occupied and the position monitored for a one-hour period to obtain a large enough number of readings for calculating a best statistical fit. Occasionally during these time periods, large deviations of positions (over 100 m) were observed. It was later learned that, during April, the U.S. Department of Defence had intermittently turned on selective availability, as well as carried out a number

Figure 1.2.1

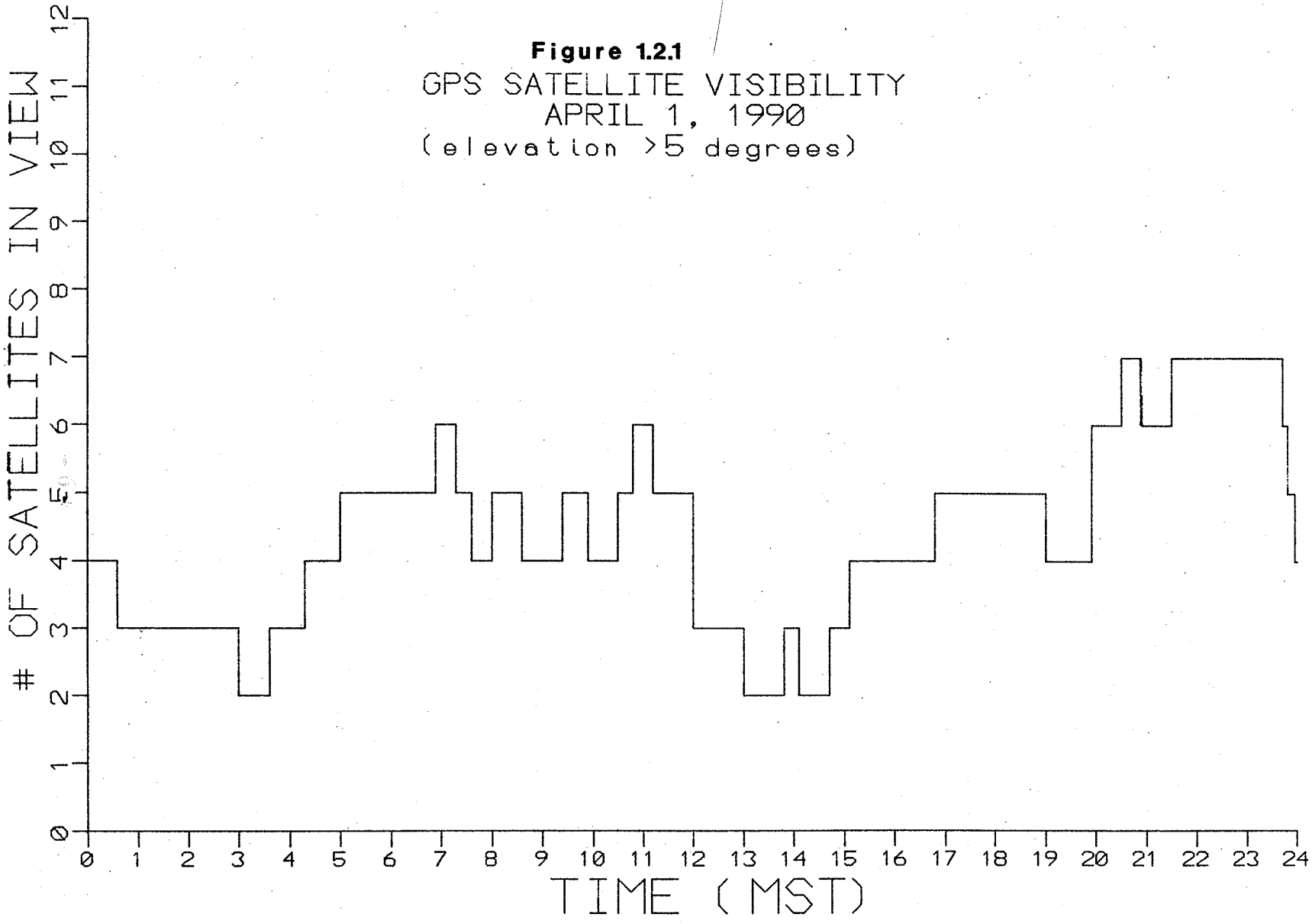
GPS SATELLITE VISIBILITY
APRIL 1, 1990
(elevation >5 degrees)
OF SATELLITES IN VIEW
0 1 2 3 4 5 6 7 8 9 10 11 12
0 1 2 3 4 5 6 7 8 9 10 11 12 13 14 15 16 17 18 19 20 21 22 23 24
TIME (MST)

of other tests on the GPS system. Hence, these data were discarded as unusable. Since the initial positions were located in mid-March before selective availability testing was begun, the quoted positions are thought to be accurate to within a 25 m circle.

The geographical locations and UTM's of all sites are listed in Table 1.2.1, and the sites are plotted on a UTM grid map in Figure 1.2.2.

TABLE 1.2.1

SITE (NAD-27)	GEOGRAPHICAL LOCATION (NAD-27)	UTM	SITE	GEOGRAPHICAL LOCATION	UTM
BH-1	N 69° 39' 45.8" W134° 23' 20.4"	N 7728200 E 523700	CPT-6	N 69° 46' 33.0" W134° 13' 01.7"	N 7740892 E 530204
BH-1A	N 69° 40' 54.7" W 134° 20' 8.3"	N 7730350 E 525650			
BH-2	N 69° 44' 21.0" W134° 16' 34.3"	N 7736776 E 527974	CPT-7	N 69° 47' 34.4" W134° 11' 22.8"	N 7742810 E 531239
BH-3	N 69° 46' 33.0" W134° 13' 01.7"	N 7740892 E 530204	CPT-8	N 69° 48' 27.5" W134° 09' 57.3"	N 7744466 E 532132
BH-4	N 69° 48' 27.5" W134° 09' 57.3"	N 7744466 E 532132	CPT-9	N 69° 49' 50.5" W134° 07' 43.2"	N 7747056 E 533530
BH-5	N 69° 52' 34.4" W134° 03' 19.2"	N 7752174 E 536273	CPT-10	N 69° 50' 43.6" W134° 06' 18.1"	N 7748715 E 534415
BH-6	N 69° 43' 21.8" W 134° 23' 14.5"	N 7734900 E 523600			
BH-7	N 69° 42' 39.6" W 134° 29' 30.2"	N 7733550 E 519670			
BH-8	N 69° 43' 0.1" E 134° 18' 54.2"	N 7734250 E 526500			
CPT-2	N 69° 43' 15.2" W134° 18' 20.1"	N 7734724 E 526862	CPT-12	N 69° 51' 56.9" W134° 04' 19.8"	N 7751000 E 535645
CPT-3	N 69° 43' 36.7" W134° 17' 45.4"	N 7735394 E 527227	CPT-13	N 69° 52' 34.4" W134° 03' 19.2"	N 7752174 E 536273
CPT-4	N 69° 44' 21.0" W134° 16' 34.3"	N 7736776 E 527974	CPT-14	N 69° 52' 56.0" W134° 02' 43.5"	N 7752849 E 536644
CPT-5	N 69° 45' 31.3" W134° 14' 41.2"	N 7738969 E 529162			

Figure 1.2.2 Borehole locations

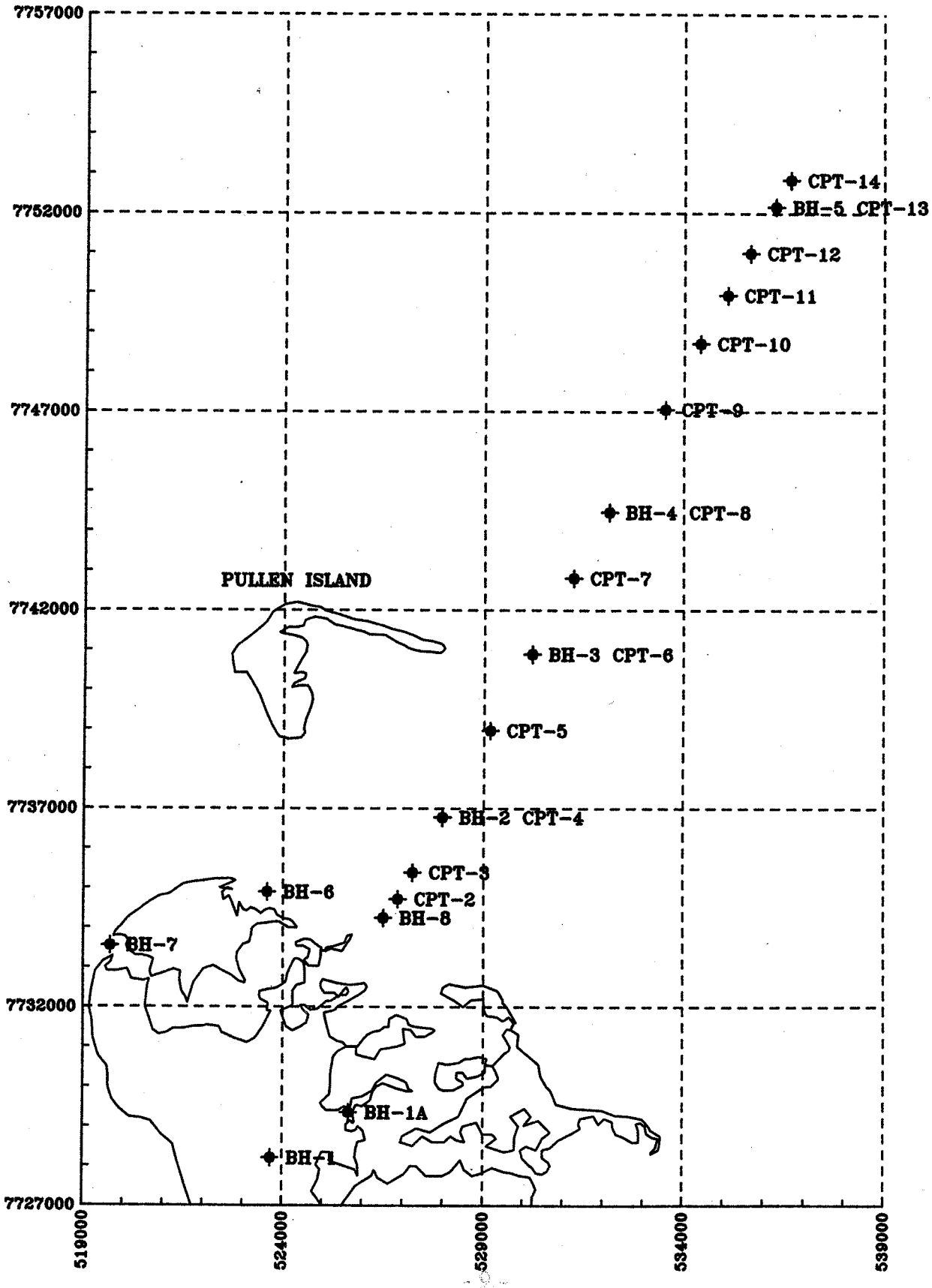

1.3 DRILLING METHODS

S.R. Dallimore, D. Gillespie, F.M. Nixon and J. Shimeld

Three separate drill rigs were utilized for the studies reported in this Open File Report. The deep boreholes completed in the spring used a skid-mounted Containerized Drill System (CDS) equipped with a HT-700 top drive rotary drill. The shallow boreholes utilized a ATV mounted CME 750 top-drive rotary drill. A helicopter portable CME 700 top-drive rotary drill was used for the single summer borehole (90BH1A).

Drilling services were provided by Foundex Explorations Ltd. and Midnight Sun Drilling through a joint venture called Arctic Investigations Ltd.

Deep borehole program

The CDS system utilized standard fluid drilling technology with a recirculation system to reduce environmental disturbance. Sampling was carried out with an HQ wireline coring system with two 1.5 m long triple tube core barrels, one of which was spring mounted (retractor barrel) and one of standard design. Both core barrels cut core of 63 mm nominal diameter. Two drilling fluids were utilized; a non-toxic, mineral oil-based mud produced by Technifluid Ltd. and a more conventional brine-based mud. The oil-based mud was abandoned after two boreholes (90BH2 and 90BH5) due to continued problems maintaining circulation and side-wall integrity.

An electrically powered, drilling fluid chiller unit, owned by Gulf Canada Resources Ltd., was utilized in the deep borehole program to control the temperature of the drilling fluids and reduce down-hole thermal disturbance. This system operated very successfully by maintaining oil-based mud temperatures below -4°C, and brine-based mud temperature at about 0°C. Temperatures of the drilling mud in the mud supply and return tanks were monitored continuously during drilling with an 8 channel data logger. Mud temperature plots for Boreholes 90BH2, 90BH4 and 90BH5 are shown on Figures 1.3.1 to 1.3.3.

The configuration for the CDS system showing the mud circulation system, the drill container and the lay out of the science trailer are shown on Figure 1.3.4.

Figure 1.3.1

MUD TEMPERATURES
90BH2

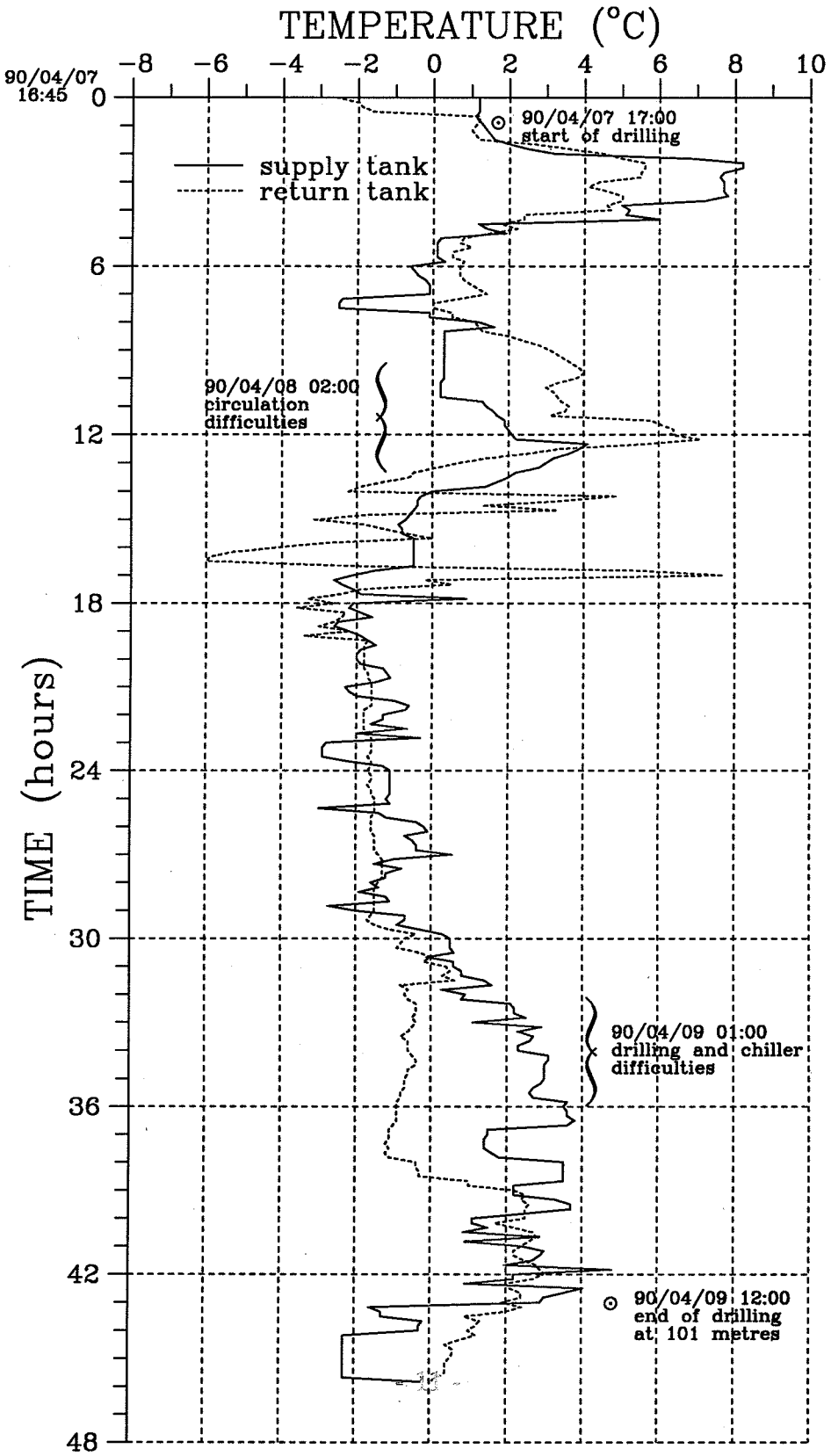

Figure 1.3.2

MUD TEMPERATURES
90BH4

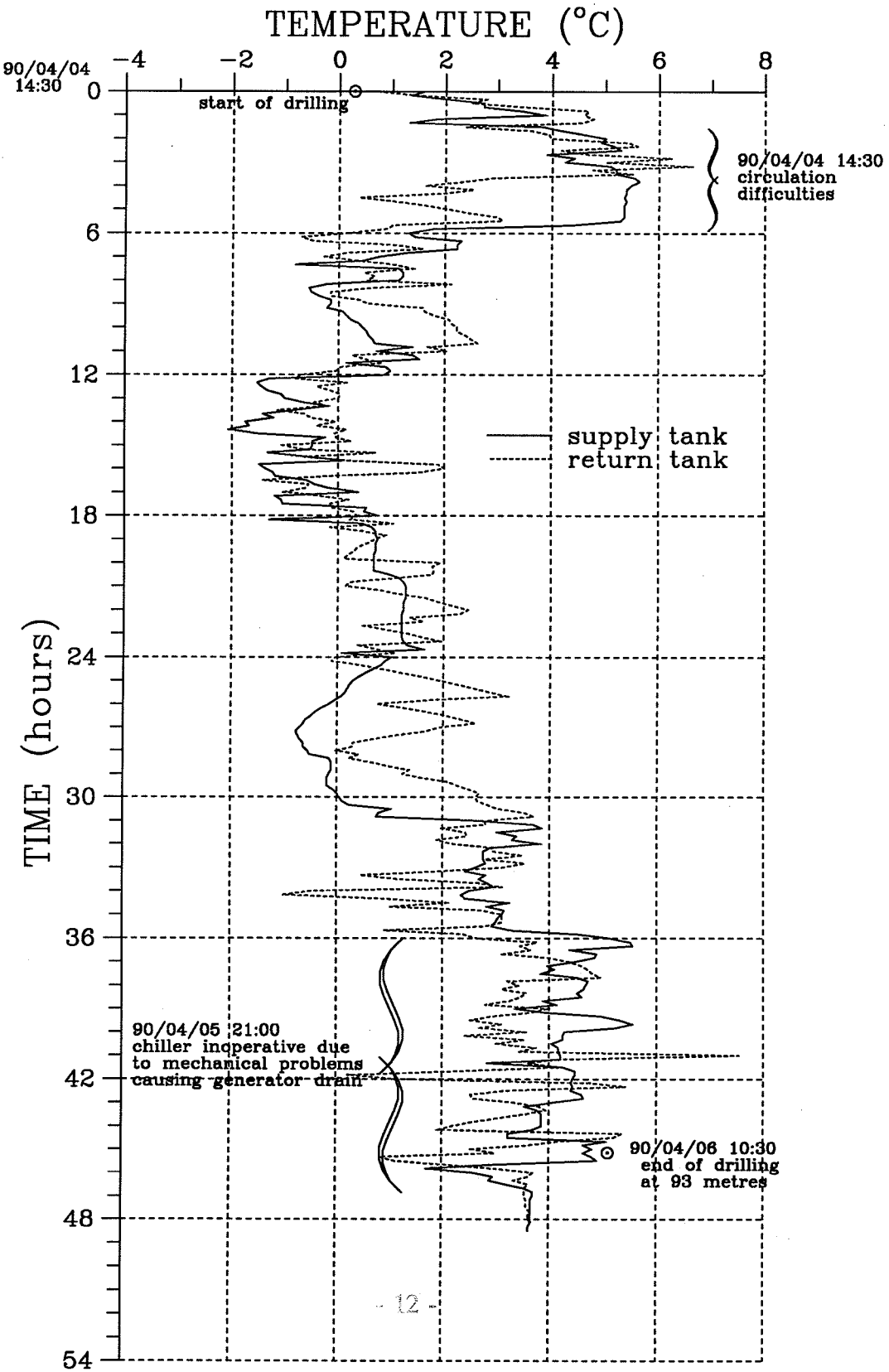

Figure 1.3.3

MUD TEMPERATURES 90BH5

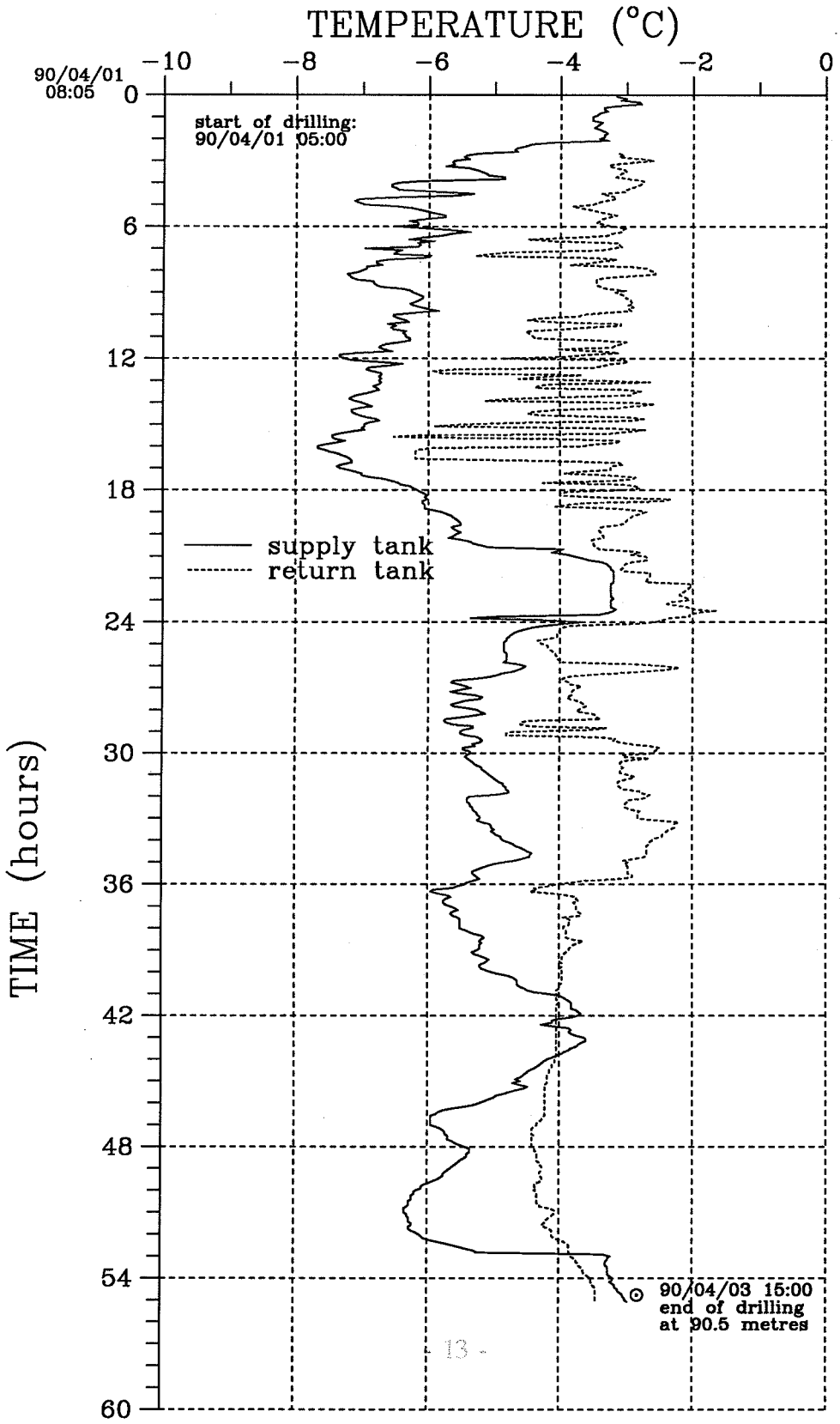

Figure 1.3.4 Layout of drilling containers and mud circulation system

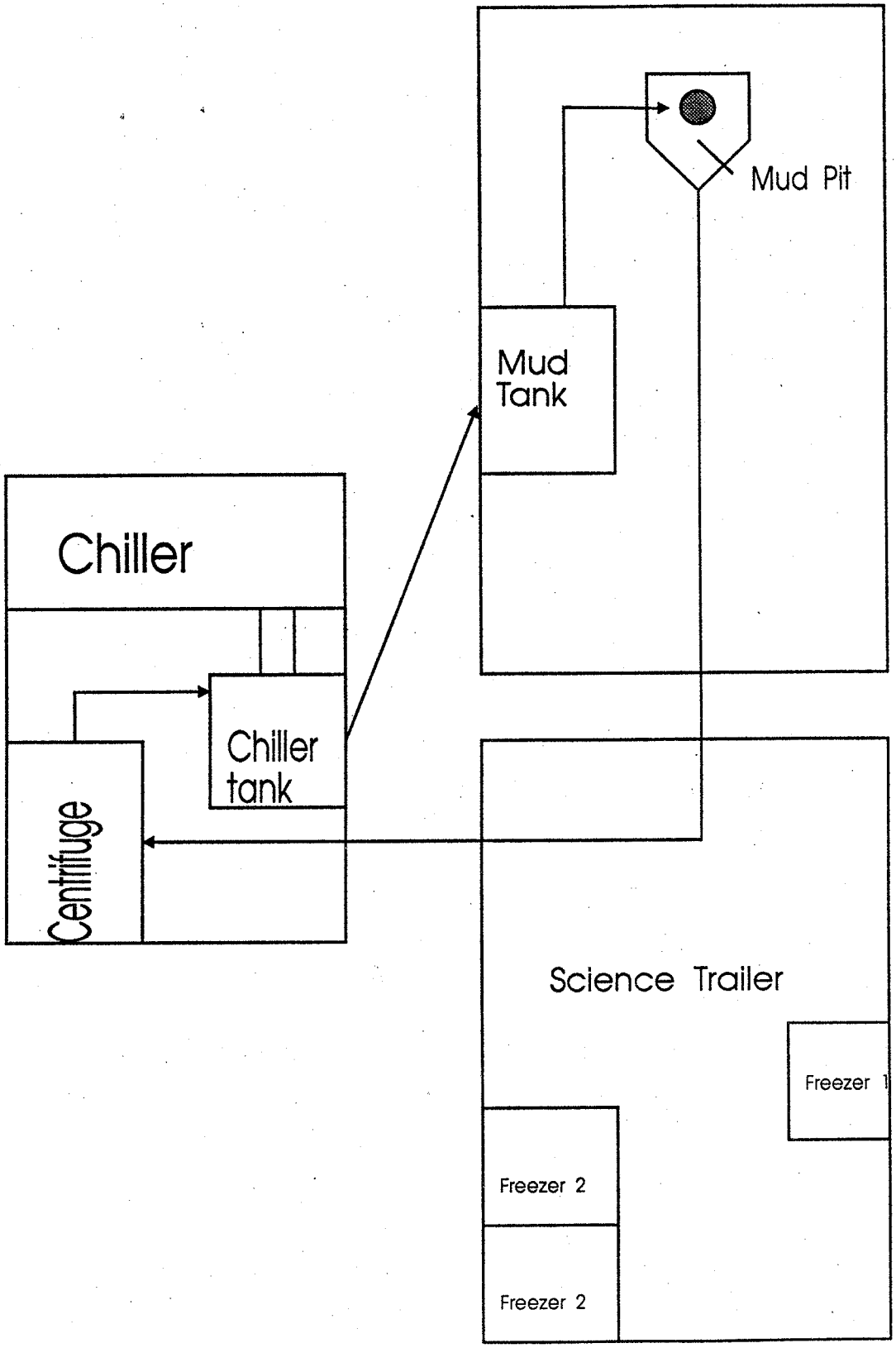

Shallow borehole program

The shallow boreholes drilled in the spring and the summer utilized a dry coring technique. Continuous samples were collected for each of these boreholes with a 90 cm long CRREL core barrel attached to continuous flight augers. Core yielded by this technique were 10 cm in diameter.

1.4 SAMPLE HANDLING

S.R. Dallimore and D. Gillespie

Deep borehole program

Nearly all of the core collected during the deep borehole program were retrieved with a spring mounted 'retractor barrel'. This barrel was capable of collecting excellent samples in variable lithologies and ice-bonding conditions. Once brought to the surface, samples were removed from the core barrel and logged immediately. This procedure involved a quick visual inspection of the core, a measurement of the core temperature with a temperature probe, and an estimation of the strength of cohesive sediments with a pocket penetrometer. At this time an assessment was made of the condition of the sample in terms of both physical disturbance and sensitivity to thermal degradation. Based on this estimate, physically undisturbed core samples were classified according to ice-bonding as the following: 1) well bonded, 2) partially bonded (thermally sensitive) or 3) unbonded.

Subsequent to their collection and classification, a considerable effort was made to store, transport and receive core in Inuvik without substantially altering the ice-bonding conditions of the samples. For the unbonded and partially bonded samples this was achieved by storing the samples in scientific freezers placed at the drill site (Figure 1.3.4). Temperatures in the freezers were held at just above freezing for the unbonded sediments (+1 to +3°C) and at about -2°C for the partially bonded sediments. Well-bonded samples were allowed to cool to the inside temperature of the science trailer which was usually less than -5°C. All samples were generally transported within 12 hours of their collection in insulated chests by truck or helicopter.

Temperatures of the unbonded and partially bonded samples during field storage and transportation were monitored with data loggers.

Onshore boreholes

Samples from the North Head coastal boreholes and 90BH1 and 90BH1A were all considered to be well-bonded. Generally these samples were placed in core boxes and allowed to cool to air temperature. Since air temperatures were generally -20°C when drilling the spring boreholes, little physical disturbance was noted in the samples. However, for 90BH1A, drilled in the summer, samples were allowed to thaw.

1.5 FIELD LABORATORY STUDIES

A. Wilkinson and L. Maurice

A field laboratory was set up in Inuvik at the Inuvik Research Centre (IRC), of the Science Institute of the Northwest Territories. All tests considered to be susceptible to either temperature changes or contamination after sampling were carried out at this facility. Because Inuvik was more than 150 km away from the drilling site, a number of logistical problems had to be overcome to ensure adequate communication with field staff, as well as the efficient and timely transportation of core. Radio-telephone communications to the drilling rig, the truck or helicopter and the laboratory ensured that the delivery of the cores was always anticipated by laboratory personnel. Upon arrival, cores were immediately placed in scientific freezers according to the thermal category assigned at the field site. Core intervals were logged on an 'inventory of core received' sheet, along with the thermal category for storage. These records were checked against photocopies of the 'drill core field inventory' sheets and 'core recovery logs' delivered with the cores.

Testing in the Inuvik Research Centre was carried out according to the sensitivity of a particular test to thermal or mechanical disturbance. Tests included thermal conductivity, acoustic properties, bulk density, sediment logging, photography, strength, water content, salinity, grain size and plasticity. A flow chart of the procedures, showing storage conditions for the different core types and the hierarchy for testing is shown on Figure 1.5.1. Details regarding the specialized procedures undertaken as part of the thermal conductivity program and physical property program are described in Appendix B.

A paper archive was maintained for each borehole at the field lab and subsequently after shipping of core to other laboratories. This was based on a logical sequence of operations associated with each core length, from drilling recovery, storage, field measurements and transport to Inuvik. Every aspect of the investigations in Inuvik had an associated paper record of observations and results, a copy of which was filed by the investigator each day. A summary chart of each core length, sequenced by depth for each borehole, was initialled as the reports were filed to provide an operational overview. Examples of data recording sheets are given in Appendix B.

Figure 1.5.1
CORE PROCESSING IN INUVIK RESEARCH CENTRE

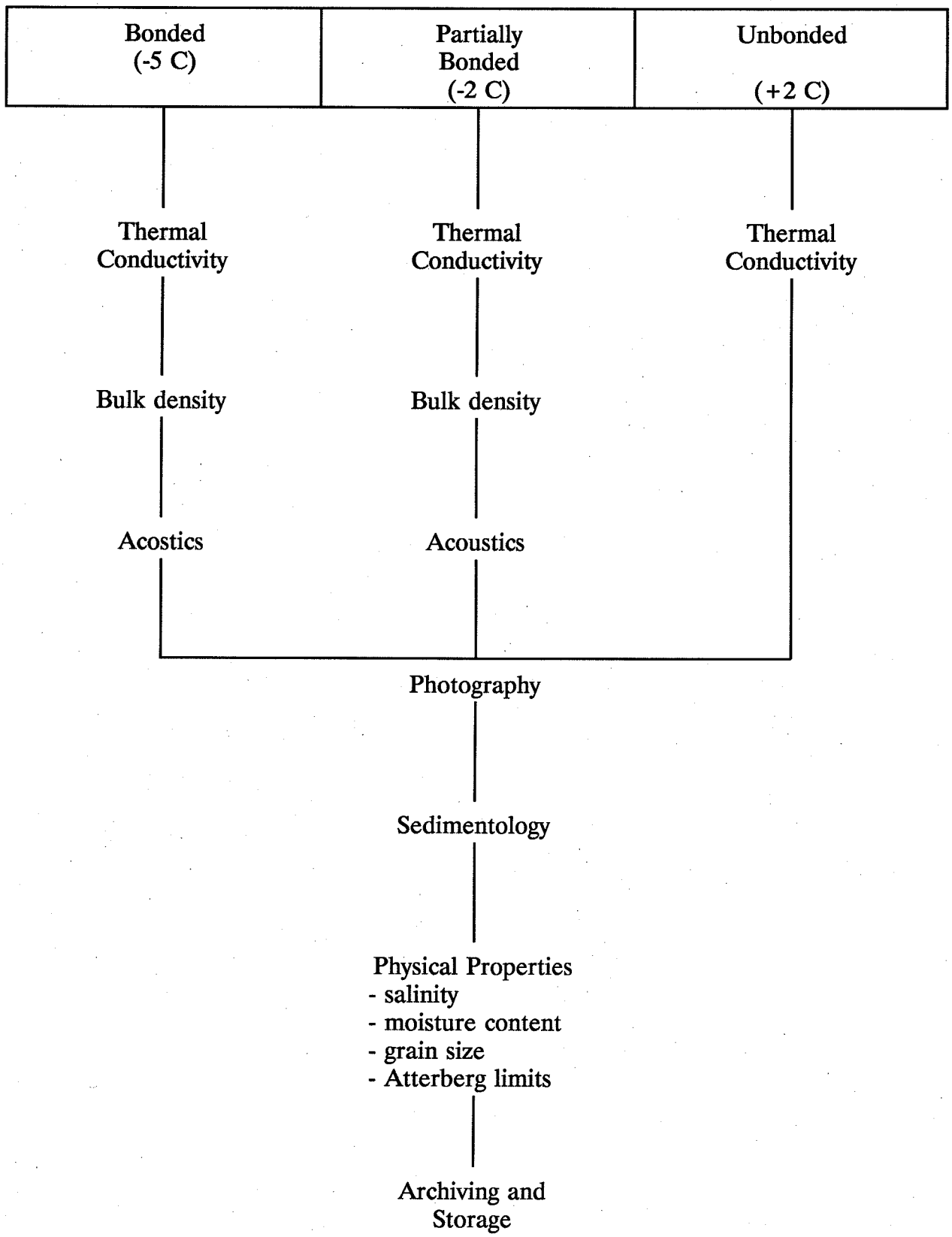

CHAPTER 2

ONSHORE-OFFSHORE TRANSECT: QUATERNARY GEOLOGY

2.1 ONSHORE GEOLOGY

S.R. Dallimore and J.-S. Vincent

2.1.1 Regional Overview

The Quaternary geology of Richards Island and the Tuktoyaktuk Peninsula area has been reviewed by Rampton (1988). Coastal sections on northern Richards Island and Hooper Island have revealed a relatively complex stratigraphic setting. A simplified diagram of the lithostratigraphic units observed on land beneath glacial sediments of presumably the Early Wisconsinan Toker Point Stade is presented in Figure 2.1.1. The ages of these sediments are not well constrained, however numerous radiocarbon age determinations on organic material in these sediments have consistently yielded non-finite ages (greater than 35,000 to 40,000 YBP).

The Kendall sediments comprise the oldest unit observed in the area. The environment of deposition of these interbedded sands, silts and clays, on the basis of the abundance of marine shells, indicates that these sediments are of marine origin. The Kendall sediments are overlain by the Hooper clay which contains abundant and well preserved marine macrofossils. The Hooper clay is widespread throughout the Tuktoyaktuk Coastlands; however, in the vicinity of Mason Bay on northern Richards Island, it is only occasionally exposed, usually close to sea level.

Two distinct sand units are present above the Hooper clay, and have been assigned respectively to the Kidluit Formation and the Kittigazuit Formation by Rampton (1988). The Kidluit Formation, which immediately overlies the Hooper clay, is thought to be fluvial. On Richards Island it is typically grey in colour with numerous fluvial bedforms and abundant detrital organics and wood-rich horizons. Kittigazuit Formation sands, which occur above the Kidluit sands, are brown. Their most diagnostic features are the presence of large scale planar cross beds, uniform grain size and, a scarcity of organics. Rampton (1988) has suggested a deltaic depositional environment for this unit, however, some evidence also points to an eolian depositional environment.

Glacial deposits related to the Toker Point Stade, of presumed Early Wisconsinan age, overly the Kittigazuit Formation unconformably. On Richards Island these sediments include widespread bodies of till and local occurrences of glaciofluvial sands and gravel.

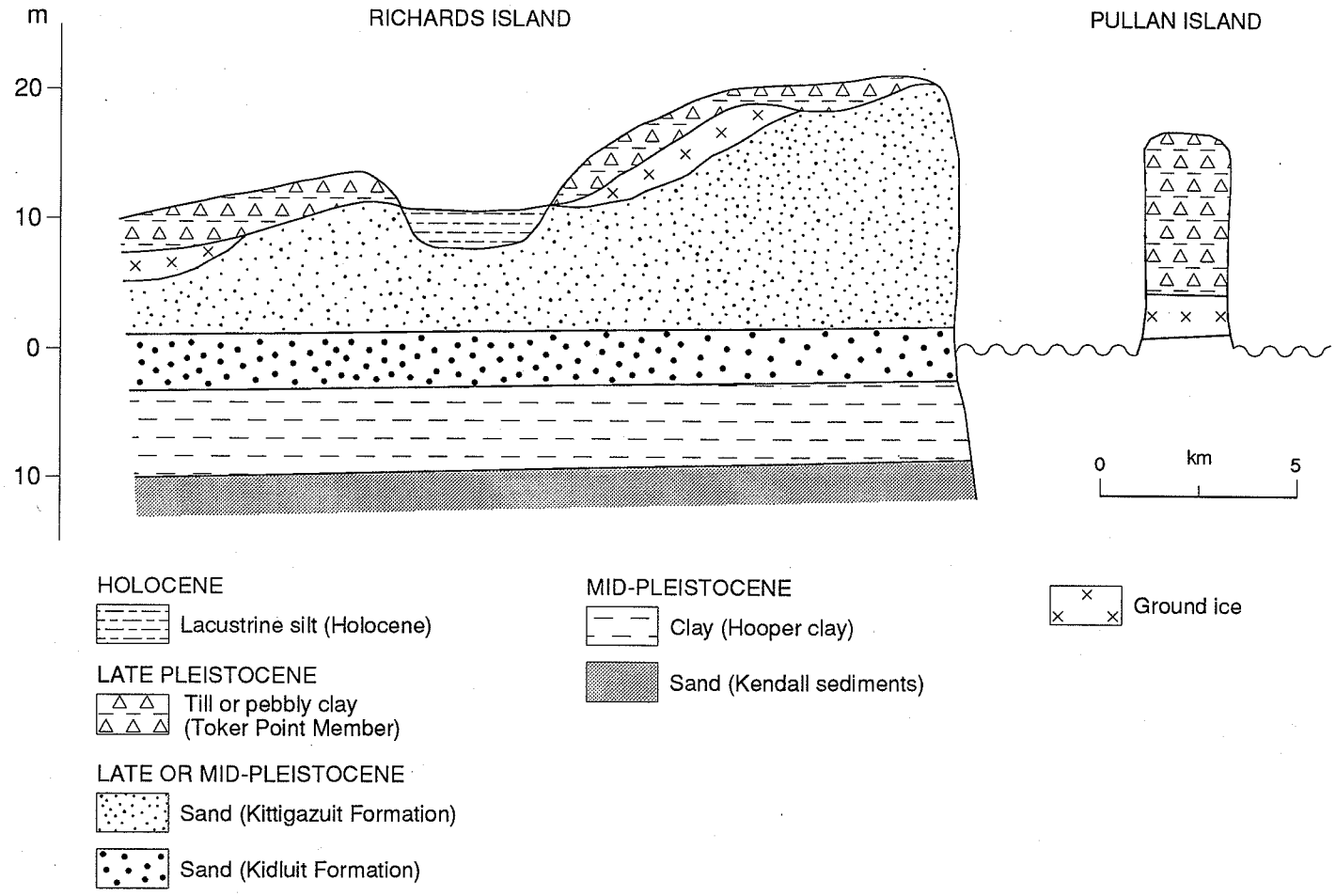

Figure 2.1.1 Generalized stratigraphy of coastal bluffs in vicinity of northern Richards I.

The glacial episode which deposited these sediments also caused substantial glaciotectonic deformation of the underlying sediments. In some areas of Richards Island, localized thrusting and folding of thick packages of sediment are common. The thickness and character of the till on Richards Island are variable. On northern Richards Island it is commonly re-worked to form a lag gravel deposit.

2.1.2 Description of coastal exposures in the vicinity of the transect landfall

A simplified surficial geology map of northern Richards Island showing areas of recent coastal change is presented on Figure 2.1.2. East of North Head in the vicinity of the landfall of the transect, eroding coastal bluffs are between 5 and 18 m high. The main surficial units consist of a thin clay diamicton or gravel lag, underlain by massive brown sands. The character of the diamicton is variable. It is absent in some locations, but in others it may be up to 10 m thick. The diamicton is either Toker Point till or till re-worked by solifluction and other processes. The underlying sand commonly contains planar cross stratification and is assigned to the Kittigazuit Formation. Individual co-planar bedding sets may greater than 10 m high, dipping 5 to 35 degrees mainly to the east but with intersecting sets dipping in other directions. The Kittigazuit sand is generally very uniform in grain size with only rare thin silty sand interbeds and very occasional thin detrital organic bands. Paleoecological analysis of an organic-rich bed in an exposure in the vicinity of Mason Bay has revealed a relatively diverse plant and insect macrofossil assemblage thought to reflect terrestrial depositional conditions (J.V. Matthews Jr., Plant Macrofossil report, 88-29; Fossil Arthropod report, 88-14).

Ground ice content of the Kittigazuit Formation sand is generally low although the diamicton may contain substantial amounts of excess ice and even massive ice. Where the ice content of the diamicton is high, retrogressive thaw flow slides are common (Fig. 2.1.2).

Stratigraphic units present in an exposure along a peninsula just northeast of borehole 90BH1A are visible on Figure 2.1.3. This exposure is typical of many on the small islands and embayments in the area. The Kittigazuit sand is the dominant material having well developed planar cross beds dipping between 4 and 30 degrees. It is overlain by a 10 to 20 cm thick boulder lag which is thought to be a till remnant. This unit is in turn overlain by 1 to 3 m of eolian sand with abundant in situ rootlets.

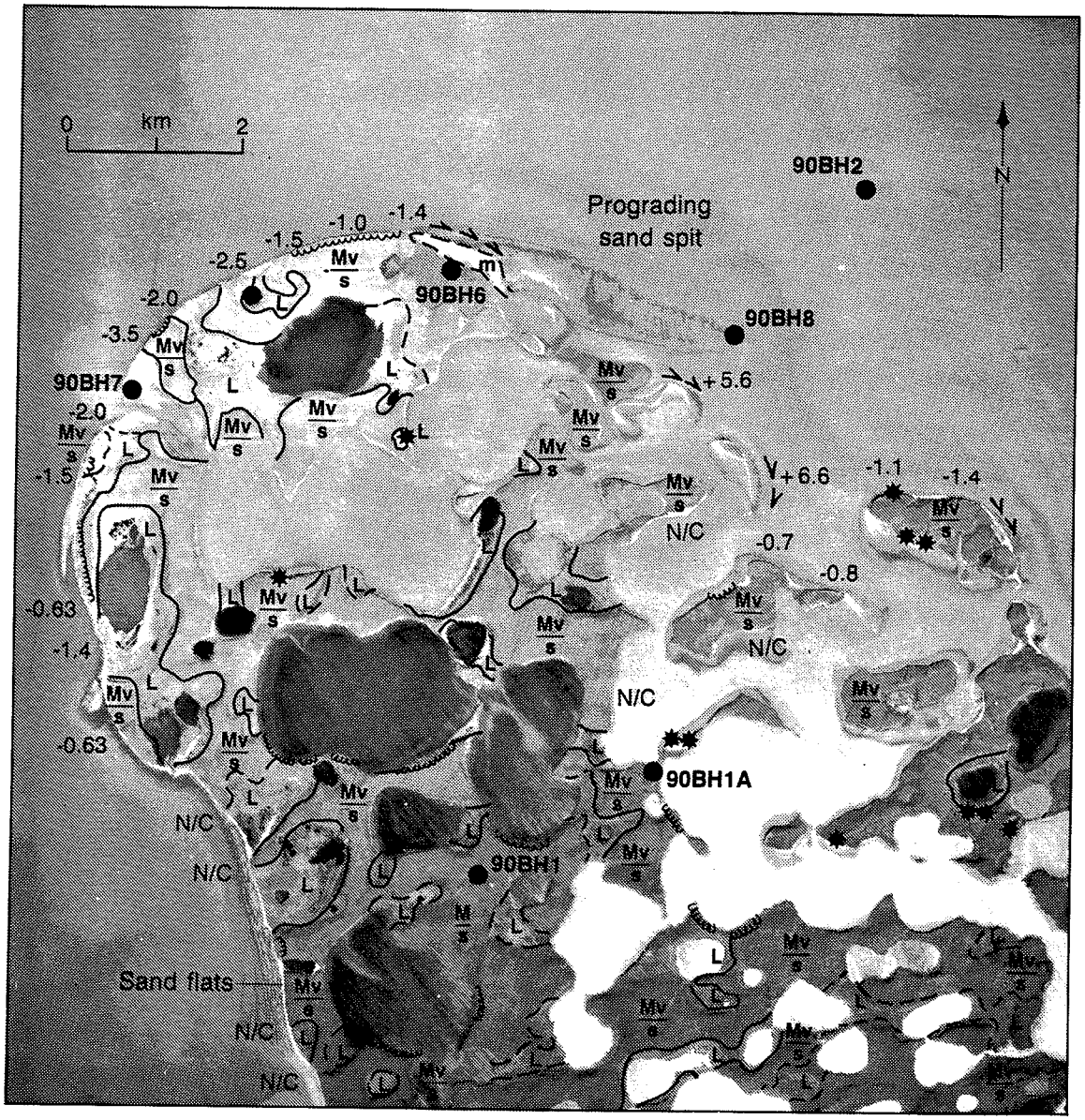

Marine sands and silts . . . . . **m**
Lacustrine sediments . . . . . **L**
Discontinuous veneer of glacial till over pre-Wisconsinan sands . . . . **Mv/s**
Glacial till over pre-Wisconsinan sands . . . . . **Mv/s**

Stable coastline . . . . . N/C
Average coastal retreat (m/yr) . . . . -1.4
Recent eolian activity . . . . . ✸
Borehole . . . . . ● **90BH2**
Retrogressive-thaw flow slides . . . . .
Sedimentation . . . . . → →

Figure 2.1.2 Surficial geology of northern Richards Island

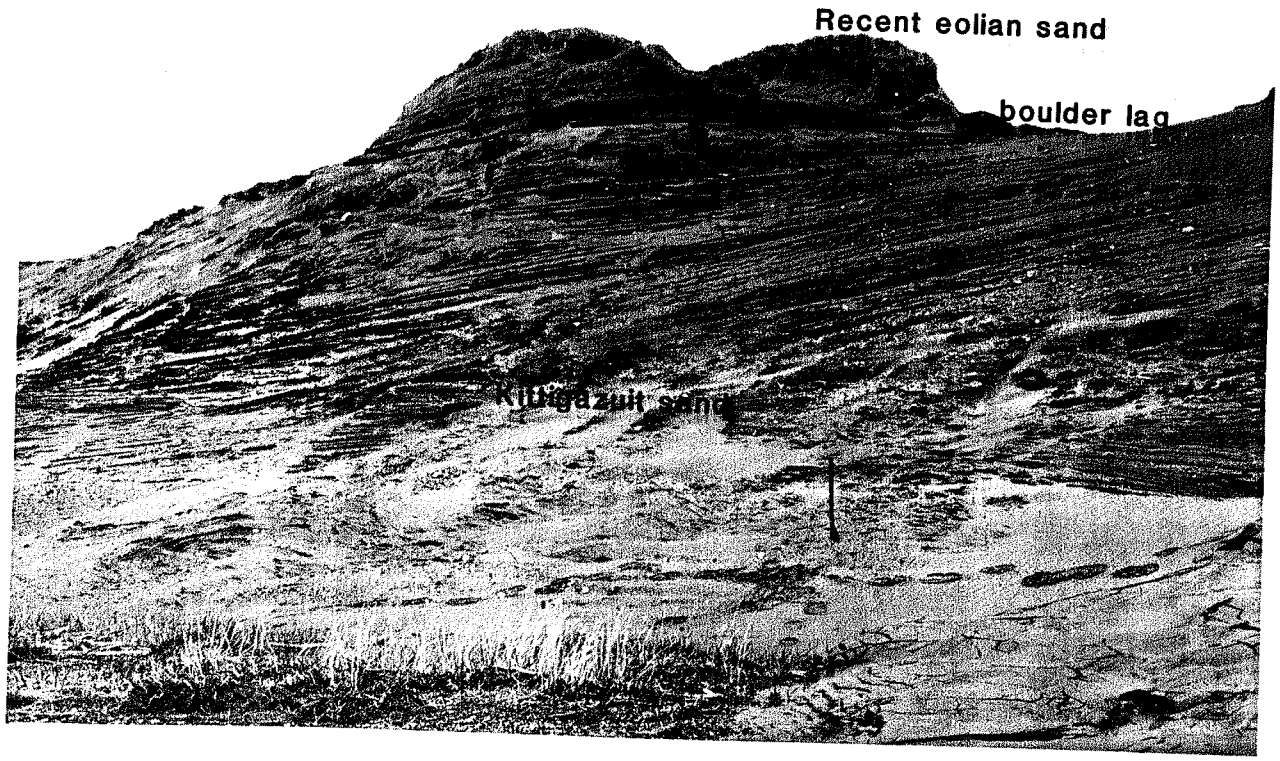

Figure 2.1.3 Photo showing geology of exposure near borehole 90BH1A (ice axe for scale).

REFERENCES

Rampton, V.N., 1988. Quaternary geology of the Tuktoyaktuk coastlands, Northwest Territories, Geological Survey of Canada, Memoir 423, 98 pgs.

Matthews, J.V. Jr. 1988. Plant Macrofossil report 88-29 and Fossil Arthropod report 88-14. Internal GSC report

2.2 OFFSHORE GEOLOGY

S.M. Blasco and J.F. Lewis

2.2.1 Offshore Geological model

A model of the surficial geology of the upper 100m of the Beaufort Shelf (Figure 2.2.1) has been proposed for the area north of Richards Island (Blasco et al. 1988; 1990). At the base of the sequence, Unit E consists of a thick, medium to fine-grained sand with silt interbeds. This unit is thought to vary considerably in depositional character across the shelf, however, northwest of Richards Island, it is characterized by prograded delta lobes with some evidence of alternating terrestrial and nearshore marine conditions. Dating in this unit is limited, however it is thought to be Late Wisconsinan.

Unit D which disconformably overlies Unit E, consists of interbedded silt and clay with an observed maximum thickness of 40 m. Seismic profiles suggest that this unit represents delta-margin depositional conditions. A radiocarbon age determination of 21,620 ± 630 YBP (B-6276) at the base of Unit D suggests that this unit is Late Wisconsinan in age (Hill et al., 1985).

Unit C consists mainly of sand with a broad spatial distribution and consistent thickness (30-40 m). Sedimentary structures, lithologies and seismic stratigraphy suggest that it represents a broad coastal glacial outwash plain. However, it is recognised that this unit varies considerably in depositional regime and may locally contain deltaic deposits and peat as well as possible diamicton. Dating of organic matter found in Unit C suggest that it may be Late Wisconsinan to early Holocene in age.

A major regional unconformity separates Unit C from overlying Units B and A. This unconformity is thought to be related to the most recent marine transgression in the area with Unit B consisting of a sequence of interbedded sands, silts and clays deposited in a nearshore setting. Unit A consists of a veneer of Holocene marine muds thought to have been deposited in water depths greater than 10 m.

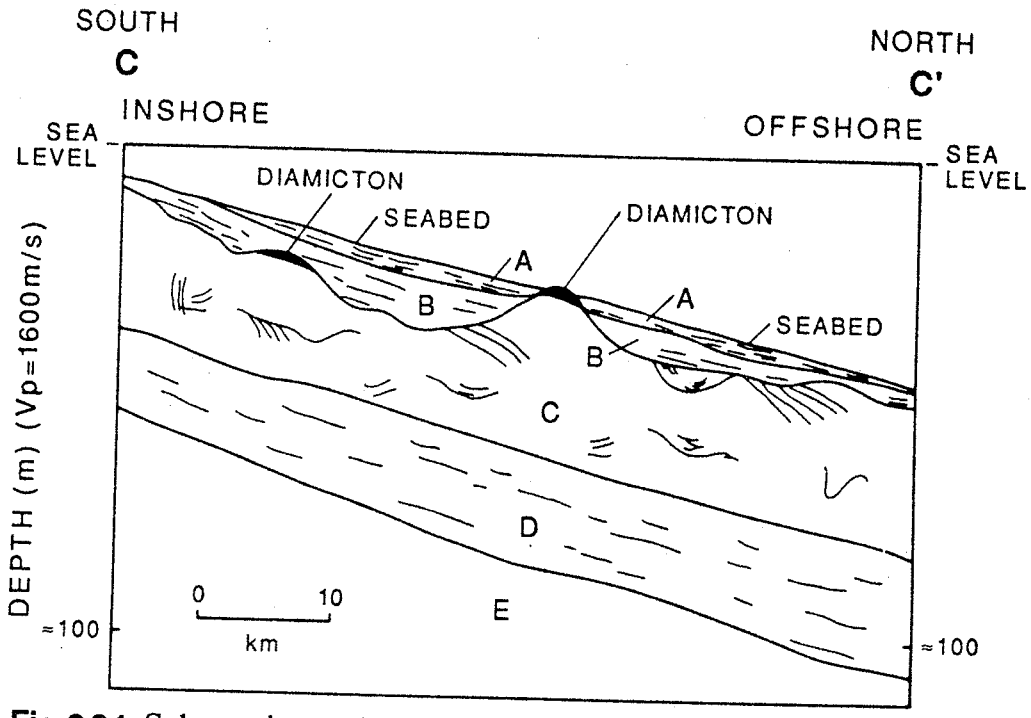

Fig. 2.2.1: Schematic north-south cross-section across the Beaufort Shelf north of Richards Island showing stratigraphy of the upper 100 m of sediment below seabed. Unit A is Holocene marine clay; Unit B is transgressive interbedded sand, silt, and clay; Unit C is a glaciofluvial outwash sand complex; Unit D is inner-shelf marine clays; and Unit E is an underlying glaciofluvial outwash sand. The top of Unit C forms a regional erosional unconformity with associated coarse lag deposits (diamicton).

2.2.2. Seismostratigraphy Along the Transect

Introduction

Bathymetry, subbottom profiles, and analogue single channel reflection seismic records (both boomer and small airgun array) were acquired along the proposed onshore-offshore transect from the 3 m to beyond the 10 m water depth contour. These data were analyzed, interpreted and integrated into a line drawing representing the cross-section of the onshore-offshore transect (Lewis, 1989). The nearshore section (3-10 m water depth) is illustrated in Enclosure 2.2.1, and was used as the basis for selecting borehole locations.

Shallow Seismostratigraphy

Within the upper 100 m of sediment along the borehole transect, four regionally mappable seismostratigraphic units (units B, C, D, and E) have been identified. An additional unit, Unit A, which consists of soft, surficial, recent marine silty clays, blankets the shelf as a thin veneer seaward of the 10 m isobath. Unit A is not present along the borehole transect proper but pinches out at the seabed at the northern end of the cross-section (see Enclosure 2.2.1). Acoustically, Unit A is transparent. Internal reflections are rare and were either never present or have since been destroyed by ice scouring. The contact with underlying Unit B is gradational over 1 to 3 m, and is not normally recognized as a distinct reflective horizon.

Unit B, which consists of spatially discontinuous interbedded stiff silty clays, silts and sands is a transgressive unit deposited under high energy, nearshore conditions related to rising sea level. Unit B outcrops on the seabed along most of the transect. Deposition of these sediments continues today in water depths less than approximately 10 m. Although the thickness of this unit varies locally, along the transect, Unit B appears as depression infill up to 14 m thick. The infill averages 10 m in thickness, thins shoreward, and pinches out offshore at the northern end of the transect. Acoustically, the unit has greater internal reflectivity than unit A, and may be relatively transparent, but usually consists internally of horizontal, laterally discontinuous reflectors. Lateral continuity of reflectors in the upper part of Unit B adjacent to the seabed may be disrupted by ice scouring. Inshore, the internal character of Unit B (and underlying units) is masked by the presence of shallow gas at depths of 2 to 10 m below seabed. Unit B rests unconformably on Unit C sediments.

Unit C consists of a complex of coastal plain sands and silty sands deposited as regressive sediments under lower sea level conditions. Unit C underlies Unit B along much of the cross-section, but outcrops on the seabed at the northern end. A high amplitude, well defined, laterally continuous, smooth reflector usually defines the B/C contact. At intervals along the borehole transect this contact is less clearly defined and may be masked by the presence of shallow gas within overlying Unit B. This B/C contact represents a regional disconformity to erosional unconformity where the upper surface of Unit C has been truncated. The thickness of Unit C averages about 30 m and decreases shorewards from about 40 m at the northern end to approximately 20 m at the southern end of the seismic section. Acoustically, Unit C is characterized internally by numerous, laterally discontinuous, small scale irregular reflectors that represent the complex cut-and-fill structures of laterally migrating channel systems. Bottomset, topset and foreset reflectors are occasionally observed. The base of Unit C and the contact with Unit D is poorly defined on most seismic reflection profiles, and is inferred to be the base of the cut and fill pattern characteristic of this unit.

Unit D consists of transgressive marine clays and silts which unconformably underlie Unit C. The thickness of Unit D decreases shorewards from approximately 15 m at the northern end of the transect to about 10 m at the southern nearshore end of the seismic section. Acoustically, this unit is transparent and is characterized by either a lack of internal reflections or weak horizontal reflections. Unit D rests unconformably on Unit E sediments.

Unit E is a regionally mappable, regressive sand unit underlying Unit D. The unconformity between these two units is marked by a laterally discontinuous, low to high amplitude, smooth reflector similar in character to the reflector marking the B/C contact. The thickness of Unit E is unknown as the penetration and resolution of single channel seismic reflection systems rarely extend beyond the top of this unit. Below the Unit D/E unconformity the upper surface of Unit E is acoustically characterized by small scale, irregular reflectors representing an incised and infilled channelled surface.

Subsea Permafrost

Ice-bearing sediments are identified on shallow seismic reflection profiles as high amplitude, laterally discontinuous, irregular 'hummocky' reflectors and, as high amplitude,

continuous, smooth, horizontal reflectors (Blasco, 1984). Ice bearing sediments identified by seismic reflection techniques are referred to as acoustically defined permafrost or APF. Along the borehole transect hummocky acoustic events occur only within Unit C and, in particular at the northern end of the cross-section. The distribution of these acoustic events would suggest that ice-bearing sediments occur as random bodies within Unit C. Such bodies occur within 4 m of the seabed at the northern end of the borehole transect, but are mostly concentrated at 8 to 12 m subseabed. Like shallow gas the occurrence of shallow ice-bearing sediments masks the underlying seismostratigraphy. As the acoustic character of units B and C are evident along much of the section, these units are probably not ice-bearing along the central part of the transect. Shallow gas-masking in the nearshore precludes any discussion about the distribution about ice-bearing sediments in this zone. The smooth reflector identified as the D/E contact along the section indicates both a lithologic change from clay to sand and the presence of ice-bearing sediments.

Nearshore Seismostratigraphy

Shallow reflection seismic data are non-existent shoreward of the 3 m isobath. Previously postulated geologic models suggest that either there is stratigraphic continuity from onshore to offshore and units C, D, and E are correlative with the Kittigazuit, Kidluit, Hooper and Kendall onshore sequences, or that the offshore units pinch out in the nearshore zone and are not found onshore.

Borehole Locations

Borehole locations were selected along the transect corridor to confirm the existence and stratigraphic character of the offshore units B, C, D, and E, to confirm the speculated distribution of ice-bearing sediments, and to provide the evidence to determine whether stratigraphic continuity or pinchout controls the shallow nearshore sediment sequence. Selected borehole locations are identified on Enclosure 2.2.1.

REFERENCES

Blasco, S.M., 1984. Perspective on the distribution of subsea permafrost on the Canadian Beaufort continental shelf. In: International Conference on Permafrost, 4th, Fairbanks, AK. Final Proceedings, National Academy Press, Washington, D.C., p. 38-86.

Blasco, S.M., Fortin, G., Hill, P.R., O'Connor, M.J., and Brigham-Grette, J., 1990. The late Neogene and Quaternary stratigraphy of the Canadian Beaufort continental shelf. In: Grantz, A., Johnson, L., and Sweeney, J.F., (eds.), The Geology of North America, v.L: The Arctic Ocean region, Geological Society of North America, Boulder Colorado.

Hill, P.R., Mudie, PJ., Moran, K., and Blasco, S.M., 1985. A sea-level curve for the Canadian Beaufort Shelf. Canadian Journal of Earth Sciences, v.22, p.1383-1393.

Lewis, J.F., 1989. Regional surficial geology of the south central Canadian Beaufort Shelf - draft report submitted to the Geological Survey of Canada, Atlantic Geoscience Centre, April 1989.

Pelletier, B.R., ed., 1984. Marine science atlas of the Beaufort Sea, sediments. Geological Survey of Canada, Misc. Report 38, 27 p.

2.3 SEDIMENTOLOGY

K. A. Jenner and S. M. Blasco

2.3.1 Sedimentary Unit Characteristics

Four sedimentary units - B, C, D and E - representing two clay and two sand units were identified from the onshore-offshore borehole transect and are presented in Figures 2.3.1 to 2.3.6. A detailed stratigraphic study of the sediments comprising Units B, C, D and E (Figures 2.3.7 to 2.3.10) was undertaken to document the nature of the contacts between the units and to characterize the lateral variability of distinct sedimentary subfacies within the clay/sand units to further aid in the future interpretation of the depositional regimes. The lateral distribution of these units is depicted in the attached fence diagram (Enclosure 2.3.1).

Unit B

Unit B, where encountered in the onshore-offshore borehole transect, comprises approximately 15 m of dark grey to black, moderately to extensively bioturbated silty clay with graded silt and fine sand interbeds toward the top of the unit. Internal laminae are either distinct or vague depending on the degree of bioturbation. Unit B was sampled in two of the six boreholes (90BH02 and 90BH03) from the spring and summer drilling programs. The upper contact of Unit B with Unit A (surficial marine clays found further offshore) was not observed and, in general, Unit B outcrops on the seafloor along the nearshore section of the transect.

Three distinct subfacies have been identified within Unit B (Figure 2.3.7). The uppermost subfacies -B_1- is comprised of an upward coarsening, fine grained, dark grey to black sand with interbedded, occasionally graded, bioturbated silt and clay. In 90BH02 the sand in subfacies B_1 is darker in colour and contains a higher concentration of disseminated organics. The basal boundary of this subfacies is gradational over several centimeters and is distinguished by the absence of sandy interbeds. Subfacies B_2 is characterized by very dark grey to black, moderately bioturbated, interlaminated and occasionally graded silt and clay with rare, fine grained, sand-infilled burrows and abundant scattered shell fragments. The upper and lower boundaries of this subfacies are also gradational over several centimeters

as a result of a change in the degree of bioturbation. In 90BH03 subfacies B_2 is additionally distinguished by a basal light brown, dry, organic-rich silty clay designated as a transitional unit between Unit B and Unit C. The basal subfacies in 90BH02 and the intermediate subfacies in 90BH03 -B_3- is differentiated from subfacies B_2 by a substantially higher degree of bioturbation with a resulting vague, primary bedding.

Unit C

Unit C comprises 12 to 35 m of fine to medium grained, dark grey to grey brown, well-sorted, massive to trough cross-bedded sand. This unit typically fines upward from basal medium grained sand to upper fine grained sand. Unit C in the offshore was sampled in three of the six boreholes (90BH02, 90BH03 and 90BH05). In two of the three boreholes (90BH03 and 90BH05) Unit C can be subdivided into three laterally correlative sedimentary subfacies (Figure 2.3.8). The upper part of Unit C (subfacies C_1) is characterized by grey-brown, fine grained sand with both wavy and planar silt, and sharp-based clayey silt interlaminae. In 90BH03 subfacies C_1 is capped by a black, silt diamict with scattered granules and pebbles (Figure 2.3.4). In 90BH05 subfacies C_1 is coarser grained when compared with the other boreholes, containing thin medium sand interbeds near the top of the subfacies, which become more frequent toward the base. Rare wood fragments, disseminated black organics and scattered pebbles were additionally observed in this subfacies. The base of subfacies C_1 in 90BH03 is gradational into a lower, dark grey to grey-brown, well-sorted fine to medium grained sand (subfacies C_2). This contact is not distinct but is defined by a subtle, downward coarsening of grain size. In 90BH05 subfacies C_1 and C_2 are separated by a 1 m thick unit of trough cross-laminated fine sand.

The Kittigazuit Formation and Kidluit Formation, in the two onshore boreholes (90BH1 and 90BH1A), comprise 35 m of fine grained, dark grey to grey brown, parallel laminated to trough cross-bedded sand. Borehole 90BH01 was excluded from further examination because only the upper 0.80 m of Kittigazuit Formation was intersected. In 90BH1A the Kittigazuit Formation is characterized by fine grained, grey brown sand with interbedded, wavy silt laminae and rare, low angle cross-bedding. Stratigraphic similarity would suggest the it is laterally equivalent to subfacies C_1 noted earlier in the offshore boreholes (Figure 2.3.8). The Kidluit Formation comprises fine grained, grey sand with

distinct trough cross-laminae and low angle cross-bedding. Stratigraphic similarity would suggest it is laterally equivalent to subfacies C_3 in the offshore boreholes. The Kittigazuit and Kidluit sands appear to be correlative with Unit C in the offshore and are therefore designated as Unit C in the following discussion. Further work however, is necessary to determine the exact relationship between these onshore and offshore units.

The sedimentary character of subfacies C_2 changes toward the distal end of the onshore-offshore transect. On land (90BH1A) subfacies C_2 is absent. In 90BH03 it is preserved as a 2 m thick, medium grained sand. Further offshore, at 90BH05, subfacies C_2 is characterized by a much thicker 15 m interval of interbedded fine and medium grained sand with a sharp basal contact (Figure 2.3.8).

Subfacies C_3 consists of dark grey, fine sand distinguished by higher concentrations of disseminated organics and well developed planar and trough cross-laminations. The thickest record of this subfacies is preserved onshore in borehole 90BH1A. Further offshore in boreholes 90BH03 and 90BH05 the subfacies is thinner but still displays the same distinctive sedimentary characteristics (Figure 2.3.8).

Of the four boreholes which sampled Unit C, 90BH02 located close to the coastline just south of Pullen Island is characterised by a distinctive facies which interrupts the lateral continuity of the subfacies identified in the remaining boreholes. The cored portion of Unit C represents a single facies of fine grained, olive-green, organic-rich, finely laminated to structureless, micaceous sand with rare pebbles, shell fragments and woody material (Figure 2.3.8).

Unit D

Unit D consists of 7 to 10 m of very dark grey to black, laminated and bioturbated silty clay, graded silt and rare fine grained sand. It is distinguished by internal s-type microfolding and subvertical microfaulting with displacements on a mm-size scale. Unit D in the offshore was intersected in four of the six boreholes (90BH2, 90BH3, 90BH4 and 90BH5) drilled during the spring and summer 1990 drilling programs, but was not cored completely in three of these.

Based on the available core, three subfacies can be identified within the unit, and these are presented graphically in Figure 2.3.9. In all boreholes the upper portion of Unit D -

subfacies D_1 - comprises dark grey, moderately to extensively bioturbated, laminated silt and silty clay. Black, organic-rich burrow-infills give this subfacies a mottled appearance. Individual silt beds have a sharp base, often with burrowed boundaries, and predominantly graded. In boreholes 90BH02 and 90BH03 subfacies D_1 is subvertically microfaulted with displacements ranging from 0.1 to 1.0 cm. The basal boundary between subfacies D_1 and D_2 is distinct, being based on the appearance of deformed bedding within the underlying subfacies; however the sedimentary characteristics of the two subfacies remains unchanged across the subfacies boundary.

The Hooper clay, identified in the onshore borehole (90BH1A), comprises 6 m of grey, bioturbated silty clay with shells and interbedded fine grained, olive grey sand toward the base. Stratigraphic similarity suggests that Hooper clay is laterally equivalent to Units D_1 and D_3 noted earlier in the offshore boreholes (Figure 2.3.9). The Hooper clay appears to be correlative with Unit D in the offshore and is therefore designated as Unit D in the following discussion. Further work however, is necessary to determine the exact relationship between these onshore and offshore units.

Subfacies D_2 exists in four of the five boreholes (90BH02, 90BH03, 90BH04 and 90BH05) which sampled Unit D (Figure 2.3.9). Proximal to the coastline in borehole 90BH02 subfacies D_2 is recorded as a single, thick, microfolded and microfaulted, bioturbated silty clay sequence. Further offshore the character of subfacies D_2 changes and in 90BH03, 90BH04 and 90BH05 this subfacies is defined by an upper dark grey, bioturbated, extensively microfolded and microfaulted silty clay, and an underlying bioturbated silty clay devoid of deformation and a lower, thin, bioturbated silty-clay with a moderate to low degree of deformation. The basal contact of subfacies D_2 is gradational over several centimeters into subfacies D_3.

Subfacies D_3 exists in four of the five boreholes (90BH1A, 90BH03, 90BH04 and 90BHO5) which sampled Unit D (Figure 2.3.9). Like subfacies D_1, subfacies D_3 is comprised of dark grey, bioturbated, laminated silt and silty-clay, but is distinguished by a downward increase in the number and thickness of silt/fine sand interbeds. These interbeds have a sharp base, are commonly graded and occasionally contain shell fragments.

Unit E

Unit E consists of fine grained, dark grey, well-sorted sand containing some dirty organic-rich interbeds toward the base of the unit. Unit E in the offshore was sampled in three of the six boreholes (90BH02, 90BH04 and 90BH05). The upper contact of Unit E was sampled in only two boreholes (90BH02 and 90BH04) and neither the middle of Unit E nor the basal contact was cored.

Based on these data Unit E has been subdivided into three subfacies with considerable uncertainty concerning their lateral extent (Figure 2.3.10). Subfacies E_1 exists in 90BH02, 90BH04 and 90BH05 and consists of very fine grained, grey to olive-grey sand with rare organic-rich laminae and some black, mafic-rich concentrations. Subfacies E_1 is found at the top of boreholes 90BH02 and 90BH04 and toward the base of the cored interval in 90BH05 (Figure 2.3.10). The basal contact of this subfacies was not cored.

The Kendall sand, identified in the onshore borehole (90BH1A), comprises 0.30 m of fine grained, olive grey sand. Stratigraphic similarity suggests that the Kendall sand is laterally equivalent to Unit E_1 noted earlier in the offshore boreholes (Figure 2.3.10), and appears to be correlative with Unit E in the offshore. However, further work is necessary to determine the exact relationship between these onshore and offshore units.

Subfacies E_2 occurs in boreholes 90BH02 and 90BH04 and is characterized by very dark grey-brown to black fine sand containing graded silt beds or interlaminated silty clay. In borehole 90BH02 subfacies E_2 is micaceous and contains fine wood fragments.

Subfacies E_3 is found only at the top of borehole 90BH05 and comprises fine grained, dark olive-grey sand with distinct planar cross-laminated and rare trough cross-laminated, organic-rich laminae. The base of this subfacies and the lower contact between Unit E and Unit F was not intersected.

2.3.2 Nature of Sedimentary Contacts

Three sedimentary contacts (B/C, C/D and D/E) were observed from the suite of six cores drilled during the spring and summer 1990 programs. Each contact is described independently in order to characterize the nature of the change between sedimentary units.

Contact B/C was cored in boreholes 90BH02 and 90BH03. In borehole 90BH02 the boundary is sharp. Very dark grey to black clayey silt of Unit B is gradational into a basal

6 cm organic-rich silty, very fine grained sand which displays an abrupt sedimentary contact and a distinct colour change, in contrast to the underlying grey sand of Unit C. The sedimentary contact at the base of Unit B in borehole 90BH03 is also sharp; however Unit B does not directly overlie Unit C. The basal 0.38 m of Unit B coarsens downwards from a very dark grey clayey silt into a fine grained silty sand containing plant fragments. This unit forms an abrupt contact with an underlying lighter grey, dry silty clay containing disseminated, light organics throughout (which does not resemble Unit B nor Unit C) and has been designated as a transitional unit between Units B and C. This transitional unit forms a sharp contact with the underlying fine grained, dark grey sand of Unit C.

Contact C/D was sampled in boreholes 90BH1A and 90BH02 and in both cores the boundary is sharp. In 90BH1A fine grained, medium to dark grey, laminated sand of Unit C is in abrupt contact with the underlying dark grey, stiff silty clay of Unit D. Similarly, in 90BH02 the base of Unit C is defined by a black 0.02 m bed of woody material which forms a very sharp boundary and distinct colour change with underlying dark grey, laminated silty clay of Unit D.

The D/E contact was sampled in boreholes 90BH1A, 90BH02 and 90BH04 and in all cores it is gradational over tens of centimeters. In 90BH1A the gradational zone spans 0.25 m and is characterized by interbedded, sharp-based, bioturbated dark grey silty clay of Unit D and medium grained olive-grey, organic-rich sand of Unit E. Both the thickness and number of sand beds increases toward the base of the basal contact. The base of Unit D, defined as the bottom of the last clay interbed, forms a sharp contact with Unit E. The gradational zone between units D and E in 90BH02 spans 2.33 m but is differentiated from the gradational zone of 90BH1A by thicker, less repetitive clay/sand interbeds. Two interbeds comprise the gradational zone: an upper 0.81 m thick fine sand bed representative of Unit E and a lower 1.42 m thick burrow-mottled sandy silt interbed of Unit D. Like the basal contact between units D and E, individual bedding contacts within the gradational zone are sharp and distinctive as a result of abrupt change in lithology and colour. In borehole 90BH04 the D/E gradational zone spans 8.01 m and like borehole 90BH1A comprises fine grained, dark grey, interlaminated to interbedded, well-sorted sand and very dark grey bioturbated, occasionally graded, silt and silty clay. The cyclicity and thickness of sand interbeds increases toward the base of the gradational zone and the colour of the sand

changes from dark grey to a distinctive honey-brown. The base of this clay/sand zone forms a very sharp contact into a black, dry, fissile, organic-rich, 1.08 m thick mud which forms the base of the gradational zone. The lower contact of this mud with Unit E is sharp.

2.3.3 B/D, C/E Unit Comparisons

Units B and D comprise the two silty clay sequences identified along the onshore-offshore borehole transect; Units C and E comprise the two sandy sequences. In this section the similarities and differences between the two clay and two sand units are discussed to further understand the spatial distribution of these units, and to gain insight into any patterns of cyclic sedimentation.

Lithologically units B and D comprise a similar very dark grey, bioturbated silty clay with numerous shell fragments and some graded silt beds. Considerable variance between these units exists upon detailed examination. Unit B coarsens upward in locations both proximal and distal to the coastline and has been further divided into subfacies on the basis of visible changes in the degree of bioturbation and the preservation of primary bedding. Conversely, Unit D fines upward and the degree of bioturbation in Unit D is relatively consistent. Subfacies within Unit D reflect the presence of microfolding and microfaulting and a distinct lower gradational zone coarsens downward toward a sharp basal contact with Unit E.

A representative comparison of subfacies between units C and E is difficult because of the limited borehole recovery of Unit E. A visual lithological comparison highlights certain differences, rather than similarities, between the two units. Unit C comprises fine grained, dark grey-brown, clean sand which is further differentiated into subfacies by a distinct, fine to medium grained sand interval and a trough cross-bedded sand interval. Conversely, Unit E is predominantly comprised of fine grained, dark olive-grey, dirty organic-rich sand (exclusive of borehole 90BH1A which intersected 0.30 m of fine grained brown sand). The only occurrence of green-grey, dirty sand in Unit C exists in borehole 90BH02. This sand visually resembles the sands of Unit E and does not conform to other desciptions of Unit C sands identified in the remaining boreholes.

2.3.4 Lateral Unit Continuity

Each of the sedimentary units - B, C, D and E - is characterized by a diagnostic combination of texture, internal structure and colour. Subfacies within these units are defined by a single but unique sedimentary characteristic. Accordingly, subfacies may be laterally correlative along the onshore-offshore transect or may be absent in one or more of the boreholes (refer to Figures 2.3.7 to 2.3.10). Individual sedimentary units however, are correlative throughout the six boreholes. The fence diagram in Enclosure 2.3.1 shows the extent of this lateral continuity. The only parameter which changes laterally is the thickness of the units. While unit thicknesses are not available in those boreholes where the interval was not sampled, Unit D is shown to thin landward and Unit B pinches out in the nearshore section of the transect. Conversely, the thickness of Unit C does not appear to change along the transect.

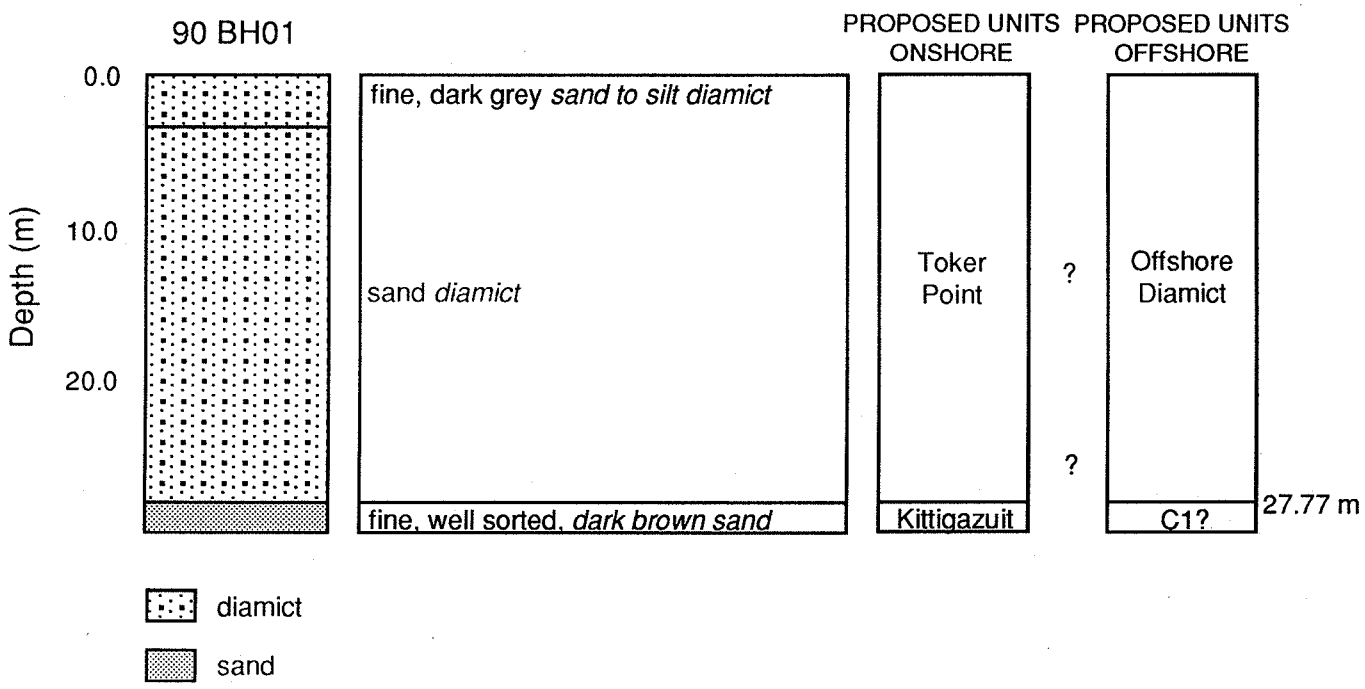

Figure 2.3.1. Borehole 90BH01

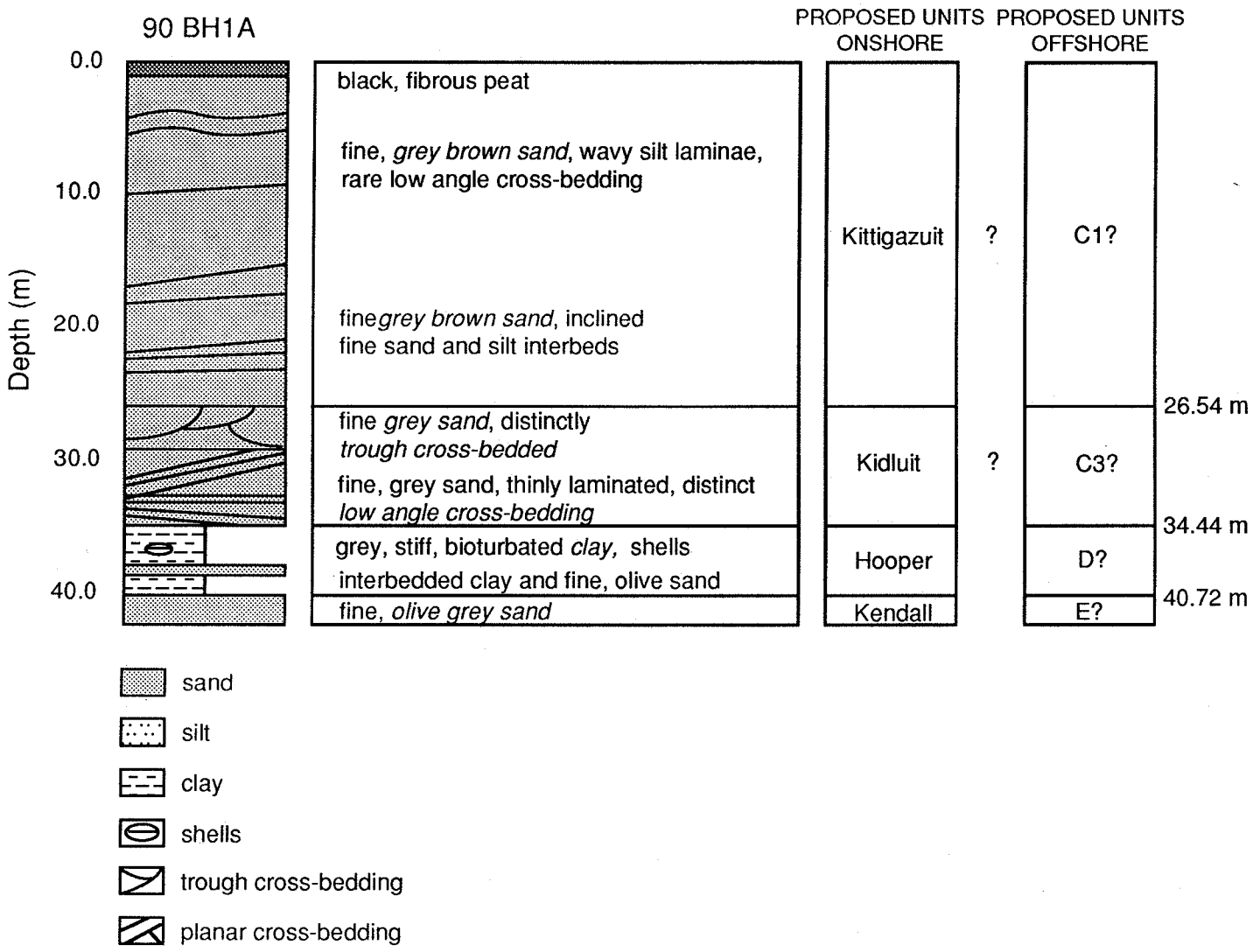

Figure 2.3.2. Borehole 90BH1A

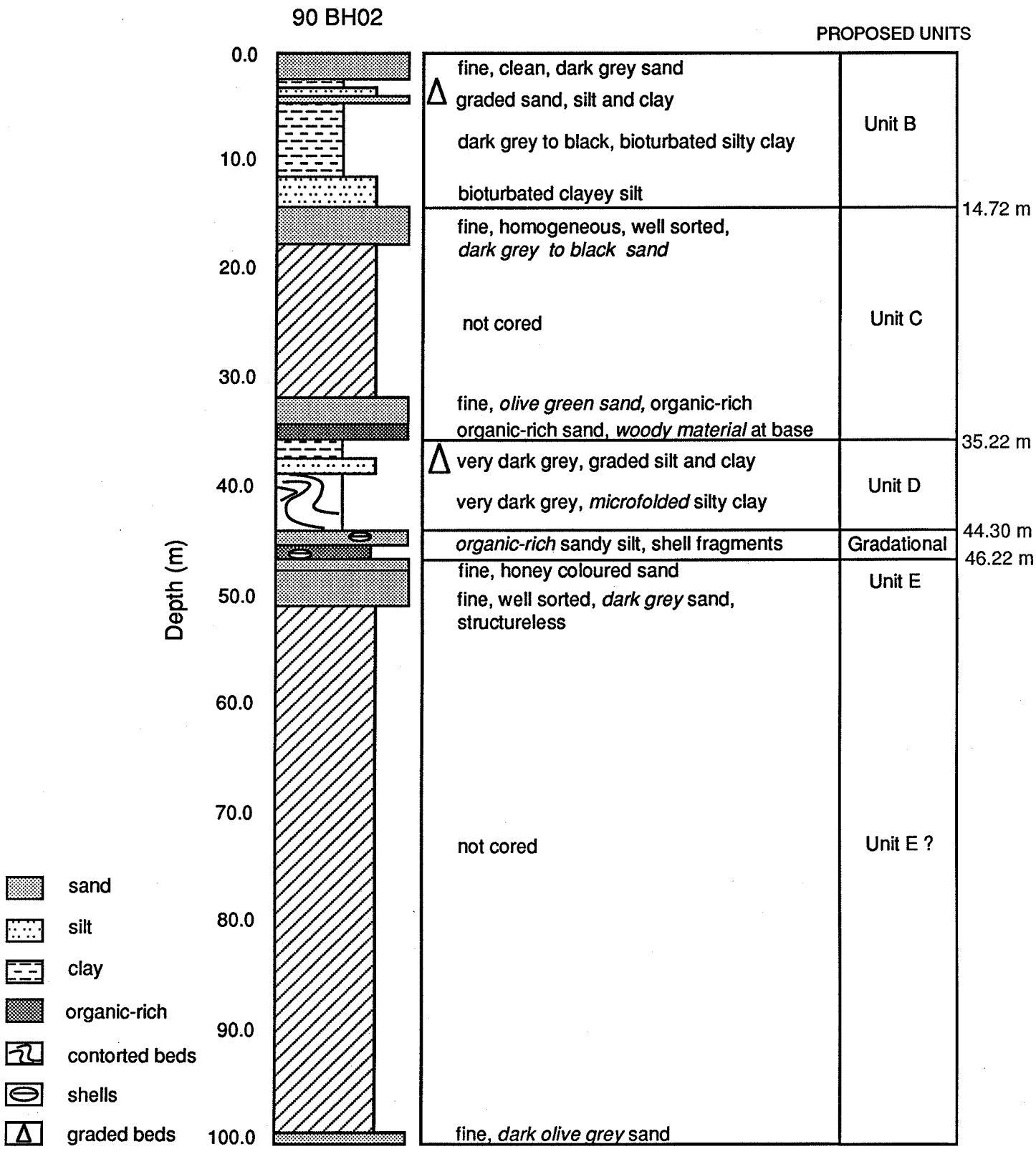

Figure 2.3.3. Borehole 90BH02

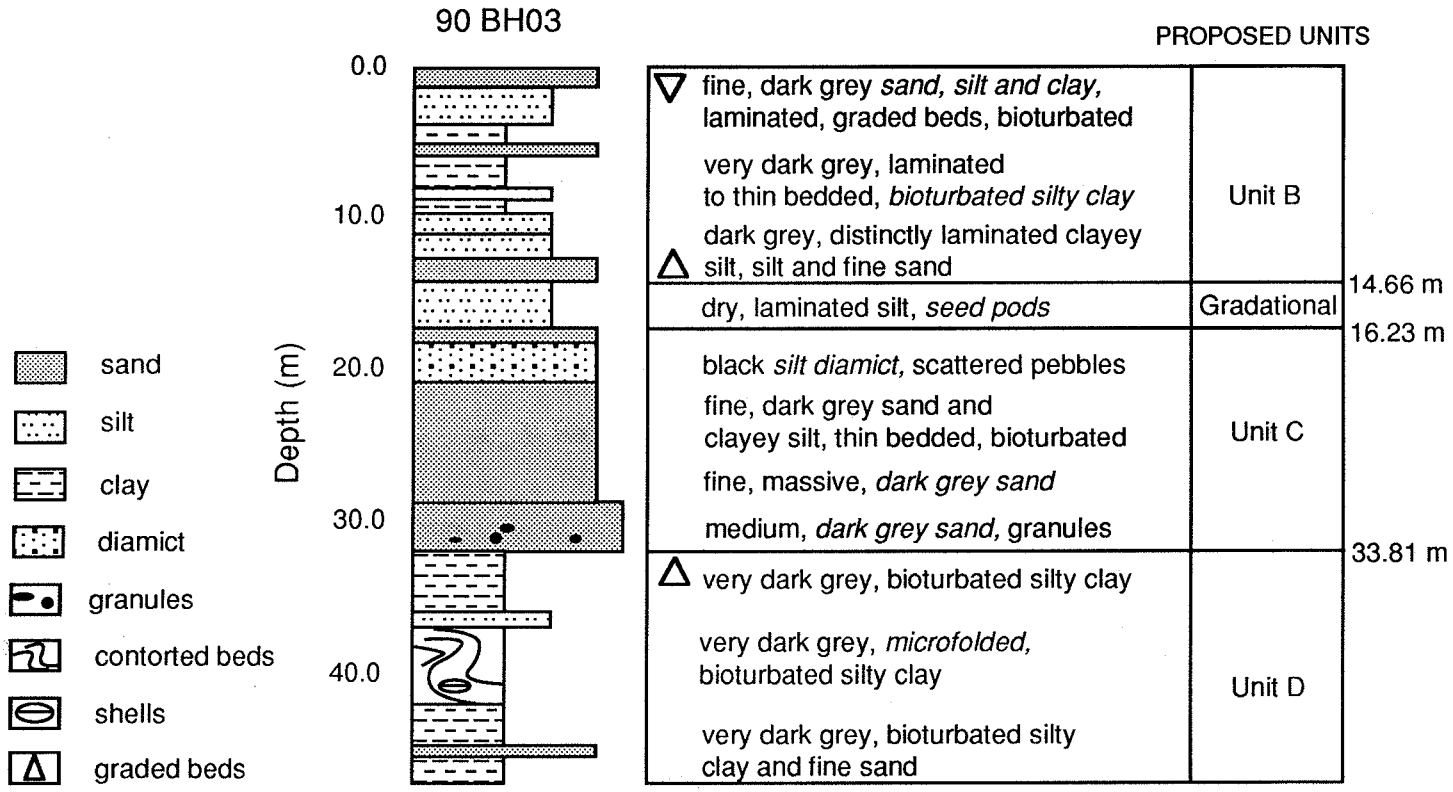

Figure 2.3.4. Borehole 90BH03

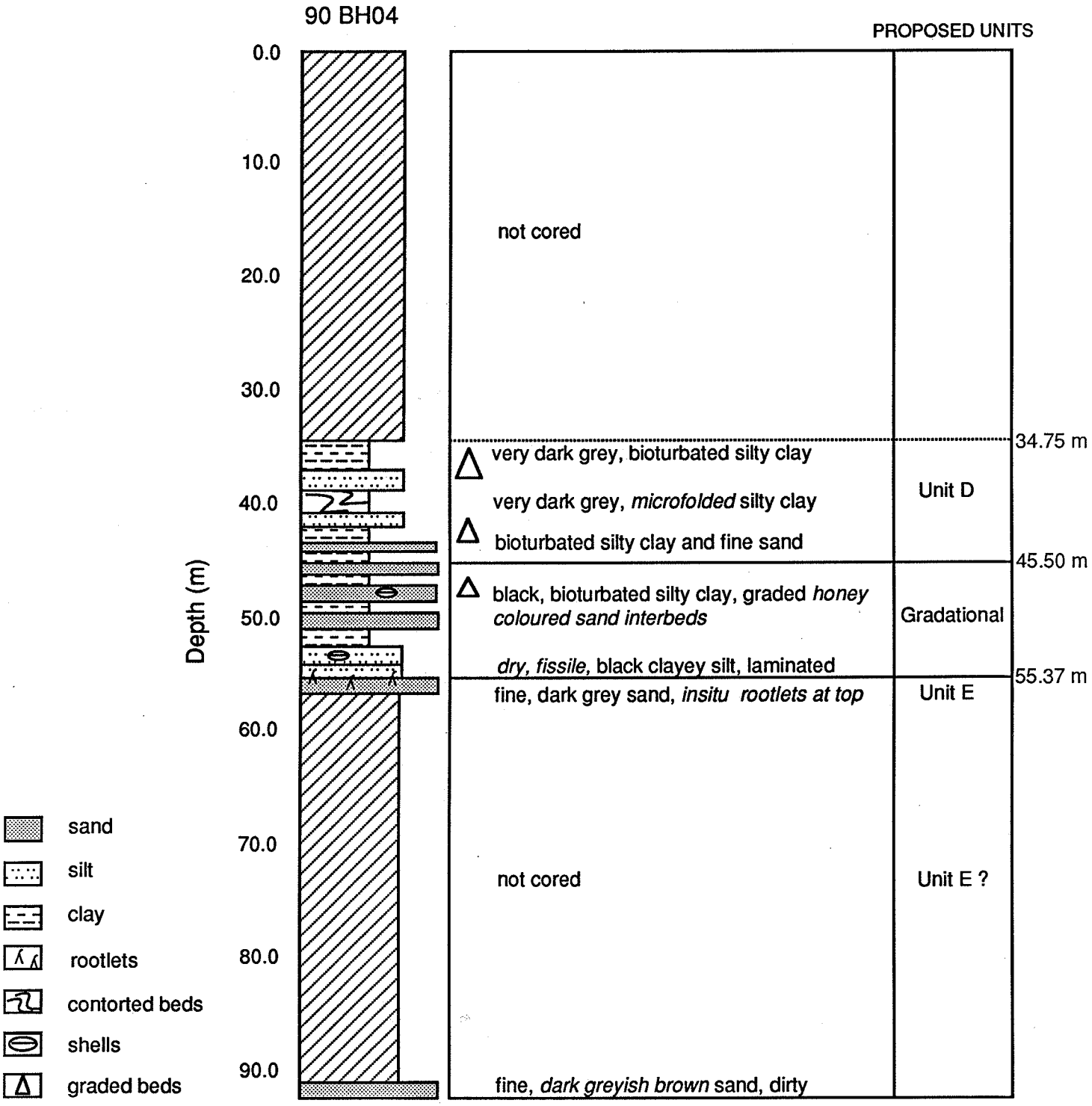

Figure 2.3.5. Borehole 90BH04

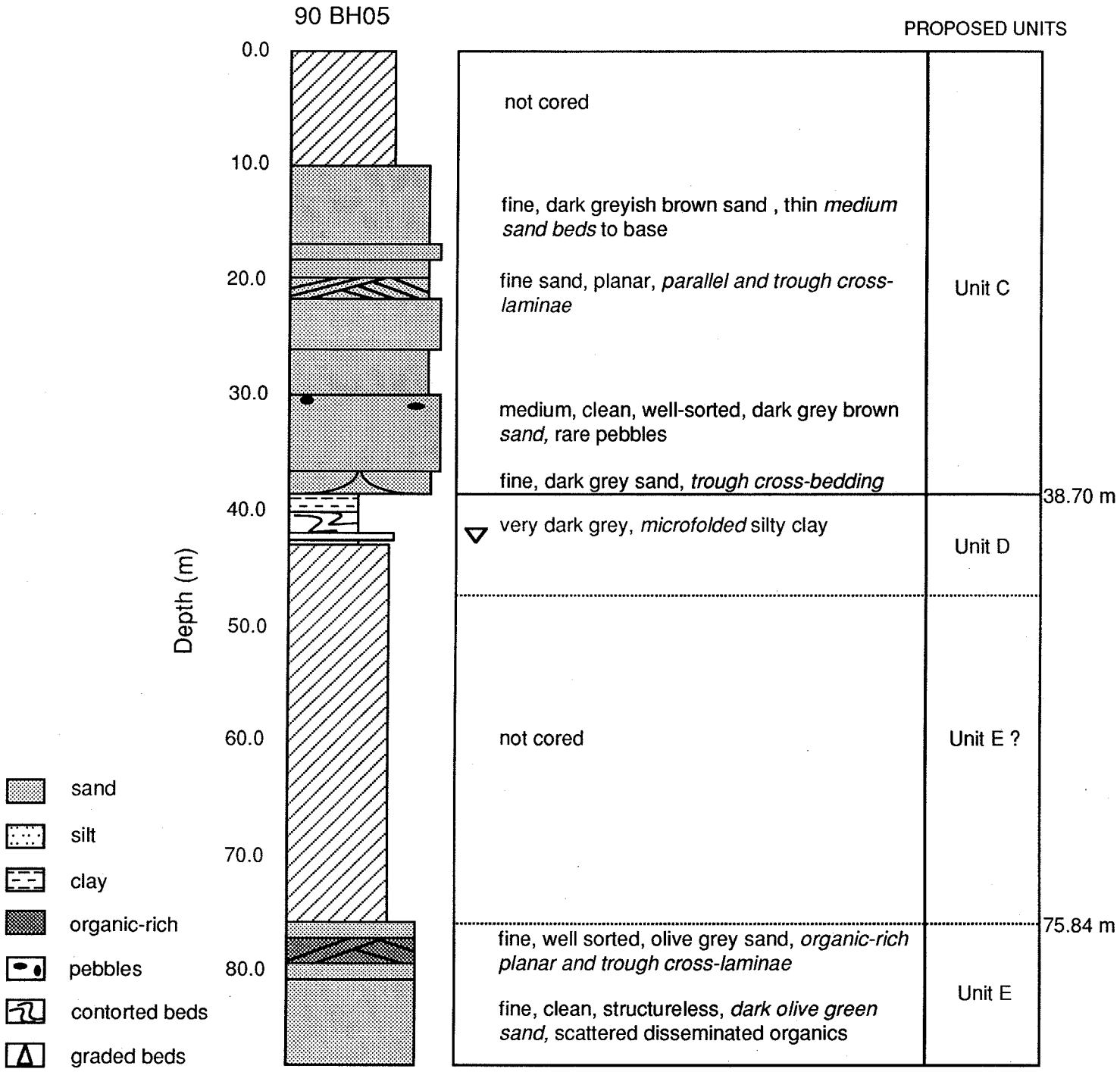

Figure 2.3.6. Borehole 90BH05

UNIT B COMPARISONS - ONSHORE-OFFSHORE TRANSECT

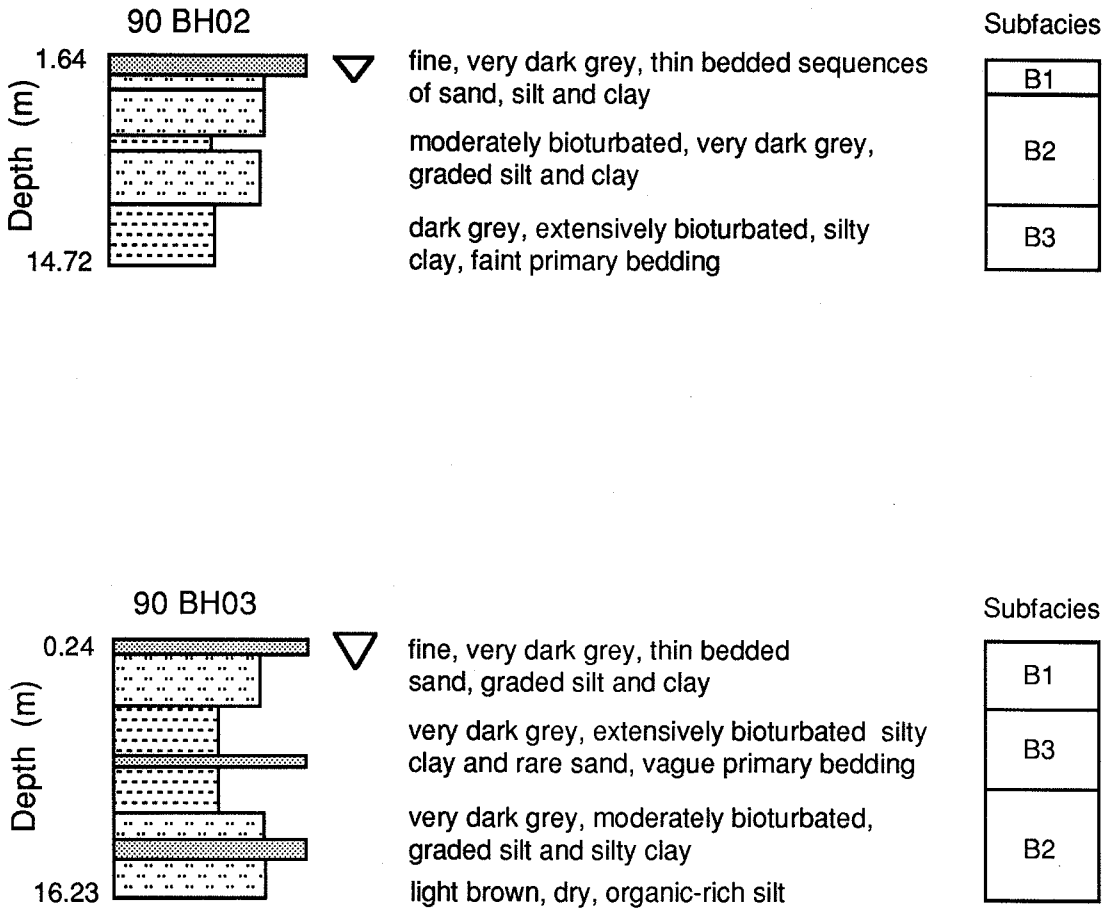

Figure 2.3.7. Onshore-offshore transect borehole comparisons of Unit B.

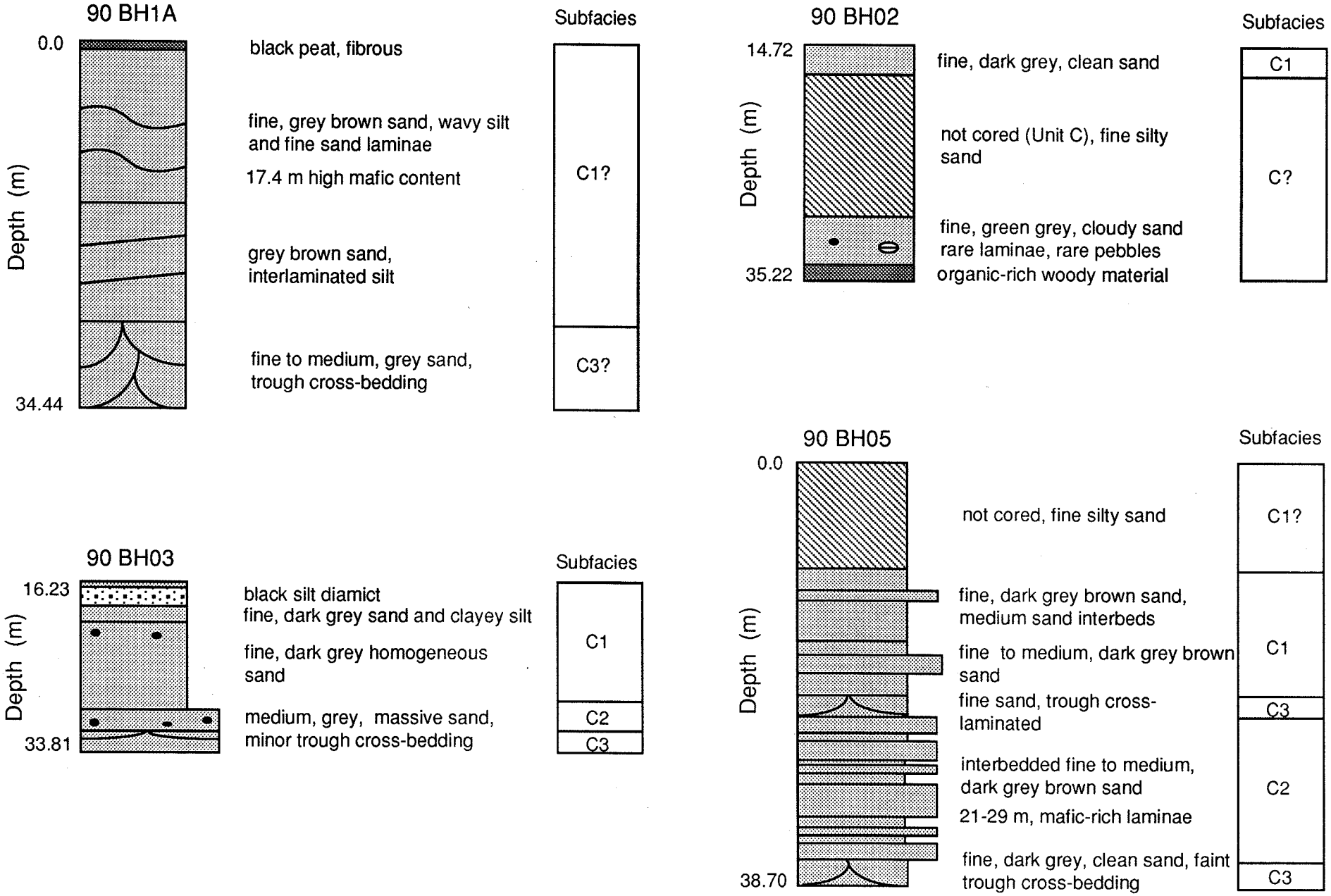

Figure 2.3.8. Spring and Summer 1990 borehole comparisons of Unit C.

UNIT D COMPARISONS - ONSHORE-OFFSHORE TRANSECT

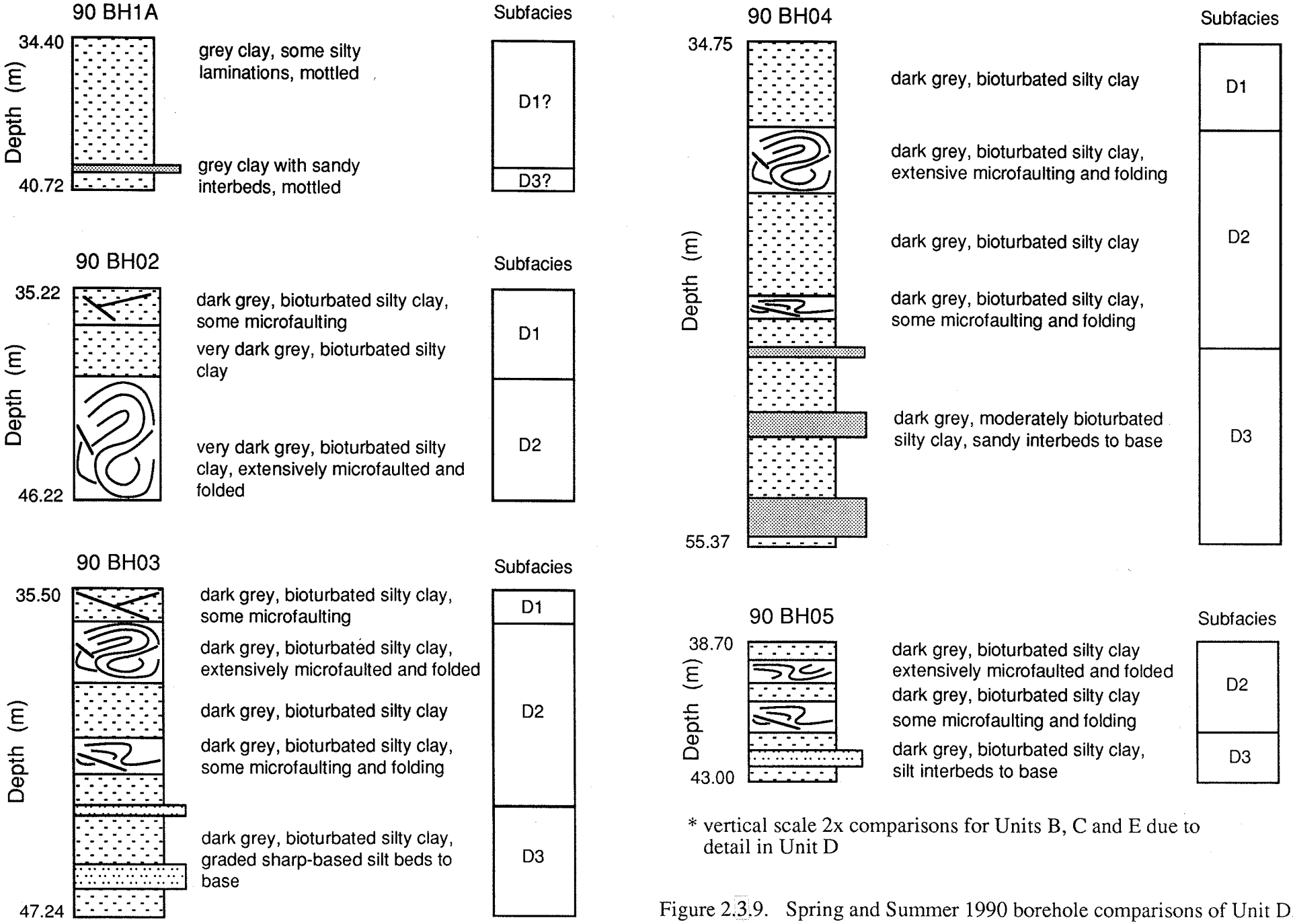

* vertical scale 2x comparisons for Units B, C and E due to detail in Unit D

Figure 2.3.9. Spring and Summer 1990 borehole comparisons of Unit D.

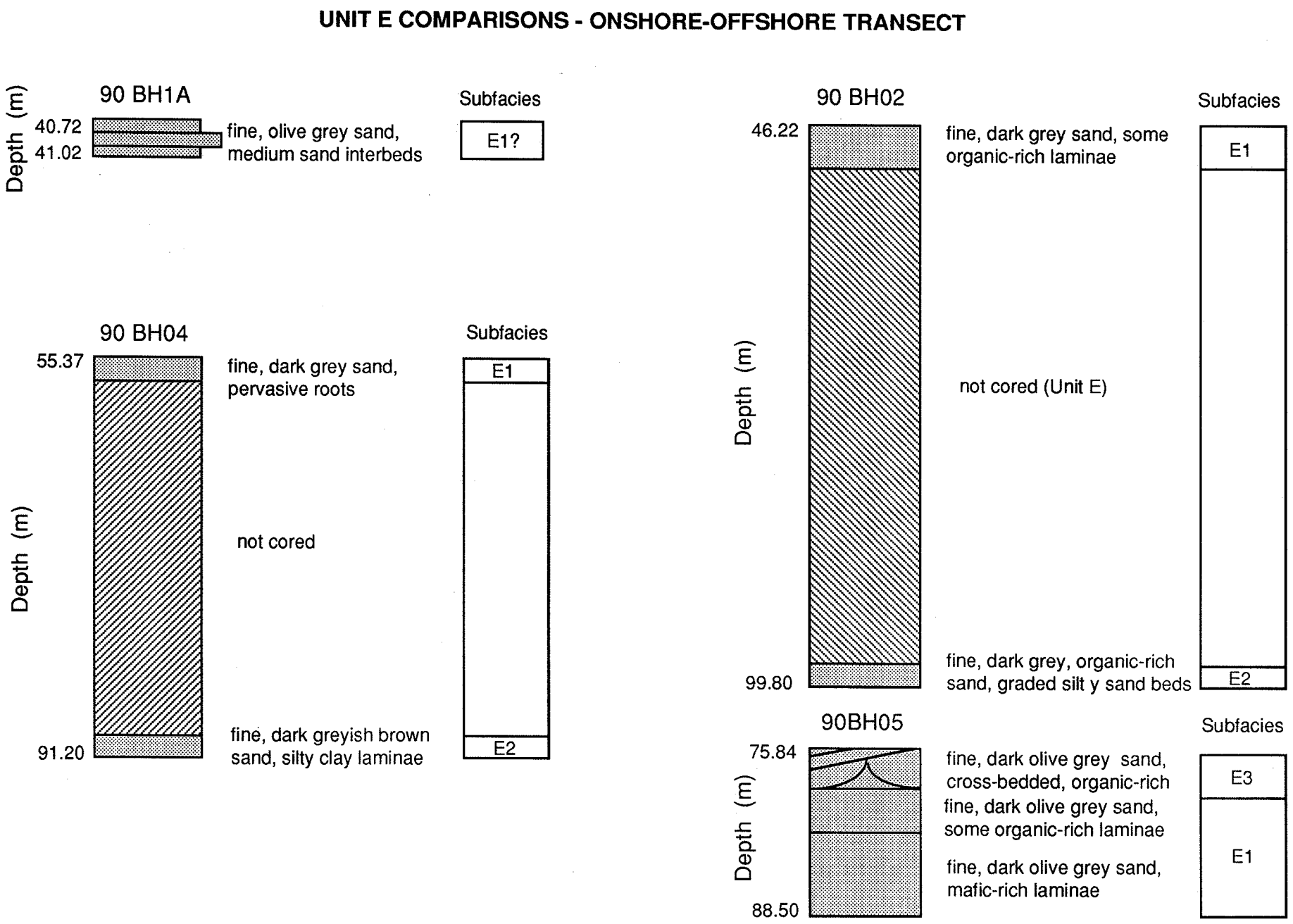

Figure 2.3.10. Spring and Summer 1990 borehole comparisons of Unit E.

2.4 MINERALOGY OF SAND UNITS

S.R. Dallimore and D.G. Paré

The investigation of the heavy and light mineralogy of sands can prove useful in interpreting the environment of deposition and post-depositional changes which may be due to diagenesis. In addition, the mineralogy may also provide diagnostic criteria for proving correlation of sand sequences between boreholes. This was particularly important in the onshore-offshore transect study since several of the subfacies identified are very similar in their physical appearance.

2.4.1 Sample preparation and point counting

In total twenty-six samples were investigated from representative sand intervals in five of the six boreholes. For each sample, heavy mineral concentrates (>3.3 specific gravity) and light minerals were separated from the 63-250 micron fractions for mounting in Araldite on glass slides. Three hundred grains were counted on each slide using a binocular microscope equipped with an analyzer and nicol. Because of the diversity of the grain shape and character for the heavy minerals, approximately 30 mineral classes were used to accommodate the 21 different mineral varieties observed. Fifteen mineral varieties were tabulated for the light minerals.

Summary tables listing each mineral variety are shown on Tables 2.4.1 and 2.4.2. These tables are based on the actual 300 grain point count data and are thus in increments of 0.3%. Based on experience from many similar investigations of this nature, these data are considered reliable to ±1%. In the case of the light mineral table it should be noted that a number of mineral varieties are included which might normally be considered heavy minerals (ie. epidote, goethite, diopside, and hypersthene). This is thought to be a result of the heavy mineral separation process, in which minerals having specific gravity values of close to 3.3 were present in both heavy and light slides.

On the basis of both heavy and light grain mineralogy it was possible to separate the samples into three groups. For the most part these agreed with the tentative unit and subfacies assignments on the basis of sediment properties described in Section 2.2. Group 1 is made up of Kittigazuit Formation sand from onshore borehole 90BH1A and

Table 2.4.1
Light Mineral Report, s.g.> 3.3, 300 grain count, Araldite mount (n = 1.57)

Sample	QZ	QZ+HE	FX	CA	EP	ER	GO	DI	HY	BZ	HBg	HBb	MI	LF	UK
90BH1A 4.8	84.0	8.0	0.0	0.0	2.3	0.0	4.0	0.0	0.0	0.0	0.0	0.0	0.0	0.0	1.7
90BH1A 14.4	60.0	12.0	0.0	0.0	14.0	0.0	2.3	1.7	0.0	0.0	4.0	0.0	2.0	0.0	4.0
90BH1A 24.5	65.0	9.7	0.0	0.0	6.0	2.0	6.3	2.0	2.0	0.0	0.0	0.0	0.0	0.0	6.0
90BH1A 27.7	68.0	4.0	0.0	0.0	10.0	0.0	4.0	0.0	0.0	0.0	2.0	0.0	6.0	0.0	6.0
90BH1A 33.3	52.0	12.0	4.0	0.0	20.0	0.0	4.0	0.0	0.0	0.0	0.0	0.0	1.7	0.0	6.3
90BH1A 40.8	62.0	10.0	2.0	0.0	8.0	2.0	4.0	0.0	2.0	0.0	0.0	0.0	2.0	2.0	6.0
90BH2 14.80	68.3	13.0	0.7	0.0	2.3	0.0	0.0	2.7	0.0	0.0	3.7	0.7	0.0	0.0	8.7
90BH2 32.00	53.7	22.7	0.3	0.0	7.0	0.0	2.0	2.7	0.3	0.0	3.0	2.0	1.3	0.0	5.0
90BH2 47.50	62.7	7.0	0.3	0.0	13.7	0.3	2.0	1.7	2.0	0.0	2.7	1.3	0.0	0.0	6.3
90BH2 50.40	60.7	11.3	0.3	0.0	12.3	1.3	1.3	2.3	0.7	0.0	1.3	1.3	0.3	0.0	6.7
90BH2 99.40	57.7	17.0	0.3	0.3	5.0	0.0	2.0	4.7	2.0	0.0	2.0	0.0	2.0	0.0	7.0
90BH3 21.80	77.0	9.0	1.0	0.0	3.7	0.0	2.0	0.3	0.0	0.0	1.3	0.0	2.0	0.0	3.7
90BH3 28.90	76.7	4.7	3.3	2.7	2.0	0.3	2.0	1.3	0.3	0.0	1.0	0.0	1.0	0.0	4.7
90BH4 56.30	78.3	12.7	0.0	1.3	0.7	0.0	0.0	1.7	0.0	0.0	1.3	0.0	0.3	0.3	3.3
90BH5 12.30	89.7	2.0	1.3	0.3	0.3	0.0	0.7	0.3	0.3	0.0	0.0	2.0	0.3	0.3	2.3
90BH5 16.35	94.0	0.7	1.0	0.3	0.3	0.0	0.0	0.0	0.0	0.0	0.0	1.0	0.0	0.3	2.3
90BH5 19.85	89.3	3.0	0.3	0.7	0.3	0.0	1.0	0.7	0.0	0.0	0.3	1.0	0.3	0.0	3.0
90BH5 21.80	83.3	2.7	1.7	4.3	0.3	0.0	1.7	0.0	1.7	0.0	0.0	1.0	0.0	0.0	3.3
90BH5 24.30	78.7	0.3	3.7	1.3	9.0	0.0	1.0	0.3	0.7	0.0	1.0	1.3	0.3	0.0	2.3
90BH5 26.95	76.7	2.3	2.0	0.7	8.7	2.3	0.3	1.0	0.0	0.0	1.3	0.3	0.0	0.0	4.3
90BH5 29.51	76.0	3.0	6.3	0.0	7.3	0.3	2.0	0.7	0.0	0.0	1.3	0.0	0.0	0.0	3.0
90BH5 32.77	62.7	3.3	5.0	0.0	18.3	0.0	1.0	0.3	0.0	0.0	1.7	1.7	1.0	0.0	5.0
90BH5 76.86	51.0	9.0	2.3	1.3	22.0	0.3	1.7	2.3	1.3	0.0	0.0	1.0	2.7	0.0	5.0
90BH5 79.40	79.3	0.7	1.0	9.7	1.0	0.0	1.7	0.0	0.0	0.0	0.0	0.0	2.0	0.0	4.7
90BH5 84.97	71.0	7.7	0.7	0.7	13.0	0.0	2.0	1.0	0.0	0.0	1.3	0.7	0.3	0.0	1.7
90BH5 88.07	71.0	11.0	0.7	1.3	5.0	0.0	2.3	0.7	0.0	0.0	0.3	0.0	0.7	0.0	7.0

analysis by Consorminex Inc.

LIST OF MINERAL CODES

QZ QUARTZ, QZ+HE QUARTZ with HEMATITE coating, FX FELDSPARS, CA CALCITE, EP EPIDOTE, Er EPIDOTE rounded, GO GOETHITE yellow brown, DI DIOPSIDE, HY HYPERSTHENE, BZ BRONZITE, HBg HORBLENDE green, HBb HORNBLENDE brown, MI MICA, LF LITHIC FRAGMENT, UK UKNOWN.

Table 2.4.2
Light Mineral Report, s.g.≤ 3.3, 300 grain count, Araldite mount (n = 1.57)

Sample	QZ	QZ+HE	FX	CA	EP	ER	GO	DI	HY	HBg	HBb	MI	LF	UK
Group 1/Kittigazuit/Subfacies C1														
BH1 4.8	84.0	8.0	0.0	0.0	2.3	0.0	4.0	0.0	0.0	0.0	0.0	0.0	0.0	1.7
BH1 14.4	60.0	12.0	0.0	0.0	14.0	0.0	2.3	1.7	0.0	4.0	0.0	2.0	0.0	4.0
BH1 24.5	65.0	9.7	0.0	0.0	6.0	2.0	6.3	2.0	2.0	0.0	0.0	0.0	0.0	6.0
BH2 1480	68.3	13.0	0.7	0.0	2.3	0.0	0.0	2.7	0.0	3.7	0.7	0.0	0.0	8.7
BH2 3200	53.7	22.7	0.3	0.0	7.0	0.0	2.0	2.7	0.3	3.0	2.0	1.3	0.0	5.0
BH5 1230	89.7	2.0	1.3	0.3	0.3	0.0	0.7	0.3	0.3	0.0	2.0	0.3	0.3	2.3
BH5 1635	94.0	0.7	1.0	0.3	0.3	0.0	0.0	0.0	0.0	0.0	1.0	0.0	0.3	2.3
BH5 1985	89.3	3.0	0.3	0.7	0.3	0.0	1.0	0.7	0.0	0.3	1.0	0.3	0.0	3.0
BH5 2180	83.3	2.7	1.7	4.3	0.3	0.0	1.7	0.0	1.7	0.0	1.0	0.0	0.0	3.3
Group 2/Kidluit/Subfacies C2 & C3														
BH1 27.7	68.0	4.0	0.0	0.0	10.0	0.0	4.0	0.0	0.0	2.0	0.0	6.0	0.0	6.0
BH1 33.3	52.0	12.0	4.0	0.0	20.0	0.0	4.0	0.0	0.0	0.0	0.0	1.7	0.0	6.3
BH3 2180	77.0	9.0	1.0	0.0	3.7	0.0	2.0	0.3	0.0	1.3	0.0	2.0	0.0	3.7
BH3 2890	76.7	4.7	3.3	2.7	2.0	0.3	2.0	1.3	0.3	1.0	0.0	1.0	0.0	4.7
BH5 2430	78.7	0.3	3.7	1.3	9.0	0.0	1.0	0.3	0.7	1.0	1.3	0.3	0.0	2.3
BH5 2695	76.7	2.3	2.0	0.7	8.7	2.3	0.3	1.0	0.0	1.3	0.3	0.0	0.0	4.3
BH5 2951	76.0	3.0	6.3	0.0	7.3	0.3	2.0	0.7	0.0	1.3	0.0	0.0	0.0	3.0
BH5 3277	62.7	3.3	5.0	0.0	18.3	0.0	1.0	0.3	0.0	1.7	1.7	1.0	0.0	5.0
Group 3/Kendall/Unit E														
BH1 40.8	62.0	10.0	2.0	0.0	8.0	2.0	4.0	0.0	2.0	0.0	0.0	2.0	2.0	6.0
BH2 4750	62.7	7.0	0.3	0.0	13.7	0.3	2.0	1.7	2.0	2.7	1.3	0.0	0.0	6.3
BH2 5040	60.7	11.3	0.3	0.0	12.3	1.3	1.3	2.3	0.7	1.3	1.3	0.3	0.0	6.7
BH2 9940	57.7	17.0	0.3	0.3	5.0	0.0	2.0	4.7	2.0	2.0	0.0	2.0	0.0	7.0
BH4 5630	78.3	12.7	0.0	1.3	0.7	0.0	0.0	1.7	0.0	1.3	0.0	0.3	0.3	3.3
BH5 7686	51.0	9.0	2.3	1.3	22.0	0.3	1.7	2.3	1.3	0.0	1.0	2.7	0.0	5.0
BH5 7940	79.3	0.7	1.0	9.7	1.0	0.0	1.7	0.0	0.0	0.0	0.0	2.0	0.0	4.7
BH5 8497	71.0	7.7	0.7	0.7	13.0	0.0	2.0	1.0	0.0	1.3	0.7	0.3	0.0	1.7
BH5 8807	71.0	11.0	0.7	1.3	5.0	0.0	2.3	0.7	0.0	0.3	0.0	0.7	0.0	7.0

analysis by Consorminex Inc.

LIST OF MINERAL CODES

QZ QUARTZ, QZ+HE QUARTZ with HEMATITE coating, FX FELDSPARS, CA CALCITE, EP EPIDOTE, Er EPIDOTE rounded, GO GOETHITE yellow brown, DI DIOPSIDE, HY HYPERSTHENE, HBg HORBLENDE green,HBb HORNBLENDE brown, MI MICA, LF LITHIC FRAGMENT, UK UKNOWN.

subfacies C_1 sands from the offshore boreholes. Group 2 is made up of the onshore Kidluit Formation sand and offshore subfacies C_1 and C_2 sands. Group 3 is made up of sediments from the Kendall sand and subfacies E_1, E_2, E_3 sands from the offshore boreholes.

2.4.2 Light Minerals

The frequency distribution of the light minerals present in each borehole is given in Table 2.4.1, and for each group in Table 2.4.2. Averages for each group are presented graphically in Figure 2.4.1. The three sand groups generally contained similar light mineral assemblages characterized by a dominance of quartz grains. Group 1 sands had the highest content of quartz and hematite-covered quartz, typically exceeding 85% and averaging about 91%. Other mineral varieties were generally less than 2%, thus allowing classification of this Unit as an orthoquartzite according to Pettijohn (1957). Group 2 sands averaged 87% quartz together with quartz containing hematite inclusions, approximately 4% feldspar grains, and less than 2% other mineral varieties. Most samples in this Unit would be classified as subarkoses according to Pettijohn (1957). Group 3 sands showed more sample-to-sample variability with some samples being classified as orthoquartzites and others as subarkoses.

2.4.3 Heavy Minerals

The three groups described previously, contained distinct heavy mineral assemblages both in terms of the variety of minerals present and in terms of their character and form. A simplified overview of the relative percentages of the major heavy minerals is summarized by borehole in Table 2.4.3, and for each group in Table 2.4.4. A graph of the averages for each group is shown in Figure 2.4.2. Group 2 samples stand out from the other groups primarily on the basis of very high pyrite and siderite values, lower garnet and ilmenite values, and marginally lower values in many other minerals. Pyrite is also present in a variety of forms including botryoidal and framboidal grains, and some goethite-covered grains. Group 3 sands can be distinguished from Group 1 sands by higher garnet, diopside, and ilmenite values and lower goethite and hypersthene values.

Because pyrite and siderite may be associated with secondary mineralization related to diagenesis, the heavy mineral data has also been investigated with these minerals

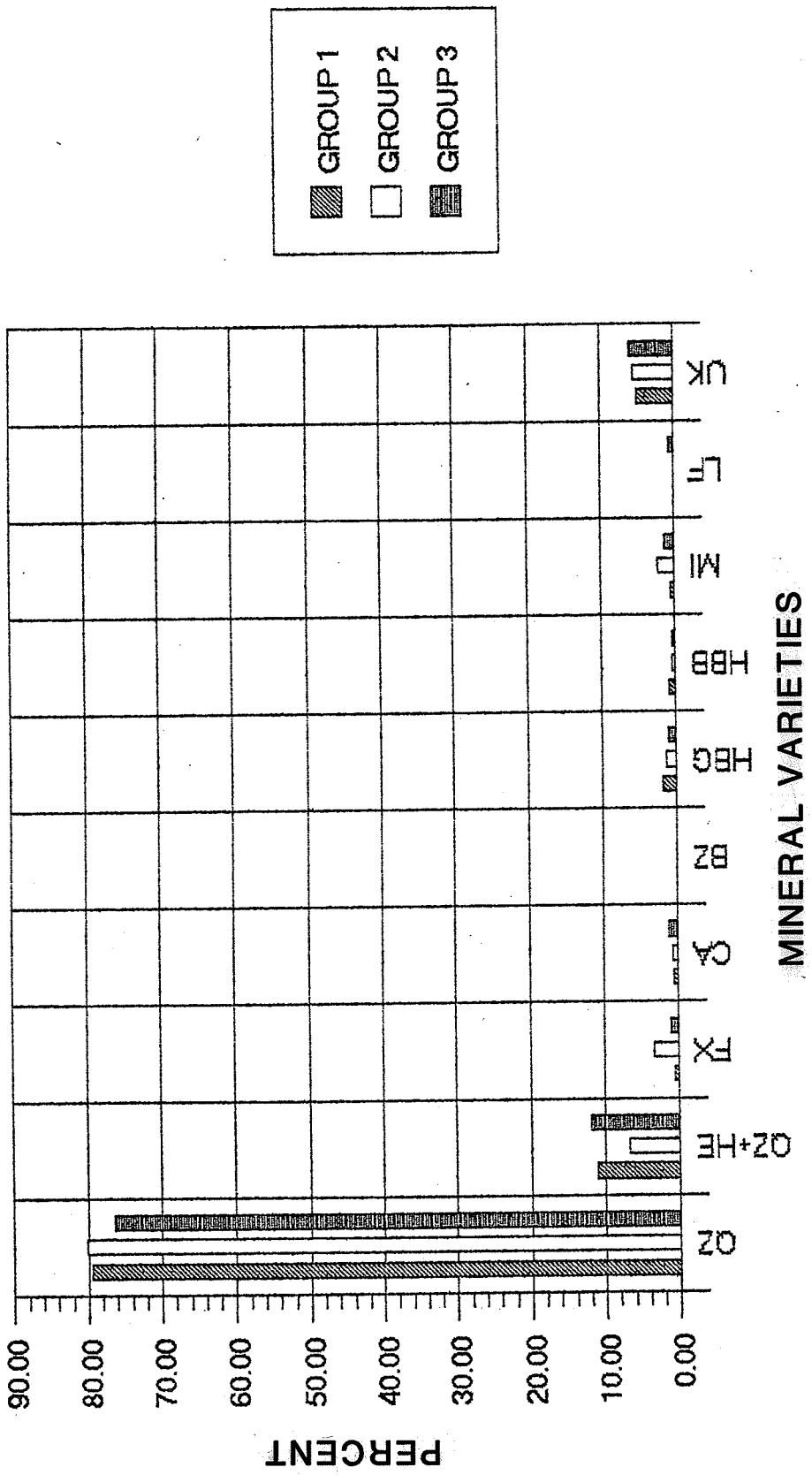

Figure 2.4.1 Light Mineral averages by group

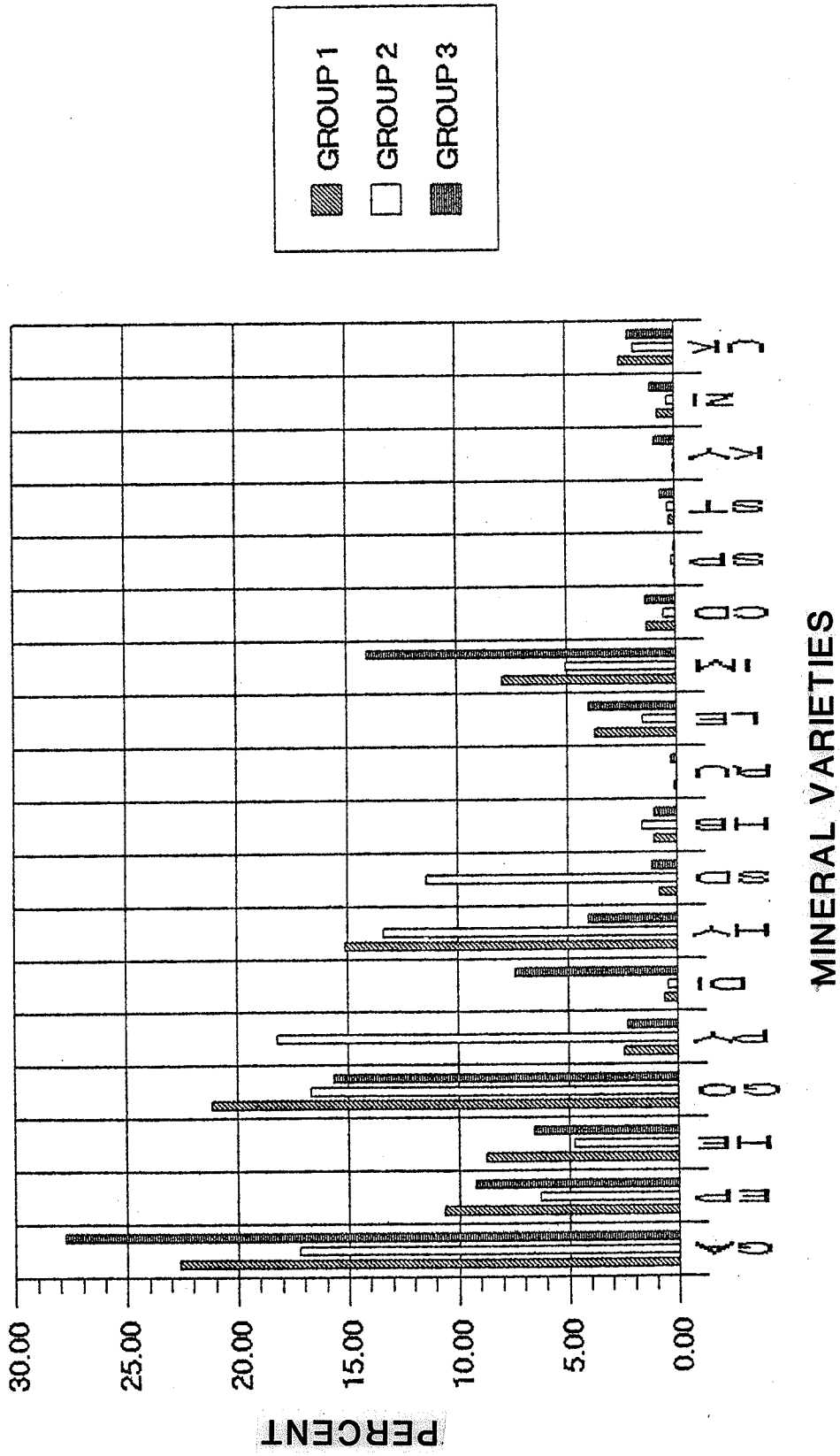

Figure 2.4.2 Heavy Mineral averages by group

Table 2.4.3
Heavy Mineral Report, s.g. > 3.3, 300 grain count, Araldite mount (n = 1.57)

Sample	GA	Gr	EP	Er	Ea	HE	Hr	GO	PY	Pg	Pb	Pe	DI	HY	BZ	SD	Sm	HBg	HBb	RU	LE	IM	CD	SP	ST	KY	MZ	ZI	Ze	UK
90BH1A 4.8	14.7	1.3	3.7	9.7		5.7	6.3	25.7	0.0	0.3	0.0	0.0	0.0	14.0	0.0	0.0	0.0	0.7	0.0	0.3	2.7	9.0	1.0	0.0	0.3	0.0	0.0	0.7	0.7	3.3
90BH1A 14.4	30.7	0.3	1.0	5.3		5.0	1.7	22.3	0.0	0.0	0.0	0.0	0.0	15.0	0.0	0.7	0.0	0.7	0.0	0.0	2.3	10.3	0.7	0.0	1.3	0.0	0.0	0.7	0.0	2.0
90BH1A 24.5	29.3	0.7	2.3	7.0		8.0	2.0	29.3	0.0	0.0	0.0	0.0	0.0	12.3	0.0	0.0	0.0	0.0	0.0	0.0	2.3	4.0	0.0	0.0	0.3	0.0	0.0	0.3	0.0	2.0
90BH1A 27.7	6.0	0.3	7.7	1.3		5.7	0.3	18.0	1.0	6.0	6.0	0.0	0.7	5.0	0.0	29.7	3.0	0.7	0.0	0.0	2.7	2.7	1.3	0.0	0.0	0.3	0.0	0.0	0.0	1.7
90BH1A 33.3	12.3	0.7	9.7	1.3		9.3	0.3	26.3	0.7	1.3	0.0	0.0	0.3	17.7	0.0	0.3	0.0	3.0	0.3	0.0	2.7	7.7	0.0	0.7	0.7	0.0	0.0	0.7	0.3	3.7
90BH1A 40.8	16.3	0.7	8.7	1.3		7.3	0.0	25.3	0.0	0.7	0.0	0.0	0.7	17.0	0.0	0.0	0.0	1.0	0.0	0.0	1.7	15.7	0.0	0.0	1.3	0.3	0.0	0.0	0.3	1.7
90BH2 14.80	18.7	1.3	8.3	9.3	0.0	3.7	2.3	9.0	1.0	0.0	3.0	0.0	0.7	22.3	0.0	0.7	0.0	0.0	0.0	0.0	5.3	6.7	3.3	0.3	0.0	0.3	0.0	0.3	0.0	3.3
90BH2 32.00	19.0	0.7	7.0	2.0	0.7	12.0	0.7	20.7	0.0	0.7	0.3	0.0	0.7	15.3	0.0	1.0	0.0	0.0	0.0	0.0	4.0	7.3	4.0	0.0	0.0	0.0	0.0	0.3	1.0	2.7
90BH2 47.50	18.7	0.7	9.3	3.3	0.7	7.3	0.3	15.7	0.0	0.0	0.7	0.0	0.3	20.0	0.0	0.7	0.0	1.3	0.0	0.0	5.7	9.3	2.7	0.0	0.0	0.0	0.0	0.3	0.7	2.3
90BH2 50.40	23.0	0.0	4.0	1.3	0.3	7.3	0.0	30.3	0.0	0.3	0.0	0.0	0.0	17.7	0.0	0.3	0.0	0.3	0.0	0.0	3.7	4.3	2.3	0.0	1.0	0.3	0.0	0.3	0.0	3.0
90BH2 99.40	13.0	0.3	9.0	1.7	0.3	10.3	0.0	10.3	0.0	0.7	1.0	0.0	0.3	8.7	0.0	6.0	0.0	0.0	0.0	0.0	3.7	26.0	3.3	0.0	1.0	0.0	0.0	0.3	1.3	2.7
90BH3 21.80	19.3	0.0	3.7	0.3	0.3	3.7	0.3	16.3	2.7	13.7	5.0	0.0	0.7	19.3	0.0	5.7	0.0	0.0	0.0	0.0	0.3	5.0	0.3	0.3	0.7	0.0	0.0	0.3	0.3	1.7
90BH3 28.90	20.0	0.0	4.7	0.7	0.0	4.7	0.0	7.3	8.3	5.0	5.7	1.3	0.0	5.7	0.0	25.0	0.0	0.3	0.0	0.0	3.0	4.3	2.0	0.0	0.0	0.0	0.0	0.0	0.0	2.0
90BH4 56.30	29.7	0.0	8.0	6.0	1.3	2.0	0.7	0.0	0.3	0.0	12.7	0.0	1.0	11.0	0.0	0.3	0.0	1.7	0.0	0.3	7.7	11.3	0.7	0.0	0.7	1.3	0.0	0.7	1.0	1.7
90BH5 12.30	30.7	0.3	6.3	1.7	0.7	3.0	2.7	22.3	0.0	1.0	0.7	0.0	0.0	10.7	0.0	0.3	0.0	1.3	0.0	0.7	3.0	9.0	0.7	0.0	0.7	0.3	0.0	0.0	0.0	4.0
90BH5 16.35	22.3	0.0	5.3	2.3	0.0	10.0	0.0	15.7	0.7	3.7	0.3	0.0	0.0	15.0	0.0	0.0	2.3	3.0	0.3	0.0	3.7	11.0	0.7	0.3	0.0	0.0	0.0	0.3	1.7	1.3
90BH5 19.85	14.3	0.0	6.3	1.3	0.0	8.0	0.3	24.0	0.3	5.3	1.3	0.0	1.0	18.0	0.0	0.7	0.7	1.3	0.0	0.0	5.7	8.3	0.3	0.0	0.0	0.0	0.0	0.0	0.7	2.0
90BH5 21.80	18.7	0.3	13.3	2.0	0.0	5.7	1.3	21.3	0.3	2.3	1.0	0.0	3.0	13.0	0.0	1.3	0.0	2.0	0.0	0.0	4.3	5.7	1.3	0.0	0.0	0.3	0.0	0.3	0.3	2.0
90BH5 24.30	23.3	0.3	4.7	0.3	0.0	4.0	0.0	16.0	5.7	15.0	5.3	0.0	0.0	13.7	0.0	1.0	2.0	2.3	0.0	0.0	0.0	4.0	0.0	0.0	0.3	0.0	0.0	0.0	0.0	2.0
90BH5 26.95	11.7	0.0	2.7	0.3	0.0	2.0	0.0	13.3	11.7	14.7	5.0	0.0	0.7	18.3	0.0	4.0	4.0	2.7	0.0	0.0	0.7	6.3	0.0	0.0	0.3	0.0	0.0	0.3	0.3	1.0
90BH5 29.51	14.3	0.3	8.0	1.0	0.0	3.0	0.3	19.0	2.3	13.0	1.3	0.0	1.3	16.0	0.0	3.7	8.3	3.0	0.0	0.0	1.3	2.3	0.3	0.0	0.3	0.3	0.0	0.0	0.0	0.3
90BH5 32.77	29.3	0.0	3.0	0.7	0.0	3.3	1.0	17.3	1.7	8.0	5.3	0.0	0.0	11.0	0.0	4.3	0.0	0.7	0.0	0.0	1.7	8.0	0.7	0.3	0.3	0.0	0.0	0.7	0.0	2.7
90BH5 76.86	26.7	0.0	9.3	0.3	0.0	5.0	0.0	20.0	0.7	0.7	0.0	0.0	1.3	10.3	0.0	0.0	2.7	1.0	0.0	0.0	4.7	12.7	1.0	0.3	0.3	1.7	0.0	0.7	0.0	0.7
90BH5 79.40	43.0	0.3	3.0	2.7	0.3	2.7	2.0	15.7	0.3	0.3	0.0	0.0	0.7	7.0	0.0	0.3	0.0	0.7	0.7	1.0	3.0	11.0	1.0	0.0	1.0	1.0	0.0	0.3	0.0	2.0
90BH5 84.97	33.7	0.3	6.7	0.0	0.0	5.3	0.0	17.3	0.0	0.7	0.0	0.0	0.0	4.0	0.0	0.3	0.0	2.0	0.0	0.7	4.3	15.0	1.0	0.3	0.7	2.0	0.3	1.3	1.3	2.7
90BH5 88.07	43.3	0.0	4.3	0.7	0.3	5.7	3.0	6.3	0.0	0.3	0.3	0.0	0.0	4.3	0.0	0.0	0.0	1.0	0.0	0.7	1.7	21.3	0.3	0.0	0.0	1.7	0.3	1.0	0.7	2.7

	GA	Gr	EP	Er	Ea	HE	Hr	GO	PY	Pg	Pb	Pe	DI	HY	BZ	SD	Sm	HBg	HBb	RU	LE	IM	CD	SP	ST	KY	MZ	ZI	Ze	UK

analysis by Consorminex Inc.

LIST OF MINERAL CODES

GA GARNET angular, Gr GARNET rounded, EP EPIDOTE angular, Er rounded, Ea Allanite, HE HEMATITE irregular, Hr HEMATITE rounded, Go GOETHITE yellow brown, Py PYRITE fresh, Pg goethite covered, Pb botryoidal/framboidal, Pe euhedral, DI diopside, HY hyperstene, BZ bronzite, SD SIDERITE x-tal aggregate, Sm SIDERITE massive, Hg HORNBLENDE green, HORNBLENDE brown, RU RUTILE red, LE LEUCOXENE, IM ILMENITE, CD CHLORITOID, SP TITANITE, ST STAUROLITE, KY KYANITE, MZ MONAZITE, ZI ZIRCON angular, Ze ZIRCON euhedral, UK UNKNOWN.

Table 2.4.4
Heavy Mineral Report, s.g. > 3.3, 300 grain count, Araldite mount (n = 1.57)

Sample	GA	Gr	EP	Er	Ea	HE	Hr	GO	PY	Pg	Pb	Pe	DI	HY	SD	Sm	HBg	HBb	RU	LE	IM	CD	SP	ST	KY	ZI	Ze	Uk
Group 1/Kittigazuit/Subfacies C1																												
BH1A 4.8	14.7	1.3	3.7	9.7		5.7	6.3	25.7	0.0	0.3	0.0	0.0	0.0	14.0	0.0	0.0	0.7	0.0	0.3	2.7	9.0	1.0	0.0	0.3	0.0	0.7	0.7	3.3
BH1A 14.4	30.7	0.3	1.0	5.3		5.0	1.7	22.3	0.0	0.0	0.0	0.0	0.0	15.0	0.7	0.0	0.7	0.0	0.0	2.3	10.3	0.7	0.0	1.3	0.0	0.7	0.0	2.0
BH1A 24.5	29.3	0.7	2.3	7.0		8.0	2.0	29.3	0.0	0.0	0.0	0.0	0.0	12.3	0.0	0.0	0.0	0.0	0.0	2.3	4.0	0.0	0.0	0.3	0.0	0.3	0.0	2.0
BH2 14.80	18.7	1.3	8.3	9.3	0.0	3.7	2.3	9.0	1.0	0.0	3.0	0.0	0.7	22.3	0.7	0.0	0.0	0.0	0.0	5.3	6.7	3.3	0.3	0.0	0.3	0.3	0.0	3.3
BH2 32.00	19.0	0.7	7.0	2.0	0.7	12.0	0.7	20.7	0.0	0.7	0.3	0.0	0.7	15.3	1.0	0.0	0.0	0.0	0.0	4.0	7.3	4.0	0.0	0.0	0.0	0.3	1.0	2.7
BH5 12.30	30.7	0.3	6.3	1.7	0.7	3.0	2.7	22.3	0.0	1.0	0.7	0.0	0.0	10.7	0.3	0.0	1.3	0.0	0.7	3.0	9.0	0.7	0.0	0.7	0.3	0.0	0.0	4.0
BH5 16.35	22.3	0.0	5.3	2.3	0.0	10.0	0.0	15.7	0.7	3.7	0.3	0.0	0.0	15.0	0.0	2.3	3.0	0.3	0.0	3.7	11.0	0.7	0.3	0.0	0.0	0.3	1.7	1.3
BH5 19.85	14.3	0.0	6.3	1.3	0.0	8.0	0.3	24.0	0.3	5.3	1.3	0.0	1.0	18.0	0.7	0.7	1.3	0.0	0.0	5.7	8.3	0.3	0.0	0.0	0.0	0.0	0.7	2.0
BH5 21.80	18.7	0.3	13.3	2.0	0.0	5.7	1.3	21.3	0.3	2.3	1.0	0.0	3.0	13.0	1.3	0.0	2.0	0.0	0.0	4.3	5.7	1.3	0.0	0.0	0.3	0.3	0.3	2.0
Group 2/Kidluit/Subfacies C2 & C3																												
BH1A 27.7	6.0	0.3	7.7	1.3		5.7	0.3	18.0	1.0	6.0	6.0	0.0	0.7	5.0	29.7	3.0	0.7	0.0	0.0	2.7	2.7	1.3	0.0	0.0	0.3	0.0	0.0	1.7
BH1A 33.3	12.3	0.7	9.7	1.3		9.3	0.3	26.3	0.7	1.3	0.0	0.0	0.3	17.7	0.3	0.0	3.0	0.3	0.0	2.7	7.7	0.0	0.7	0.7	0.0	0.7	0.3	3.7
BH3 21.80	19.3	0.0	3.7	0.3	0.3	3.7	0.3	16.3	2.7	13.7	5.0	0.0	0.7	19.3	5.7	0.0	0.0	0.0	0.0	0.3	5.0	0.3	0.3	0.7	0.0	0.3	0.3	1.7
BH3 28.90	20.0	0.0	4.7	0.7	0.0	4.7	0.0	7.3	8.3	5.0	5.7	1.3	0.0	5.7	25.0	0.0	0.3	0.0	0.0	3.0	4.3	2.0	0.0	0.0	0.0	0.0	0.0	2.0
BH5 24.30	23.3	0.3	4.7	0.3	0.0	4.0	0.0	16.0	5.7	15.0	5.3	0.0	0.0	13.7	1.0	2.0	2.3	0.0	0.0	0.0	4.0	0.0	0.0	0.3	0.0	0.0	0.0	2.0
BH5 26.95	11.7	0.0	2.7	0.3	0.0	2.0	0.0	13.3	11.7	14.7	5.0	0.0	0.7	18.3	4.0	4.0	2.7	0.0	0.0	0.7	6.3	0.0	0.0	0.3	0.0	0.3	0.3	1.0
BH5 29.51	14.3	0.3	8.0	1.0	0.0	3.0	0.3	19.0	2.3	13.0	1.3	0.0	1.3	16.0	3.7	8.3	3.0	0.0	0.0	1.3	2.3	0.3	0.0	0.3	0.3	0.0	0.0	0.3
BH5 32.77	29.3	0.0	3.0	0.7	0.0	3.3	1.0	17.3	1.7	8.0	5.3	0.0	0.0	11.0	4.3	0.0	0.7	0.0	0.0	1.7	8.0	0.7	0.3	0.3	0.0	0.7	0.0	2.7
Group 3/Kendall/Unit E																												
BH1A 40.8	16.3	0.7	8.7	1.3		7.3	0.0	25.3	0.7	0.0	0.0	0.7	17.0	0.0	0.0	0.0	1.0	0.0	0.0	1.7	15.7	0.0	0.0	1.3	0.3	0.0	0.3	1.7
BH2 47.50	18.7	0.7	9.3	3.3	0.7	7.3	0.3	15.7	0.0	0.7	0.0	0.3	20.0	0.0	0.7	0.0	1.3	0.0	0.0	5.7	9.3	2.7	0.0	0.0	0.0	0.3	0.7	2.3
BH2 50.40	23.0	0.0	4.0	1.3	0.3	7.3	0.0	30.3	0.3	0.0	0.0	0.0	17.7	0.0	0.3	0.0	0.3	0.0	0.0	3.7	4.3	2.3	0.0	1.0	0.3	0.3	0.0	3.0
BH2 99.40	13.0	0.3	9.0	1.7	0.3	10.3	0.0	10.3	0.7	1.0	0.0	0.3	8.7	0.0	6.0	0.0	0.0	0.0	0.0	3.7	26.0	3.3	0.0	1.0	0.0	0.3	1.3	2.7
BH4 56.30	29.7	0.0	8.0	6.0	1.3	2.0	0.7	0.0	0.3	0.0	12.7	0.0	1.0	11.0	0.3	0.0	1.7	0.0	0.3	7.7	11.3	0.7	0.0	0.7	1.3	0.7	1.0	1.7
BH5 76.86	26.7	0.0	9.3	0.3	0.0	5.0	0.0	20.0	0.7	0.7	0.0	0.0	1.3	10.3	0.0	2.7	1.0	0.0	0.0	4.7	12.7	1.0	0.3	0.3	1.7	0.7	0.0	0.7
BH5 79.40	43.0	0.3	3.0	2.7	0.3	2.7	2.0	15.7	0.3	0.3	0.0	0.0	0.7	7.0	0.3	0.0	0.7	0.7	1.0	3.0	11.0	1.0	0.0	1.0	1.0	0.3	0.0	2.0
BH5 84.97	33.7	0.3	6.7	0.0	0.0	5.3	0.0	17.3	0.0	0.7	0.0	0.0	0.0	4.0	0.3	0.0	2.0	0.0	0.7	4.3	15.0	1.0	0.3	0.7	2.0	1.3	1.3	2.7
BH5 88.07	43.3	0.0	4.3	0.7	0.3	5.7	3.0	6.3	0.0	0.3	0.3	0.0	0.0	4.3	0.0	0.0	1.0	0.0	0.7	1.7	21.3	0.3	0.0	1.7	0.3	1.0	0.7	2.7

analysis by Consorminex Inc.

LIST OF MINERAL CODES

GA GARNET angular, Gr GARNET rounded, EP EPIDOTE angular, Er rounded, Ea Allanite, HE HEMATITE irregular, Hr HEMATITE rounded, GO GOETHITE yellow brown, PY PYRITE fresh, Pg goethite covered, Pb botryoidal/framboidal, Pe euhedral, DI diopside, HY hyperstene, SD SIDERITE x-tal aggregate, Sm SIDERITE massive, HBg HORNBLENDE green, HBb HORNBLENDE brown, RU RUTILE red, LE LEUCOXENE, IM ILMENITE, CD CHLORITOID, SP TITANITE, ST STAUROLITE, KY KYANITE, ZI ZIRCON angular, Ze ZIRCON euhedral, UK UNKNOWN.

removed (Figure 2.4.3). Of interest in this comparison is the apparent similarity of values for the remaining minerals for Group 1 and 2 sands.

2.4.4 Discussion

In general terms the various sand units investigated in this study are remarkable in their similarities rather than their differences. The light minerals present in each group indicate that the various subfacies of Units C and E are mature sediments with a dominance of quartz grains and only trace amounts of feldspar and lithic fragment grains. The heavy mineralogy of subfacies C_2 and C_3 appear to be distinct from subfacies C_1 on the basis of higher siderite and pyrite concentrations. These higher concentrations,as well as the presence of botryoidal and framboidal pyrite grains which are easily disturbed during primary grain transport, suggest that secondary mineral growth possibly resulting from diagenesis may have occurred in subfacies C_2 and C_3. When siderite and pyrite are removed from the averages for the various subfacies of Unit C there is almost no statistical difference between them. Higher garnet, diopside and ilmenite, and lower goethite concentrations provide a clear discrimination on the basis of heavy minerals of the various subfacies of Unit E relative to those of Unit C. This may be the only solid evidence of variable depositional conditions or providence of the sands units based solely on mineralogy.

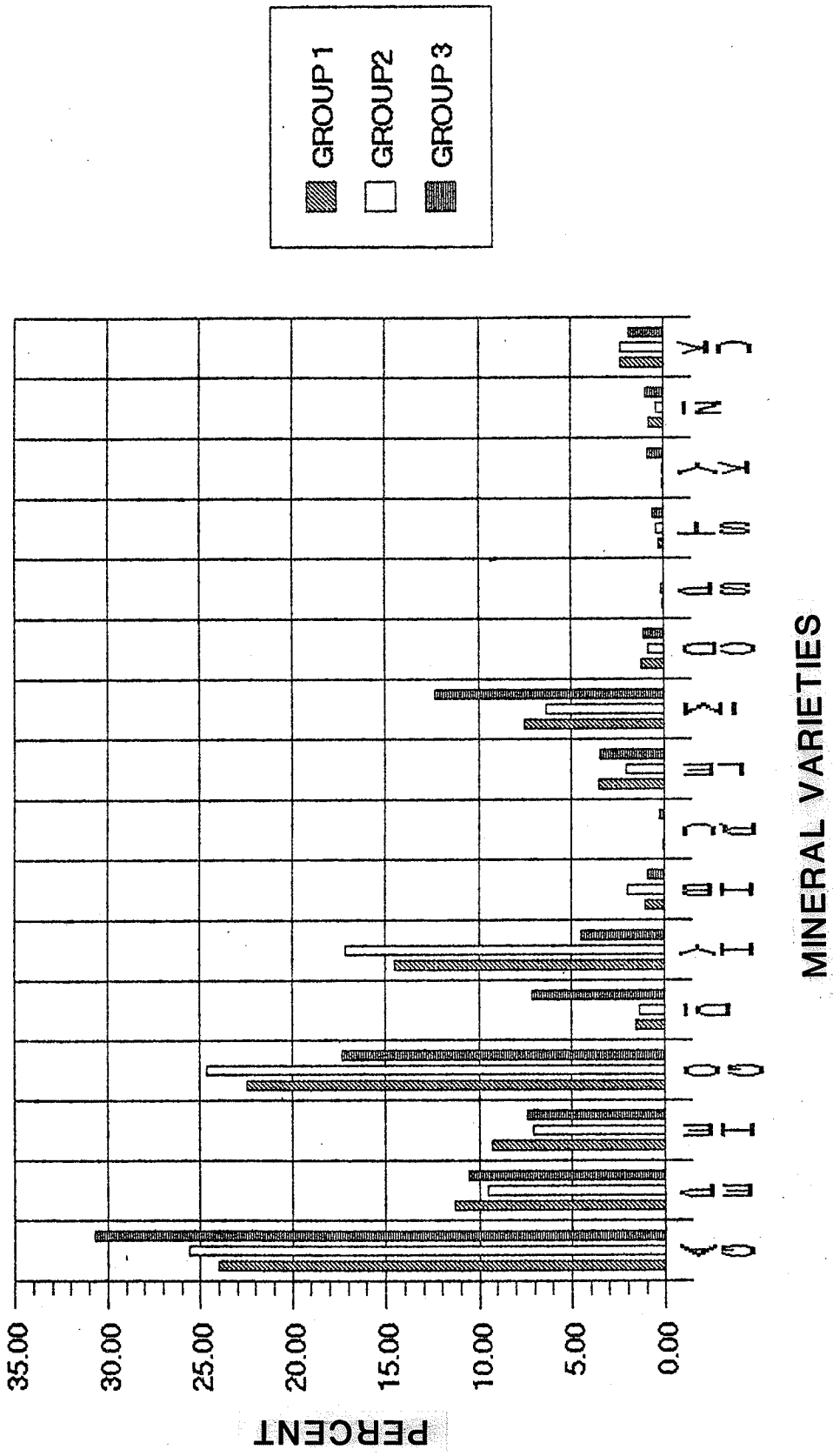

Figure 2.4.3 Heavy Mineral averages by group with Siderite and Pyrite removed

REFERENCES

Pettijohn, F.J., 1957. Sedimentary Rocks. Harper and Row, London, 718 p.

2.5 GRAIN TEXTURE OF SAND UNITS

J.A. Hanright

2.5.1 Introduction

In order to further the stratigraphic and sedimentologic investigation of sand sequences collected in boreholes from Richards Island and areas offshore, a study of grain characteristics was undertaken using a Scanning Electron Microscope (S.E.M.). This technique allows recognition of differences in grain markings and sedimentological characteristics which can aid in the differentiation of sand units.

Samples from boreholes 90BH1A and 90BH5 were chosen for the investigation of physical characteristics and grain surface textures using the S.E.M.. Six samples were selected from each core so that the major sand units along the entire core were investigated.

Untreated samples were mounted on metal specimen stubs. The stubs were then coated with a gold-palladium alloy and examined using a Cambridge Instruments S-200 S.E.M.. Each sample was photographed at magnifications ranging between x 57.6 and x 247, depending on the grain size of the sample. About 30 to 40 grains were captured on each electromicrograph. The sample was then scanned at magnifications up to about x 4000 in order to examine smaller features. An attempt was made to qualitatively determine the most dominant grain surface characteristics of each sample. Notes were made of other unusual or outstanding features.

2.5.2 Analysis

Observing the samples at lower magnifications revealed differences between samples in grain size, degree of sorting and, most notably, the degree of rounding of the grains. At higher powers it was possible, in some instances, to recognize differences in the surface texture and markings on the sand grains. Tables 2.5.1 and 2.5.2 summarize the information derived from the S.E.M. work for boreholes 90BH1A and 90BH5, respectively.

2.5.3 Discussion

It was possible to separate 9 of the 12 samples into three distinct groups, each with their own attributes (Table 2.5.3).

Table 2.5.1 Characteristics of S.E.M. samples from Borehole 1A

	SHAPE	ROUNDNESS	SIZE	SORTING
BH1A 4.8	Equant to oblate	Subrounded to subangular	Medium to very fine sand	well sorted
Notes: Grains with rounded edges abundant. Some have frosted appearance and many have dish-shaped concavities.				
BH1A 8.6	Equant	Rounded to subangular	Medium to very fine sand	well sorted
Notes: Grains with rounded edges abundant. Almost all grains have frosted appearance and many have dish-shaped structures.				
BH1A 24.5	Equant to oblate	Well rounded to subangular	Medium to very fine sand	well sorted
Notes: All grains exhibited rounded edges. Frosted grains are abundant, some with dish shaped concavities.				
BH1A 27.7	Equant to oblate	Subangular to very angular	Fine sand to coarse silt	moderate sorting
Notes: Most grains have sharp edges (not rounded). Several show fresh conchoidal fractures. Considerable variation in grain shape and surface textures. Silt is abundant.				
BH1A 33.3	Equant to oblate	Subrounded to very angular	Fine sand to coarse silt	well sorted
Notes: Most grains show fresh fractures, sharp edges. Some show fresh fracture surfaces. Silt particles are not common.				
BH1A 40.8	Equant	Rounded to subangular	Medium sand to coarse silt	moderate sorting
Notes: Grains tend to have well rounded edges but surface textures vary from smooth to abundant pits, some of which are V-shaped, and grooves. Silt grains are not common.				

Table 2.5.2 Characteristics of S.E.M. samples from Borehole 5.

	SHAPE	ROUNDNESS	SIZE	SORTING
BH5 16.35	Equant	Rounded to subangular	V. fine sand to coarse silt	well sorted
Notes: Many grains with rounded edges (very few with sharp, fresh edges). Some grains have dish-shaped concavities and frosted appearance. Many grains have secondary crystal growth.				
BH5 19.85	Equant	Subrounded to subangular	V. fine sand to coarse silt	very well sorted
Notes: Most edges appear rounded. Some grains with frosted appearance. Fresh fractures are infrequent.				
BH5 24.30	Equant	Subrounded to very angular	Medium sand to coarse silt	moderate sorting
Notes: Many grains with fresh conchoidal fractures and sharp edges. Some show V-shaped pits. Subrounded grains are infrequent.				
BH5 32.77	Equant	Rounded to Angular	Medium sand to coarse silt	moderate sorting
Notes: Many fresh conchoidal fractures. Grains frequently have sharp edges. Rounded grains do not have frosted appearance.				
BH5 79.40	Equant	Subrounded to subangular	Medium to fine sand	very well sorted
Notes: Homogeneous sample in terms of shape and rounding. Fracture surfaces have dulled edges and are not fresh looking. Surface textures are smooth to irregular.				
BH5 88.07	Spherical to plate-shaped	Subrounded to angular	Fine sand to v. fine silt	poorly sorted
Notes: . Larger grains have dish-shaped features and frosted appearance and rounded edges. Angular grains with sharp edges abundant. Some secondary crystal growth.				

Table 2.5.3 Sample groupings

	Samples	Geologic formation/subfacies
Group 1	BH1A 4.8 BH1A 8.6 BH1A 24.5 BH5 16.35 BH5 19.85	Kittigazuit Kittigazuit Kittigazuit C1 C1
Group 2	BH1A 27.7 BH1A 33.3 BH5 24.30 BH5 32.70	Kidluit Kidluit C2 C2
Group 3	BH1A 40.8 BH5 79.40 BH5 88.07	Kendall Unit E Unit E

Group 1 (Kittigazuit sand - subfacies C_1)

In the first group, 90BH1A 4.8 m, 90BH1A 8.6 m and 90BH1A 24.5 2 m were of a coarser texture than 90BH5 16.35 m and 90BH5 19.85 m, but in other respects exhibited similar characteristics. Sedimentological logs (see section 2.3) of 90BH1A identify samples at depths of 4.8 m, 8.6 m, and 24.5 m as Kittigazuit Formation sands. Logs of 90BH5 indicate that samples 16.35 m and 19.85 m are from subfacies C_1.

Few, if any, angular grains or fresh fracture surfaces were noted from this group. Even grains classified as sub-angular exhibited dulled, rounded edges under close inspection. All of these samples were well sorted except for one which was very well sorted (Figure 2.5.1). In addition, a number of the grain surface textures of these samples appeared similar. Grains with a frosted texture were common and these grains often also exhibited dish-shaped concavities on their surfaces (Figure 2.5.2).

Group 2 (Kidluit sand - subfacies C_2)

Within the second group, sedimentological logs (see section 2.3) indicate that samples from 90BH1A are from the Kidluit Formation and those from 90BH5 are from subfacies C_2. This group of samples has very different characteristics from those of the first group. In samples 90BH1A 27.7 m, 90BH1A 33.3 m, 90BH5 24.30 m and 90BH5 32.77 m, grains which have sharp edges and fresh fractures are common. In general, these samples contain many more angular grains than those in the first group (Figure 2.5.3). Many of these grains have conchoidal fractures and broken plates (Figure 2.5.4). Some rounded grains are found in these samples, however they are not abundant and they do not frequently exhibit the frosted surface texture and dish-shaped features that are a feature of the first group. The samples from this group also tend to be only moderately sorted (one is well sorted). Those from 90BH1A are slightly finer in texture than those from 90BH5.

Group 3 (Kendall sediments - Unit E)

Of the remaining samples 90BH1A 40.8 m (Kendall Formation from the sedimentological logs) and 90BH5 79.40 m (identified as unit E from the sedimentological logs) show some similar tendencies with each other and with the samples from the first group. Both samples have grains which are distinctly rounded; also, freshly broken surfaces

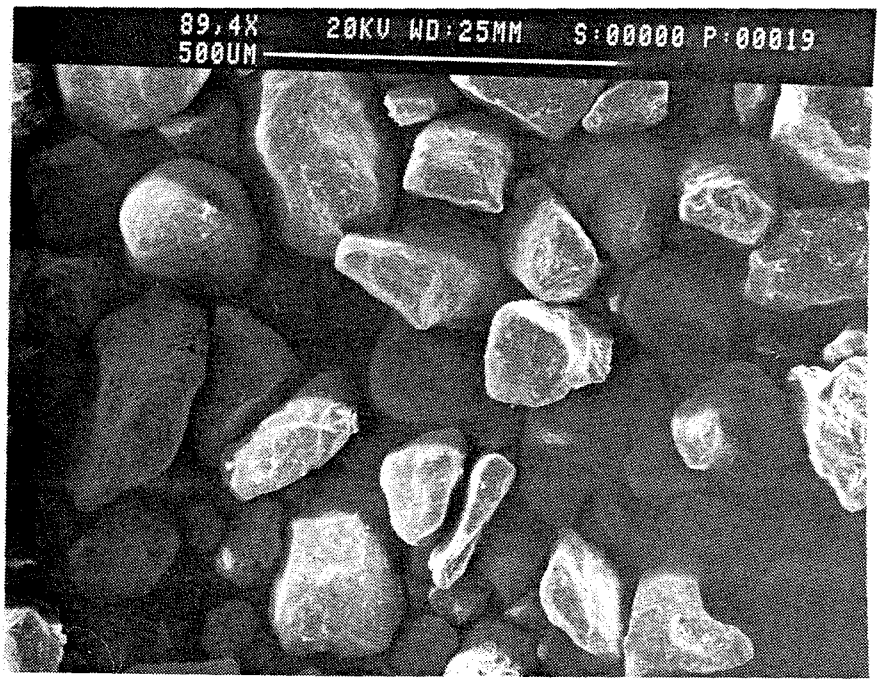

Figure 2.5.1. This photo shows the rounded grains and good sorting typical of group 1.

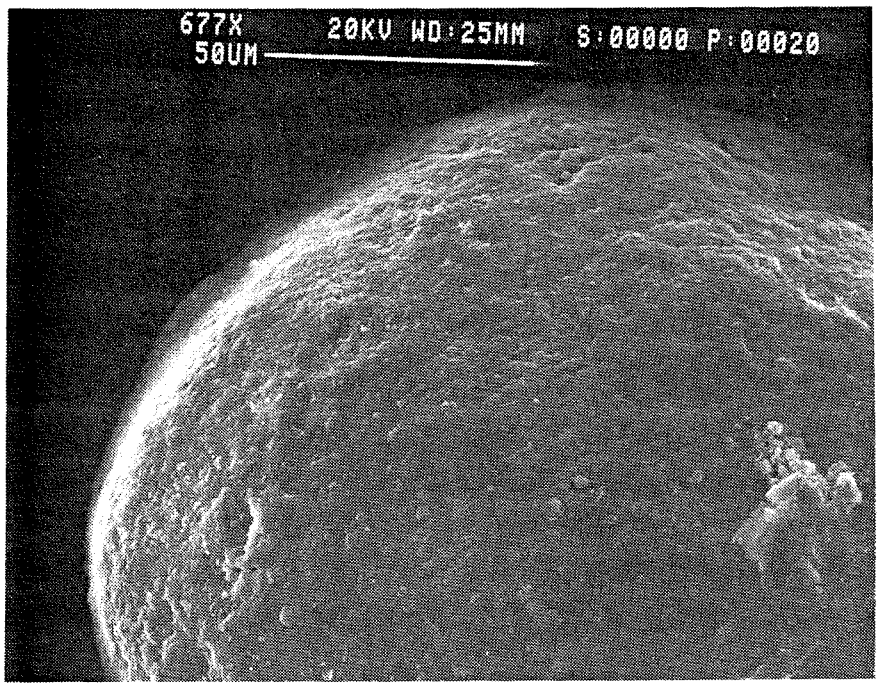

Figure 2.5.2. Rounded grains and dish-shaped concavities are common features of the samples in group 1.

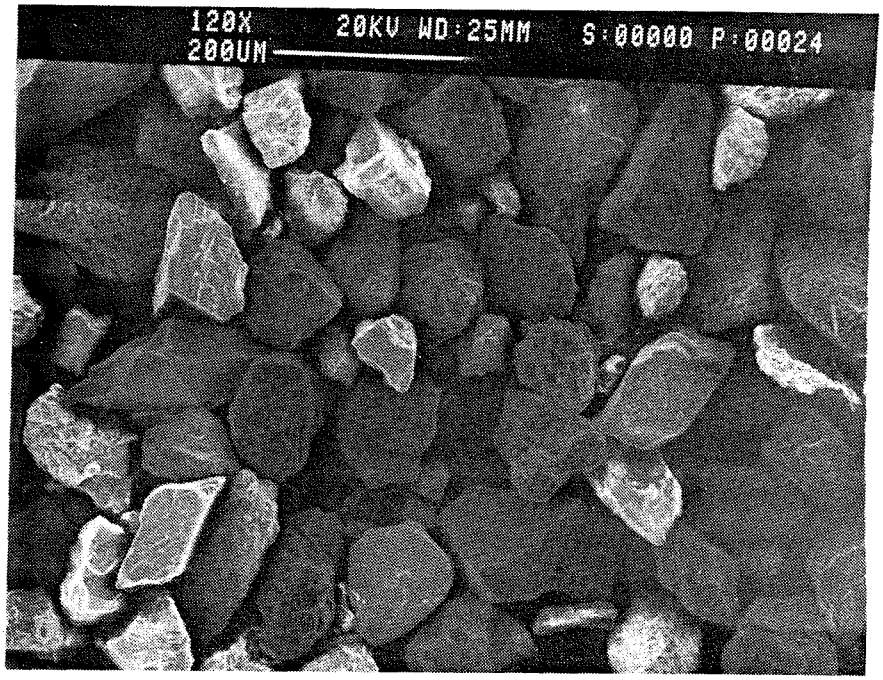

Figure 2.5.3. The angular grains and relatively poor sorting of samples from group 2 are shown in this photo.

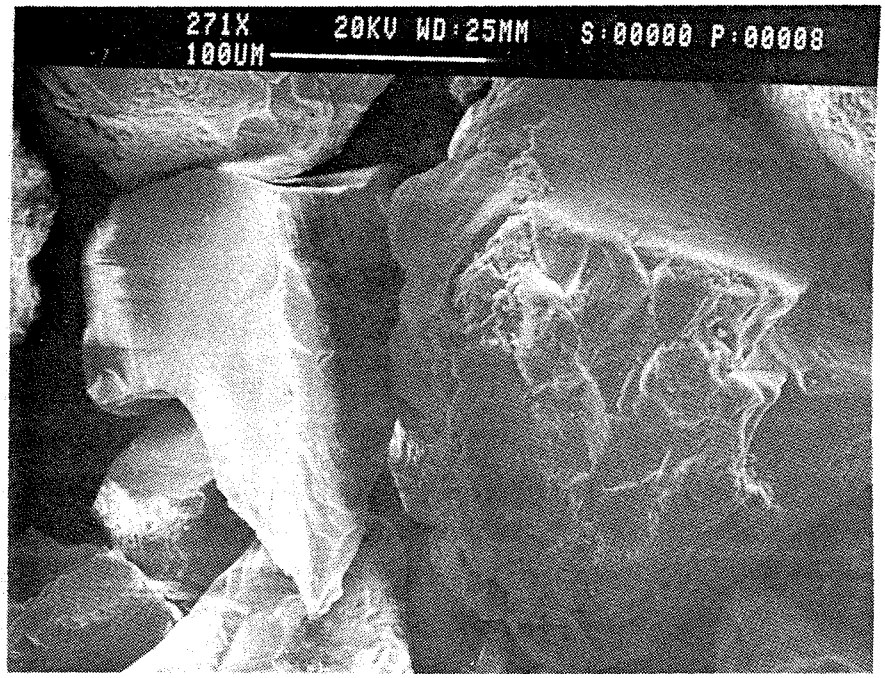

Figure 2.5.4. Conchoidal fractures and broken plates are shown on many on many of the grains of group 2.

are absent. However, close examination revealed that many of the sub-angular grains from 90BH1A 40.8 m and particularly 90BH5 79.40 m had the scars of old fractures and broken plates, which have been subdued and dulled (Figure 2.5.5). The grain surface textures showed a variety of features from smooth to very pitted and irregular. No single grain-surface characteristic appeared to be dominant.

Sample 90BH5 88.07 m (unit E from sedimentological logs) shares some of the same features as those in groups 1 and 2. Angular grains tend to be dominant, yet the fresh looking fractures that are a feature of the second group are absent. Some of the larger rounded grains have the frosted surface texture apparent on grains of the first group. Like samples 90BH1A 40.8 m and 90BH5 79.40 m, there are a variety of surface textures from smooth to very irregular.

2.5.4 Depositional Environment

Grain surface characteristics may, in some cases, be used to tentatively interpret transportational and depositional environments of sand grains. However grains with similar features may be found in different environments and, as Krinsley and Doornkamp (1973) explain, no single mechanical mark provides diagnostic evidence of a specific environment. Thus, grain surface textural characteristics alone are normally considered insufficient for interpreting depositional environments. However, they may help to differentiate stratigraphic units and can provide supporting evidence for interpretations of the environment of deposition.

Grain rounding and dish-shaped features tend to be indicative of eolian transport (Krinsley and Doornkamp, 1973). As discussed by Hill and Nadeau (1984), in cold environments, the amount of rounding may vary depending on the wind intensity and the time the grain resided in the environment, so that dish-shaped concavities are generally the best indicator of a cold desert eolian deposit. Many of the grains of group 1 (Kittigazuit Formation and subfacies C_1) show varying degrees of roundness as well as dish-shaped concavities which suggest these sand grains may have been derived from a cold eolian environment.

Angular grains which exhibit conchoidal fractures suggests a glacial environment, although there may be some degree of mechanical rounding of the larger grains as they are

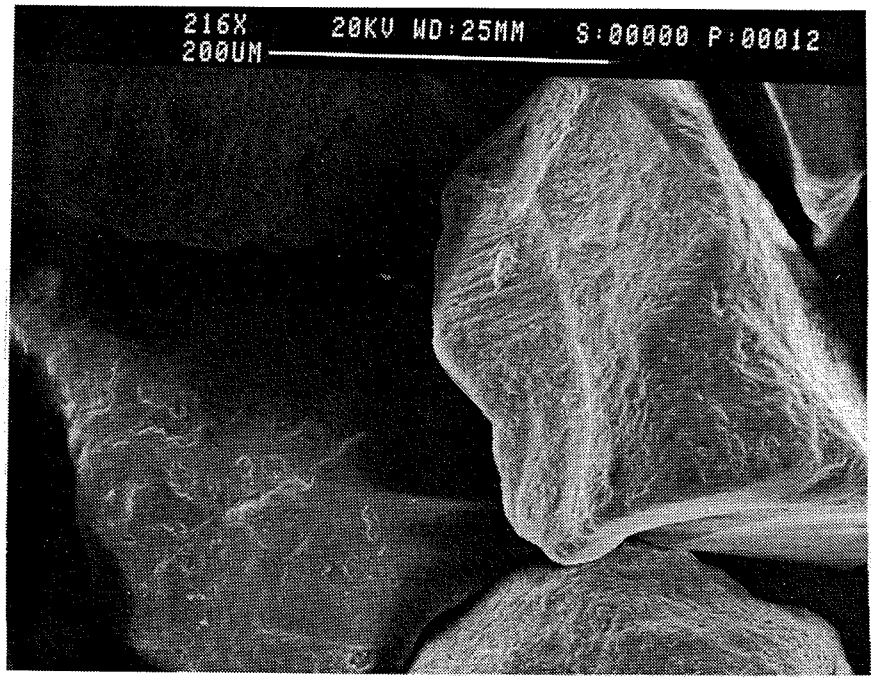

Figure 2.5.5. Rounded conchoidal fractures were visible on some of the grains from BH5 79.40m. Note also the variability in grain surface textures.

transported away from the ice front (Krinsley and Doornkamp, 1973). The characteristics of the second group of samples (Kidluit Formation and subfacies C_2) generally shows many angular grains with conchoidal fracturing, thus it appears these samples may be obtained from a glaciogenic deposit. However, Mazullo and Ritter (1991) argue that grains deposited in a glacial environment may be rounded or angular, and that source rock composition is the primary influence on surface grain textures in a glacial environment.

It is not possible to speculate on the genesis of the remainder of the samples. The variability in grain surface features may be a reflection of a polygenetic history and/or it may have resulted from diagenesis which has obscured the original characteristics formed during transportation of the grains.

REFERENCES

Hill, P.R., and Nadeau, O.C., 1984. Grain-surface textures of Late Wisconsinan sands from the Canadian Beaufort Shelf. Journal of Sedimentary Petrology, v.54, p.1349-1357.

Krinsley, D., and Doornkamp, J.C., 1973. Atlas of Quartz Sand Surface Textures. Cambridge University Press, England, 91 p.

Mazzullo, J., and Ritter, C., 1991. Influence of sediment source on the shapes and surface textures of glacial quartz sand grains. Geology, v.19, p.384-388.

2.6 GEOCHEMISTRY

R.E. Cranston

2.6.1 Introduction

There are a number of indicators that methane is present in marine sediments and that it is presently being released or has been released in the past. Seismic records often show bright spots, enhanced reflections, acoustic turbidity and acoustic blanking. Sidescan records reveal circular pock marks, up to 100's of metres in diameter and 10's of metres deep, thought to be caused by gas eruptions at the sea floor. Methane can be measured by collecting seawater and sediment samples and passing a gaseous sample through chromatography equipment.

Hot and cold seafloor vents allow unique biological communities to exist, often not following normal photosynthetic processes. Instead, bacteria are gathering energy from methane and hydrogen sulfide gas being released at the vent. Anthropogenic activities in harbours and estuaries supply sufficient organic carbon to support anaerobic conditions in the sediment column, allowing bacteria to produce methane which is often seen bubbling from the seafloor.

In addition to methane production by biogenic processes, most methane escaping from marine sediments is produced by thermogenic mechanisms in buried hydrocarbon reserve areas, where time, heat and pressure convert buried organic matter to hydrocarbon products, some of which are alkane hydrocarbons such as methane, ethane, propane and butane. Once produced, these gases can migrate from the production zone through permeable sediments. However, as the methane moves upward, an oxidative sulfate flux moves in the opposite direction and consumes methane by oxidizing it to carbon dioxide. If the methane flux exceeds the sulfate flux, gas will form bubbles at some depth and either escape from the sediment column or form gas hydrate deposits. Both forms of methane pose hazards to offshore exploration and development as well as to the global greenhouse warming problem. Methane is a greenhouse gas which is accumulating in the atmosphere relatively more quickly than other greenhouse gases, including carbon dioxide (Cicerone and Oremland, 1988).

Gas hydrate deposits are known to occur in marine sediments where gas bubbles occur and the total pressure is in the range of 30 to 60 atmospheres at temperatures of 0 to 10 degrees Celsius. The formation conditions are very sensitive to gas composition which can include varying amounts of alkanes, carbon dioxide, hydrogen sulfide, hydrogen and nitrogen species. One litre of wet sediment can contain more than 100 litres of methane at standard temperature and pressure in a hydrate structure. This corresponds to 10 % organic carbon in the sediment on a dry weight basis. Such deposits are often referred to as bottom simulating reflectors on seismic records. Based on these occurrences, it has been estimated that more carbon is held in gas hydrate deposits than all known fossil fuel deposits (Kvenvolden, 1988).

As part of the onshore-offshore transect project, sediment samples were collected and stored in gas-tight containers. In addition, small sediment samples were recovered to investigate the oxidation potential and organic carbon content of the sediment column. The main geochemical concern was the balance between concentrations of methane and dissolved sulfate. If significant amounts of methane are present, dissolved sulfate is reduced to sulfide during the microbial oxidation of methane.

2.6.2. Methods

Gas sample jars were used to store about 0.5 L of wet sediment for methane and higher alkane analyses. Eleven samples were recovered and analyzed by gas chromatography at the Cape Breton Coal Research Lab operated by CANMET, in Sydney, N.S. The results are reported as headspace concentrations in ppm(volume), where the headspace volume was approximately equal to the wet sample volume.

Forty additional samples were stored in 20 ml scintillation vials for dissolved sulfate and solid phase organic carbon analyses. In order to recover pore water from the sediment, 5 ml of deionized water was thoroughly mixed with a 10 g portion of wet sediment. The diluted pore water was recovered using a refrigerated centrifuge and filtered through 0.5 um pore diameter membrane filters. Sulfate concentrations were determined by adding excess barium to precipitate barium sulfate, while the remaining barium concentration was determined by atomic absorption spectroscopy. Because of the dilution-extraction step and natural dilution due to fresh water, the original salinity was not known, but major cation

concentrations were determined in the diluted sample. Final sulfate results are reported as the amount of sulfate depletion in the pore water. This was calculated from the salinity estimate, from the amount normally found in oxidized seawater, and from the amount found in the diluted pore water.

Organic carbon analyses were done on dried sediment samples that were digested with 10% hydrochloric acid to remove carbonate carbon. Carbon concentrations were determined using a Leco WR-112 carbon combustion analyzer.

2.6.3 Results

Table 2.6.1 contains results for the gas, sulfate and organic carbon analyses. Gas results, in ppmv in the headspace, are listed in two columns under methane and C2+, i.e. higher alkane which includes ethane, propane, butane and isobutane. Sulfate results are recorded as the amount of sulfate depletion relative to the amount of sulfate expected in fully oxidized pore water. The results are corrected for natural salinity variations and for the dilution step used in the pore water extraction procedure. Organic carbon values are recorded as the percentage of organic carbon in dry sediment samples. Field logs were used to identify corresponding geological units for each sample interval.

Table 2.6.2 contains mean concentrations (with standard deviations and number of observations) for each geological unit from the results presented in Table 2.6.1.

2.6.4 Discussion

In oxidized sediments, sulfate depletion will be less than 5% of the total available sulfate. In moderately reduced or sub-oxic sediments, sulfate depletion will reach 50%, while in strongly reduced sediment, where biogenic methane is present in significant amounts, sulfate depletion will approach 100% as widespread oxidation of methane coupled with reduction of sulfate occurs. From the results in Table 2.6.2, sulfate concentrations in Unit C were an average of only 3% lower than concentrations expected for oxidized pore water. An average of 6% of the sulfate was depleted in Unit B, while 7% was missing in Unit E and 8% in Unit D. The low amount of sulfate depletion in all units indicates that anoxic conditions were not present. A t-test to measure whether means are significantly different showed that Unit C had significantly less sulfate removed than did either Units B

TABLE 2.6.1 Megatransect Redox and Gas Results

Site	Geological Unit	Subsample Depth (m)	Sulfate Depletion (%)	Organic Carbon (%)	Methane (ppmv)	C2+ (ppmv)
BH-2	B	2.95	7	1.68		
	B	4.27	7	0.78		
	B	5.29	7	1.29		
	B	6.74	7	1.22		
	B	10.30	11	1.33		
	B	11.88	7	1.43		
	C	15.30	7	0.27		
	C	32.30	4	0.31	<0.01	<0.01
	D/E	45.10	7	0.89	0.16	0.01
BH-3	B	drill mud	-	17.7	<0.01	<0.01
	B	1.37	4	1.91		
	B	3.65	4	1.20		
	B	5.00	4	0.97		
	B	6.40	0	1.24		
	B	7.90	4	0.27		
	B	8.84	7	1.24		
	B	9.15	0	0.90		
	B	10.17	0	1.00		
	B	11.20	7	1.25		
	B	12.47	11	1.15		
	B	13.90	7	0.67		
	B	15.00	7	0.98		
	C	16.70	7	0.24		
	C	17.30	4	0.64		
	C	21.20	4	0.66	0.02	<0.01
	D	37.50	11	1.48		
	D	45.72	15	1.18		
BH-4	D	34.70	7	1.31		
	D	38.80	7	1.27	0.56	<0.01
	D	42.56	7	1.32		
	D	50.29	7	1.35	1.32	<0.01
	E	90.80	7	0.28	<0.01	<0.01
BH-5	C	9.91	4	0.97		
	C	10.90	0	0.54		
	C	14.00	0	0.38		
	C	16.31	0	0.75	<0.01	<0.01
	C	21.60	4	0.15		
	C	33.80	0	0.13	<0.01	<0.01
	D	41.35	7	1.40	1.43	<0.01
	E	79.40	7	0.18	<0.01	<0.01

TABLE 2.6.2 Summary of Geochemical Data *

Geological Unit	Sulfate Depletion (%)	Organic Carbon (%)	Methane (ppmv)
B	6 +/- 3 (18)	1.1 +/- 0.4 (18)	(0)
C	3 +/- 3 (11)	0.5 +/- 0.3 (11)	0.01 +/.005 (4)
D	8 +/- 3 (8)	1.3 +/- 0.2 (8)	0.9 +/- 0.6(4)
E	7 +/- 0 (2)	0.2 +/- 0.1 (2)	0.01 +/- 0 (2)

* (mean values +/- std dev, no. of observations)

or D, i.e. Unit C tended to be marginally more oxidized than B or D.

Organic carbon means in Table 2.6.2 indicate that Unit C had significantly lower organic carbon concentrations than either Units B or D (based on t-test applied to means). Methane concentrations in headspace were found to be highest in Unit D. Unfortunately, no gas samples were collected for Unit B, and the number of observations for the gas samples were too limited to carry out meaningful significance tests.

Unit D was most depleted in sulfate and contained more organic carbon and methane than did other units. This suggests that minor amounts of biogenic methane was being produced in Unit D. The absence of higher alkanes (C2+ in Table 2.6.1) suggests that biogenic methane is present rather than deeper thermogenic gas which would include higher hydrocarbon gases.

Biogenic gas production in harbours and coastal basins produce headspace concentrations of methane exceeding 10,000 ppmv, whereas the highest value found in bore hole samples was less than 2 ppmv. The possibility of gas hydrates in this area have been speculated from seismic data and from offshore drilling results. Under the temperature and pressure conditions present in the study, methane hydrate would occur at depths of 400 to 600 m downcore. The deepest megatransect gas sample came from 91 m downhole at a water depth of 6 m. It is impossible to speculate whether gas hydrates occur at these sites based on the gas analyses reported in Table 2.6.1.

2.6.5 Conclusion

Geochemical results from onshore-offshore transect samples show that minor amounts of biogenic methane were found in the oxic and mildly reducing sediments. The highest methane concentrations were 4 orders of magnitude lower than is normally found in strongly reducing sediments or in areas where deeper thermogenic gas is migrating through the sediment column. There was not a sufficient amount of gas in the upper 100 m of the sediment column to speculate whether gas hydrates occurred at depth in this region.

REFERENCES

Cicerone, R.J. and R.S. Oremland, 1988. Biogeochemical aspects of atmospheric methane. Global Biogeochemical Cycles, vol. 2, 299-327.

Kvenvolden, K., 1988. Methane hydrate - a major reservoir of carbon in the shallow geosphere? Chemical Geology, vol 71, 41-51.

2.7 WATER-COLUMN TEMPERATURE, SALINITY AND CONDUCTIVITY MEASUREMENTS

J.A. Hunter, P.J. Kurfurst and S.M. Birk

Measurements of temperature, salinity and electrical conductivity were made at most cone penetrometer sites (CPT sites) along the onshore-offshore transect line. These surveys were conducted to provide supplementary data on the oceanographic conditions to aid in interpreting shallow sediment temperature and salinity variations. Sites CPT-9 to CPT-14 were occupied on April 3/90, and sites CPT-2 to CPT-8 were occupied on April 6/90.

At all sites, measurements were made at 0.5 m intervals down to seabottom. Data was collected using a YSI Model 33 S-C-T meter using a YSI 3300 Conductivity/Temperature Probe. Reading accuracies are as follows:

Temperature	± 0.1°C
Salinity	± 0.7 ppt
Conductivity	± 3%

The results are plotted in the following figures; each site is identified by a CPT site number and can be located by the site listing in section 1.2.

In the onshore regions, where low salinities occurred, difficulty was experienced in keeping the probe ice-free during a run; repeat measurements were made as checks. Nevertheless, exceedingly low salinity and/or conductivity readings may indicate probe icing and may be in error. As well, all readings taken at depths less than 2 m are within the hole drilled through the sea ice and are probably not representative.

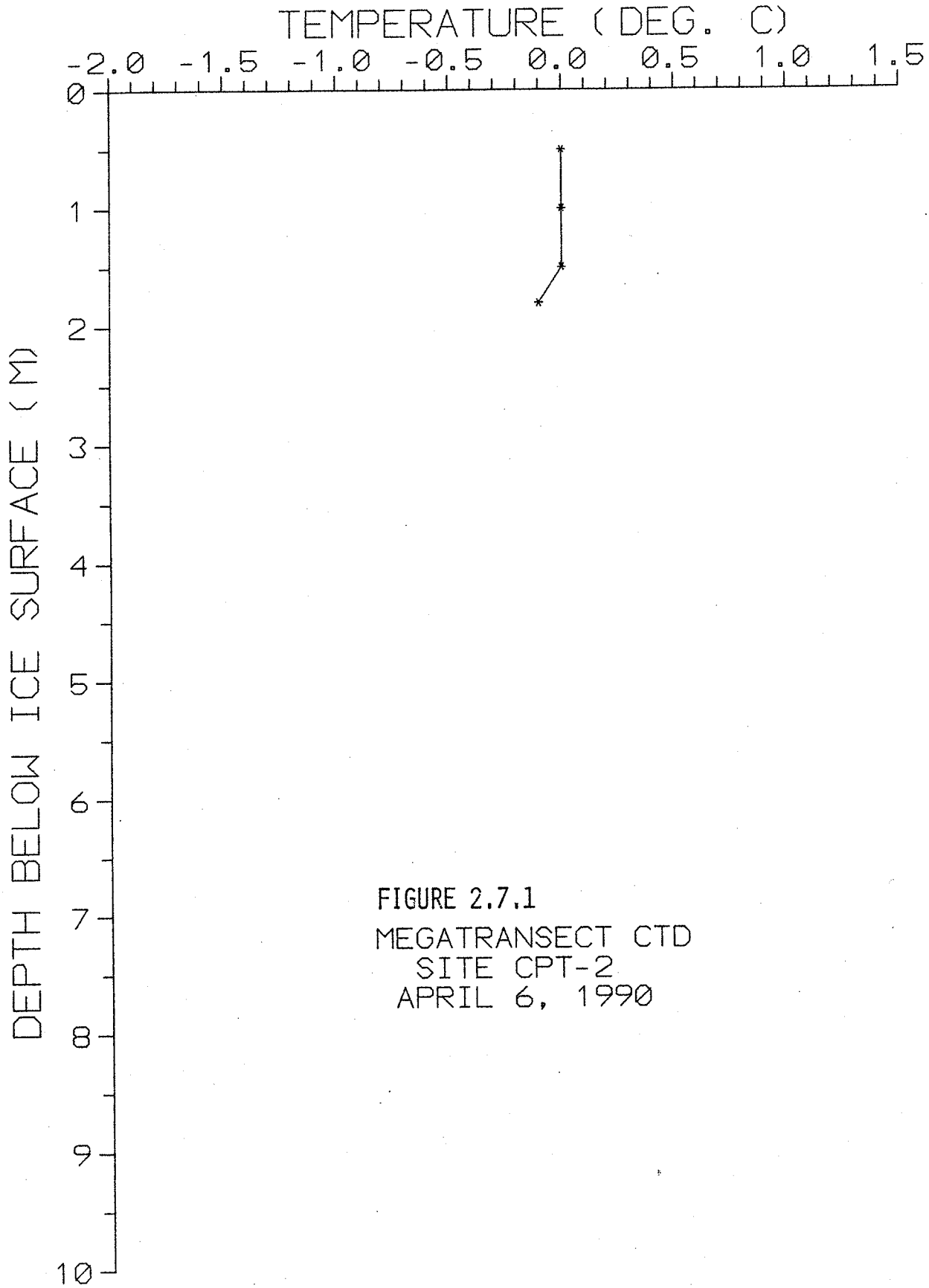

FIGURE 2.7.1
MEGATRANSECT CTD
SITE CPT-2
APRIL 6, 1990

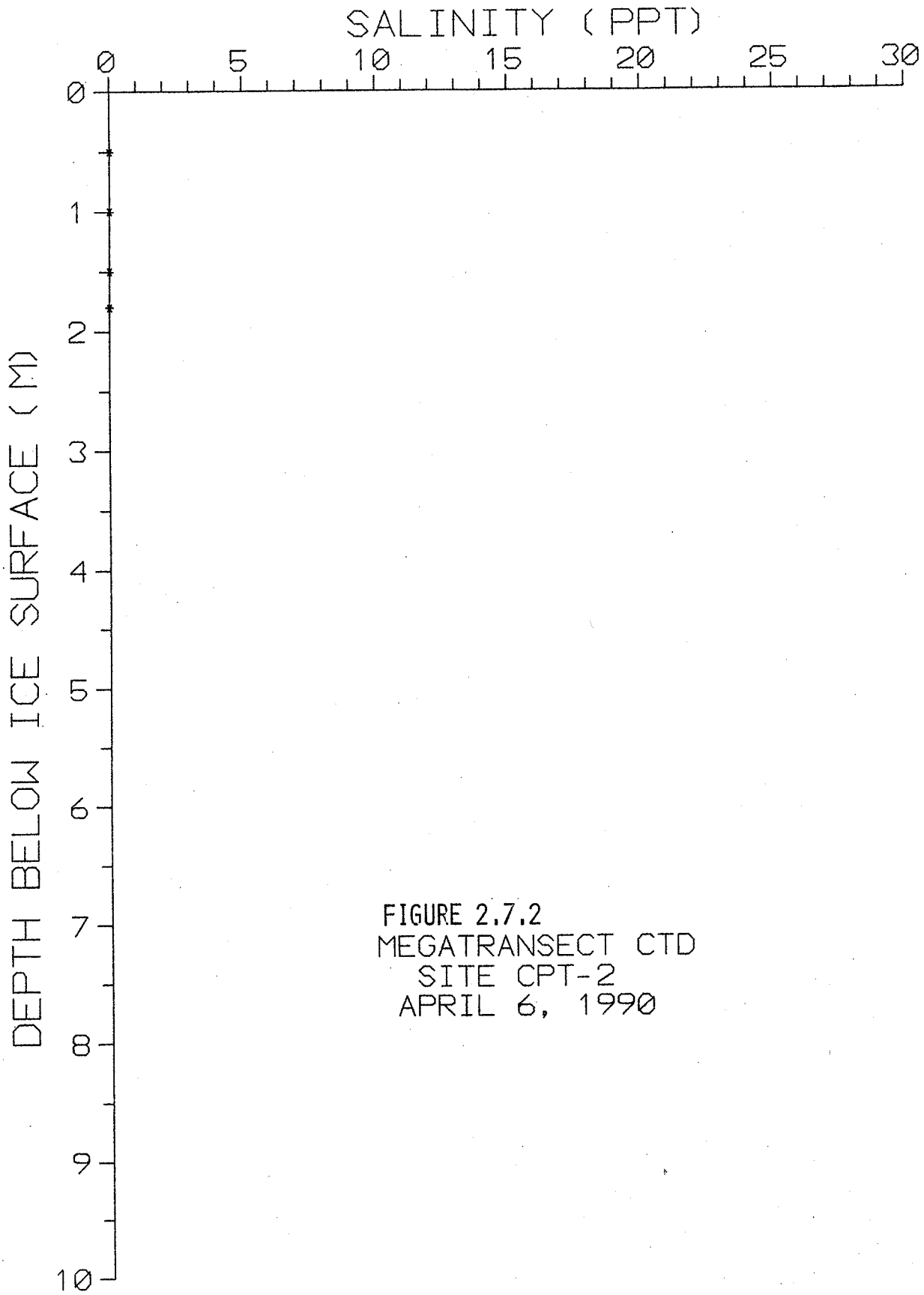

FIGURE 2.7.2
MEGATRANSECT CTD
SITE CPT-2
APRIL 6, 1990

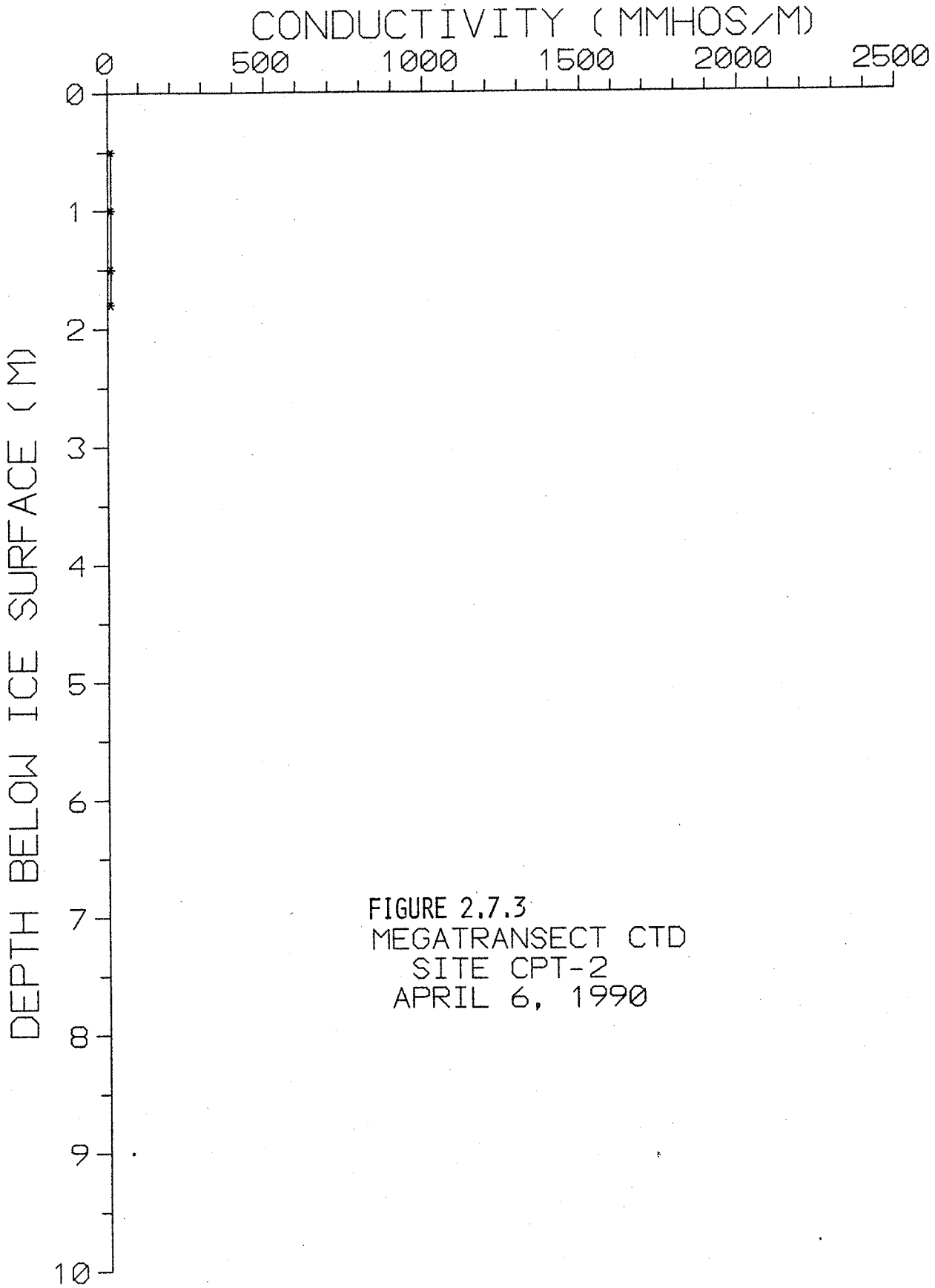

FIGURE 2.7.3
MEGATRANSECT CTD
SITE CPT-2
APRIL 6, 1990

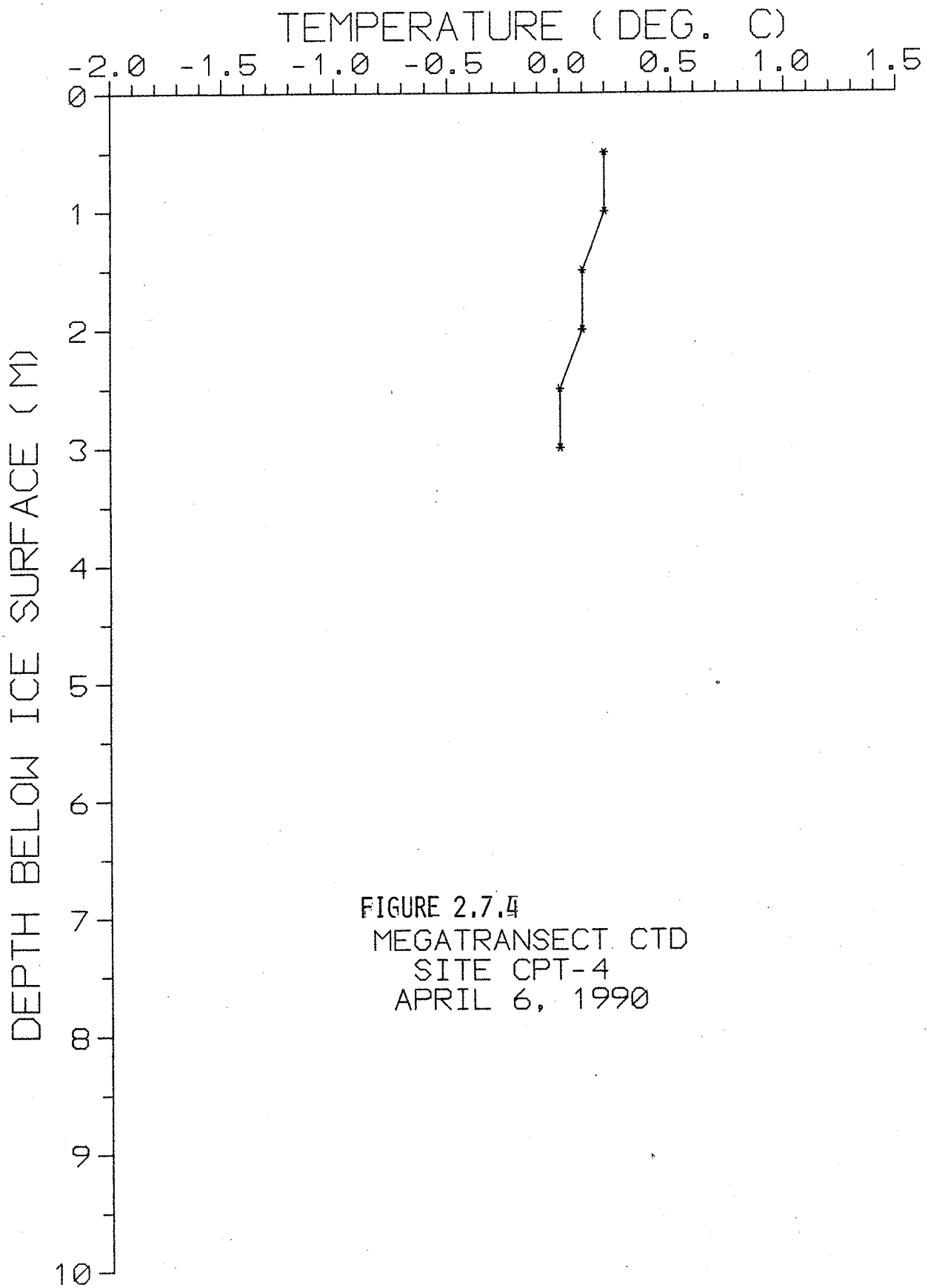

FIGURE 2.7.4
MEGATRANSECT CTD
SITE CPT-4
APRIL 6, 1990

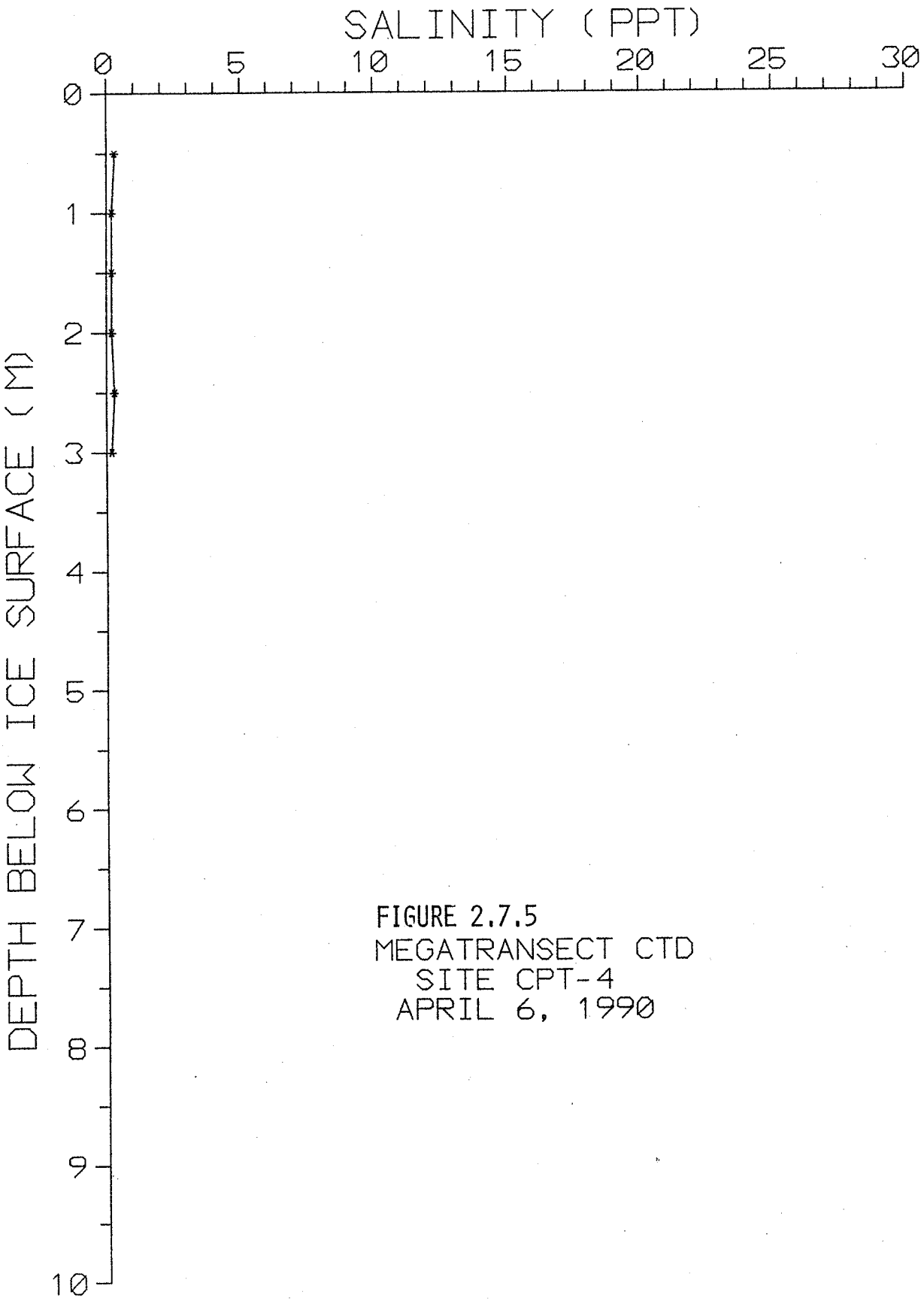

FIGURE 2.7.5
MEGATRANSECT CTD
SITE CPT-4
APRIL 6, 1990

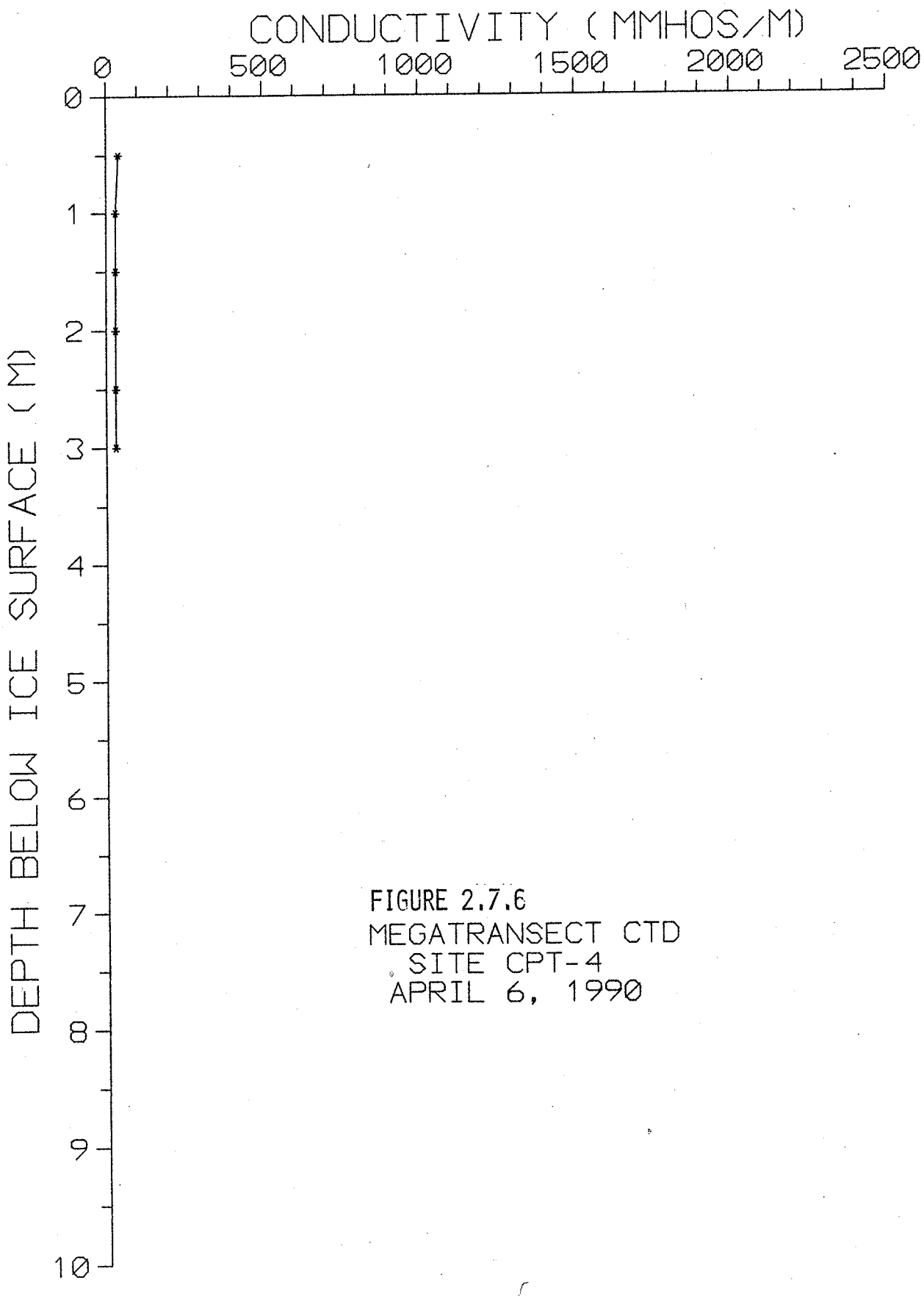

FIGURE 2.7.6
MEGATRANSECT CTD
SITE CPT-4
APRIL 6, 1990

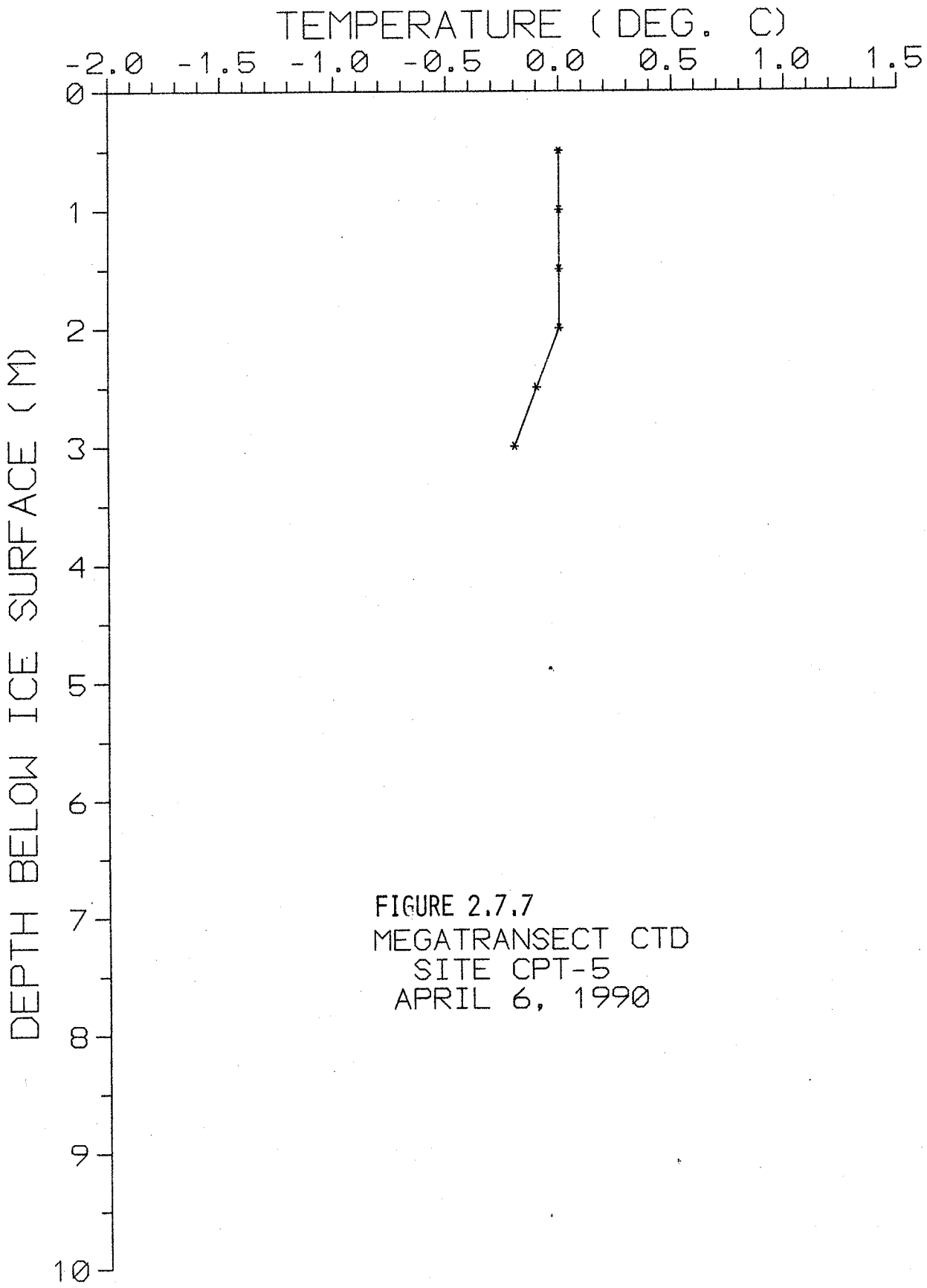

FIGURE 2.7.7
MEGATRANSECT CTD
SITE CPT-5
APRIL 6, 1990

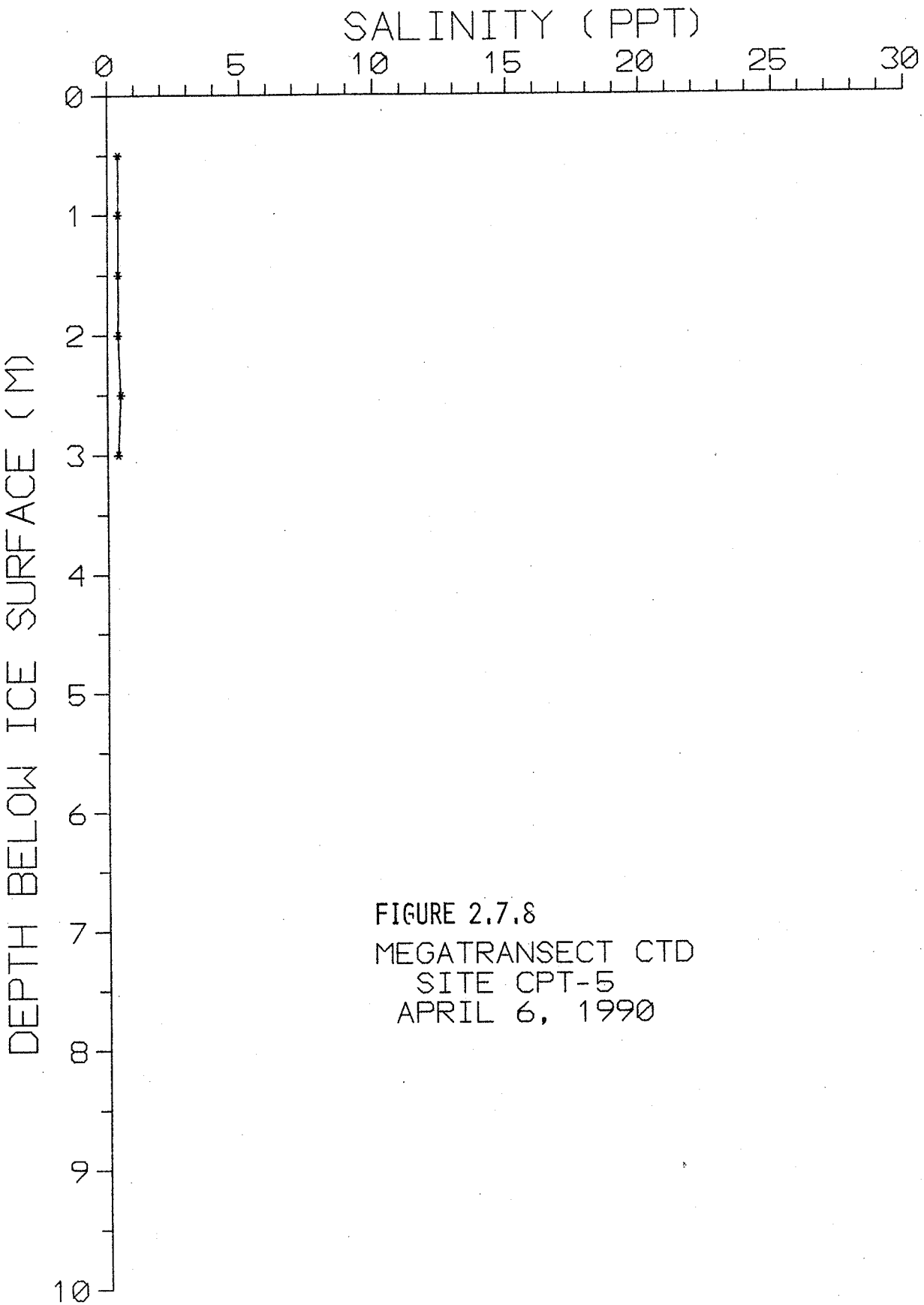

FIGURE 2.7.8
MEGATRANSECT CTD
SITE CPT-5
APRIL 6, 1990

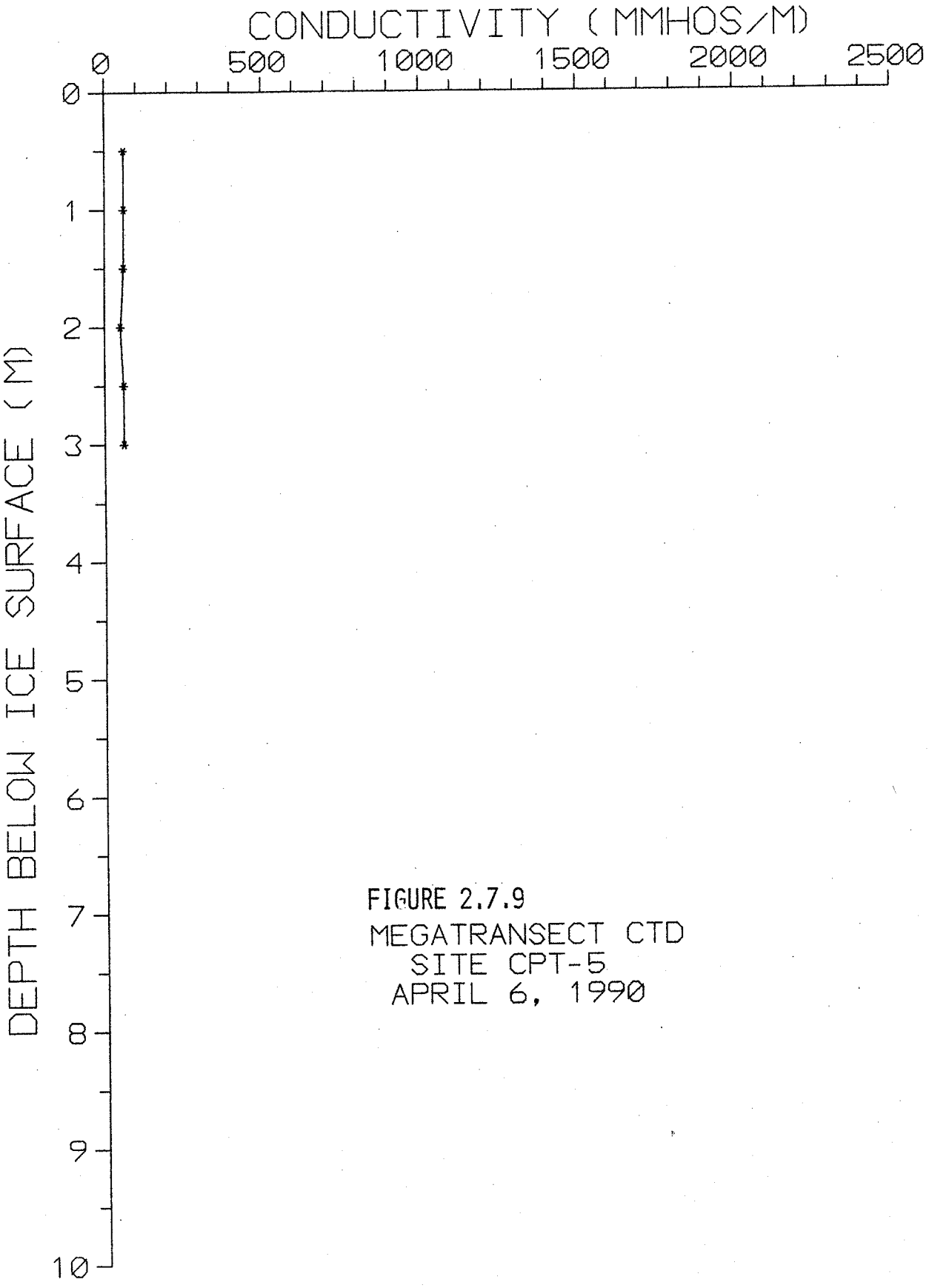

FIGURE 2.7.9
MEGATRANSECT CTD
SITE CPT-5
APRIL 6, 1990

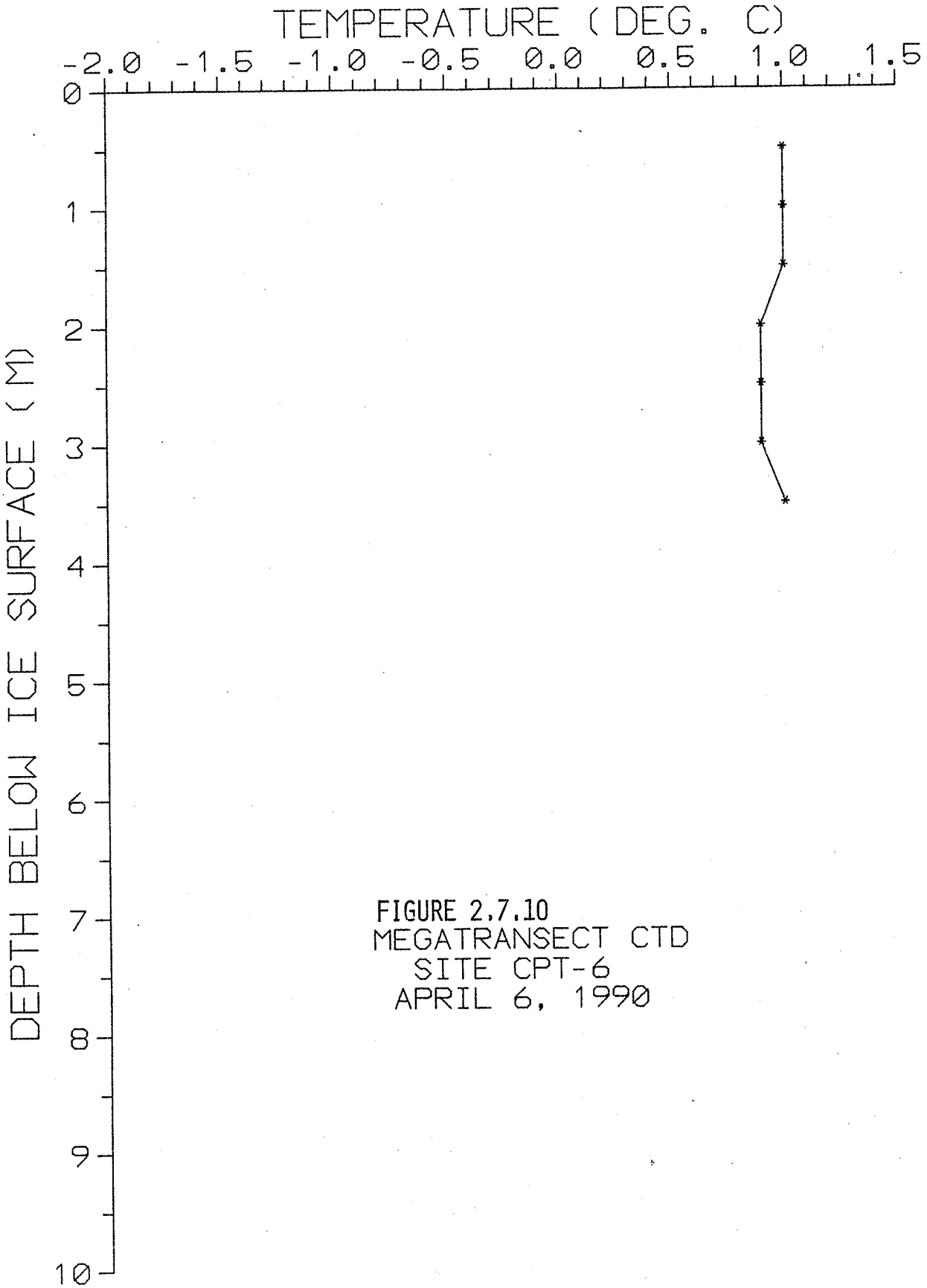

FIGURE 2.7.10
MEGATRANSECT CTD
SITE CPT-6
APRIL 6, 1990

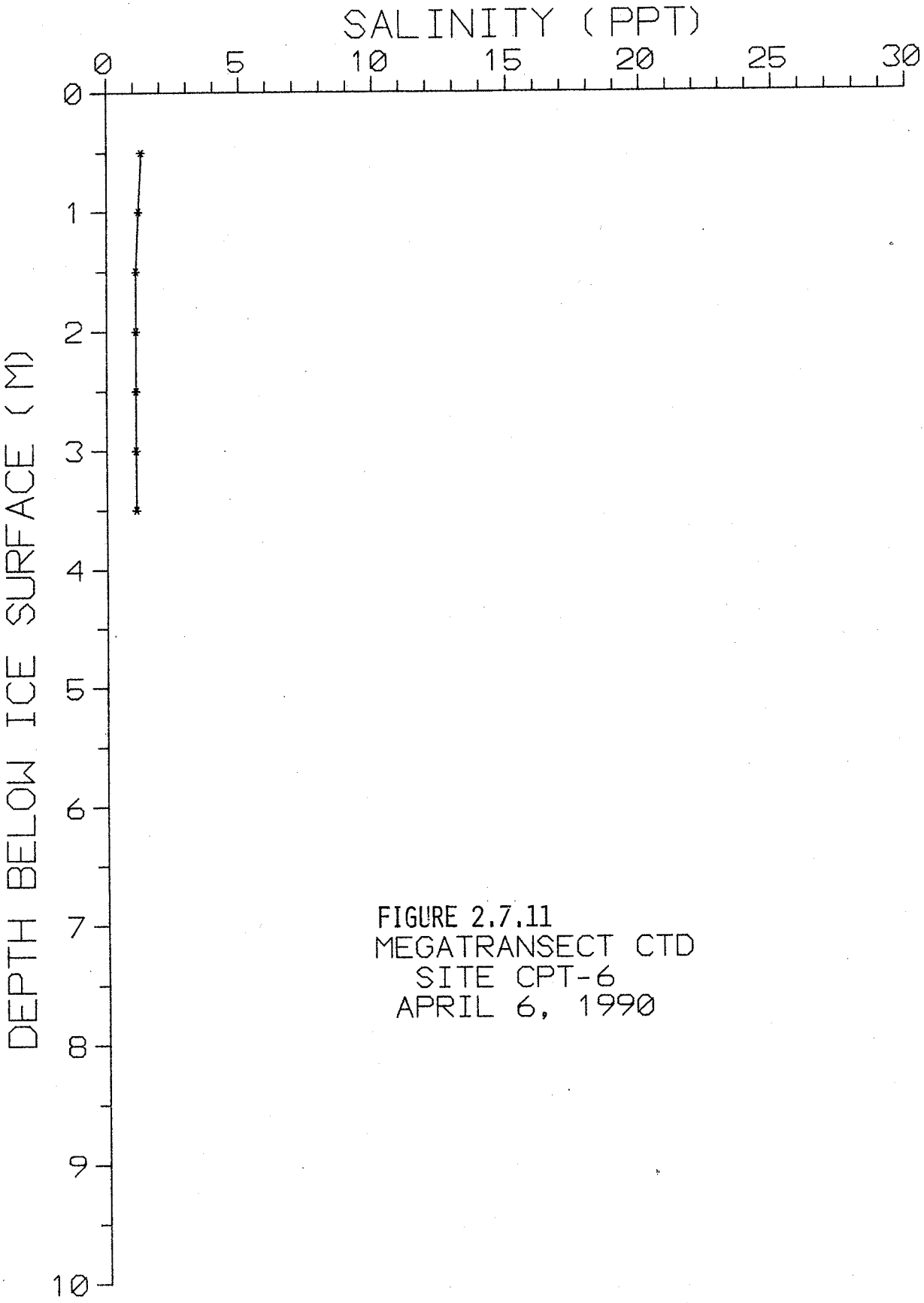

FIGURE 2.7.11
MEGATRANSECT CTD
SITE CPT-6
APRIL 6, 1990

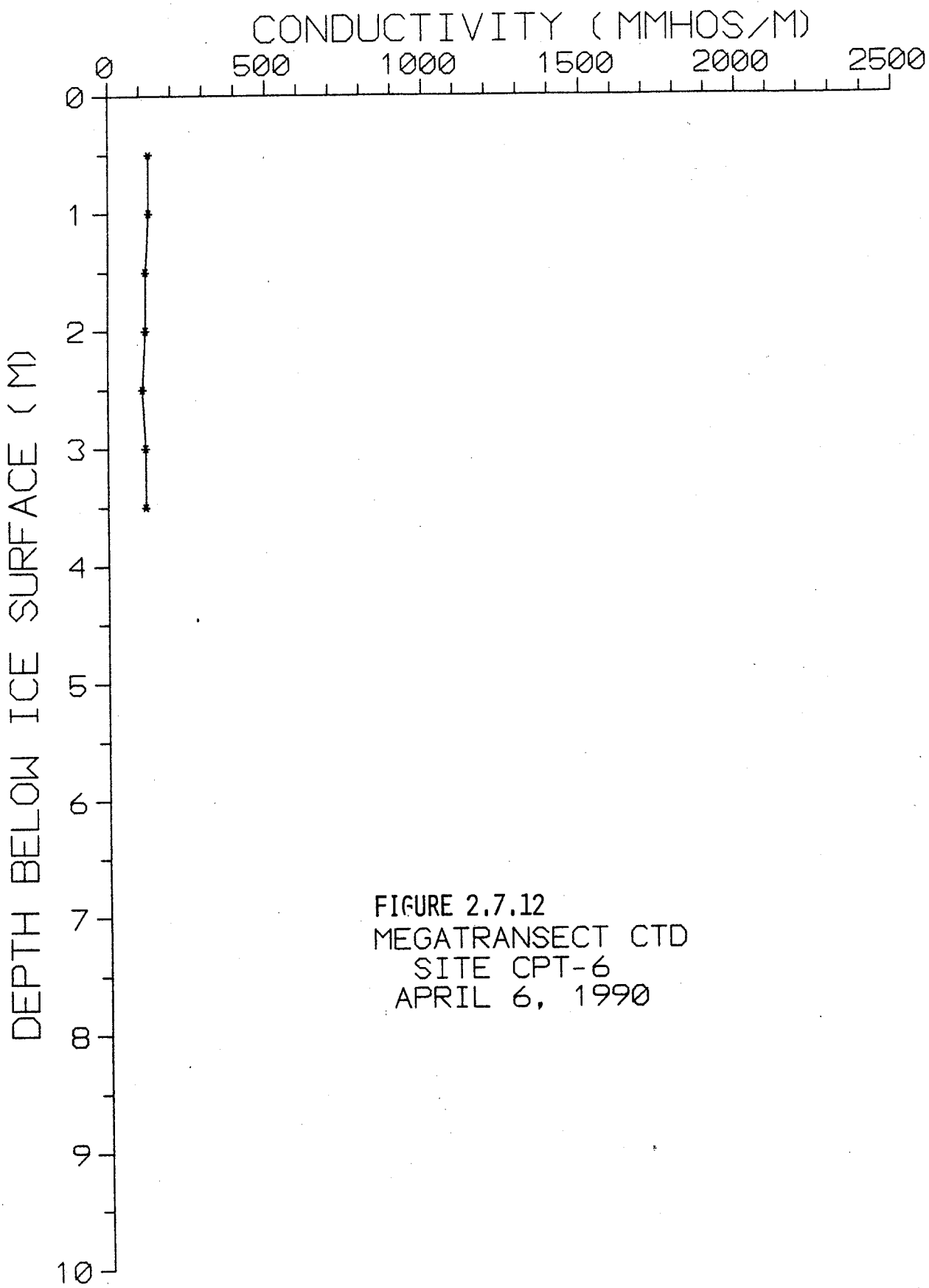

FIGURE 2.7.12
MEGATRANSECT CTD
SITE CPT-6
APRIL 6, 1990

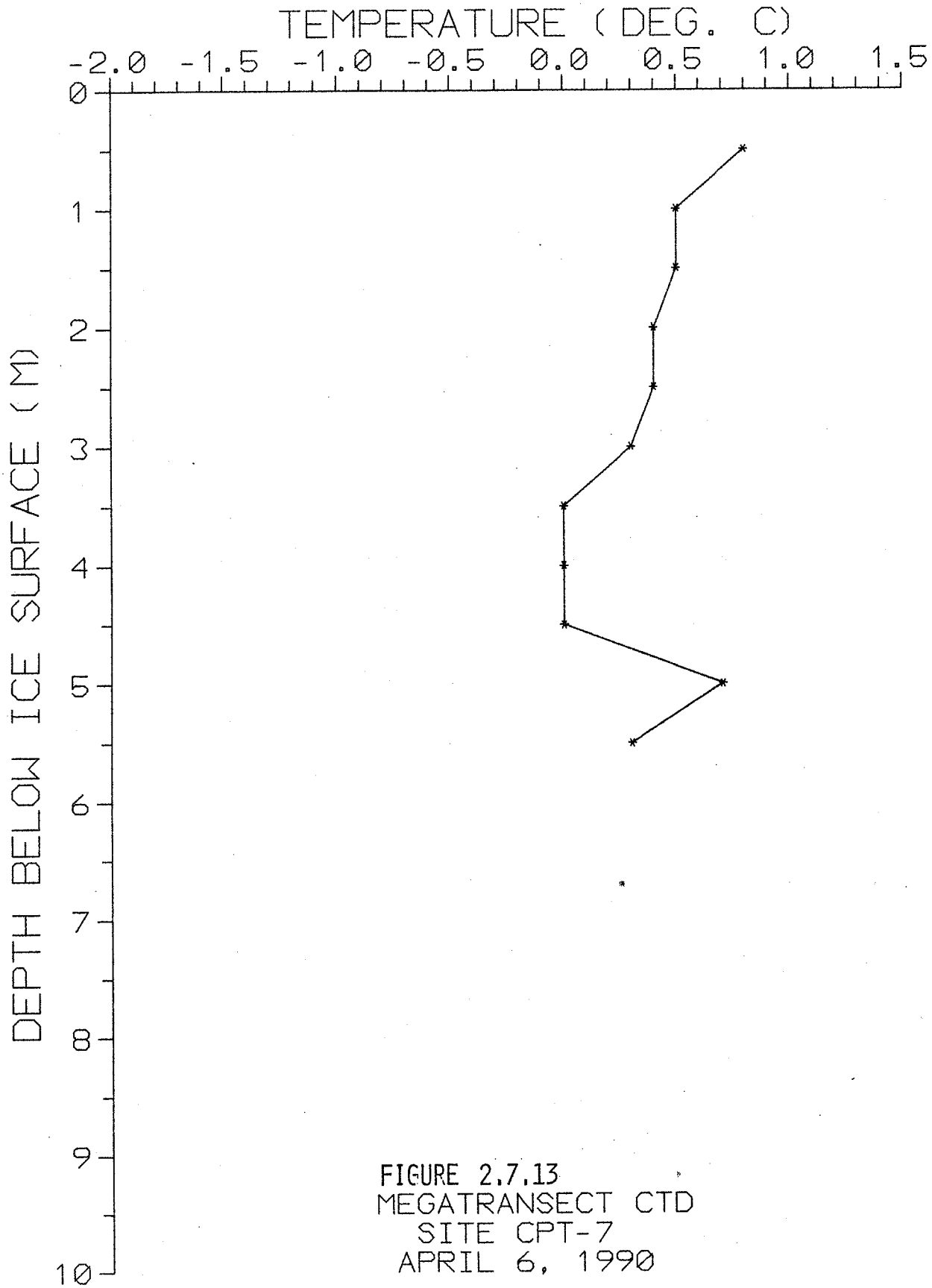

FIGURE 2.7.13
MEGATRANSECT CTD
SITE CPT-7
APRIL 6, 1990

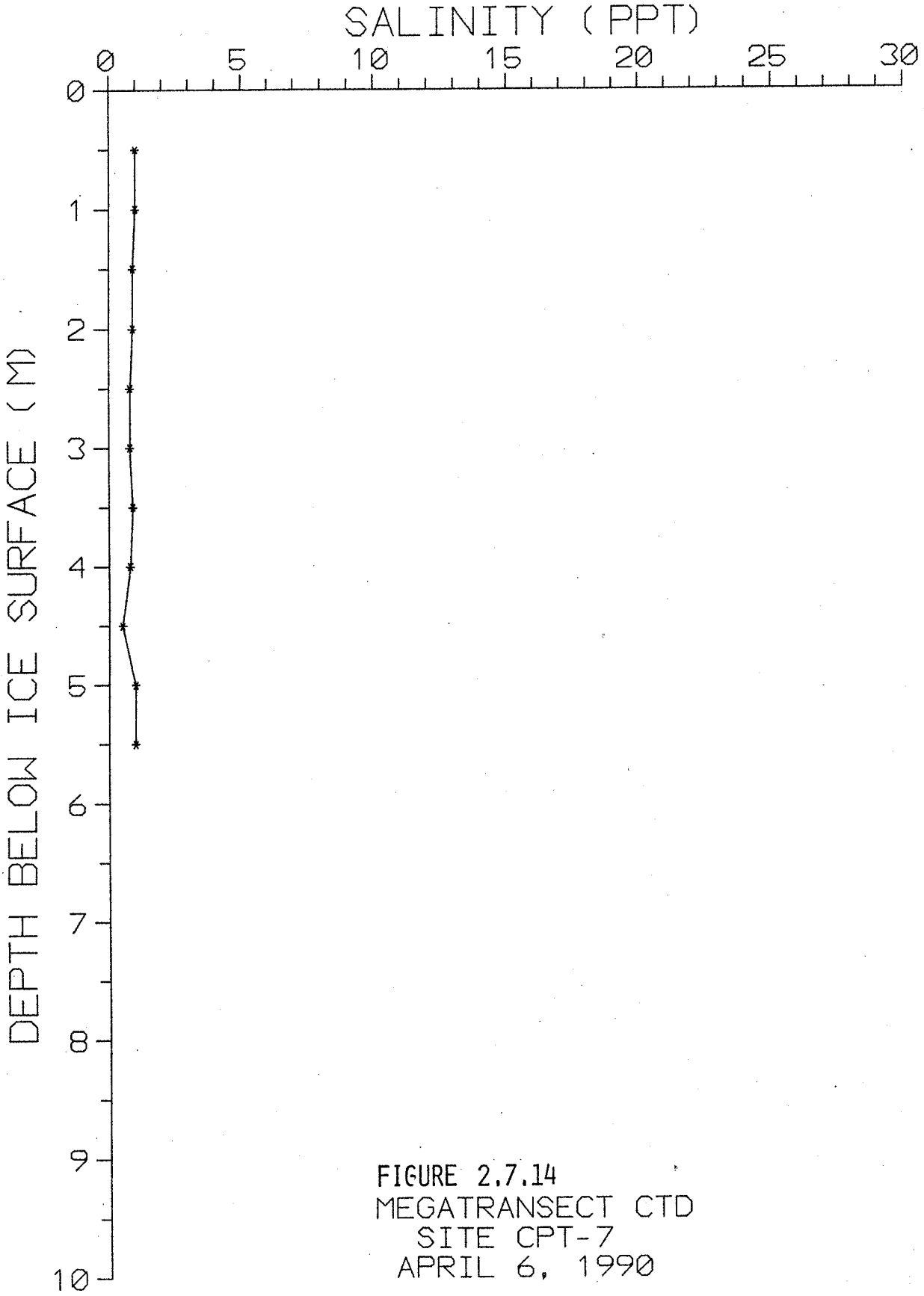

FIGURE 2.7.14
MEGATRANSECT CTD
SITE CPT-7
APRIL 6, 1990

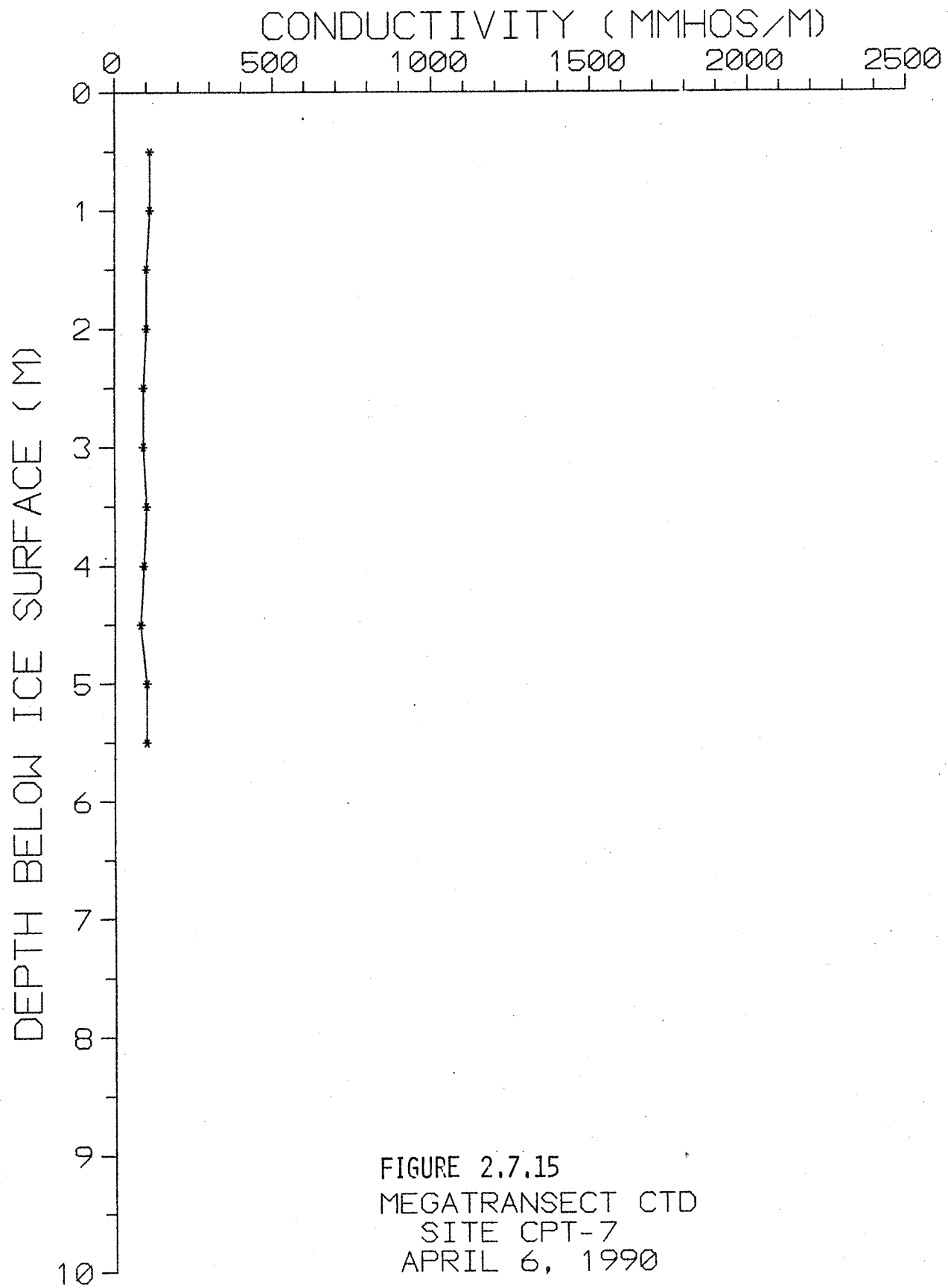

FIGURE 2.7.15
MEGATRANSECT CTD
SITE CPT-7
APRIL 6, 1990

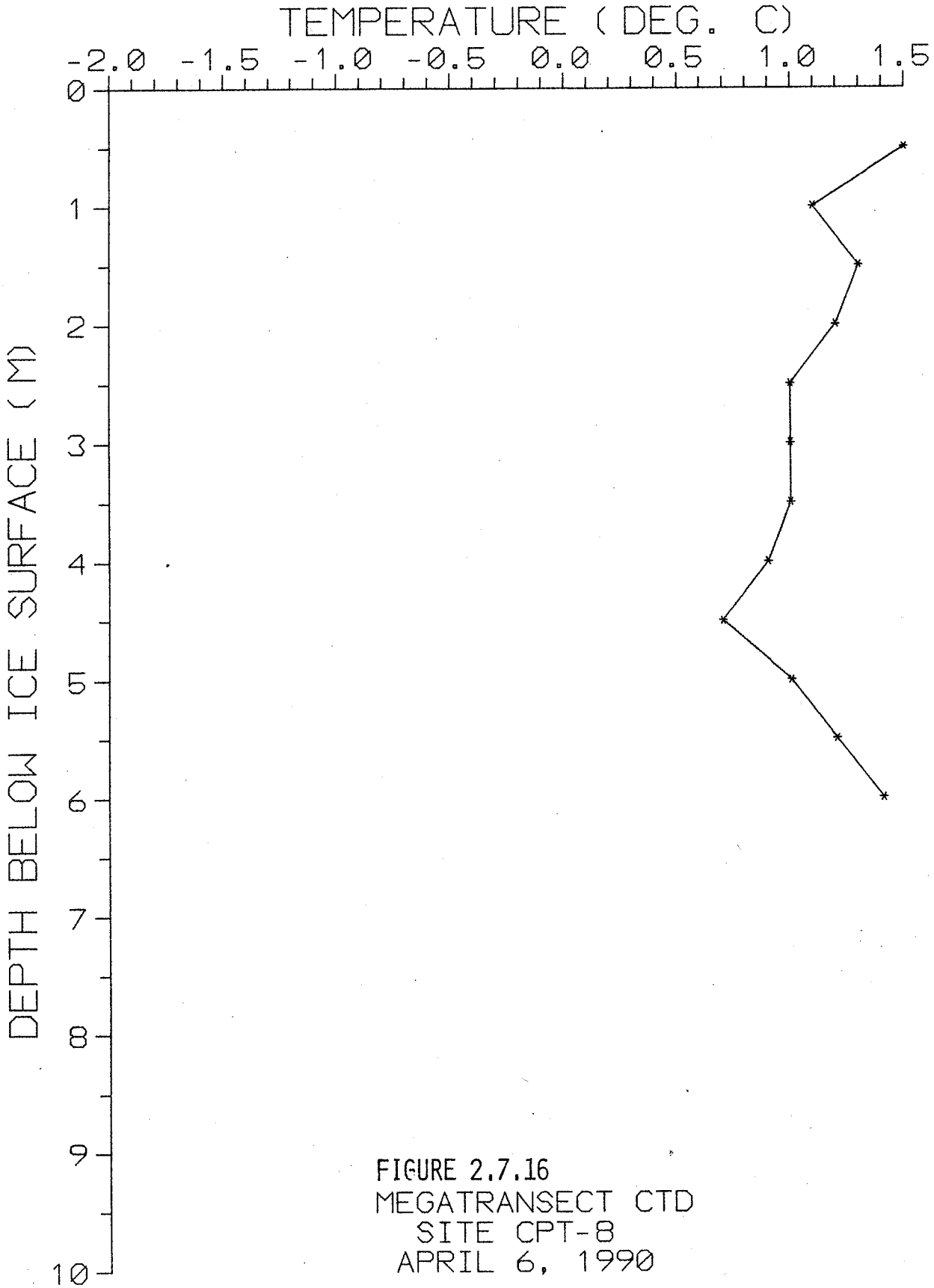

FIGURE 2.7.16
MEGATRANSECT CTD
SITE CPT-8
APRIL 6, 1990

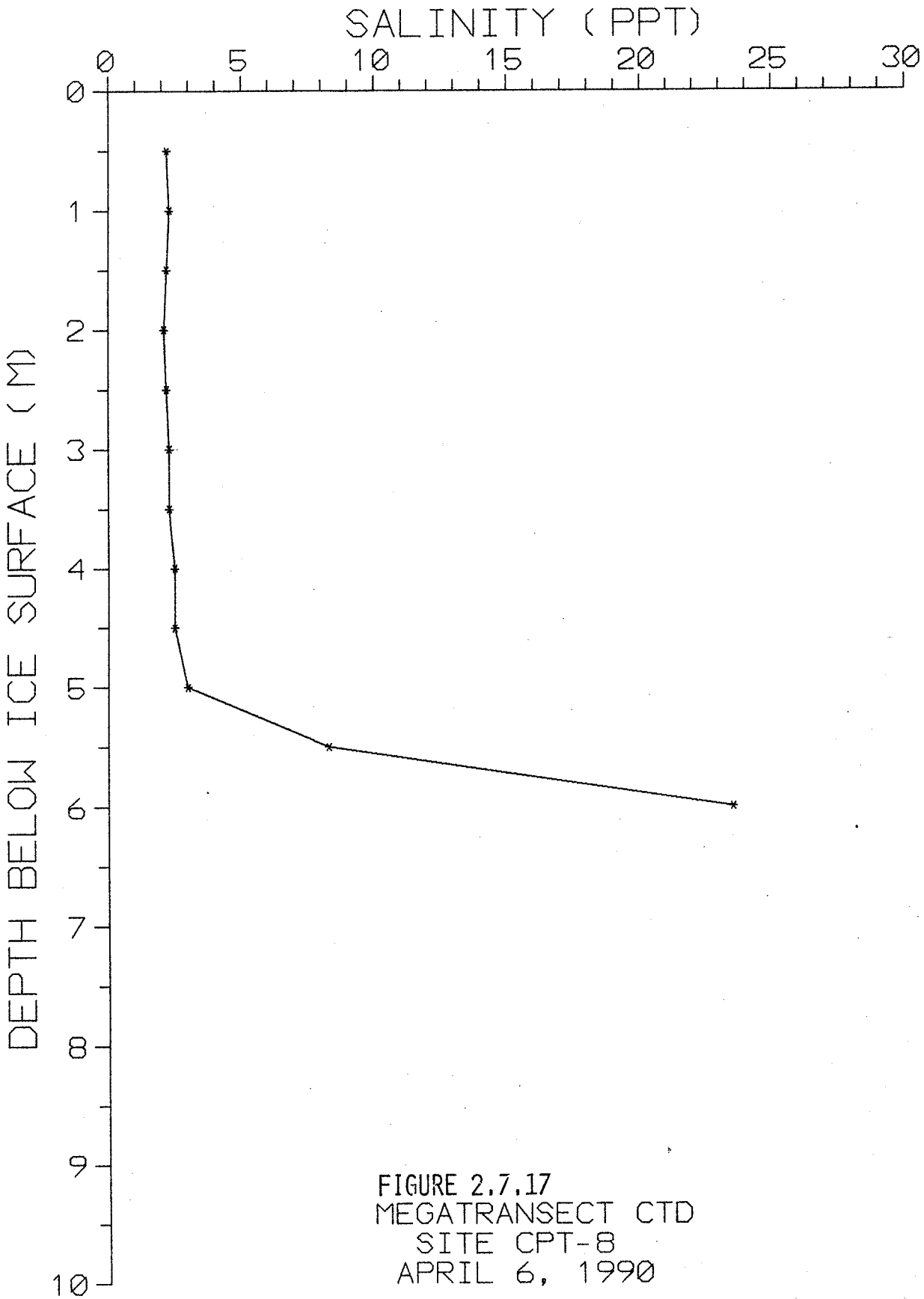

FIGURE 2.7.17
MEGATRANSECT CTD
SITE CPT-8
APRIL 6, 1990

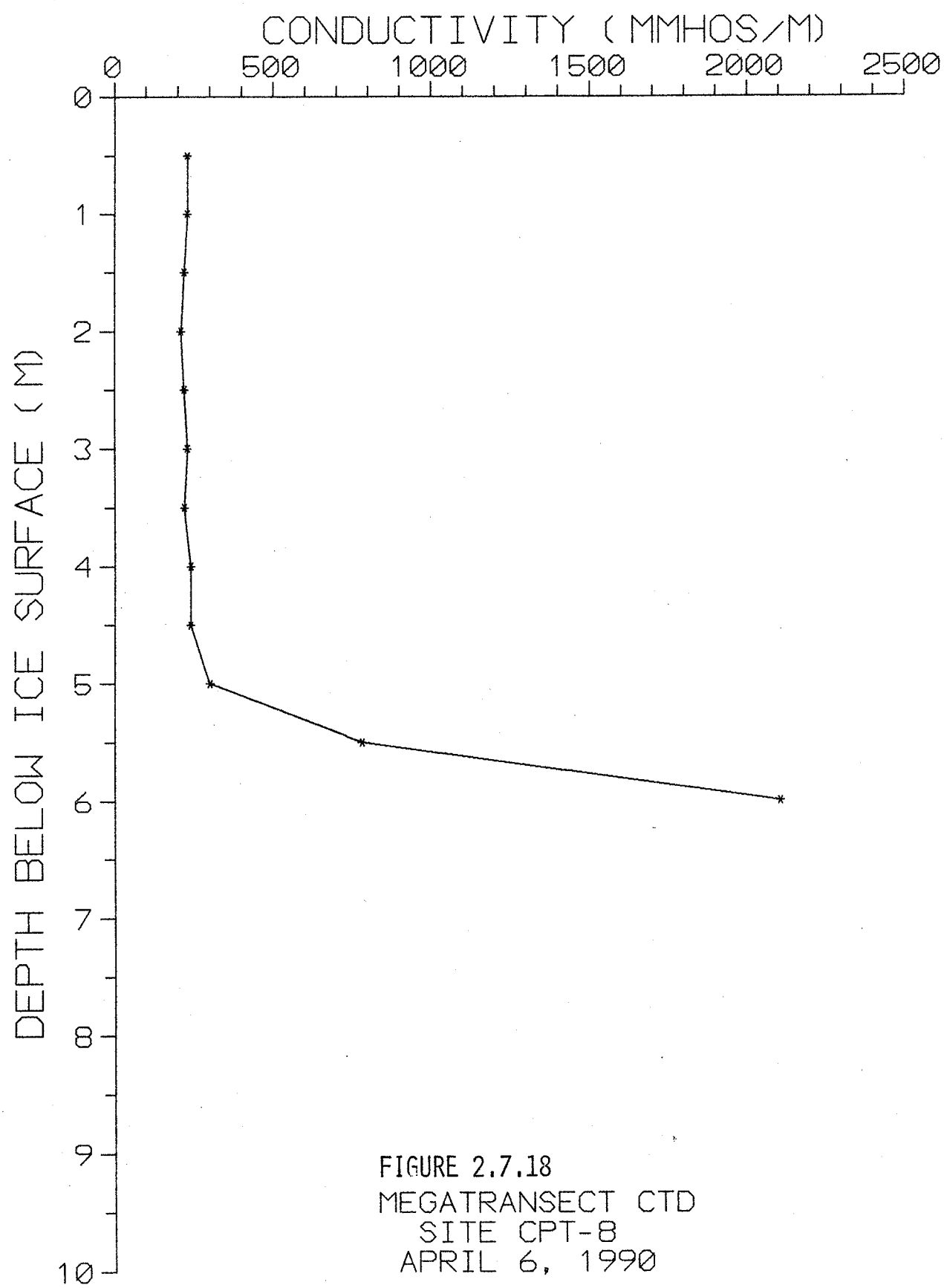

FIGURE 2.7.18
MEGATRANSECT CTD
SITE CPT-8
APRIL 6, 1990

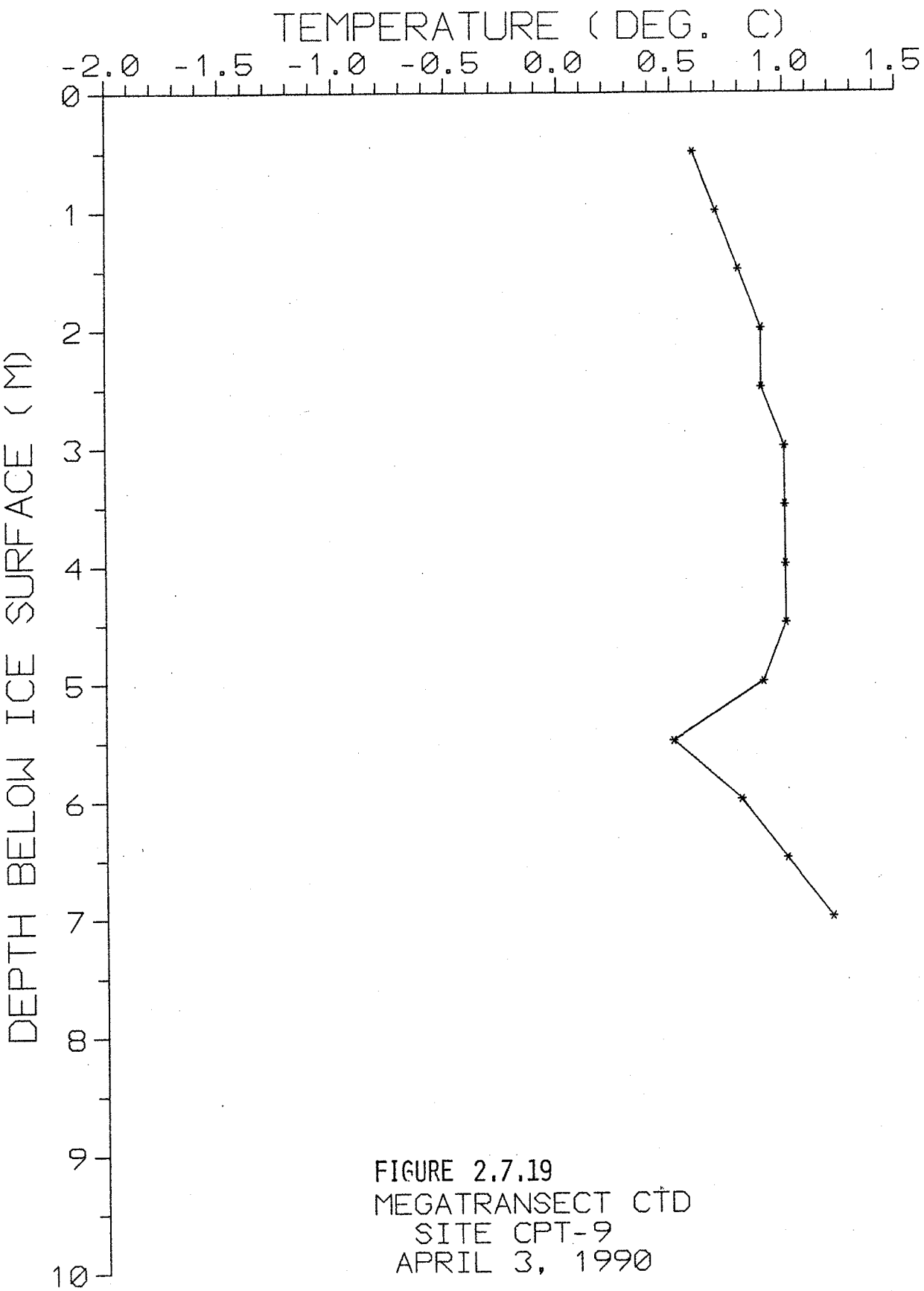

FIGURE 2.7.19
MEGATRANSECT CTD
SITE CPT-9
APRIL 3, 1990

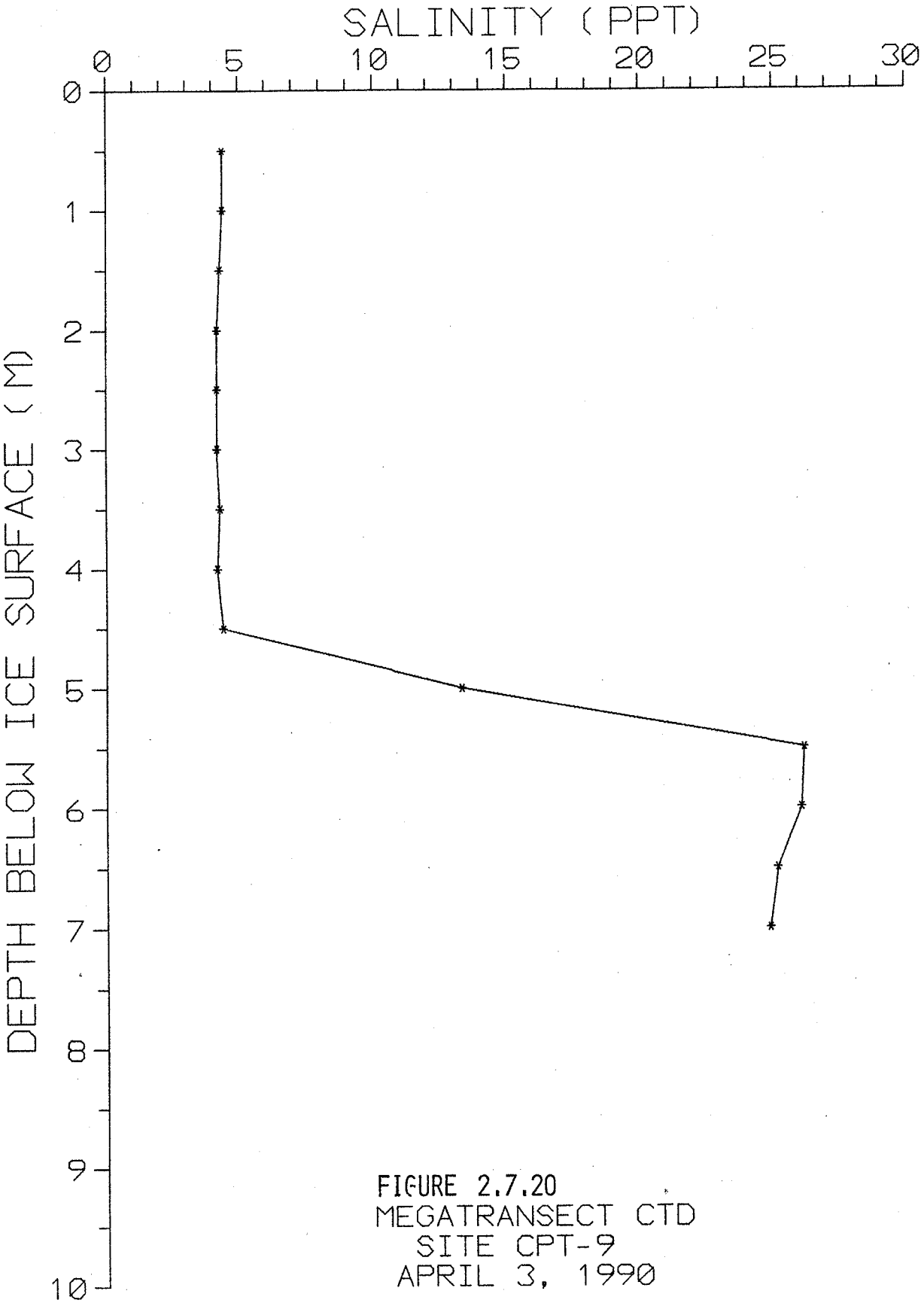

FIGURE 2.7.20
MEGATRANSECT CTD
SITE CPT-9
APRIL 3, 1990

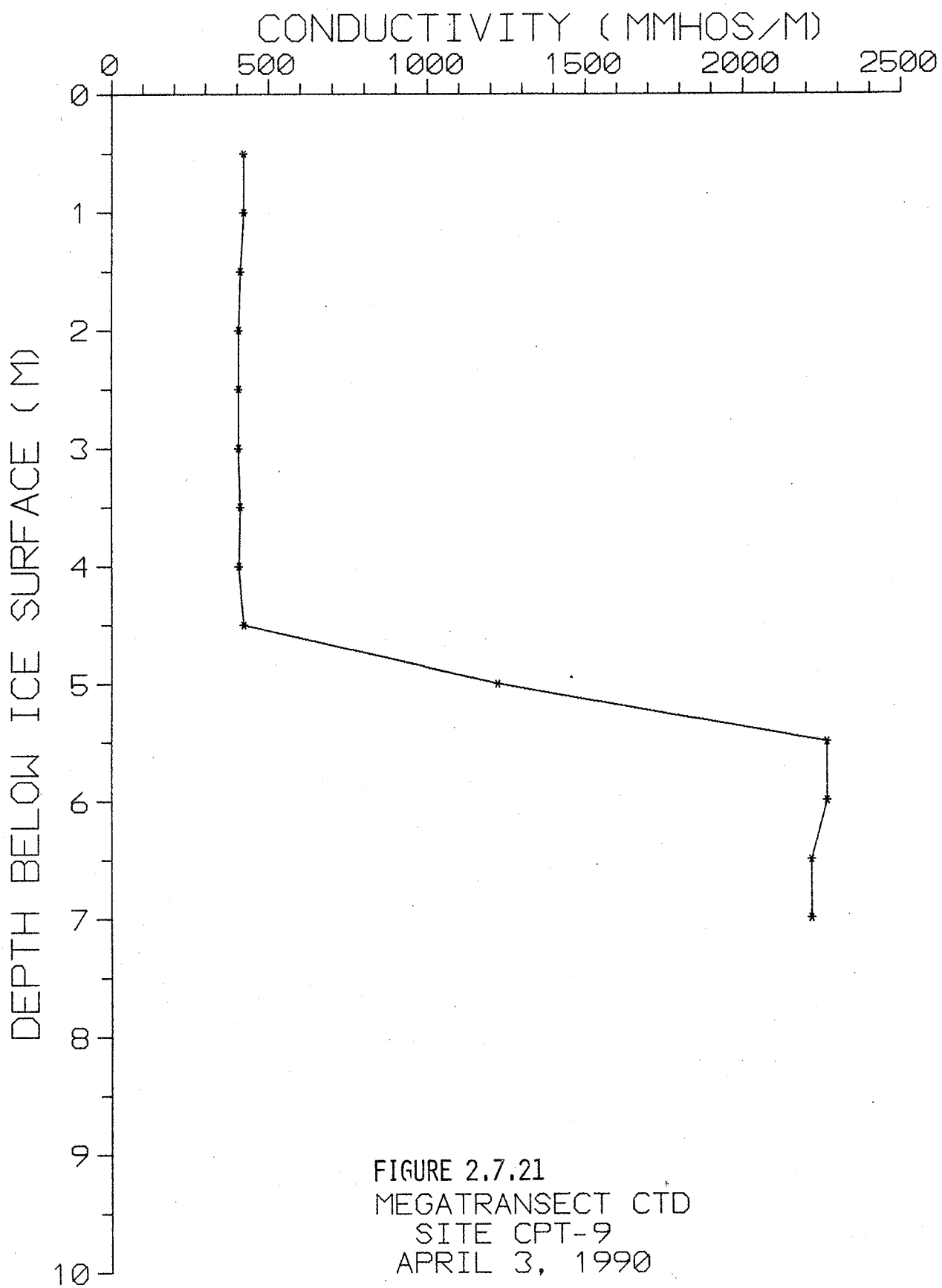

FIGURE 2.7.21
MEGATRANSECT CTD
SITE CPT-9
APRIL 3, 1990

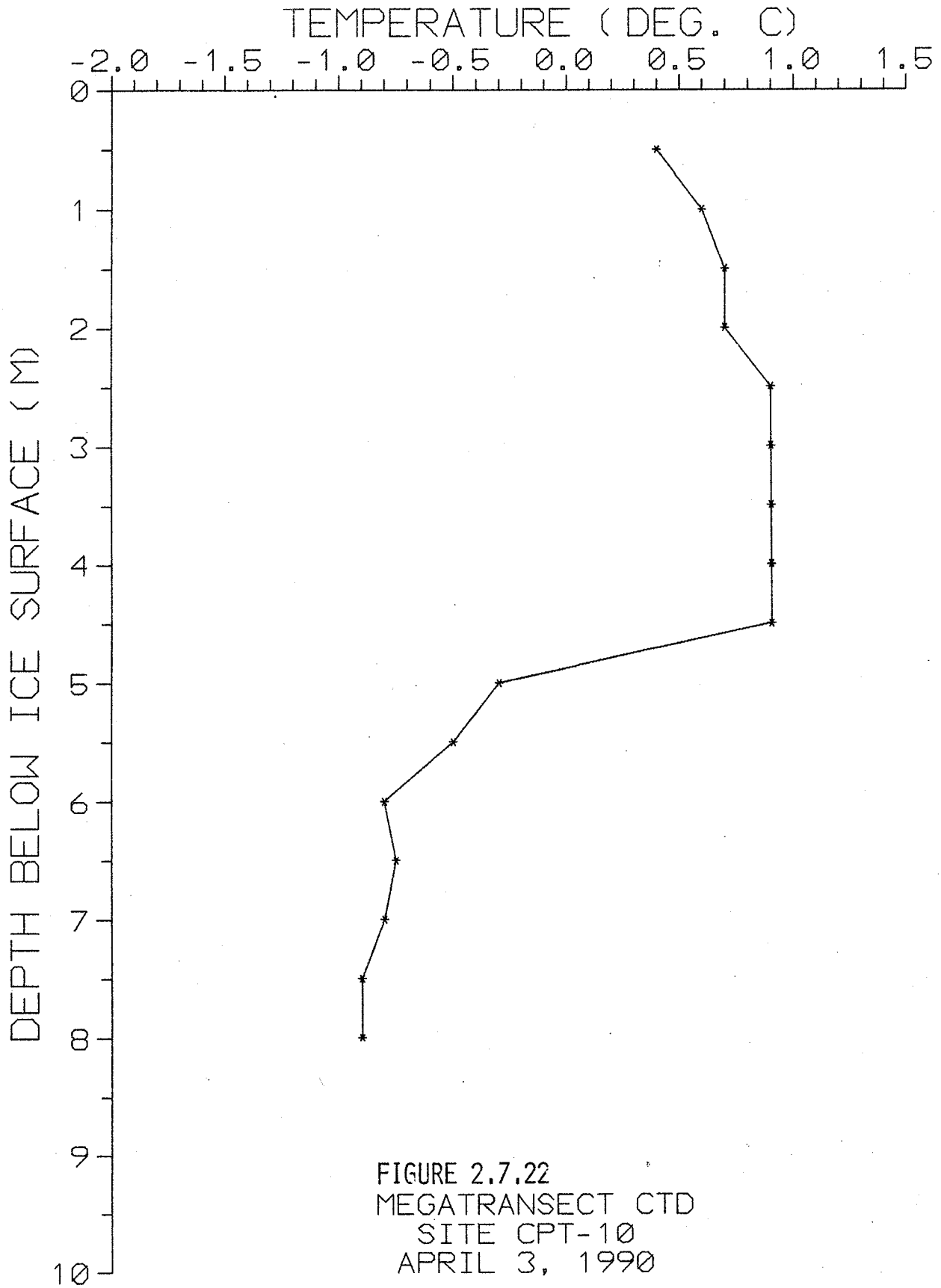

FIGURE 2.7.22
MEGATRANSECT CTD
SITE CPT-10
APRIL 3, 1990

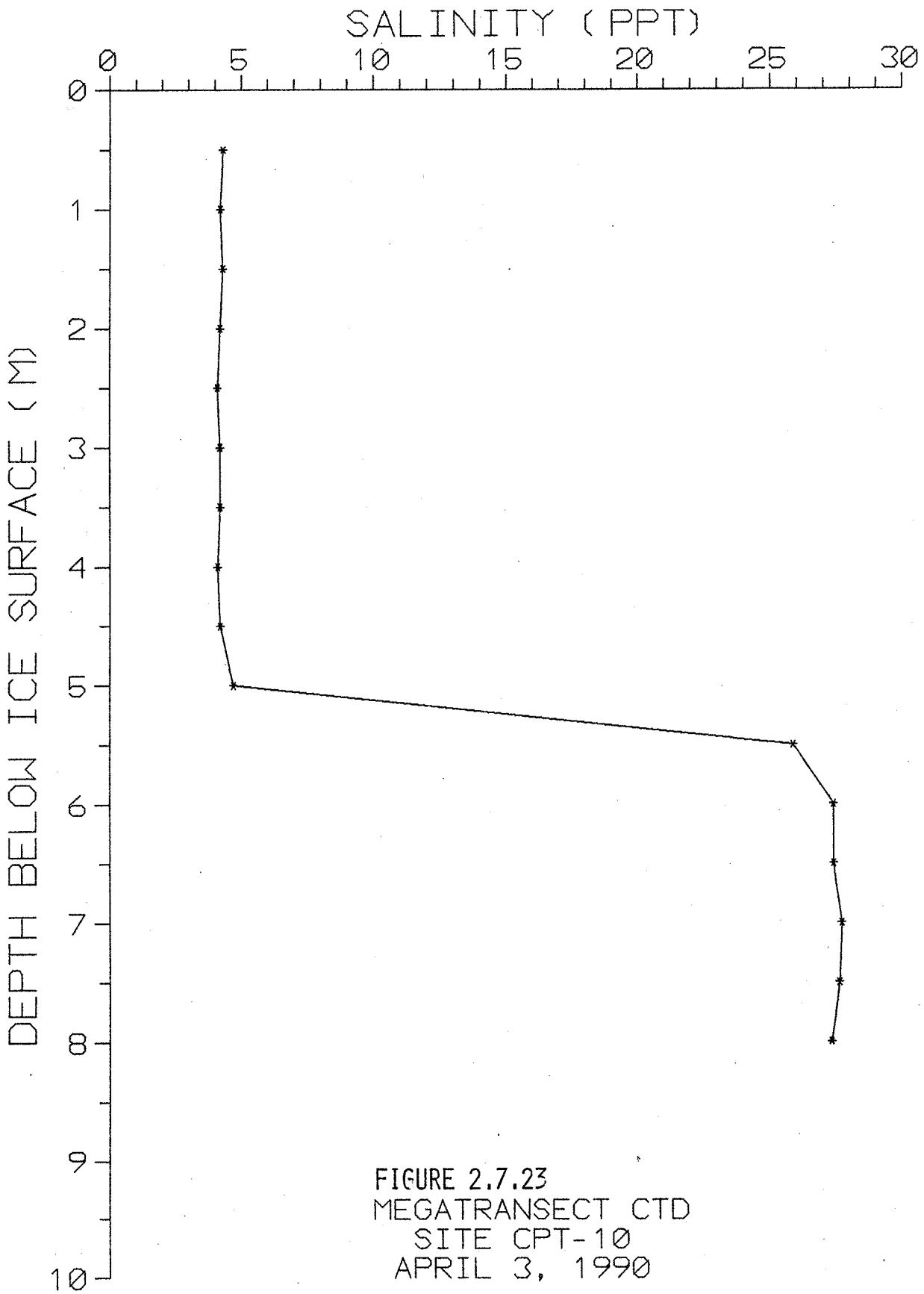

FIGURE 2.7.23
MEGATRANSECT CTD
SITE CPT-10
APRIL 3, 1990

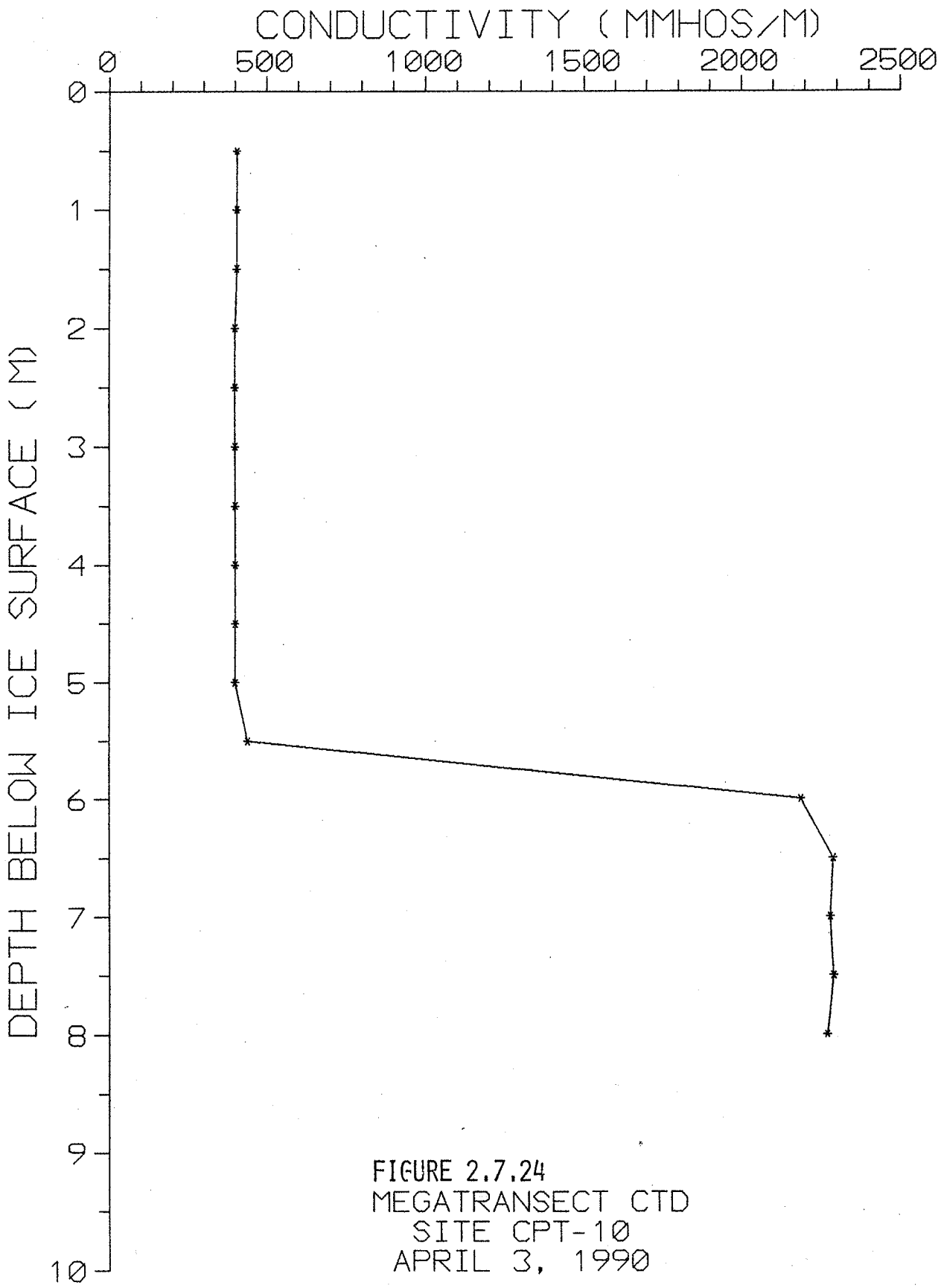

FIGURE 2.7.24
MEGATRANSECT CTD
SITE CPT-10
APRIL 3, 1990

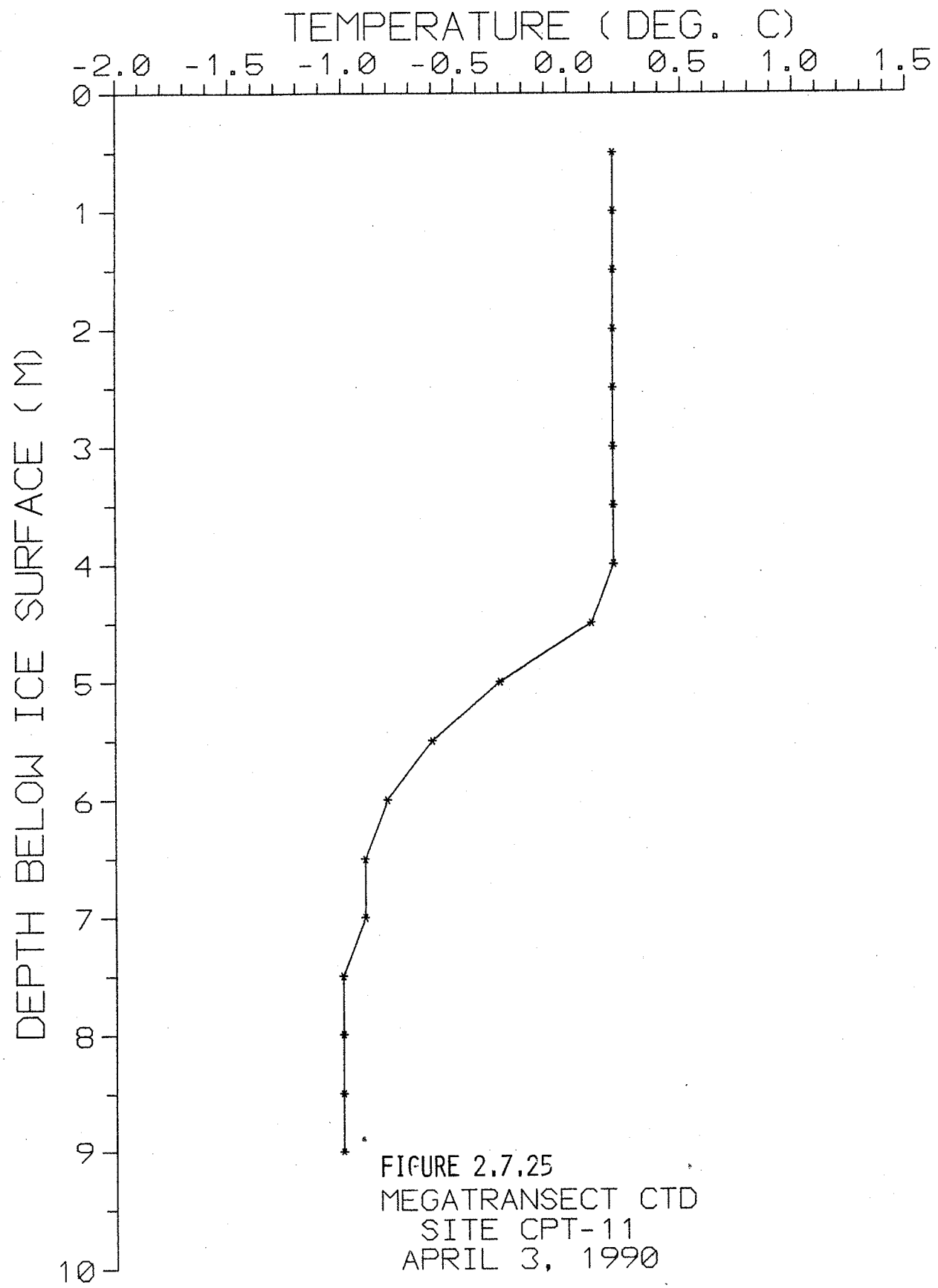

FIGURE 2.7.25
MEGATRANSECT CTD
SITE CPT-11
APRIL 3, 1990

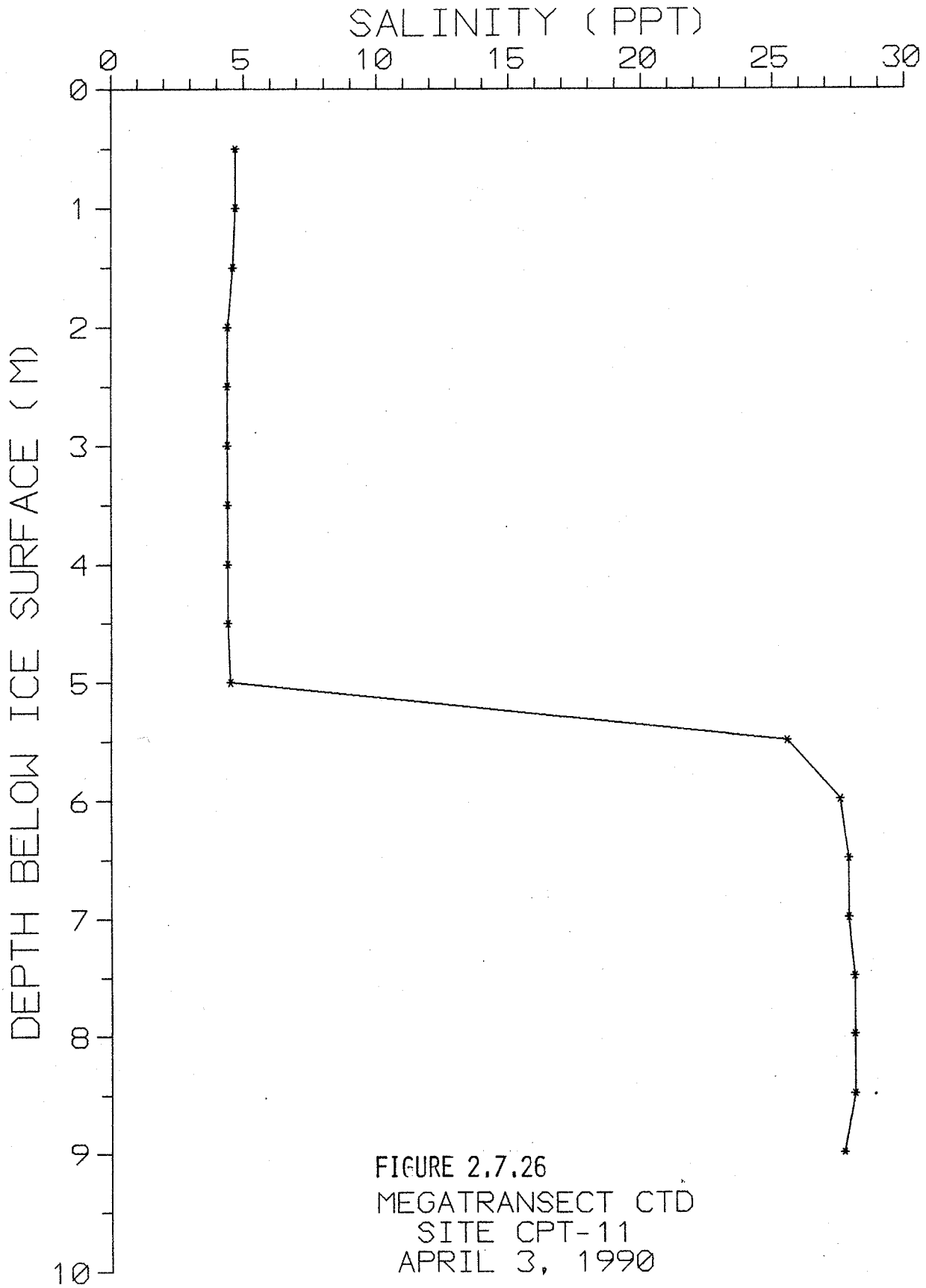

FIGURE 2.7.26
MEGATRANSECT CTD
SITE CPT-11
APRIL 3, 1990

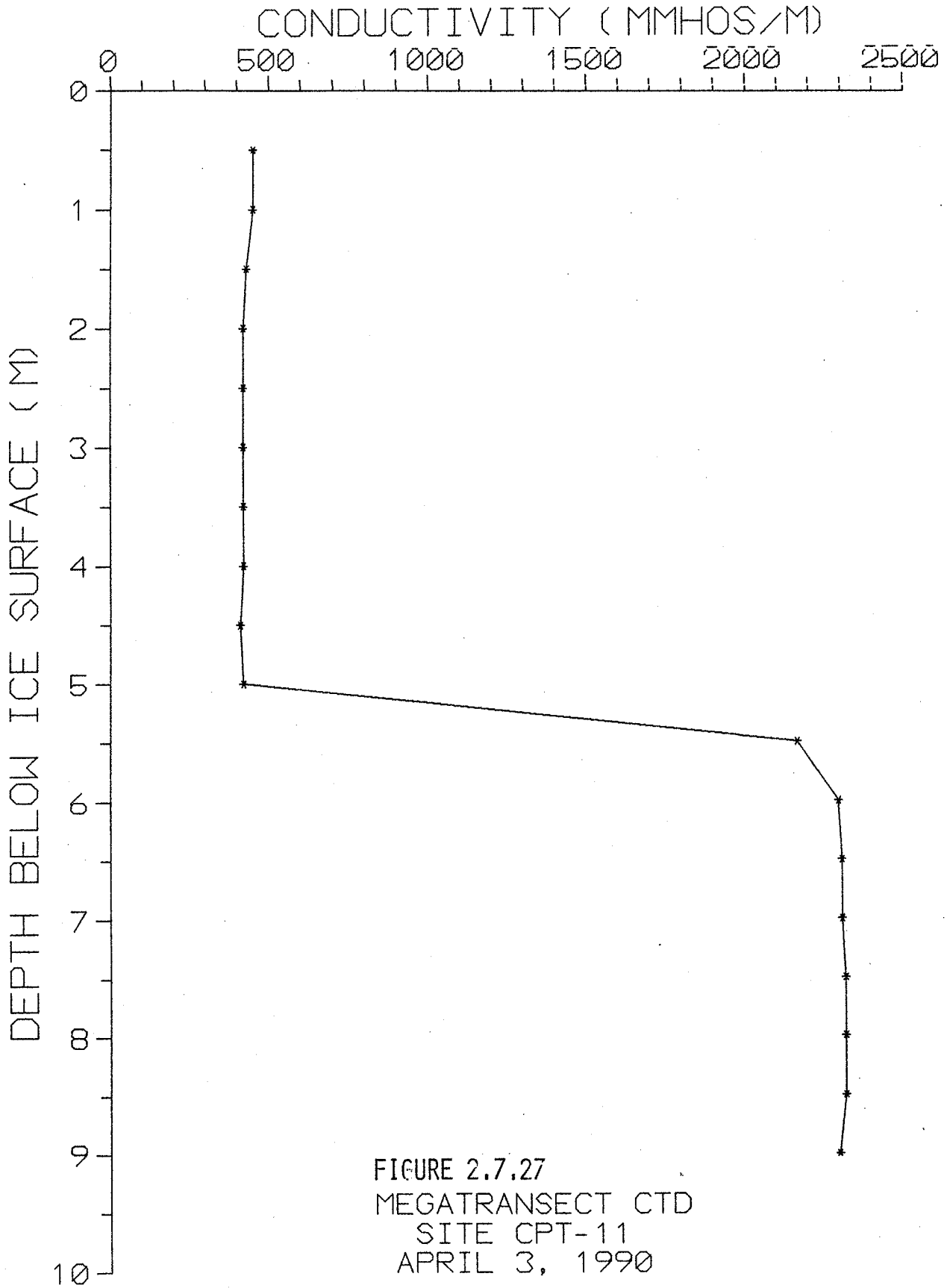

FIGURE 2.7.27
MEGATRANSECT CTD
SITE CPT-11
APRIL 3, 1990

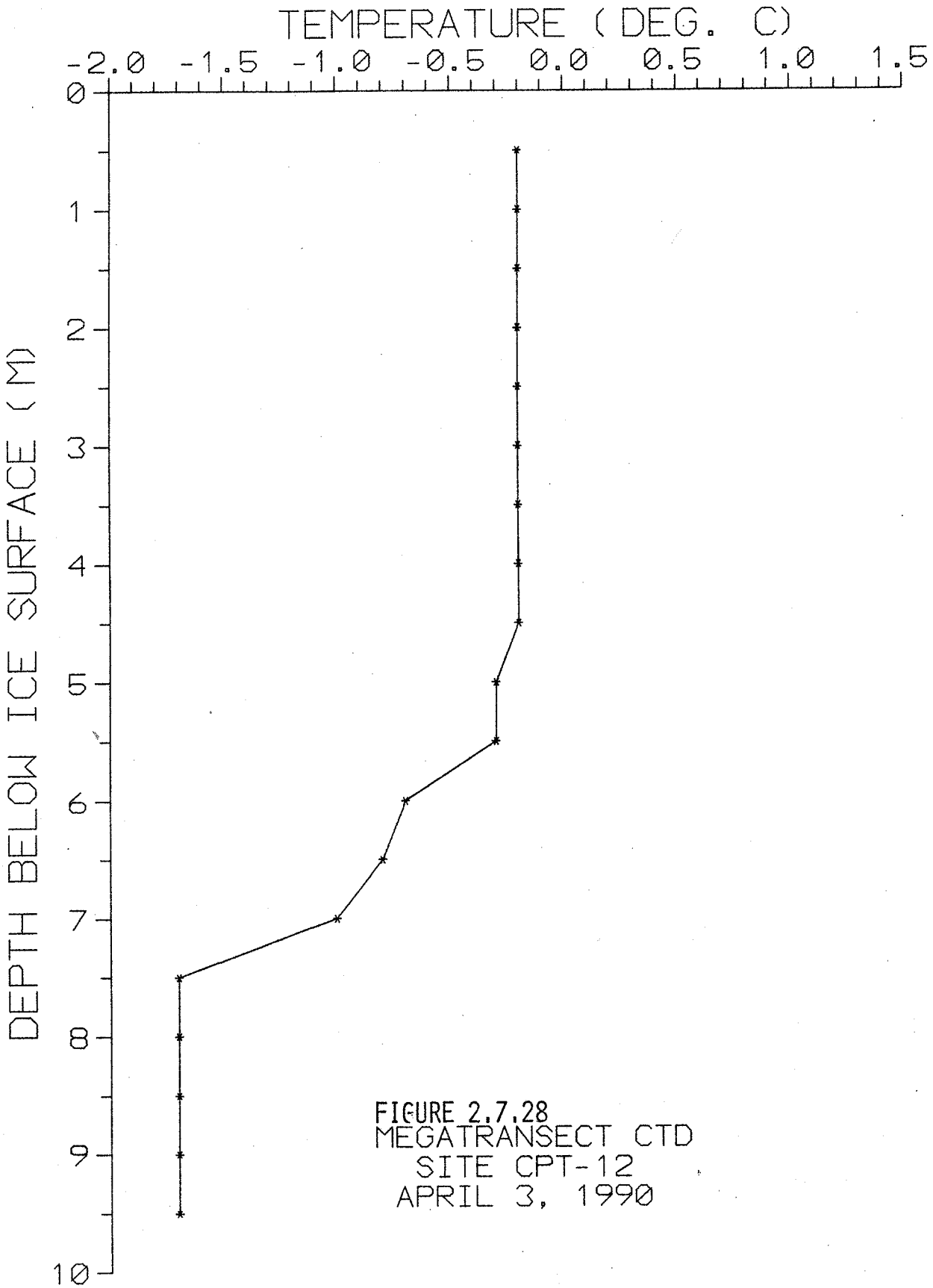

FIGURE 2.7.28
MEGATRANSECT CTD
SITE CPT-12
APRIL 3, 1990

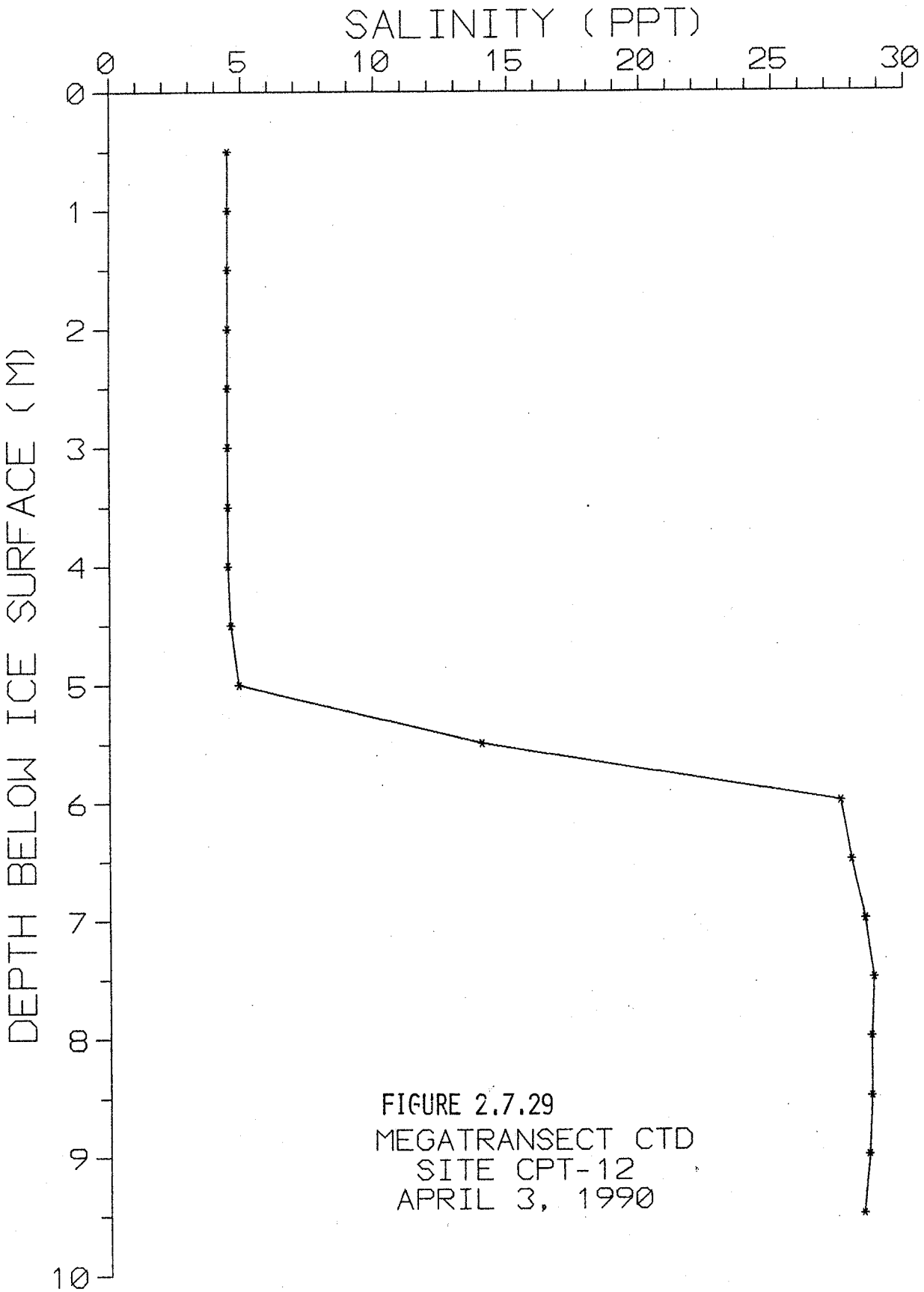

FIGURE 2.7.29
MEGATRANSECT CTD
SITE CPT-12
APRIL 3, 1990

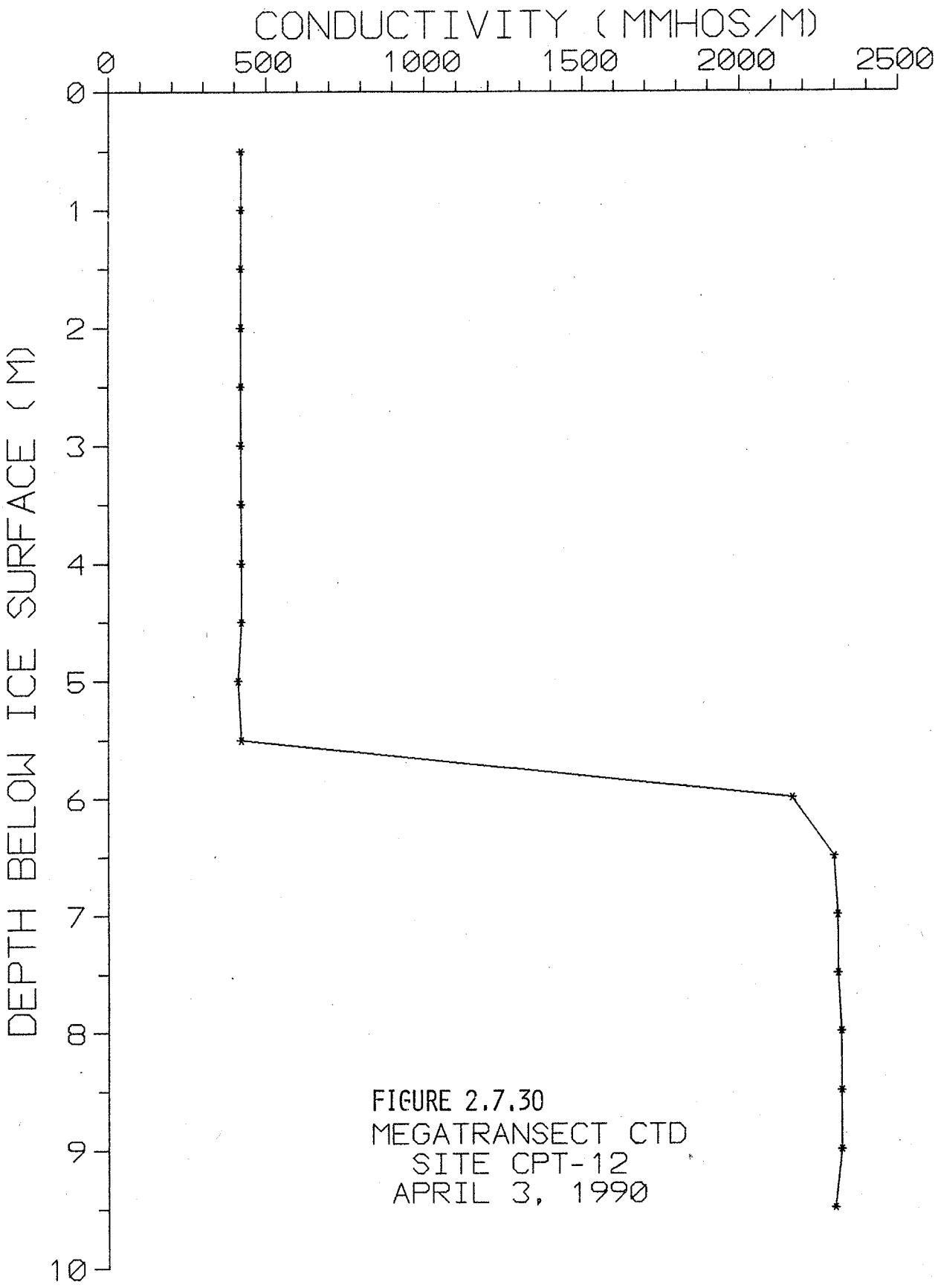

FIGURE 2.7.30
MEGATRANSECT CTD
SITE CPT-12
APRIL 3, 1990

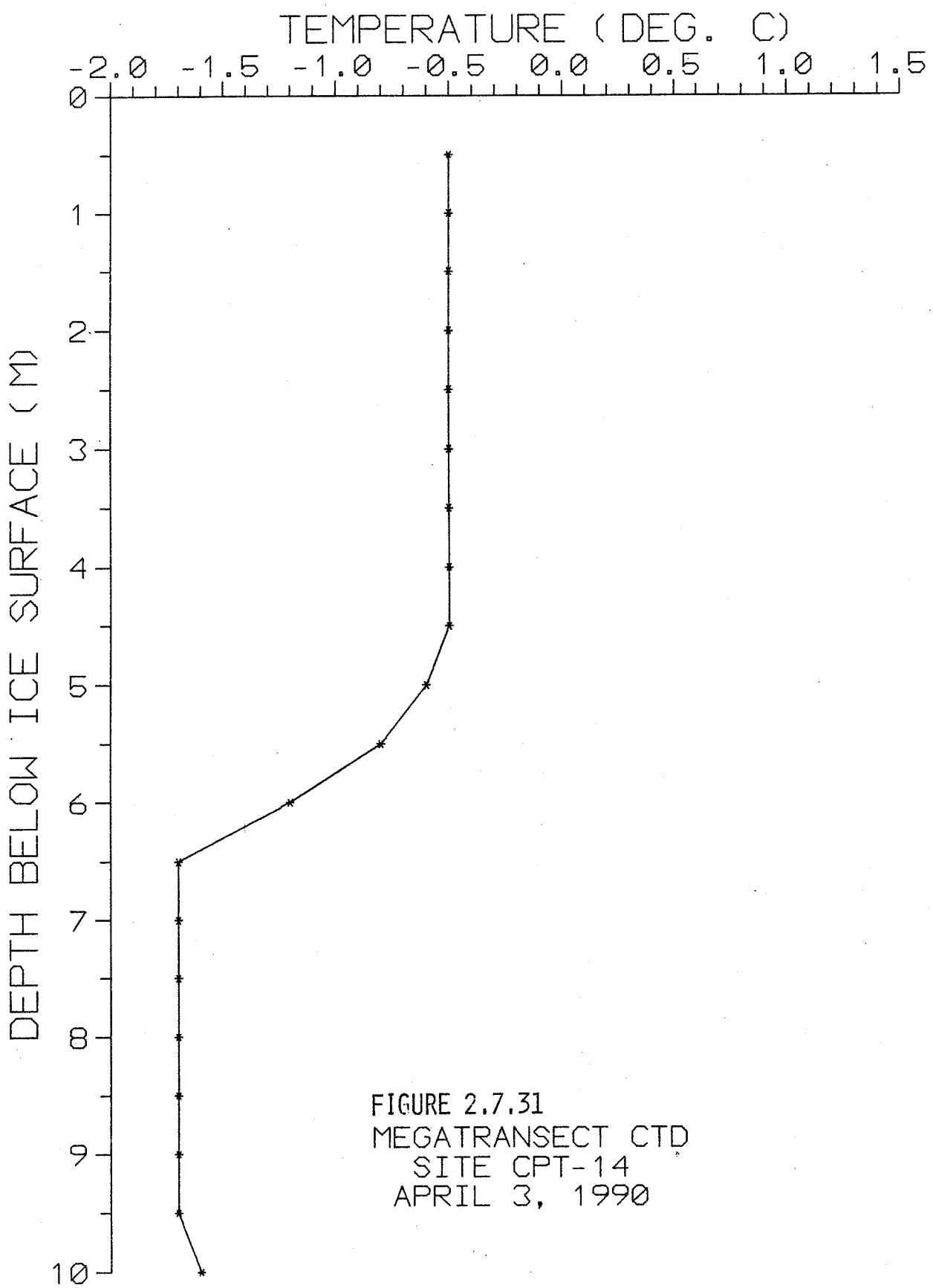

FIGURE 2.7.31
MEGATRANSECT CTD
SITE CPT-14
APRIL 3, 1990

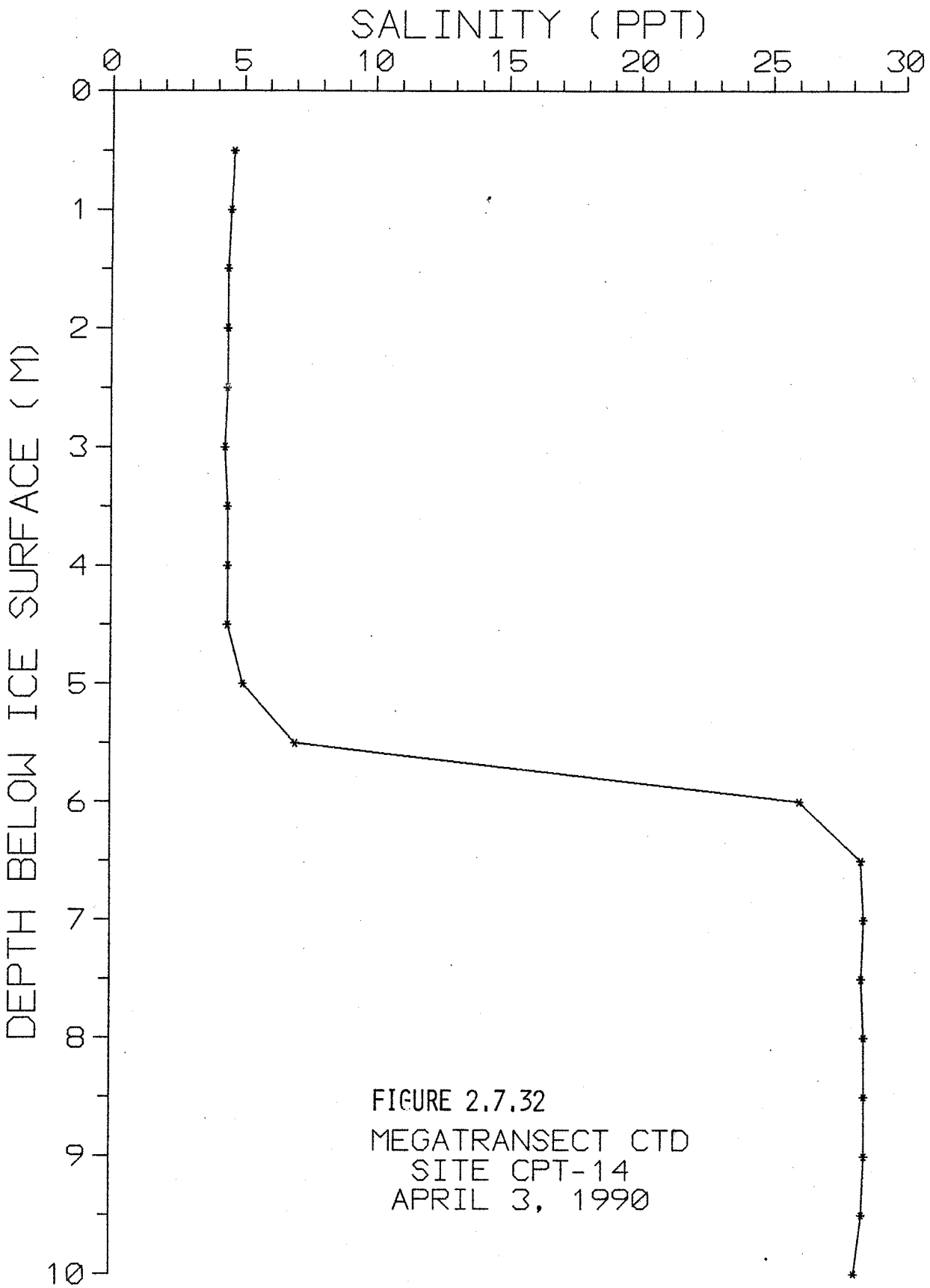

FIGURE 2.7.32
MEGATRANSECT CTD
SITE CPT-14
APRIL 3, 1990

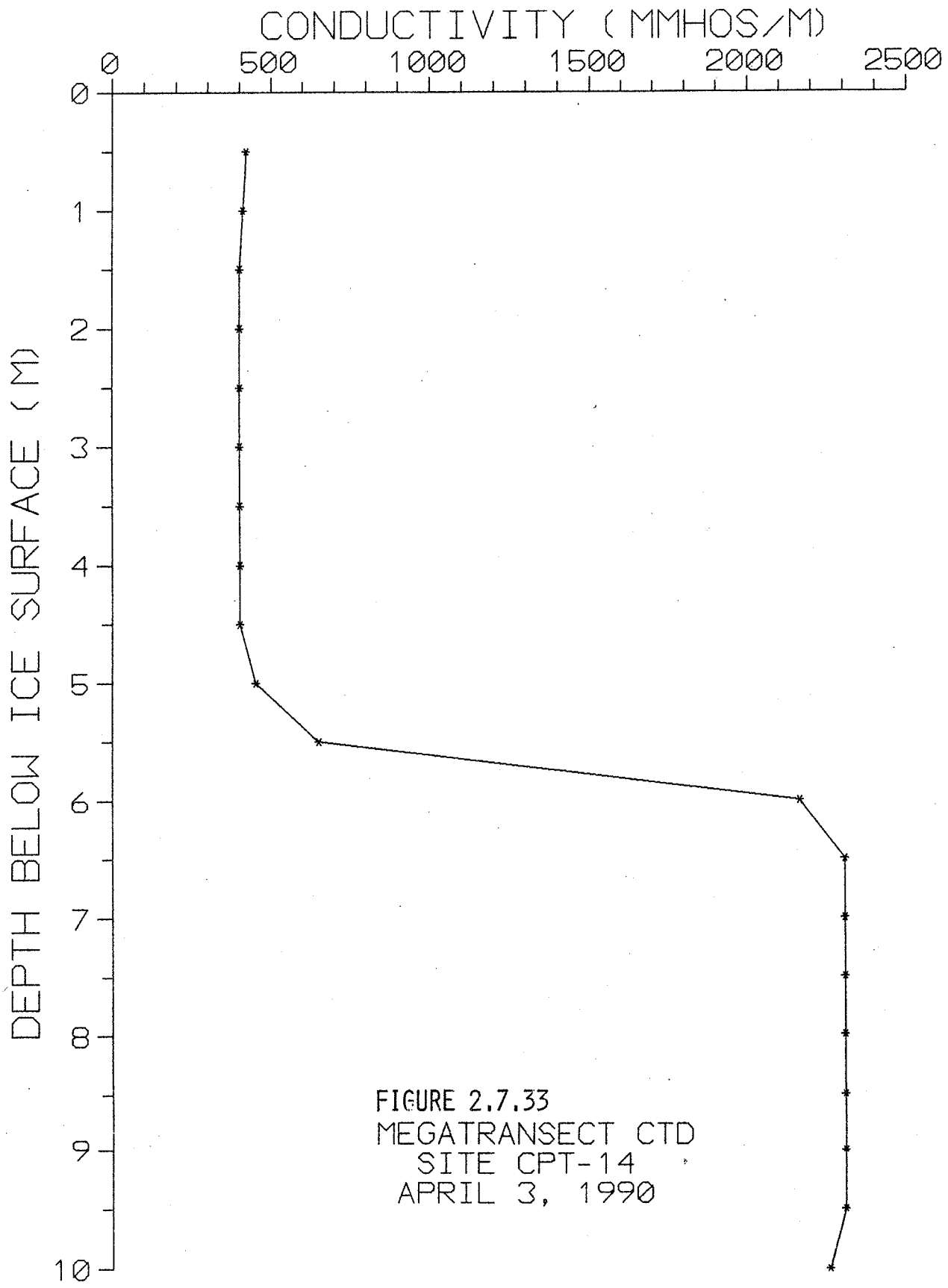

FIGURE 2.7.33
MEGATRANSECT CTD
SITE CPT-14
APRIL 3, 1990

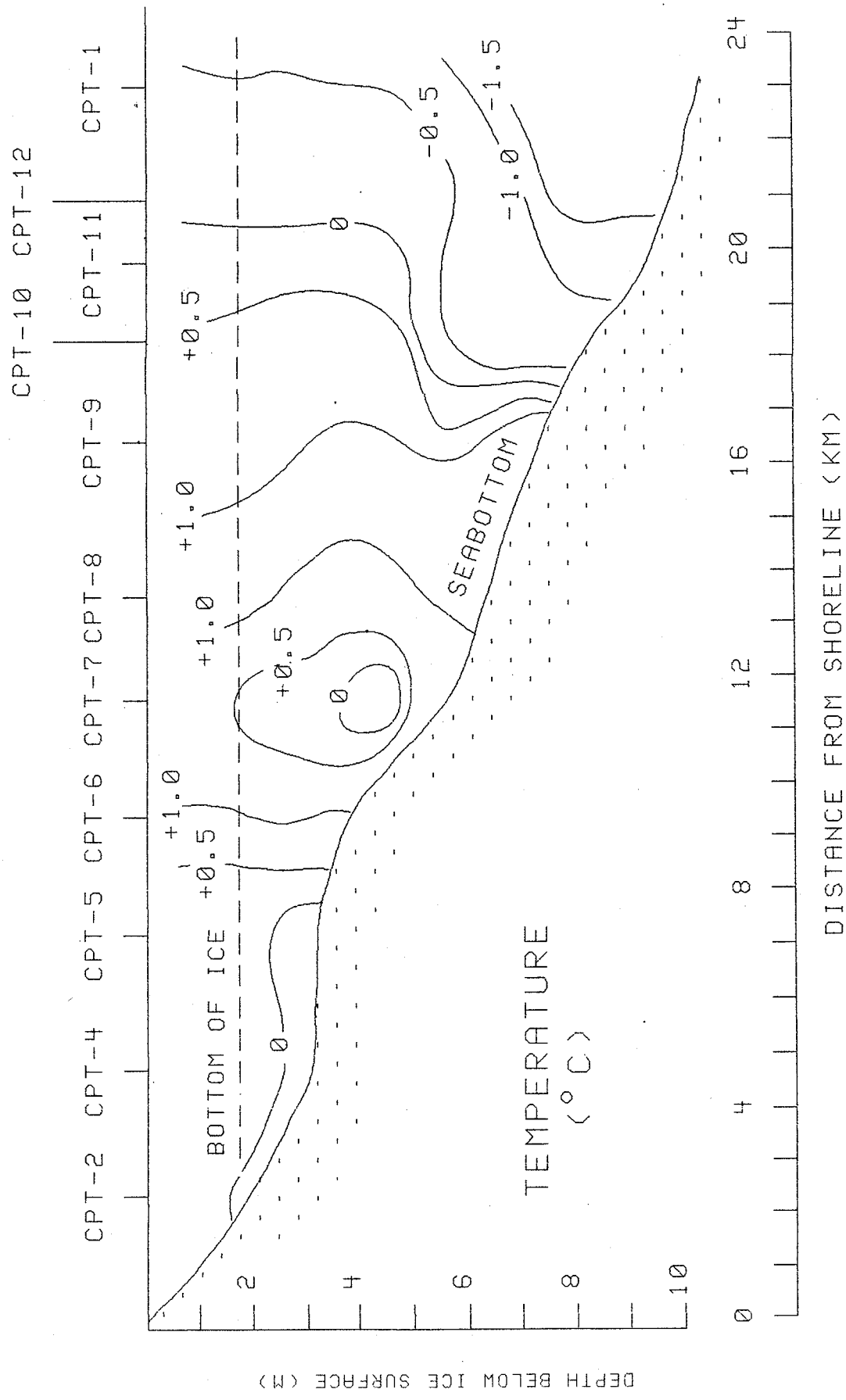
CPT-10 CPT-12
CPT-1
CPT-2 CPT-4 CPT-5 CPT-6 CPT-7 CPT-8 CPT-9 CPT-11
BOTTOM OF ICE
SEABOTTOM
TEMPERATURE
(°C)
+1.0
+0.5
0
-0.5
-1.0
-1.5
DEPTH BELOW ICE SURFACE (M)
DISTANCE FROM SHORELINE (KM)
0
4
8
12
16
20
24
2
4
6
8
10

FIGURE 2.7.34

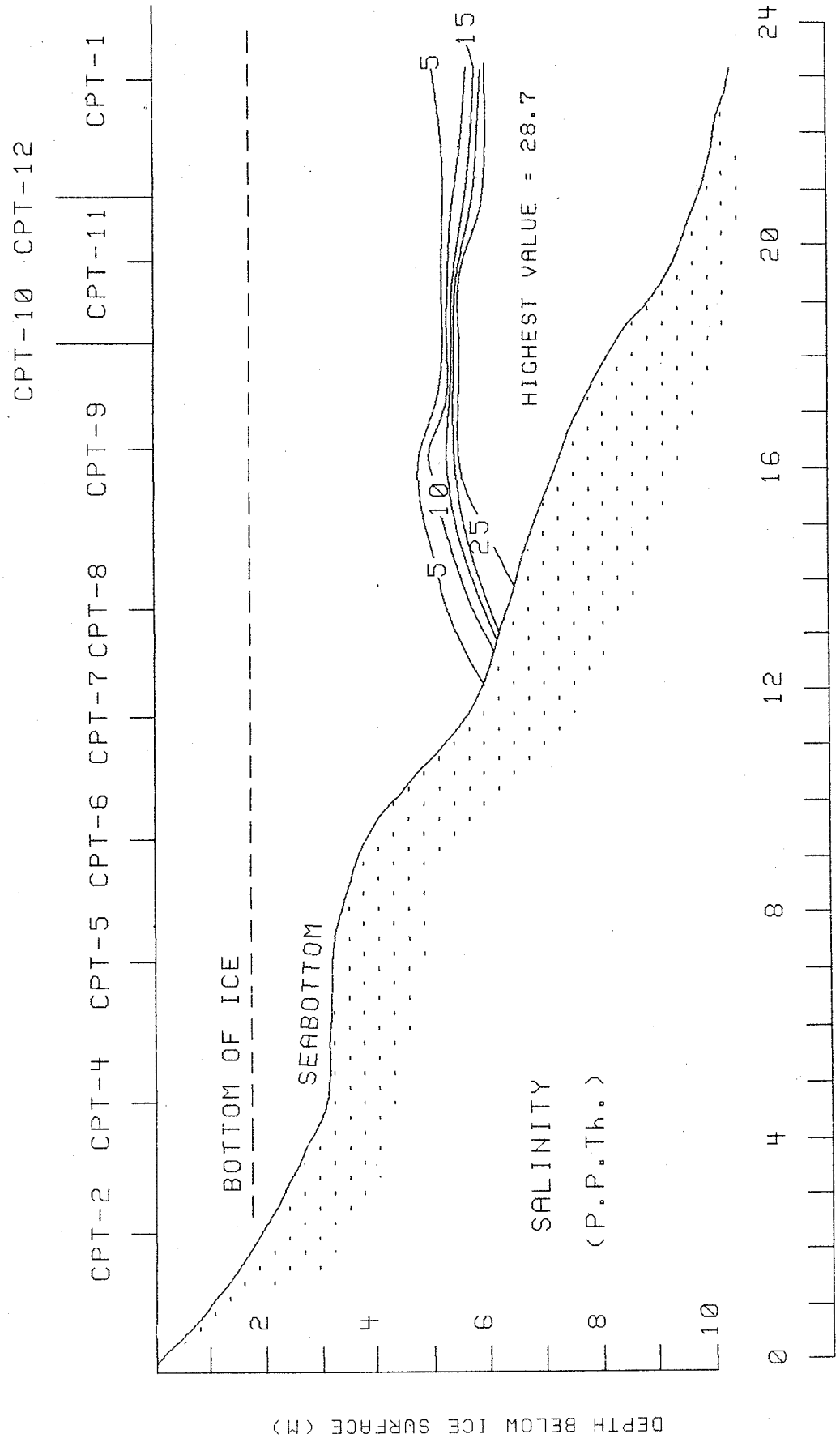
CPT-10 CPT-12
CPT-1
CPT-11
CPT-9
CPT-8
CPT-7
CPT-6
CPT-5
CPT-4
CPT-2
BOTTOM OF ICE
SEABOTTOM
SALINITY
(P.P.Th.)
HIGHEST VALUE = 28.7
5
15
10
5
25
DEPTH BELOW ICE SURFACE (M)
2
4
6
8
10
0
4
8
12
16
20
24
DISTANCE FROM SHORELINE (KM)

FIGURE 2.7.35

CHAPTER 3

ONSHORE-OFFSHORE TRANSECT: GEOPHYSICS

3.1 BOREHOLE GEOPHYSICAL LOGGING

J.A. Hunter, P.J. Kurfurst, S.M. Birk, R.A. Burns and R.L. Good

Geophysical borehole logging consists of lowering probes down the borehole to measure various physical properties of the surrounding material as a function of depth. Some logs can be run in cased boreholes, others require open-hole conditions. Geophysical logs are used to supplement core examination, to substitute for core loss or intermittent sampling, and to infer conditions beyond the thin column of core actually sampled.

Three types of geophysical logging were carried out in the boreholes immediately after drilling and casing were completed. These were:

1. Electrical conductivity (induction)
2. Natural gamma
3. Seismic downhole (interval velocity)

Conductivity and natural gamma logs

The conductivity (Figures 3.1.1a to 3.1.1e) and gamma logs (Figures 3.1.2a to 3.1.2e) were obtained using an EM-39 unit which is a small, portable, digital logging system manufactured by Geonics Limited. Both logs can be run in a plastic-cased borehole (either dry or fluid-filled). The EM-39 system was chosen because of the logistic advantages of running induction logs compared with electrical resistivity logs, which can only be obtained in a fluid-filled, uncased borehole.

The conductivity probe utilizes a coaxial coil geometry with an intercoil spacing of 50 cm; estimates of the radius of penetration into the formation are in the range of 1-1.5 m. The manufacturer states that the tool is unaffected by conductive borehole fluid in a 5 cm plastic casing. Measurement accuracies are in the range of 5%.

The conductivity of unconsolidated material is strongly dependent on the chemistry and physical state of the pore water. Frozen sediments with fresh pore water are characterized by low conductivities; in contrast, unfrozen, saline sediments are highly conductive. In this environment, conductivity logs are useful indicators of changes in the physical state of the pore water, and of the salinity of the sediments.

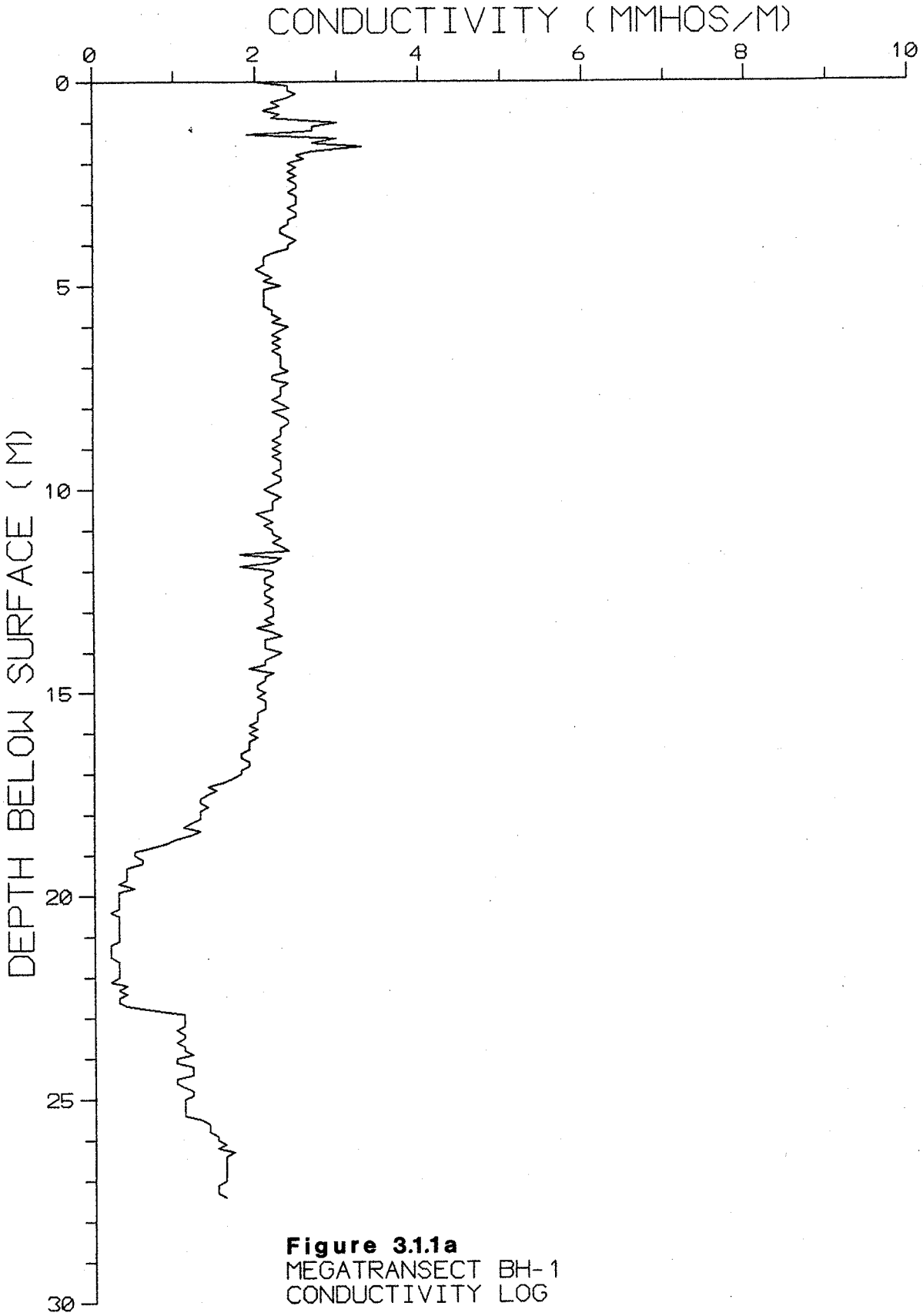

Figure 3.1.1a
MEGATRANSECT BH-1
CONDUCTIVITY LOG

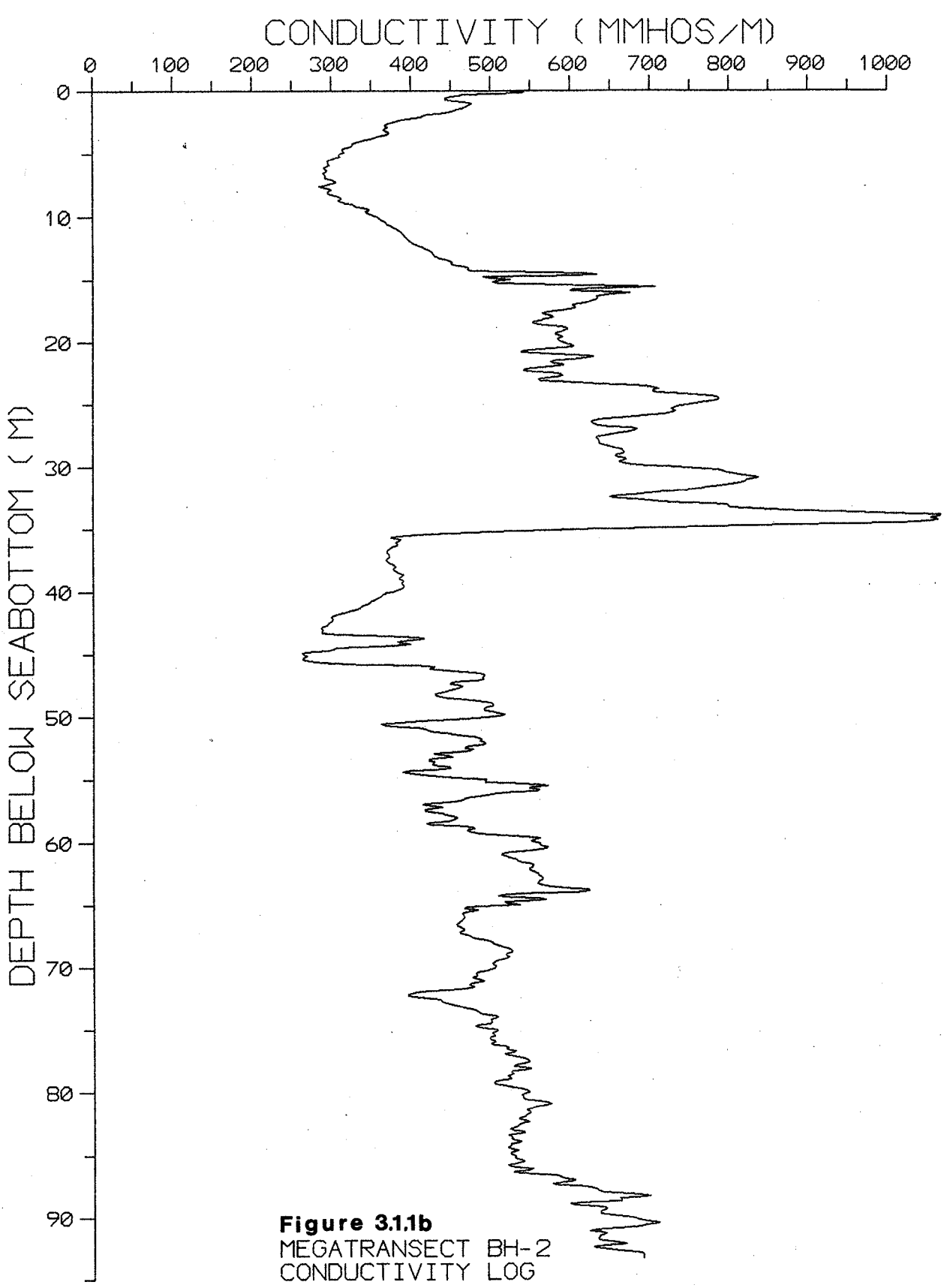

Figure 3.1.1b
MEGATRANSECT BH-2
CONDUCTIVITY LOG

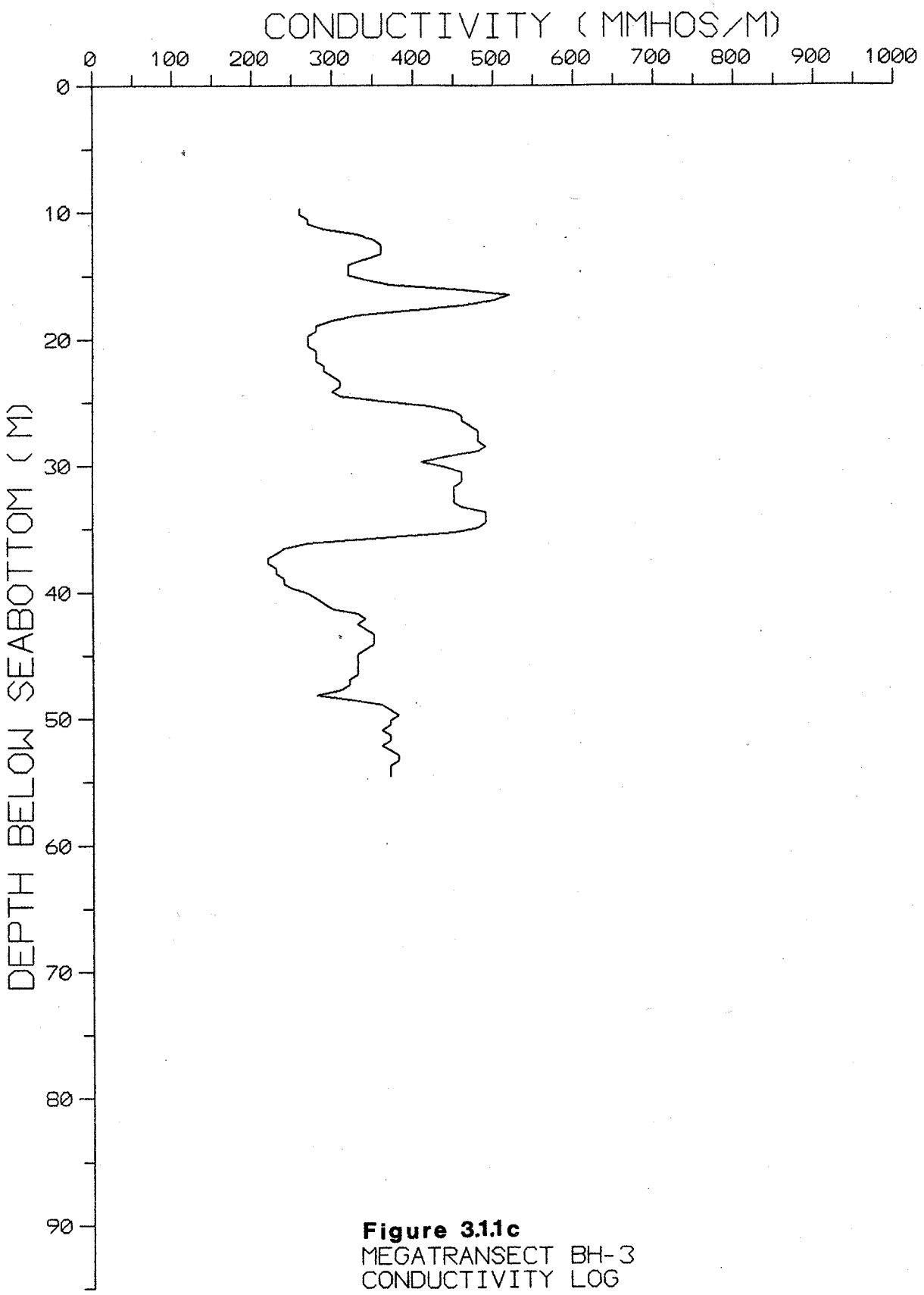

Figure 3.1.1c
MEGATRANSECT BH-3
CONDUCTIVITY LOG

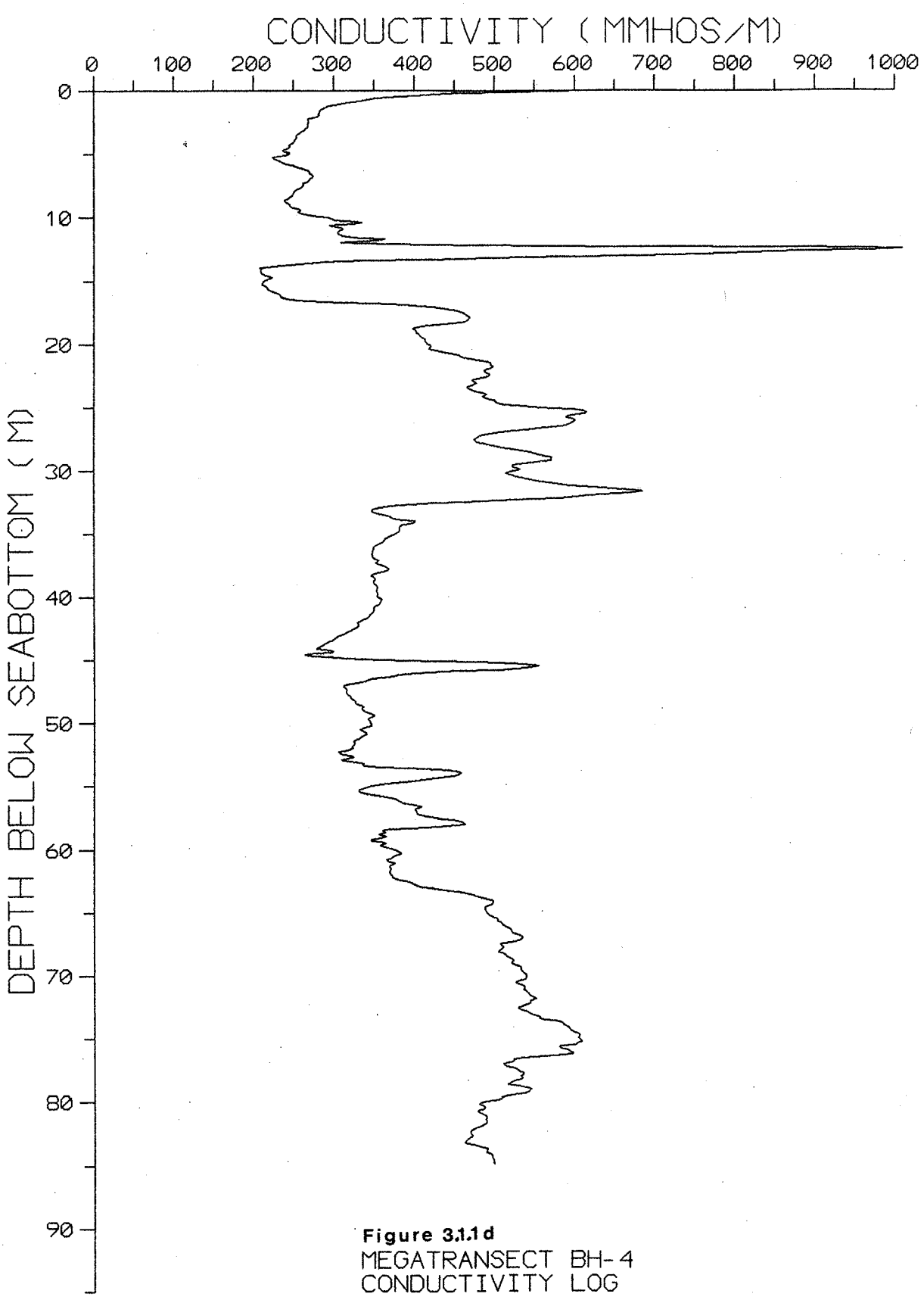

Figure 3.1.1d
MEGATRANSECT BH-4
CONDUCTIVITY LOG

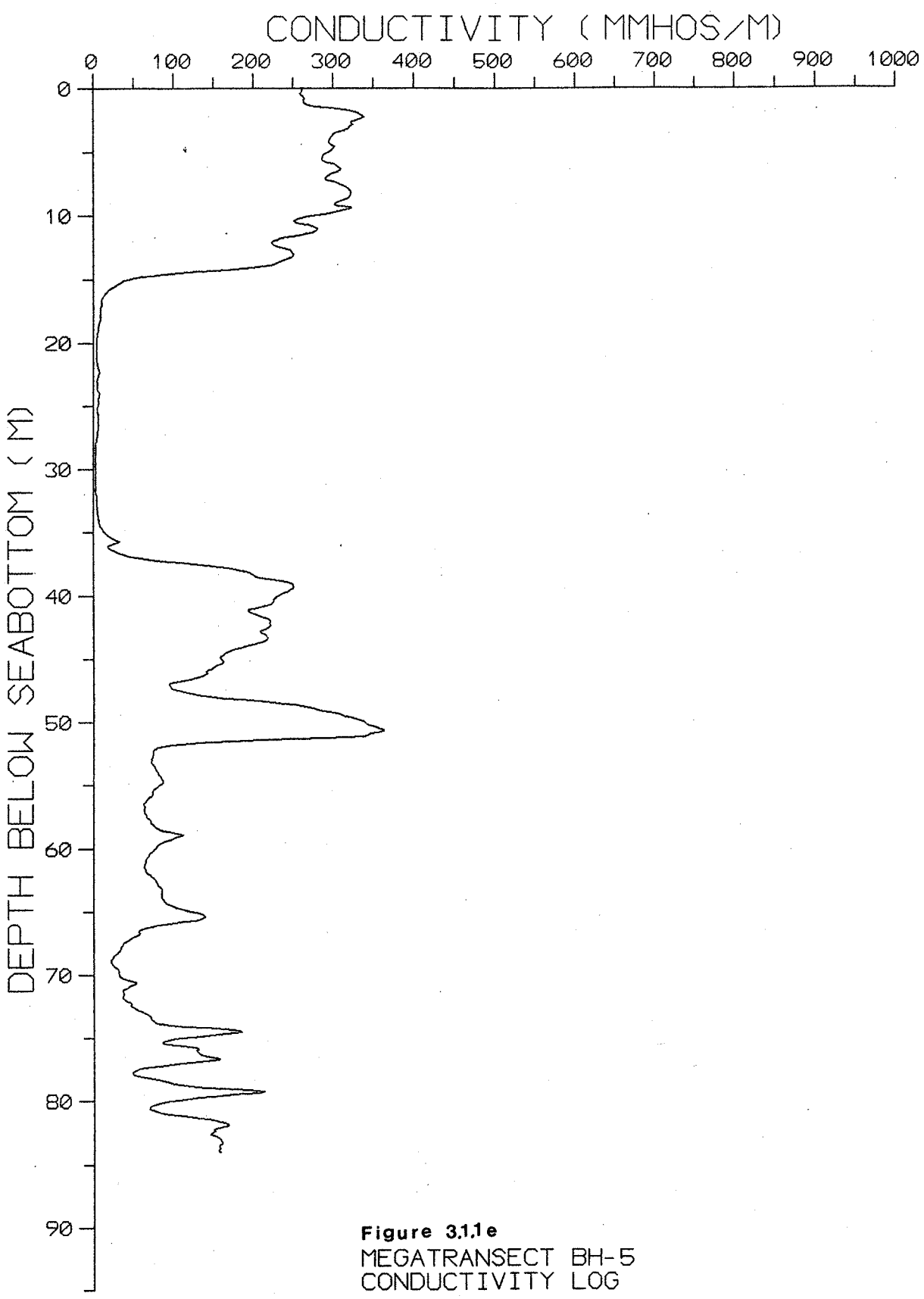

Figure 3.1.1e
MEGATRANSECT BH-5
CONDUCTIVITY LOG

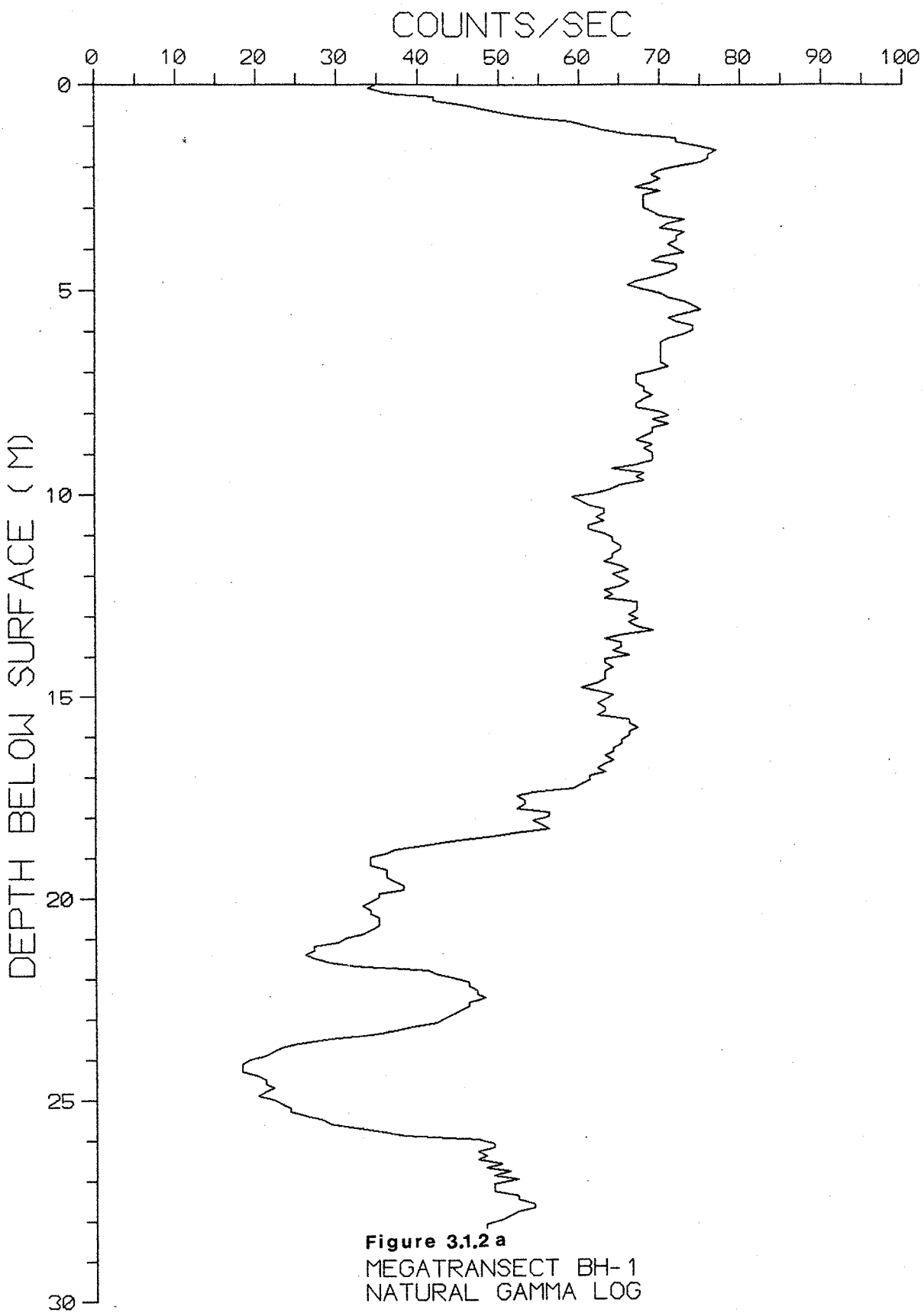

Figure 3.1.2 a
MEGATRANSECT BH-1
NATURAL GAMMA LOG

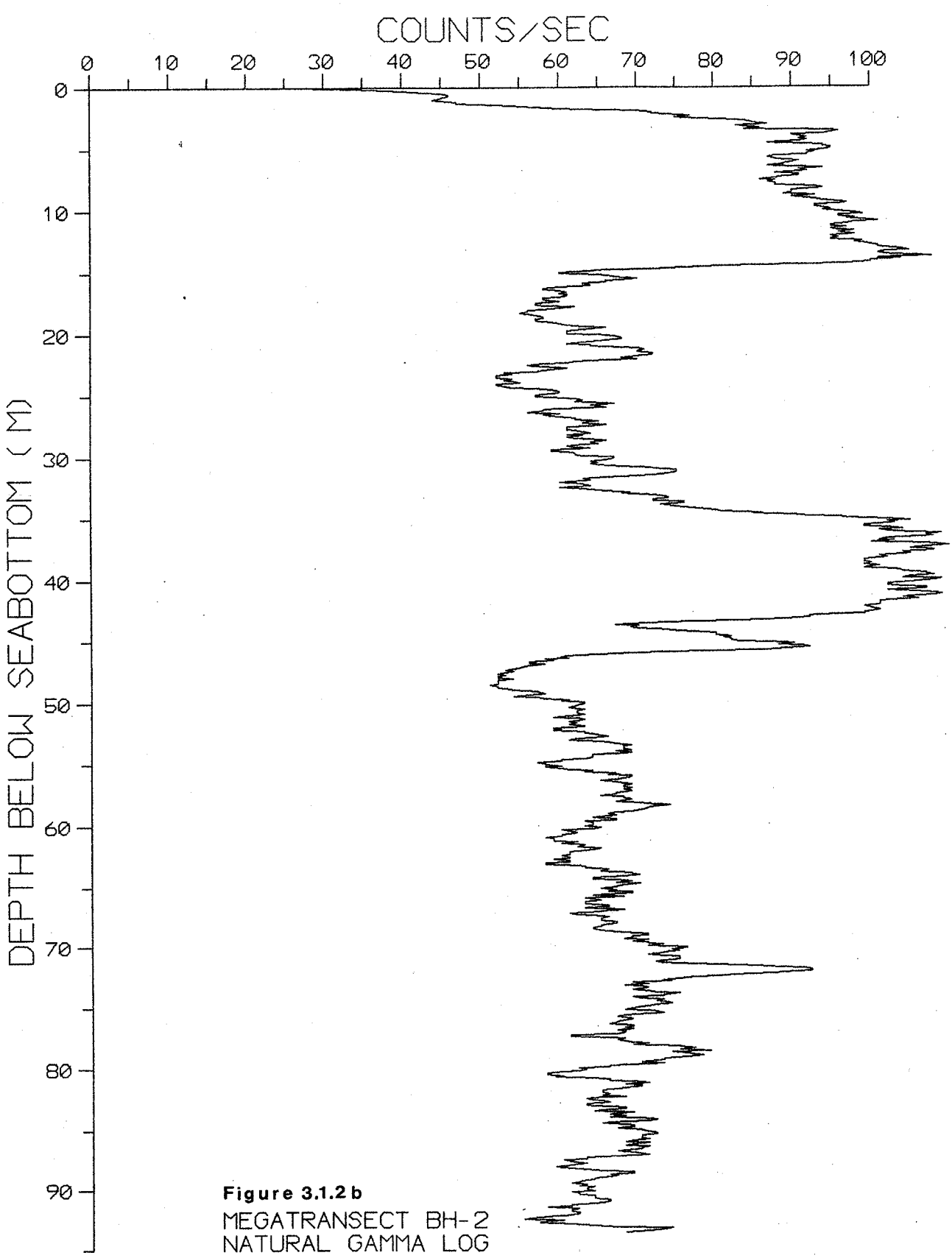

Figure 3.1.2 b
MEGATRANSECT BH-2
NATURAL GAMMA LOG

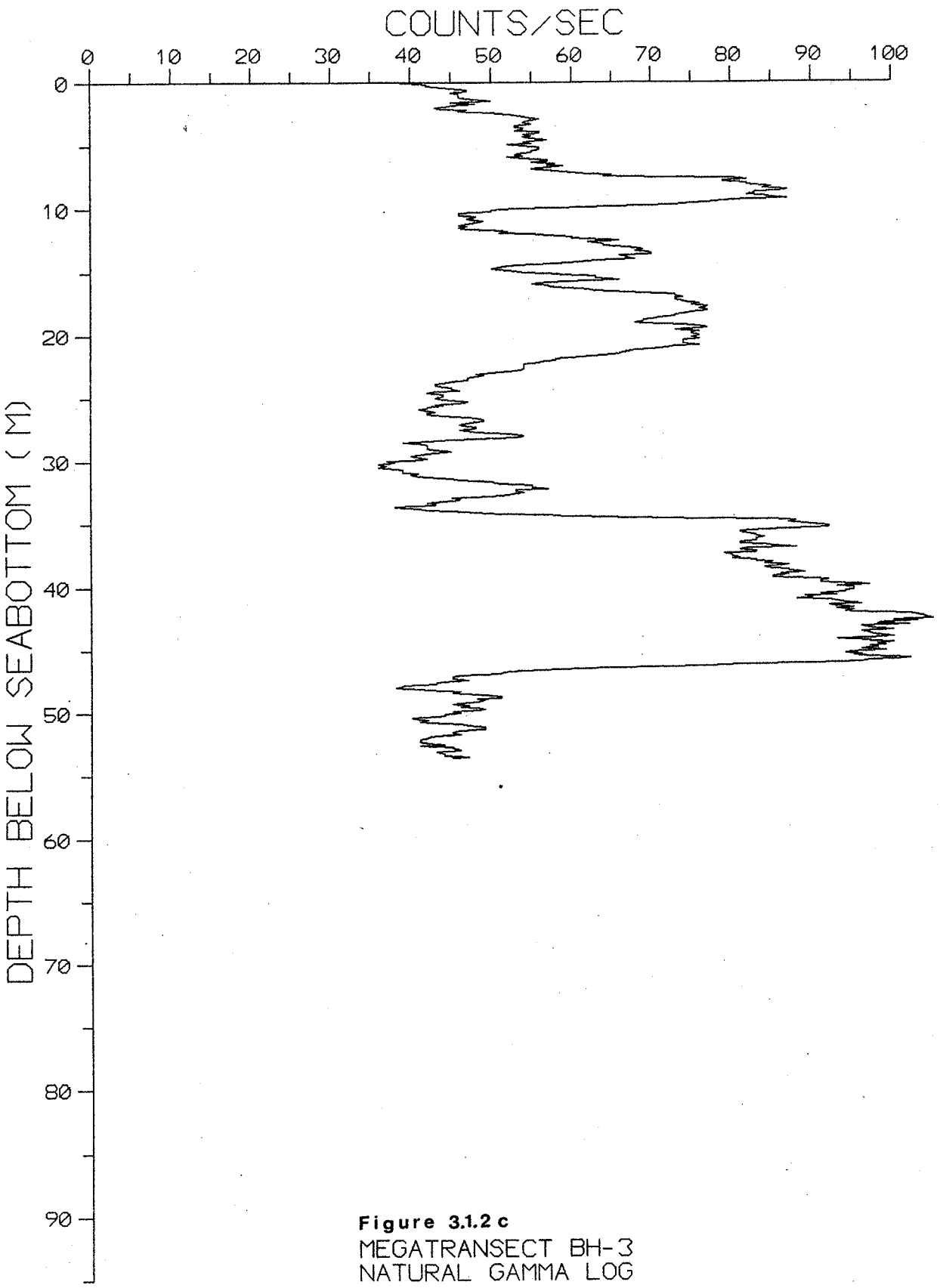

Figure 3.1.2 c
MEGATRANSECT BH-3
NATURAL GAMMA LOG

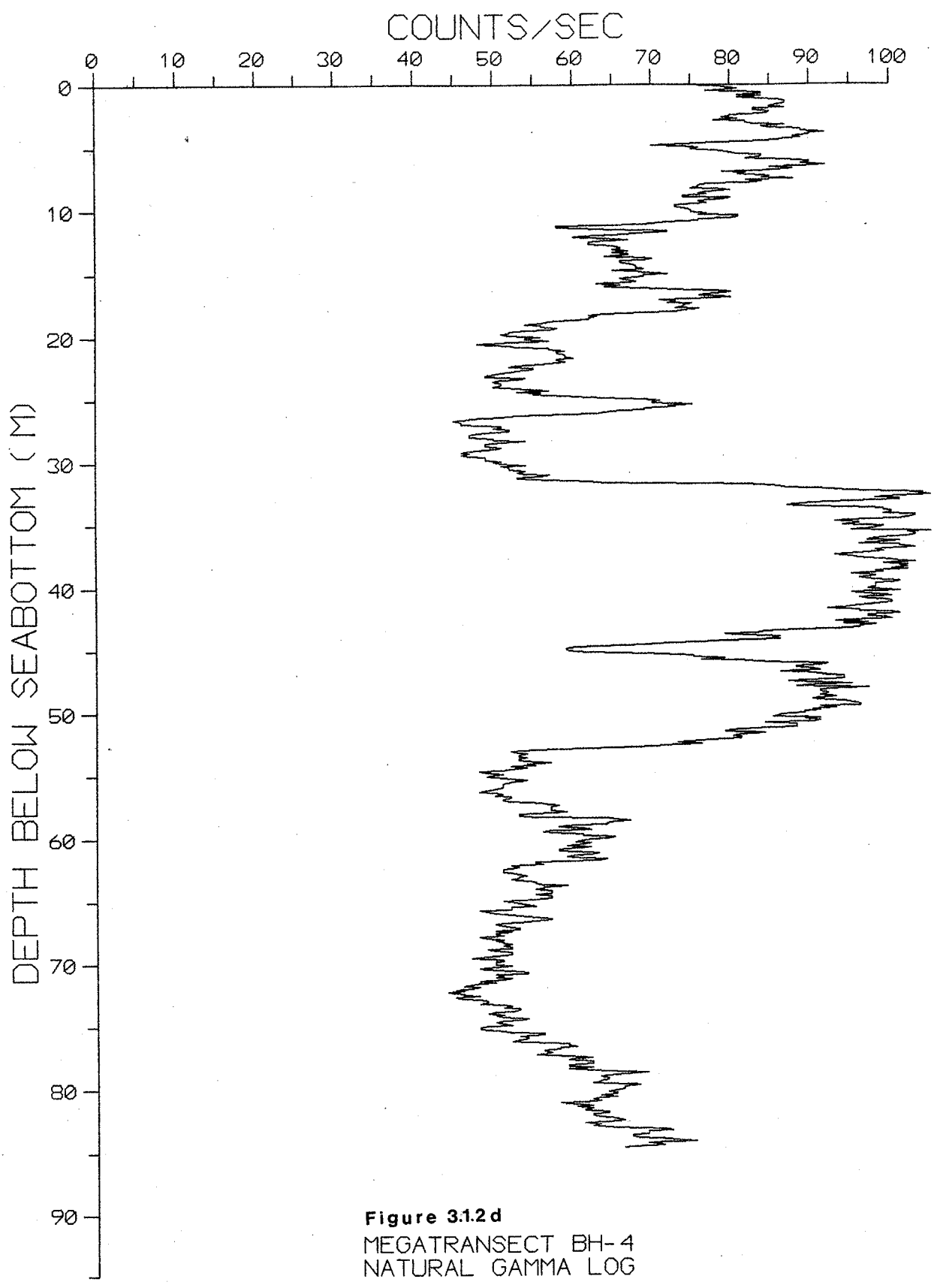

Figure 3.1.2 d
MEGATRANSECT BH-4
NATURAL GAMMA LOG

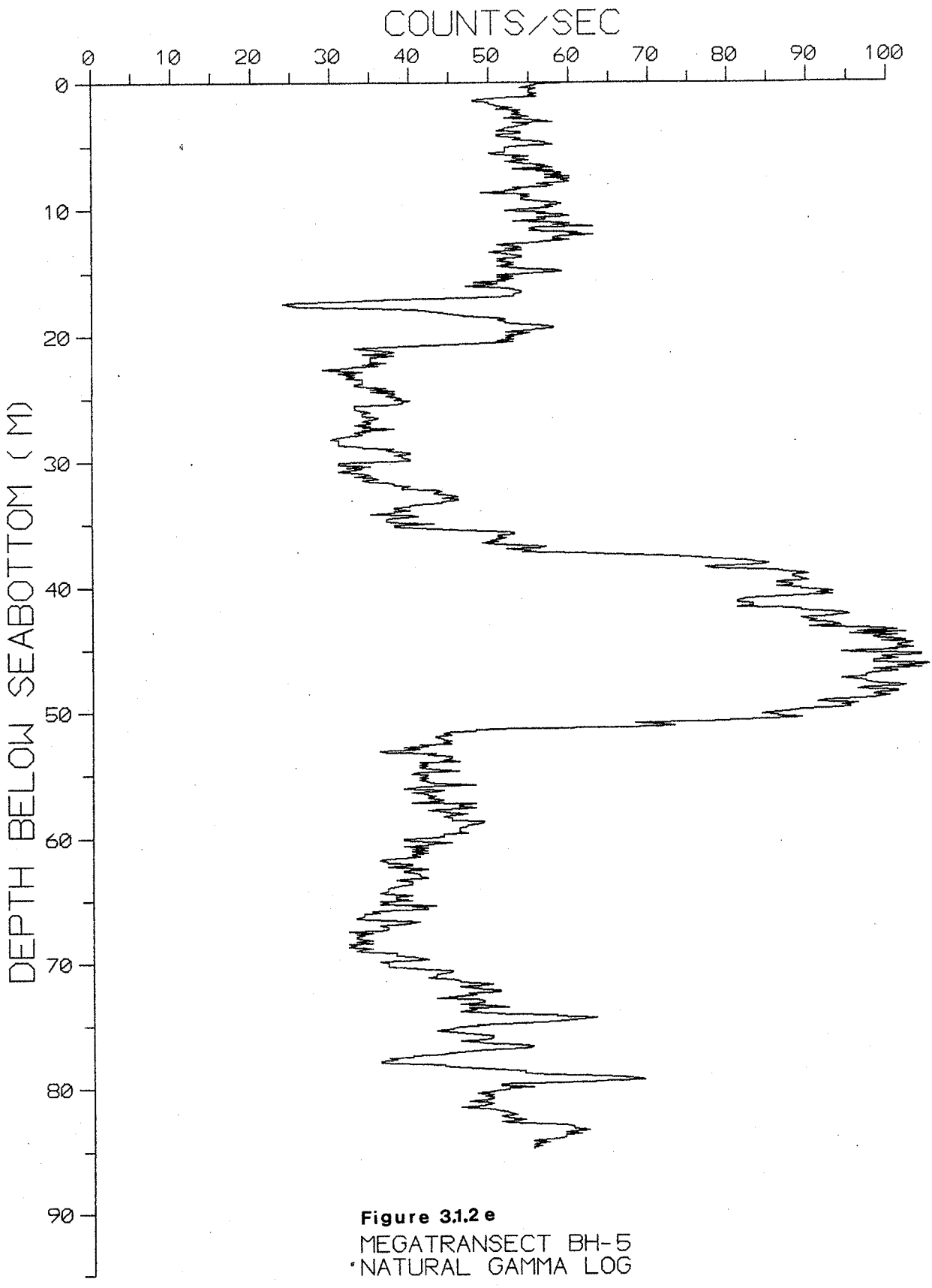

Figure 3.1.2 e
MEGATRANSECT BH-5
NATURAL GAMMA LOG

The natural gamma probe is a passive tool that measures the amount of radioactivity emitted by the sediments surrounding the borehole. In unconsolidated sediments, the log mainly reflects the clay content, since radioactive isotopes (potassium, uranium and thorium) tend to concentrate in the clay minerals. Gamma logs are also good indicators of the presence of massive ice, which is characterized by count rates of essentially zero. Since an external calibration of the natural gamma probe was not possible, the data obtained should be interpreted in a qualitative way; that is, low gamma readings are associated with coarse-grained sediments, and high readings are associated with fine-grained sediments.

More than one run of both the conductivity and gamma tool were made in each hole. In boreholes 90BH3 and 90BH4, an error of the order of 1 m in the zero position of the cable was observed after one run of lowering and raising of the tool in the borehole. In these cases it was assumed that slippage occurred on the well-head counter on the up-going run due to ice build-up on the pulley under conditions of blowing snow. Hence only the down-going run was selected for publication.

The conductivity log of 90BH3 begins at 9.6 m below seabottom, as a result of interference from the steel casing above that point.

Downhole seismic logs

The seismic downhole system used in this project was developed at the Geological Survey of Canada. It consists of a 12-channel hydrophone array, with a 0.5 m spacing between detectors, which is lowered in increments down the borehole, and is used to record the seismic signals generated by a source on surface. The source was a small explosive charge that was detonated on the seabottom at an offset of 6 m from the hole. Each shot results in a 12-channel record. In boreholes 90BH3 and 90BH5, records were obtained with a spacing of 1 m between successive positions of the array (i.e. with a 10 hydrophone overlap between shots), to provide the redundancy of data that is used in a statistical interpretation technique. Due to time constraints, records from 90BH2 and 90BH4 were obtained with a 5 m spacing between successive positions of the array (2 hydrophone overlap between shots).

First arrival travel times were picked for all data sets, and used to calculate interval velocities. The 3-point velocity fits shown in this report (Figures 3.1.3a to 3.1.3d) correspond

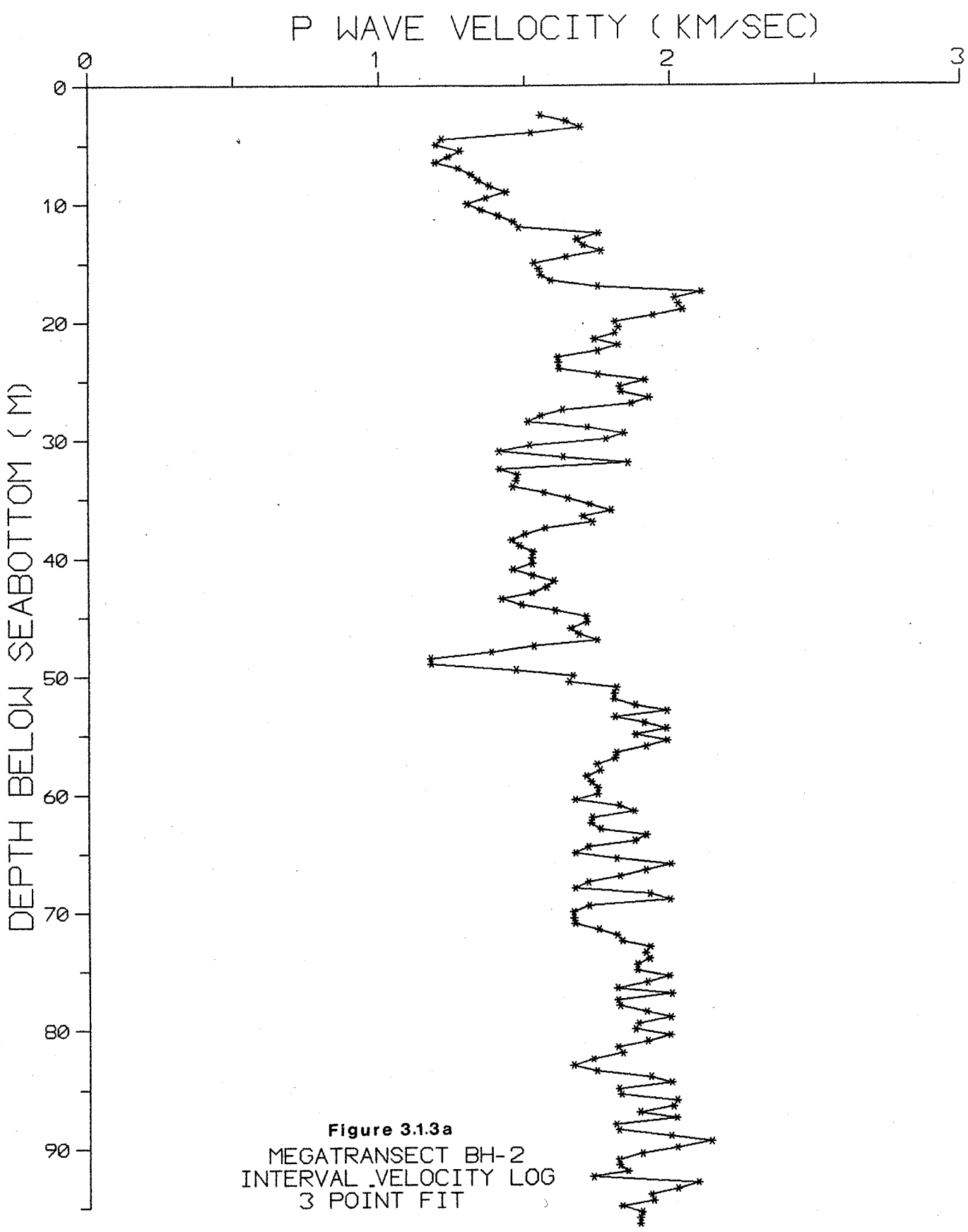

Figure 3.1.3a

MEGATRANSECT BH-2
INTERVAL VELOCITY LOG
3 POINT FIT

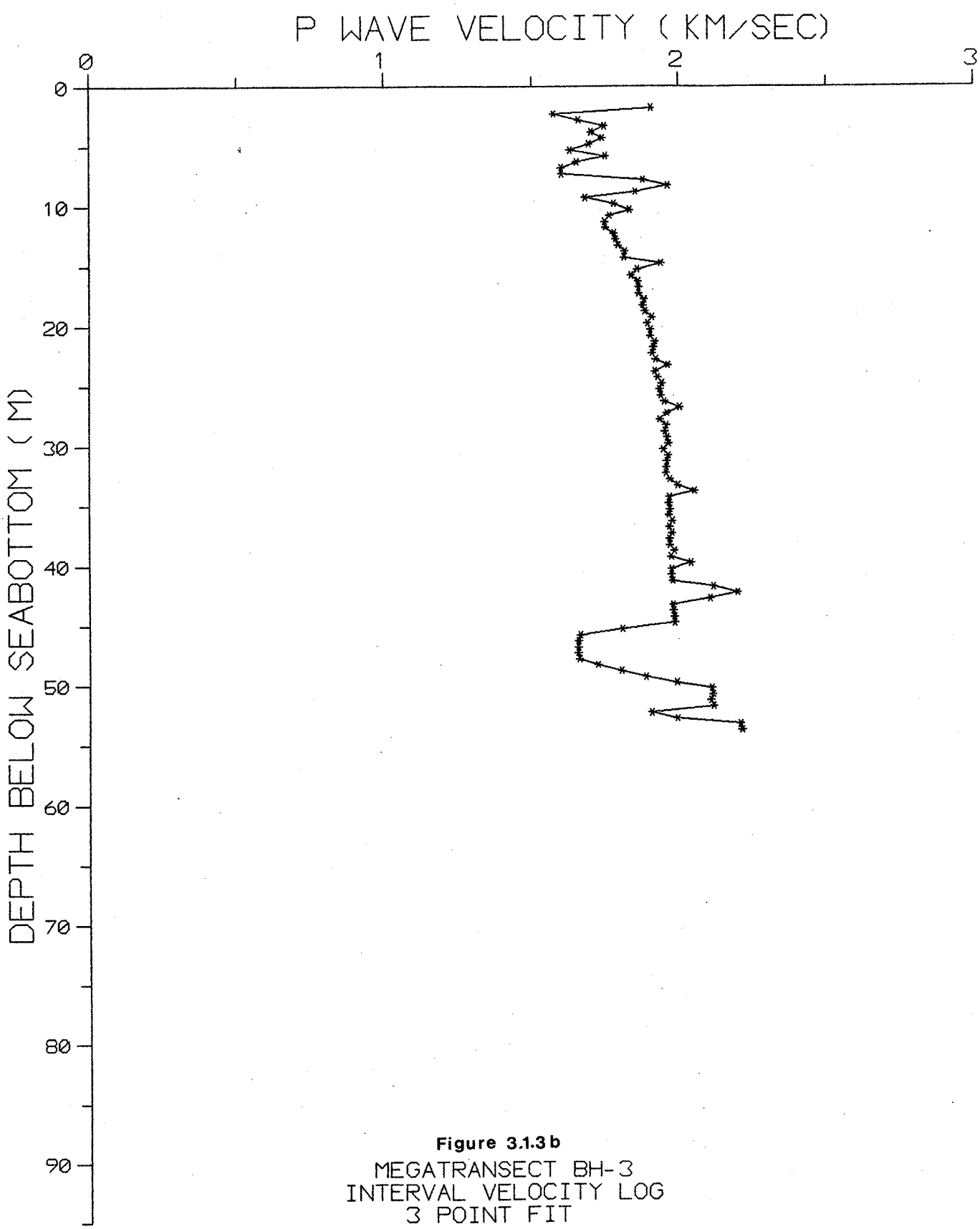

Figure 3.1.3 b

MEGATRANSECT BH-3
INTERVAL VELOCITY LOG
3 POINT FIT

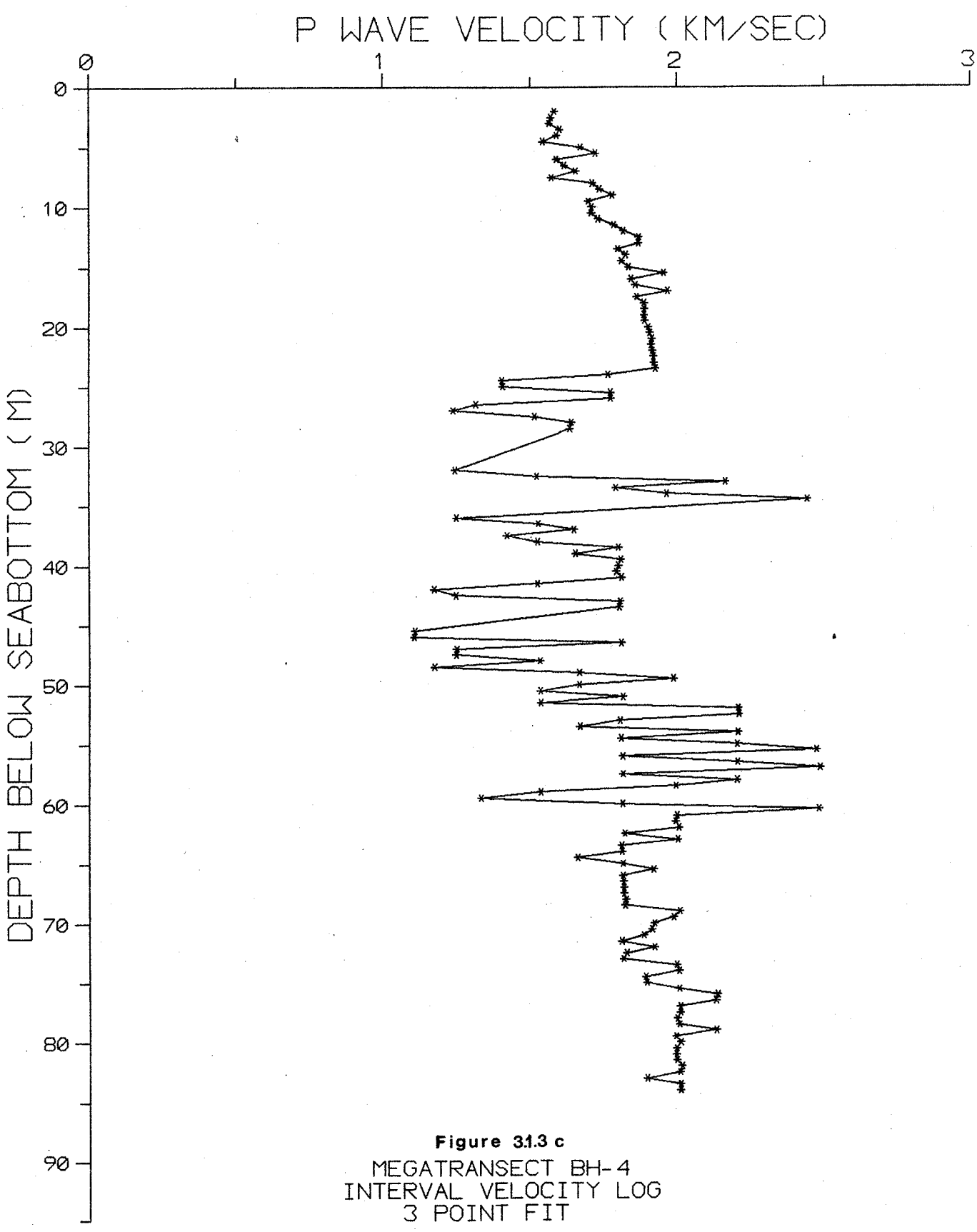

Figure 3.1.3 c

MEGATRANSECT BH-4
INTERVAL VELOCITY LOG
3 POINT FIT

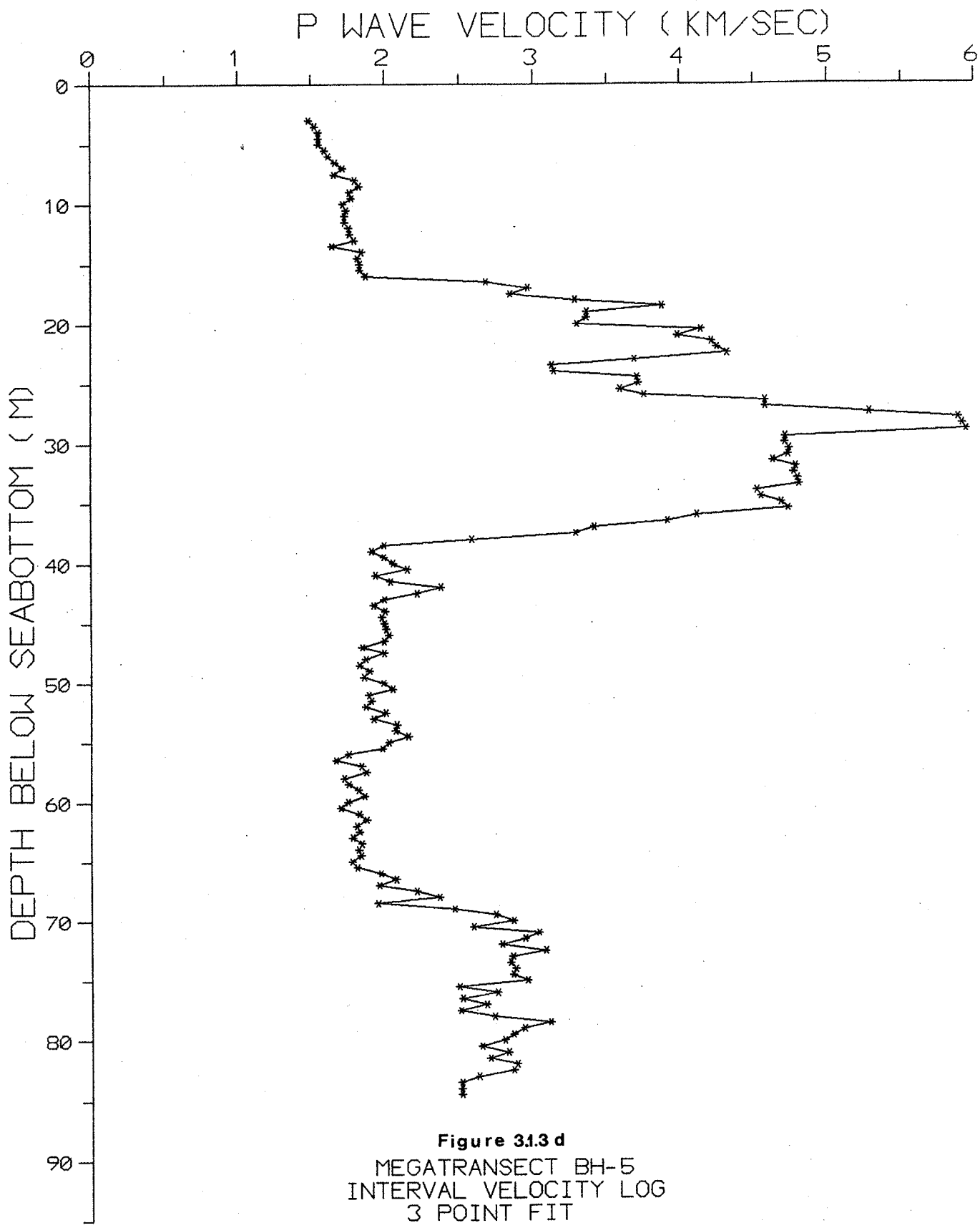

Figure 3.1.3 d

MEGATRANSECT BH-5
INTERVAL VELOCITY LOG
3 POINT FIT

to the interval velocities over a 1 m downhole distance. Considerable deviation from a straight-line ray-path between source and receiver can occur, due to refraction effects in the presence of large velocity contrasts; hence, these data have been corrected for ray-bending using an iterative technique.

Velocity values less than 1.4 km/sec may indicate the presence of gas. Velocity values in the range of 2.0-2.2 km/sec may indicate marginal ice-bonding. Velocity values greater than 2.5 km/sec indicate ice-bonding. A high velocity zone in 90BH5, where values exceed 5.0 km/sec, suggests that the sand is in grain-to-grain contact and bonded with interstitial ice. Similar velocities are observed for frozen sands and frozen sandstone in laboratory studies, and have occasionally been observed in refraction surveys on land in the Tuktoyaktuk Peninsula and offshore on the Beaufort Sea Shelf.

The redundant data sets obtained in 90BH3 and 90BH5 and the statistical techniques that can be applied to these data are considered to result in higher quality results than those obtained for 90BH2 and 90BH4.

Velocity values were compiled in histogram form for all data (Figure 3.1.4) and for each geological unit as defined in Chapter 2.3 (Figures 3.1.5 to 3.1.8). Unit B gives values grouping between 1.65 km/sec and 1.9 km/sec. Unit C shows the largest spread of values; it is suggested that velocity values of non-ice-bonded Unit C group between 1.70 km/sec and 2.0 km/sec. The skewed distribution with a predominant grouping in the range 1.4-1.7 km/sec may represent minor quantities of gas. Values of Unit C above 2.0 km/sec probably represent various degrees of ice-bonding. Values in the range of 3.0 to 4.8 km/sec are typical of ice-bonded sands on land in the Mackenzie Delta region. Unit D exhibits two velocity groupings; a minor one occurring in the range of 1.4-1.55 km/sec, and a larger one in the 1.8 to 2.1 km/sec range. The high velocity range is unusual for non-bonded clayey silts and may suggest partial ice-bonding or overconsolidation. Unit E has two distinct velocity ranges, 1.65-2.1 km/sec and 2.4 to 2.9 km/sec; the higher zone reflects the ice-bonded materials found in 90BH5.

A compilation of all data from all units, shown in histogram form indicates a strong grouping of velocities in the range 1.45-2.1 km/sec for non-ice-bonded and low ice-content materials. Other significant groupings appear at velocities greater than 2.4 km/sec suggest the presence of ice-bonded materials.

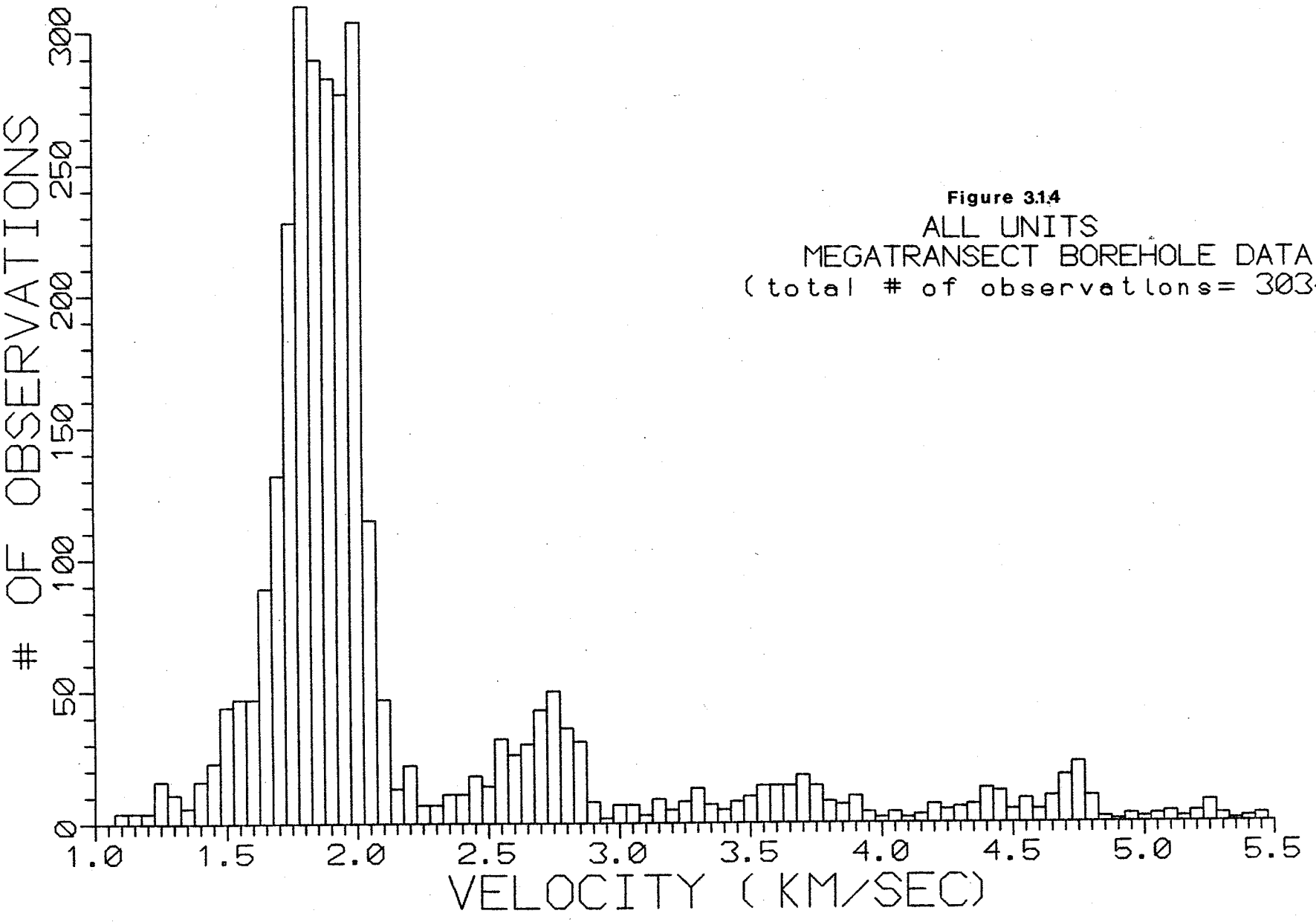

Figure 3.14

ALL UNITS
MEGATRANSECT BOREHOLE DATA
(total # of observations= 3034)

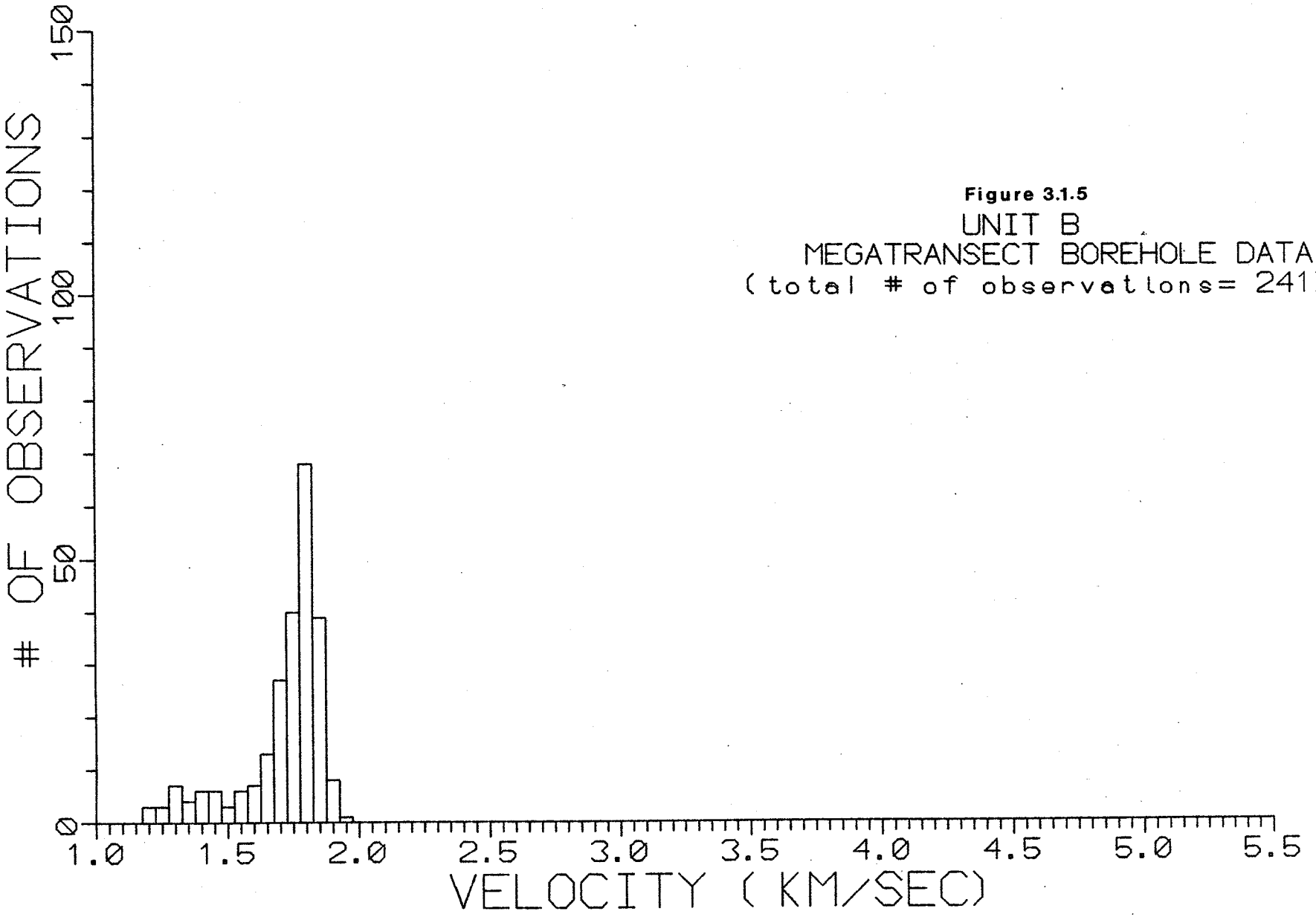

Figure 3.1.5

UNIT B
MEGATRANSECT BOREHOLE DATA
(total # of observations= 241)

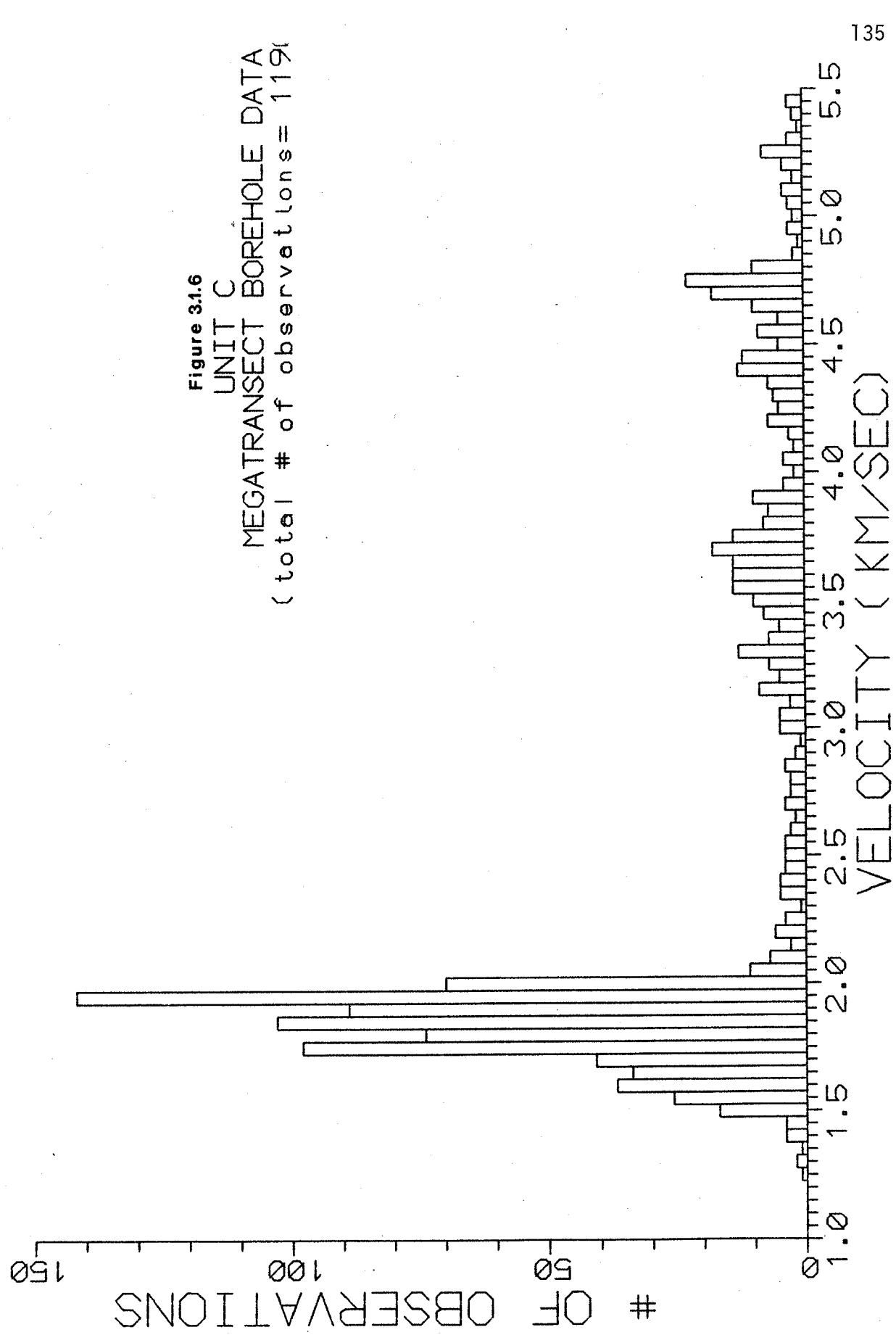
UNIT C
MEGATRANSECT BOREHOLE DATA
(total # of observations= 119
OF OBSERVATIONS
0
50
100
150
1.0
1.5
2.0
2.5
3.0
3.5
4.0
4.5
5.0
5.5
VELOCITY (KM/SEC)

Figure 3.1.6

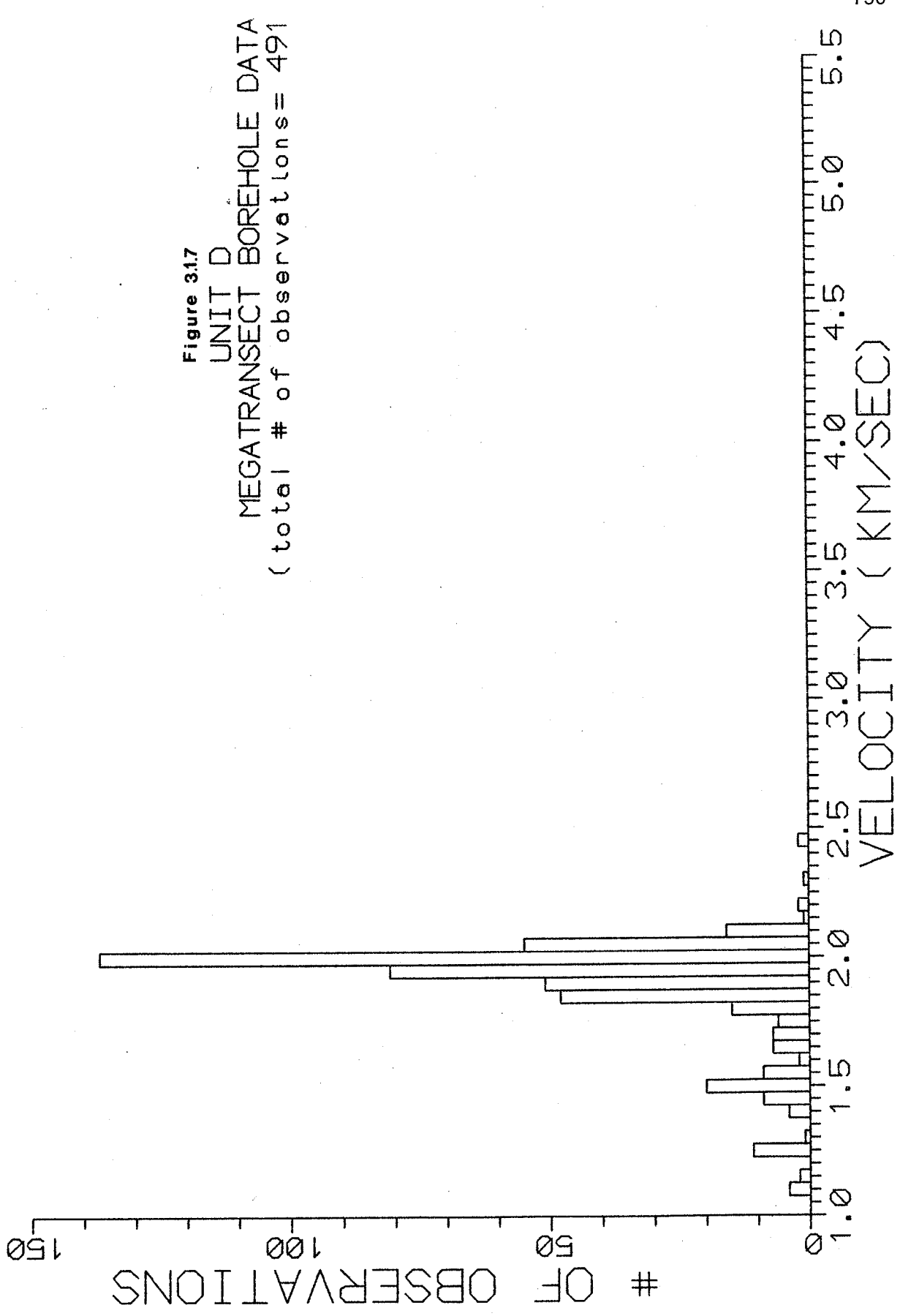
UNIT D
MEGATRANSECT BOREHOLE DATA
(total # of observations= 491
OF OBSERVATIONS
0
50
100
150
1.0
1.5
2.0
2.5
3.0
3.5
4.0
4.5
5.0
5.5
VELOCITY (KM/SEC)

Figure 3.1.7

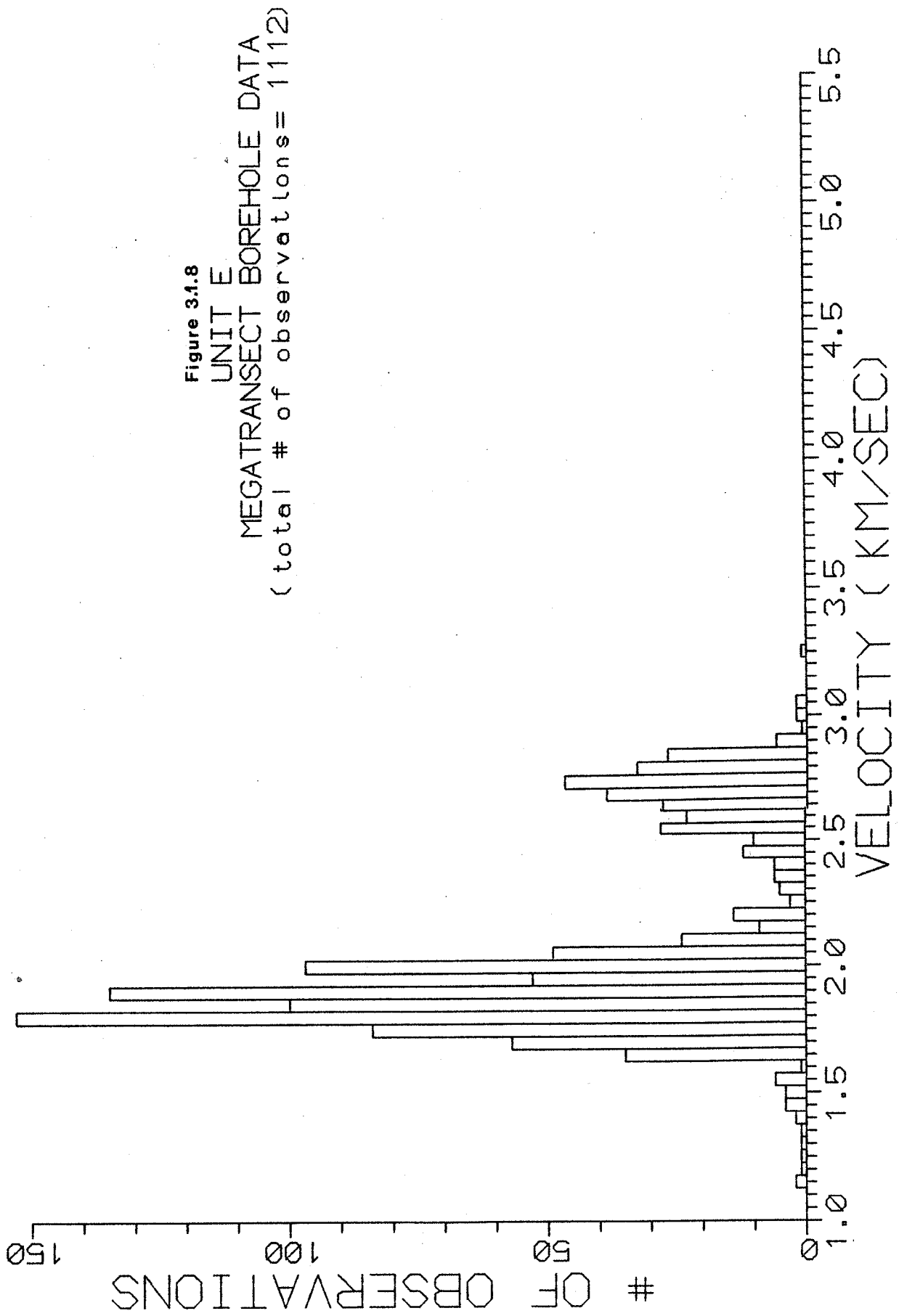
UNIT E
MEGATRANSECT BOREHOLE DATA
(total # of observations= 1112)
OF OBSERVATIONS
0
50
100
150
1.0
1.5
2.0
2.5
3.0
3.5
4.0
4.5
5.0
5.5
VELOCITY (KM/SEC)

Figure 3.1.8

3.2 GEOTHERMAL MEASUREMENTS

A.E. Taylor and V.S. Allen

A program to measure ground temperatures and sediment thermal properties was undertaken to establish the present geothermal regime, to provide data on which to base further geothermal analyses and to constrain thermal modelling, and to complement the geological and geotechnical investigations.

The geothermal program consisted of the instrumentation of each borehole with a precision temperature-measuring cable, and a water temperature measuring cable placed through the sea ice. An automatic data logger was attached to both cables and left for almost a month.

This setup was sufficient to establish the present ground temperature regime and to delineate the extent of permafrost, the sub-0°C sediment. The principal rationale for the use of data loggers was to monitor the thermal recovery of the hole from effects of drilling and to permit an assessment of the temperatures representative of undisturbed seabed. This is particularly important for holes penetrating permafrost where frozen zones may be thawed, or unfrozen zones may be frozen in the drilling and circulation process; generally a much longer period of monitoring is required when latent heat is involved. Also, these loggers permit the detection of ice motion that may result in cables being pulled partly or entirely out of the holes. Seawater temperatures are the upper boundary condition to the ground thermal regime in the offshore and were measured at each site.

In September, 1989, a similar geotechnical hole had been instrumented with a temperature cable at the Gulf/Esso Isserk wellsite. As Isserk lies some 10 km northwest of 90BH5 in this project, its data are complimentary to the Transect project and are included here.

3.2.1 Multithermistor cables

Temperature cables were made to standardized Geological Survey of Canada specifications of cable design, wiring and plug termination by Hardy BBT Ltd., Calgary. Measuring from the "zero" mark to be placed at the seabed, the spacing of thermistors was specified as 1, 3, 6, 10, 15, 20, 25, 30 m and every 10 m metres to 100 m. Yellow Springs

Inc. type YSI 44033 thermistors were wired into a 25 conductor polyurethane jacketed cable at designated intervals and over-molded with polyurethane for physical protection and to ensure waterproofness. A suitable length (10 m to 30 m) of leader cable was left above the zero mark to allow for the expected water depth and ice thickness and to permit the logger to be left some distance from the hole; this section was covered with braided electronic shielding for protection against abuse at the surface, particularly by animals. A 5 kg (approximate) sinker bar was provided for attachment at the lower end of the cable. Water temperature cables were made by the same procedure, and consisted of four thermistors spaced at 2 m intervals.

3.2.2 Thermistor calibration

Manufacturer's specifications of these thermistors include an "interchangeability" of 0.1 K. Thermistors used in the cables at 90BH3, 90BH5 and the upper 24 m at 90BH4 were first calibrated in our Ottawa laboratory. This precision calibration was undertaken to a resolution of better than 0.001 K, and to an absolute accuracy of +/- 0.01 K traceable to standards at the National Research Council of Canada. Three constants determined in this procedure define the thermistor resistance-temperature conversion unique to a particular thermistor, and each thermistor was identified with a serial number. Staggered delivery of the some 250 thermistors required by the project did not allow time for all thermistors to be calibrated in this way. However, an ice bucket check on the completed cable was done by Hardy BBT as a final check that sensors had not been damaged in the insertion and molding operation.

3.2.3 Data loggers

Two types of data loggers were used. Seadata model 1250A is a 64-channel, cassette or solid-state memory data acquisition system that has been widely used in the Norman Wells pipeline monitoring program and at other sites of interest to the Permafrost Research Section. These were installed at 90BH1, 90BH2 and 90BH4, and at the Isserk well. Power is supplied entirely by means of internal batteries. Two prototype Brancker Research model XL-100 loggers, 64-channel instruments of a new design, were installed at 90BH3 and 90BH5. Power is supplied to these by internal rechargeable batteries and solar panels were

used to maintain the charge. Both logger types have environmental seals and plugs, and since their specifications include use in arctic temperatures, no environmental protection or insulation was used.

3.2.4 Installation of temperature cables

In all cases, the instrumented length of the cables as manufactured was somewhat longer than the available section of hole. Once the latter was known, the cable was folded back on itself from the bottom, interspersing thermistors from the lower end of the cable with ones above, and bound in several places with PVC tape; note was made of the new effective thermistor spacing and thermistor serial number, in the case of the calibrated thermistors. A 5 kg weight was attached to the bottom.

The installation of the temperature cables was the final technical activity on a hole. Following installation of the silicone fluid-filled PVC tube in a hole and the running of the downhole geophysical logs, the temperature cable was run in with the zero mark being set at the seafloor; the cable was suspended from the top of the PVC casing with a cable hanger. This casing was allowed to freeze into the ice and presumably also freeze in any frozen intervals within the sediment. Water temperature cables were installed through nearby ice holes, folding these shorter cables where required such that the bottom thermistor was at or just above the seafloor. The data logger was set up for automatic data acquisition at 2 hour intervals, and both the borehole and water temperature cables were then attached to it.

A geotechnical hole was drilled as part of a foundation testing program at the Gulf/Esso Isserk wellsite in September, 1989. The hole was drilled from the deck of the Molikpaq while the sand ballast was being filled. The hole was deepened to 34 m, a depth beyond that required for testing, and a cable was installed through the drill casing, which then was pulled out over the cable. A Seadata logger was attached and left until June, 1990.

3.2.5 Recovery of ground temperature data

Manual temperature readings using a hand-held precision multimeter were taken upon installation of the cable, and on April 16, 21 and 26, at which latter date the installations were demobilized. Data were dumped to a portable computer from the

Brancker loggers in the field on a couple of occasions during the week following installation (to monitor operation), and on April 21 and 26. Cassette tapes from the Seadata loggers were removed only on April 26. The Seadata logger at 90BH4 suffered a complete failure and no automatic data were recovered from this site.

At the Isserk site, data tapes were retrieved in November 1989, and June 1990. The time series record is complete until early 1990, when the record became unusually noisy.

Thermistor resistances R were converted to temperatures T using a 3-parameter relation,

$$T = \frac{B}{\ln R + \ln A} + C$$

where A, B and C are calibration constants (obtained from the precision calibration of the thermistors or from the manufacturer's constants).

3.2.6 Recovery of temperature cables

The last activity in the field was the demobilization of the temperature installations on April 26. Weather and sea ice conditions had been monitored for the previous week, and this was considered the latest that the installations could be safely left. Any ice motion would tend to pull the cables out of the seabed or break them and, after large movement, it might have proved difficult to relocate the data loggers.

Loggers were disconnected from the cables, manual readings were taken and an attempt was made to pull each cable out of the silicone fluid-filled tubing. At 90BH2, 90BH4 and 90BH5 the complete cable was recovered. At 90BH3, the cable was found firmly frozen in an ice plug inside the tubing about 0.7 m below the top of the sea ice. With considerable pulling effort, the tubing came free of the sea ice and, following additional effort, the cable broke around the zero mark. This suggests that the cable had frozen into the tubing at some deeper level within the seabed. The tubing itself appeared to have been already broken near the seabed. Water temperature cables were cut level with the sea ice and wood markers and frames were either burnt on site or removed with other debris to

Tuktoyaktuk.

3.2.7 Ground temperature data

Time-series of temperatures are presented in Fig. 3.2.1 to 3.2.3 for 90BH2, 90BH3 and 90BH5, respectively; however no automatic data were recovered at 90BH4 because of the logger failure. In these plots, some depths have been omitted for clarity. As expected, the 3 to 4 weeks of data acquisition appears to have been sufficient for the boreholes to recover from the thermal disturbance due to drilling. It may also be concluded, from the discussion below, that ice motion was insufficient to prevent the extraction of a good set of temperatures representative of undisturbed conditions.

Temperature-depth plots of the manual measurements (taken shortly after installation, and on April 16, 21 and 26) are presented in Figures 3.2.4-3.2.8 for 90BH1-5, respectively, and for all offshore boreholes in Fig. 3.2.9 using the final data. These profiles also illustrate the recovery of temperatures from drilling disturbances. For the final log in each borehole, surface temperatures (land surface or seabed, as appropriate) reflect the seasonal terrestrial or marine conditions, respectively. At 90BH1 on land, temperatures were measured in July and it was determined that ground temperatures decrease below the surface to about 7 m and increase at greater depths. At the offshore boreholes 90BH2-5, temperatures increase with depth for 5 to 7 m below the seabed, then decrease with depth, exhibiting an inversion between 5 and 10 m. The inversion in all cases denotes the approximate depth of most of the seasonal variation; a late summer log might show seabed temperatures somewhat higher than the inversion, while a winter log would give seabed temperatures somewhat lower than the inversion temperature.

90BH1: This cable was left to freeze permanently in this short hole. (A replacement borehole was drilled to greater depth somewhat north in the summer of 1990, but logistics have prevented any temperatures being obtained to the present).

90BH2: The cable was removed from the borehole on April 21 for several hours to accommodate geophysical logging (Fig. 3.2.1). From the time-series data, it appears that formation temperatures were increased by the drilling process; note the cooling during the

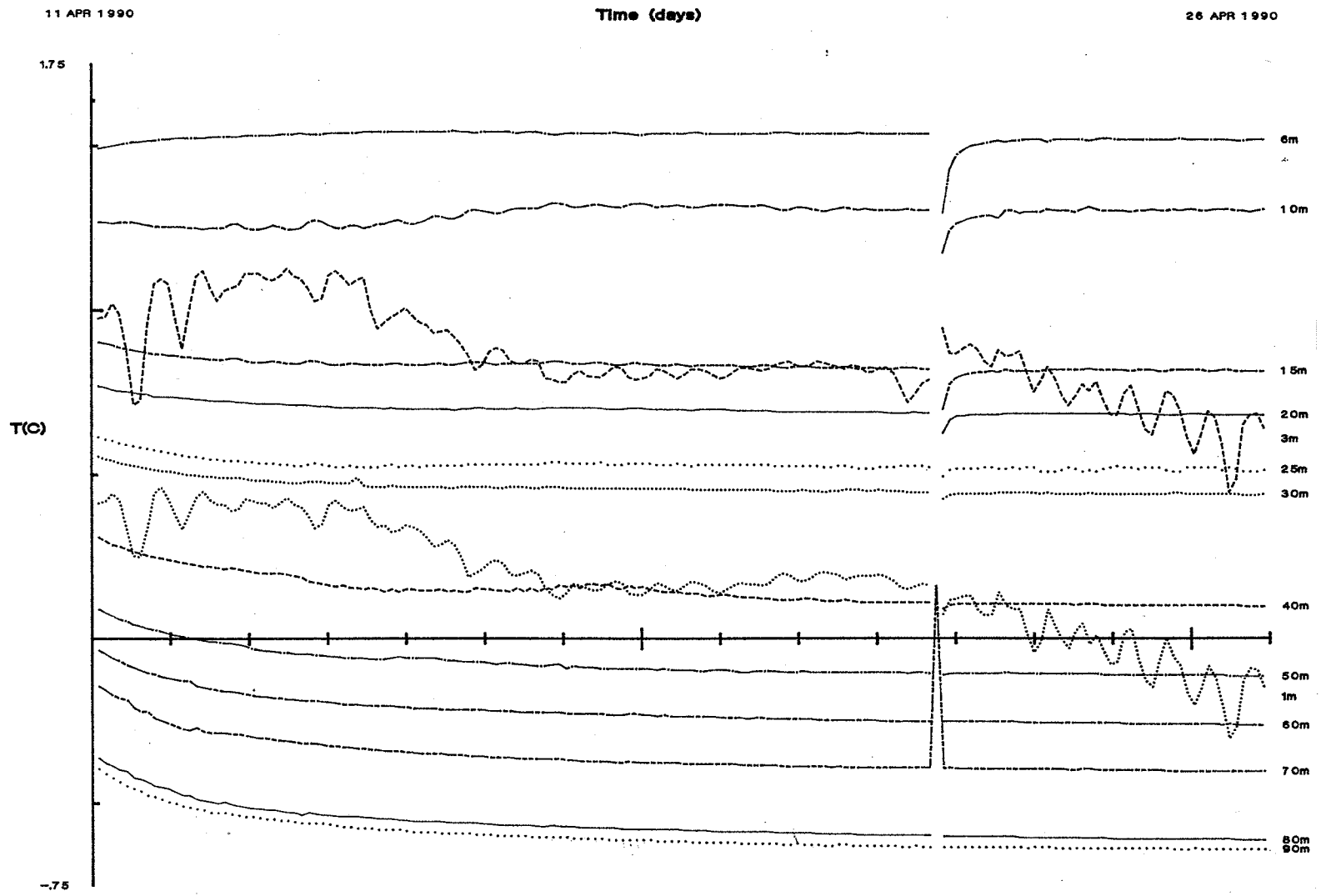

FIGURE 3.2.1 Time series of temperatures from the Seadata logger at BH2.

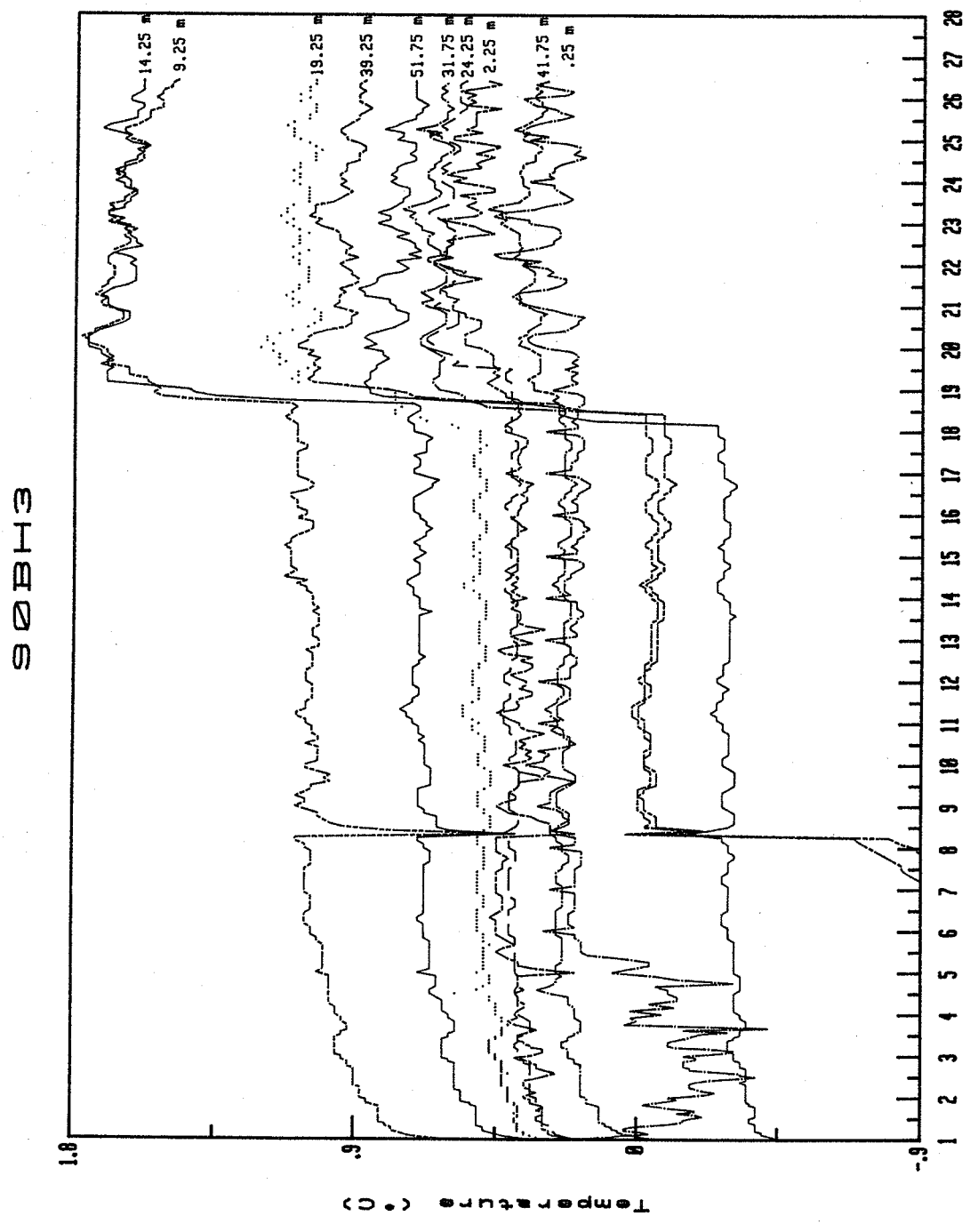

FIGURE 3.2.2 Time series of temperatures from the Brancker logger at BH3.

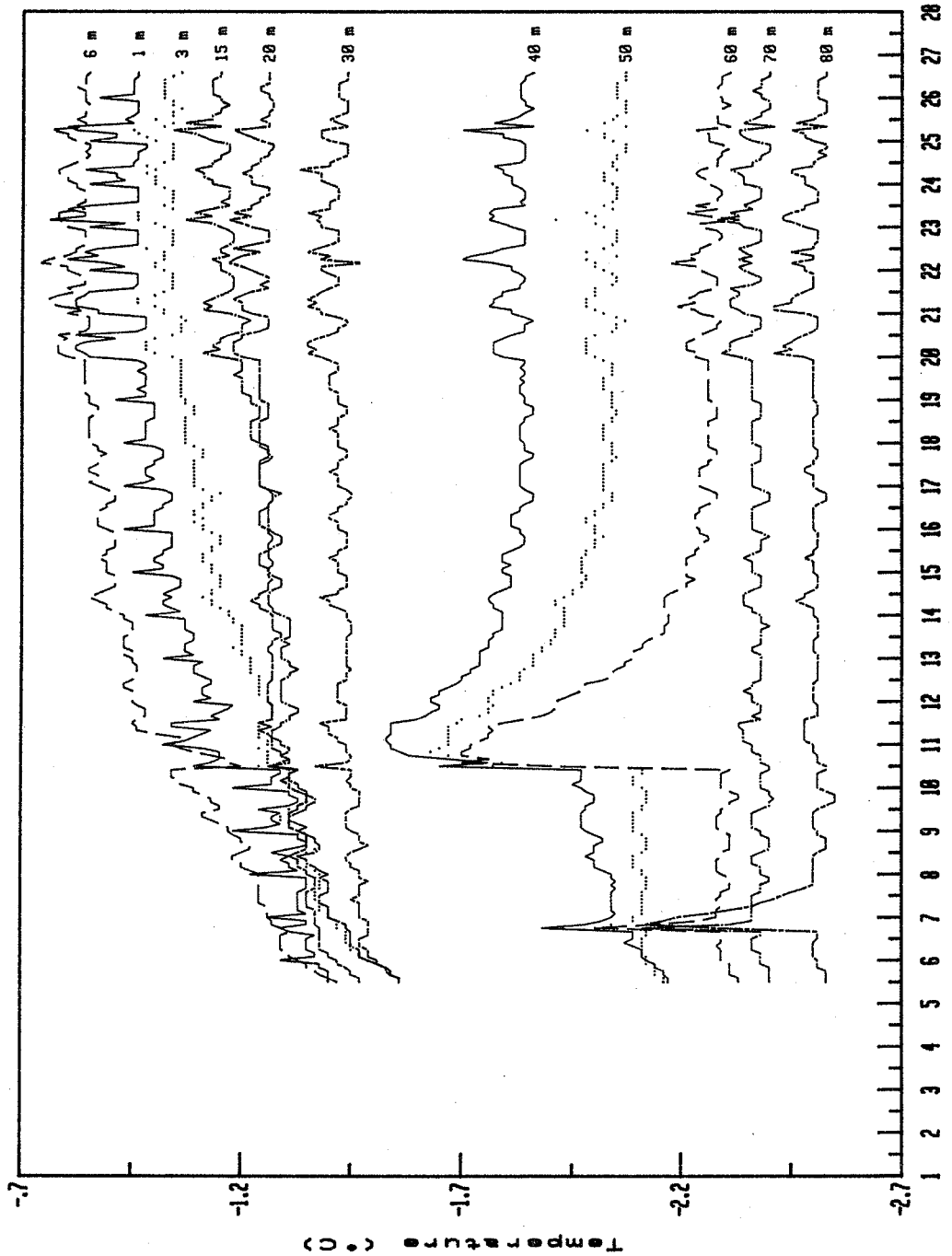

FIGURE 3.2.3 Time series of temperatures from the Brancker logger at BH5.

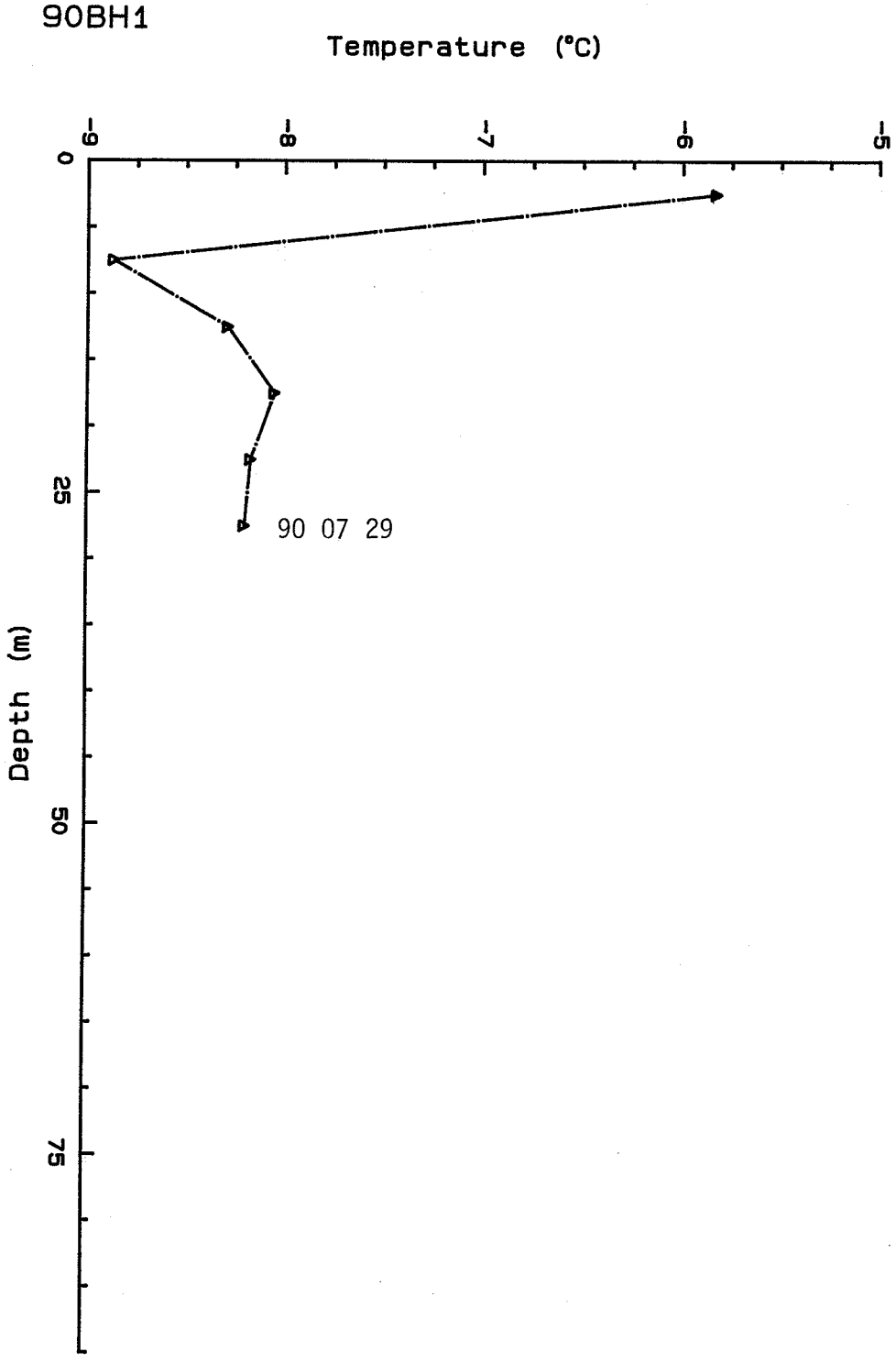

FIGURE 3.2.4 Temperature-depth plot for a measurement taken on July 29 at BH1.

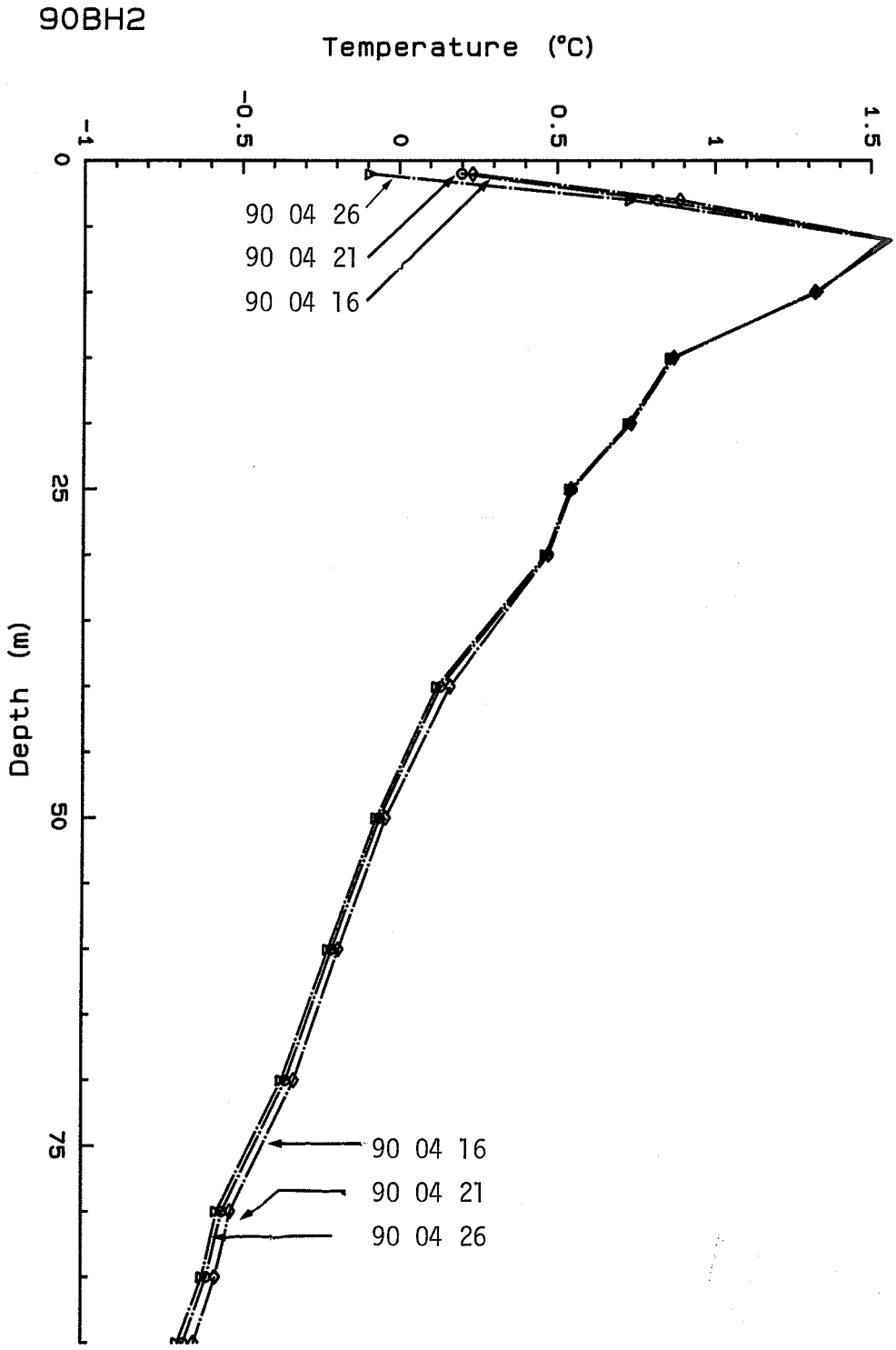

FIGURE 3.2.5 Temperature-depth plots for measurements taken on April 16, 21 and 26 for BH2.

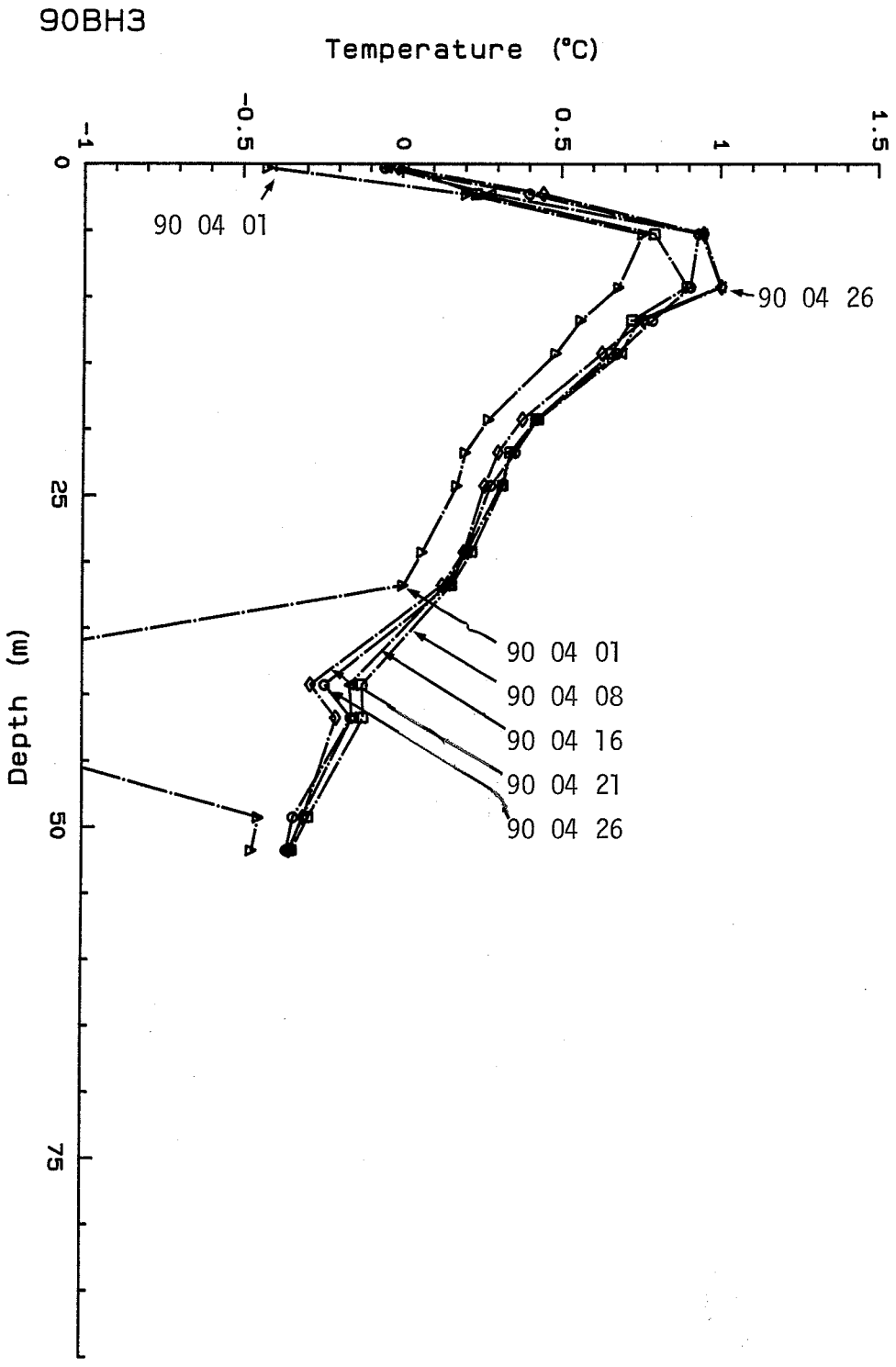

FIGURE 3.2.6 Temperature-depth plots for measurements taken shortly after installation on April 01, and on April 8, 16, 21 and 26 for BH3.

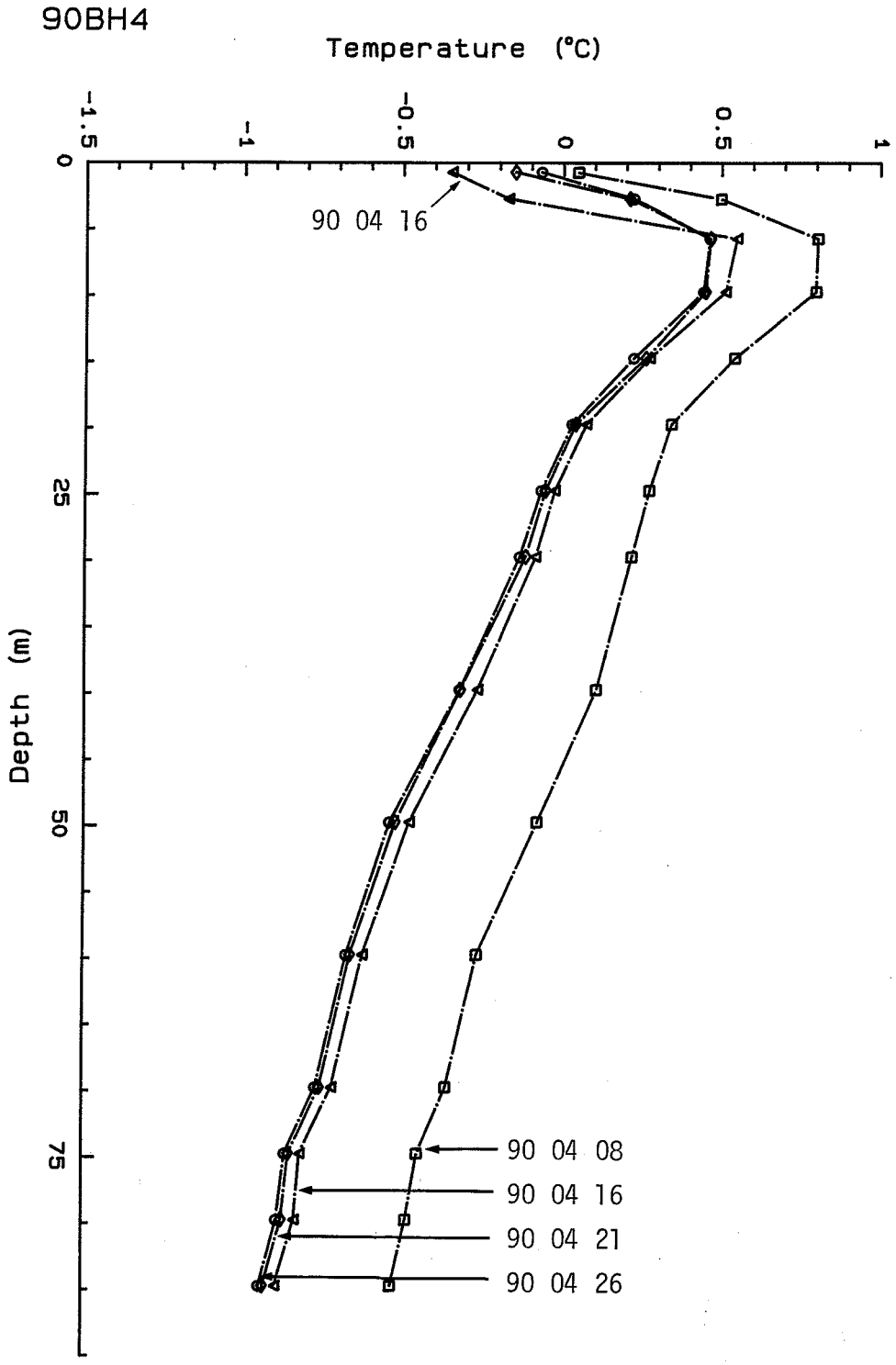

FIGURE 3.2.7 Temperature-depth plots for measurements taken shortly after installation on April 8, and on April 16, 21 and 26 for BH4.

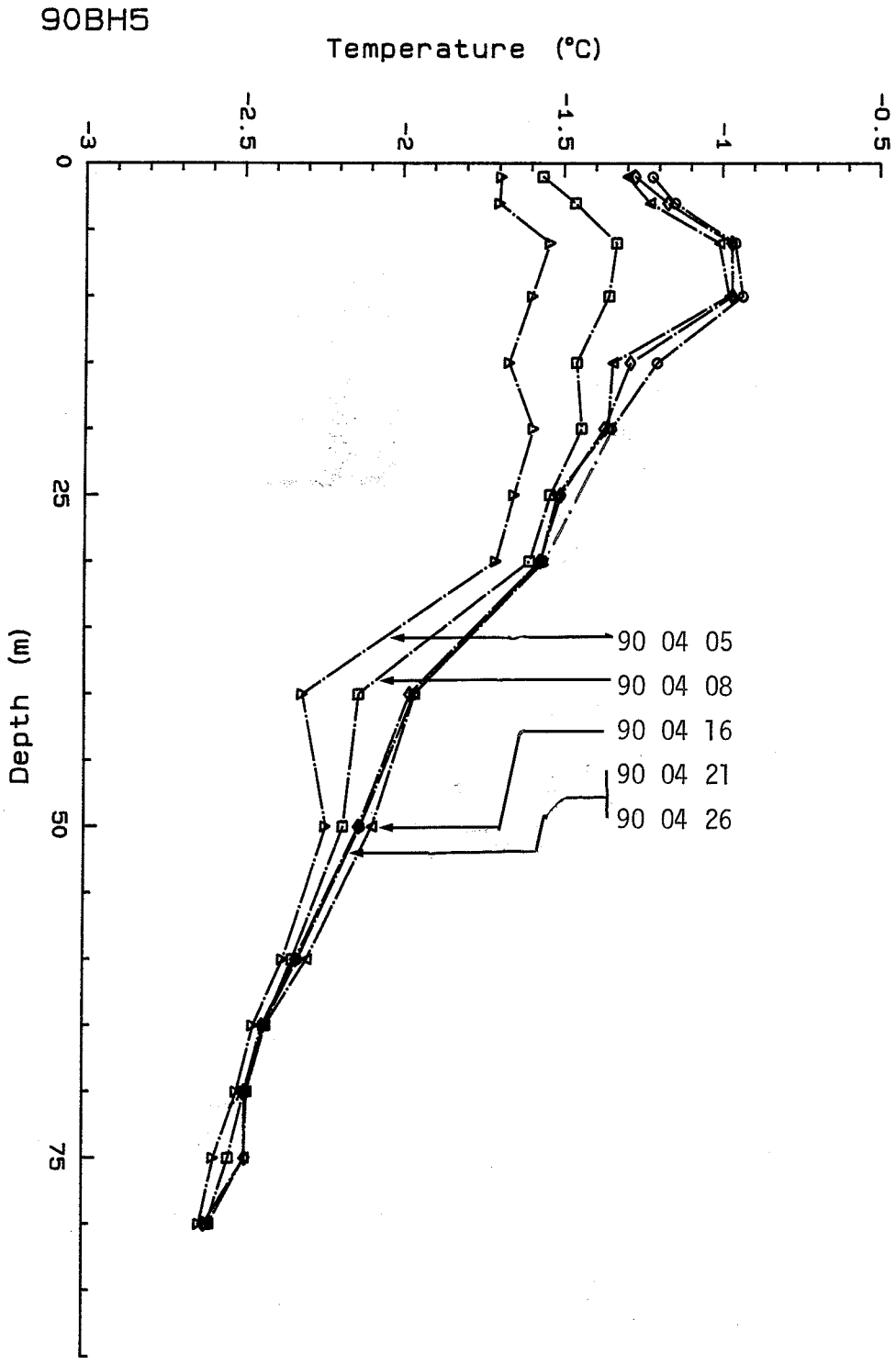

FIGURE 3.2.8 Temperature-depth plots for measurements taken shortly after installation on April 5, and on April 8, 16, 21 and 26 for BH5.

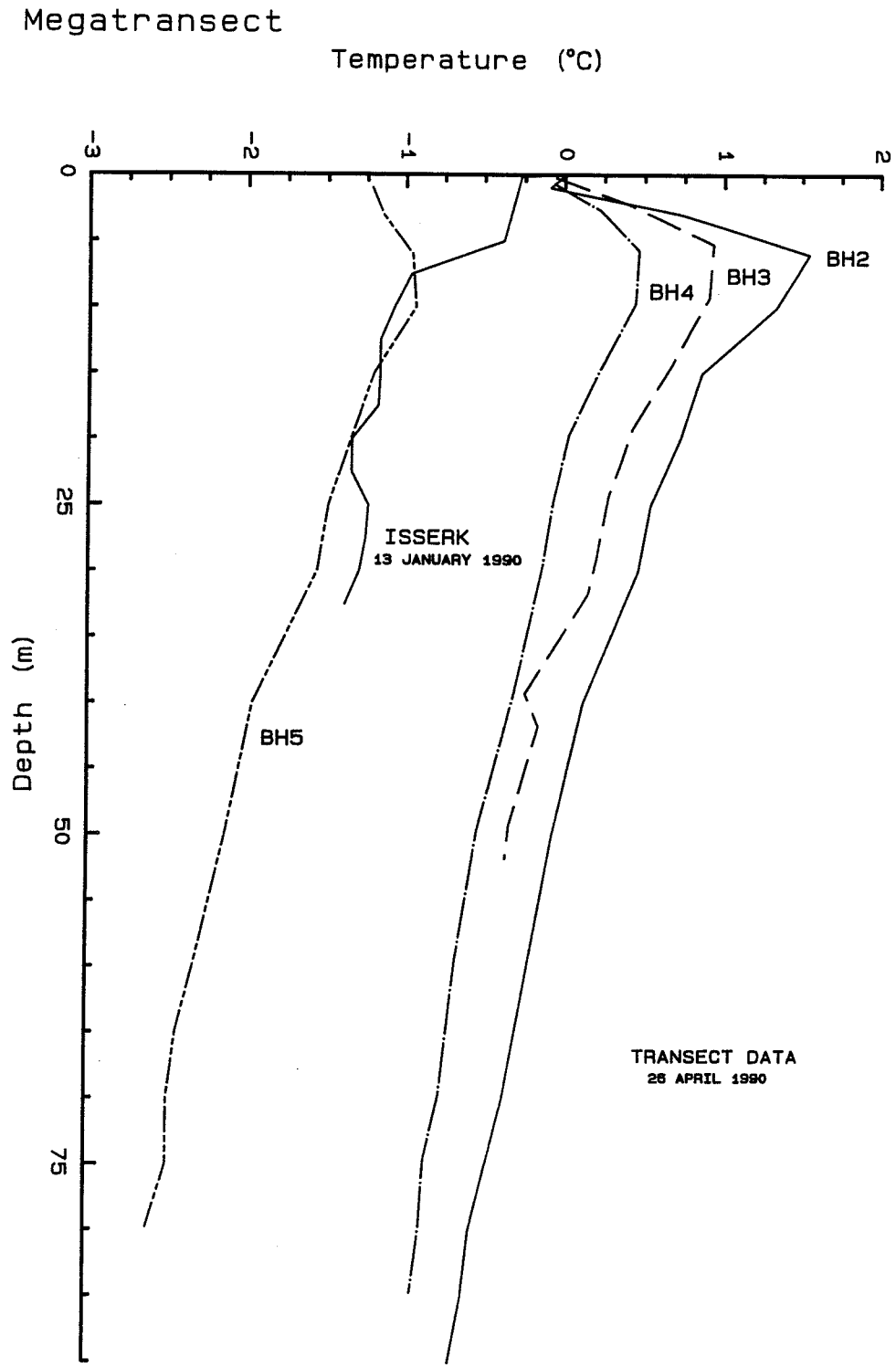

FIGURE 3.2.9 Temperature-depth plot for BH2-BH5 and Isserk.

first week, except at depths 6 and 10 m. Mud supply temperatuers were slightly positive about one third of the time during drilling of this hole (see Fig. 1.3.1). The periodic variations most noticeable in the top two sensors (1 and 3 m) appear to be related to the tidal frequency according to the record from Tuktoyaktuk (Fig. 3.2.10). The period varies, but over the 16 days represented by the data, the average is 13.3 h (1.8 cycles per day). The amplitude is less in the middle of the record, April 16-21, as is the amplitude on the tidal record. The variations at 1 and 3 m depth appear to be in phase with each other, but opposite in phase to much smaller variations between 6 and 25 m. This phase relationship would be expected if the cable were being raised and lowered in the hole, with, for instance, the upper two sensors entering a cooler regime while the deeper sensors enter a warmer regime (refer to the temperature-depth gradients in Fig. 3.2.5). However, the contrast in temperature amplitudes is disproportionately large compared with the contrast in temperature gradients if these temperature variations are to be attributed entirely to tidal lift. Also, there is poor agreement in phase with the tide record from Tuktoyaktuk. We note that the water temperature record (Fig. 3.2.11) shows a similar periodic variation approximately in phase with the Tuk tide record; this suggests some horizontal movement of water, with a mass of water having slightly higher temperatures accompanying high tide.

90BH3: Data after April 18 were noisy due to some internal electronic problem and may be disregarded; clearly the hole had attained equilibrium prior to this date (Fig. 3.2.2). Drilling cooled the borehole at all depths below 2 m. Substantial cooling is suggested around 40 m (see sensors at 39.25 and 41.75 m). This zone is also reflected in the low temperature spike in the log of April 1 (Fig. 3.2.6) and is related to depressed circulation temperatures during the drilling of this interval.

An unknown event is recorded on April 8. Temperatures in the upper 14 m temporarily decrease (except at 0.25 m), temperatures between 19 and 32 m show no change, and temperatures below 39 m increase. This is consistent with the cable being lifted and replaced to the same position (see the temperature-depth gradients in Fig. 3.2.6). The behaviour at sensors 39.25 and 41.75 is more problematical, as a long substantial trend of increasing temperatures is terminated in an abrupt, rather than asymptotic fashion on April 8. The periodic variations in all traces in Fig. 3.2.2 appear to have a 24 h cycle; see

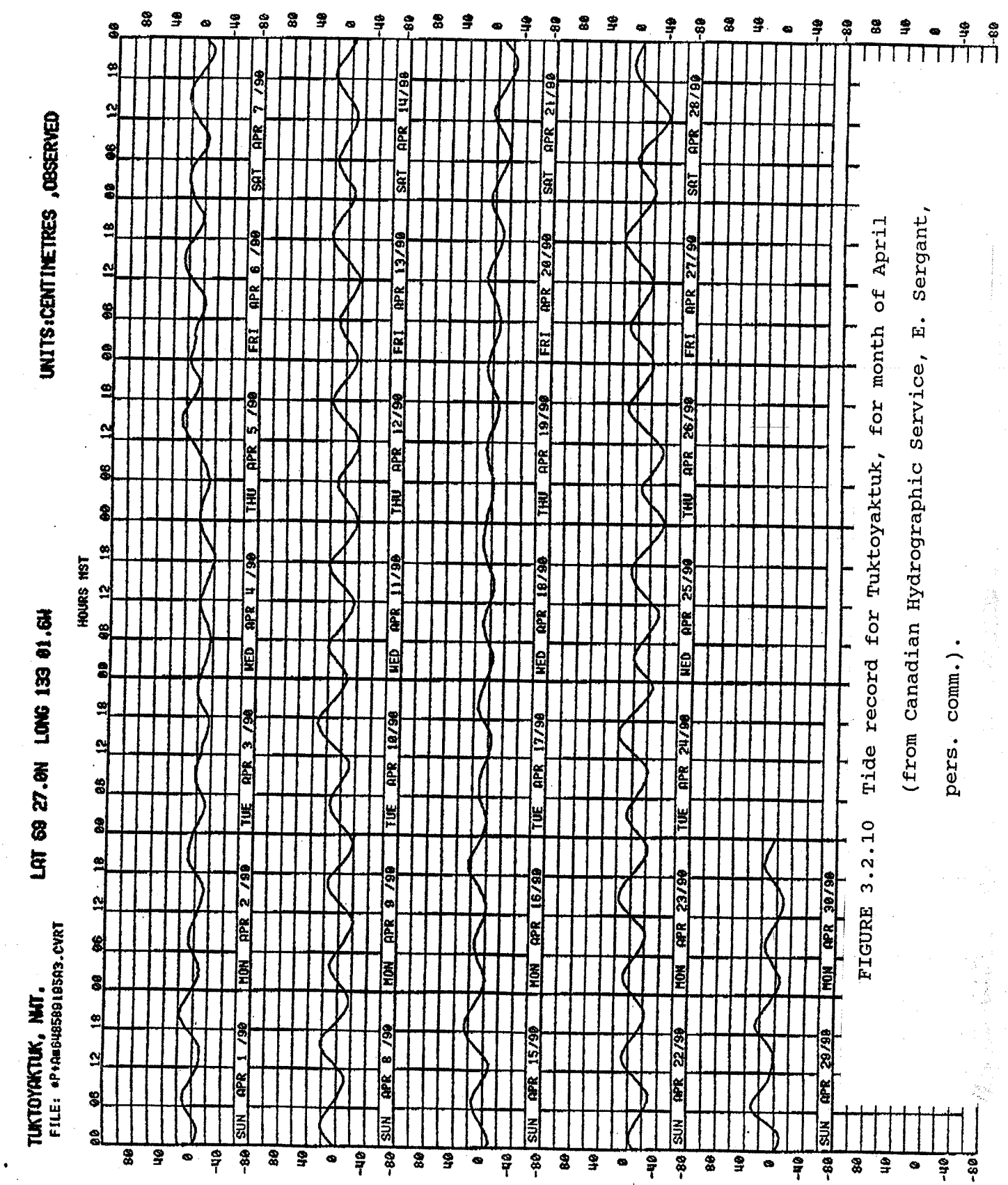

FIGURE 3.2.10 Tide record for Tuktoyaktuk, for month of April (from Canadian Hydrographic Service, E. Sergant, pers. comm.).

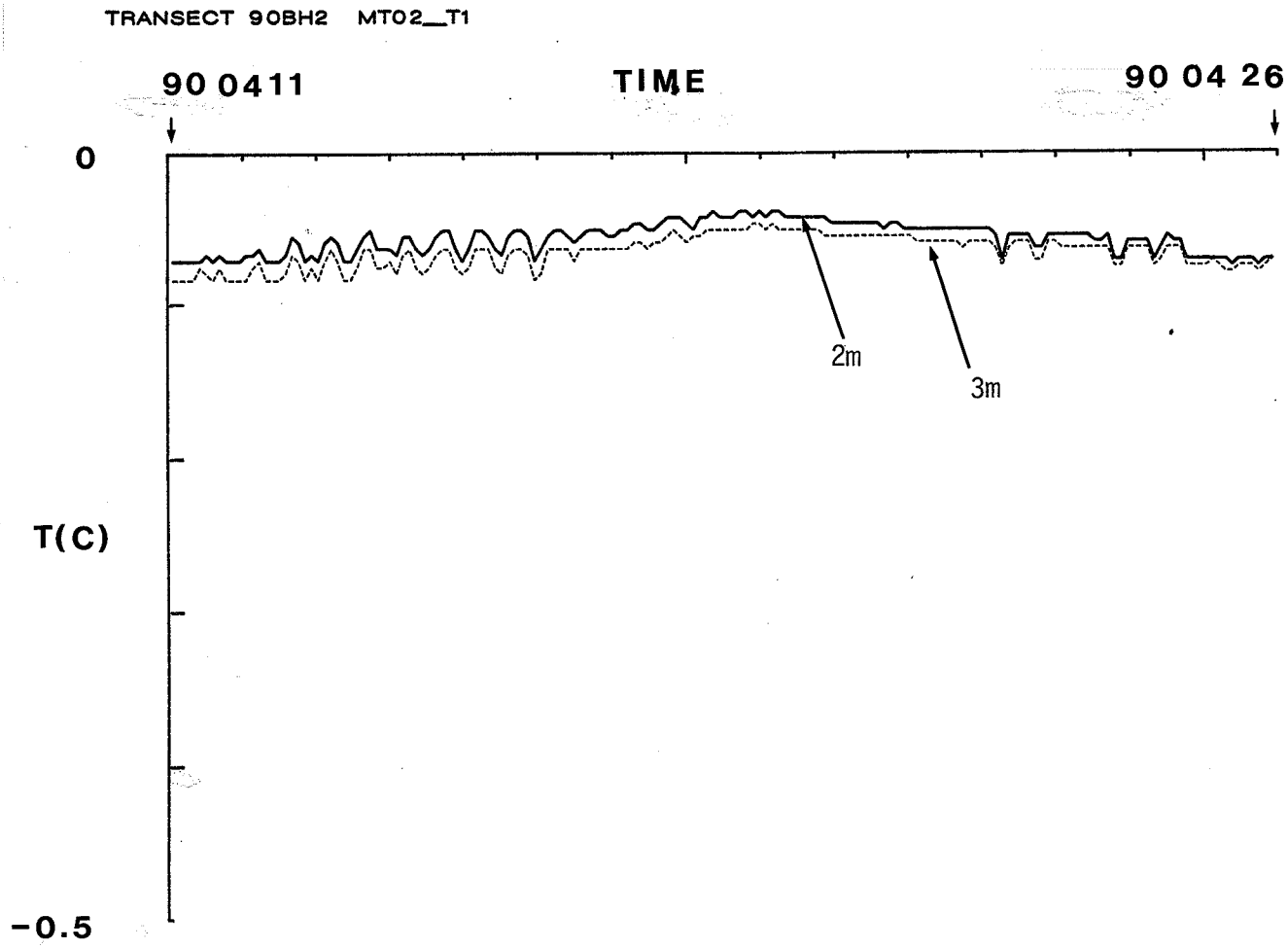

FIGURE 3.2.11 Water temperature-time series for BH2.

the discussion below for BH5.

90BH4: Fig. 3.2.7 shows that the hole cooled after the drilling, a result of positive mud supply temperatures initially, and towards the end of drilling (see Fig. 1.3.2). Subsequent seasonal warming is evident in the upper 5 m.

90BH5: Several features are apparent in the time-series (Fig. 3.2.3). Temperatures increase in the first week, a direct result of mud supply temperatures (Fig 1.3.3) significantly lower than sediment temperatures. On April 6, temperatures exhibit a sharp increase of about 0.2-0.3 K only at depths greater than 40 m. During an event on April 10, temperatures decrease 0.2 K at 6 m, and recover; decrease 0.1 K at 10 m and recover with an offset about 0.1 K higher; increase 0.1 K at 25 m and recover, and increase 0.3 to 0.5 K at 40 to 60 m and recover after several days. The event on April 10 may be a result of the cable being lifted. This may be visualized by looking at the April 8 log in Fig. 3.2.8. If the sensor at 60 m, for instance, were lifted some 20 m, it would enter a section of hole some 0.5 K higher, and hence record a temperature rise of that amount; the sensor at 30 m would experience little temperature change, since the hole was nearly isothermal above it. If the cable lifted in this fashion, the record suggests that the cable and tubing largely returned to its original position.

Composite plot: The final logs (April 26) at 90BH2 to 90BH5 are plotted in Fig. 3.2.9, along with the log from the Gulf/Esso geotechnical hole at Isserk. Temperatures just beneath the seabed are -0.1°C at 90BH2, 90BH3 and 90BH4, correlating with the bottom water temperatures between -0.1 and 0°C (Fig. 3.2.11-13). Seabed temperature at 90BH5 is -1.2°C, similar to the bottom water temperature measured there, -1.08°C. Estimates of the multidecadal long-term mean seabed temperatures may be obtained by extrapolating temperatures beneath the inversion (e.g. 15 to 50 m) to depth=0. Fig. 3.2.14 shows these relationships between bottom water temperature and long-term mean sediment temperatures. The multidecade trend in bottom water temperatures is a gradual decrease in temperatures in the offshore direction (or with increasing water depth). The larger change between 90BH4 and 90BH5 may be a reflection of the fact that the spacing between

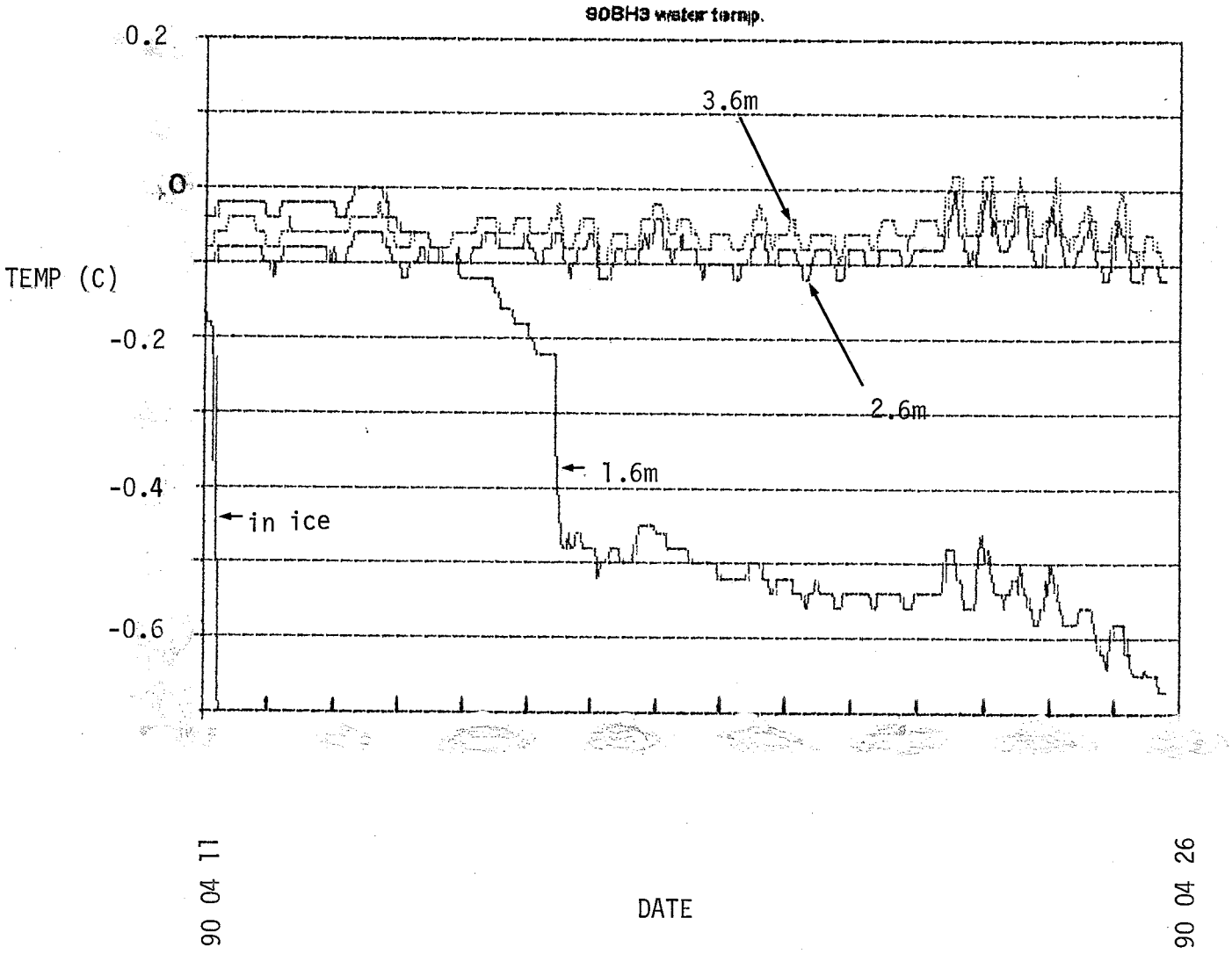

FIGURE 3.2.12 Water temperature-time series for BH3.

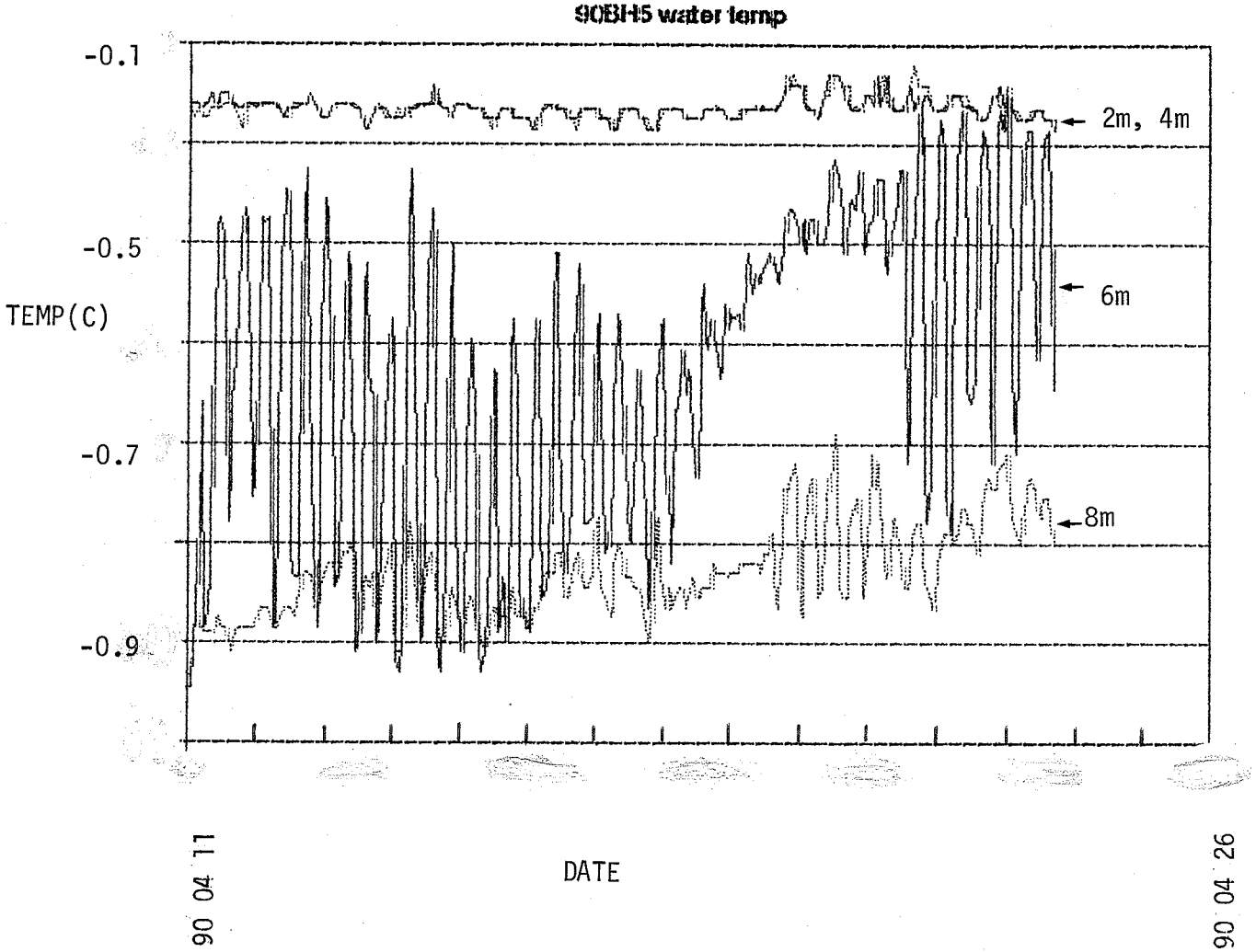

FIGURE 3.2.13 Water temperature-time series for BH5.

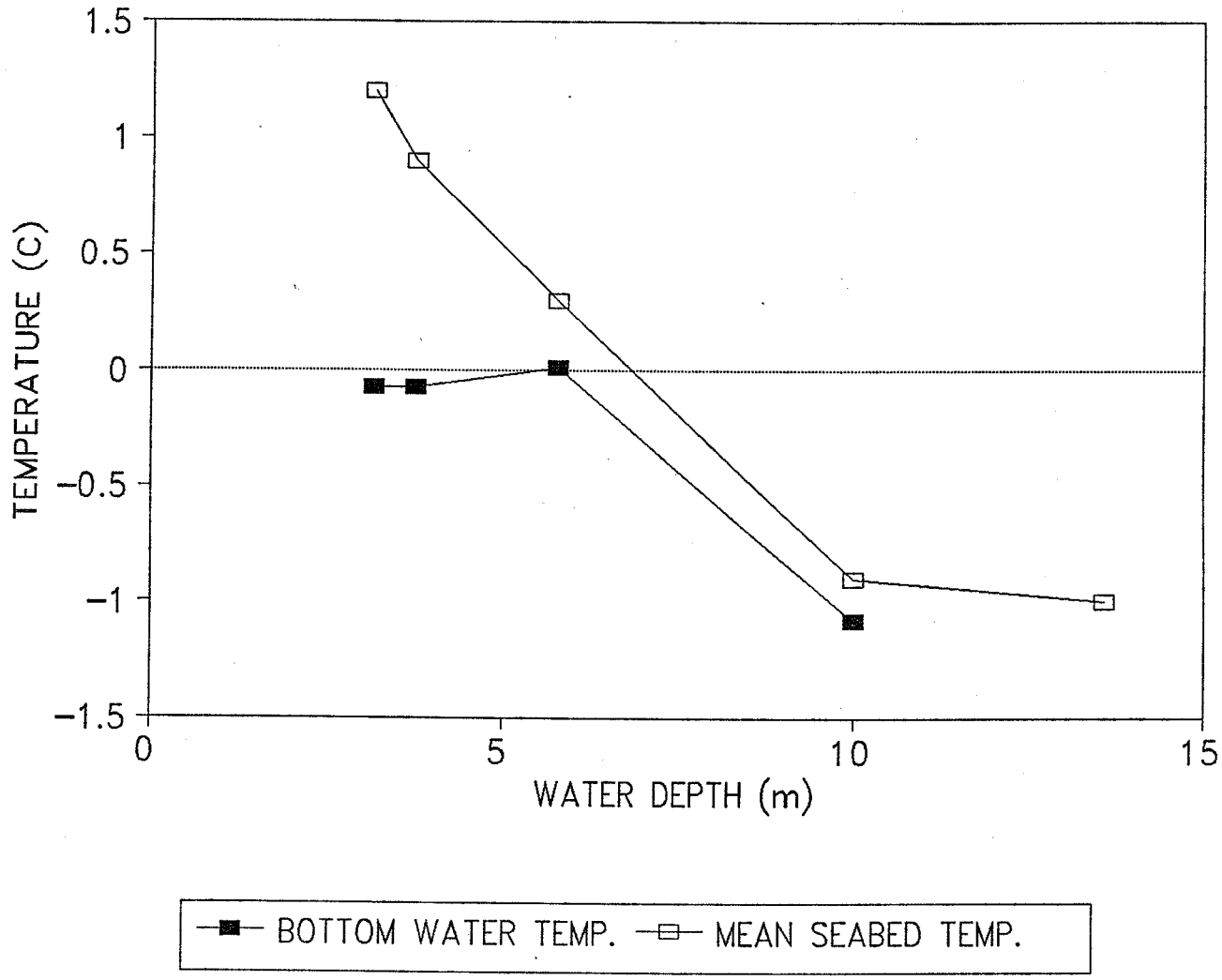

FIGURE 3.2.14 Bottom water temperatures and extrapolated mean sediment surface temperatures versus water depth.

90BH4 and 90BH5 is nearly twice that between each of 90BH2 and 90BH3 and 90BH4.

Temperatures recorded at Isserk are similar to those at 90BH5, although the temperature-depth gradient is less. The temperatures above 7 m are higher than the inversion temperature. This profile was taken while the drilling structure, the Molikpaq, was still on location. The higher temperatures reflect the late summer temperatures preserved by the several metres of sand fill placed on the seabed near the end of the previous September.

3.3 THERMAL CONDUCTIVITY

A. Wilkinson and A.E. Taylor

3.3.1 Introduction

Thermal conductivity - a measure of the ability of materials to conduct heat - was measured as a component of the onshore-offshore transect project. Thermal conductivity may be measured by the comparative steady-state method using the divided bar (Jessop, 1990). However, the absolute transient needle probe method, as originally reported by von Herzen and Maxwell (1959), is better suited to soft, or partially lithified, sea-bottom sediments.

The latter method was used both at the drill site and in the laboratory at the Inuvik Research Centre. A commercially available unit was used in the field (Thermal Property Analyzer, model 600 made by Geotherm Inc. of Uxbridge, Ontario). A system developed in-house by Taylor and Allen (1986), and Taylor, Allen and Sidhu (1990, in preparation) was used in Inuvik. The latter system was designed in-house based on the HP 200 computer and SQL software. The needle-probe method is an absolute technique with the system and software standardized by using the known conductivity of water (0.59W/mK at room temperature). With the needle probe, as with other methods, sampling should be spaced along the cores to provide a statistically valid representation for the stratigraphy. Nevertheless, unknown variability in minerals, water content, salinity, temperature and pressure make this difficult to achieve (Jessop 1990).

3.3.2 Test program

Thermal conductivity, and Time Domain Reflectometry measurements were made on selected core samples in the field, particularly for those considered thermally sensitive. About 120 field conductivity measurements were made in the end of each core section by J. Ogilvie. All cores were transported subsequently to the Inuvik laboratory for further analysis.

On the basis of in situ core recovery temperatures it was determined that cores would be stored, and their thermal conductivities measured, in three thermal environments: frozen, around -8°C; unfrozen around +2°C; and thermally sensitive (or partially-bonded) around -

2°C. Ratcliffe (1960) recommends a temperature correction (a reduction of 0.3% per degree of excess temperature) if the thermal conductivity measurement is not carried out at the recovery temperature. The correction is small for the recovery-to-laboratory temperature differences in the onshore-offshore transect analyses, at conditions close to the phase change, thermal conductivities and other physical properties of sediments are highly temperature-dependent.

Monitoring of the thermal history of the sediment samples was difficult in transport. After receiving the samples in Inuvik, it was essential to allow them to return to equilibrium in a thermally controlled environment prior to running the needle probe measurements. Two modified domestic freezers were used for "active" needle probe measurements. They were set up in Room 110 so that they were accessible for the probe leads and data acquisition units. A third freezer and a scientific Revco freezer were located in the shipping bay. These acted as holding compartments for incoming unfrozen, and partially bonded cores, respectively. Well-frozen cores were kept in the cold room at -8°C until their thermal conductivities were measured in the active freezers which were reset to -8°C after the warmer cores had been measured.

The cores were placed horizontally in the appropriate thermal category freezer. Advance notice of the time of arrival of the cores and the core temperature at the drill site allowed laboratory personnel to fine-tune the active freezers using a thermal mass of ice/water pails. This shortened the time required for the cores to reach thermal equilibrium and, hence, the delay before the cores were released for subsequent acoustic testing, sedimentological logging, and physical property tests. Ideally a shipment would fill an active freezer; if not then thermal mass water/ice pails were left in the freezer under the horizontal cores. Before closing the freezer a suite of nine holes was drilled with a 6 cm long by 0.5 mm diameter bit through the PVC casings, and into the sediments if frozen, in order to receive needle probes of the same dimensions. Usually 3-4 cores were drilled at 20-30 cm intervals. Each probe contained a thermistor bead half-way down a heater wire loop.

Attaining thermal equilibrium often took several hours in which time the freezers were not opened. The internal temperatures of the freezers (and the room) were monitored every four hours using a portable YSI thermometer which was connected sequentially to

the thermometer sensor cable leading out of each freezer.

Thermal equilibrium was monitored at each sensor position. When the ambient temperature change of the core at each probe in the suite was low compared to the temperature rise due to the calibrated heat input, the acquisition unit began the run. The first two minutes of the program recorded the ambient temperature change at each probe location to enable correction for any residual temperature drift. After two minutes a calibrated unit of heat (from a current of approximately 100 ma) was applied to each probe for six minutes and the temperature of the sediment, as the heat accumulated and decayed, recorded as a function of time. The temperature rise is indirectly proportional to the thermal conductivity of the sediment in which the probe is placed. Occasionally, when repeated measurements were done, it was noted that the conductivity of frozen samples tended to increase with successive measurements. This may have arisen from a modification of the ice-bonded sediment in contact with the probe, and so, generally, only the initial measurement was considered representative.

After completion of each run the probes were removed, and the holes in the casing were taped to prevent moisture loss. The three or four cores were then transferred, if frozen, for acoustic testing in the cold room, or directly to the sedimentology team in the shipping bay work area.

It was agreed that when the duration to reach thermal stability for geothermal measurements would hold up unduly other thermally destructive analysis then a 15 cm section of each core was cut out and retained intact in its freezer for later geothermal testing. This procedure was only necessary for about ten cores because of the delivery rate of cores and the co-operation of the other analyses teams. Approximately 600 thermal conductivity measurements were made in the Inuvik Research Centre laboratory.

3.3.3 Results

Data from each borehole were compiled in spreadsheets (see Appendix C) according to depth, lithology, geological unit and test conditions. From these data sets various plots were drawn and are presented here. Graphs of thermal conductivity against depth (to 100 m) for each borehole, indicate that the majority of measurements were made in sediments down to 60 m, predominantly in the 30 - 50 m range (Fig. 3.3.1-3.3.6). In

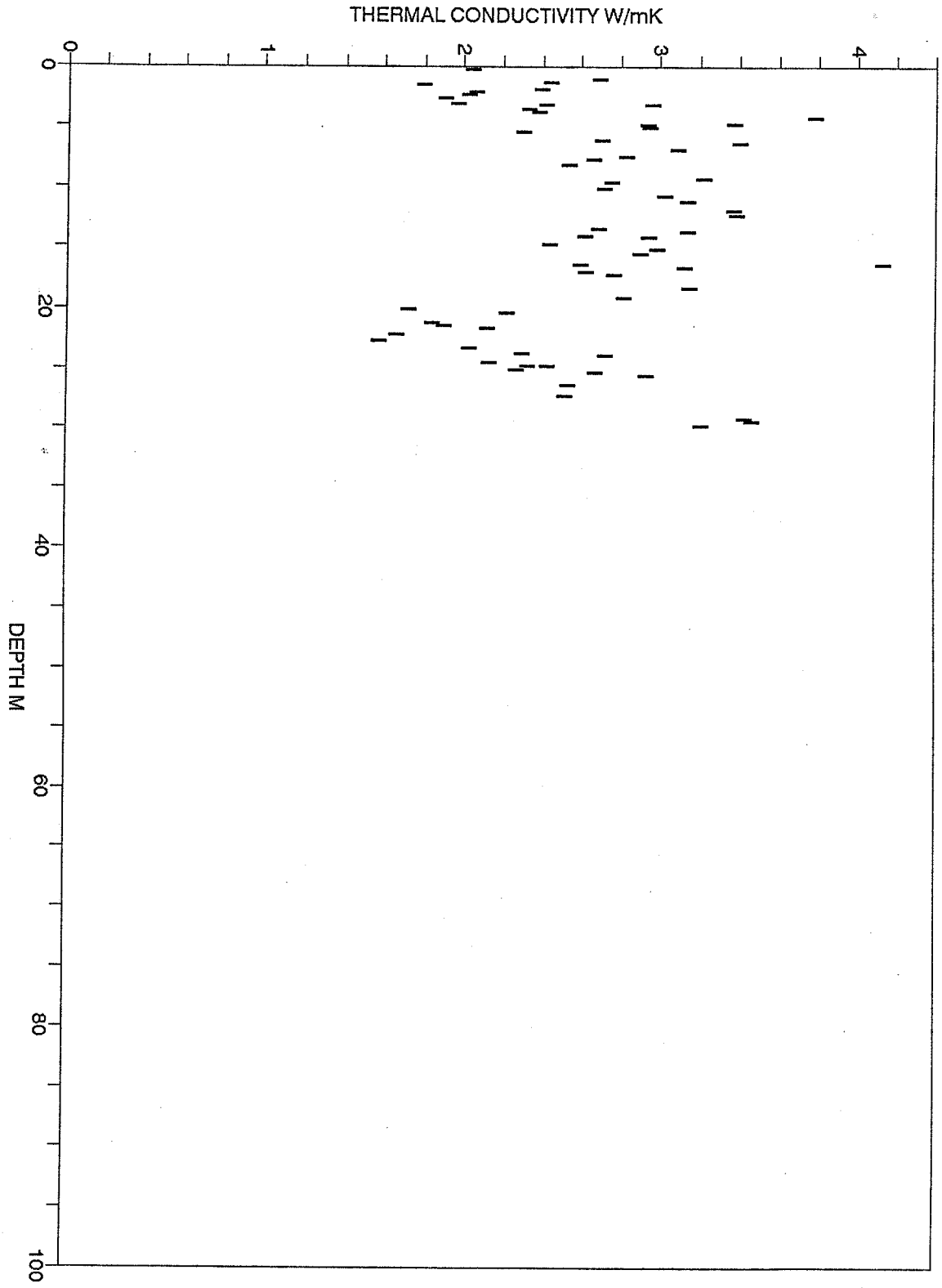

FIGURE 3.3.1 Thermal conductivity vs. depth for BH1

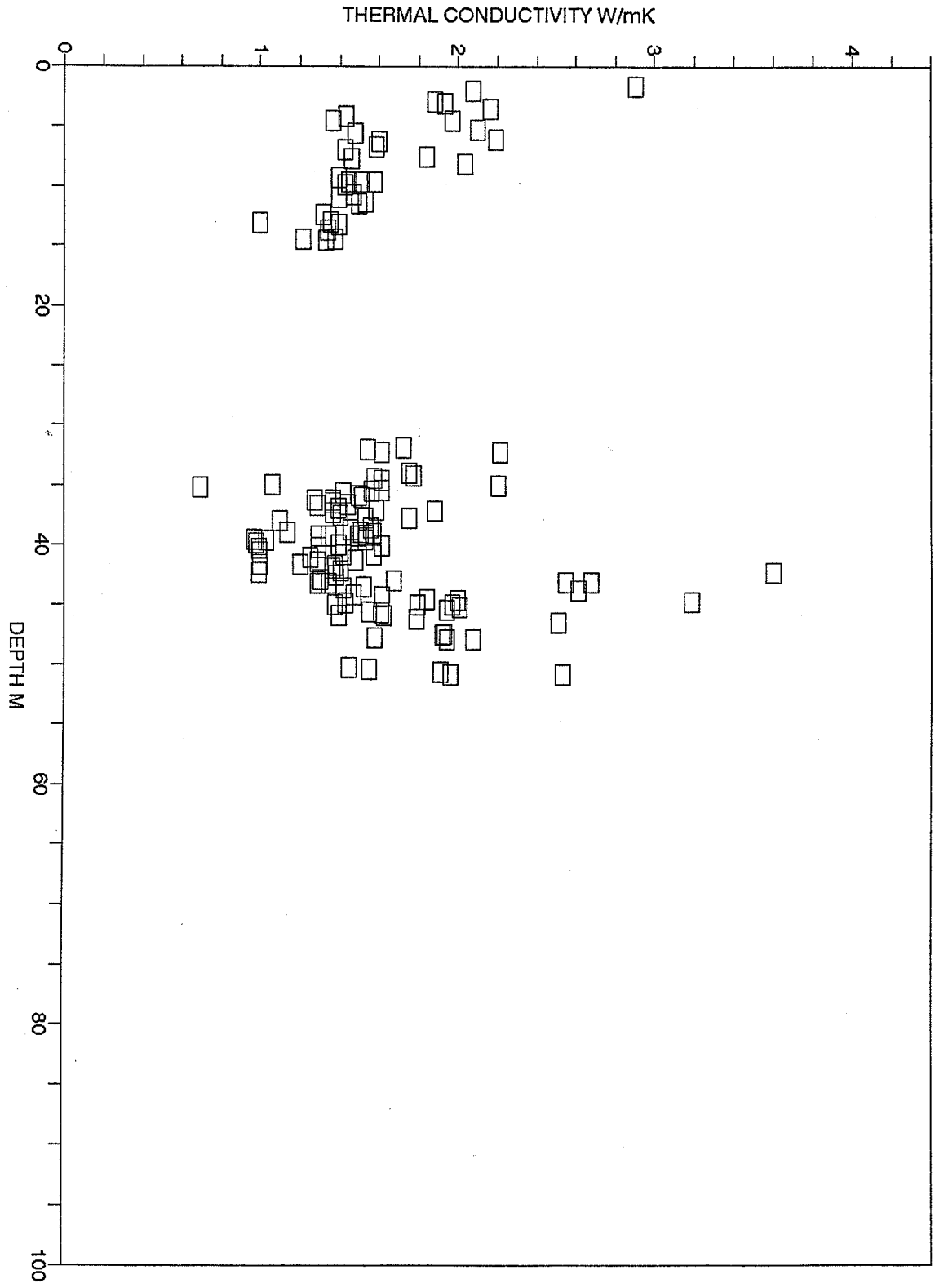

FIGURE 3.3.2 Thermal conductivity vs. depth for BH2.

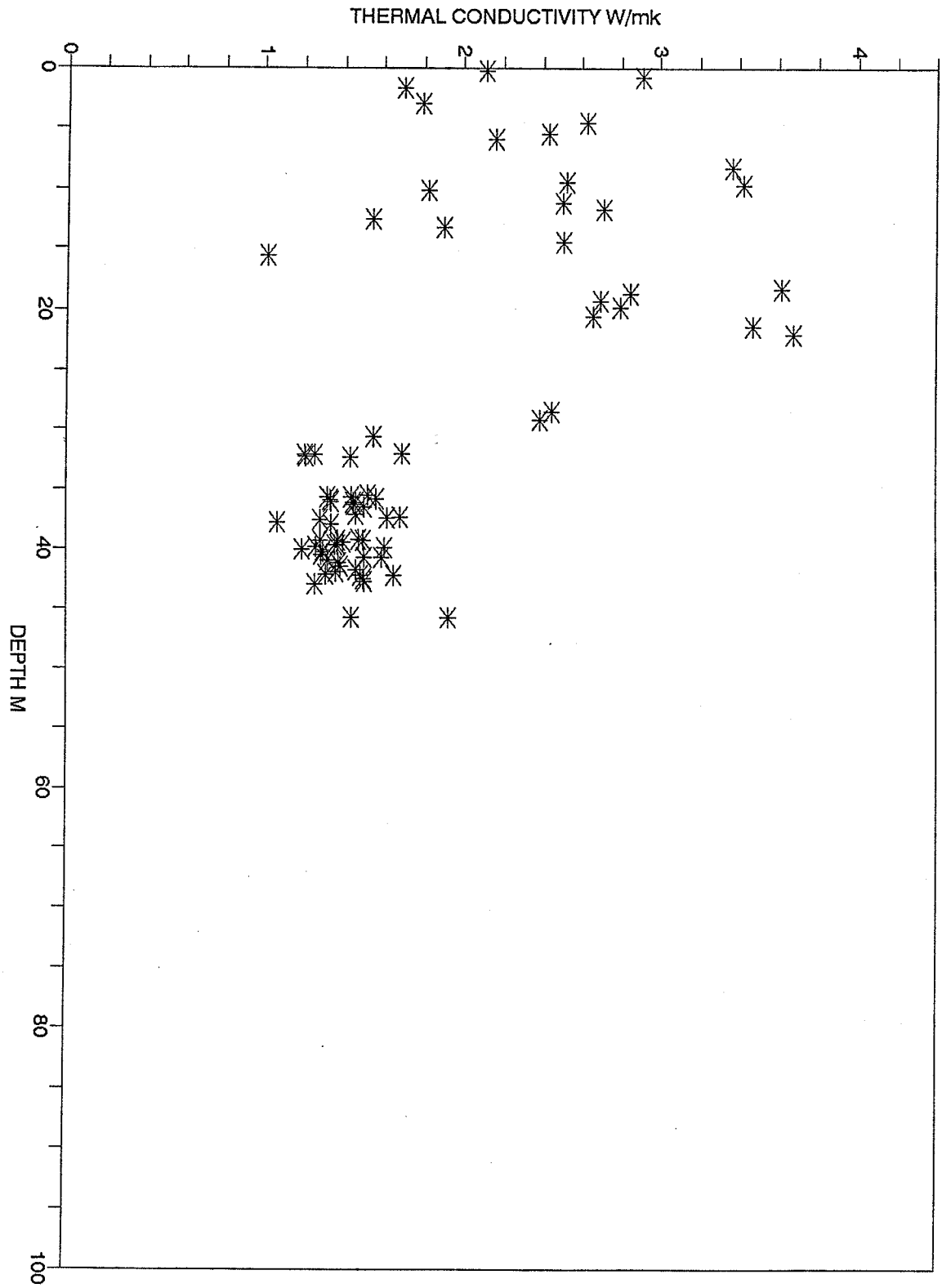

FIGURE 3.3.3 Thermal conductivity vs. depth for BH3.

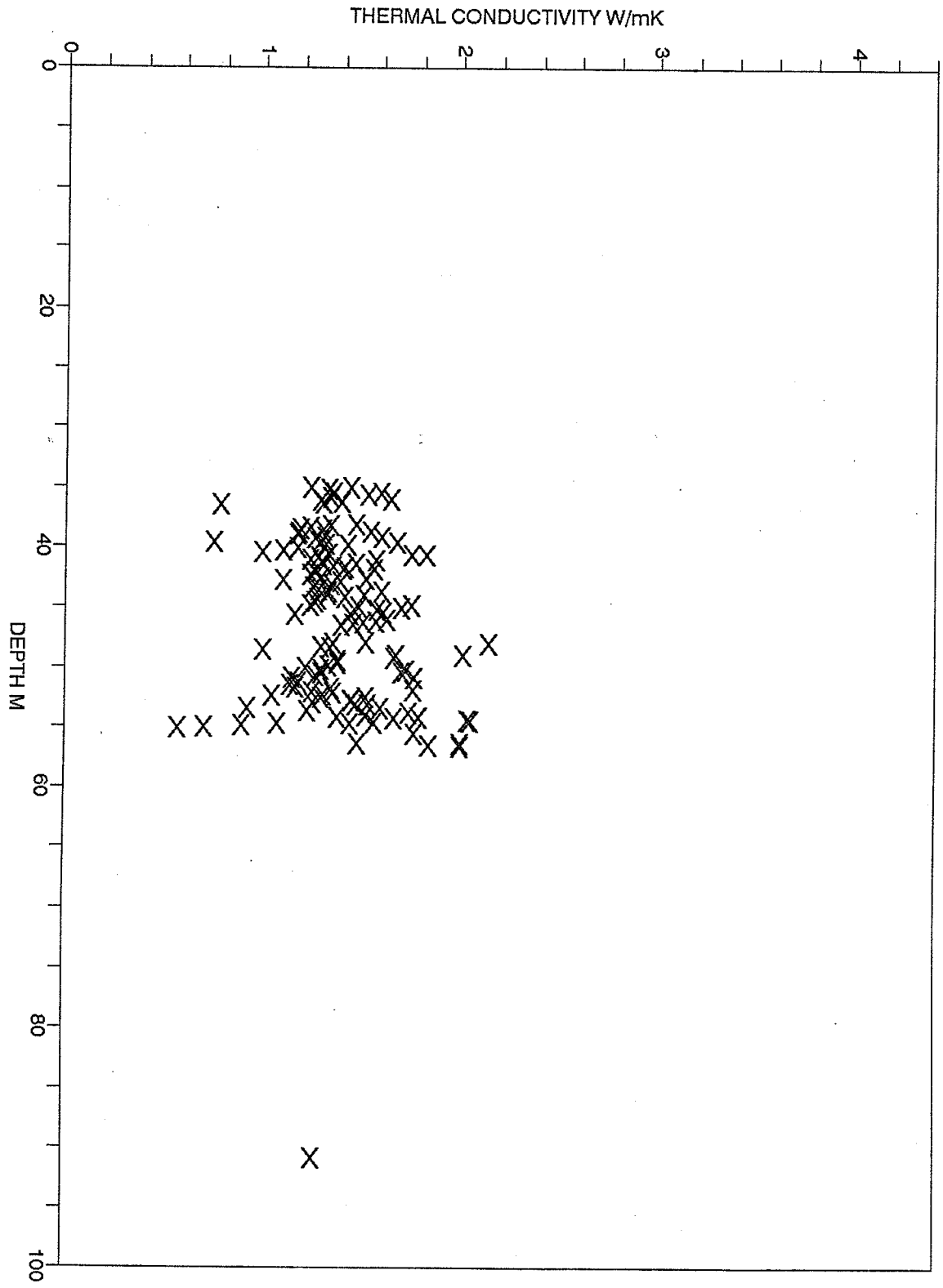

FIGURE 3.3.4 Thermal conductivity vs. depth for BH4.

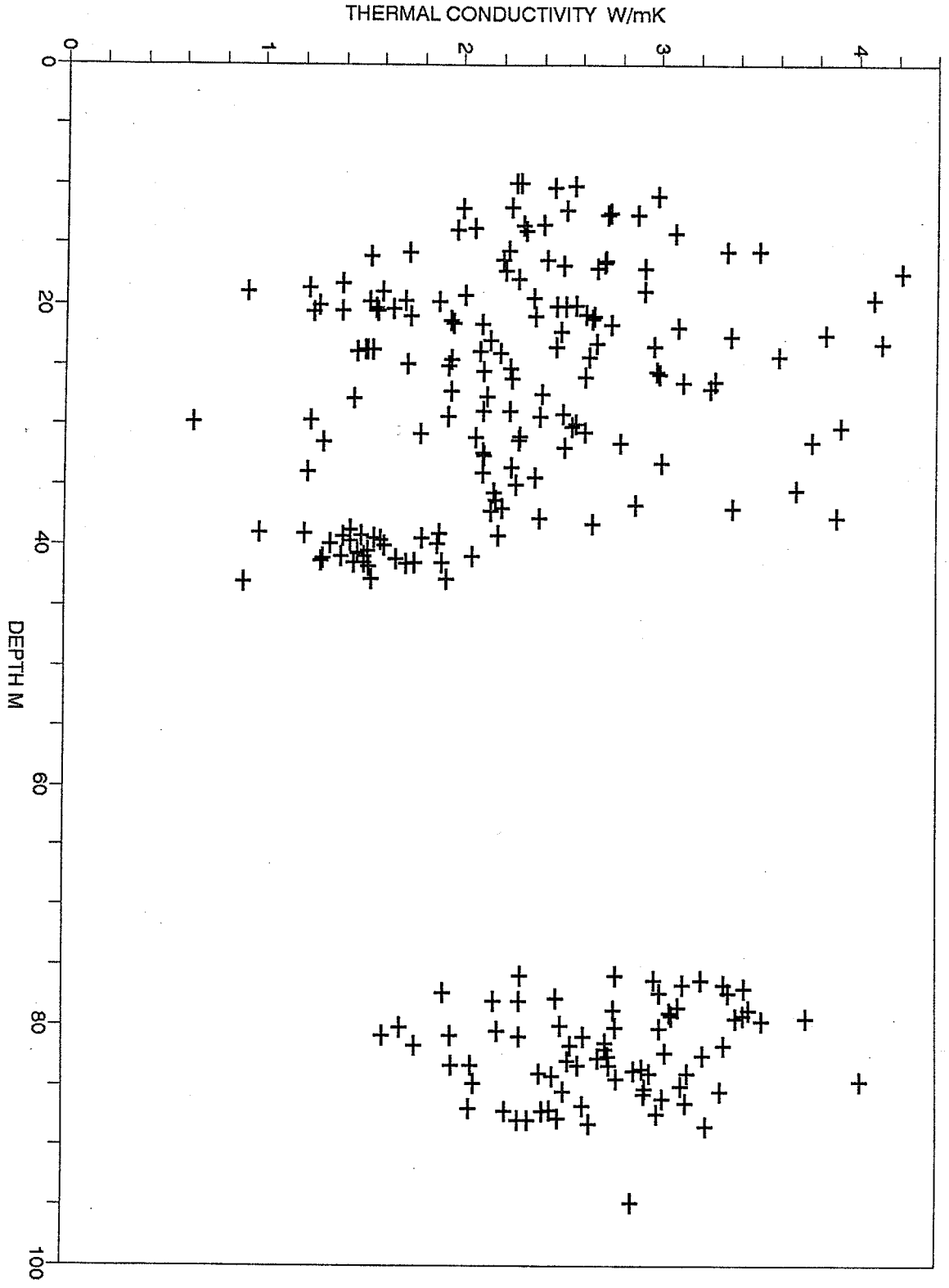

FIGURE 3.3.5 Thermal conductivity vs. depth for BH5.

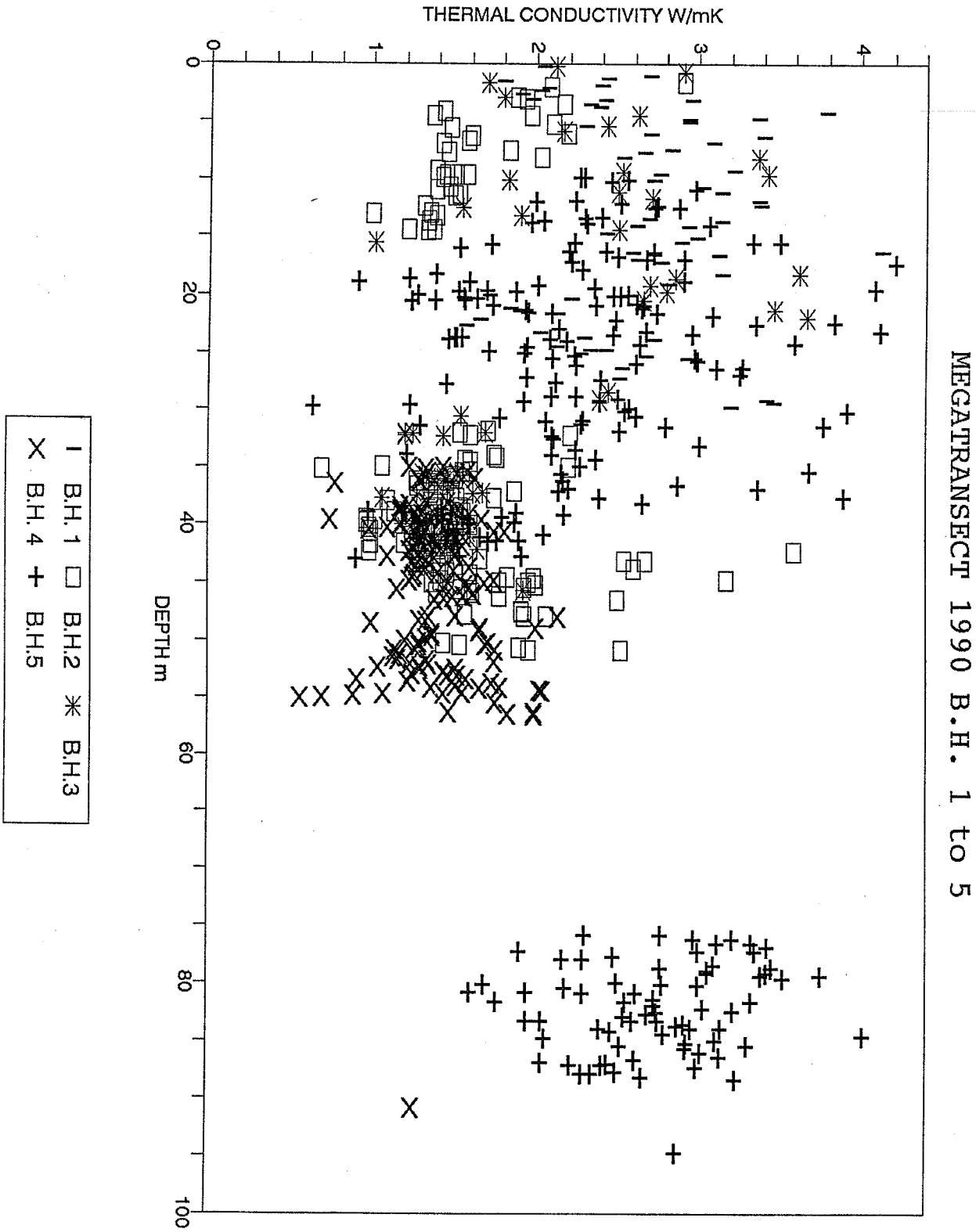

FIGURE 3.3.6 Thermal conductivity vs. depth for BH1-BH5.

addition, these data are presented in less detail on the summary logs (Appendix A), allowing review of lithology and ice-bonding conditions.

The average thermal conductivity of each geological unit for each borehole is shown in Table 3.3.1. The marine clays (unit D) show an average thermal conductivity of 1.49 W/mK. By contrast Unit C (glaciofluvial/deltaic sands) shows an average conductivity of 2.26W/mK. It should be noted in particular, that higher conductivities generally occur in the more frozen sediments of boreholes 1 and 5. Thermal conductivity of ice is almost four times that of water and may explain the higher conductivities in the frozen sediments.

Frequency distributions of the principal sediment types within each core are plotted (Fig. 3.3.7-3.3.11). The reader should note the higher conductivities of the coarse grained sand and the lower thermal conductivity of the large proportion of silty clay, probably associated with their higher water contents and finer grain size.

The transect thermal conductivities support the 1981-1983 conclusions on shallower samples from the Beaufort Shelf (Taylor and Allen 1987). They found shallow sediment conductivities up to 50% higher than those reported for deep-ocean sediments. At this stage of analysis the mineral content (e.g. quartz and clay fractions), grain size and ice-bonding would appear to be the major determinant of thermal conductivities in the sediments in the onshore-offshore transect.

MEGATRANSECT 1990

TABLE 3.3.1. Average thermal conductivities and test conditions for Megatransect boreholes 1-5

BH #	UNIT	AVERAGE CONDUCTIVITY W/mK	STANDARD DEVIATION W/mK	TEST CONDITIONS
1	B			
2	B	1.62	0.37	unfrozen
3	B	2.55	1.22	unfrozen
4	B			
5	B			
ALL	B	2.08		
1	C	2.65	0.54	frozen
2	C	1.61	0.04	unfrozen
3	C	2.33	0.89	unfrozen
4	C			
5	C	2.45	0.82	frozen
ALL	C	2.26		
1	D			
2	D	1.48	0.43	unfrozen
3	D	1.43	0.15	unfrozen
4	D	1.34	0.19	unfrozen
5	D	1.56	0.28	frozen
ALL	D	1.49		
1	E			
2	E	1.86	0.40	frozen
3	E			
4	E	1.45	0.31	unfrozen
5	E	2.79	0.58	frozen
ALL	E	2.03		

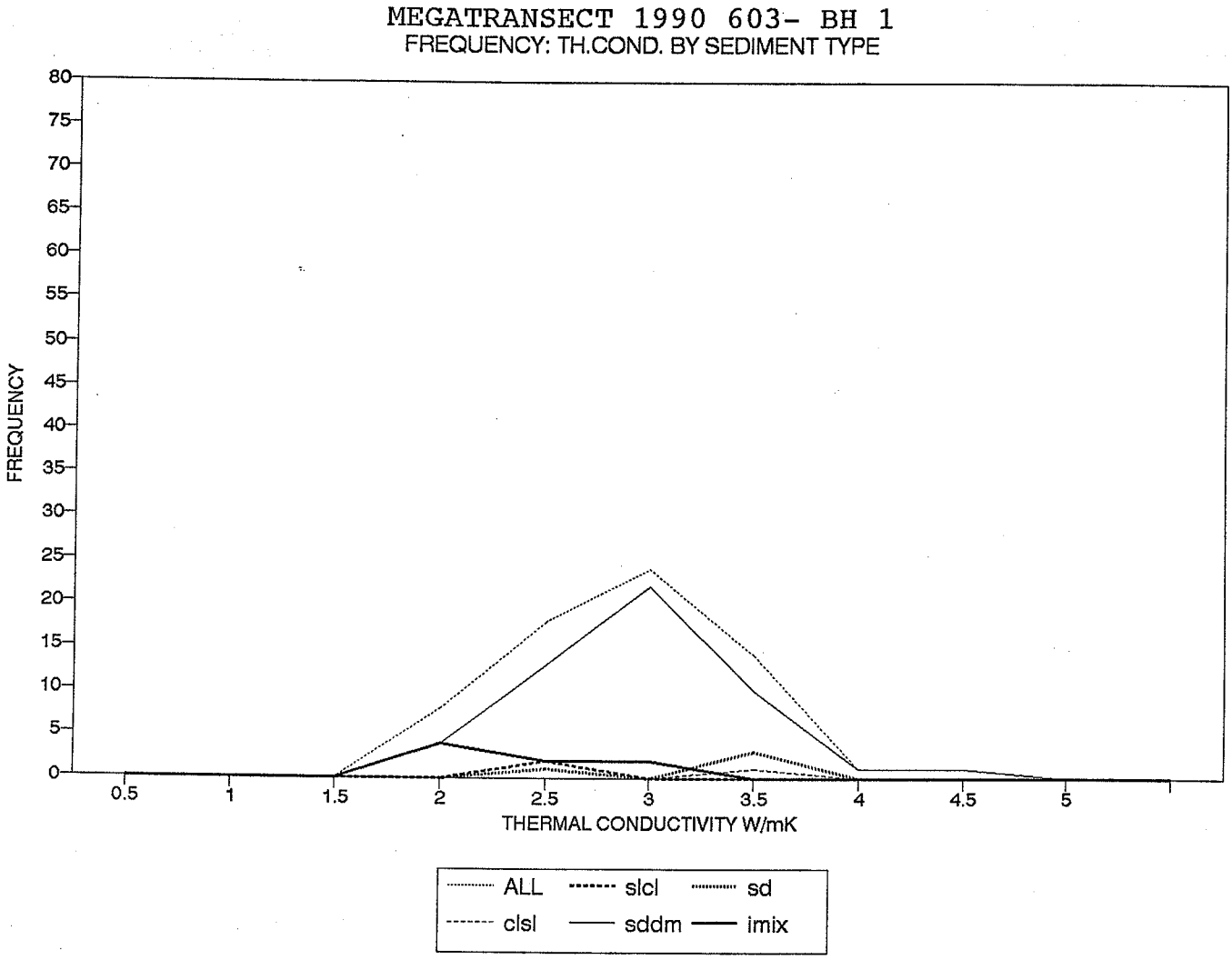

FIGURE 3.3.7 Frequency of thermal conductivity values by sediment type for BH1.

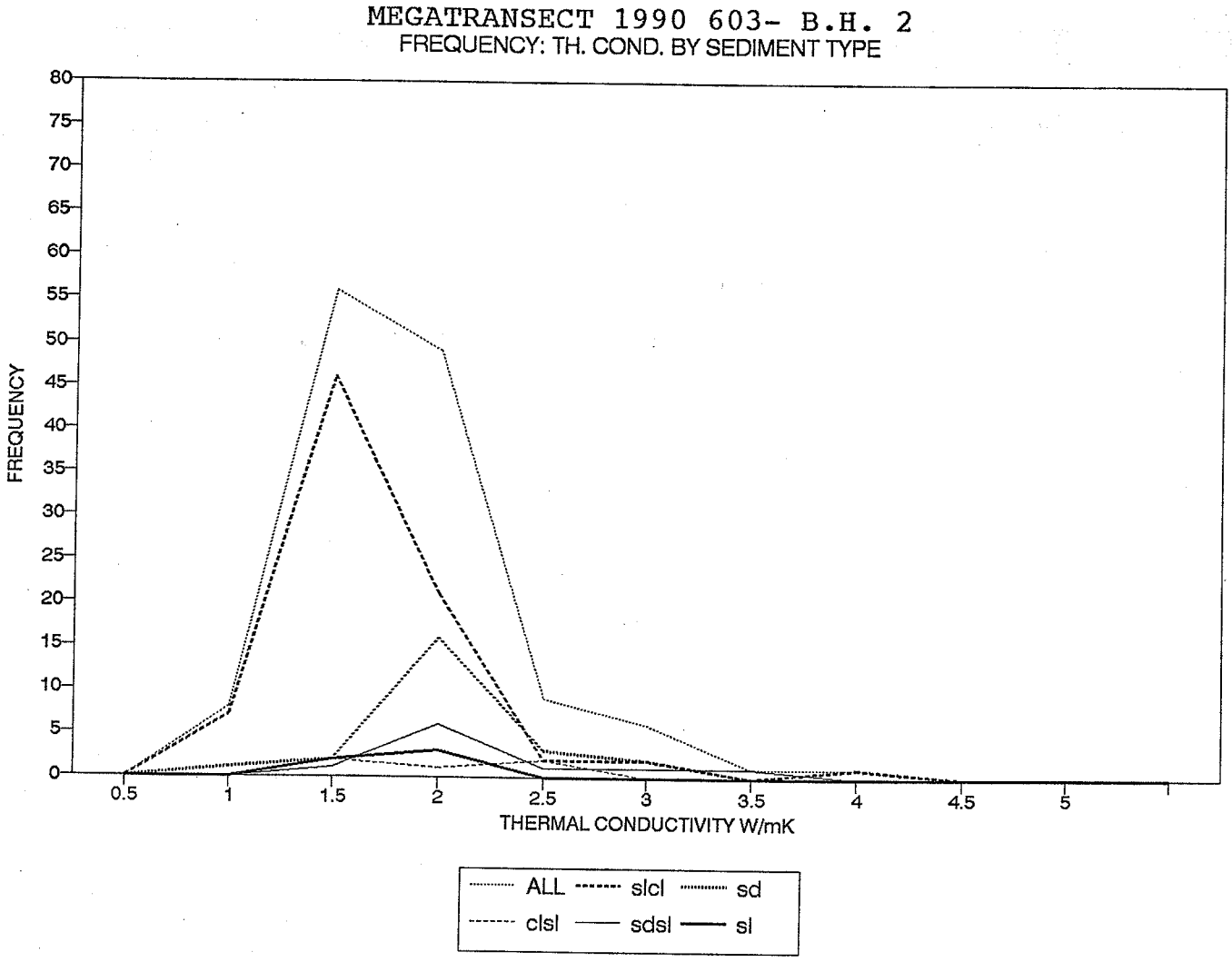

FIGURE 3.3.8 Frequency of thermal conductivity values by sediment type for BH2.

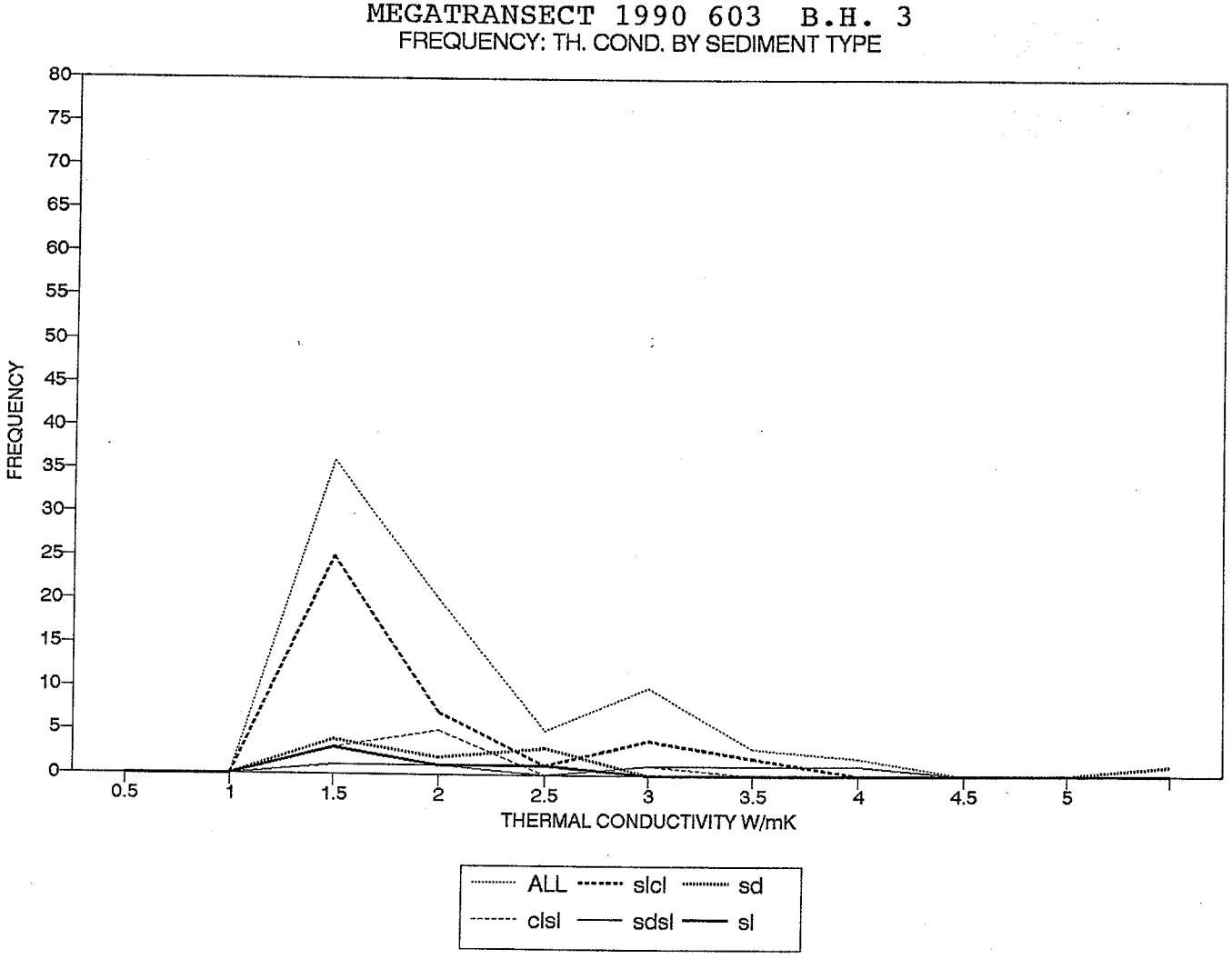

FIGURE 3.3.9 Frequency of thermal conductivity values by sediment type for BH3.

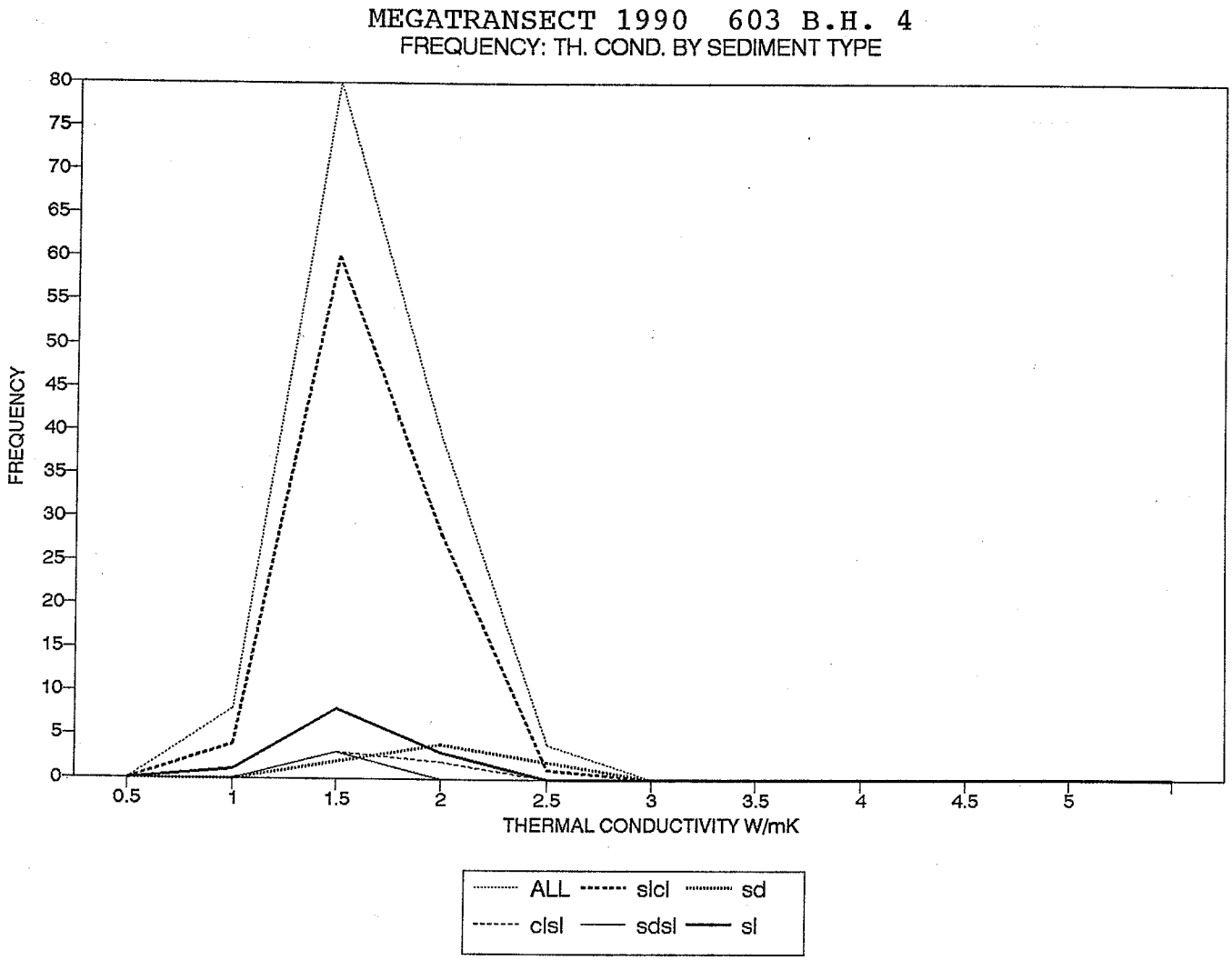

FIGURE 3.3.10 Frequency of thermal conductivity values by sediment type for BH4.

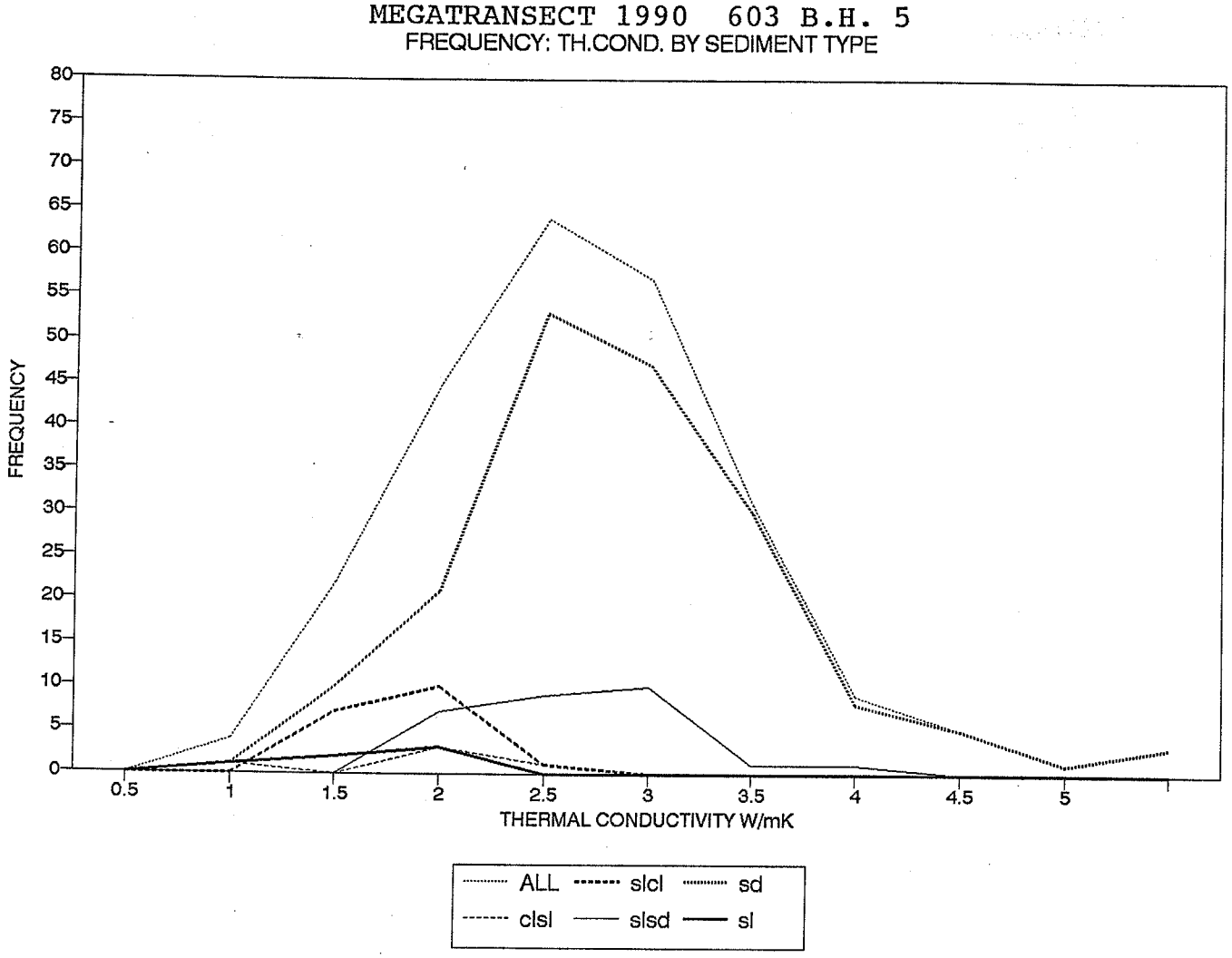

FIGURE 3.3.11 Frequency of thermal conductivity values by sediment type for BH5.

REFERENCES

Jessop, A.M., 1990. Thermal Geophysics. Developments in Solid Earth Geophysics 17, Elsevier.

Ratcliffe, E.H., 1960. The thermal conductivities of ocean sediments. J. Geophys. Res., 65: 1535-1541.

Taylor, A.E. and Allen, V.S., 1986. Geothermal Program on the CCGS NAHIDIK, cruises 1981-83, Canadian Beaufort Sea. Energy, Mines and Resources Canada, Earth Physics Branch, Internal Report 86-05.

Talylor, A.E. and Allen, V.S., 1987. Shallow sediment temperature perturbations and sediment thermal conductivities, Canadian Beaufort Shelf. Can. J. Earth Sci., 24: 2223-2234.

Von Herzen, R.P. and Maxwell, A.E., 1959. The measurement of thermal conductivity of deep-sea sediments by a needle probe method. J. Geophys. Res., 64: 1557-1563.

3.4 AN EXAMINATION OF TIME DOMAIN REFLECTOMETRY DATA

D.E. Patterson

Measurements of the apparent dielectric constant, K_a, and reflection coefficient at long travel times, ρ_∞, were made on core samples from boreholes 90BH3 and 90BH5. This type of information is routinely collected to determine the phase composition of ice-bonded sediments, an important consideration for determining geotechnical conditions. The following sections describe the methodolgy for these investigations and suggest improvements for subsequent work.

Methodology

Polaroid film is used to record the TDR's crt display (travel time versus voltage reflection coefficient) and determinations of K_a are made from travel time measurements using equation 1.

$$K_a = \left[\frac{c\ tt}{L}\right]^2 \tag{1}$$

The K_a values are converted to volumetric water contents (%), Θ, using equation 2 (Smith and Tice, 1988).

$$\Theta = -1.458x10^{-1} + 3.868x10^{-2}K_a - 8.502x10^{-4}K_a^2 + 9.920x10^{-6}K_a^2 \tag{2}$$

The values of ρ_∞ can be converted to estimates of the electrical conductivity, σ using equation 3:

$$\sigma = \left[\frac{1-\rho_\infty}{1+\rho_\infty}\right] \frac{c\epsilon_o}{L} \frac{Z_1}{Z_o} \tag{3}$$

where c is the free space velocity; ϵ_o is the free space permittivity and Z_1 is the impedance of the transmission line (300 Ω) and Z_o equals 50 Ω.

Results and recommendations for further work

Tables 3.4.1 and 3.4.2 summarize the results from the two boreholes. These tables show:

1. K_a values for two probe lengths (5.05 and 7.55 cm) where appropriate,
2. Reflection coefficient values, ρ, and
3. Θ values as determined from equation 1.

Figures 3.4.1 and 3.4.2 show the K_a profiles for boreholes 3 and 5 respectively, and Figures 3.4.3 and 3.4.4 show the salinity profiles determined from measurements on sediment samples.

The K_a values for borehole 3 (see Table 3.4.1 and Figure 3.4.1) generally show significant variation with depth, with K_a values generally in the 17-30 range. These values, and their associated water contents, largely represent differences in lithological units. The K_a values were often determined using two probe lengths. In general, the between-probe measures are consistent; however, sometimes significant differences do exist. The between-probe differences for any depth are most likely due to a combination of:

1. gaps around the lines which occur during probe insertion and/or,
2. uncertainties in determining travel time (too coarse a time-base scale on TDR results in short traces on polaroid).

The salinity values for borehole 3 are quite high. No association between salinity and K_a nor salinity and ρ_∞ was found.

The K_a values for borehole 5 (see Table 3.4.2 and Figure 3.4.2) are much lower than those of borehole 3. There was some difficulty determining K_a for this borehole since the trace lengths on the polaroids were generally very short; these are noted as such in Table 3.4.2. This uncertainty in K_a estimates can be alleviated by changing to a finer time-base scale setting on the TDR and/or using a longer TDR probe. As for borehole 3, no association between salinity and K_a nor salinity and ρ_∞ was found, although a decrease in both K_a and salinity was noted in the upper 18 m of the borehole.

There are, however, general comments which can be made regarding the TDR data itself. Firstly, the TDR traces are generally too short on the polaroid records and this affects the certainty in dielectric constant and water content estimates. This can be

Table 3.4.1 K_a - Θ values for Borehole 90BH3

Borehole	Depth (m)	Ka 5.05 cm	Ka 7.55 cm	ρ	Θ 5.05 cm	Θ 7.55 cm
90BH3	.76	23.00		-.62	.4148	
90BH3	1.37		33.96	-.50		.5758
90BH3	1.88	20.70		-.55	.3786	
90BH3	3.65	17.29		-.48	.3201	
90BH3	4.40		17.96	-.55		.3321
90BH3	5.00	25.00	26.68	-.58	.4448	.4694
90BH3	5.40		25.30	-.58		.4492
90BH3	6.40	21.20	24.00	-.52	.3866	.4299
90BH3	8.70	27.00	24.00	-.62	.4740	.4299
90BH3	9.15	16.00	20.30	-.57	.2961	.3720
90BH3	10.17	33.60	28.10	-.65	.5703	.4899
90BH3	10.90	36.00	28.10	-.67	.6076	.4899
90BH3	11.21	33.60	29.50	-.65	.5703	.5100
90BH3	12.35	36.00	29.50	-.69	.6076	.5100
90BH3	14.66	25.00		-.65	.4448	
90BH3	16.13	33.60	28.07	-.70	.5703	.4895
90BH3	19.15	17.60	19.10	-.40	.3257	.3519
90BH3	20.44	15.20	18.52	-.49	.2805	.3420
90BH3	21.34	17.60	16.85	-.50	.3257	.3120
90BH3	22.04	23.00	21.50	-.60	.4148	.3914
90BH3	28.20	6.10	10.96	.05	.0608	.1891
90BH3	30.50	10.90	10.10	.80	.1876	.1684
90BH3	31.95					
90BH3	35.50	25.00	28.10	-.65	.4448	.4899
90BH3	35.70		28.10	-.67		.4899
90BH3	36.17	33.60	28.10	-.67	.5703	.4899
90BH3	36.96	17.60	20.30	-.53	.3257	.3720
90BH3	37.50	19.40	20.30	-.56	.3570	.3720
90BH3	38.64	16.00	16.85	-.53	.2961	.3120
90BH3	39.25	17.60	17.96	.50	.3257	.3321

Table 3.4.2 K_a - Θ values for Borehole 90BH5

Borehole	Depth (m)	Ka 5.05 cm	ρ	Θ 5.05 cm
90BH5	9.92	11.60		.2040
90BH5	12.50	16.00		.2961
90BH5	14.00	14.44		.2653
90BH5	15.47	11.56	-.48	.2030 trace too short
90BH5	16.31	10.23		.1715 trace too short
90BH5	17.00			trace too short
90BH5	17.88	9.00	.43	.1407
90BH5	19.72	4.00	.47	
90BH5	20.10	5.76		.0507 trace too short
90BH5	20.40	7.84	.54	.1100
90BH5	20.97	5.76	.70	.0507
90BH5	23.20			trace too short
90BH5	29.73			trace too short
90BH5	29.73			trace too short
90BH5	31.35		.45	trace too short
90BH5	75.84	5.76	.10	.0507 trace too short
90BH5	76.20	11.56	-.05	.2030 trace too short
90BH5	77.93	5.76	.17	.0507 trace too short
90BH5	78.66	7.84	-.01	.1100 trace too short
90BH5	80.12	9.00	-.05	.1407 trace too short
90BH5	80.82	12.96	-.68	.2343 trace too short
90BH5	80.93	9.00	-.21	.1407 trace too short
90BH5	81.66	4.00	.30	trace too short
90BH5	83.28	12.96	-.15	.2343 trace too short
90BH5	83.28	10.20	-.24	.1708
90BH5	84.72	11.56	-.39	.2030 trace too short
90BH5	84.72	9.00	-.34	.1407 trace too short
90BH5	85.50	5.76	-.17	.0507 trace too short
90BH5	87.00	11.56	-.25	.2030 trace too short
90BH5	87.08	16.00	-.52	.2961 trace too short
90BH5	87.78	10.24	-.26	.1718

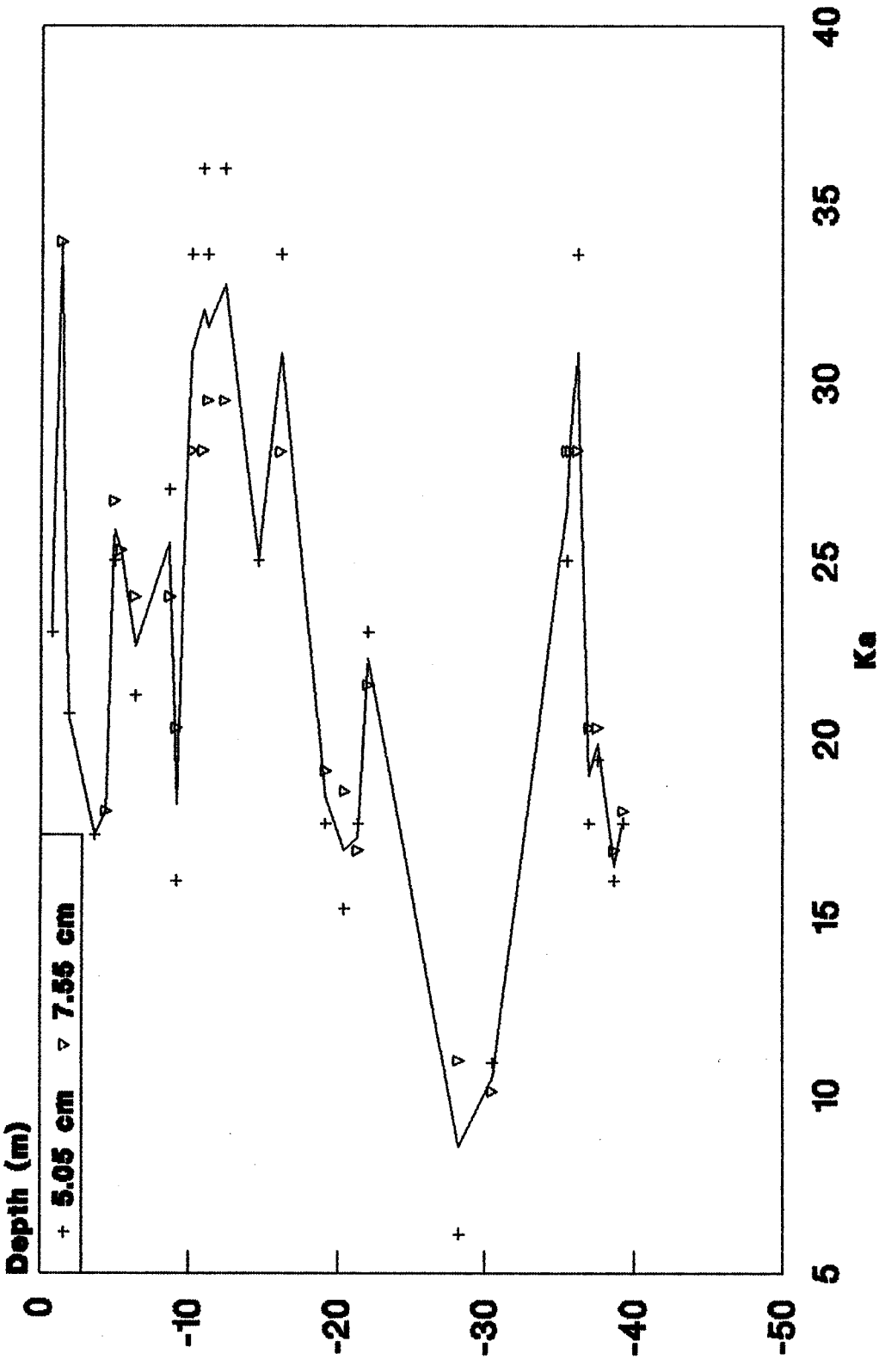

Figure 3.4.1 Ka, Borehole 3

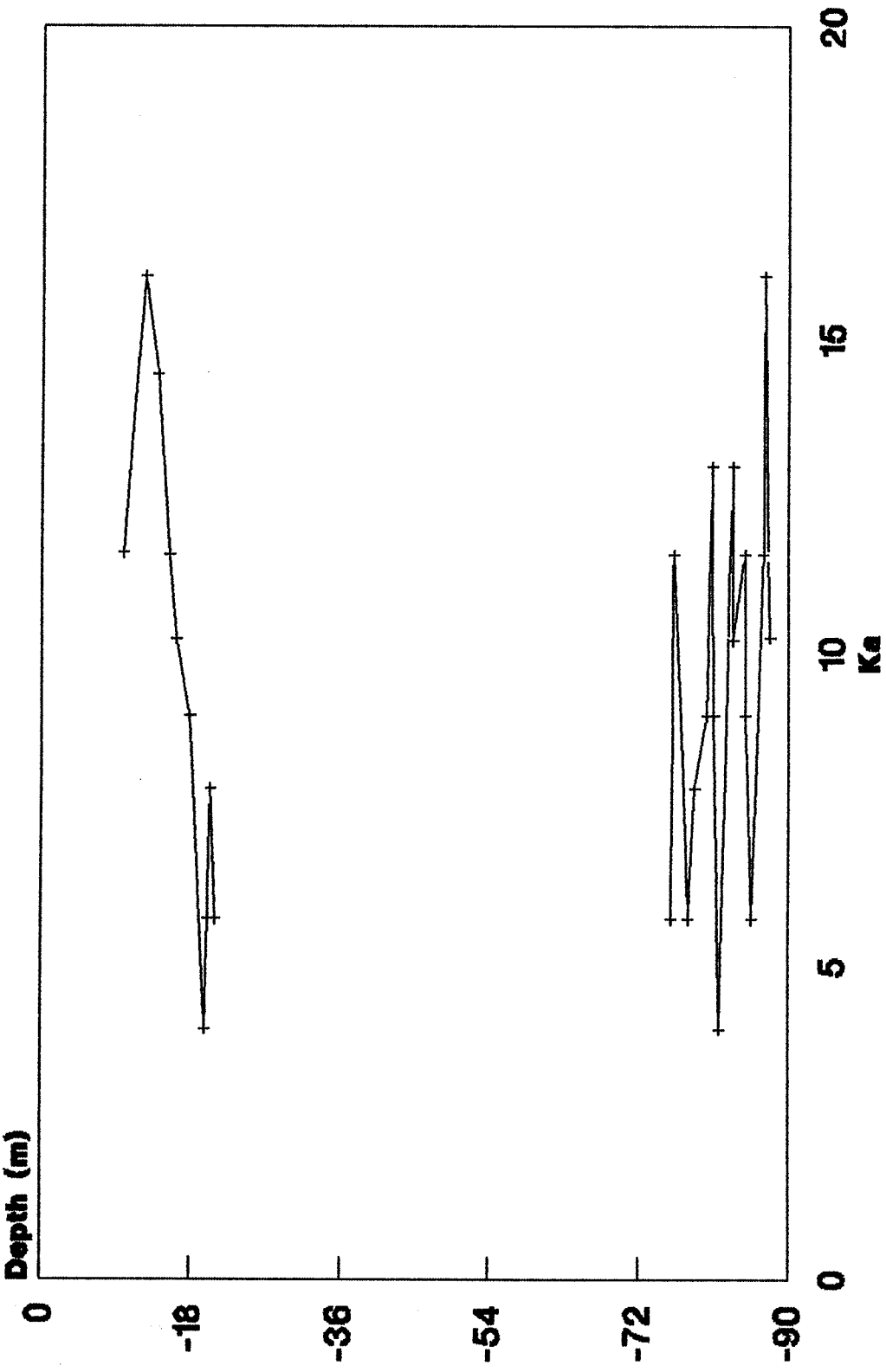

Figure 3.4.2 Ka, Borehole 5

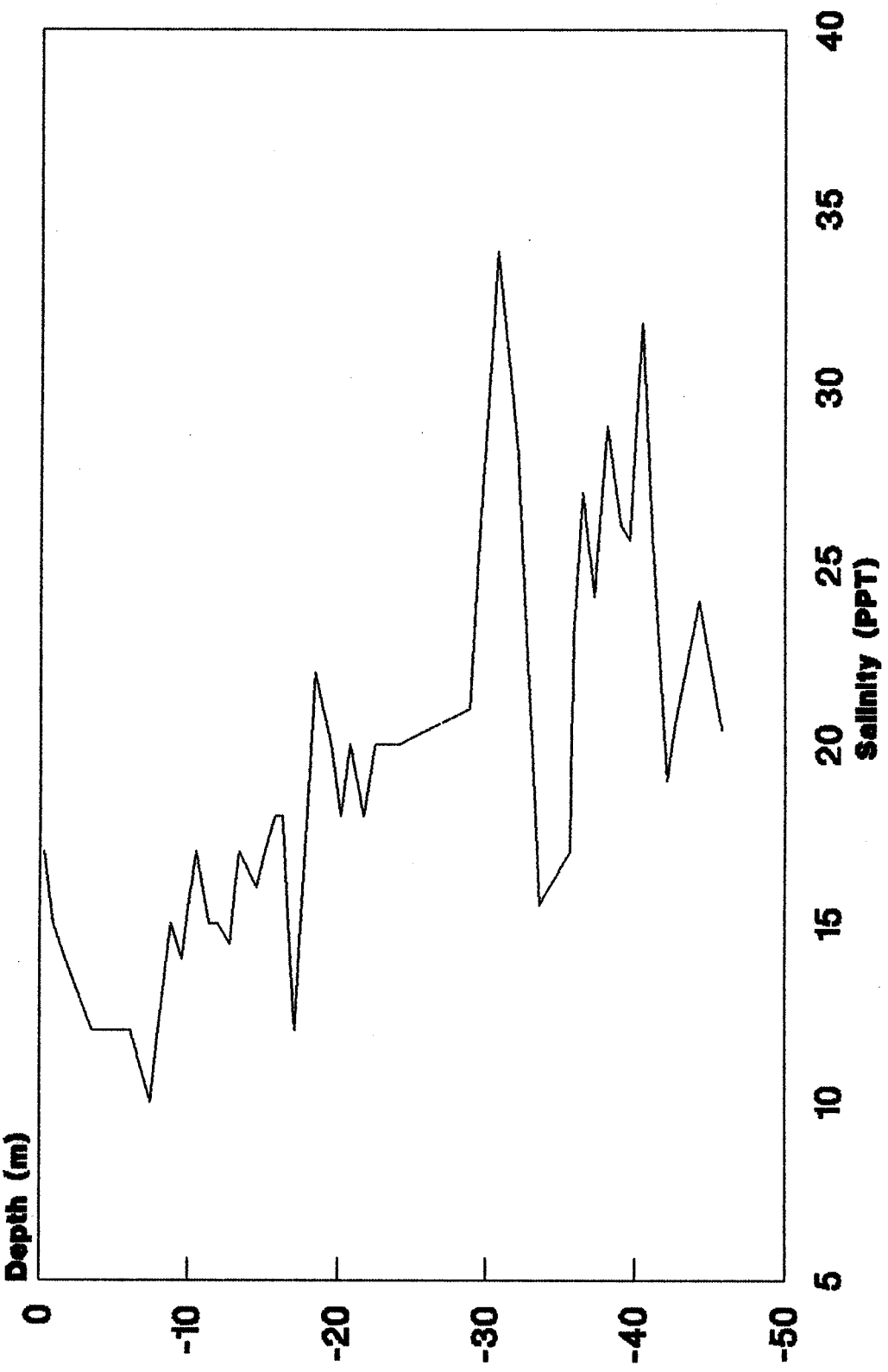

Figure 3.4.3 Salinity, Borehole 3

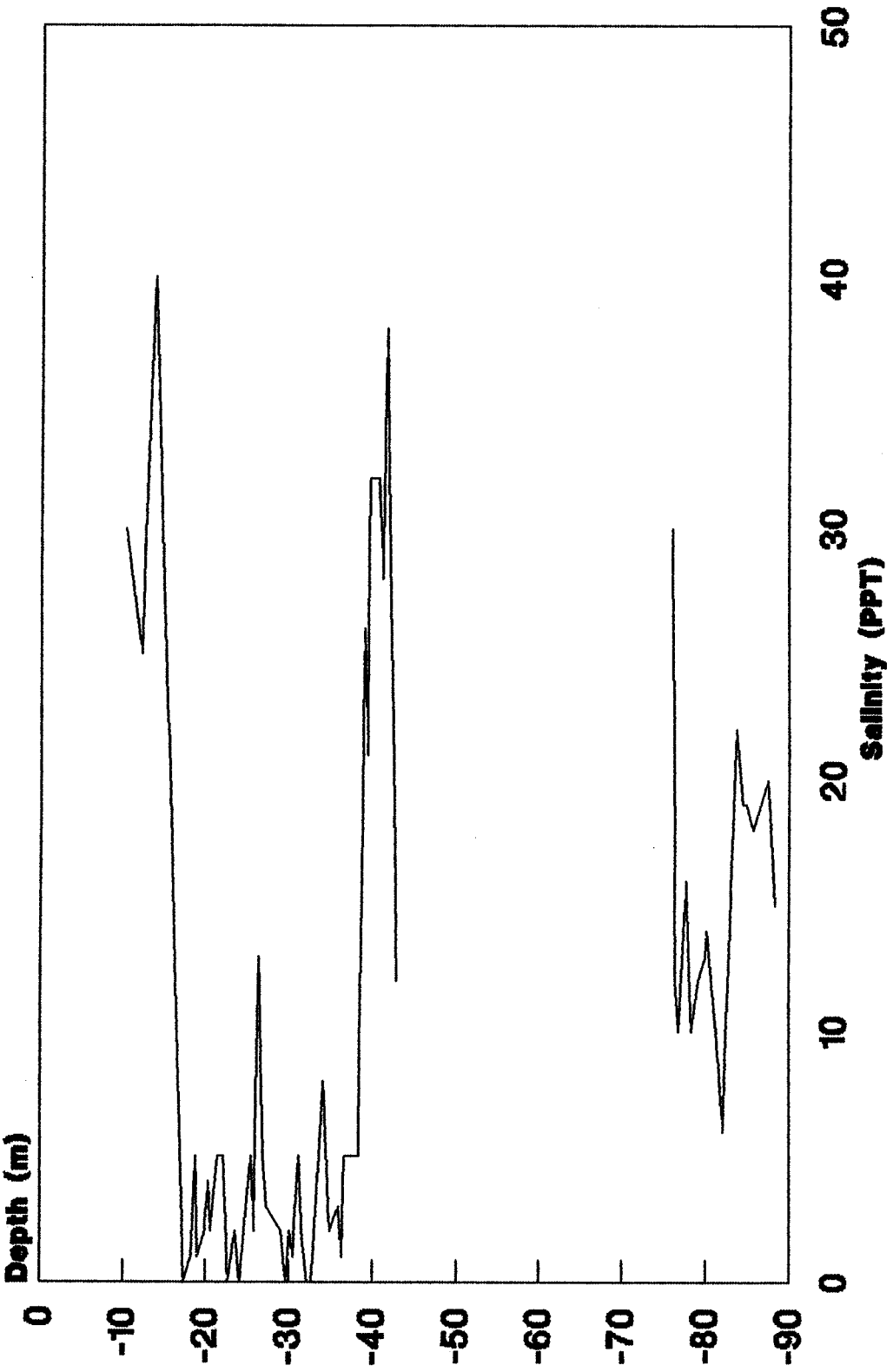

Figure 3.4.4 Salinity, Borehole 5

improved in several ways:

1. use of longer probes
2. finer time-base scale setting
3. increased magnification of TDR's crt on polaroid (reference graticules must be visible; often accomplished by over-exposure)

Secondly, the reflection coefficient data does not appear to be a viable method of determining salinity because of the effects that water content, mineralogy and temperature have upon the electrical conductivity. If electrical conductivity measurements were desired in themselves, a tri-lead coaxial cage line could be used as the TDR probe, thus removing the influence of the balun transformer used in the present design. This type of transmission line also offers the possibility of making accurate estimates of dielectric constant and water content estimates.

REFERENCE

Smith, M.W. and A.R. Tice 1988. Measurement of the unfrozenwater content of soils: Comparison of NMR and TDR methods, U.S. Army Cold Regions Research and Engineering Laboratory, CRREL Report 88-18, Oct. 1988, 11 pp.

CHAPTER 4

ONSHORE-OFFSHORE TRANSECT: GEOTECHNICAL RESULTS

4.1 PHYSICAL PROPERTIES OF STRATIGRAPHIC UNITS

S.R. Dallimore and D.E. Patterson

A summary of the physical property testing completed for each of the onshore-offshore boreholes is presented in the detailed borehole logs in Appendix A and in spread sheet form in Appendix D. A brief summary of the properties of each of the major units is presented in the following sections.

Onshore boreholes

Toker Point Till

The Toker Point till was only intersected in borehole 90BH1. The till at this location is a poorly sorted diamicton with approximately 50% sand, 30% silt and 20% clay (Figure 4.1.1). Less than 2% of the particles by weight are composed of pebbles up to 2 cm in diameter. The till has a low plasticity and is classified as a low plastic clay by the Unified Soil Classification System. Frozen bulk density of the till averages about 1.8 g/cm^3. Volumetric excess ice contents were found to range from 5 to 15%, yielding gravimetric water contents substantially higher than the liquid limit of the sediment. Salinities were consistently less than 2 ppt.

Kittgazuit and Kidluit Formations

The Kittigazuit and Kidluit Formations encountered in boreholes 90BH1 and 90BH1A were almost identical in their physical properties. Both are well sorted, primarily fine to medium grained sand (Figure 4.1.2), with only occasional silty layers. Ice contents and gravimetric water contents are generally low, and salinities average less than 3ppt.

Hooper Clay

The Hooper clay identified in borehole 90BH1A is a poorly sorted silt with less than 30% clay sized particles and less than 5% sand sized particles (Figure 4.1.3). According to the Unified Soil Classification System, the Hooper clay would be classified as a low plastic silt (Ml). Ice contents and gravimetric water contents are generally low. Salinities varied from 5 to 35 ppt with the average being about 20 ppt.

Figure 4.1.1 Toker Point Till

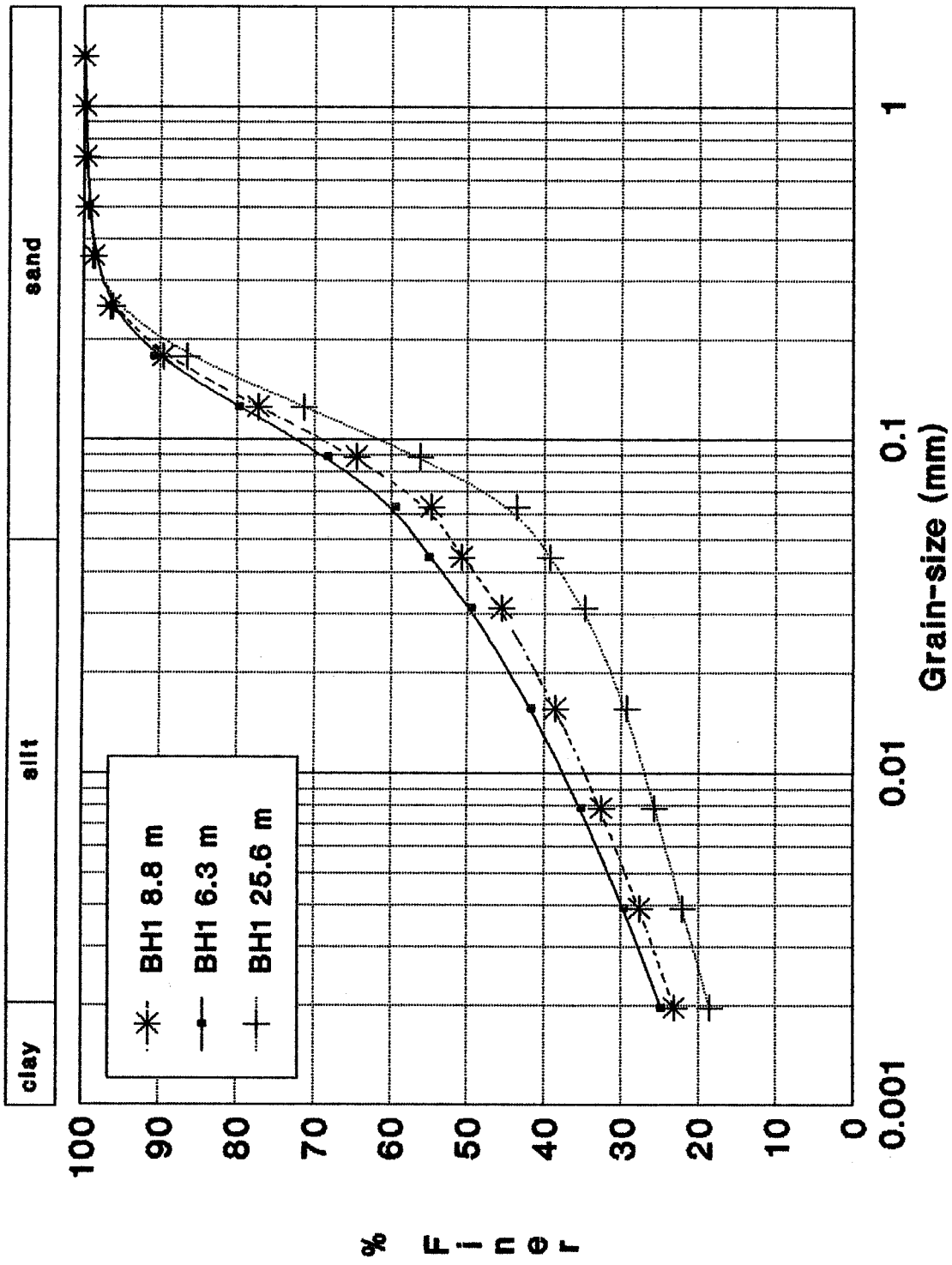

Figure 4.1.2 Kittigazuit/Kidluit Unit

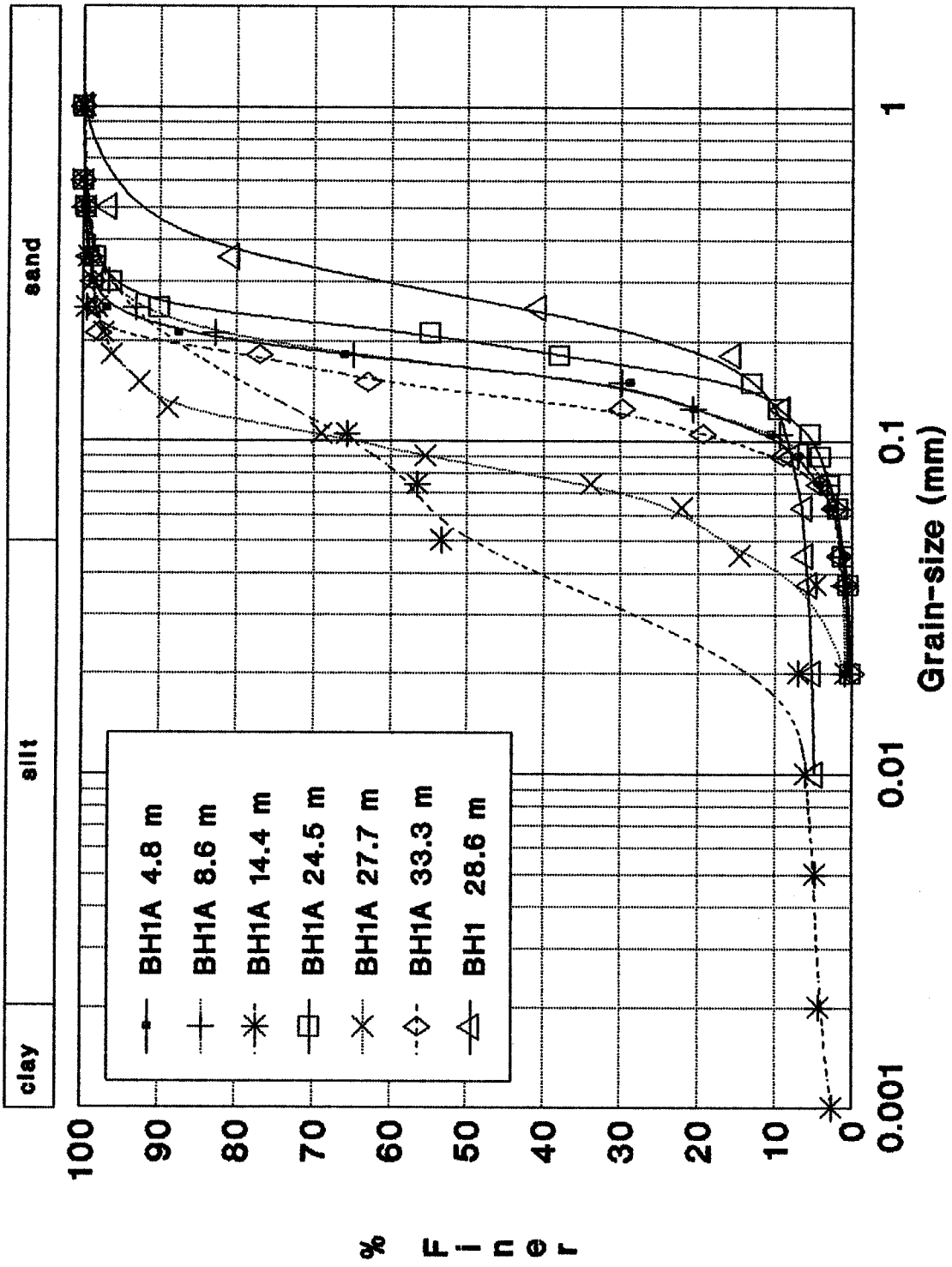

Figure 4.1.3 Hooper Clay

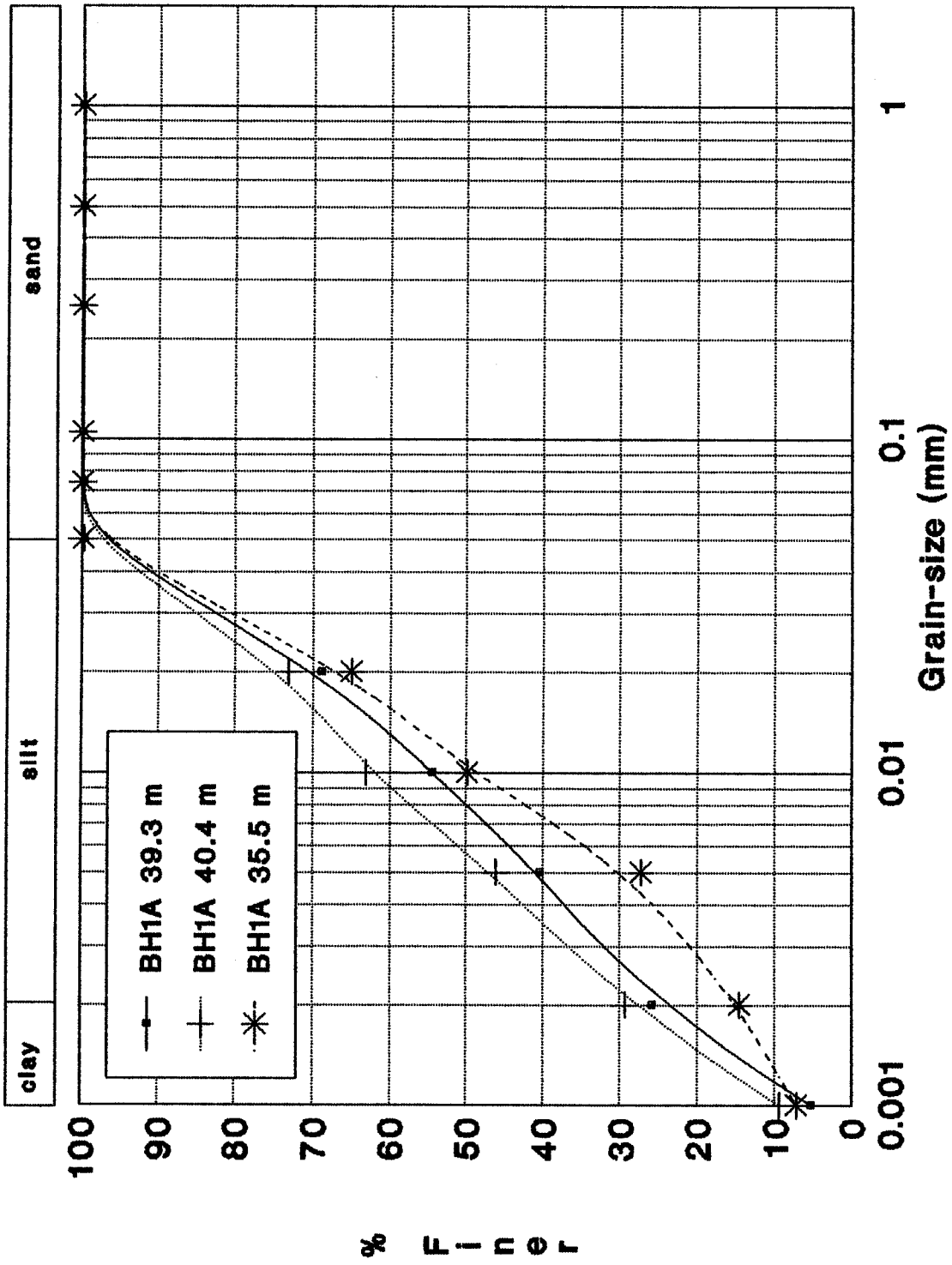

Offshore boreholes

Unit B

Grain size analyses conducted on samples from Unit B intersected in boreholes 90BH2 and 90BH3 suggest that it varies from a well sorted sand to poorly sorted clayey silt according to the Unified Soil Classification System (Figure 4.1.4). In most cases, Unit B is a low plastic clay (Cl) according to the Unified Soil Classification System. Water contents are variable as are salinities which range from 10 ppt to 28 ppt. Unit B in borehole 90BH2 is characterized by an interesting salinity profile. Salinities in from the seafloor down average about 25 ppt for the first 2 m, decrease rapidly to approximately 13 ppt at 12m, and then increase to about 20 ppt close to the contact with Unit C. This trend is confirmed by data from the downhole conductivity log run in 90BH2 (see Appendix A). A similar trend was observed in salinity mesasurements from 90BH3.

Unit C

Unit C was found to vary in grain size (Figure 4.1.5) reflecting the various subfacies described in Section 2.2. The silt diamicton in borehole 90BH3 comprises almost identical grain size characteristics to the Toker Point till. Subfacies C1, C2, C3 are well sorted sands with occasional poorly sorted silty sand interbeds. A 6 m thick gravel layer encountered at the top of Unit C in borehole 90BH4 was not sampled.

Salinities in Unit C were also variable. In borehole 90BH5 a thin ice-bonded layer was encountered at the seafloor with salinities of 15ppt (see Section 4.3 and Appendix A). Beneath this layer Unit C was unbonded to an estimated depth of 10m. Although this layer was not sampled, data from the conductivity log suggested it is characterized by high pore water salinities. The partially ice-bonded layer intersected from 10 m to 16 m was characterized by salinities from 25 to 40 ppt. The abrupt transition from partially ice-bonded to well ice-bonded sediment at 16 m was marked by an abrupt decrease in salinity to values less than 5 ppt.

In the remainder of the offshore boreholes Unit C was unbonded and characterized by variable salinities from 12 to 40 ppt.

Figure 4.1.4 Unit B

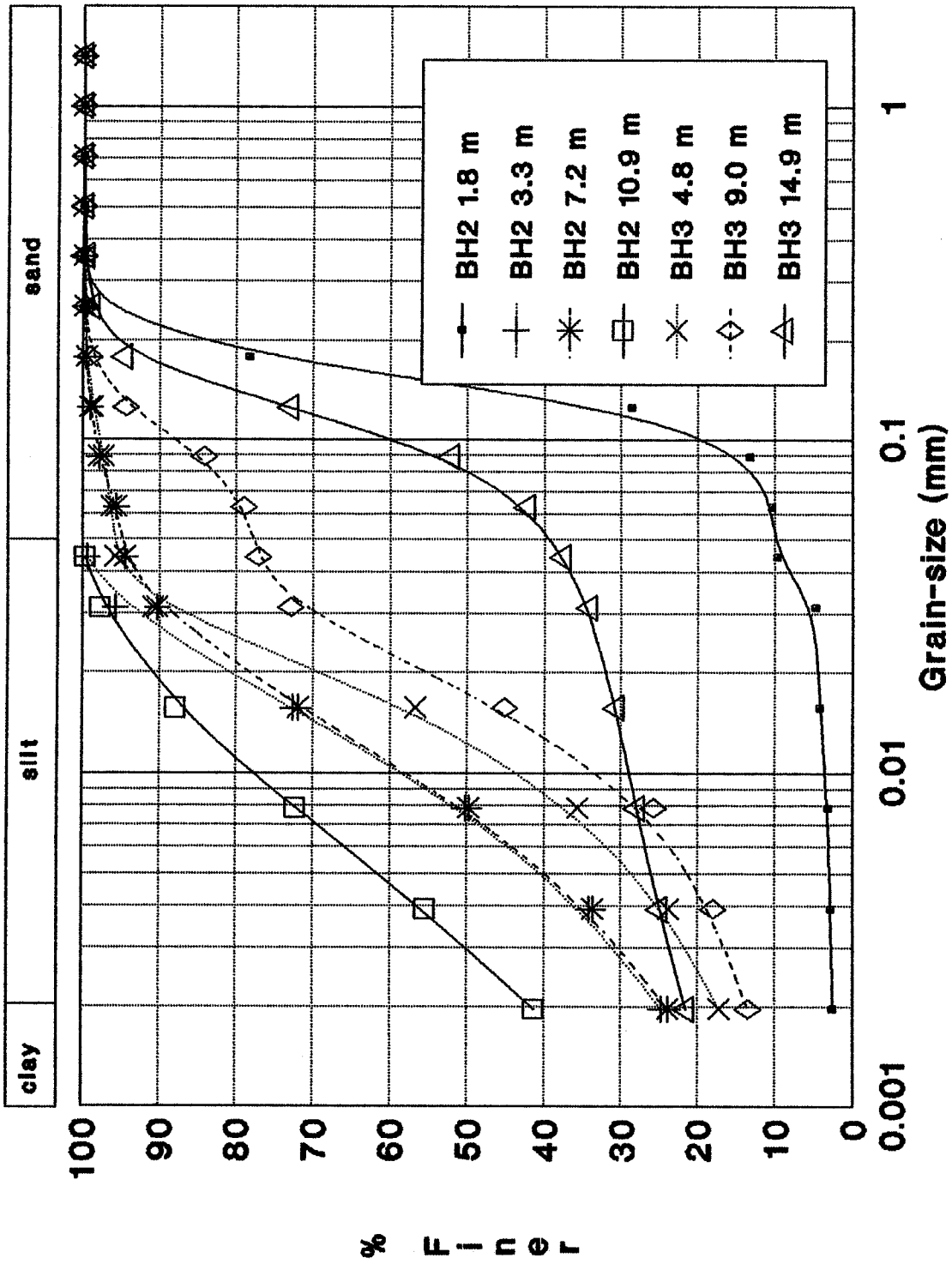

Figure 4.1.5a Unit C

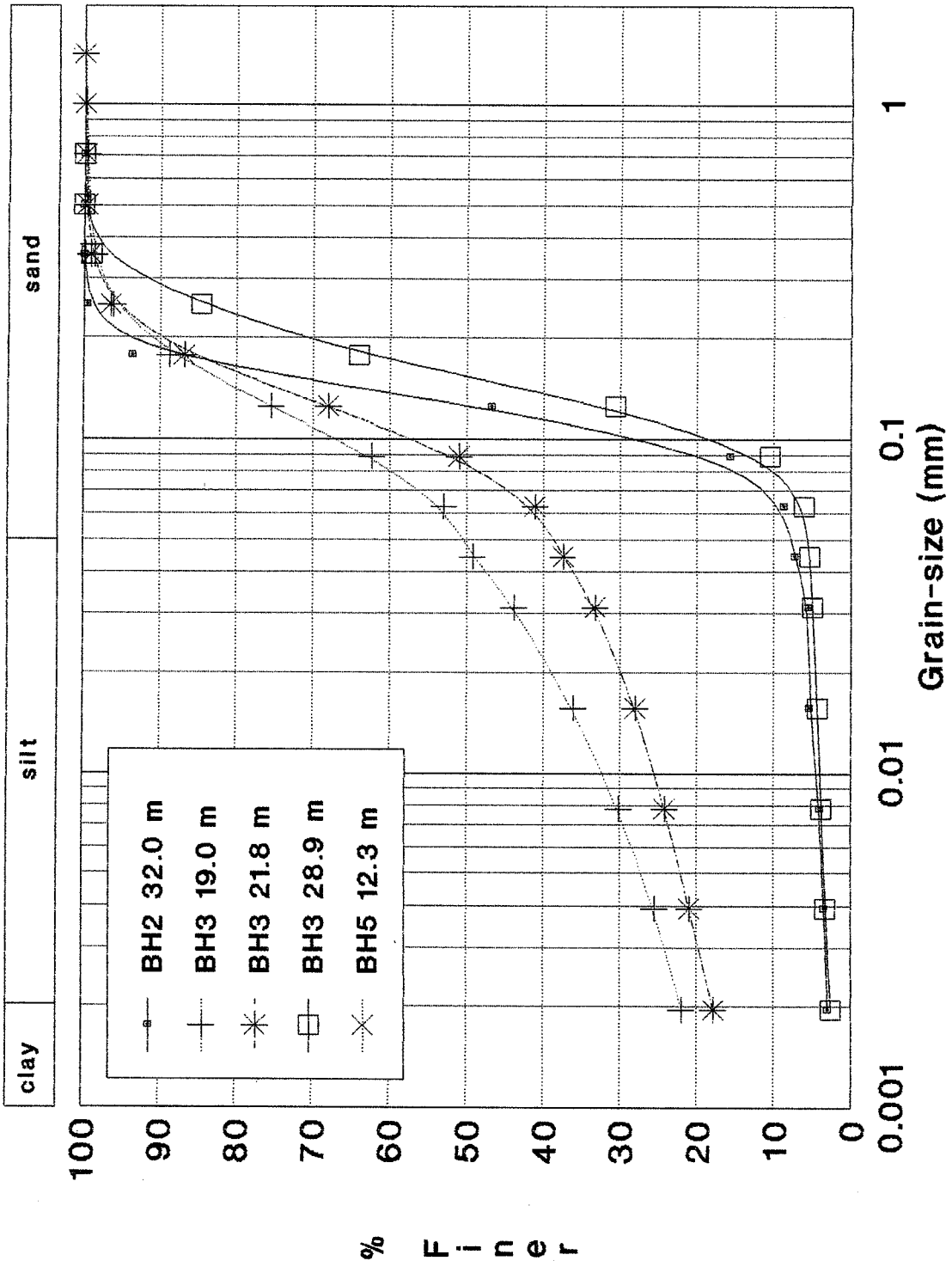

Figure 4.1.5b Unit C

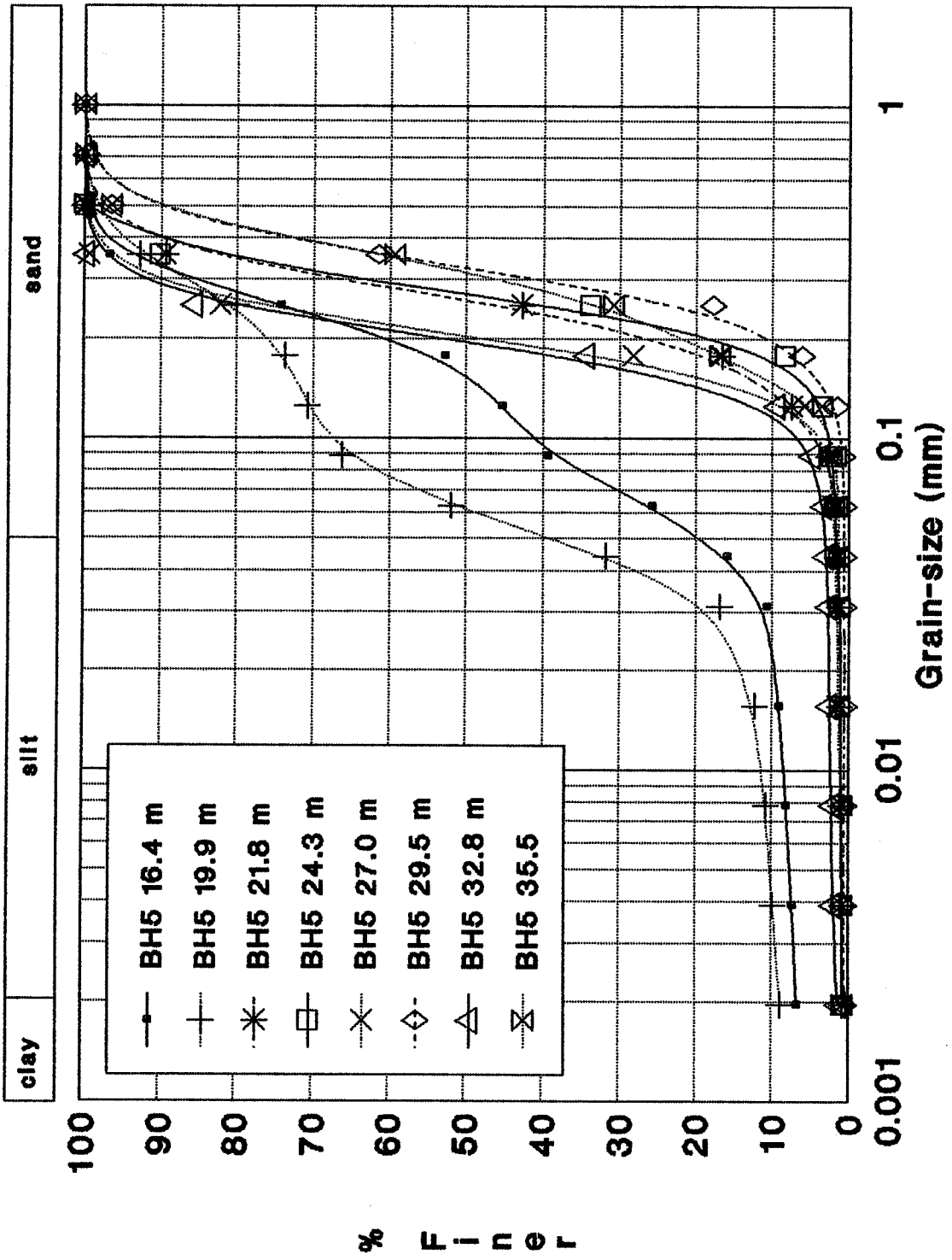

Unit D

Unit D is a relatively uniform clayey silt, consisting of approximately 35% clay, 60% silt and generally less than 5% sand. Most samples of Unit C would be classified as low plastic silts (Ml) according to the Unified Soil Classification System. Water contents showed some variability but were generally between the plastic and liquid limits. Salinities averaged about 20 ppt with some values as high as 48 ppt (Figure 4.1.6).

Unit E

Unit E was only intermittently sampled; however, it appears to be quite uniform consisting of a well sorted, fine grained sand (Figure 4.1.7). Measured pore water salinities were variable and surprisingly high with values up to 62 ppt.

Figure 4.1.6a Unit D

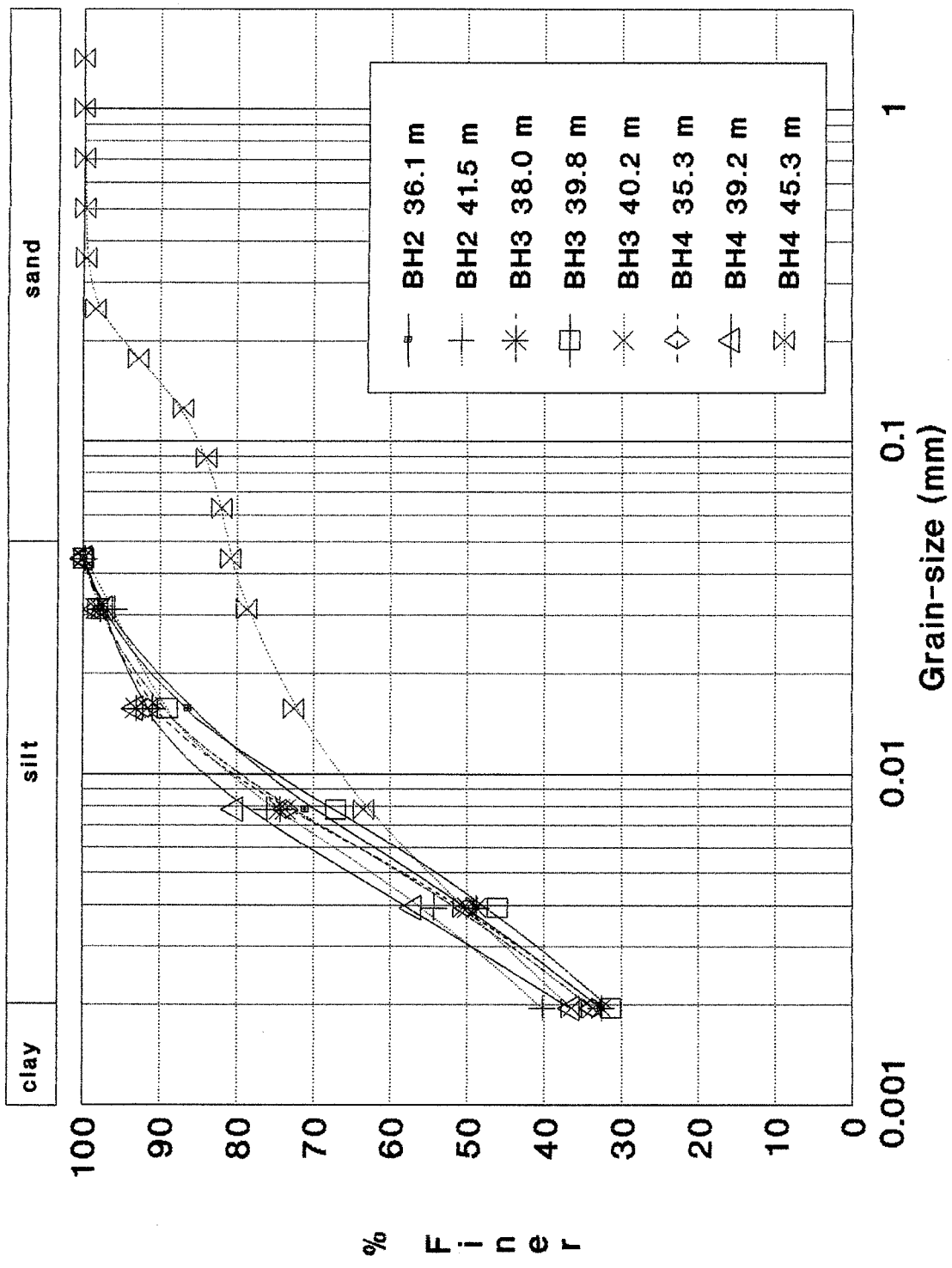

Figure 4.1.6b Unit D

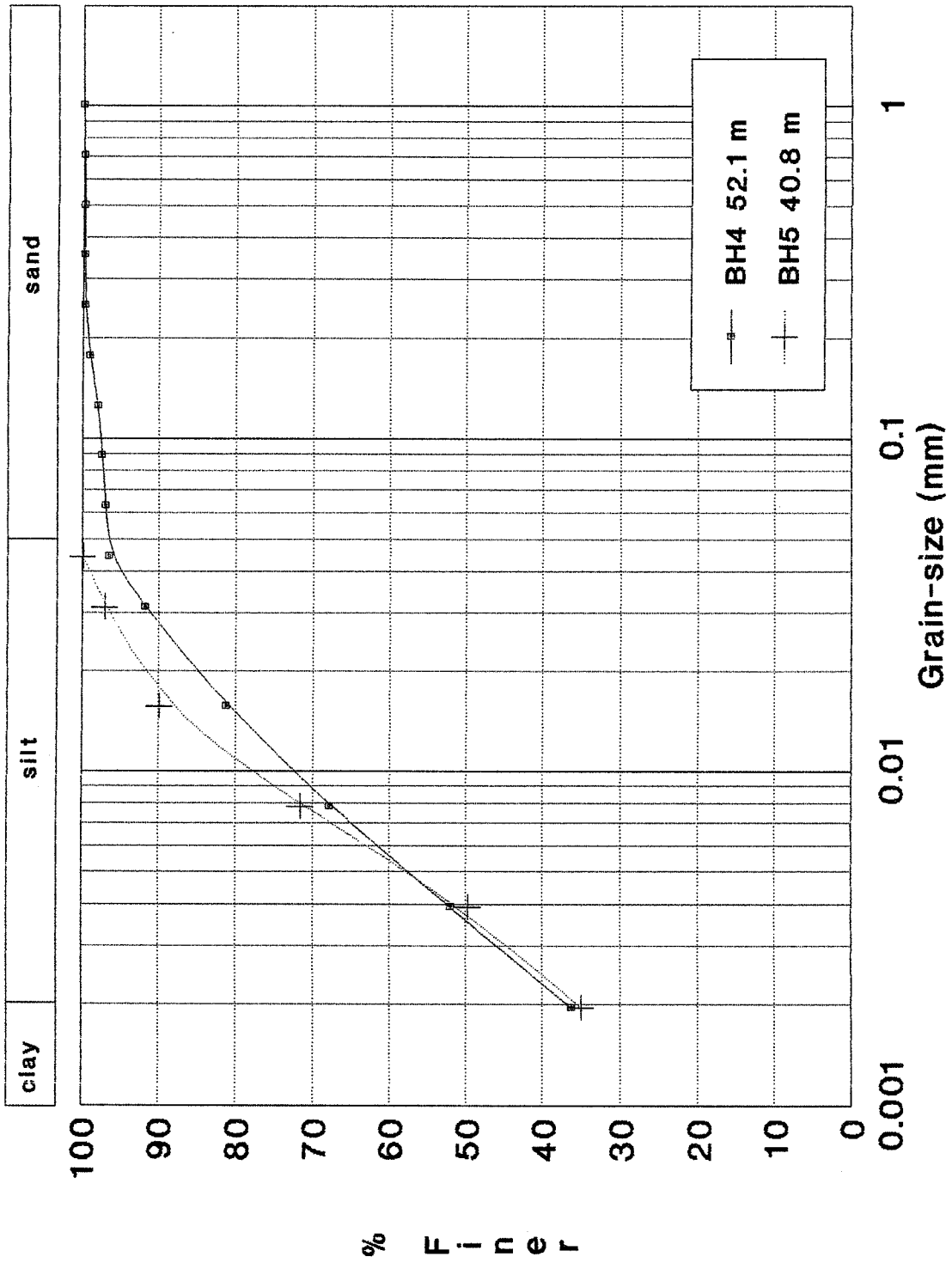

Figure 4.1.7a Unit E

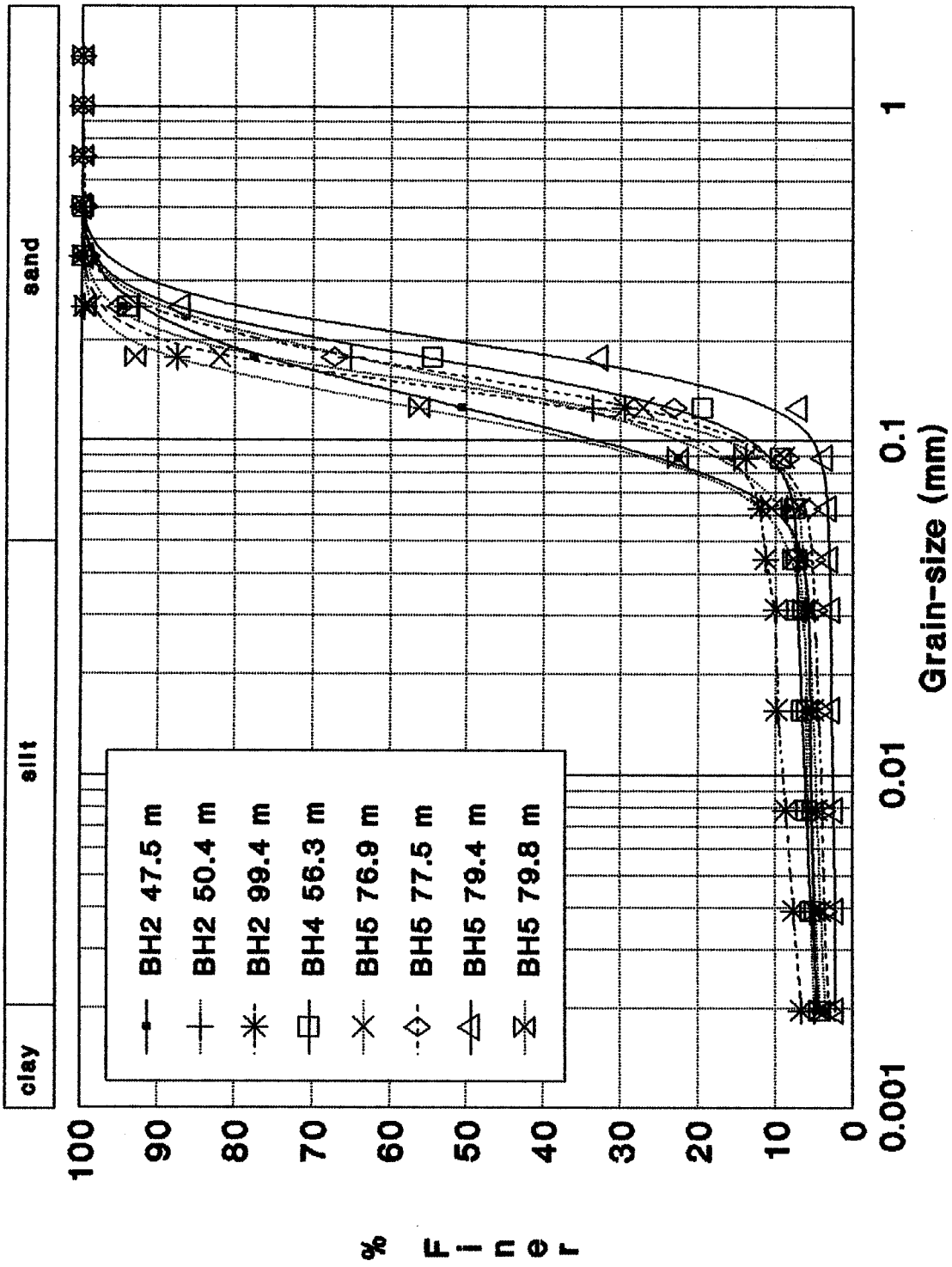

Figure 4.1.7b Unit E

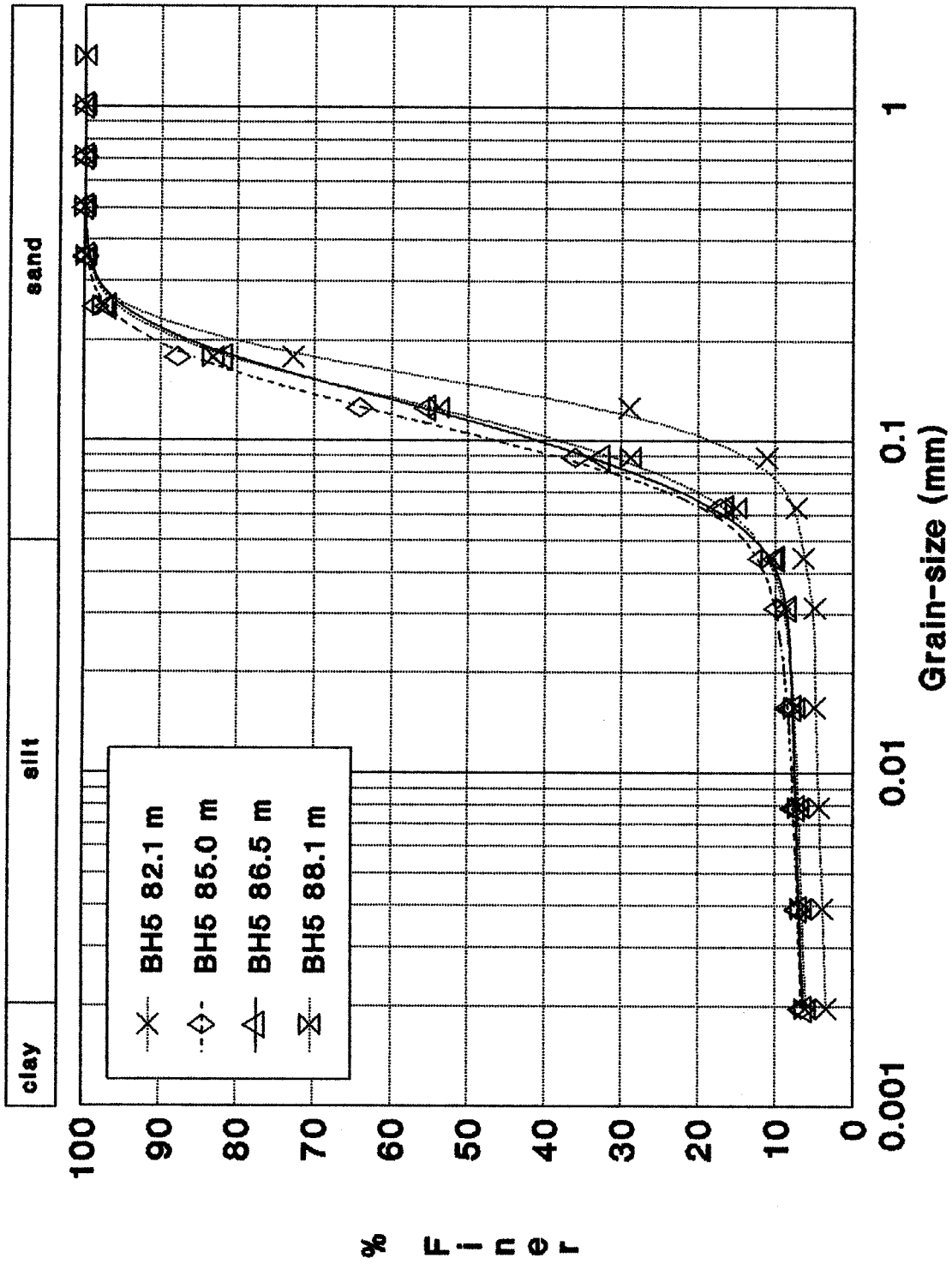

4.2 CONE PENETRATION TESTING OF UNIT B

P.J. Kurfurst and D.J. Woeller

The cone penetration testing program was carried out from the sea-ice east of North Head, Richards Island, N.W.T. along the route of the onshore-offshore transect between March 25 and 31, 1990. The locations of the CPT sites in relation to the borehole locations are shown in Fig. 1.2.2. The positions of all sites are summarized in Table 1.2.1.

4.2.1 Field Equipment and Procedures

Electric Cone Penetrometer

The cone penetration tests (CPT) were carried out by ConeTec Investigations Ltd. of Vancouver, using an integrated electronic cone system. A 10-ton subtraction type cone was used for all of the soundings. This cone has a tip area of 10 cm^2 and friction sleeve area of 150 cm^2, and is designed with an equal end area friction sleeve and a tip end area ratio of 0.85. Figure 4.2.1 shows the subtraction cone used for the seismic, temperature, salinity and resistivity testing.

The cone used during the program was capable of recording the following parameters at specific depth intervals:

- Tip Resistance (Qc)
- Sleeve Friction (Fs)
- Dynamic Pore Pressure (Ut)
- Temperature (T)
- Cone Inclination (i)
- Shear (S) and Compressional (P) Wave Velocities
- Salinity
- Resistivity

The above parameters, excluding the S and P wave velocities, were printed simultaneously on a printer and stored on a cassette cartridge for future analysis and reference.

The pore pressure element on the cone is located directly behind the cone tip. The pore pressure element is 5.0 mm thick and is made of porous plastic. Each of the elements used were saturated in glycerin under vacuum pressure prior to penetration. Pore pressure

dissipations were recorded at 5 second intervals during pauses in the penetration.

A complete set of baseline readings were taken prior to, and at the completion of each sounding to determine temperature shifts and any zero load offsets in order to make corrections to the cone data as necessary. These corrections are extremely important, especially when the loads are relatively low, as inaccurate corrections are the single largest source of error with respect to the accuracy of cone data.

Prior to performing a CPT sounding, a hole was augered through the ice and steel casing was set 1 to 1.5 m below the mud line in order to prevent the buckling of the cone rods during penetration. The cone was pushed using a specially modified " CME 750 " drill rig with a down pressure capacity of 10 tons. The drill rig was supplied and operated by Midnight Sun Drilling Co. Ltd. from Whitehorse, Yukon.

The cone penetration tests were performed to depths varying between about 3 and 25 m below the top of sea ice; the mudline was between 2 and 11 m below the top of sea ice. The top of the sea ice is referred to as zero datum and all test holes are referenced to this datum. It should be noted that minor discrepancies were observed between the depths to the mudline determined from the cone tests and those measured during drilling. These differences are thought to have resulted from tidal effects and minor errors with zero reference on the cone traces. Table 4.2.1 presents a summary of all tests performed.

Temperature Monitoring

The ground temperatures were recorded using fast acting resistance temperature devices (RTD) located in the outer portion of the cone body. This location was chosen so that the sensor was as close to the soil as possible and far away from any self-heating components within the cone. To establish the ground temperature at a specific depth, the change in temperature with time was recorded for intervals ranging between 8 and 14 minutes. After reviewing the temperature data, it was concluded that a dissipation time of about 10 minutes was optimal.

Seismic Cone Penetration Testing

The seismic cone penetration test (SCPT) uses the standard electric cone equipped with a velocity seismometer. The seismometers used in the cones for this program were

Table 4.2.1 Summary of tests performed

DATE	HOLE NO.	DEPTH FROM TOP OF ICE TO MUDLINE (m)	PENETRATION BELOW MUDLINE (m)	REMARKS
03/26/90	CPT-6	3.65	20.65	Pore Fluid Salinity
				Stopped on Dense Sand
03/26/90	CPT-6A	3.65	20.35	Down Hole Seismic, Resistivity and Temperature Tests
				Stopped on Dense Sand
03/27/90	CPT-4A	2.9	19.0	Down Hole Seismic, Resistivity and Temperature Tests
				Stopped on Dense Sand
03/27/90	CPT-4	2.9	19.0	Pore Fluid Salinity
				Stopped on Dense Sand
03/28/90	CPT-13A	10.65	13.7	Stopped on Dense Sand (permafrost)
03/29/90	CPT-12	9.85	18.1	Pore Fluid Salinity
				Stopped on Dense Sand
03/30/90	CPT-8A	6.65	26.0	Stopped on Dense Sand
03/30/90	CPT-8	6.65	24.5	Pore Fluid Salinity
				Stopped on Dense Sand
03/31/90	CPT-3A	2.3	15.0	Down Hole Seismic Tests
				Stopped on Dense Sand
03/30/90	CPT-3	2.3	15.0	Pore Fluid Salinity
				Stopped on Dense Sand

Geospace GSC-14-L3 with a natural frequency of 28 Hz. The seismometer is mounted horizontally and is oriented during testing in alignment with the shot hole (energy source). Figure 4.2.1 illustrates the seismic cone used for this project.

During selected cone soundings, downhole seismic testing was carried out to determine shear (S) and compressional (P) waves arrival times. The shot hole was located 1.5 m from the cone sounding hole and Mark II seismic caps were used as an energy source. The caps were detonated electrically just below the mudline. The seismic impulse was detected by the seismometer and was recorded on a 4-channel digital oscilloscope. Detonation of the caps electrically provided reference times and allowed for the precise timing of S and P wave arrivals.

Overconsolidation Ratio

The overconsolidation ratio (OCR) was computed for sediments at the CPT-4 location using pore pressure data collected from CPT-4 and CPT4A sites. The PPD method (Sully et al., 1988) was used to calculate the difference in penetration pore pressures recorded on, and behind the cone tip, and to predict the overconsolidation ratio of cohesive soils penetrated during the cone penetration test.

Chemi-Cone Penetration Testing

The chemi-cone penetration test (CCPT) uses the standard electric cone equipped with a groundwater sampling module, located directly behind the cone. During pauses in penetration (typically at 1 m intervals), the pump is cycled and a sample of groundwater or seawater is pulled into a chamber where both conductivity and temperature measurements are made. Using the conductivity and temperature data collected, the salinity of the water sample can be computed.

Resistivity Cone

The resistivity cone penetration test (RCPT) was the standard electric cone equipped with a resistivity module located directly behind the cone. Bulk resistivity measurements of the soil were taken at 5 cm intervals during the cone sounding.

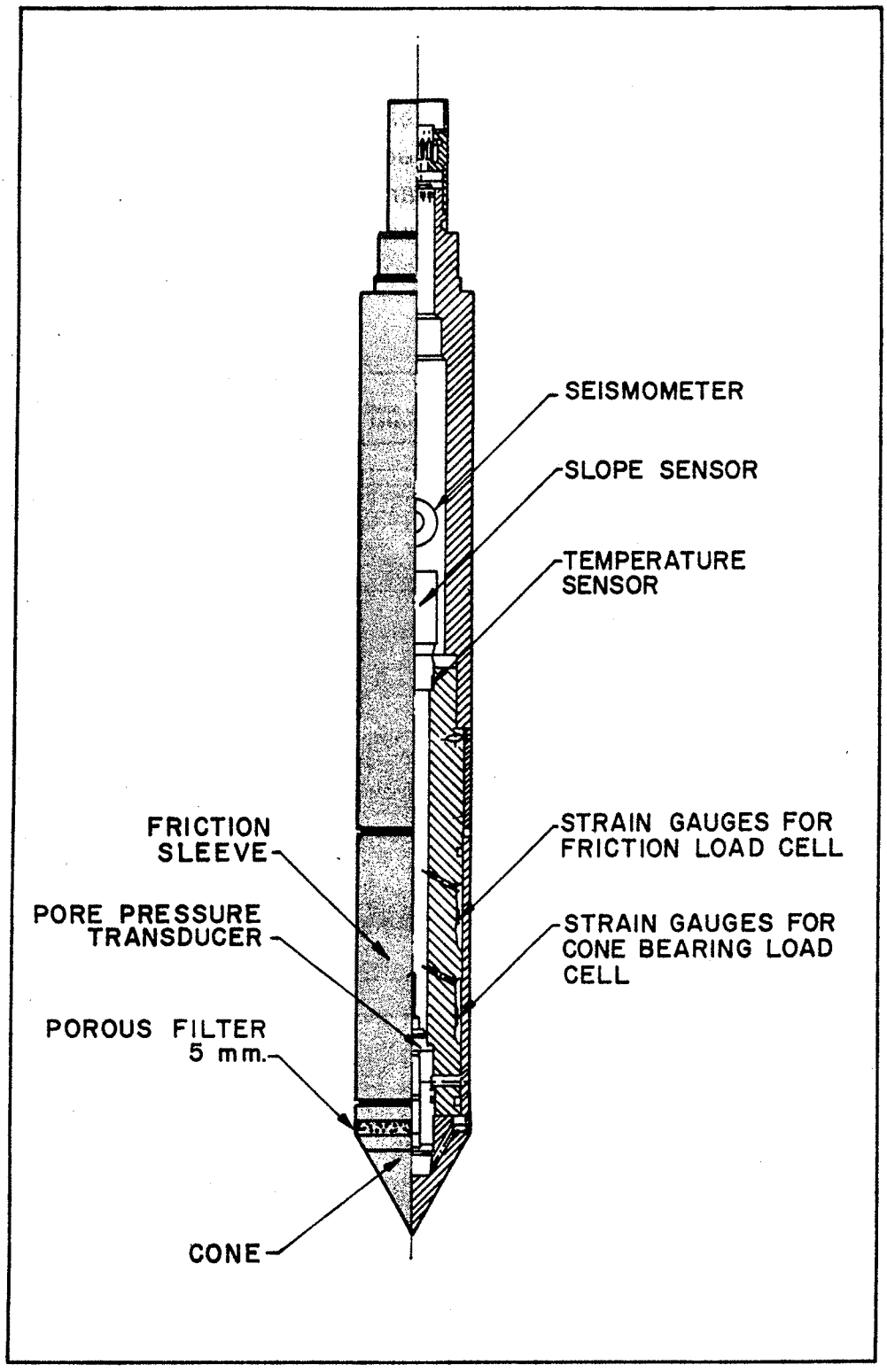

Figure 4.2.1 SEISMIC CONE PENETROMETER

4.2.2 Cone Penetration Test Data and Interpretation

Soil Data

The cone penetration test data are presented in graphical form as Figures 4.2.3 to 4.2.10 and are referenced to the top of sea ice. The thickness of the sea-ice ranged between 1.5 m and 1.8 m at the various test locations.

The stratigraphic interpretation is based on relationships between cone bearing (Qc), sleeve friction (Fs) and dynamic pore pressure (Ut). The friction ratio (Rf) is a calculated parameter (sleeve friction divided by cone bearing) which is used to infer soil behaviour type. Generally, cohesive soils have high friction ratios, low cone bearings and generate large excess pore water pressures. Cohesionless soils have lower friction ratios, high cone bearings and generate little or no excess pore water pressures.

The interpretation of soil data was done using correlation charts developed by Robertson (1989) and illustrated in Figure 4.2.2. It should be noted that it is not always possible to clearly identify a soil type based on Qc, Fs and Ut parameters. Occasionally soils fall within different soil categories on these charts. In these situations, experience and judgement based on an assessment of the pore pressure dissipation data have been used to infer the soil type.

Based on the results of CPT (Figures 4.2.3 to 4.2.10), the soils in the study area consist of either soft silts (CPT 6, 8 and 12) or compact to dense sands (CPT 3, 4 and 13) from the mudline down to depths varying between 1.0 m and 5 m. These deposits are underlain by a stratum of stiff clayey silt with occasional seams of fine sand. A deposit of compact to dense sand with trace amounts of silt was found below the clayey silt to depths of 26 m below the mudline.

The clayey silts have a relatively high shear strength, in part due to overconsolidation. The dynamic pore pressure response recorded during the soundings also indicates overconsolidation of these silts. The sands are relatively dense possibly due to some degree of overconsolidation.

The cone penetration tests were stopped on dense sand layers or at the contact with permanently frozen ground. This contact can be detected by the pore pressure and temperature response, as illustrated by the record from CPT-13. There is an obvious spike in the pore pressure at 12.45 m depth with corresponding temperature of -0.5°C.

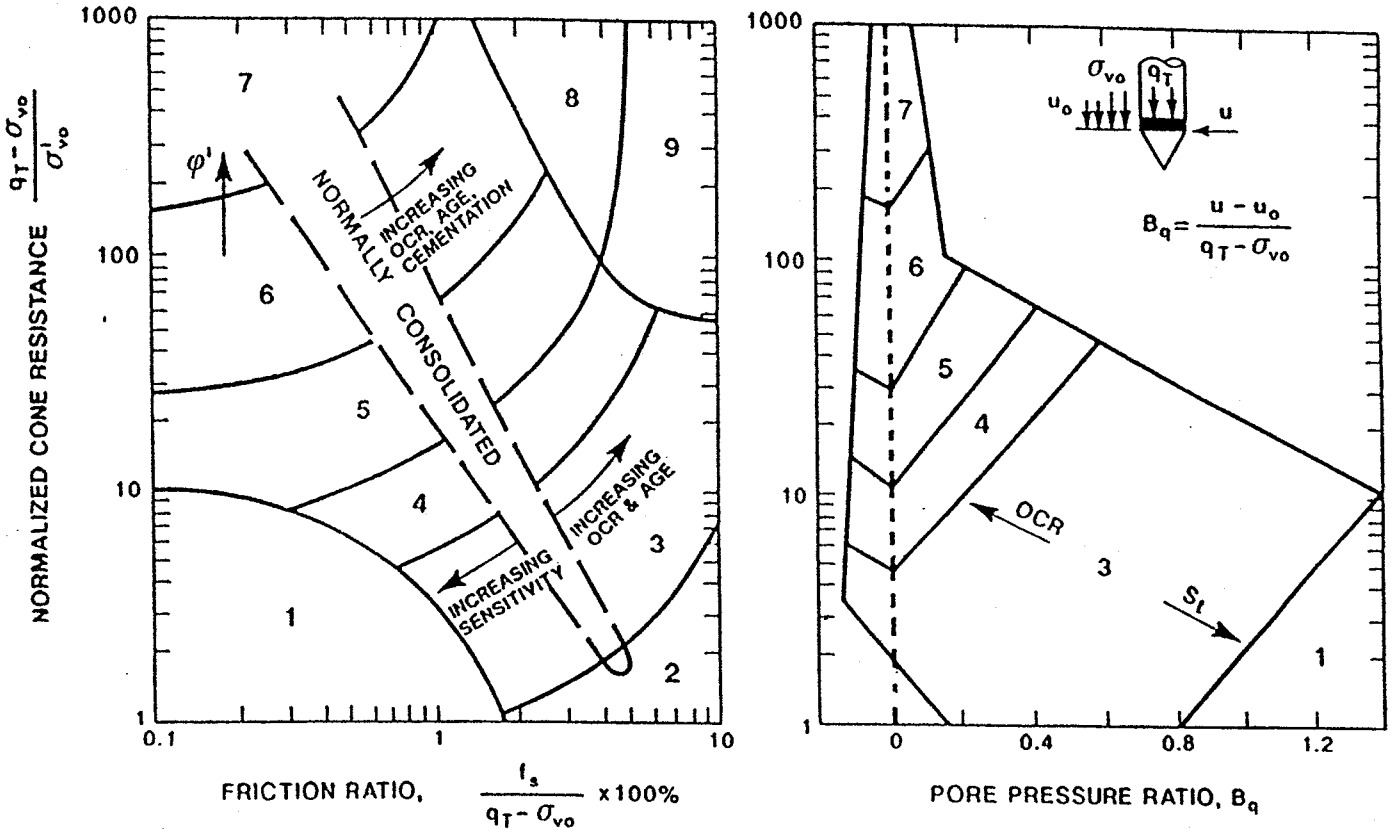

1. SENSITIVE FINE GRAINED
2. ORGANIC SOILS - PEATS
3. CLAYS - CLAY TO SILTY CLAY
4. SILT MIXTURES - CLAYEY SILT TO SILTY CLAY
5. SAND MIXTURES - SILTY SAND TO SANDY SILT
6. SANDS - CLEAN SAND TO SILTY SAND
7. GRAVELLY SAND TO SAND
8. VERY STIFF SAND TO CLAYEY* SAND
9. VERY STIFF FINE GRAINED*

(*) HEAVILY OVERCONSOLIDATED OR CEMENTED

Figure 4.2.2 Proposed soil behaviour type classification chart based on normalized CPT and CPTU data.

Figure 4.2.3

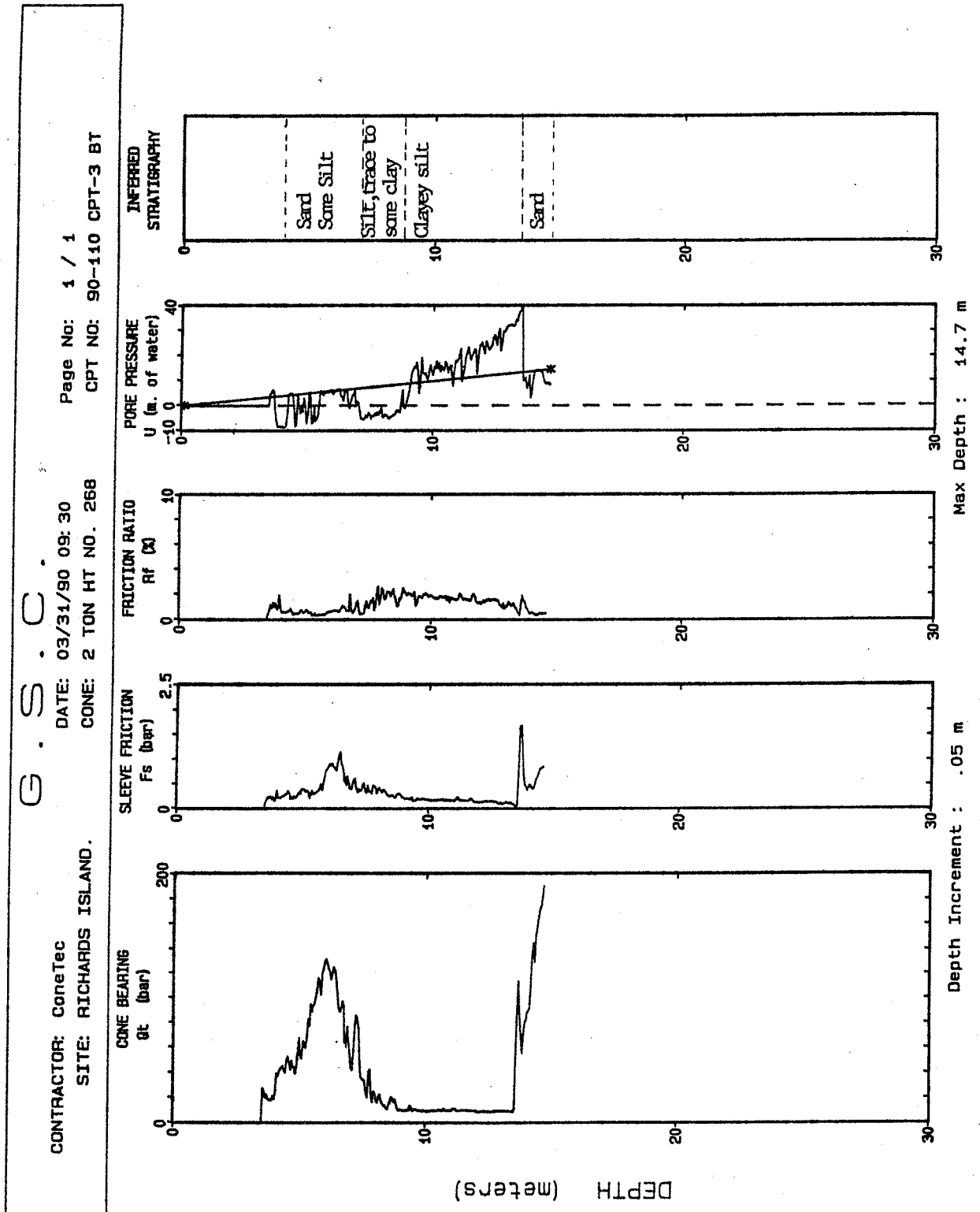
G . S . C .
CONTRACTOR: ConeTec
SITE: RICHARDS ISLAND.
DATE: 03/31/90 09:30
CONE: 2 TON HT NO. 268
Page No: 1 / 1
CPT NO: 90-110 CPT-3 BT
CONE BEARING
Qt (bar)
SLEEVE FRICTION
Fs (bar)
FRICTION RATIO
Rf (%)
PORE PRESSURE
U (m. of water)
INFERRED
STRATIGRAPHY
Sand
Some Silt
Silt, trace to some clay
Clayey silt
Sand
DEPTH (meters)
Depth Increment : .05 m
Max Depth : 14.7 m

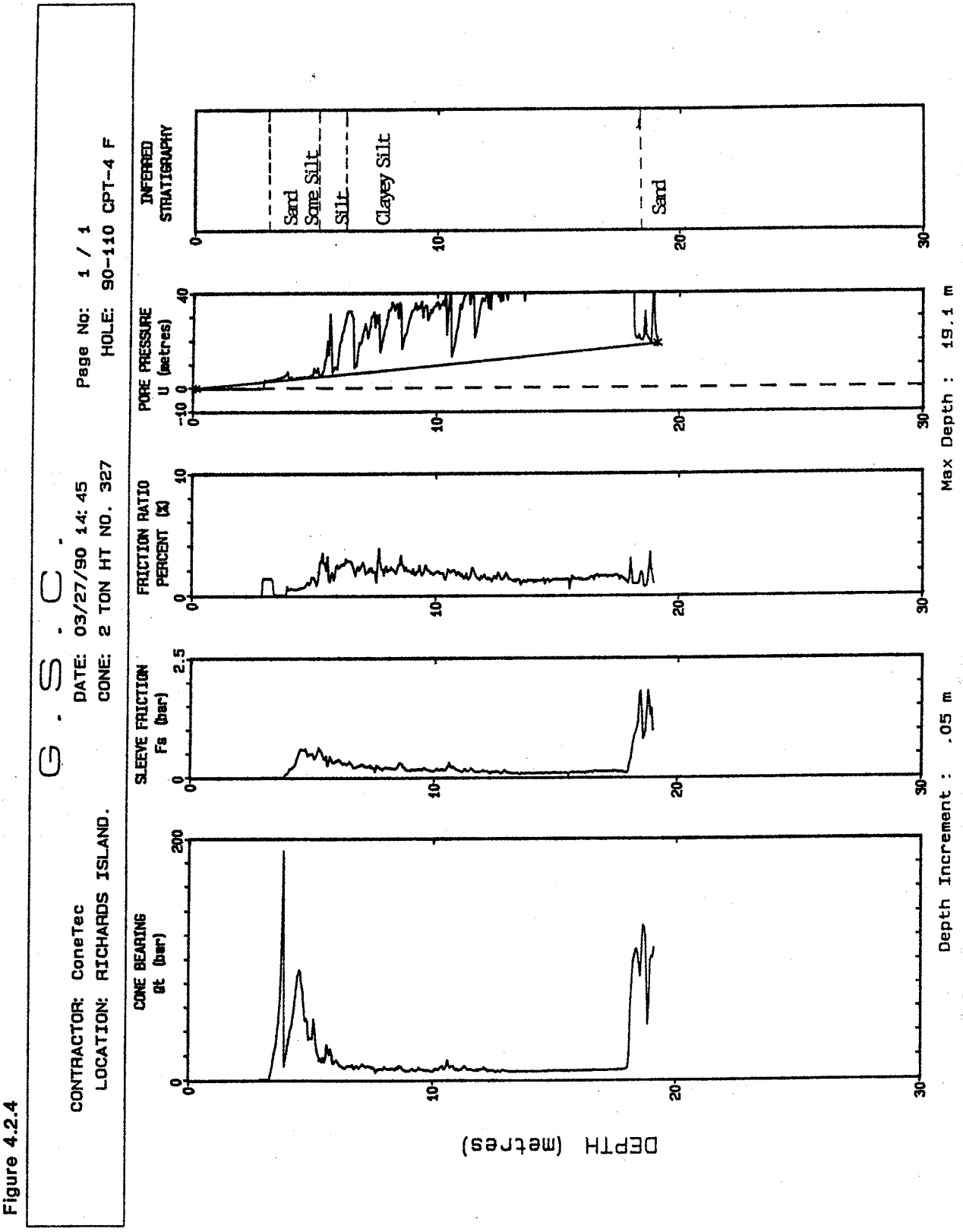
G . S . C .
CONTRACTOR: ConeTec
LOCATION: RICHARDS ISLAND.
DATE: 03/27/90 14:45
CONE: 2 TON HT NO. 327
Page No: 1 / 1
HOLE: 90-110 CPT-4 F
CONE BEARING
qt (bar)
SLEEVE FRICTION
Fs (bar)
FRICTION RATIO
PERCENT (%)
PORE PRESSURE
U (metres)
INFERRED
STRATIGRAPHY
Sand
Some Silt
Silt
Clayey Silt
Sand
DEPTH (metres)
Depth Increment : .05 m
Max Depth : 19.1 m

Figure 4.2.4

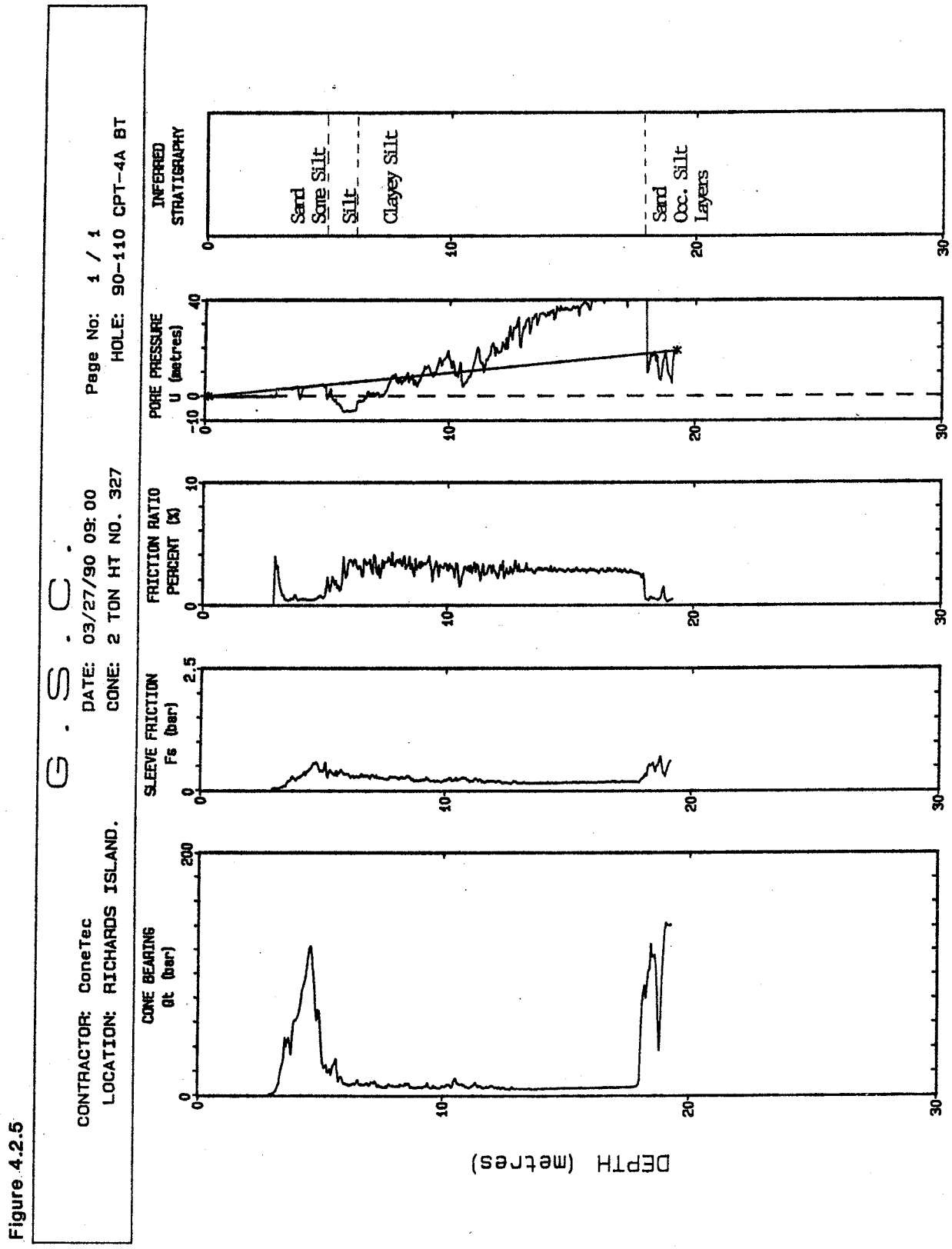
G . S . C .
CONTRACTOR: ConeTec
LOCATION: RICHARDS ISLAND.
DATE: 03/27/90 09:00
CONE: 2 TON HT NO. 327
Page No: 1 / 1
HOLE: 90-110 CPT-4A BT
CONE BEARING
Qt (bar)
SLEEVE FRICTION
Fs (bar)
FRICTION RATIO
PERCENT (%)
PORE PRESSURE
U (metres)
INFERRED
STRATIGRAPHY
Sand
Some Silt
Silt
Clayey Silt
Sand
Occ. Silt
Layers
DEPTH (metres)
Depth Increment : .05 m
Max Depth : 19.25 m

Figure 4.2.5

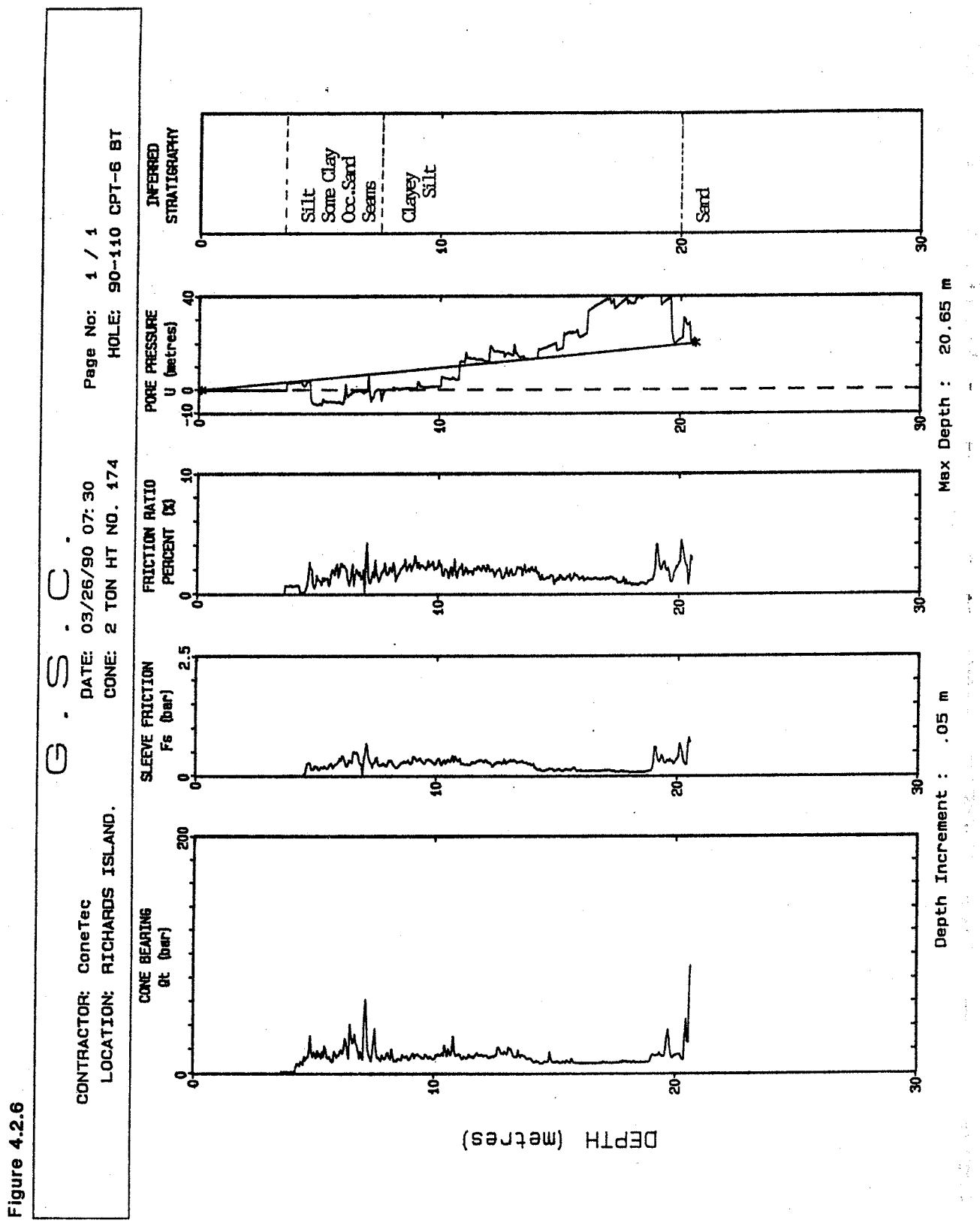
G . S . C .
CONTRACTOR: ConeTec
LOCATION: RICHARDS ISLAND.
DATE: 03/26/90 07:30
CONE: 2 TON HT NO. 174
Page No: 1 / 1
HOLE: 90-110 CPT-6 BT
CONE BEARING
Qt (bar)
SLEEVE FRICTION
Fs (bar)
FRICTION RATIO
PERCENT (%)
PORE PRESSURE
U (metres)
INFERRED
STRATIGRAPHY
Silt
Some Clay
Occ.Sand
Seams
Clayey
Silt
Sand
DEPTH (metres)
Depth Increment : .05 m
Max Depth : 20.65 m

Figure 4.2.6

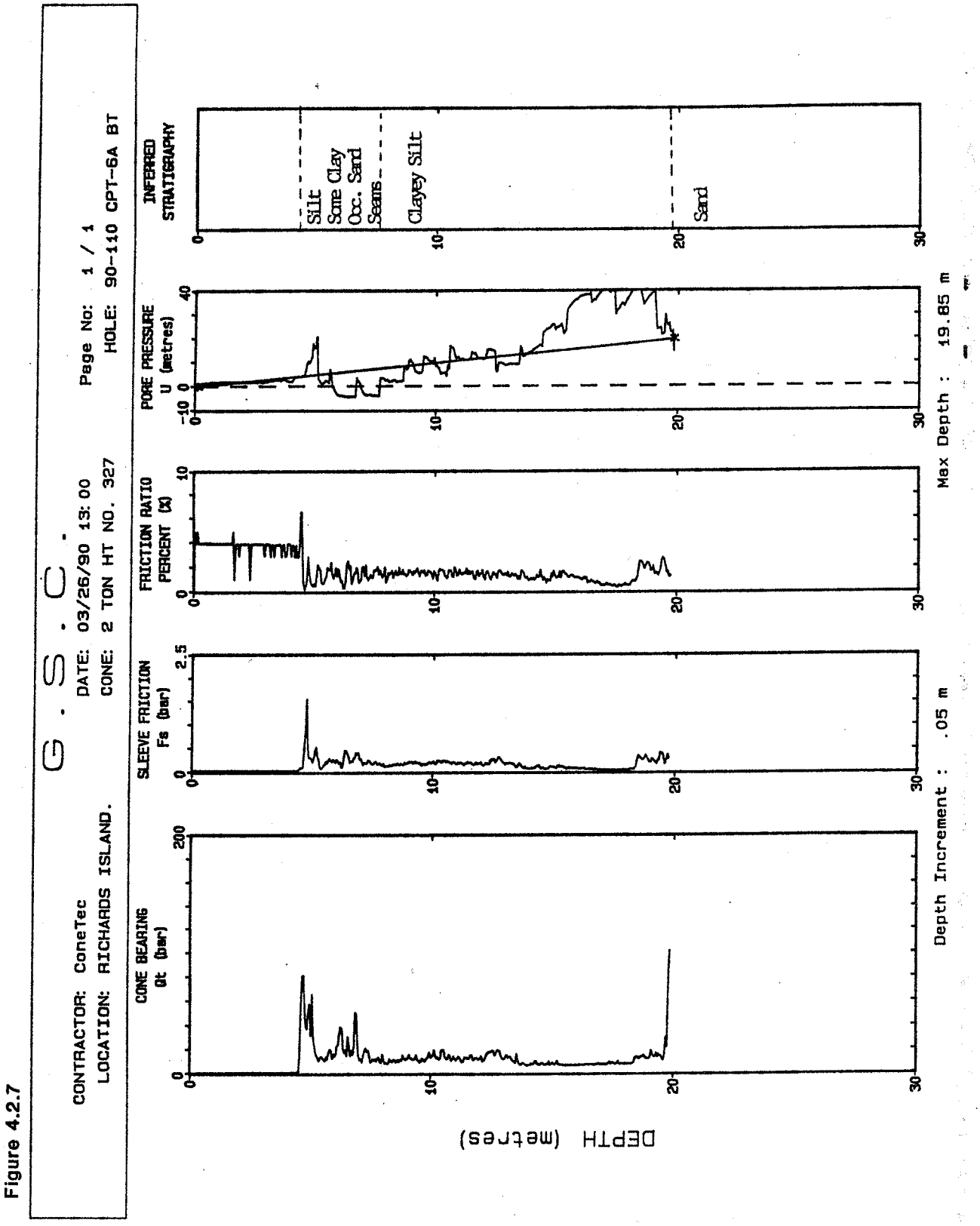
G . S . C .
CONTRACTOR: ConeTec
LOCATION: RICHARDS ISLAND.
DATE: 03/26/90 13:00
CONE: 2 TON HT NO. 327
Page No: 1 / 1
HOLE: 90-110 CPT-6A BT
CONE BEARING Qt (bar)
SLEEVE FRICTION Fs (bar)
FRICTION RATIO PERCENT (%)
PORE PRESSURE U (metres)
INFERRED STRATIGRAPHY
Silt
Some Clay
Occ. Sand
Seams
Clayey Silt
Sand
DEPTH (metres)
Depth Increment : .05 m
Max Depth : 19.85 m

Figure 4.2.7

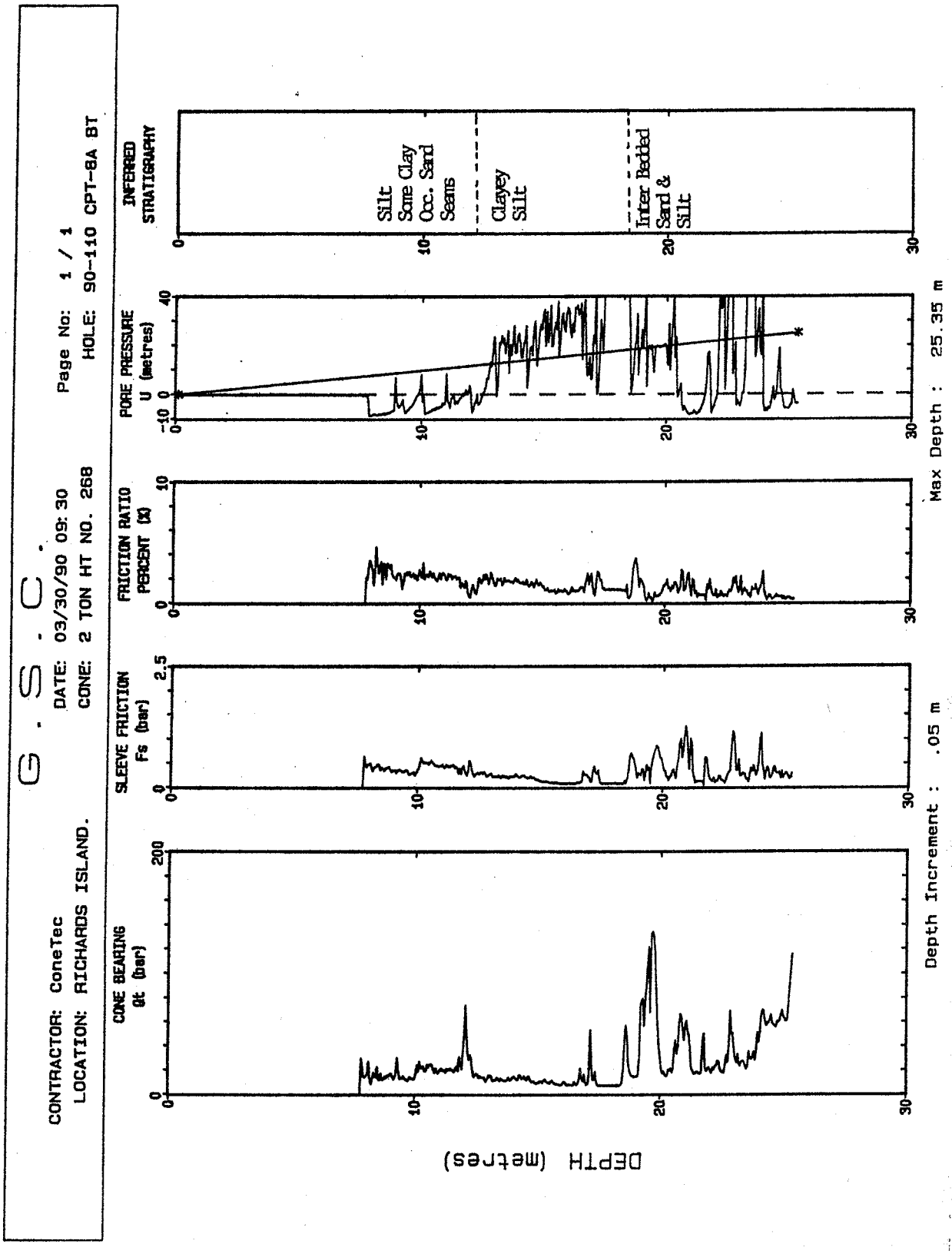
G . S . C .
CONTRACTOR: ConeTec
LOCATION: RICHARDS ISLAND.
DATE: 03/30/90 09:30
CONE: 2 TON HT NO. 268
Page No: 1 / 1
HOLE: 90-110 CPT-8A BT
CONE BEARING
Qt (bar)
SLEEVE FRICTION
Fs (bar)
FRICTION RATIO
PERCENT (%)
PORE PRESSURE
U (metres)
INFERRED
STRATIGRAPHY
Silt
Some Clay
Occ. Sand
Seams
Clayey
Silt
Inter Bedded
Sand &
Silt
DEPTH (metres)
Depth Increment : .05 m
Max Depth : 25.35 m

Figure 4.2.8

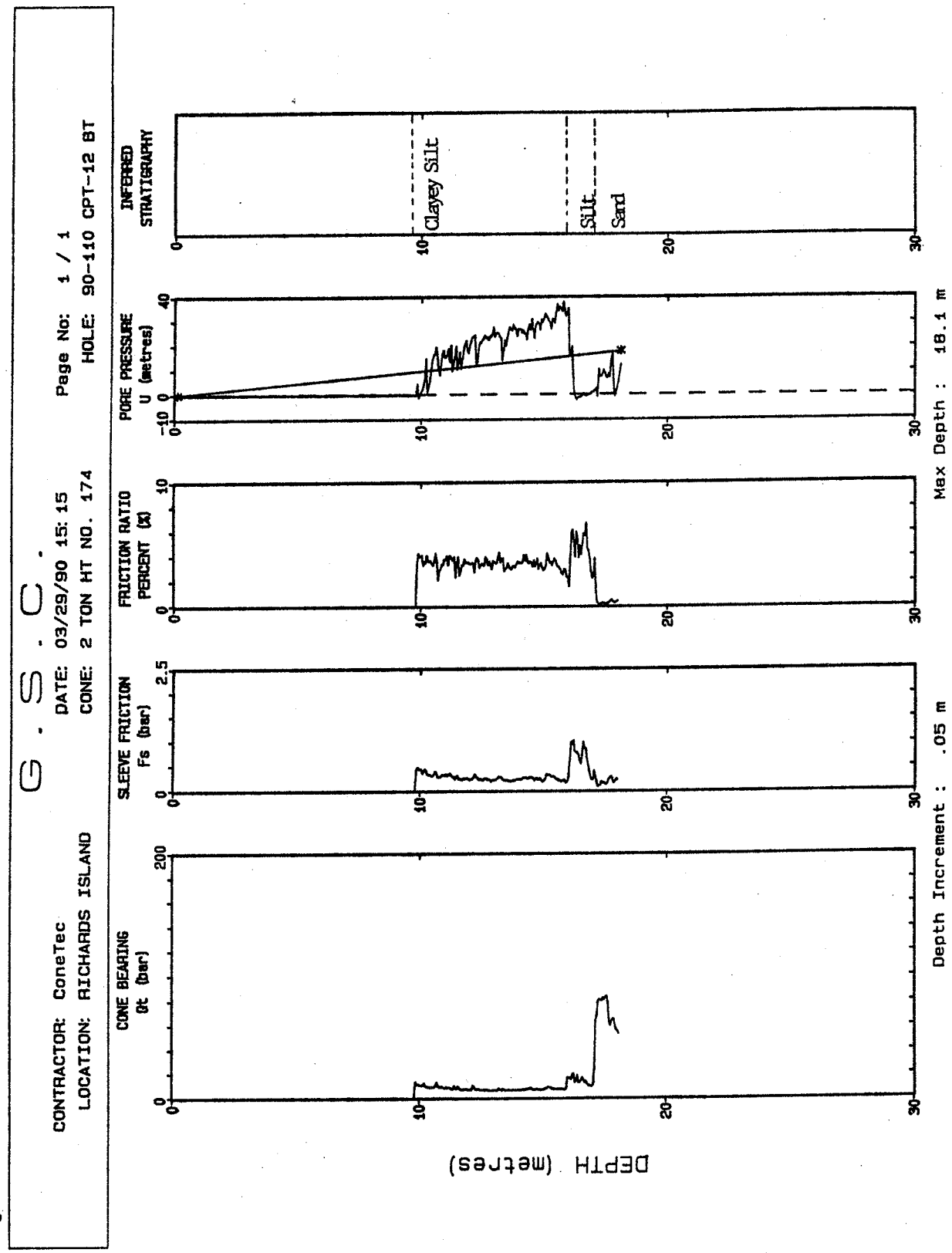
G . S . C .
CONTRACTOR: ConeTec
LOCATION: RICHARDS ISLAND
DATE: 03/29/90 15:15
CONE: 2 TON HT NO. 174
Page No: 1 / 1
HOLE: 90-110 CPT-12 BT
CONE BEARING
Qt (bar)
SLEEVE FRICTION
Fs (bar)
FRICTION RATIO
PERCENT (%)
PORE PRESSURE
U (metres)
INFERRED
STRATIGRAPHY
Clayey Silt
Silt
Sand
DEPTH (metres)
Depth Increment : .05 m
Max Depth : 18.1 m

Figure 4.2.9

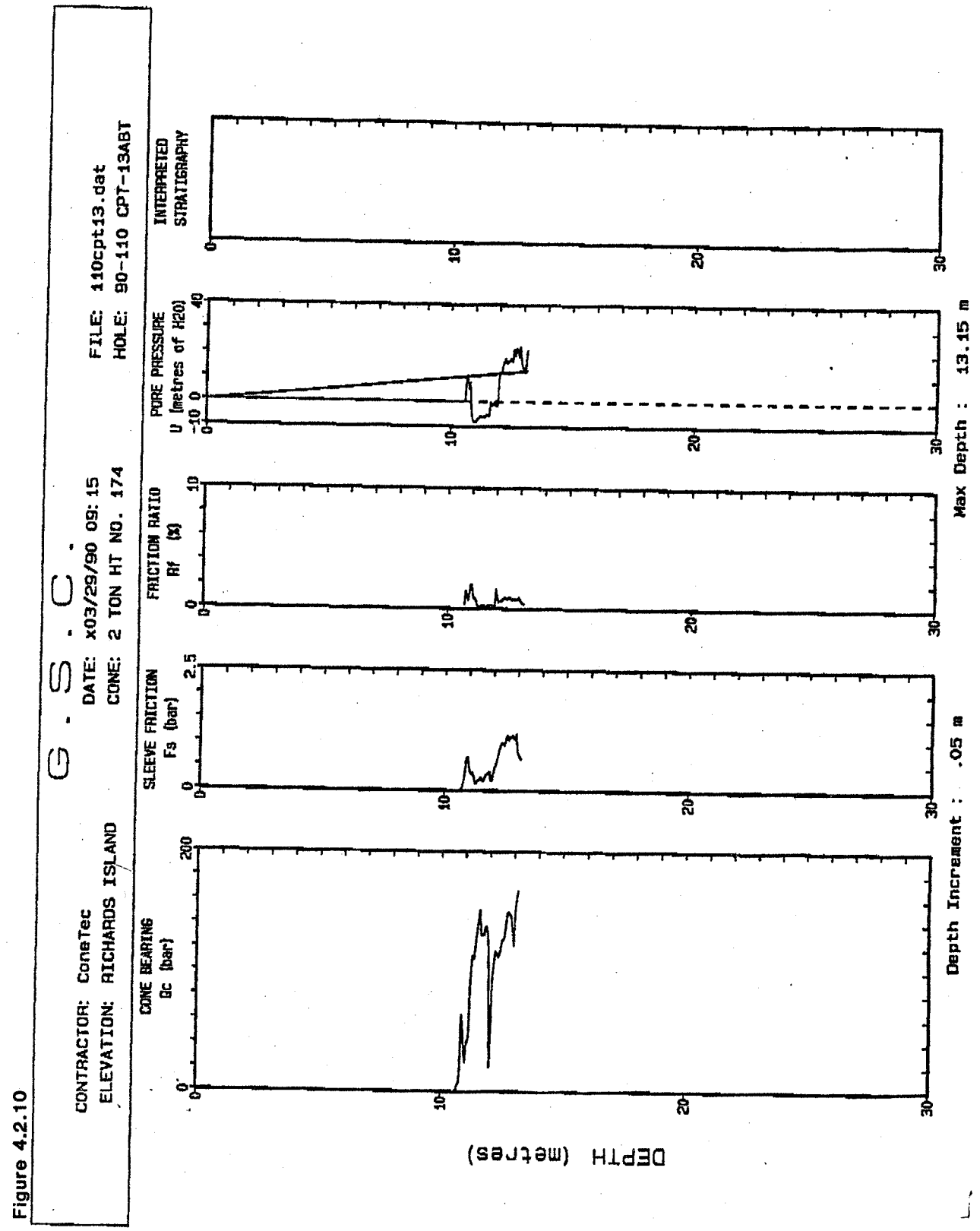
G . S . C .
CONTRACTOR: ConeTec
ELEVATION: RICHARDS ISLAND
DATE: x03/29/90 09:15
CONE: 2 TON HT NO. 174
FILE: 110cpt13.dat
HOLE: 90-110 CPT-13ABT
CONE BEARING Qc (bar)
SLEEVE FRICTION Fs (bar)
FRICTION RATIO Rf (%)
PORE PRESSURE U (metres of H20)
INTERPRETED STRATIGRAPHY
DEPTH (metres)
Depth Increment : .05 m
Max Depth : 13.15 m

Figure 4.2.10

Spikes in both the Qc and Ut profiles just below the mudline for depths of about 0.2 to 0.3 m were recorded at several test locations. These increases reflect a seasonally frozen layer of corresponding thickness at the mudline. Temperatures of the sea water and the soils at the mudline range from -0.5°C to 1.6 °C, and the salinities of the seawater at the mudline vary between 5 to 10 ppt. The negative (below 0 °C) temperatures and the low salinities account for the freezing of the soil at these locations during the winter season.

Using the PPD method for data collected at CPT-4, the OCR in the clayey silt is estimated to be about 6.5 near the mudline, decreasing to about 1.5 at the sand contact. Plots of the penetration pore pressures, OCR and Su/P' (ratio of undrained shear strength to pore water pressure) versus depth are presented as Figures 4.2.11 to 4.2.13.

Temperature Data

To obtain accurate equilibrium ambient temperatures, dissipation times from 8 to 14 minutes are required as temperatures fluctuate significantly depending on the type of material being penetrated. Penetration through cohesionless soils with high sleeve friction values generates significant heat causing temperatures to rise above the ambient temperature.

Temperature measurements taken during selected soundings vary depending on hole location relative to Richards Island and depth below the mudline. Temperature dissipation tests were carried out at varying intervals of depth in 4 of the cone holes (CPT 3A, 6A, 8A and 13A) in order to determine accurate ambient temperatures. Plots showing the variation of temperatures with depth for 3A, 6A and 8A are shown in Figure 4.2.14 to 4.2.16. Only two readings were taken at the CPT-13A location where temperatures of -1.6 and -0.5°C were recorded at the mudline and at a depth of 12.45 m, respectively. The temperature profiles show that ground temperatures tend to increase with depth below the mudline from -0.5 to 1.9 °C. The ambient temperature of the sea water at the mudline is relatively constant at about -0.4 °C with the exception of CPT-13A site.

Seismic Data

Based on the results of the seismic tests performed at SCPT 3A, 4A and 6A sites, it was determined that the average compressional wave velocity for the soils penetrated was

Figure 4.2.11 PORE PRESSURE VS DEPTH

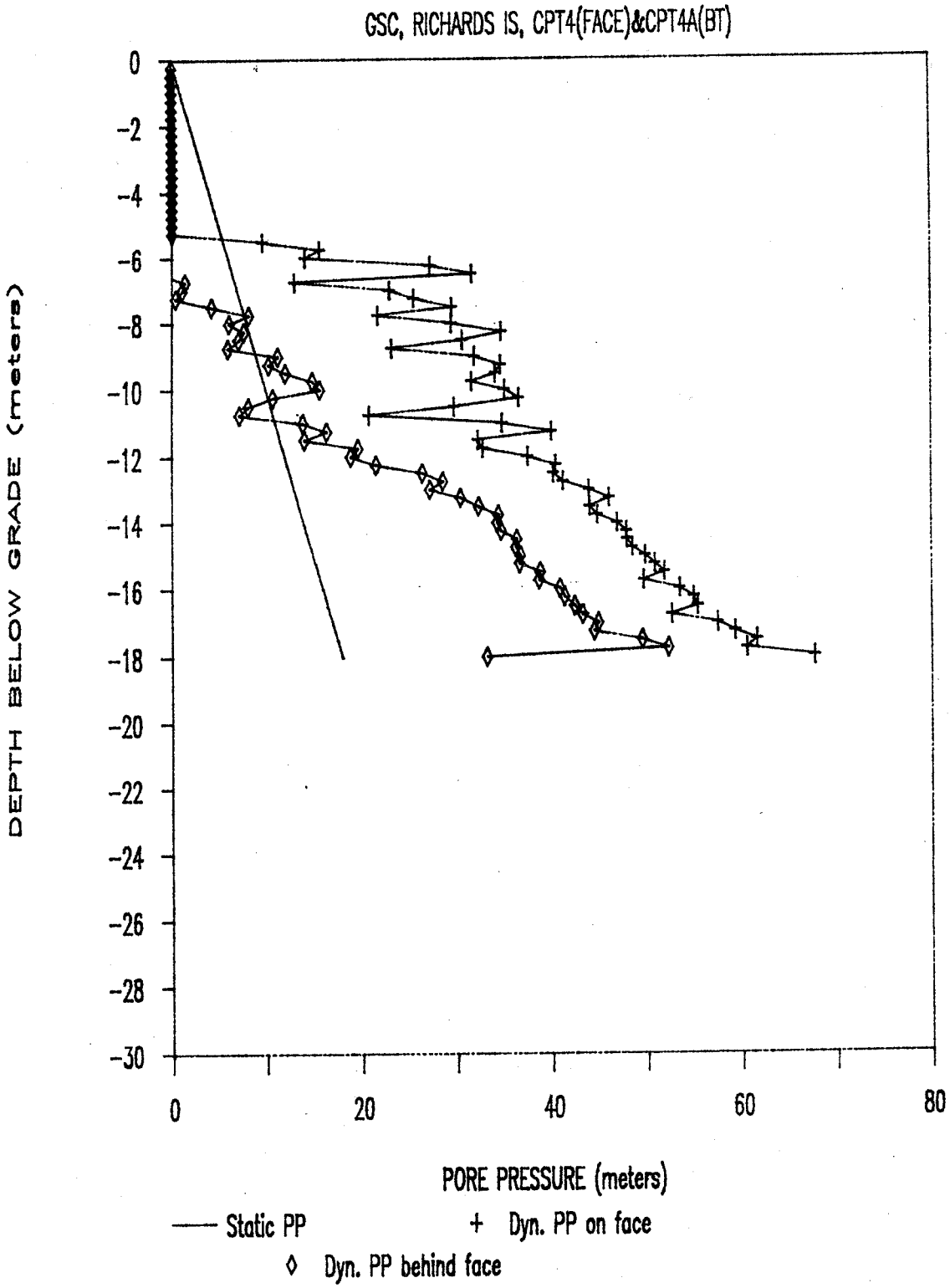

Figure 4.2.12 OVER CONSOLIDATION RATIO VS DEPTH

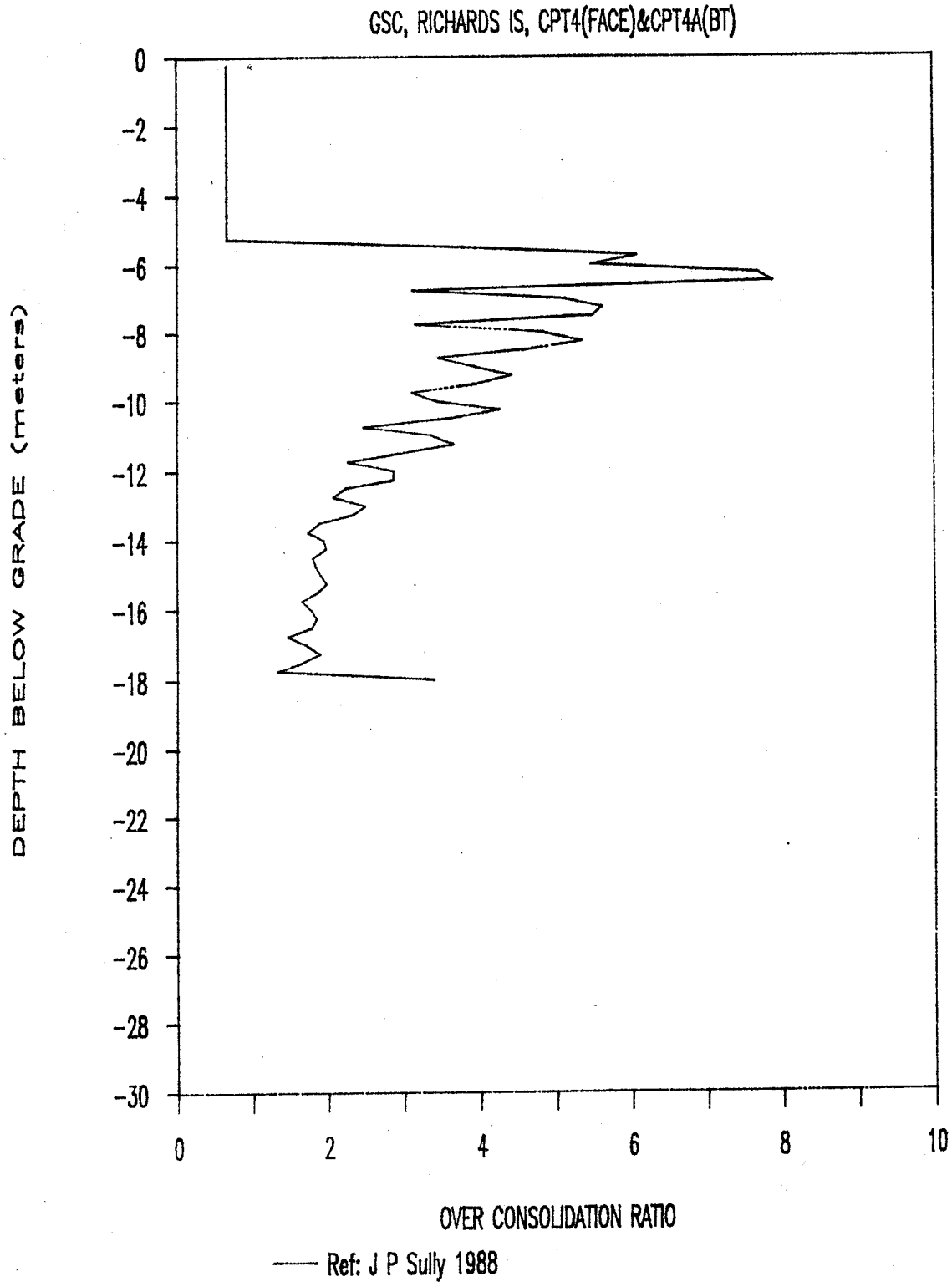

Figure 4.2.13 Su/P' VS DEPTH

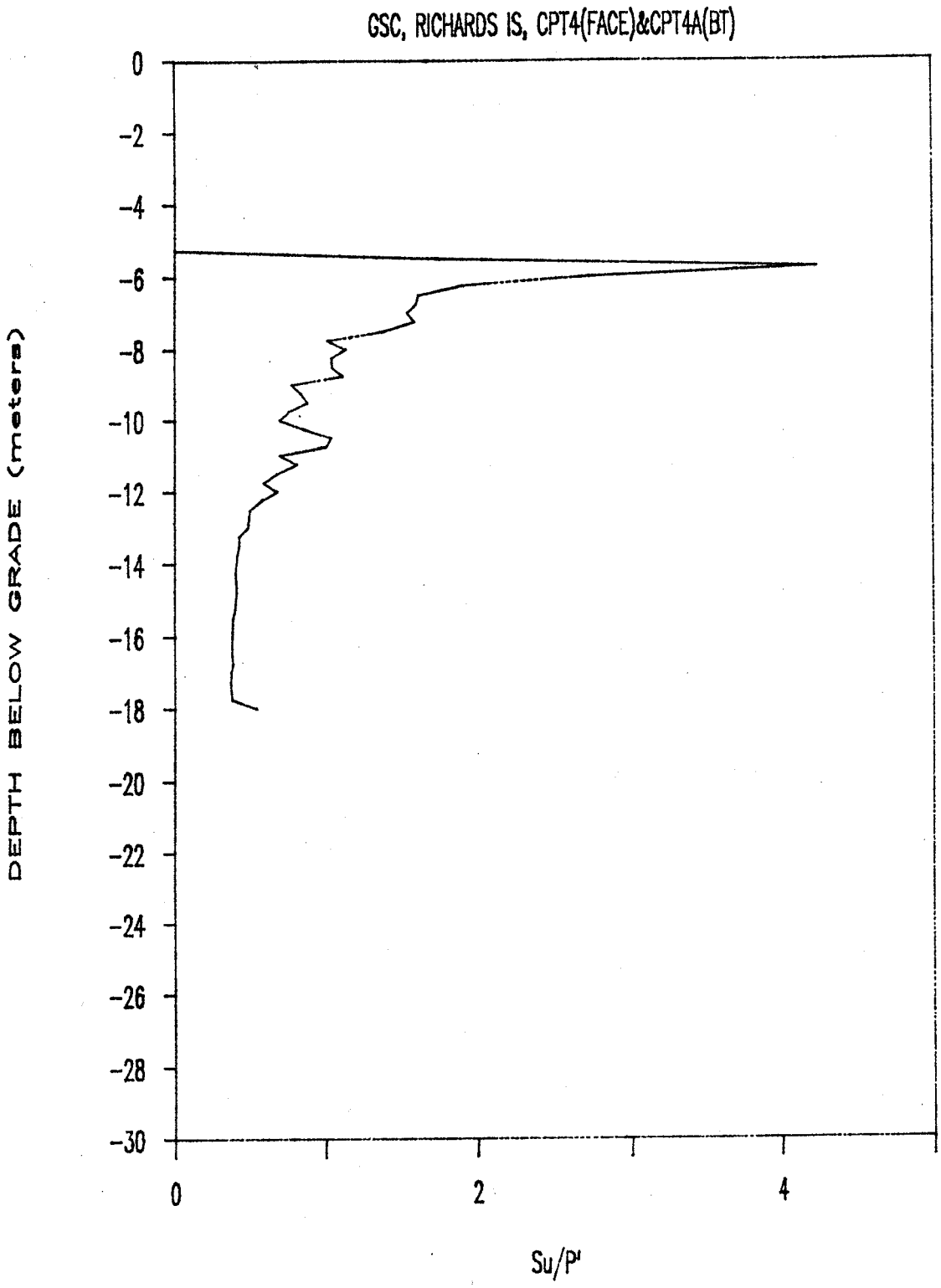

Figure 4.2.14 TEMPERATURE VS DEPTH

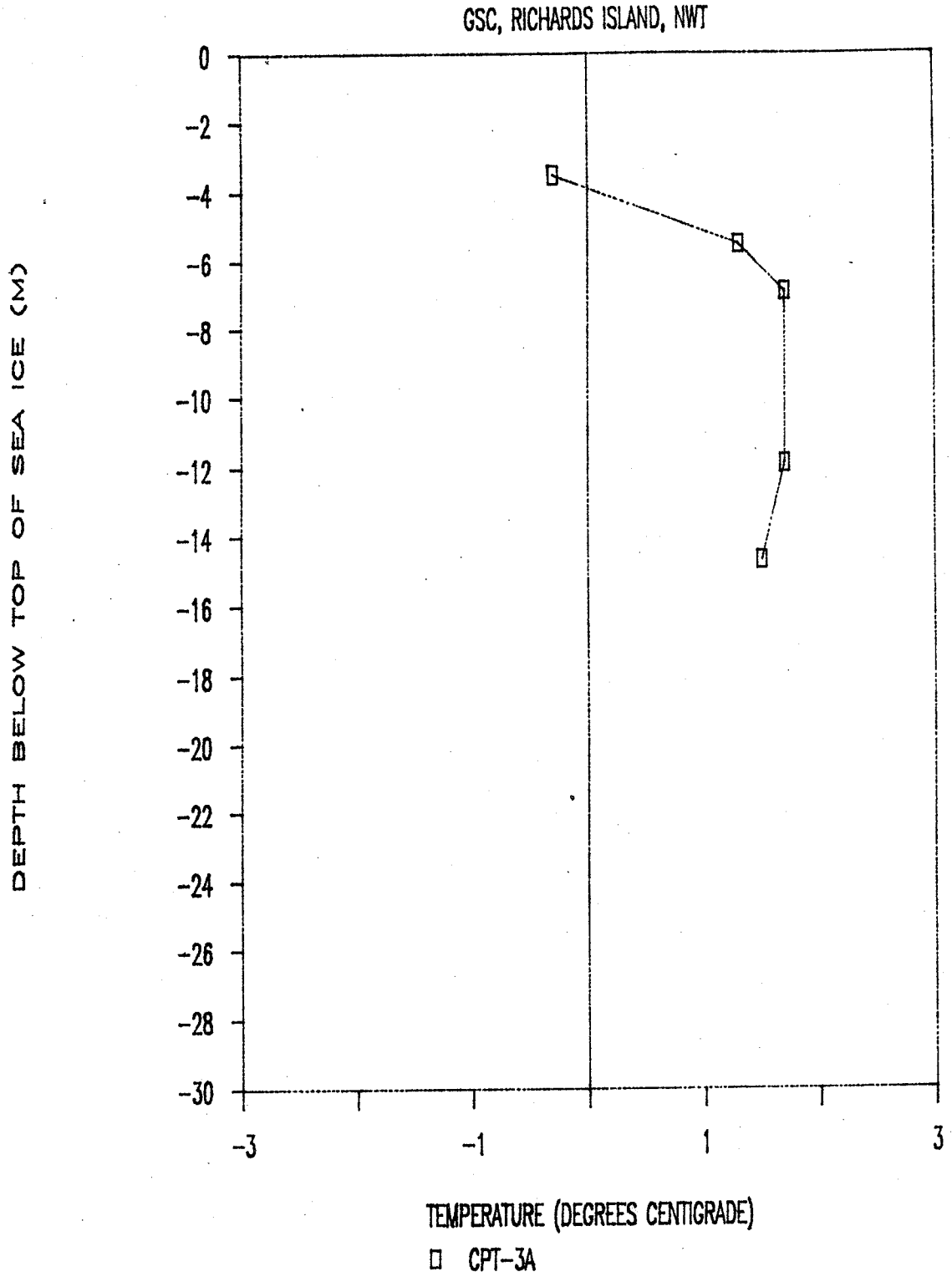

Figure 4.2.15 TEMPERATURE VS DEPTH

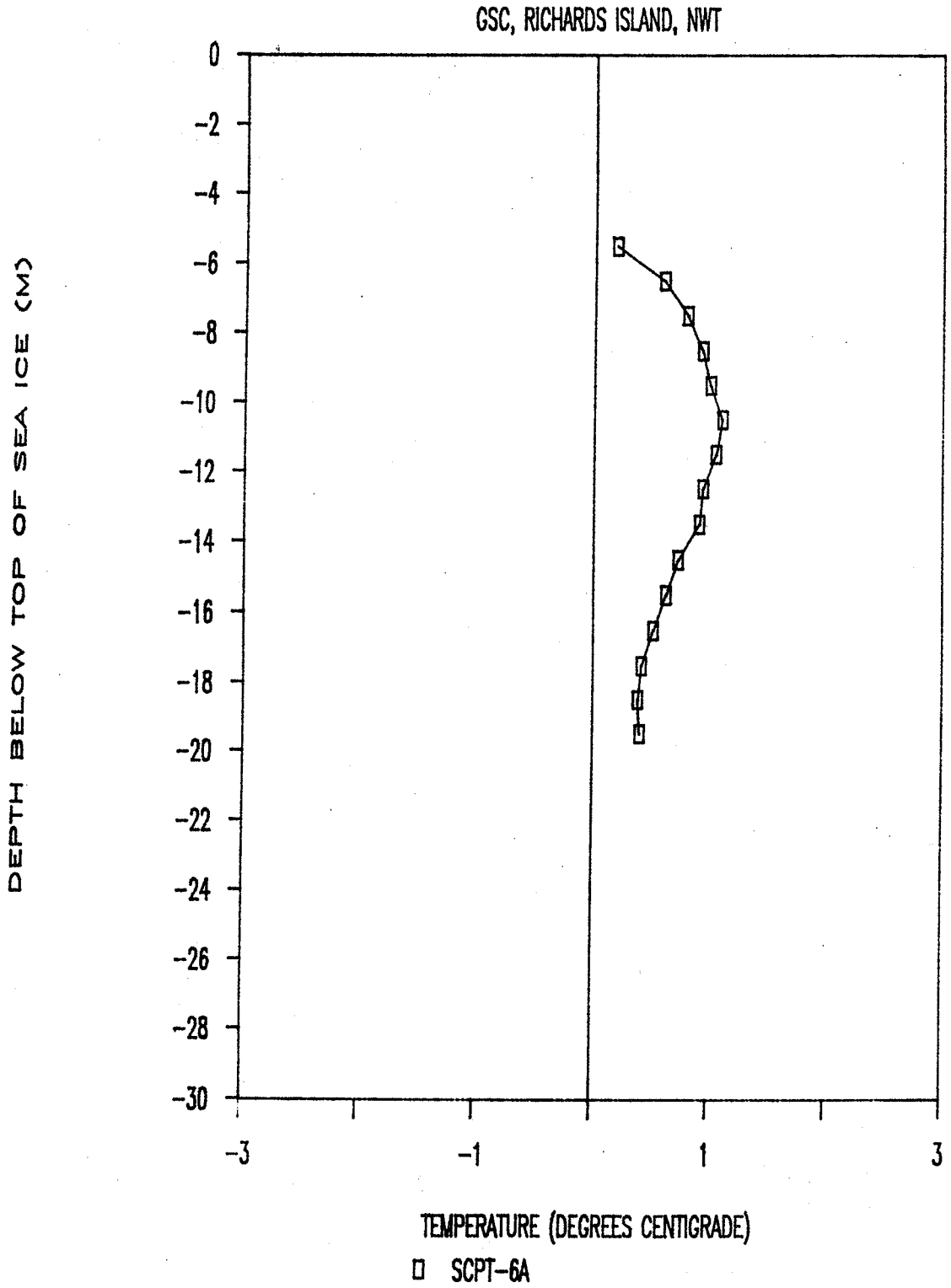

Figure 4.2.16 TEMPERATURE VS DEPTH

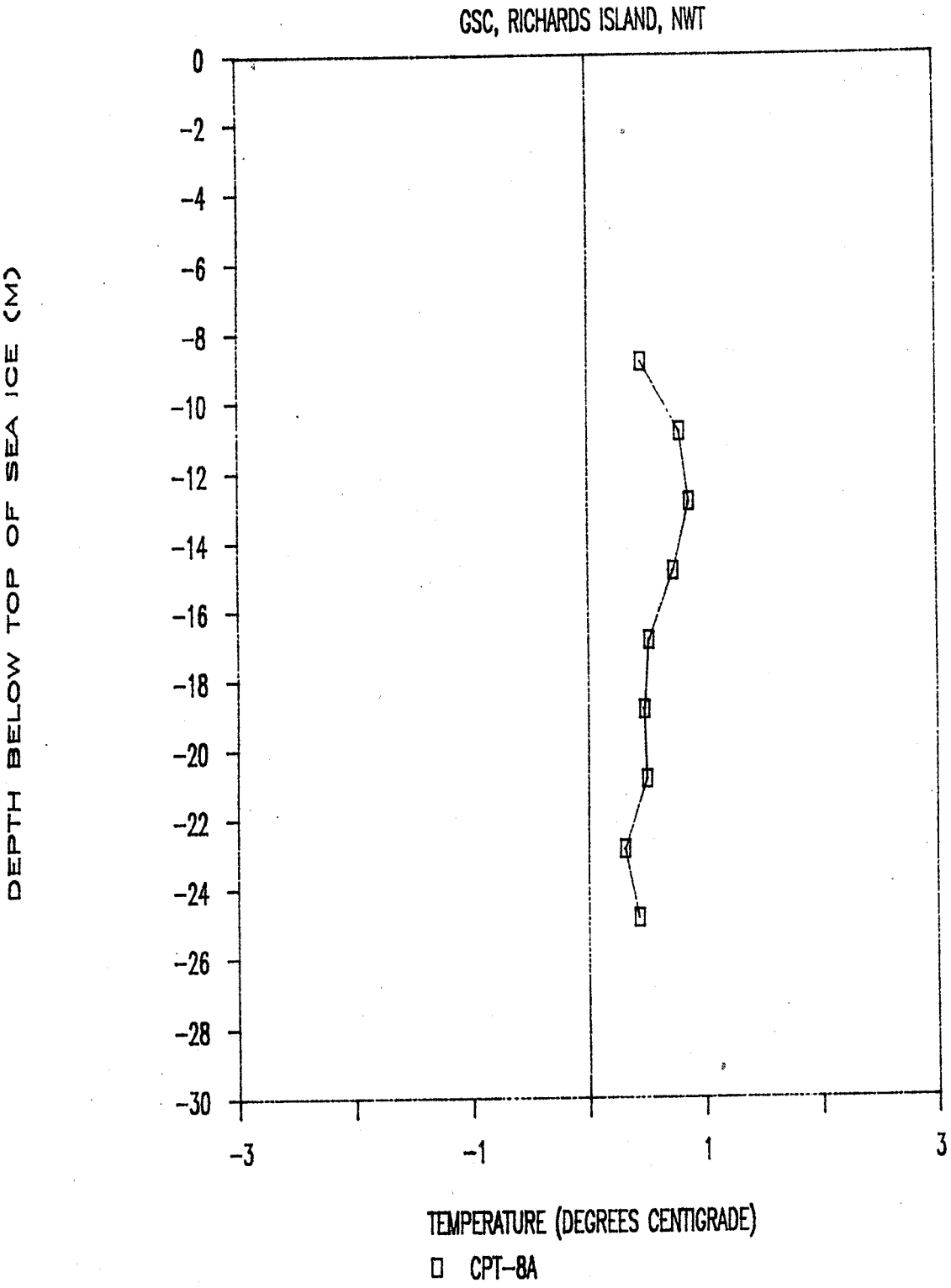

1500 to 1600 m/s and the average shear wave velocity was 150 to 160 m/s. The records of the downhole seismic data are presented in Figures 4.2.17 to 4.2.19.

Salinity Data

Results of tests performed at CPT 3, 4, 6 and 12 sites show that the salinity of the seawater at the mudline ranged between 5 and 10 ppt. The salinities of the soil pore fluid varied depending on the soil type. Generally, pore fluid contained within the silts and clayey silts has a higher salinity than the pore fluid contained within the sands. This phenomenon is largely due to the clay mineralogy and the lower ion exchange capacity of clay minerals. The salinities of the pore fluid ranged between 10 and 30 ppt, the largest values being recorded within the normally consolidated clayey silt stratum. Profiles showing the variation in salinity with depth are shown in Figures 4.2.20 to 4.2.23.

Resistivity Data

Measurements carried out at CPT 4 and CPT 6 sites show that the resistivity of the seawater at the mudline ranged between 0.7 and 0.8 ohm-m. The bulk resistivities of the soil varied depending on the soil type. Generally, resistivities of the silts and clayey silts were lower than resistivities of the sands. The bulk resistivity of the clayey silts ranged between 1 and 3 ohm-m. The largest resistivities were recorded in the sands with values as high as 5 ohm-m. Profiles showing the variation in bulk resistivity with depth are shown as Figures 4.2.24 and 4.2.25.

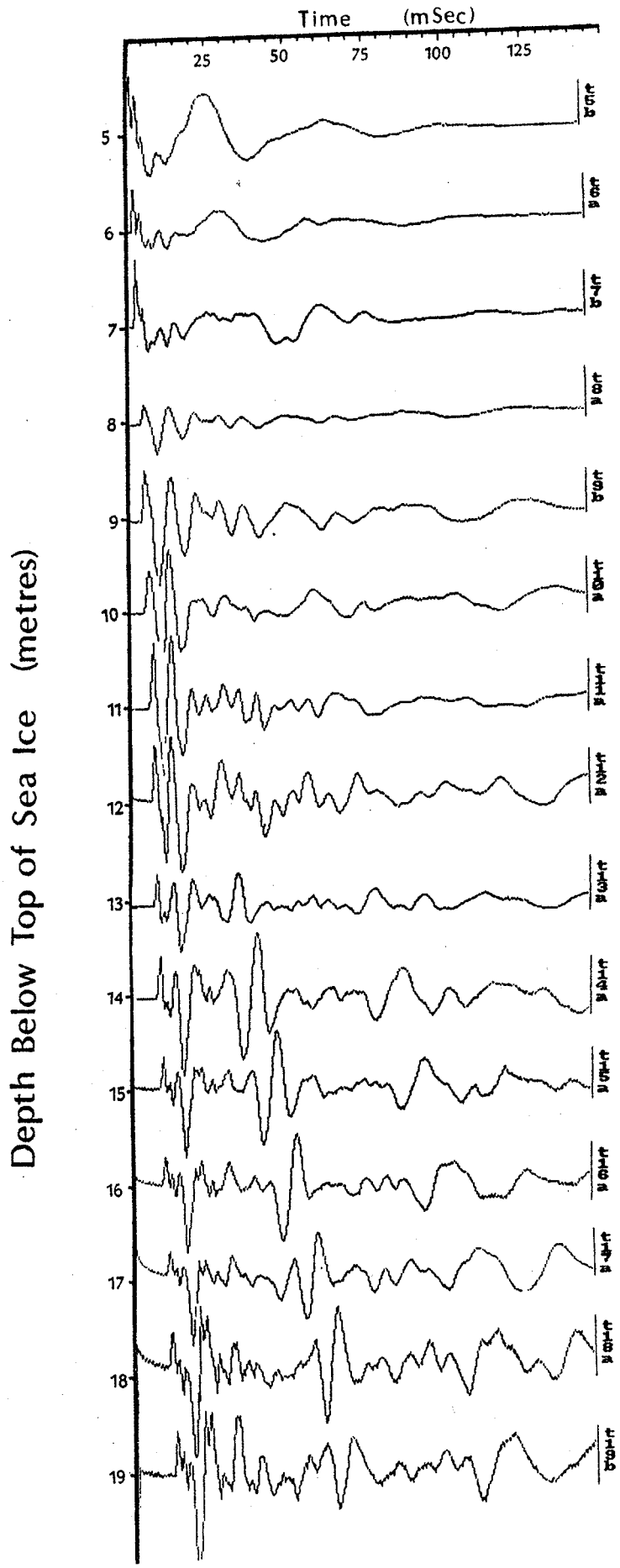

Figure 4.2.17
Down Hole Seismic Data
CPT-4A
March 27, 1990
Richards Island, N.W.T.

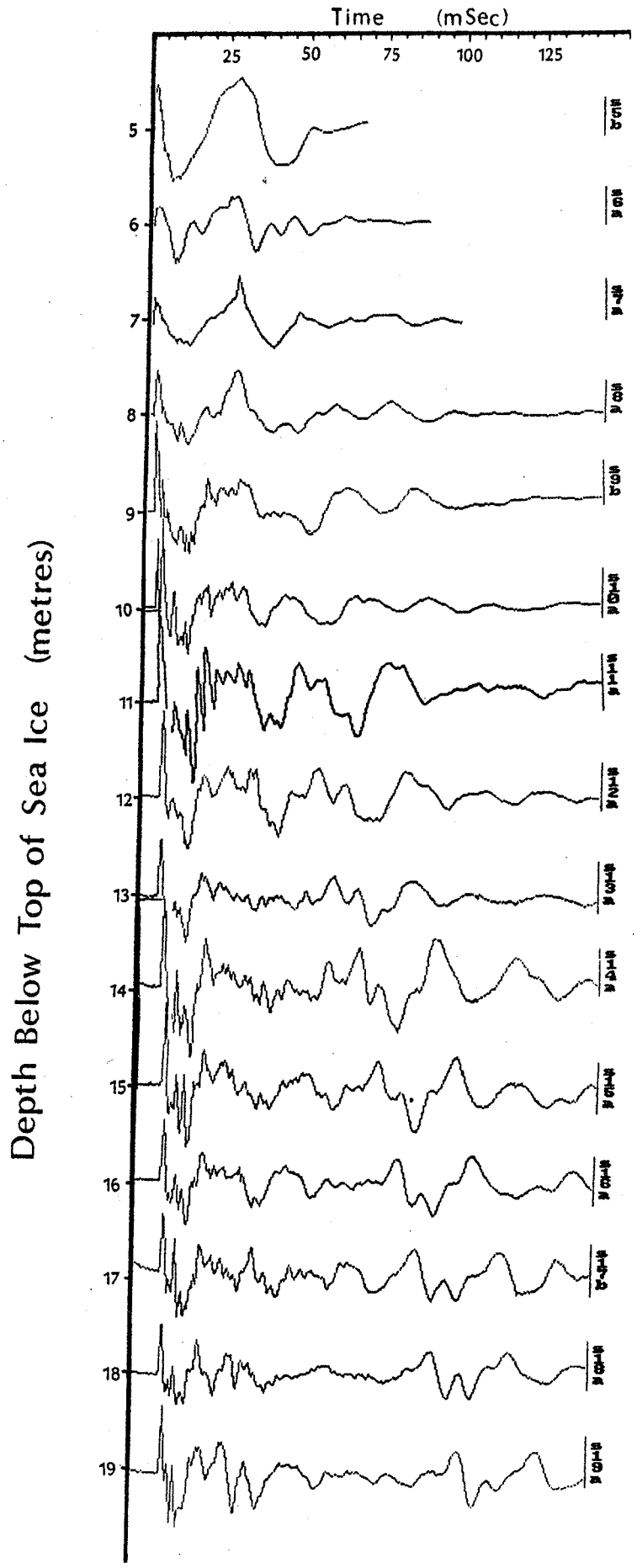

Figure 4.2.18
Down Hole Seismic Data
CPT-6A
March 26, 1990
Richards Island, N.W.T.

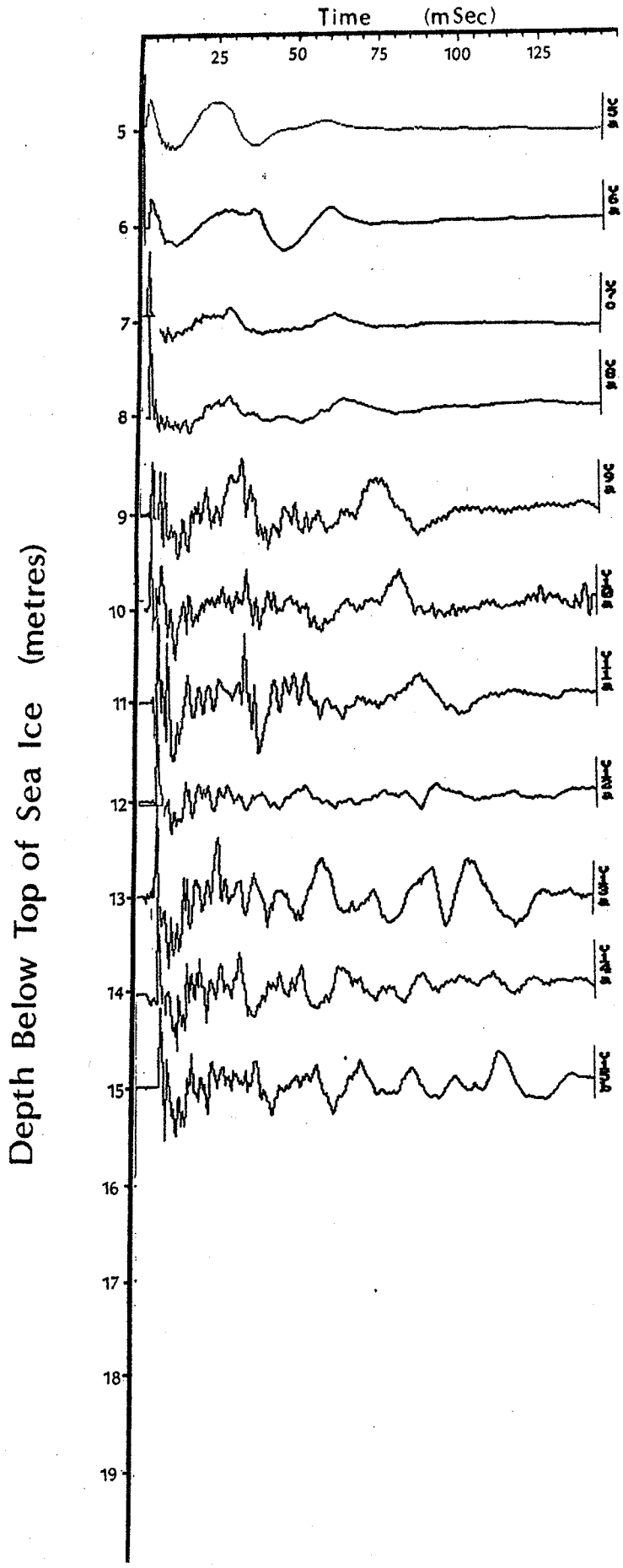

Figure 4.2.19
Down Hole Seismic Data
CPT-3A
March 31, 1990

Figure 4.2.20 SALINITY VS DEPTH

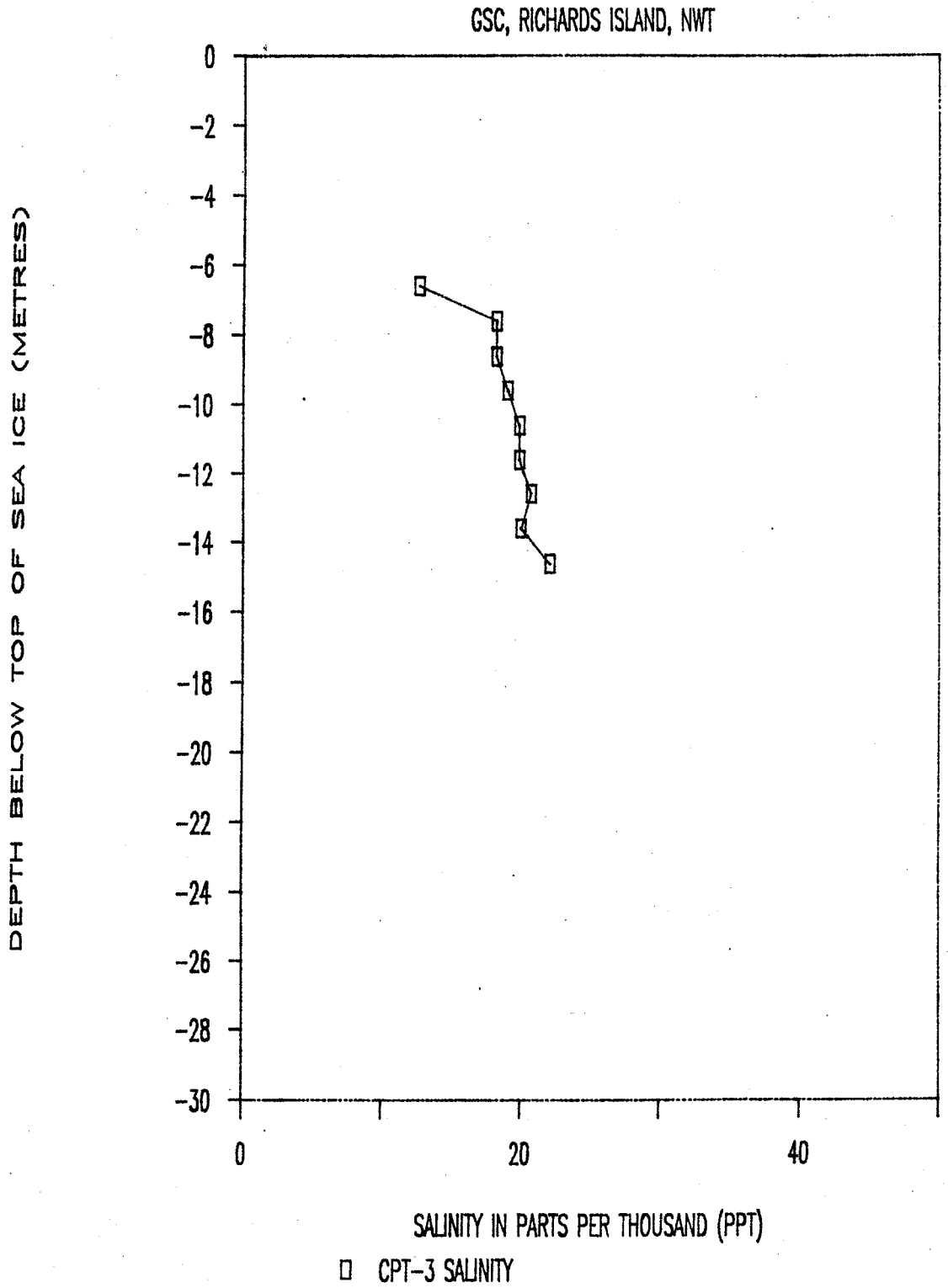

Figure 4.2.21 SALINITY VS DEPTH

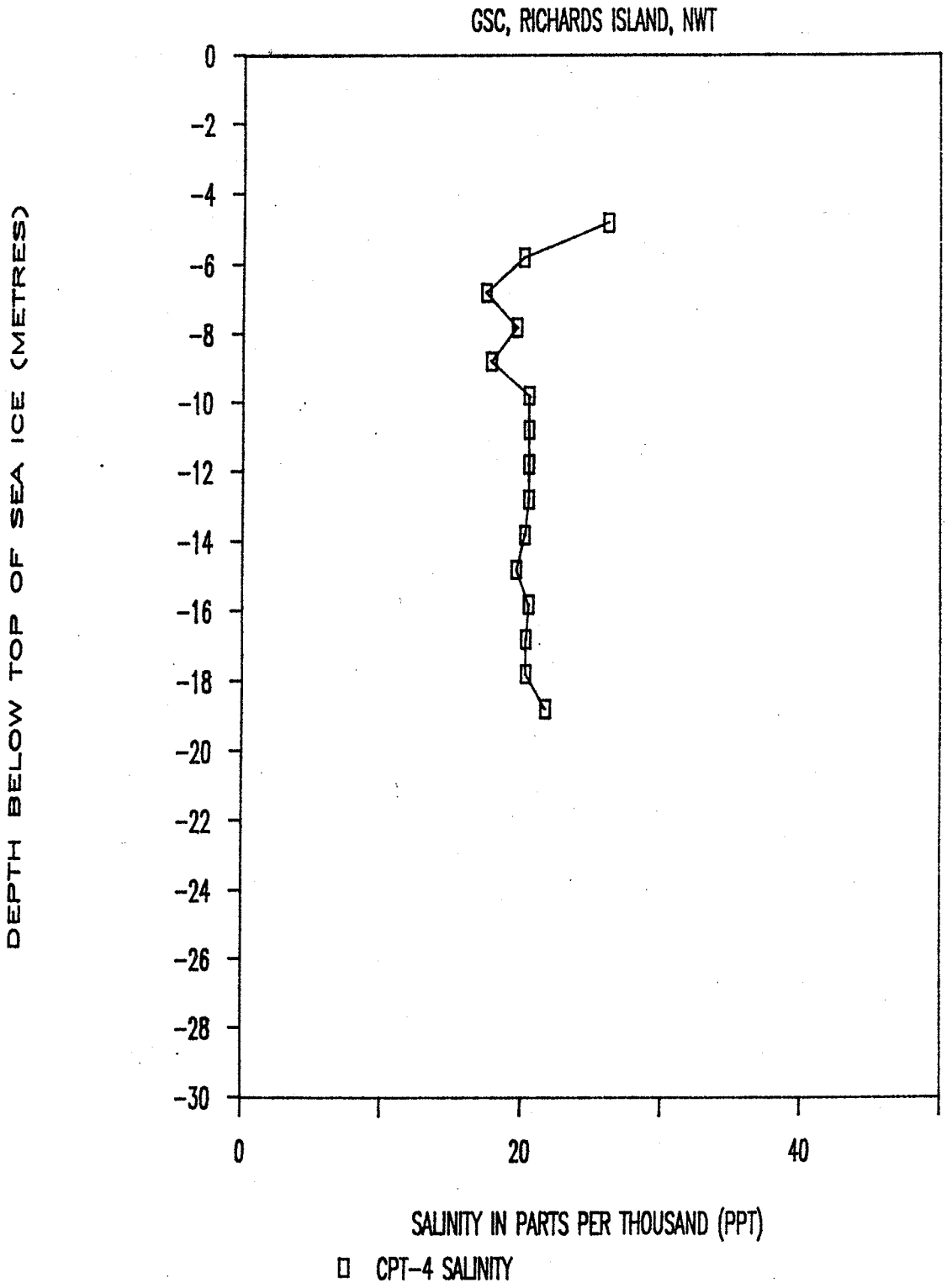

Figure 4.2.22 SALINITY VS DEPTH

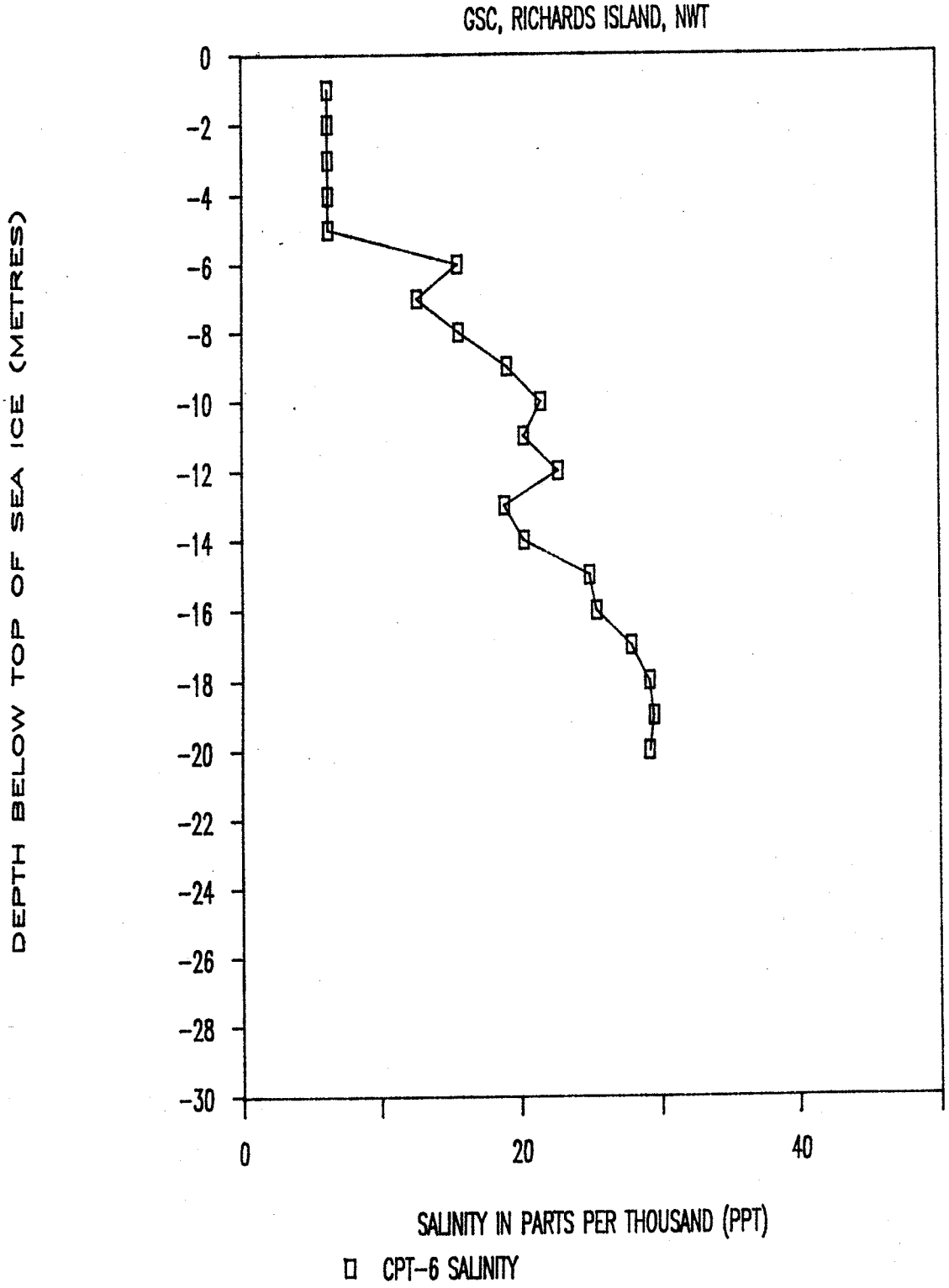

Figure 4.2.23 SALINITY VS DEPTH

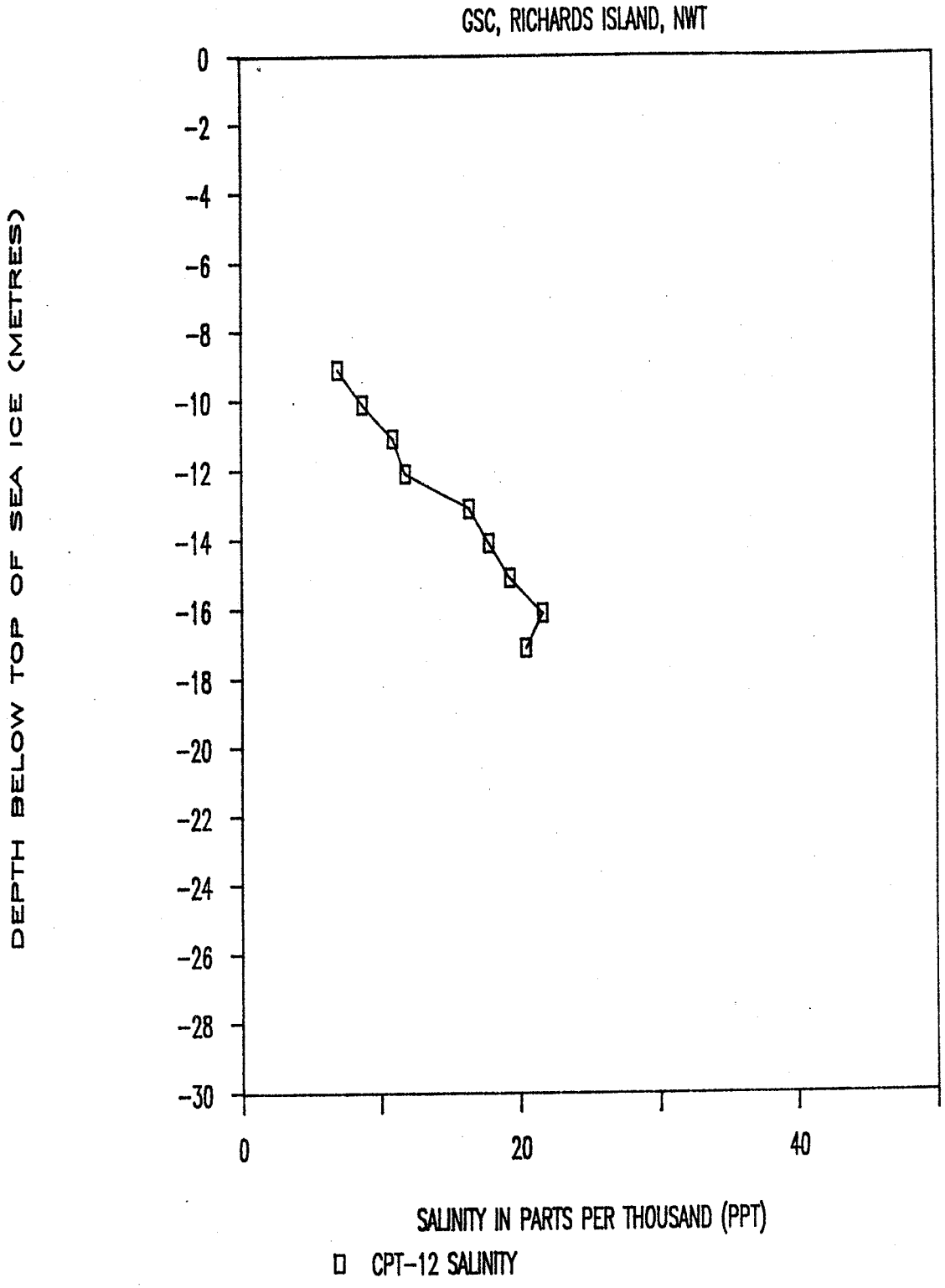

Figure 4.2.24 RESISTIVITY VS DEPTH

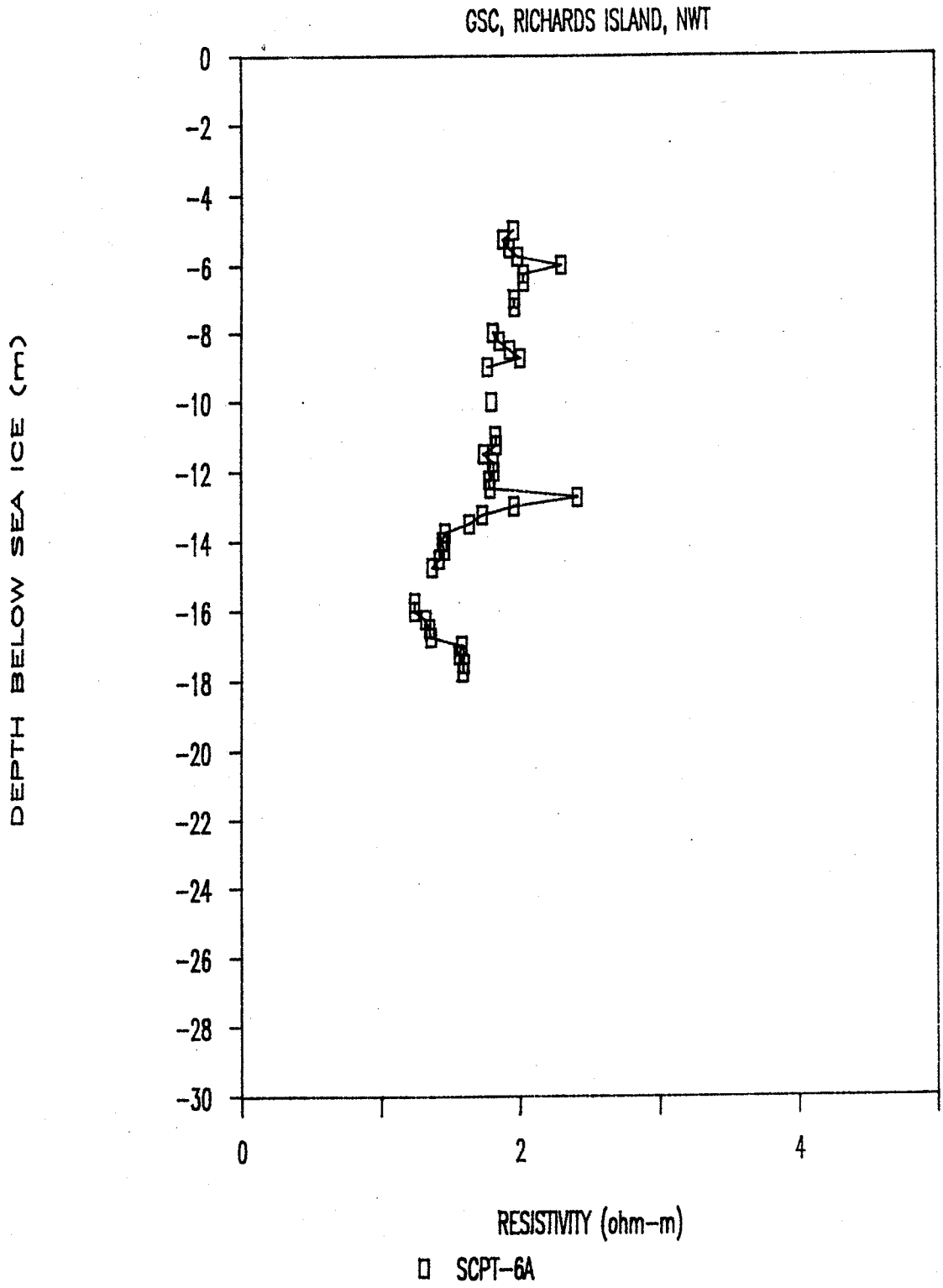

Figure 4.2.25 RESISTIVITY VS DEPTH

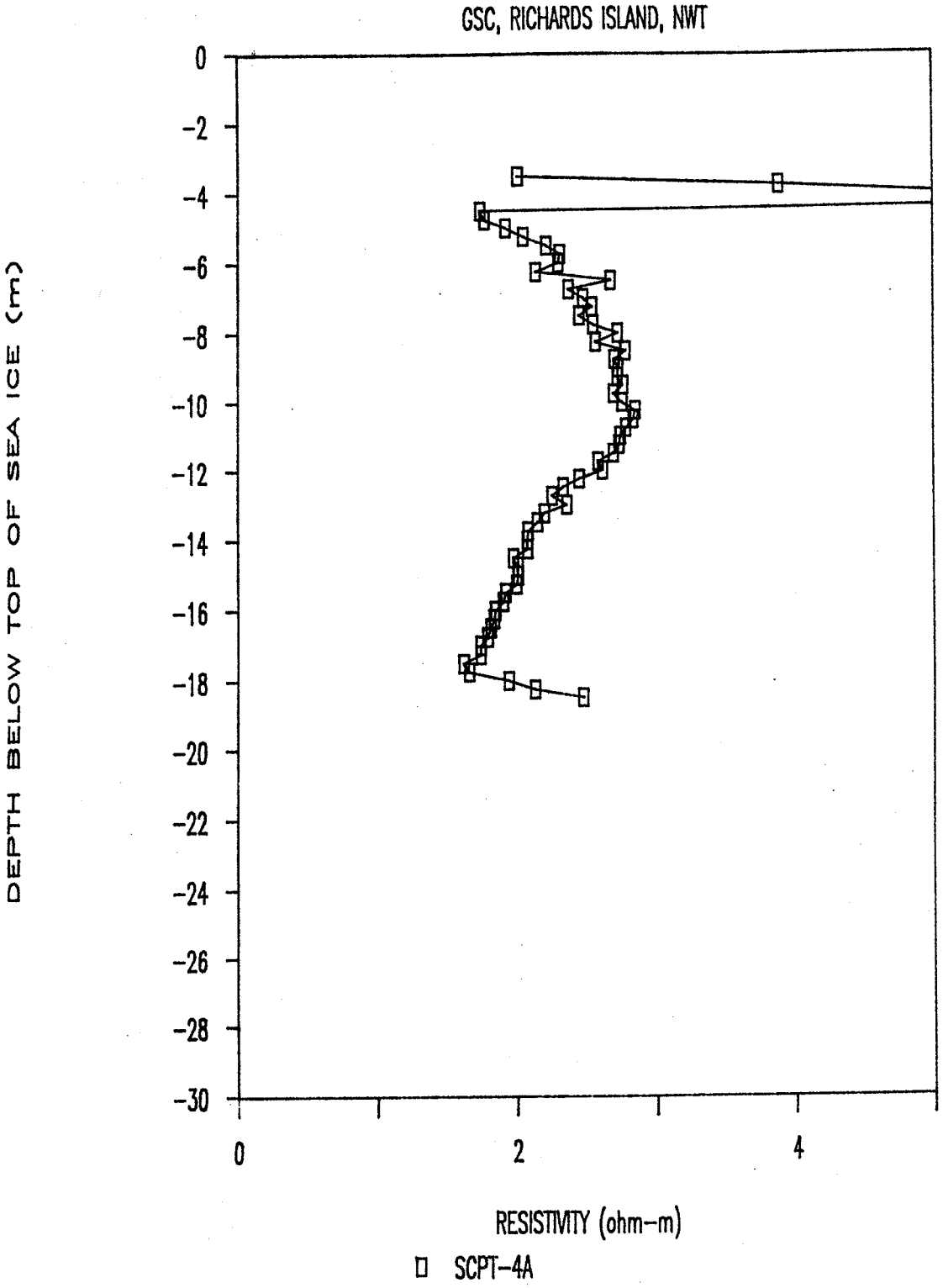

REFERENCES

American Society for Testing and Materials (ASTM) (1984). Standard test method for laboratory determination of pulse velocities and ultrasonic elastic constants of rock; Annual book of standards, V. 04.08, No. 02845-83.

Robertson, P.K. (1990). Soil classification using the cone penetration test; Can. Geotech. Journal, V. 27, No. 1, p. 151-158.

Sully, J.P., Campanella, R.G., and Robertson, P.K. (1988). Interpretation of penetration pore pressures to evaluate stress history in clays; Proceedings, 1st Int. Symp. on Penetration Testing, V. 2, p. 993-999.

4.3 ICE BONDING AND EXCESS ICE

S.R. Dallimore

Onshore boreholes

Sediments encountered in the onshore boreholes, 90BH1 and 90BH1A, were found to be well ice-bonded. Borehole 90BH1, drilled slightly inland from the coast at the top of a low hill, encountered substantial thicknesses of ice-rich sediment and massive ice at depth. In borehole 90BH1A, drilled close to the shore, ice-rich zones were limited mainly to the upper 2 m with only occasional visible excess ice at depth in the form of random ice lenses and veins. At both sites a 50 cm thick ice layer was encountered at about 50 to 80 cm depth. This layer occurred in organic rich silts and is thought to be at the base of the active layer representing ground ice accumulation at the top of permafrost.

The massive ice in 90BH1 occurred at the base of an 11 m thick silt diamicton, thought to be Toker Point till, and above a lower sand interpreted to be the Kittigazuit Formation. This massive ice body was about 11 m thick, and consisted mainly of 1 to 2 m thick ice layers with thin diamicton and sand layers. The ice was generally bubble-free with crystals varying from 1 mm to 20 mm in size. Sediment inclusions were common, with small isolated clasts and discrete bands of sediment-rich ice. Salinities of the massive ice were less than 1 ppt, and two oxygen-isotope determinations indicate that the $\delta^{18}O$ values for the ice are about -30‰. The sediment contained in the ice changed from clay diamicton above 24m to mostly sand below this level.

Offshore boreholes

Because the temperature conditions of shallow offshore permafrost are normally close to the freezing point, the identification of ice bonding in drill core is often very difficult. In most sediments the change from bonded to unbonded conditions can be expected to be gradational, depending on the amount of pore ice present in the sediment. Thus, for marginally frozen permafrost the physical consequences of ice bonding may not be obvious without detailed laboratory testing. In most standard geotechnical investigations the thermal disturbance caused by drilling can be expected to cause substantial warming of in situ temperatures which may cause permafrost degradation. In addition, since bonding is

influenced by the salinity of the pore fluids in the sediment, brine-based drilling fluids can cause changes in ice-bonding due to contamination.

As described in previous sections, for the deep boreholes along the onshore-offshore transect a considerable effort was made to reduce drilling disturbance by chilling and monitoring the temperatures of the drilling fluid, and by experimenting with several different drilling fluids.

Boreholes 90BH2, 90BH3 and 90BH4

Thermal measurements in these boreholes confirm the presence of permafrost at depth, as well as a thin seasonally frozen layer at the sea bed. Observations of ice bonding are limited to the bottom of boreholes 90BH2 and 90BH4, in Unit E, from depths of 85 to 95 m. In both cases partial ice bonding was speculated by field loggers who detected variable drilling resistance and possible ice bonding in core samples. Because of poor sample recovery and the long retrieval time to bring the samples to the surface, these observations are not considered reliable on their own. However, as discussed in Section 3.1, downhole seismic velocities can also provide an indication of ice bonding with values above 2.0 km/sec generally being assumed to indicate partial ice bonding for sands. In the case of 90BH2 the velocities are variable from 1.8 to 2.0 km/sec, while for 90BH4 velocities are consistently above 2.0 beneath 76 m depth (See Appendix A). Since the field observations and the seismic velocity information are supportive it is thought that partial ice bonding occurred in the bottom of both boreholes. An interesting zone of possible ice bonding can be inferred in borehole 90BH4, based on high seismic velocities observed from 50 to 61m depth. Some of these zones correlate with low salinity values measured on core samples. However, no ice bonding was observed in core samples.

Borehole 90BH5

In borehole 90BH5 the ice-bonded layer at the sea bed was apparently thicker than at the other offshore holes, causing refusal on the CPT push at this site. A shelby tube sample of this layer revealed bonded sand (Unit C) with no visible excess ice. The sample yielded excess water (less than 5% by volume) upon thawing, with pore water salinities of about 15 ppt.

Unbonded sand of Unit C was encountered beneath the seasonally bonded layer to an estimated depth of 10 m. At this depth the first signs of partial ice bonding were observed in core samples. An abrupt change from partially ice-bonded sand to well bonded sand was observed at about 16 m depth corresponding with a rapid drop in pore water salinities. The remainder of the hole was well bonded except for the fine grained silts and clays of Unit D, which were unbonded.

Excess ice in borehole 90BH5 was observed in Unit C with significant ice-rich sediment in the zone of 17 to 20 m depth. Discrete ground ice layers were observed from 17.15 to 17.27 m, from 18.25 to 18.6 m and from 18.6 to 18.95 m. Ground ice layers contained 60-80 % ice by volume with measured gravimetric water contents as high as 81.5%. The ice was typically bubble-free and cloudy in appearance with disseminated sand grains giving it a brown colour. Salinities of the ground ice and the well ice-bonded Unit C sand were less than 5 ppt.

Unit E sand was well bonded throughout with no visible excess ice being observed. Water contents in this unit were low reflecting the low ice contents. Salinities were observed to vary from 10 to 30 ppt.

4.4 DYNAMIC PROPERTIES OF ICE-BONDED SEDIMENTS

P.J. Kurfurst and J.G. Bisson

Acoustic wave propagation tests were made in order to compare the laboratory-measured acoustic wave velocities on specific samples with those measured in situ, and to provide a basis for calculating the elastic constants required for design purposes by engineers. The measurements were carried out on two sets of frozen ice-bonded samples from boreholes 90BH1 and 90BH5 (24 and 33 samples respectively). These measurements were made at temperatures similar to those measured in the field, using an OYO 5217-A Sonic viewer. Prior to the tests, all specimens were cut to approximately 12 or 20 cm length (maintaining a constant diameter/length ratio), measured, weighed and the bulk density was determined.

Using the first arrival technique, the compressional (V_p) and shear wave (V_s) velocities were calculated as follows:

$$V_p = L_p/T_p, \text{ and} \quad (1)$$

$$V_s = L_s/T_s \quad (2)$$

Where V = pulse propagation velocity (m/s),

L = pulse travel distance (m),

T = effective pulse-travel time (s)

Ultrasonic elastic constants (E, μ, G, K) were calculated using formulas recommended by the American Society for Testing and Materials, Standard D2845-83 (ASTM, 1984):

$$E = [\rho\, V_s^2\, (3\, V_p^2 - 4\, V_s^2)]/(V_p^2 - V_s^2) \quad (3)$$

where E = Young's modulus (Pa),

ρ = density (kg/m^3);

$$\mu = (V_p^2 - 2\, V_s^2)/[2\, (V_p^2 - V_s^2)] \quad (4)$$

where μ = Poisson's ratio;

$$G = p\, V_s^2 \quad (5)$$

where G = shear modulus (or modulus of rigidity) (Pa);

$$K = \rho\, (3\, V_p^2 - 4\, V_s^2)/3 \quad (6)$$

where K = bulk modulus (or modulus of volumetric elasticity) (Pa).

The results of the tests are summarized in Tables 4.4.1 and 4.4.2.

Table 4.4.1

Sample #	Interval (m)	Diameter (cm)	Length (cm)	Weight (g)	Bulk Density (g/cm^3)	Tp (us)	Vp (m/s)	Ts (us)	Vs (m/s)	Poisson's Ratio	Rigidity Modulus (GPa)	Young's Modulus (GPa)	Volumetric Elasticity (GPa)
90BH1-1	19.04-19.24	10.00	20.0	2668.7	1.699	68.0	2941.2	133.6	1497.0	0.33	3.81	10.09	9.62
90BH1-2	18.02-18.22	10.00	20.0	2892.8	1.842	63.2	3164.6	132.8	1506.0	0.35	4.18	11.31	12.87
90BH1-3	10.28-10.48	10.00	20.0	2743.0	1.746	62.4	3205.1	131.2	1524.4	0.35	4.06	10.99	12.53
90BH1-4	12.23-12.43	10.00	20.0	2840.5	1.808	64.0	3125.0	134.4	1488.1	0.35	4.00	10.84	12.32
90BH1-5	9.25-9.45	10.00	20.0	2693.3	1.715	67.2	2976.2	144.0	1388.9	0.36	3.31	9.00	10.78
90BH1-6	27.17-27.34	10.00	17.0	1796.1	1.345	56.8	2993.0	104.8	1622.1	0.29	3.54	9.15	7.33
90BH1-7	5.28-5.48	10.00	20.0	2667.0	1.698	82.4	2427.2	146.0	1369.9	0.27	3.19	8.07	5.75
90BH1-8	3.10-3.30	10.00	20.0	2588.4	1.648	68.8	2907.0	144.0	1388.9	0.35	3.18	8.60	9.69
90BH1-9	1.06-1.24	10.00	18.0	2051.6	1.451	78.0	2307.7	134.0	1343.3	0.24	2.62	6.51	4.24
90BH1-10	6.32-6.52	10.00	20.0	2739.4	1.744	68.8	2907.0	142.4	1404.5	0.35	3.44	9.27	10.15
90BH1-11	20.24-20.44	10.00	20.0	1757.8	1.119	78.0	2564.1	143.2	1396.6	0.29	2.18	5.63	4.45
90BH1-12	24.68-24.88	10.00	20.0	1807.9	1.151	84.0	2381.0	133.6	1497.0	0.17	2.58	6.05	3.09
90BH1-13	16.26-16.46	10.00	20.0	2891.1	1.840	64.8	3086.4	132.0	1515.2	0.34	4.23	11.33	11.90
90BH1-14	14.62-14.82	10.00	20.0	2852.6	1.816	68.0	2941.2	136.0	1470.6	0.33	3.93	10.47	10.47
90BH1-15	2.02-2.22	10.00	20.0	2624.5	1.671	64.8	3086.4	116.8	1712.3	0.28	4.90	12.52	9.38
90BH1-16	8.02-8.22	10.00	20.0	2693.0	1.714	64.8	3086.4	114.4	1748.3	0.26	5.24	13.24	9.34
90BH1-17	21.21-21.41	10.00	20.0	1536.7	0.978	65.6	3048.8	136.0	1470.6	0.35	2.12	5.71	6.27
90BH1-18	22.01-22.21	10.00	20.0	1533.7	0.976	79.2	2525.3	136.0	1470.6	0.24	2.11	5.25	3.41
90BH1-19	4.62-4.82	10.00	20.0	2338.2	1.488	60.0	3333.3	124.8	1602.6	0.35	3.82	10.32	11.44
90BH1-20	23.38-23.58	10.00	20.0	1835.5	1.168	63.2	3164.6	127.2	1572.3	0.34	2.89	7.72	7.85
90BH1-21	25.04-25.24	10.00	20.0	1528.3	0.973	64.8	3086.4	128.8	1552.8	0.33	2.35	6.24	6.14
90BH1-22	26.28-26.48	10.00	20.0	1809.3	1.152	59.2	3378.4	119.2	1677.9	0.34	3.24	8.67	8.82
90BH1-23	28.32-28.52	10.00	20.0	2997.1	1.908	51.2	3906.3	106.4	1879.7	0.35	6.74	18.19	20.12
90BH1-24	14.10-14.30	10.00	20.0	2831.9	1.803	56.0	3571.4	115.2	1736.1	0.35	5.43	14.62	15.75

Table 4.4.2

Sample #	Interval (m)	Diameter (cm)	Length (cm)	Weight (g)	Bulk Density (g/cm^3)	Tp (us)	Vp (m/s)	Ts (us)	Vs (m/s)	Poisson's Ratio	Rigidity Modulus (GPa)	Young's Modulus (GPa)	Volumetric Elasticity (GPa)
90BH5-1	18.775-18.90	6.10	12.50	359.0	1.016	8.0	15625.0	76.0	1644.7	0.49	2.75	8.21	244.32
90BH5-2	20.27-20.392	6.10	12.20	637.1	1.787	44.0	2772.7	92.0	1326.1	0.35	3.14	8.49	9.55
90BH5-3	19.82-19.942	6.10	12.20	686.7	1.926	46.0	2652.2	96.0	1270.8	0.35	3.11	8.40	9.40
90BH5-4	18.28-18.402	5.90	12.20	383.9	1.151	36.0	3388.9	65.6	1859.8	0.28	3.98	10.23	7.91
90BH5-5	17.28-17.403	6.10	12.30	664.1	1.847	36.8	3342.4	67.2	1830.4	0.29	6.19	15.92	12.39
90BH5-6	22.42-22.546	6.10	12.60	718.2	1.950	41.6	3028.8	72.0	1750.0	0.25	5.97	14.93	9.93
90BH5-7	22.08-22.202	6.10	12.20	687.0	1.927	39.2	3112.2	84.0	1452.4	0.36	4.06	11.06	13.24
90BH5-8	29.60-29.722	6.10	12.20	702.0	1.969	31.2	3910.3	45.6	2675.4	0.06	14.09	29.87	11.31
90BH5-9	36.67-36.795	6.10	12.50	723.5	1.980	33.6	3720.2	60.0	2083.3	0.27	8.60	21.86	15.95
90BH5-10	38.09-38.212	5.90	12.20	712.6	2.136	34.4	3546.5	62.4	1955.1	0.28	8.17	20.93	15.98
90BH5-11	32.51-32.633	6.10	12.30	688.0	1.914	30.4	4046.1	56.0	2196.4	0.29	9.23	23.84	19.02
90BH5-12	37.19-37.312	6.10	12.20	686.5	1.925	31.2	3910.3	60.0	2033.3	0.31	7.96	20.93	18.83
90BH5-13	36.075-36.197	6.10	12.20	680.2	1.908	32.0	3812.5	56.0	2178.6	0.26	9.05	22.77	15.66
90BH5-14	35.57-35.693	6.10	12.30	683.5	1.901	31.2	3942.3	56.8	2165.5	0.28	8.92	22.90	17.66
90BH5-15	34.915-35.037	6.10	12.20	732.3	2.054	31.2	3910.3	60.8	2006.6	0.32	8.27	21.85	20.38
90BH5-16	80.0-80.122	6.10	12.20	685.9	1.924	46.4	2629.3	140.0	871.4	0.44	1.46	4.20	11.35
90BH5-17	27.29-27.412	6.10	12.20	716.9	2.011	32.0	3812.5	62.4	1955.1	0.32	7.69	20.31	18.98
90BH5-18	25.16-25.282	6.10	12.20	650.1	1.823	31.2	3910.3	50.0	2440.0	0.18	10.86	25.64	13.40
90BH5-19	84.73-85.854	6.10	12.40	719.5	1.985	46.4	2672.4	136.0	911.8	0.43	1.65	4.73	11.98
90BH5-20	76.58-76.702	6.10	12.20	682.1	1.913	43.2	2824.1	132.0	924.2	0.44	1.63	4.71	13.08
90BH5-21	77.66-77.782	6.10	12.20	681.2	1.911	58.0	2103.4	196.0	622.4	0.45	0.74	2.15	7.47
90BH5-22	88.26-88.382	6.10	12.20	719.9	2.019	52.0	2346.2	248.0	491.9	0.48	0.49	1.44	10.46
90BH5-23	81.87-81.992	6.10	12.30	692.4	1.926	40.8	3014.7	107.2	1147.4	0.42	2.54	7.18	14.12
90BH5-24	76.37-76.492	6.10	12.30	669.9	1.864	43.2	2847.2	84.0	1464.3	0.32	4.00	10.55	9.78
90BH5-25	83.80-83.922	6.10	12.20	739.3	2.073	45.2	2699.1	108.0	1129.6	0.39	2.65	7.38	11.58
90BH5-26	87.10-87.222	6.10	12.20	693.6	1.945	48.8	2500.0	118.0	1033.9	0.40	2.08	5.81	9.39
90BH5-27	84.46-84.582	6.10	12.20	715.1	2.006	46.4	2629.3	192.0	635.4	0.47	0.81	2.38	12.79
90BH5-28	78.79-78.912	6.10	12.20	699.1	1.961	51.2	2382.8	128.0	953.1	0.40	1.78	5.00	8.76
90BH5-29	86.68-86.802	6.10	12.20	715.3	2.006	48.0	2541.7	112.0	1089.3	0.39	2.38	6.61	9.79
90BH5-30	85.70-85.822	6.10	12.20	736.5	2.066	47.2	2584.7	110.4	1105.1	0.39	2.52	7.00	10.44
90BH5-31	82.96-83.082	6.10	12.20	733.6	2.057	45.6	2675.4	105.6	1155.3	0.39	2.75	7.61	11.07
90BH5-32	30.08-30.202	6.10	12.20	718.2	2.014	32.8	3719.5	50.0	2440.0	0.12	11.99	26.92	11.88
90BH5-33	30.58-30.702	6.10	12.20	688.8	1.932	32.8	3719.5	54.0	2259.3	0.21	9.86	23.82	13.58

4.5 CONSOLIDATION TESTING OF UNIT D

H.A. Christian, J. Landva and S.M. Blasco

4.5.1 Test procedure

A laboratory testing program was carried out by Jacques, Whitford and Associates Ltd. under contract to the Atlantic Geoscience Centre to determine the consolidation characteristics of Unit D. Three core samples from borehole 90BH2 at depths of 39.3 m, 40.4 m and 42.2 m were chosen for investigation. Two subsamples were carefully trimmed from each sample to produce test specimens A through F which were 5 cm in diameter and 2 cm or 1.75 cm in height. After trimming, initial measurements were taken for dimensions, weights and water contents. Preparation of the specimens proved to be difficult due to extensive internal fissuring with no preferred orientation which resulted in a blocky fabric that easily disintegrated. The moisture contents of specimens E and F from 42.2 m sample averaged about 30% while the other specimens averaged about 36%.

Loading procedures for each test included ten load increments and two unloading increments. Load increments were nominally 100 percent of the previous load from 49 kPa to 6322 kPa with additional itermediate loads of 2354 kPa and 4534 kPa. Loading steps were maintained to at least the end of primary consolidation as defined by time versus dial reading plots for each load increment; the longer durations of some loadings permitted a proper determination of secondary consolidation coefficients.

4.5.2 Results

All specimens exhibited high levels of overconsolidation with specimens A, B and E, F having overconsolidation ratios (OCR) above 2.2 and specimens C and D having values of about 1.7. Test results are summarized in Table 4.5.1 and summary plots of void ratio vs. log vertical stress (e-log p') and consolidation coefficient vs log vertical stress (C_v-log p') for each specimen are given in Figures 4.5.1 to 4.5.6. Required variables for these plots were calculated from the test data using a spreadsheet program. The curves of e-log p' were determined from the time vs displacement relationship at the end of primary consolidation. Times (t_{90}'s or t_{50}'s) for primary consolidation were small, and it was found to be more accurate to use the square root time method to determine the consolidation coefficients

Table 4.5.1. Summary of Consolidation Test Results

BOREHOLE	SPECIMEN	SUB-BOTTOM DEPTH (m)	DEPTH BSL (m)	W_n (%)	P_o' (kPa)	P_c' (kPa)	OCR
90BH2	A	39.3	42.3	36.1	340	740	2.2
90BH2	B	39.4	42.4	37.0	340	840	2.5
90BH2	C	40.1	43.1	36.3	350	560	1.6
90BH2	D	40.3	43.1	34.5	350	660	1.9
90BH2	E	42.2	45.2	29.5	390	1000	2.6
90BH2	F	42.3	45.3	31.5	390	900	2.3

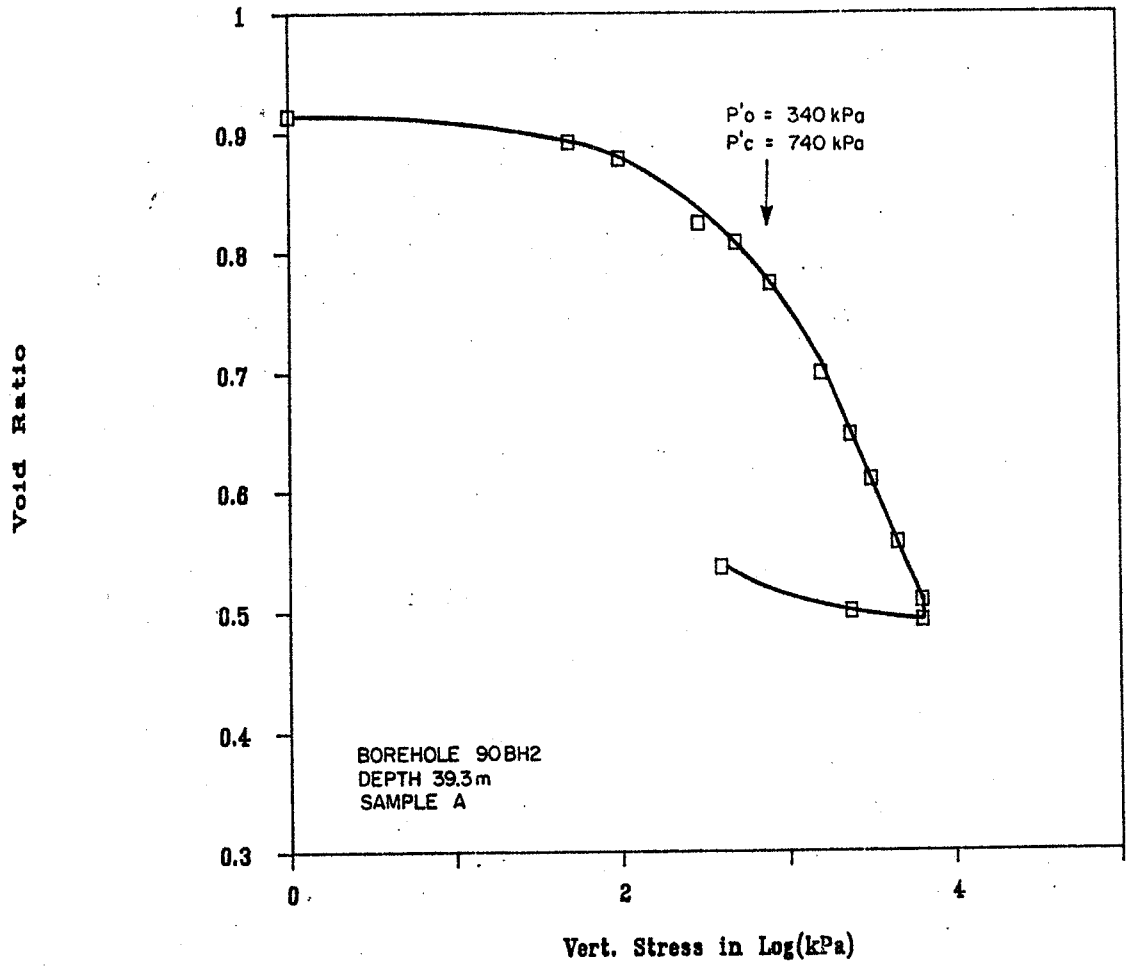

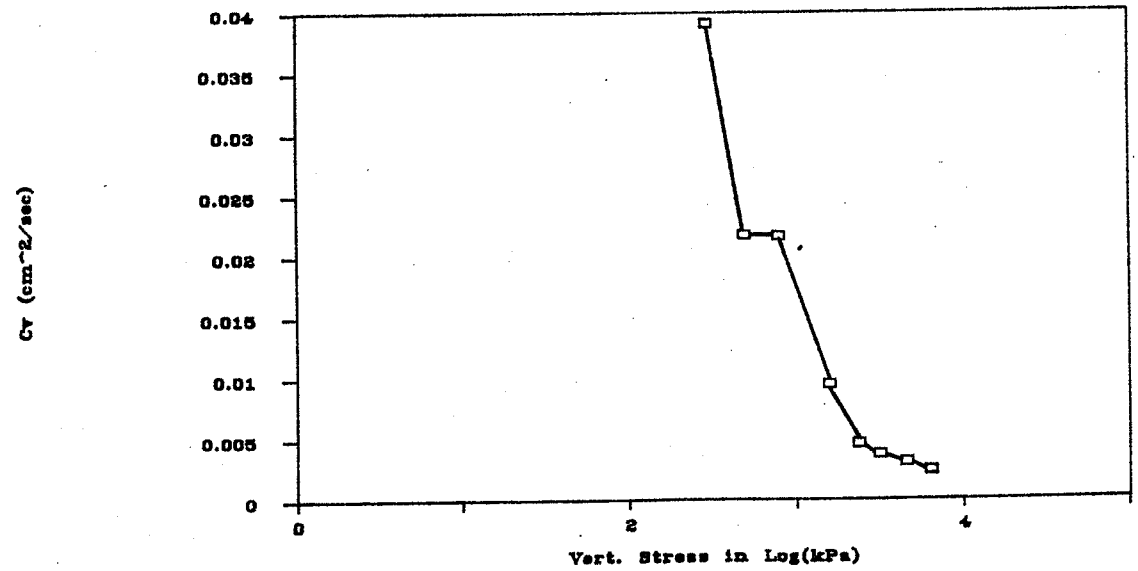

Figure 4.5.1 Consolidation test results, specimen A

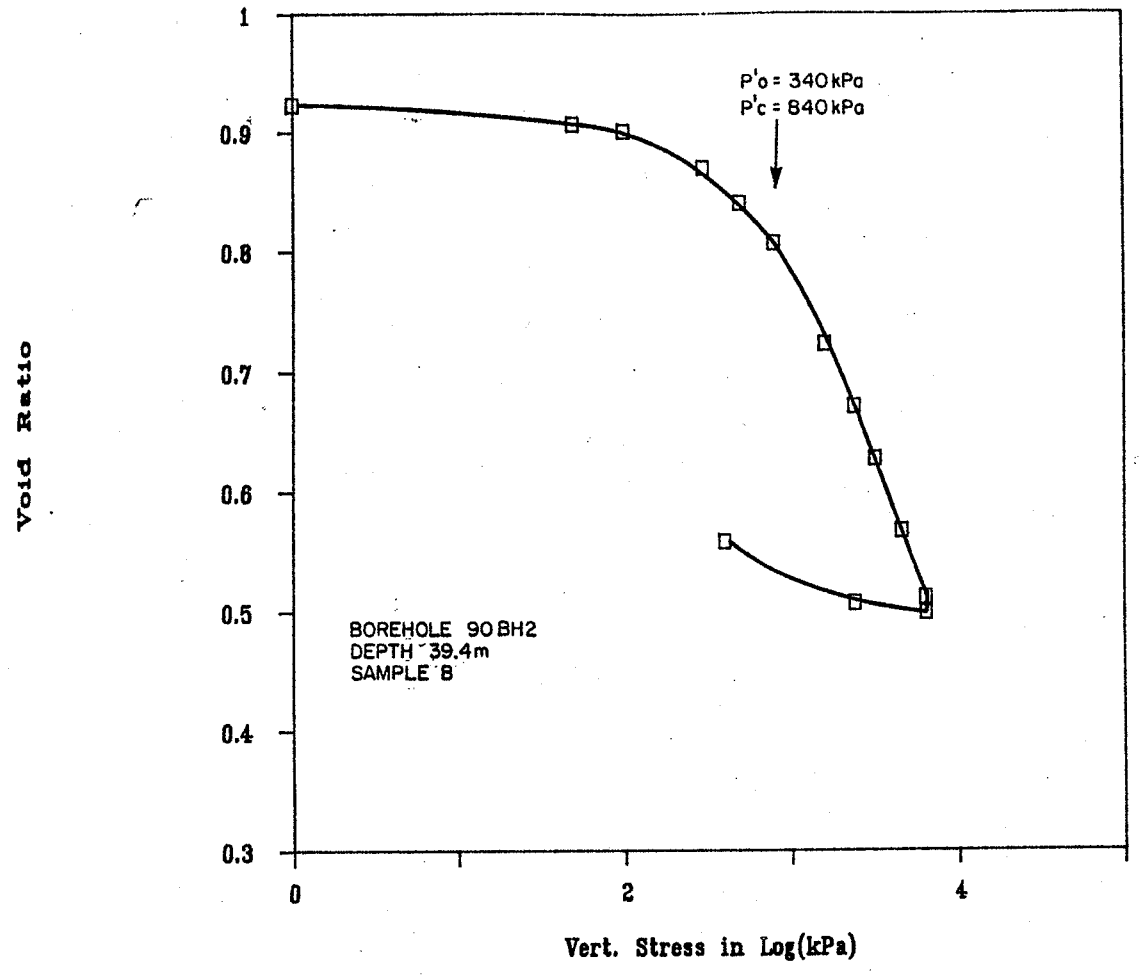

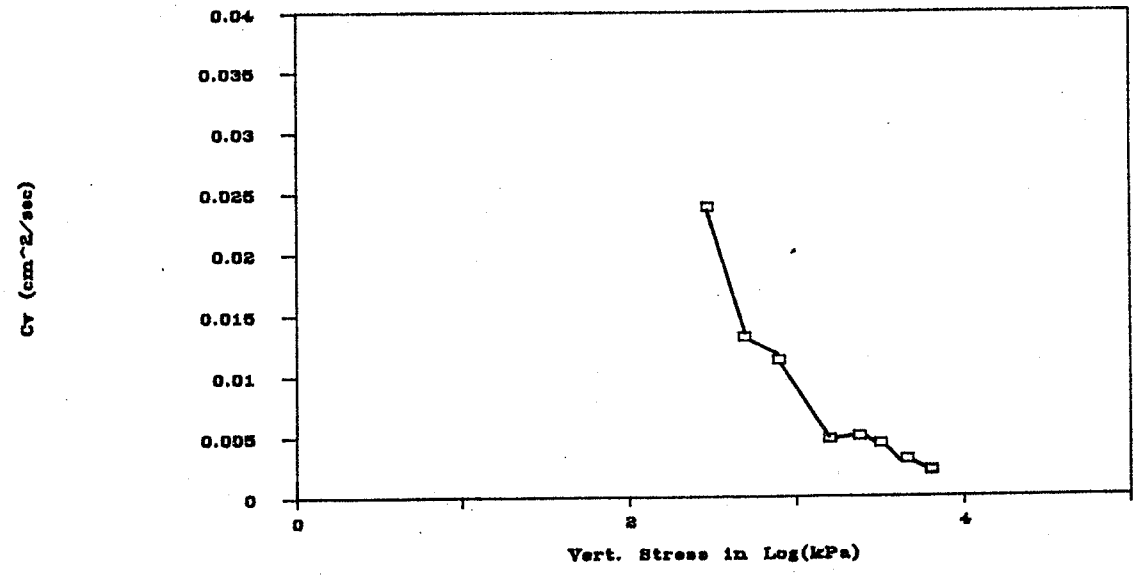

Figure 4.5.2 Consolidation test results, specimen B

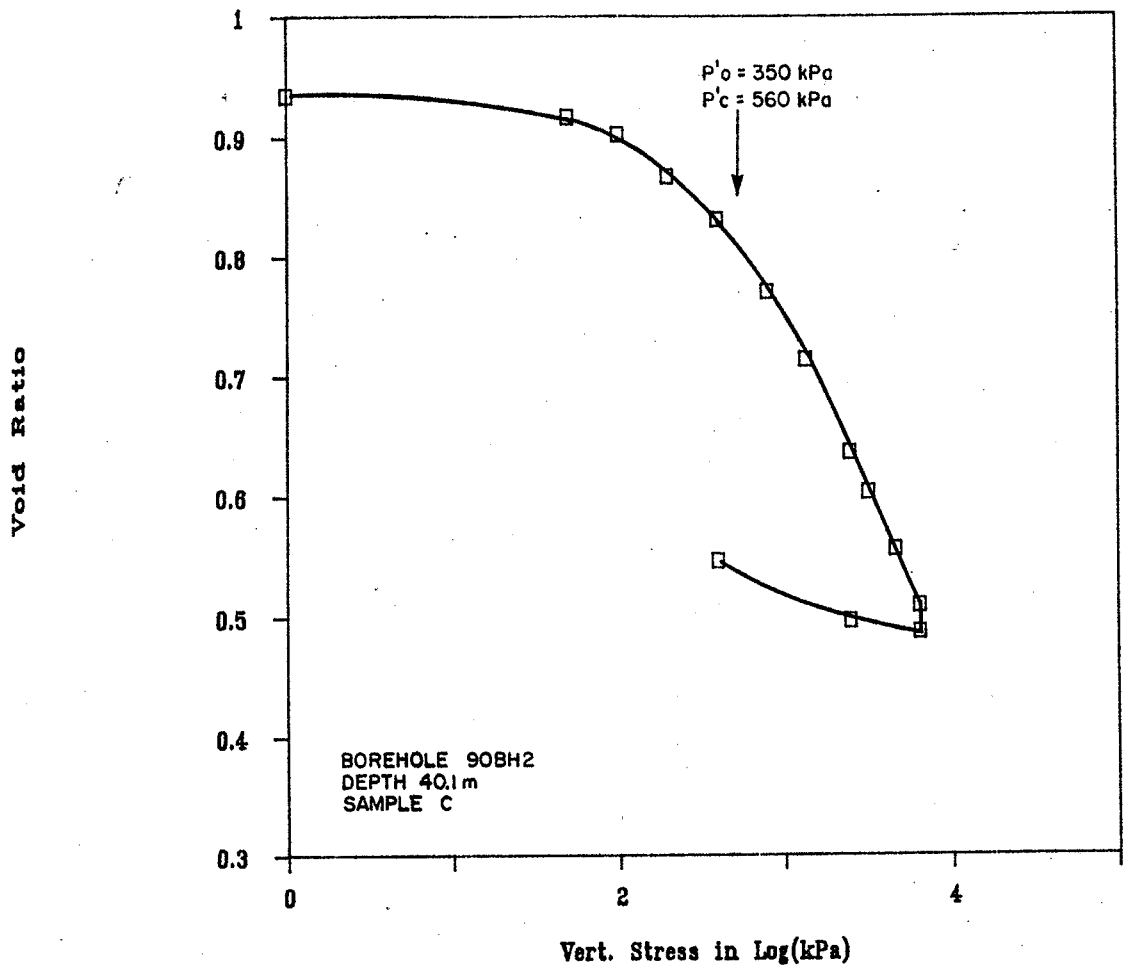

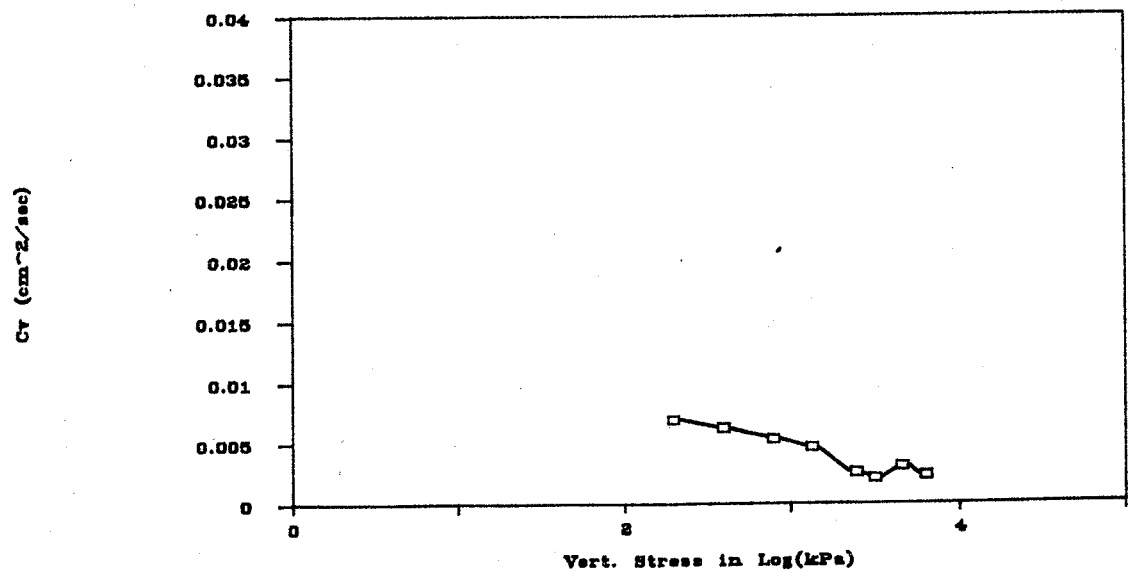

Figure 4.5.3 Consolication test results, specimen C

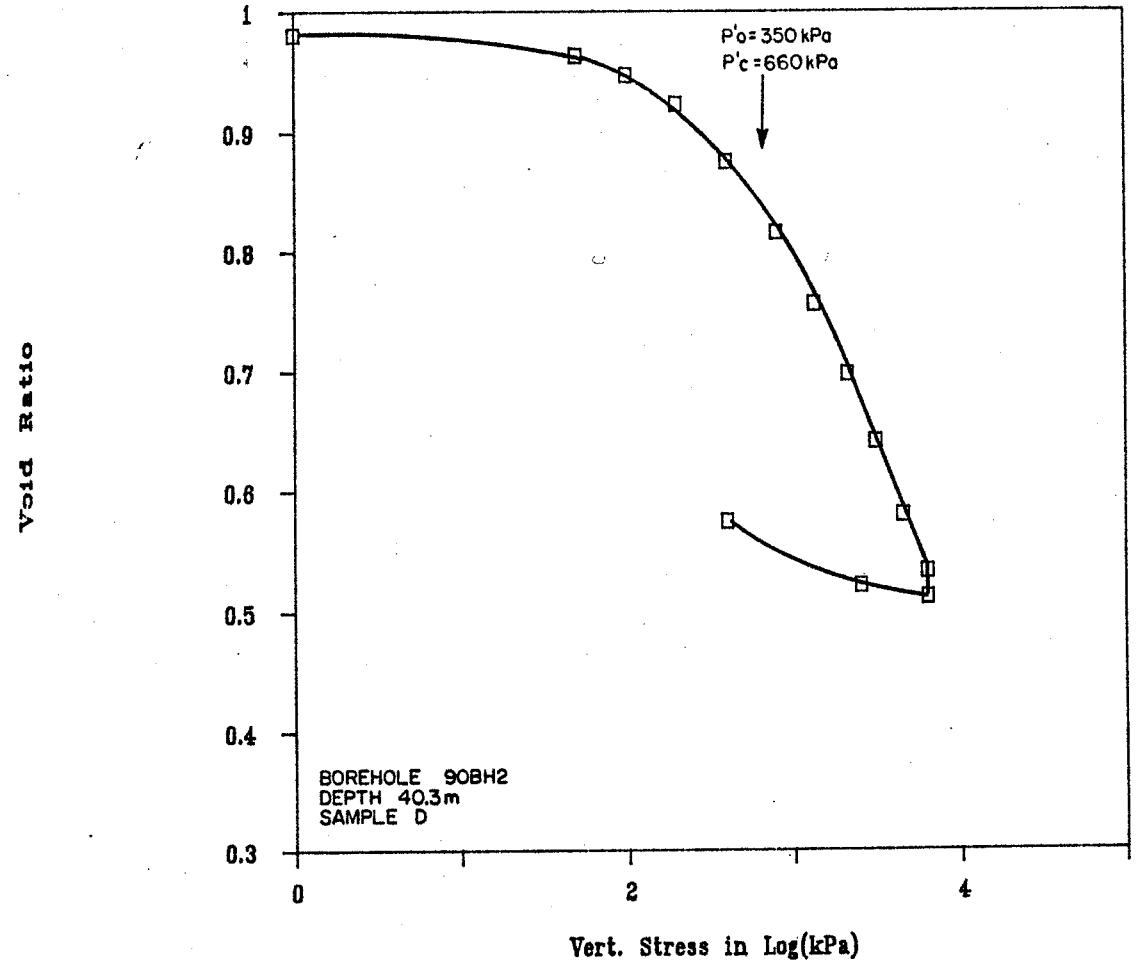

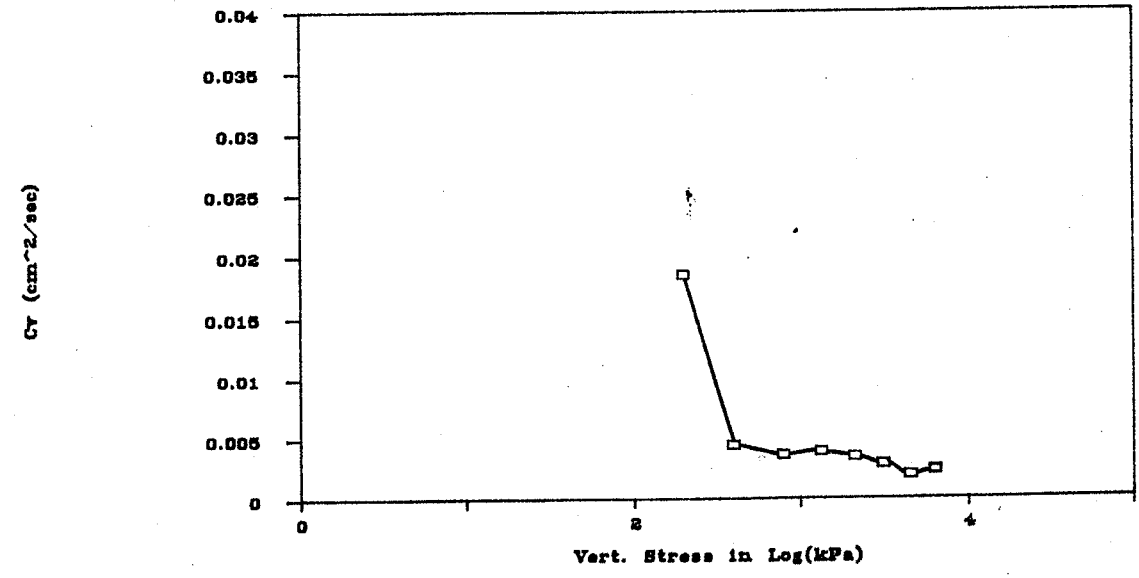

Figure 4.5.4 Consolidation test results, specimen D

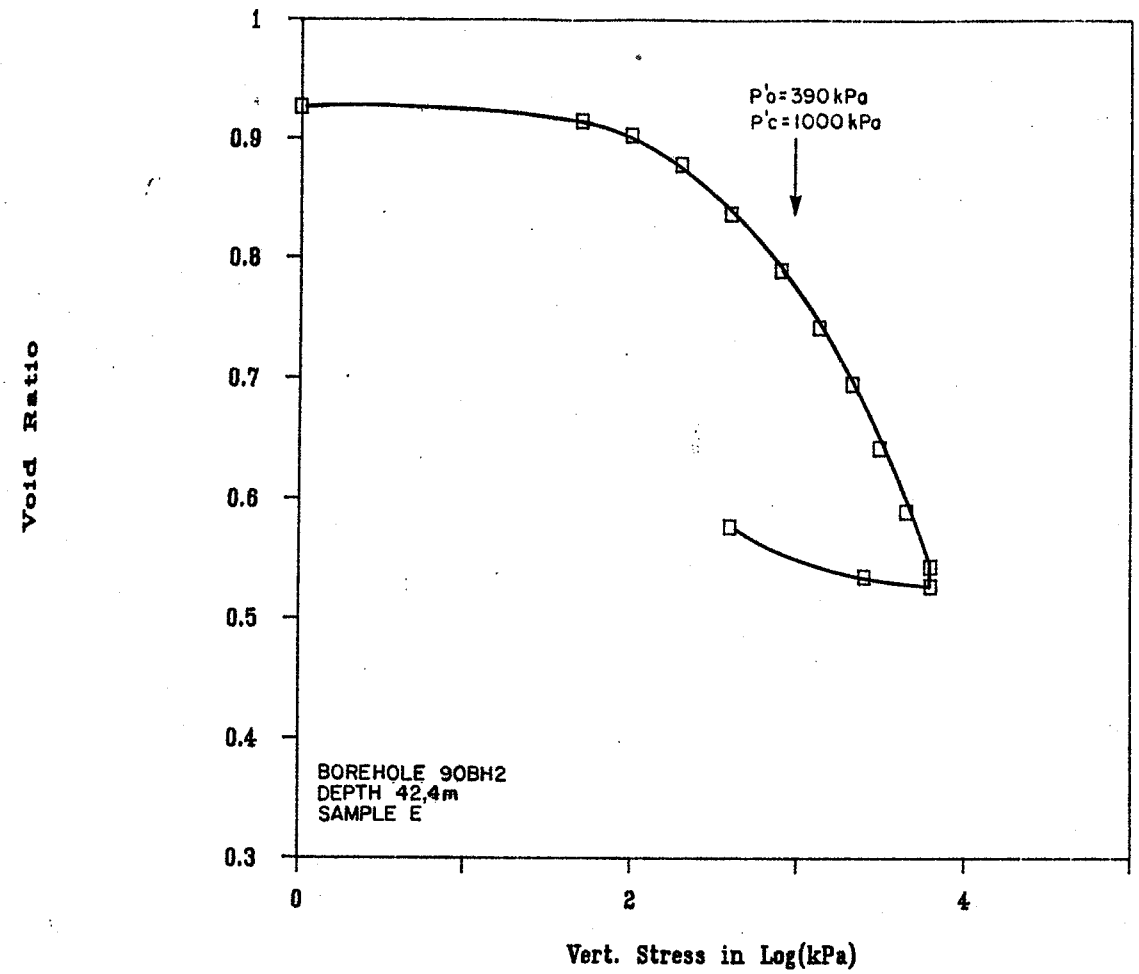

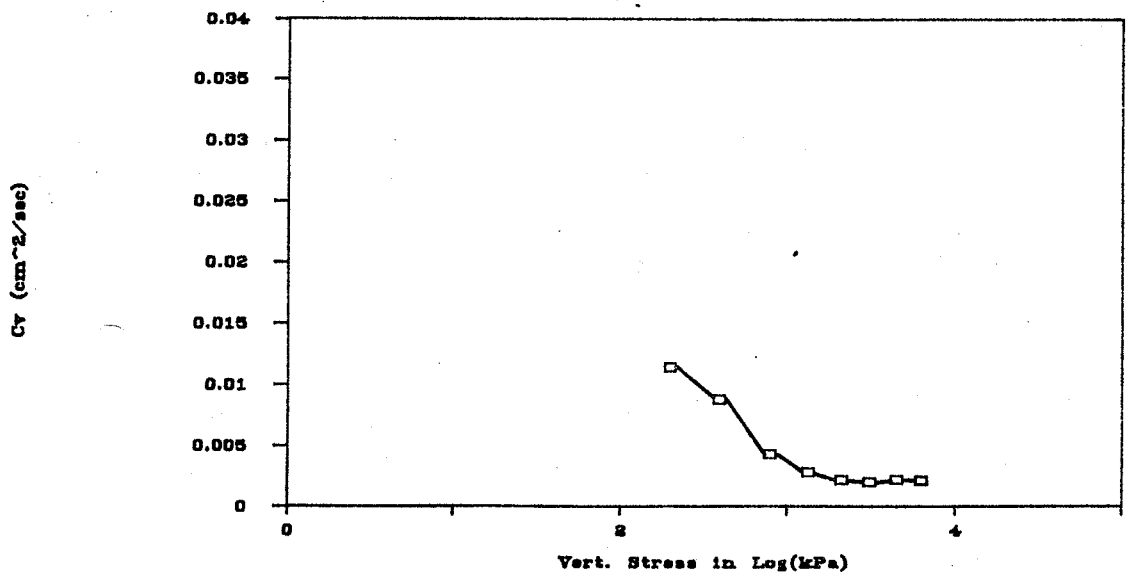

Figure 4.5.5 Consolidation test results, specimen E

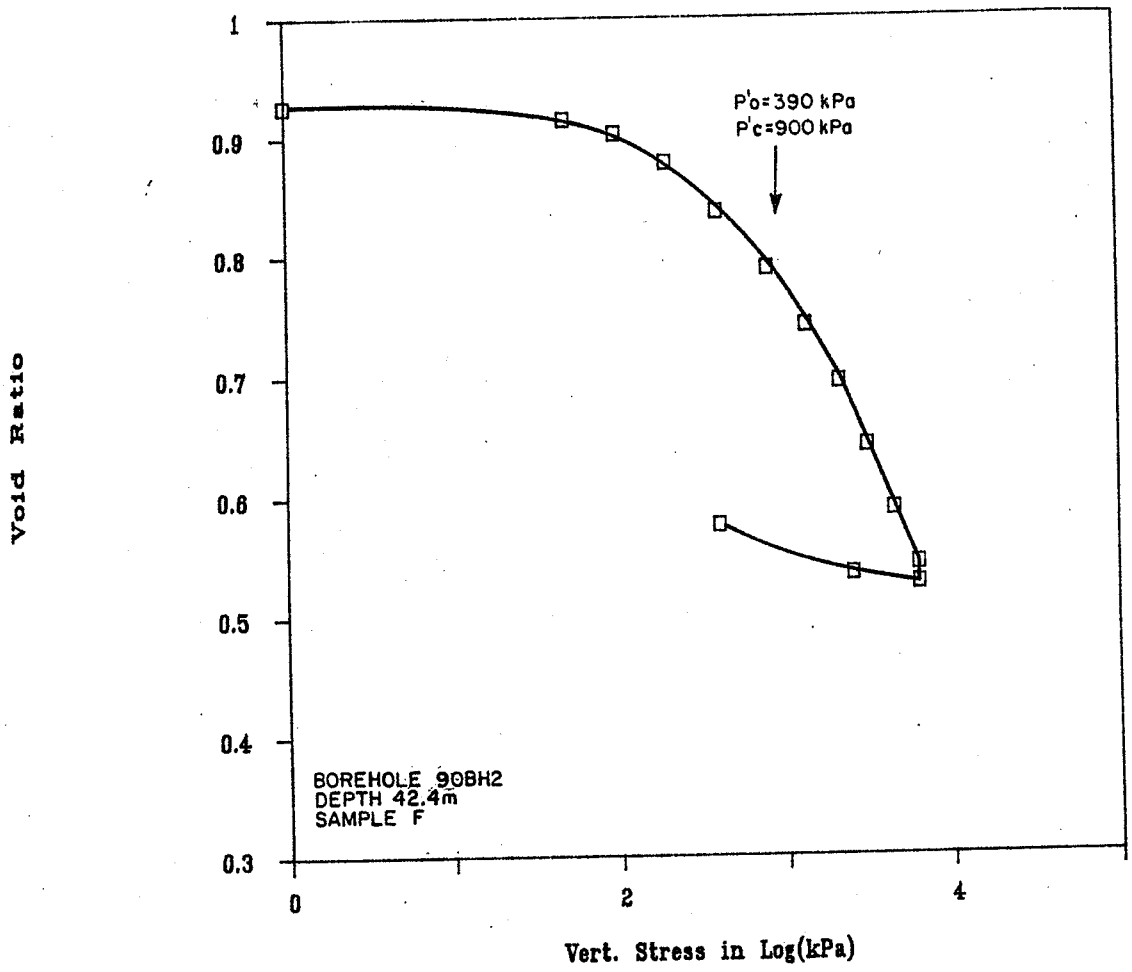

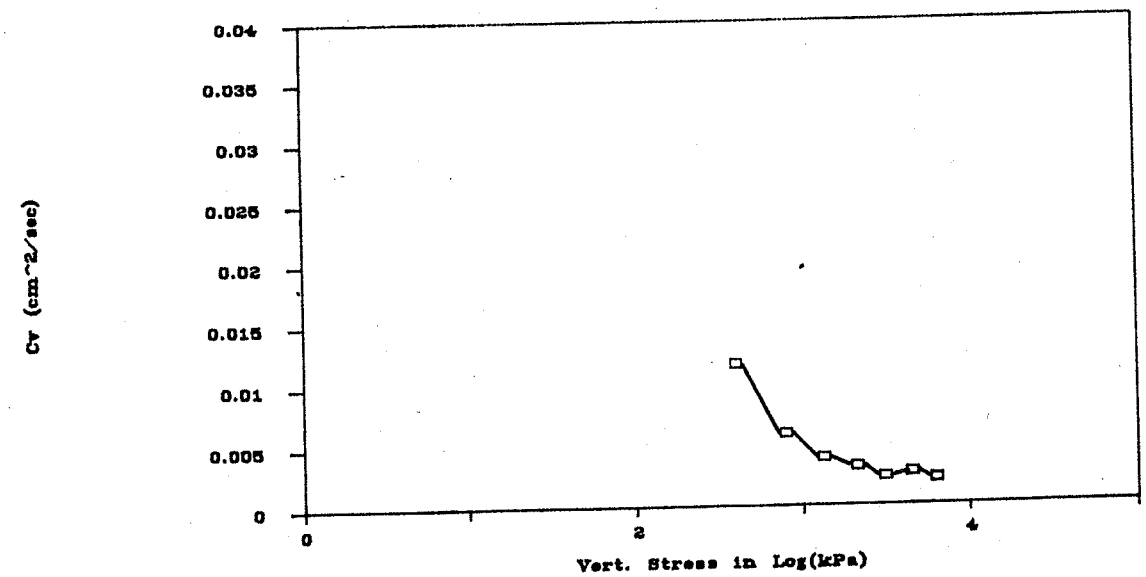

Figure 4.5.6 Consolidation test results, specimen F

rather than the log time method. Preconsolidation pressures (P'_c) determined using Casagrande's method are shown in Figures 4.5.1 to 4.5.6.

4.5.3 Discussion

Based on the stratigraphic correlations established from the 5 offshore boreholes it is thought that each sample was from subfacies D_1 of Unit D (see Section 2.2). Samples from layers above and below specimens A, B, C, and D consisted of moderately bioturbated, very dark grey to black, laminated and fissured silty clay containing interbedded sharp-based graded silt beds (<1 cm thick). Logging of cores immediately upon retrieval revealed limited in situ subvertical microfaults having offsets in the bedding of 1 to 10 mm. Core samples containing specimens E and F were more intensively bioturbated with fewer interbeds and no observed microfaulting. Internal inspection of the cores during preparation of the consolidation test specimens also revealed that all specimens were intensely fissured and broke apart readily.

Grain size analyses of a sample from 90BH2 41.5 m suggest that the sediment was composed of about 40 % clay and 60 % silt (see Figure 4.1.6a). Water contents measured in the field laboratory in Inuvik were similar to the values reported in Table 4.5.1 and confirmed that specimens E and F had lower values than those in the other specimens. Preconsolidation pressures were well defined on the e-log p' curves by a sharp transition in compressibility, indicating that the sediment was sampled with a minimum of disturbance.

CHAPTER 5

ONSHORE-OFFSHORE TRANSECT: SUMMARY

CHAPTER 5
ONSHORE-OFFSHORE TRANSECT: SUMMARY

S.R. Dallimore

5.1 Geology

A simplified cross section of geological conditions encountered along the transect is given on Figure 5.1. Based on available data compiled in geological studies to date, it is apparent that the stratigraphic sequence encountered offshore, beneath the Holocene transgressive unconformity, correlates with the sequence on land. Sedimentary unit characteristics, mineralogy and grain surface texture of the sands and geotechnical similarities, suggest that distinct subfacies recognised in each unit can be traced between boreholes. Although continuous sediment cores were not collected in each borehole, downhole geophysical logs confirmed lithologic characteristics and stratigraphic boundaries.

The data presented in this report suggests that offshore subfacies C_1 of Unit C is equivalent to the Kittigazuit Formation described on land and subfacies C_2 and C_3 are equivalent to Kidluit Formation. There is also evidence to suggest that the diamicton encountered offshore in borehole 90BH3 is similar in grain size and character to the Toker Point till identified in borehole 90BH1. Unit D is thought to be equivalent to the Hooper clay and Unit E to the Kendall sediments. It must be emphasized however, that further work is necessary to determine the exact relationship between the units and the major discrepancies in the tentative ages assigned to them. Due to the complex origin of Unit C, and possibly Unit E, it is also possible that important facies may have not have been sampled or may be absent at the borehole locations investigated. For instance the marine seismic section (Figure 2.2.2) shows complex cut and fill structures at the top of Unit C related to the Holocene marine transgression. As described in Chapter 6, the incorporation of lake basins in the nearshore zone indicates that these areas may have distinct sediment associations and temperature conditions.

5.2 Permafrost Conditions

The ground temperature conditions are presented along an idealized cross section of the onshore/offshore transect in Figure 5.2. Ground temperatures on land and in the

Figure 5.1 ONSHORE - OFFSHORE STRATIGRAPHY

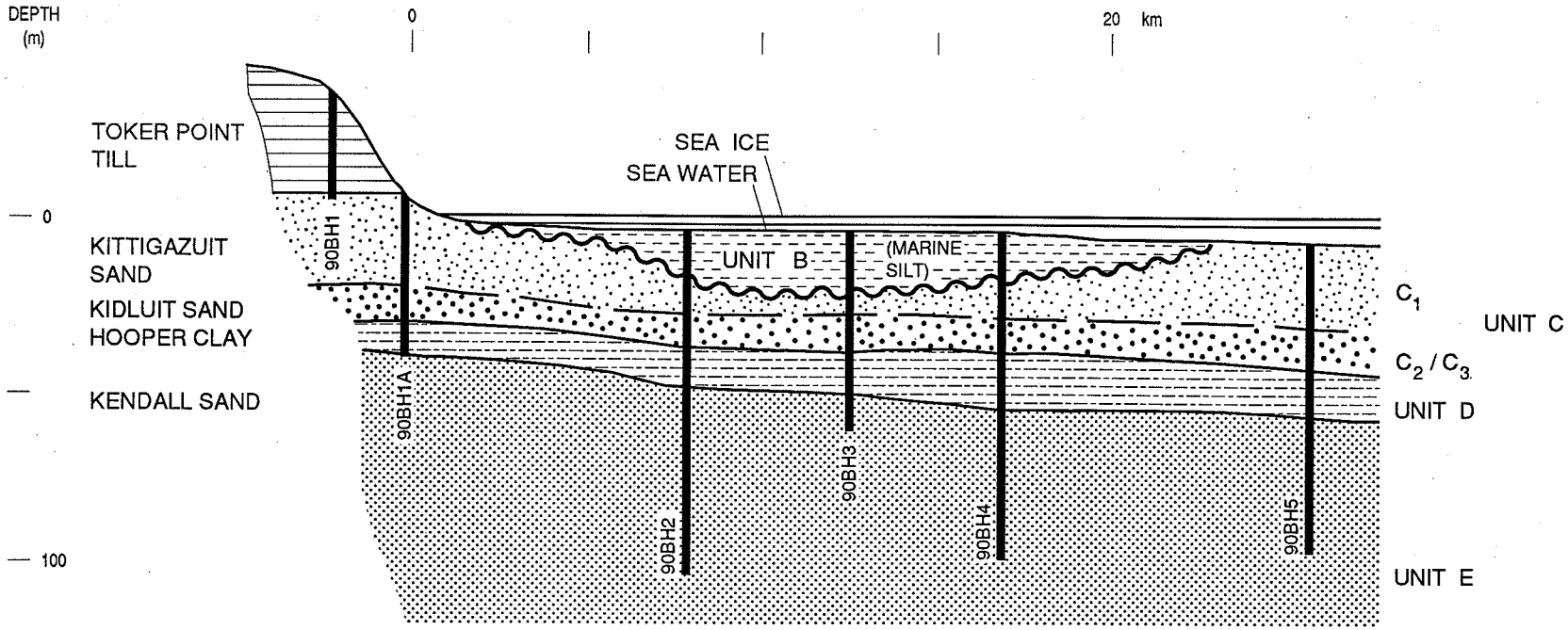

Figure 5.2 TEMPERATURE SECTION

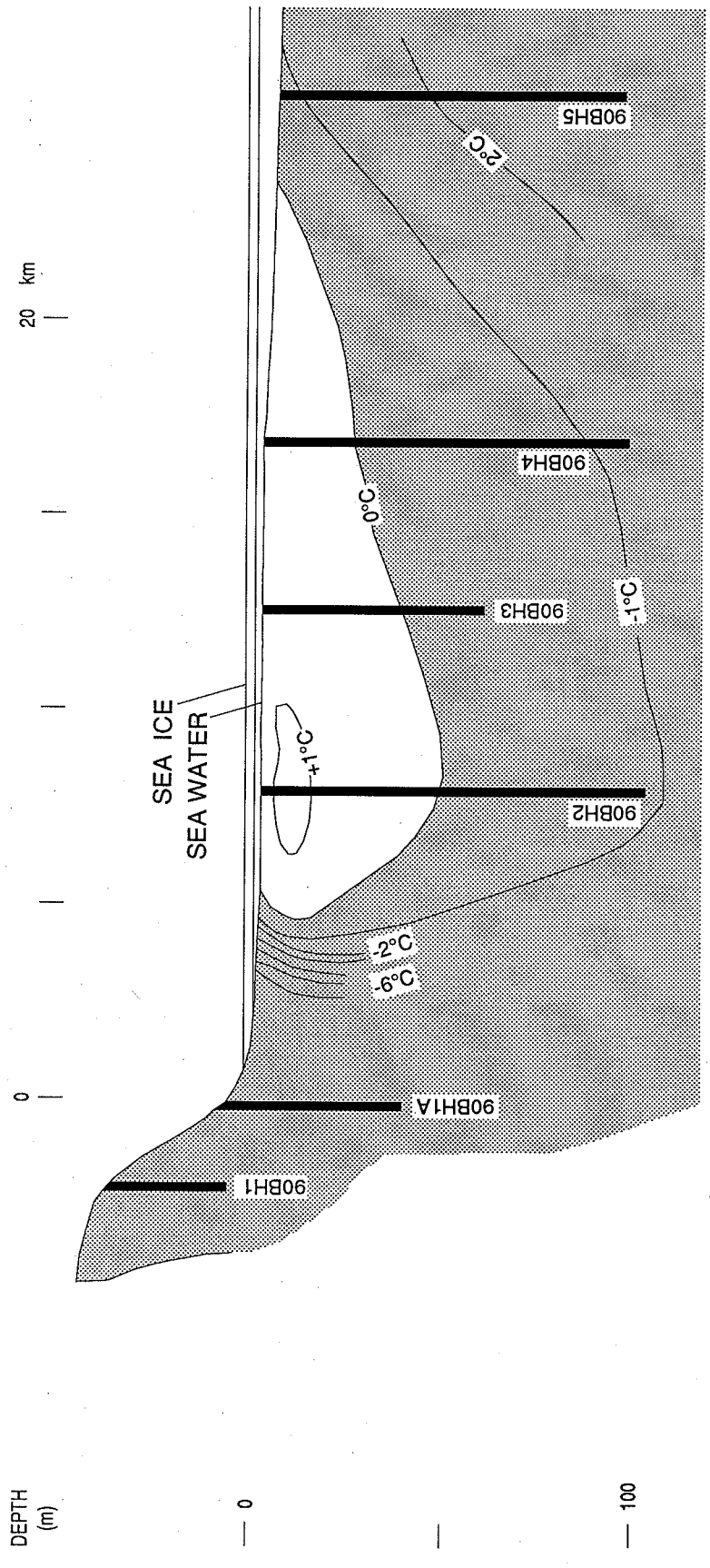

shallow nearshore area where the sea ice freezes to the bottom in the winter are relatively cold, with mean annual ground surface temperatures averaging between -6 and -9°C. The warmest ground temperatures and deepest thawing were encountered in borehole 90BH2 in approximately 3 m water depth. Further offshore of this point ground temperatures cooled, with the 0°C isotherm intersecting the sea bottom between borehole 90BH4 and 90BH5.

The ice bonding conditions in sediments with temperatures below 0°C are affected by the grain size and pore water salinity and are thus stratigraphically controlled. A summary of the bonding conditions showing the simplified stratigraphy and temperature conditions is shown on Figure 5.3. Unit C, which has low salinities and is well bonded onshore, was unbonded in borehole 90BH4 and at the top of 90BH5. Salinities in these zones varied from 10 to 20 ppt with a distinct trend in salinity from the sea bottom, as determined from the conductivity logs. This suggests that saline pore water has migrated into permafrost. Unit D, both onshore and offshore, has high in situ salinities typical of a marine depositional environment. Because of the high salinities and fine grain size, Unit D was unbonded in borehole 90BH4 and 90BH5 at temperatures between 0 and -2°C. The occurrence of unbonded Unit D below ice-bonded, non-saline Unit C in borehole 90BH5 and the similar salinities in Unit D in all boreholes suggests that no pore water exchange occurred in Unit D. Ice-bonding conditions in Unit E were variable, as were the observed salinities. In boreholes 90BH2 and 90BH4 the occurrence of ice bonding has been speculated for the bottom of the boreholes at temperatures close to the -1°C isotherm. Ice-bonding was more pronounced in borehole 90BH5, because Unit E was below -2°C with porewater salinity values below 20 ppt.

In the onshore boreholes the Toker Point till is very ice-rich with massive layers of nearly pure ice between the contact with the till and the underlying Kittigazuit sand. Excess ice and three thin layers of massive ice also occur in Unit C in borehole 90BH5.

5.3 Geotechnical Conditions

Correlation of the onshore and offshore stratigraphy has allowed, for the first time, estimation of geotechnical conditions of the upper 100 m of the seabed over the nearshore area. The strength and physical properties of sediments encountered along the transect

Figure 5.3 TEMPERATURE AND ICE - BONDING CONDITIONS

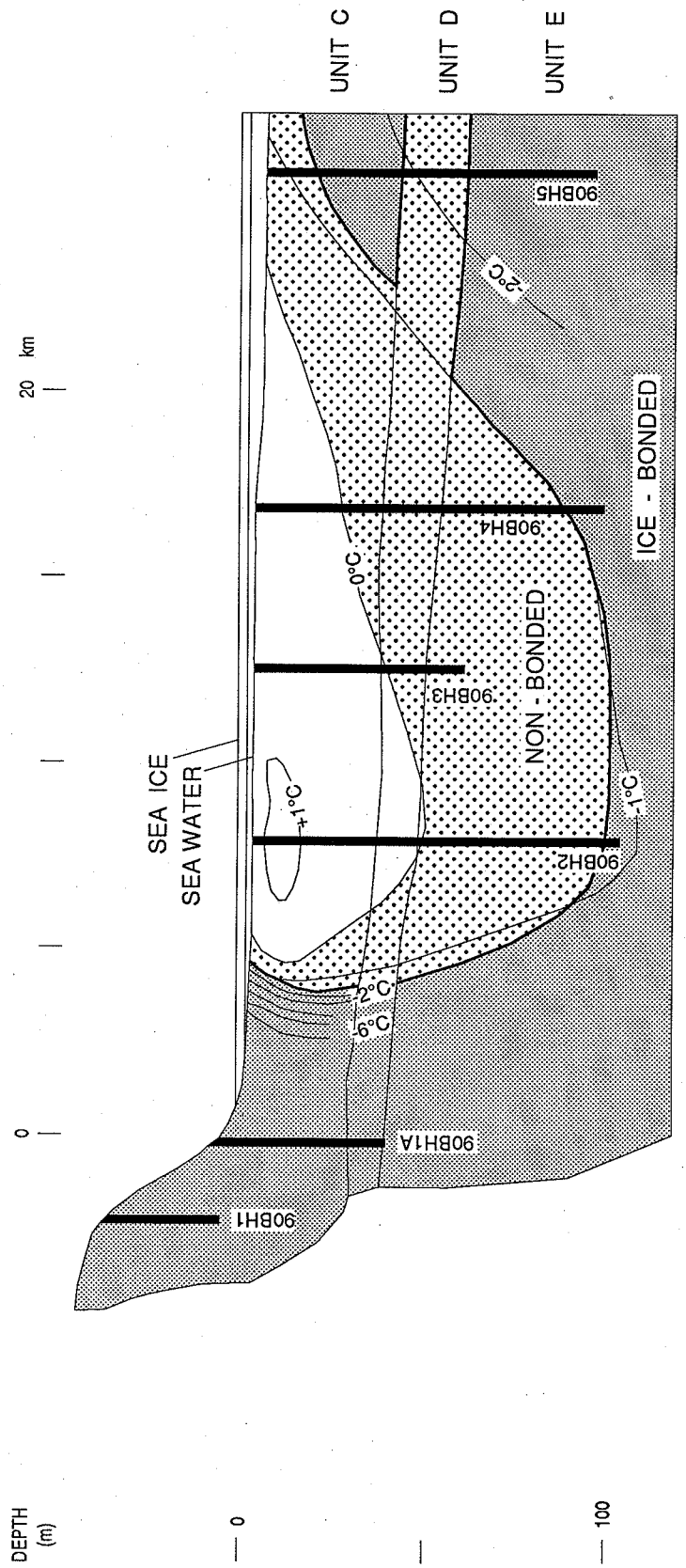

were found to be variable. Perennially frozen sediments can be expected to have variable strengths depending on the ice bonding conditions. High salinities in Unit D and occasional high salinities in units C and E may dictate that these sediments will be unbonded even at relatively cold in situ temperatures.

Unit D was found to have several subfacies characterized by unique sedimentological and physical characteristics. Consolidation testing of samples from borehole 90BH2 suggested that Unit D was highly overconsolidated. Cone penetration testing of Unit B revealed variable strength and grain size characteristics, a thin ice-bonded layer at the sea floor and high overconsolidation ratios.

5.4 Ongoing Work

The results of the onshore-offshore transect have advanced considerably understanding of the stratigraphy and permafrost setting of nearshore areas in the vicinity of northern Richards Island. In many instances the type of studies reported on here represent the preliminary results of multi-phased investigations. Over the next several years researchers will continue to study core samples, carry out experiments and undertake computer modelling. This work is expected to concentrate on three main areas; 1) investigations of the depositional history of the main stratigraphic units, 2) thermal modelling of the effects of the Holocene transgression, and 3) studies of the geotechnical properties of nearshore sediments including, consolidation state and salinity characteristics.

CHAPTER 6

NORTH HEAD COASTAL BOREHOLES

CHAPTER 6
NORTH HEAD COASTAL BOREHOLES:
Geological setting and modifications to progression of thaw

L.D. Dyke

6.1 Introduction

The thaw of ice-bonded permafrost that follows coastal retreat is dependant on the time elapsed since a terrestrial point is submerged. Thawing persists once a point on the seabottom is submerged to a depth that brings it below contact with winter bottom-fast sea ice. For the southern Beaufort Sea in the vicinity of the Mackenzie Delta, thaw will also be controlled by the duration and intensity of warming brought about by the discharge of the Mackenzie River. Initial temperature and salinity of the materials undergoing inundation will further determine the rate of thaw.

The upland terrain at the north end of Richards Island is underlain by a patchy distribution of diamicton (till) consisting of a very dark brown silty clay containing scattered pebbles. This diamicton overlies a sand unit which displays highly contorted bedding in exposures along the eroding coast at North Head. Salinities in this unit, where frozen, are generally below 10 ppt, based on borehole samples from the North Head area (Kurfurst, 1987). Therefore salinity of these sediments will not have a pronounced influence on thawing temperature. The warming of the ground temperature up to 0°C, as coastal retreat brings a terrestrial location through the zone in contact with sea ice, will increase the initial rate of thaw. Other thermal conditions at the onset of inundation, dependent on a thermal regime other than that established on the upland tundra, may result in different thermal histories.

The North Head area contains many lakes ranging between 0.5 and 2 km in the longest axis. When intercepted by coastal retreat, these lakes effectively induce sudden increments of retreat if the lake bottom elevation is below sea level. This sudden retreat will be accompanied by the incorporation of any lake bottom talik into the thawed zone that follows the retreating coast. However, this incorporation will be delayed if the residual sill between the open sea and the lake remains in water shallow enough to maintain ice bonding. Furthermore, permafrost will begin to aggrade into the lake bottom if sediment

infilling raises the lake bottom into contact with winter ice. Bathymetric changes to lake bottoms, once they become lagoons, will therefore introduce complications into subsea permafrost distribution.

If the lake bottom is above sea level, retreat across a subaerially exposed lake bottom will continue. However, the retreat rate will probably be slow enough to allow permafrost aggradation into the exposed lake bottom before it disappears. In either case the presence of lake-bottom taliks provide opportunities for permafrost aggradation in an environment otherwise undergoing permafrost degradation. of permafrost degradation.

6.2 Borehole Program

The boreholes reported on here were located to investigate the consequences of lake incorporation in the nearshore zone along a retreating coast (Fig. 6.1). The data collected from these boreholes can be used to anticipate initial conditions that may determine the later temperature and degree of ice bonding of offshore sediments once transgression occurs. These initial conditions differ from the temperatures, salinities, and stratigraphy beneath upland terrain at North Head. Boreholes 90BH6 and 90BH7 were cored continuously through ice bonded sediments and the cores stratigraphically logged (Appendix A). Borehole 90BH8 was ice-bonded and cored for the first 3.5 m. Below this depth the borehole was advanced through unfrozen sediments by augering. Geophysical logs and laboratory measurements were made as follows:

Temperature: thermistor cable with beads at 2 m spacing, starting at a depth a 1 m.

Water Salinity: salinity as g/L NaCl of water extracted from thawed core sample

Conductivity: borehole electrical conductivity log

Gamma radiation: Natural gamma log

Moisture Content: by weight of thawed pore ice

Excess Ice Content: by volume as water on top of thawed sediment in sample container

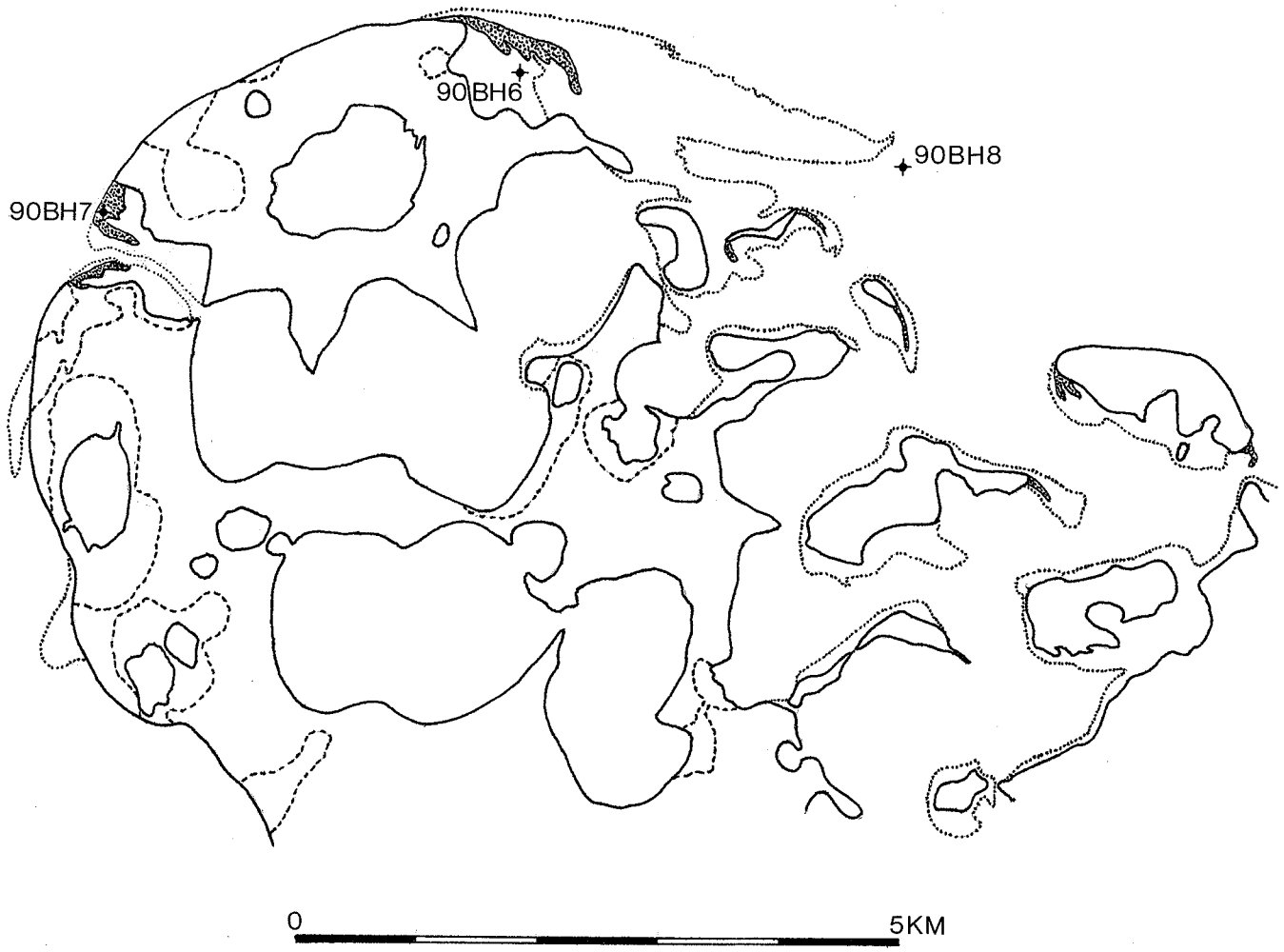

Figure 6.1 Location of boreholes, north end of Richards Island.

Summary of Boreholes

All measurements in metres

	90BH6	90BH7	90BH8
Surface ice thickness	0.6	0	1.7
Total depth below ground surface	20.55	20.45	15
Elevation of top of borehole	-0.6	about 1.0	-1.7
Ice bonded thickness	all	all	top 1.5

Borehole 90BH6

This borehole is located in the lagoon behind the prominent spit that protrudes eastwards from the northern extremity of Richards Island. A steep embankment on the south and west sides of the lagoon, together with shoreline terraces slightly elevated above the present lagoon level, suggests that the lagoon occupies a breached lake. The position of the north side of the lake is unknown. However, two borings to a depth of about 4 m on the sandy silt apron (which extends east from the spit) encountered massive sand with inclined bedding (outlined by slight changes in grain size) at a depth of about 2 m (Wolfe, 1989). This unit is tentatively thought to be the Kittigazuit Formation and its presence beneath apron sediments suggests no lake existed at the location of these boreholes. Therefore a lake may have coincided with the present lagoon.

Appendix A presents the stratigraphy of 90BH6. Massive sands containing occasional wood fragments are overlain by about 4 m of dark brown to dark grey, slightly sandy clay with scattered pebbles. This diamicton is considered to be the Early Wisconsinan Toker Point till that caps parts of the North Point upland (Rampton, 1988). Its position in this borehole is considerably below the general elevation for this till in the North Head area. Above the till is sand with occasional pebbles, grading into sand with silty bands over a total thickness of 3 m. Another 3 m of dark brown, slightly fetid sandy silt follows, capped by a final 2 m of interbedded sand and silt.

Borehole 90BH7

This borehole is located on the west side of North Head in a lake basin clearly breached by coastal erosion. Sand and gravel washover fans extend across the lake bottom from the coast a few hundred metres inland. The borehole is located on one of these, approximately 10 m inland from a line of dunes that marks the top of the beach.

The borehole log in Appendix A shows massive sands with occasional wood fragments and silt layers overlain by about 5 m of silt containing occasional pebbles. The sand sequence is interpreted as Kidluit Formation overlain by diamicton thought to be till. The diamicton is overlain by about 1 m of black, slightly fetid clay. This is interpreted as a lake bottom or lagoon setting. Temporary exposure to seawater is suggested by the moderate salinites of pore water in the black clay. Close to 2 m of sand and thin gravel layers are in abrupt contact with the clay.

Borehole 90BH8

This borehole was placed to locate the distal underwater end of the silty sand platform that extends eastward from the northernmost part of North Head. About 1.7 m of sea ice was encountered, frozen to the bottom. This ice may have been thickened by overthrusting during freeze-up as the sea ice surface was rough and buckled in the vicinity. About 1.5 m of ice-bonded sand with silty sand interbeds were encountered below this ice (Appendix A). Augering continued to a depth of 15 m but only produced a slurry of silty sand.

6.3 Interpretation

In borehole 90BH6 the sequence above the till is interpreted as a basin filling. In part, filling may have been accomplished by glaciofluvial sedimentation and completed during and after breaching by the sea. Coarser material near the top of the core may have been added recently by washover across the spit. Temperatures near the base of the borehole show upward heat flow,(Appendix A) indicating that ice bonding is deep enough to have existed for a minimum of a few hundred years. In the following paragraph, it is inferred that permafrost aggradation began at the time of lake breaching.

The high salinities of the top few metres are most likely due to concentration of solute ahead of an advancing freezing front. Evaporative concentration in subaerially exposed

sediments is also possible but seems less likely because permafrost would aggrade to the depth in a few years, too short a time to permit concentration of solutes to the depth that they are encountered. Therefore permafrost aggradation must have begun as the sediment surface came into contact with winter ice in a water body that communicated with the saline waters of the Beaufort Sea. Many freeze-thaw cycles would ensue, permitting concentration of the solute over a longer interval of time. Establishment of permanent ice bonding would then prevent the further diffusion of solute. If the lake bottom was unfrozen at the time of breaching, permafrost aggradation must have commenced shortly after breaching. If not, solutes would have had time to penetrate more deeply into the basin sediments.

Salinities and conductivities are low throughout borehole 90BH7 (Appendix A, note small range of conductivity scale) except for a peak in salinity corresponding with the black clay layer. The overall low salinities suggest either a very short exposure of a lake talik to sea water or the presence of permafrost prior to breaching.

Temperature records from the boreholes are not complete but can be used to speculate on the extent of permafrost at the time of breaching. Temperatures in borehole 90BH7 (Appendix A) indicate a gradual warming below 10 m which, if extrapolated to depth, gives about 60 m of ground below 0°C. This is thin in comparison with the several 100 m of permafrost known to exist in the area, and indicates a relatively short time for permafrost aggradation. Therefore a lake talik probably did exist at the time of breaching. The present moderate salinity of the black clay layer may have been acquired from modern storm washovers.

Electrical conductivity in borehole 90BH8 (Appendix A) rises rapidly through the ice bonded part of the borehole and becomes essentially constant at depth as unfrozen ground is reached. The entire section is probably at a salinity of roughly 20 ppt. This pervasive salinity is most easily explained if the entire borehole lies within Unit B. This is the transgressive unit derived from eroded and reworked onshore sediments and its formation would include incorporation of Beaufort Sea water.

Sediments in borehole 90BH8 are ice bonded to 1.5 m below seabottom, and are in contact with 1.7 m of winter sea ice. This amount of freezing is considerable for the amount of sea ice present and suggests that permafrost may be just beginning to form at this

location. Construction of the sandy silt platform from the west may ensure that the seabottom continues to become shallower and that permafrost continues to aggrade at this location.

6.4 Conclusions

1. Some lake basins may contain several metres of sediment fill deposited after the last glaciation in the area. Depending on exposure to storm winds, some of this basin filling may take place after the lake has been breached by coastal erosion if the lake bottom is below sea level. As coastal retreat continues, these sediments will then be incorporated into the sub-sea sedimentary sequence.

2. Present lagoons along the north coast of Richards Island are likely to be underlain by a range of thermal profiles. The degree of cooling will depend on the time elapsed since filling has brought lagoon bottoms into contact with winter ice.

3. Construction of underwater extensions of spits and bars in areas previously inundated may coincide with permafrost aggradation where the seabottom is brought into contact with sea ice. Rapid erosion of such extensions could result in anomalous shallow permafrost occurrences where the seabottom is brought below the depth of winter sea-ice growth.

REFERENCES

Kurfurst, P.J. (Editor) 1987: Geotechnical investigations of northern Richards Island, N.W.T., Geological Survey of Canada, Open File 1707, 146 p.

Rampton, V.N. 1988: Quaternary Geology of the Tuktoyaktuk Coastlands, Northwest Territories; Geological Survey of Canada, Memoir 423, 98 p.

Wolfe, S.A. 1989: Investigation of nearshore conditions across an aggrading coastal shoreline in permafrost, Richards Island, N.W.T.; M. Sc. thesis, Department of Geology, Queen's University, Kingston, Ontario K7L 3N6.

APPENDIX B

Examples of data recording sheets

FIELD LOGGING SHEET

Borehole Number: 90 BH 5

Project: Onshore/offshore transect.

Location & comments:
Set up on site by ~1500
Prep 1500 – 1900.

Date: 31/03/90

Drill: Foundex

Logged by: SRD/JWS

Shift: Day.

Increment From	Increment To	Samples #	Samples Type	Temp. (°C)	Description Sediment/Rock	Ice	NRC
					6:55pm hole augered through ice. Depth from table to mudline 39' (11.89 m)	10m water	
					started drilling @ 7:00pm		
					~~pm~~ hose frozen still waiting @ 7:30		
0	0.30m	no trace for sample			20cm of brown clay - coarse fining up from sandy, silty clay to clay w/ occas fine sand. v soft grad. contact with sand (dk brown)	excess water from malleable remelt in clay	
					Sand = 10 cm - coarsening up from silty sand to sand. shell frag at 20cm - sand unit fi firm		
0.30	0.45				shelby sample dk brown silt and sand interbeds fairly firm visible ice inclusion on top	Vx	
					9:15 PM		
5½ OD casing					Pushed casing 1' using		
5 ID casing					2100 psi × 3" ϕ = 14,800 lbs.		
					- 1¾ rod = 5,048 lbs		
					9,750 lbs		
					9:45 Driving casing ≈ 65 blows/ft 2'-3'		
					350 lbs hammer		

90 BH.5.

INVENTORY OF FIELD AND LAB TESTS

m Core Interval	FIELD TESTS Conductivity	FIELD TESTS TDR	LAB. Conductivity	LAB TESTS Acoustic	Bulk Density	Shear Vane	Photography	Sed. Logging	Sub-samples	Water Content	Salinity	A. Limits	Grain Size	Comments
23.7-24.0 BH-90-3	28/03 PH	26/03 PH	28/03 PH	28/03 JB	28/03 BH	29/03 AB	29/03 GD	29/03 GE	29/03 GH	03/04 AW	28/03 LM	29/03 GF	30/03 GF	See #1 attached sheet
20.1 - 20.4	J.O 1/04	J.O.	AET 2/04	JSB 02.04.90	JSB. 02.04.90	—	RH 2/4	PH 2/4	PH/RH 2/4	LM 02/04	LM 02/04	—	—	
20.4 - 20.97	J.O 1/04	—	AET 2/04	—	—		RH 2/4	PH 2/4	PH/RH 2/4	LM 02/04	LM 02/04	—	—	
20.97-21.60	J.O 1/04	—	AET 2/04	—	—		RH 2/4	KJ 2/4	KJ/RH 2/4	LM 02/04	LM 02/04	—	—	
21.68-22.4	J.O 1/04	—	AET 2/04	JSB .02.04.90	JSB. .02.04.90.		RAH 2/4	ICJ 2/4	RH/KJ 2/4	LM 02/04	LM 02/04	—	LM 03/04	
22.41-23.2	J.O 1/04	—	AET 2/04	JSB. .02.04.90.	JSB. .02.04.90.		RAH 2/4/90	KJ 2/4/90	RH/KJ 2/4/90	LM 02/04	LM 02/04	—	—	
23.20-23.70	J.O 02/04	—	AET 3/04	—	—		RAH 3/4/90	KAJ 3/4/90	PRH 3/4/90	LM 04/04	LM 03/04	—	—	
23.7-23.88	J.O 2/04	—	AET 2/04	—	—	—	RH 3/4/90	PH 3/4	—	—	—	—	—	
23.88-24.6	J.O 2/04	—	AET 2/04	—	—		RH 3/4/90	KAJ 3/4/90	KAJ/KAH 3/4/90	LM 02/04	LM 03/04	—	LM 03/04	
24.88-25.52	—	—	AET 3/04	JSB. 04.04.90	JSB. 04.04.90		RH 3/4/90	KAJ 3/4/90	PRH 3/4/90	LM 04/04	LM 03/04	—	—	
25.52-26.2	—	—	AET 3/04	—	—		RH 3/4/90	KAJ 3/4/90	PRH 3/4/90	LM 04/04	LM 03/04	—	—	
26.2-26.42	—	—		—	—		RH 3/4/90	KAJ 3/4/90	PRH 3/4/90	LM 04/04	LM 03/04	—	—	
26.42-27.17	—	—	AET 3/04	—	—		RH 4/4/90	KAJ 4/4/90	PRH 4/4/90	LM 04/04	LM 04/04	—	LM 05/04	
27.17-27.7	—	—	AET 3/04	JSB. 04.04.90	JSB 04.04.90		RH 3/4/90	KAJ 3/4/90	PRH 3/4/90	LM 04/04	LM 03/04	—	—	
27.7-28.77	NOT RECEIVED YET			—	—					—	—	—	—	
28.77-29.30	J.O 2/04	—		—	—		RH 4/4/90	KAJ 4/4/90	PRH 4/4/90	LM 04/04	LM 04/04	—	—	
29.3-29.73	J.O 2/04	—		JSB .03.04.90	JSB .03.04.90		RH 4/4/90	KAJ	PRH	LM 04/04	LM 04/04	—	LM 05/04	

appendix A.3

DRILL CORE FIELD INVENTORY

V.F at Hole 5 -2°C

90 BH 5.

INTERVAL (metres)	RECOVERY DATE/TIME	THERMAL CATEGORY	FIELD STORAGE	TRANSPORT METHOD	TRANSPORT DATE	COOLER/BOX NUMBER
0.0-0.20	31/03/2000	N.S. cold baby poop	bag in V.F	truck	01/04/90	Box 2
0.20-0.45	31/03/2000	N.S	bag in V.F	"	"	Box 2
0.6-1.83	01/04/0510	N.S	bag in Vic	"	"	2
1.82-3.35	0104/0525	N.S	bag in Vic's	"	"	2
9.35-9.4	01/04/90 9:30	~~unfrozen~~ thermally sensitive	bag in Vic's freezer	"	"	2
9.92-11.00	9:45	~~unfrozen~~ sensitive	Vic's freezer	"	"	2
11.90-12.50	10:00	sensitive ~~unfrozen~~	Vic's freezer	"	"	2
13.30-14.00	10:30	"	"	"	"	2
15.17-15.47	10:45	partially bonded sensitive	bagged in Vic's freezer	"	"	2
~~15.47-15.54~~	"	"	split tube in Vic's freezer	"	"	2
15.54-16.31	12:00	permafrost! ~~sensitive~~	VF	"	"	2
16.3-17.0	12:00	"	"	"	"	Box #1
17.15-17.88	13:30	~~frozen~~ sensitive	VF → #1	"	"	2
17.88-18.60	13:30	" sensitive	VF → #1	"	"	2
18.6-18.2	1:10	"	outside	"	to be sent at a later date	Box #1

? Depth. (18.62-18.92)

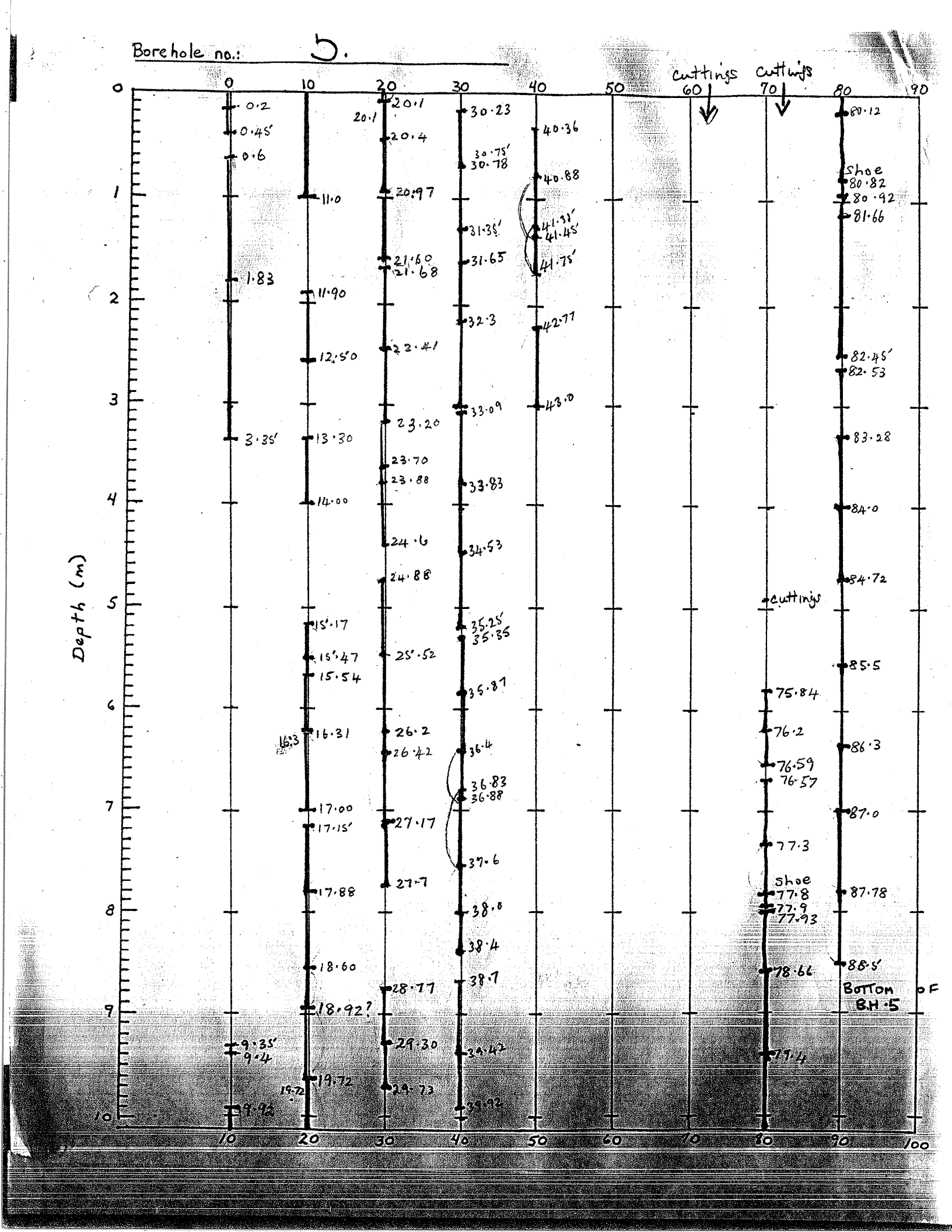
Borehole no.: 5.
Depth (m)
cuttings
cuttings
cuttings
Shoe
Shoe
Bottom of B.H. 5
0.2
0.45
0.6
1.83
3.35
9.35
9.4
9.92
11.0
11.90
12.50
13.30
14.00
15.17
15.47
15.54
16.31
16.3
17.00
17.15
17.88
18.60
18.92
19.72
19.72
20.1
20.1
20.4
20.97
21.60
21.68
22.41
23.20
23.70
23.88
24.6
24.88
25.52
26.2
26.42
27.17
27.7
28.77
29.30
29.73
30.23
30.75
30.78
31.35
31.65
32.3
33.09
33.83
34.53
35.25
35.35
36.87
36.4
36.83
36.88
37.6
38.0
38.4
38.7
39.42
39.92
40.36
40.88
41.31
41.45
41.75
42.77
43.0
75.84
76.2
76.59
76.57
77.3
77.8
77.9
77.93
78.66
79.4
80.12
80.82
80.92
81.66
82.45
82.53
83.28
84.0
84.72
85.5
86.3
87.0
87.78
88.5
0
10
20
30
40
50
60
70
80
90
100
1
2
3
4
5
6
7
8
9
10

ACOUSTIC TESTS

ample No.	Interval (.m)	Diameter (cm)	Length (cm)	Weight (g)	Bulk Density (g/cm^3)	Tp (μs)	Vp (m/s)	Ts (μs)	Vs (m/s)	Comments
) BH5-1 .60-18.92)	18.775-1890	6.0	12.5	359.0	1.02	8		76		.02.04.9
BH5-2 .1-20.4)	20.27-20.392	6.1	12.2	637.1	1.79	44		92		"
BH5-3 .72-20.1)	19.82-19.942	6.1	12.2	686.7	1.93	46		96		"
BH5-4 .88-18.60)	18.28-18.402	5.9	12.2	383.9	1.15	36.		65.6		"
BH5-5 .15-17.88)	17.28-17.403	6.1	12.3	664.1	1.85	36.8		67.2		"
BH5-6 .4-23.2)	22.42-22.546	6.1	12.6	718.2	1.95	41.6		72		"
BH5-7 .71-22.29)	22.08-22.202	6.1	12.2	687.0	1.93	39.2		84		"
BH5-8 .3-29.73)	29.60-29.722	6.1	12.2	702.0	1.97	31.2		45.6		.03-04.0
BH5-9 6.4-36.88)	36.67-36.795	6.1	12.5	723.5	1.98	33.6		60.0		"
BH5-10 .0-38.4)	38.09-38.212	5.9	12.2	712.6	2.14	34.4		62.4		"
BH5-11 .3-33.09)	32.51-32.633	6.1	12.3	688	1.91	30.4		56		"
BH5-12 .83-37.6)	37.19-37.312	6.1	12.2	686.5	1.93	31.2		60		"
BH5-13 .87-36.4)	36.075-36.197	6.1	12.2	680.2	1.91	32.0		56		"
BH5-14 .35-35.87)	35.57-35.693	6.1	12.3	683.5	1.90	31.2		56.8		"
BH5-15 .53-35.25)	34.915-35.037	6.1	12.2	732.3	2.05	31.2		60.8		"

ATLANTIC GEOSCIENCE CENTRE

CRUISE NUMBER. MEGATRANSECT	SAMPLE NUMBER. 90 BH05 11.90-12.50	TOTAL LENGTH. 0.60m ~~CM.~~
SAMPLE TYPE. HQ CORE	CALENDAR DATE. April 2 | 90	PAGE 1 OF. 1
GEOGRAPHIC LOCATION.	PROJECT NUMBER.	
SUBSAMPLED FOR. D. Gill.	SUBSAMPLED BY. RAH | KAJ	

SEDIMENT/ROCK CORE SUBSAMPLE INFO

SUBSAMPLE INTERVAL (CM.)	TEXTURE (SED SIZE)	FORAMS	SHEAR VANE	MOISTURE BULK DENSITY	SHELLS	Pore water	Pollen	Gr. Size	
12.13-12.16	Sand			✓					
12.16-12.2						✓			
12.2-12.25		✓					✓		
12.3-12.4								✓	

Borehole no.: 5. Thermal Cond. measured at lab.

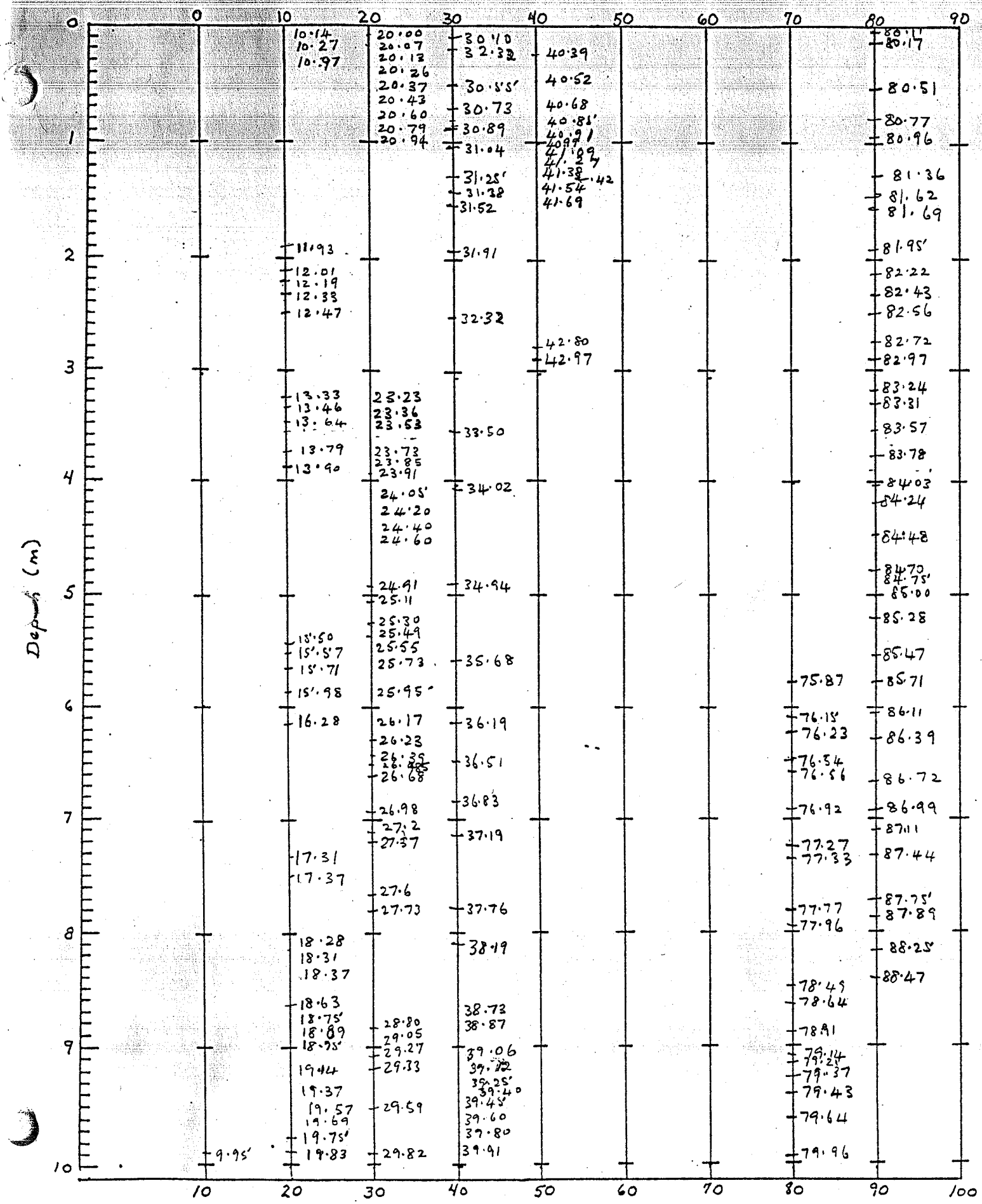

CRUISE NUMBER. MEGATRANSET	SAMPLE NUMBER. 90BB15 13.30 - 14.00	TOTAL LENGTH. 0.70m ~~CM~~
SAMPLE TYPE HQ CORE	CALENDAR DATE. April 2/90	PROJECT NUMBER.
GEOGRAPHIC LOCATION.		
DESCRIBED BY. K. JENNER	PAGE 1 OF 1	

SYMBOL LEGEND: sand; thinbd.; silt

CORE DESCRIPTION

CORE TOP

13.30 - 13.34m Thin interbeds of fs and silty sand. Sharp basal contact.

13.34 - 13.68m Homogeneous, structureless m sand. Sand clean and contains 5% mafic grains (pyroxene, hornblend etc) ~ 10% Kfsp rich. Appears to have been homogenized during drilling: invert in core centre and rare silty blebs surrounded by invert.

13.68 - 13.94m Thinbd silty sand and unbid fsand. 80% silty sand & 20% fine sand bds. Parallel bedded.

Consolidated but not firm

moderately effervescent

2.5Y 4/2

13.30 TOP

13.94

18.17 - 18.72
20.3 - 20.97

MOISTURE CONTENT TEST RESULTS

ASTM Designation D2216

Project No.: _____ Borehole No.: 90 BH 5

Project: _____

Address: _____ Date Tested: 02/04 By: LM

Depth m	Tare No.	Weight of Wet Soil g	Weight of Dry Soil g	M. C. %	Visual Description of Soil ASTM D2488 ☐ ASTM Standard Not Followed ☐	Pocket Pen. Reading
10.24-10.28	100	79.0	72.5	19.17	9.92 - 11.00	
12.13-12.16	102	92.6	85.5	15.04	11.90 - 12.50	
18.73-18.78	104	63.0	41.0	814.81	18.6 - 18.92	
19.92-19.94	106	79.1	70.6	26.65	19.72 - 20.10	
26.78-26.83	108	87.4	74.7	34.70	20.1 - 20.4	
13.60-13.63	110	104.0	95.4	15.17	13.30 - 14.00	
17.42-17.41	112	113.0	96.8	27.74	17.15 - 17.88	
18.40-18.44	114	57.7	44.2	228.81	17.88 - 18.66	
16.50-16.54	116	97.6	86.3	23.44	16.30 - 17.00	
22.73-22.77	118	94.4	83.0	25.56	22.41 - 23.20	
22.0-22.03	120	89.7	78.5	27.93	21.68 - 22.41	
21.40-21.42	124	87.8	75.7	32.88	20.97 - 21.60	
19.28-19.32	122	107.4	95.5	20.80	18.92 - 19.72	
20.48-20.51	126	70.7	61.7	38.13	20.4 - 20.97	
24.19-24.23	128	165.7	142.8	21.93	23.88 - 24.60	
39.53-39.57	132	73.1	64.6	33.33	39.42 - 39.92	
40.61-40.63	130	73.0	63.8	36.07	40.36 - 40.80	
3882-3887	134	63.0	57.1	32.06	38.7 - 39.16	
39.22-39.25	136	175.1	65.6	35.71	38.90 - 39.42	
41.10-41.14	138	70.6	62.7	32.38	40.88 - 41.45	
41.54-41.58	140	72.3	64.2	31.76	41.35 - 41.75	
36.24-36.27	148	122.9	104.3	28.22	35.87 - 36.40	
35.84-35.87	150	102.0	89.5	24.56	35.35 - 35.87	
32.62-32.64	142	97.0	853	25.16	32.30 - 33.09	
37.44-37.47	144	85.2	75.6	26.16	36.83 - 37.60	

03/04/90

SALINITY

Borehole no.	Depth (m)	Lab. no.	Salinity (‰)	
5	24.12 - 24.15	90-BH5-2412 PW	0	sand *
5	39.57 - 39.60	90-BH5-3957 PW	32	clay *
5	40.65 - 40.70	90-BH5-4065 PW	32	clay *
5	38.90 - 38.95	90-BH5-3890 PW	26	clay *
5	39.25 - 39.30	90-BH5-3925 PW	21	clay *
5	41.15 - 41.20	90-BH5-4115 PW	28	clay *
5	41.58 - 41.62	90-BH5-4158 PW	38	clay *
5	32.66 - 32.68	90-BH5-3266 PW	0	
5	35.80 - 35.84	90-BH5-3580 PW	3	
5	36.24 - 36.27	90-BH5-3624 PW	1	
5	37.49 - 37.53	90-BH5-3749 PW	5	
5	38.28 - 38.30	90-BH5-3828 PW	5	
5	25.77 - 25.79	90-BH5-2577 PW	2	
5	34.87 - 34.90	90-BH5-3487 PW	2	
5	23.45 - 23.48	90-BH5-2345 PW	2	
5	26.35 - 26.40	90-BH5-2635 PW	13	
5	25.44 - 25.46	90-BH5-2544 PW	5	
5	27.25 - 27.27	90-BH5-2725 PW	3	
5	32.09 - 32.15	90-BH5-3209 PW	0	
5	33.60 - 33.63	90-BH5-3360 PW	5	
5	34.09 - 34.11	90-BH5-3409 PW	8	
5	37.81 - 37.83	90-BH5-3781 PW	5	
5	36.48 - 36.50	90-BH5-3648 PW	50	

* used centrifuge method

APPENDIX C

Tables of thermal conductivity data

MEGATRANSECT 1990 603 B.H. 1

Site	Borehole	Depth m	Conductivity W/mK	Method	Lithology	Lith	Ambient	N69 39'45.8" Latitude N	W134 23'20.4" Longitude W	Unit
603	1	0.30	2.0417	N.P.	silty clay	slcl	-5.30	69.66272	134.38900	C
603	1	1.15	2.6929	N.P.	sandy diam.	sddm	-4.04	69.66272	134.38900	C
603	1	1.33	2.4392	N.P.	sandy diam.	sddm	-3.93	69.66272	134.38900	C
603	1	1.55	1.7932	N.P.	sandy diam.	sddm	-5.32	69.66272	134.38900	C
603	1	1.99	2.3922	N.P.	sandy diam.	sddm	-3.96	69.66272	134.38900	C
603	1	2.18	2.0653	N.P.	sandy diam.	sddm	-4.97	69.66272	134.38900	C
603	1	2.35	2.0226	N.P.	sand	sd	-3.23	69.66272	134.38900	C
603	1	2.65	1.9060	N.P.	sandy diam.	sddm	-3.54	69.66272	134.38900	C
603	1	3.15	1.9713	N.P.	sandy diam.	sddm	-3.31	69.66272	134.38900	C
603	1	3.20	2.4170	N.P.	sandy diam.	sddm	-4.52	69.66272	134.38900	C
603	1	3.23	2.9592	N.P.	sandy diam.	sddm	-4.60	69.66272	134.38900	C
603	1	3.60	2.3277	N.P.	silty clay	slcl	-4.04	69.66272	134.38900	C
603	1	3.80	2.3843	N.P.	sandy diam.	sddm	-6.12	69.66272	134.38900	C
603	1	4.33	3.7825	N.P.	sandy diam.	sddm	-4.32	69.66272	134.38900	C
603	1	4.73	3.3729	N.P.	sandy diam.	sddm	-5.07	69.66272	134.38900	C
603	1	4.84	2.9369	N.P.	sandy diam.	sddm	-4.68	69.66272	134.38900	C
603	1	5.06	2.9437	N.P.	sandy diam.	sddm	-5.06	69.66272	134.38900	C
603	1	5.40	2.3002	N.P.	sandy diam.	sddm	-5.49	69.66272	134.38900	C
603	1	6.20	2.7047	N.P.	sandy diam.	sddm	-4.61	69.66272	134.38900	C
603	1	6.40	3.4024	N.P.	sandy diam.	sddm	-5.49	69.66272	134.38900	C
603	1	6.90	3.0917	N.P.	clay-silt	clsl	-3.74	69.66272	134.38900	C
603	1	7.45	2.8283	N.P.	sandy diam.	sddm	-4.61	69.66272	134.38900	C
603	1	7.74	2.6636	N.P.	sandy diam.	sddm	-5.24	69.66272	134.38900	C
603	1	8.16	2.5374	N.P.	sandy diam.	sddm	-5.76	69.66272	134.38900	C
603	1	9.30	3.2205	N.P.	sandy diam.	sddm	-4.05	69.66272	134.38900	C
603	1	9.56	2.7614	N.P.	sandy diam.	sddm	-6.39	69.66272	134.38900	C
603	1	10.20	2.7214	N.P.	sandy diam.	sddm	-5.59	69.66272	134.38900	C

MEGATRANSECT 1990 603 B.H. 1

Site	Borehole	Depth m	Conductivity W/mK	Method	Lithology	Lith	Ambient	N69 39'45.8" Latitude N	W134 23'20.4" Longitude W	Unit
603	1	10.70	3.0235	N.P.	sandy diam.	sddm	-4.56	69.66272	134.38900	C
603	1	11.20	3.1395	N.P.	sandy diam.	sddm	-3.97	69.66272	134.38900	C
603	1	11.90	3.3779	N.P.	sandy diam.	sddm	-5.53	69.66272	134.38900	C
603	1	12.30	3.3873	N.P.	sandy diam.	sddm	-3.95	69.66272	134.38900	C
603	1	13.43	2.6935	N.P.	sandy diam.	sddm	-4.96	69.66272	134.38900	C
603	1	13.73	3.1406	N.P.	sandy diam.	sddm	-5.55	69.66272	134.38900	C
603	1	13.99	2.6193	N.P.	sandy diam.	sddm	-4.99	69.66272	134.38900	C
603	1	14.15	2.9441	N.P.	sandy diam.	sddm	-5.21	69.66272	134.38900	C
603	1	14.70	2.4369	N.P.	sandy diam.	sddm	-3.49	69.66272	134.38900	C
603	1	15.10	2.9897	N.P.	sandy diam.	sddm	-3.72	69.66272	134.38900	C
603	1	15.40	2.9004	N.P.	sandy diam.	sddm	-4.61	69.66272	134.38900	C
603	1	16.20	4.1307	N.P.	sandy diam.	sddm	5.17	69.66272	134.38900	C
603	1	16.40	2.5969	N.P.	sandy diam.	sddm	-4.57	69.66272	134.38900	C
603	1	16.60	3.1250	N.P.	sandy diam.	sddm	-3.65	69.66272	134.38900	C
603	1	17.00	2.6292	N.P.	sandy diam.	sddm	-5.21	69.66272	134.38900	C
603	1	17.20	2.7750	N.P.	sandy diam.	sddm	-3.89	69.66272	134.38900	C
603	1	18.20	3.1507	N.P.	sandy diam.	sddm	-3.90	69.66272	134.38900	C
603	1	19.10	2.8243	N.P.	sandy diam.	sddm	-4.53	69.66272	134.38900	C
603	1	20.05	1.7232	N.P.	sandy diam.	sddm	-4.43	69.66272	134.38900	C
603	1	20.35	2.2186	N.P.	sandy diam.	sddm	-7.25	69.66272	134.38900	C
603	1	21.13	1.8483	N.P.	ice w/ sandy diam.	isddm	-4.80	69.66272	134.38900	C
603	1	21.42	1.9037	N.P.	ice w/ sandy diam.	isddm	-4.69	69.66272	134.38900	C
603	1	21.60	2.1295	N.P.	ice	i	-3.00	69.66272	134.38900	C
603	1	22.15	1.6642	N.P.	ice+sed.	ise	-4.10	69.66272	134.38900	C
603	1	22.73	1.5780	N.P.	ice+sed.inclus.	ise	-3.75	69.66272	134.38900	C
603	1	23.33	2.0338	N.P.	sandy diam.	sddm	-5.75	69.66272	134.38900	C
603	1	23.71	2.2994	N.P.	sandy diam.	sddm	-5.26	69.66272	134.38900	C

MEGATRANSECT 1990 603 B.H. 1

Site	Borehole	Depth m	Conductivity W/mK	Method	Lithology	Lith	Ambient	N69 39'45.8" Latitude N	W134 23'20.4" Longitude W	Unit
603	1	23.90	2.7320	N.P.	sandy diam.	sddm	-4.56	69.66272	134.38900	C
603	1	24.49	2.1321	N.P.	sandy diam.	sddm	-3.99	69.66272	134.38900	C
603	1	24.79	2.3305	N.P.	sandy diam.	sddm	-4.25	69.66272	134.38900	C
603	1	24.80	2.4329	N.P.	ice+sed.	ise	-4.69	69.66272	134.38900	C
603	1	25.00	2.2717	N.P.	sandy diam.	sddm	-4.56	69.66272	134.38900	C
603	1	25.30	2.6796	N.P.	sandy diam.	sddm	-4.59	69.66272	134.38900	C
603	1	25.52	2.9375	N.P.	ice w/ sed. incl.	ise	-5.40	69.66272	134.38900	C
603	1	26.30	2.5396	N.P.	sandy diam.	sddm	-1.67	69.66272	134.38900	C
603	1	27.25	2.5226	N.P.	ice w/silt-sand	islsd	-4.34	69.66272	134.38900	C
603	1	29.20	3.4319	N.P.	sand	sd	-2.40	69.66272	134.38900	C
603	1	29.44	3.4679	N.P.	sand	sd	-1.21	69.66272	134.38900	C
603	1	29.70	3.2136	N.P.	sand	sd	-1.13	69.66272	134.38900	C

MEGATRANSECT 1990 603 BH 2

Site	Borehole	Depth m	Conductivity W/mK	Method	Lithology	Lith	Ambient	N69 44'21.0" Latitude N	W134 16'34.3" Longitude W	Uni
603	2	1.67	2.9870	T.P.A.	f. sand	sd	1.65	69.73917	134.27619	B
603	2	2.02	1.9930	T.P.A.	sand-silt-clay	sdslcl	1.99	69.73917	134.27619	B
603	2	2.98	1.8030	T.P.A.	silt	sl	3.21	69.73917	134.27619	B
603	2	3.10	1.9303	N.P.	silt	sl	0.27	69.73917	134.27619	B
603	2	3.56	2.0670	T.P.A.	silt-clay	slcl	2.27	69.73917	134.27619	B
603	2	4.20	1.4324	N.P.	silt+clay	slcl	-1.27	69.73917	134.27619	B
603	2	4.51	1.3644	N.P.	silt70%,clay	slcl	-0.99	69.73917	134.27619	B
603	2	4.54	1.9020	T.P.A.	clayey silt	clsl	3.02	69.73917	134.27619	B
603	2	5.32	2.0410	T.P.A.	clayey silt	clsl	3.52	69.73917	134.27619	B
603	2	5.52	1.4760	N.P.	clayey silt	clsl	-0.66	69.73917	134.27619	B
603	2	6.12	2.0940	T.P.A.	silt-clay	slcl	2.22	69.73917	134.27619	B
603	2	6.25	1.6004	N.P.	silt+clay	slcl	0.36	69.73917	134.27619	B
603	2	6.77	1.5410	T.P.A.	silty clay	slcl	2.65	69.73917	134.27619	B
603	2	6.99	1.4273	N.P.	silty clay	slcl	-0.32	69.73917	134.27619	B
603	2	7.57	1.7870	T.P.A.	silty clay	slcl	1.83	69.73917	134.27619	B
603	2	7.68	1.4590	N.P.	silt-clay	slcl	0.53	69.73917	134.27619	B
603	2	8.21	1.9520	T.P.A.	clayey silt	clsl	2.67	69.73917	134.27619	B
603	2	9.35	1.3952	N.P.	silt70%,clay	slcl	-0.27	69.73917	134.27619	B
603	2	9.67	1.5260	T.P.A.	silty clay	slcl	2.67	69.73917	134.27619	B
603	2	9.70	1.4483	N.P.	silt-clay	slcl	-0.34	69.73917	134.27619	B
603	2	9.73	1.4960	T.P.A.	silty clay	slcl	1.32	69.73917	134.27619	B
603	2	9.96	1.4272	N.P.	silt	sl	-1.37	69.73917	134.27619	B
603	2	10.73	1.4250	T.P.A.	silty clay	slcl	2.35	69.73917	134.27619	B
603	2	10.95	1.3950	N.P.	silty clay	slcl	-0.01	69.73917	134.27619	B
603	2	11.34	1.4960	T.P.A.	silty clay	slcl	2.82	69.73917	134.27619	B
603	2	11.46	1.4990	N.P.	silty clay	slcl	-0.92	69.73917	134.27619	B
603	2	12.44	1.2950	T.P.A.	silty clay	slcl	2.55	69.73917	134.27619	B

MEGATRANSECT 1990 603 BH 2

Site	Borehole	Depth m	Conductivity W/mK	Method	Lithology	Lith	Ambient	N69 44'21.0" Latitude N	W134 16'34.3" Longitude W	Uni
603	2	13.02	1.3499	N.P.	silty clay	slcl	0.60	69.73917	134.27619	B
603	2	13.05	1.3730	T.P.A.	silty clay	slcl	1.58	69.73917	134.27619	B
603	2	13.17	1.3962	N.P.	silty clay	slcl	0.52	69.73917	134.27619	B
603	2	13.69	1.3360	T.P.A.	silty clay	slcl	2.33	69.73917	134.27619	B
603	2	14.36	1.2154	N.P.	silty clay	slcl	-0.05	69.73917	134.27619	B
603	2	14.39	1.3730	T.P.A.	silty clay	slcl	0.93	69.73917	134.27619	B
603	2	14.52	1.3330	N.P.	clayey silt	clsl	-0.15	69.73917	134.27619	B
603	2	31.90	1.7232	N.P.	fine sand,loose	sd	0.16	69.73917	134.27619	C
603	2	32.00	1.5412	N.P.	fine sand,loose	sd	0.43	69.73917	134.27619	C
603	2	32.20	1.6124	N.P.	fine sand,loose	sd	-0.92	69.73917	134.27619	C
603	2	32.27	2.2510	T.P.A.	fine sand	sd	-0.28	69.73917	134.27619	C
603	2	33.93	1.7539	N.P.	fine sand	sd	0.70	69.73917	134.27619	C
603	2	34.25	1.7694	N.P.	fine sand	sd	0.36	69.73917	134.27619	C
603	2	34.40	1.5753	N.P.	fine sand	sd	0.41	69.73917	134.27619	C
603	2	34.60	1.6136	N.P.	fine sand	sd	-0.69	69.73917	134.27619	C
603	2	34.93	1.0631	N.P.	fine sand	sd	-3.96	69.73917	134.27619	C
603	2	35.00	2.2046	N.P.	fine sand	sd	-2.99	69.73917	134.27619	C
603	2	35.20	0.6919	N.P.	fine sand	sd	-2.96	69.73917	134.27619	C
603	2	35.37	1.6124	N.P.	silty clay	slcl	-3.65	69.73917	134.27619	D
603	2	35.47	1.5660	T.P.A.	silty clay	slcl	0.27	69.73917	134.27619	D
603	2	35.60	1.4147	N.P.	silty clay	slcl	-1.49	69.73917	134.27619	D
603	2	35.90	1.4992	N.P.	silty clay	slcl	-0.54	69.73917	134.27619	D
603	2	36.00	1.5146	N.P.	silty clay	slcl	-1.67	69.73917	134.27619	D
603	2	36.20	1.2741	N.P.	silty clay	slcl	0.19	69.73917	134.27619	D
603	2	36.24	1.3360	T.P.A.	silty clay	slcl	-0.66	69.73917	134.27619	D
603	2	36.40	1.3641	N.P.	silty clay	slcl	-1.21	69.73917	134.27619	D
603	2	36.57	1.4373	N.P.	silty clay	slcl	0.21	69.73917	134.27619	D

MEGATRANSECT 1990 603 BH 2

Site	Borehole	Depth m	Conductivity W/mK	Method	Lithology	Lith	Ambient	N69 44'21.0" Latitude N	W134 16'34.3" Longitude W	Uni
603	2	36.69	1.2852	N.P.	silty clay	slcl	0.31	69.73917	134.27619	D
603	2	36.90	1.3990	N.P.	silty clay	slcl	-0.52	69.73917	134.27619	D
603	2	37.02	1.6010	T.P.A.	silty clay	slcl	-0.09	69.73917	134.27619	D
603	2	37.10	1.8787	N.P.	silty clay	slcl	-2.93	69.73917	134.27619	D
603	2	37.30	1.3647	N.P.	silt,silty clay	slcl	-1.91	69.73917	134.27619	D
603	2	37.50	1.3996	N.P.	silt,silty clay	slcl	-2.09	69.73917	134.27619	D
603	2	37.70	1.7507	N.P.	silt,silty clay	slcl	-3.09	69.73917	134.27619	D
603	2	37.77	1.5480	T.P.A.	silty clay	slcl	0.18	69.73917	134.27619	D
603	2	37.95	1.0959	N.P.	silty clay	slcl	-2.79	69.73917	134.27619	D
603	2	38.50	1.5870	T.P.A.	silty clay	slcl	0.37	69.73917	134.27619	D
603	2	38.65	1.4523	N.P.	silty clay	slcl	-2.67	69.73917	134.27619	D
603	2	38.90	1.5032	N.P.	silty clay	slcl	-1.96	69.73917	134.27619	D
603	2	38.95	1.1373	N.P.	silty clay	slcl	-1.67	69.73917	134.27619	D
603	2	39.05	1.5704	N.P.	silty clay	slcl	-2.10	69.73917	134.27619	D
603	2	39.10	1.5297	N.P.	silty clay	slcl	-1.94	69.73917	134.27619	D
603	2	39.25	1.3414	N.P.	silty clay	slcl	-1.70	69.73917	134.27619	D
603	2	39.25	1.2926	N.P.	silty clay	slcl	-2.76	69.73917	134.27619	D
603	2	39.27	1.5090	T.P.A.	silty clay	slcl	0.99	69.73917	134.27619	D
603	2	39.44	0.9695	N.P.	silty clay	slcl	-2.03	69.73917	134.27619	D
603	2	39.45	1.5241	N.P.	silty clay	slcl	-2.19	69.73917	134.27619	D
603	2	39.60	1.0262	N.P.	silty clay	slcl	-1.20	69.73917	134.27619	D
603	2	39.90	0.9734	N.P.	silty clay	slcl	-1.29	69.73917	134.27619	D
603	2	40.00	1.3937	N.P.	silty clay	slcl	-1.96	69.73917	134.27619	D
603	2	40.04	1.6490	T.P.A.	silty clay	slcl	0.30	69.73917	134.27619	D
603	2	40.15	1.2969	N.P.	silty clay	slcl	-2.01	69.73917	134.27619	D
603	2	40.35	0.9924	N.P.	silty clay	slcl	-1.47	69.73917	134.27619	D
603	2	40.55	0.9999	N.P.	silty clay	slcl	-1.55	69.73917	134.27619	D

MEGATRANSECT 1990 603 BH 2

Site	Borehole	Depth m	Conductivity W/mK	Method	Lithology	Lith	Ambient	N69 44'21.0" Latitude N	W134 16'34.3" Longitude W	Uni
603	2	40.75	1.4206	N.P.	silty clay	slcl	-3.10	69.73917	134.27619	D
603	2	40.81	1.5980	T.P.A.	silty clay	slcl	1.47	69.73917	134.27619	D
603	2	41.05	1.2531	N.P.	silty clay	slcl	-0.73	69.73917	134.27619	D
603	2	41.20	1.4740	N.P.	silty clay	slcl	0.79	69.73917	134.27619	D
603	2	41.40	1.2846	N.P.	silty clay	slcl	0.65	69.73917	134.27619	D
603	2	41.60	1.2010	N.P.	silty clay	slcl	-1.65	69.73917	134.27619	D
603	2	41.64	1.0350	T.P.A.	silty clay	slcl	0.34	69.73917	134.27619	D
603	2	41.75	1.3731	N.P.	silty clay	slcl	-0.97	69.73917	134.27619	D
603	2	41.95	1.3619	N.P.	silty clay	slcl	0.43	69.73917	134.27619	D
603	2	42.15	1.4054	N.P.	silty clay	slcl	-0.62	69.73917	134.27619	D
603	2	42.32	0.9926	N.P.	silty clay	slcl	-1.79	69.73917	134.27619	D
603	2	42.34	2.8910	T.P.A.	silty clay	slcl	-0.06	69.73917	134.27619	D
603	2	42.60	1.3799	N.P.	silty clay	slcl	-2.16	69.73917	134.27619	D
603	2	42.90	1.2987	N.P.	silty clay	slcl	-1.75	69.73917	134.27619	D
603	2	43.00	1.6692	N.P.	silty clay	slcl	-1.95	69.73917	134.27619	D
603	2	43.12	2.3320	T.P.A.	silty clay	slcl	-0.29	69.73917	134.27619	D
603	2	43.13	2.2664	T.P.A.	silty clay	slcl	0.55	69.73917	134.27619	D
603	2	43.20	1.3453	N.P.	silty clay	slcl	-2.32	69.73917	134.27619	D
603	2	43.25	1.2858	N.P.	silty clay+sand lenses	slclsd	-2.30	69.73917	134.27619	D
603	2	43.45	1.5219	N.P.	silty clay+sand lenses	slclsd	-1.71	69.73917	134.27619	D
603	2	43.65	1.4139	N.P.	silty clay+sand lenses	slclsd	-1.69	69.73917	134.27619	D
603	2	43.85	2.6137	N.P.	silty clay+sand lenses	slclsd	-2.59	69.73917	134.27619	D
603	2	44.15	1.4695	N.P.	silt+clay	slcl	-2.26	69.73917	134.27619	D
603	2	44.30	1.6095	N.P.	fine sand	sd	-0.39	69.73917	134.27619	E
603	2	44.50	1.8405	N.P.	fine sand	sd	-0.42	69.73917	134.27619	E
603	2	44.67	1.9988	N.P.	sand to silt	sdsl	-1.54	69.73917	134.27619	E
603	2	44.72	2.7550	T.P.A.	sand-silt	sdsl	2.77	69.73917	134.27619	E

MEGATRANSECT 1990 603 BH 2

Site	Borehole	Depth m	Conductivity W/mK	Method	Lithology	Lith	Ambient	N69 44'21.0" Latitude N	W134 16'34.3" Longitude W	Uni
603	2	44.85	1.4263	N.P.	silty sand, clay	slsdcl	-3.07	69.73917	134.27619	E
603	2	44.96	1.7907	N.P.	silt?	sl	0.31	69.73917	134.27619	E
603	2	45.05	1.9685	N.P.	sandy silt	sdsl	-2.38	69.73917	134.27619	E
603	2	45.05	1.3746	N.P.	silt?	sl	-1.12	69.73917	134.27619	E
603	2	45.25	2.0052	N.P.	sandy silt	sdsl	-2.25	69.73917	134.27619	E
603	2	45.45	1.9396	N.P.	sandy silt	sdsl	-2.49	69.73917	134.27619	E
603	2	45.58	1.5350	T.P.A.	sand-silt	sdsl	1.33	69.73917	134.27619	E
603	2	45.70	1.6043	N.P.	sandy silt	sdsl	-2.05	69.73917	134.27619	E
603	2	45.95	1.3975	N.P.	sandy silt	sdsl	-1.92	69.73917	134.27619	E
603	2	46.00	1.6165	N.P.	sandy silt	sdsl	-1.33	69.73917	134.27619	E
603	2	46.20	1.7903	N.P.	clay+sand	clsd	-1.92	69.73917	134.27619	E
603	2	46.57	2.5150	T.P.A.	sand-silt	sdsl	-1.37	69.73917	134.27619	E
603	2	47.45	1.9226	N.P.	fine sand	sd	-1.33	69.73917	134.27619	E
603	2	47.63	1.9209	N.P.	fine sand	sd	-0.42	69.73917	134.27619	E
603	2	47.79	1.5769	N.P.	fine sand	sd	-0.95	69.73917	134.27619	E
603	2	47.94	1.9362	N.P.	fine sand	sd	-2.68	69.73917	134.27619	E
603	2	47.97	2.0760	T.P.A.	f. sand	sd	-0.29	69.73917	134.27619	E
603	2	50.25	1.4427	N.P.	sand?	sd	-2.97	69.73917	134.27619	E
603	2	50.40	1.5464	N.P.	sand?	sd	-2.97	69.73917	134.27619	E
603	2	50.60	1.9092	N.P.	sand?	sd	-2.32	69.73917	134.27619	E
603	2	50.87	2.5300	T.P.A.	f. sand	sd	-1.18	69.73917	134.27619	E
603	2	50.90	1.9621	N.P.	fine sand	sd	-1.96	69.73917	134.27619	E

MEGATRANSECT 1990 603 - B.H. 3

Site	Borehole	Depth m	Conductivity W/mK	Method	Lithology	Lith	Ambient	Latitude	Longitude W	Unit
603	3	32.07	1.2609	N.P.	f.-m. sand	sd	1.87	N69 46'33.0"	W134 13'01.7"	C
603	3	32.14	1.2075	N.P.	f.-m. sand	sd	1.74	N69 46'33.0"	W134 13'01.7"	C
603	3	32.21	1.2112	N.P.	f.-m. sand	sd	1.52	N69 46'33.0"	W134 13'01.7"	C
603	3	32.28	1.4412	N.P.	f.-m. sand	sd	1.22	N69 46'33.0"	W134 13'01.7"	C
603	3	35.50	1.5390	T.P.A.	silt	sl	1.94	N69 46'33.0"	W134 13'01.7"	C
603	3	35.53	1.5276	N.P.	silt	sl	1.35	N69 46'33.0"	W134 13'01.7"	D
603	3	35.60	1.3205	N.P.	silty clay	slcl	1.32	N69 46'33.0"	W134 13'01.7"	D
603	3	35.67	1.4454	N.P.	silty clay	slcl	0.56	N69 46'33.0"	W134 13'01.7"	D
603	3	35.70	1.8530	T.P.A.	silty clay	slcl	1.15	N69 46'33.0"	W134 13'01.7"	C
603	3	35.73	1.5725	N.P.	silty clay	slcl	2.28	N69 46'33.0"	W134 13'01.7"	D
603	3	35.84	1.3378	N.P.	silt	sl	2.32	N69 46'33.0"	W134 13'01.7"	D
603	3	35.95	1.3473	N.P.	silty clay	slcl	2.38	N69 46'33.0"	W134 13'01.7"	D
603	3	36.04	1.4525	N.P.	silt	sl	2.16	N69 46'33.0"	W134 13'01.7"	D
603	3	36.14	1.4644	N.P.	silty clay	slcl	1.67	N69 46'33.0"	W134 13'01.7"	D
603	3	36.17	1.4592	N.P.	silt-silty clay	slcl	-2.62	N69 46'33.0"	W134 13'01.7"	D
603	3	36.17	1.6870	T.P.A.	silt-silty clay	slcl	0.45	N69 46'33.0"	W134 13'01.7"	C
603	3	36.44	1.5120	N.P.	silty clay	slcl	-1.26	N69 46'33.0"	W134 13'01.7"	D
603	3	36.96	1.6130	T.P.A.	silty clay	slcl	1.16	N69 46'33.0"	W134 13'01.7"	D
603	3	37.04	1.4702	N.P.	clay+silt	clsl	-1.05	N69 46'33.0"	W134 13'01.7"	D
603	3	37.23	1.6905	N.P.	clay+silt	clsl	0.37	N69 46'33.0"	W134 13'01.7"	D
603	3	37.42	1.6260	N.P.	clay+silt	clsl	-0.36	N69 46'33.0"	W134 13'01.7"	D
603	3	37.50	1.2750	T.P.A.	silty clay	slcl	1.03	N69 46'33.0"	W134 13'01.7"	D
603	3	37.53	1.2853	N.P.	silty clay	slcl	2.29	N69 46'33.0"	W134 13'01.7"	D
603	3	37.69	1.0662	N.P.	silty clay	slcl	2.20	N69 46'33.0"	W134 13'01.7"	D
603	3	37.90	1.6590	T.P.A.	silty clay	slcl	1.10	N69 46'33.0"	W134 13'01.7"	D
603	3	37.90	1.3463	N.P.	silty clay	slcl	1.95	N69 46'33.0"	W134 13'01.7"	D
603	3	38.64	1.5710	T.P.A.	silty clay	slcl	1.00	N69 46'33.0"	W134 13'01.7"	D
603	3	38.94	1.7370	T.P.A.	silty clay	slcl	0.54	N69 46'33.0"	W134 13'01.7"	D

MEGATRANSECT 1990 603 - B.H. 3

Site	Borehole	Depth m	Conductivity W/mK	Method	Lithology	Lith	Ambient	Latitude	Longitude W	Unit
603	3	15.50	1.0133	N.P.	sand w/clay-silt	sdsl	1.56	N69 46'33.0"	W134 13'01.7"	B
603	3	15.70	0.8020	T.P.A.	sand w/clay-silt	sdsl	0.52	N69 46'33.0"	W134 13'01.7"	B
603	3	16.13	1.1160	T.P.A.	sand w/clay-silt	sdsl	0.46	N69 46'33.0"	W134 13'01.7"	B
603	3	18.30	3.6243	N.P.	sandy diam.	sddm	1.11	N69 46'33.0"	W134 13'01.7"	C
603	3	18.57	2.8537	N.P.	silt diam.	sldm	1.07	N69 46'33.0"	W134 13'01.7"	C
603	3	18.90	2.2310	T.P.A.	silt diam.	sldm	0.60	N69 46'33.0"	W134 13'01.7"	C
603	3	19.15	2.1260	T.P.A.	silt diam.	sldm	1.06	N69 46'33.0"	W134 13'01.7"	C
603	3	19.15	2.8350	T.P.A.	silt diam.	sldm	0.59	N69 46'33.0"	W134 13'01.7"	C
603	3	19.15	2.7022	N.P.	silt diam.	sldm	1.90	N69 46'33.0"	W134 13'01.7"	C
603	3	19.48	2.3340	T.P.A.	clayey silt	clsl	0.61	N69 46'33.0"	W134 13'01.7"	C
603	3	19.81	2.8031	N.P.	silt diam.	sldm	2.01	N69 46'33.0"	W134 13'01.7"	C
603	3	20.12	2.1040	T.P.A.	clayey silt	clsl	-0.23	N69 46'33.0"	W134 13'01.7"	C
603	3	20.44	2.4380	T.P.A.	clayey silt	clsl	1.13	N69 46'33.0"	W134 13'01.7"	C
603	3	20.44	2.6620	N.P.	clayey silt	clsl	1.59	N69 46'33.0"	W134 13'01.7"	C
603	3	20.82	2.5080	T.P.A.	clayey silt	clsl	0.56	N69 46'33.0"	W134 13'01.7"	C
603	3	21.34	3.4726	N.P.	v.fine sand w/cl-slt	sdsl	1.77	N69 46'33.0"	W134 13'01.7"	C
603	3	21.34	3.5070	T.P.A.	v.fine sand w/cl-slt	sdsl	0.74	N69 46'33.0"	W134 13'01.7"	C
603	3	21.69	2.4450	T.P.A.	v.fine sand w/cl-slt	sdsl	0.77	N69 46'33.0"	W134 13'01.7"	C
603	3	22.04	3.6752	N.P.	v.fine sand w/cl-slt	sdsl	1.14	N69 46'33.0"	W134 13'01.7"	C
603	3	22.04	3.1540	T.P.A.	v.fine sand w/cl-slt	sdsl	0.26	N69 46'33.0"	W134 13'01.7"	C
603	3	22.39	2.7040	T.P.A.	v.fine sand w/cl-stl	sdsl	1.20	N69 46'33.0"	W134 13'01.7"	C
603	3	28.20	2.0800	T.P.A.	fine sand	sd	0.65	N69 46'33.0"	W134 13'01.7"	C
603	3	28.44	2.4524	N.P.	fine sand	sd	-1.18	N69 46'33.0"	W134 13'01.7"	C
603	3	29.20	2.3932	N.P.	fine sand	sd	-1.78	N69 46'33.0"	W134 13'01.7"	C
603	3	30.50	1.6640	T.P.A.	f.-m. sand	sd	1.36	N69 46'33.0"	W134 13'01.7"	C
603	3	30.53	1.5549	N.P.	f.-m. sand	sd	-0.77	N69 46'33.0"	W134 13'01.7"	C
603	3	31.95	2.1590	T.P.A.	fine sand	sd	0.71	N69 46'33.0"	W134 13'01.7"	C
603	3	31.98	1.7025	N.P.	fine sand	sd	1.74	N69 46'33.0"	W134 13'01.7"	C

MEGATRANSECT 1990 603 - B.H. 3

Site	Borehole	Depth m	Conductivity W/mK	Method	Lithology	Lith	Ambient	Latitude	Longitude W	Unit
603	3	0.24	2.1159	N.P.	fine sand	sd	0.66	N69 46'33.0"	W134 13'01.7"	B
603	3	0.76	1.9250	T.P.A.	fine sand	sd	-0.49	N69 46'33.0"	W134 13'01.7"	B
603	3	0.79	2.9075	N.P.	fine sand-silty clay	sdcl	1.90	N69 46'33.0"	W134 13'01.7"	B
603	3	1.37	2.1250	T.P.A.	clayey silt	clsl	0.29	N69 46'33.0"	W134 13'01.7"	B
603	3	1.71	1.7012	N.P.	clayey silt	clsl	0.12	N69 46'33.0"	W134 13'01.7"	B
603	3	1.88	1.8860	T.P.A.	clayey silt	clsl	-0.03	N69 46'33.0"	W134 13'01.7"	B
603	3	3.05	1.7949	N.P.	sand +silt	sdsl	0.57	N69 46'33.0"	W134 13'01.7"	B
603	3	3.65	1.9450	T.P.A.	sand +silt	sdsl	0.72	N69 46'33.0"	W134 13'01.7"	B
603	3	3.80	6.7415	N.P.	fine sand	sd	0.51	N69 46'33.0"	W134 13'01.7"	B
603	3	4.40	1.9070	T.P.A.	silty clay	slcl	0.48	N69 46'33.0"	W134 13'01.7"	B
603	3	4.53	2.6289	N.P.	silty clay	slcl	3.14	N69 46'33.0"	W134 13'01.7"	B
603	3	5.00	1.7470	T.P.A.	silty clay	slcl	3.09	N69 46'33.0"	W134 13'01.7"	B
603	3	5.40	2.4350	N.P.	silt+clay	slcl	3.35	N69 46'33.0"	W134 13'01.7"	B
603	3	5.80	1.7170	T.P.A.	silt	sl	3.12	N69 46'33.0"	W134 13'01.7"	B
603	3	5.98	2.1662	N.P.	silt	sl	-0.59	N69 46'33.0"	W134 13'01.7"	B
603	3	6.40	1.6770	T.P.A.	silt	sl	3.48	N69 46'33.0"	W134 13'01.7"	B
603	3	8.25	3.3667	N.P.	silty clay	slcl	3.59	N69 46'33.0"	W134 13'01.7"	B
603	3	8.70	1.6560	T.P.A.	silty clay	slcl	4.15	N69 46'33.0"	W134 13'01.7"	B
603	3	9.15	1.5440	T.P.A.	silty clay	slcl	4.18	N69 46'33.0"	W134 13'01.7"	B
603	3	9.40	2.5261	N.P.	silt+silty clay	slcl	-0.91	N69 46'33.0"	W134 13'01.7"	B
603	3	9.70	3.4246	N.P.	silt+silty clay	slcl	-0.12	N69 46'33.0"	W134 13'01.7"	B
603	3	10.17	1.8262	N.P.	clayey silt+silt	clsl	1.95	N69 46'33.0"	W134 13'01.7"	B
603	3	11.21	2.5038	N.P.	silt+clayey silt	slcl	3.80	N69 46'33.0"	W134 13'01.7"	B
603	3	11.71	2.7161	N.P.	silty clay	slcl	3.92	N69 46'33.0"	W134 13'01.7"	B
603	3	12.47	1.5490	N.P.	clayey silt	clsl	1.19	N69 46'33.0"	W134 13'01.7"	B
603	3	13.17	1.9032	N.P.	fine sand+clay sand	sdcl	0.99	N69 46'33.0"	W134 13'01.7"	B
603	3	14.40	2.5112	N.P.	sandy silt	sdsl	1.54	N69 46'33.0"	W134 13'01.7"	B
603	3	14.66	1.4930	T.P.A.	sandy silt	sdsl	-0.02	N69 46'33.0"	W134 13'01.7"	B

MEGATRANSECT 1990 603 - B.H. 3

Site	Borehole	Depth m	Conductivity W/mK	Method	Lithology	Lith	Ambient	Latitude	Longitude W	Unit
603	3	39.10	1.4821	N.P.	silty clay	slcl	1.68	N69 46'33.0"	W134 13'01.7"	D
603	3	39.25	1.3711	N.P.	silty clay	slcl	-1.64	N69 46'33.0"	W134 13'01.7"	D
603	3	39.25	1.2851	N.P.	silty clay	slcl	-1.99	N69 46'33.0"	W134 13'01.7"	D
603	3	39.25	2.0060	T.P.A.	silty clay	slcl	1.72	N69 46'33.0"	W134 13'01.7"	D
603	3	39.27	1.5043	N.P.	silty clay	slcl	1.32	N69 46'33.0"	W134 13'01.7"	D
603	3	39.41	1.3991	N.P.	silty clay	slcl	-1.49	N69 46'33.0"	W134 13'01.7"	D
603	3	39.60	1.3714	N.P.	silty clay	slcl	-1.52	N69 46'33.0"	W134 13'01.7"	D
603	3	39.64	1.3624	N.P.	silty clay	slcl	-3.55	N69 46'33.0"	W134 13'01.7"	D
603	3	39.75	1.5440	T.P.A.	silty clay	slcl	0.04	N69 46'33.0"	W134 13'01.7"	D
603	3	39.75	1.2633	N.P.	silty clay	slcl	-1.56	N69 46'33.0"	W134 13'01.7"	D
603	3	39.90	1.6099	N.P.	silty clay	slcl	-1.62	N69 46'33.0"	W134 13'01.7"	D
603	3	39.93	1.1919	N.P.	silty clay	slcl	-1.31	N69 46'33.0"	W134 13'01.7"	D
603	3	40.03	1.3750	T.P.A.	silty clay	slcl	3.85	N69 46'33.0"	W134 13'01.7"	D
603	3	40.06	1.2997	N.P.	clayey silt	clsl	1.99	N69 46'33.0"	W134 13'01.7"	D
603	3	40.25	1.2999	N.P.	silty clay	slcl	1.63	N69 46'33.0"	W134 13'01.7"	D
603	3	40.40	1.2957	N.P.	silty clay	slcl	1.13	N69 46'33.0"	W134 13'01.7"	D
603	3	40.40	1.4910	T.P.A.	silty clay	slcl	0.89	N69 46'33.0"	W134 13'01.7"	D
603	3	40.64	1.5979	N.P.	silty clay	slcl	1.09	N69 46'33.0"	W134 13'01.7"	D
603	3	40.67	1.5095	N.P.	silt+clay	slcl	-3.42	N69 46'33.0"	W134 13'01.7"	D
603	3	40.90	1.3216	N.P.	clayey silt	clsl	-1.27	N69 46'33.0"	W134 13'01.7"	D
603	3	41.15	1.3832	N.P.	silty clay	slcl	-1.25	N69 46'33.0"	W134 13'01.7"	D
603	3	41.33	1.3866	N.P.	silty clay	slcl	-1.35	N69 46'33.0"	W134 13'01.7"	D
603	3	41.77	1.4681	N.P.	silt+silty clay	slcl	2.54	N69 46'33.0"	W134 13'01.7"	D
603	3	41.90	1.3655	N.P.	silt+silty clay	slcl	2.55	N69 46'33.0"	W134 13'01.7"	D
603	3	42.04	1.3154	N.P.	silty clay	slcl	1.84	N69 46'33.0"	W134 13'01.7"	D
603	3	42.18	1.4905	N.P.	silt	sl	2.00	N69 46'33.0"	W134 13'01.7"	D
603	3	42.21	1.6569	N.P.	clay	cl	-1.35	N69 46'33.0"	W134 13'01.7"	D
603	3	42.41	1.5064	N.P.	clay	cl	-1.58	N69 46'33.0"	W134 13'01.7"	D

MEGATRANSECT 1990 603 - B.H. 3

Site	Borehole	Depth m	Conductivity W/mK	Method	Lithology	Lith	Ambient	Latitude	Longitude W	Unit
603	3	42.62	1.5084	N.P.	clay	cl	-1.15	N69 46'33.0"	W134 13'01.7"	D
603	3	42.85	1.2609	N.P.	silty clay	slcl	-1.30	N69 46'33.0"	W134 13'01.7"	D
603	3	45.71	1.4429	N.P.	silty clay	slcl	-2.58	N69 46'33.0"	W134 13'01.7"	D
603	3	45.72	1.9316	N.P.	silty clay	slcl	-1.28	N69 46'33.0"	W134 13'01.7"	D

MEGATRANSECT 1990 603 B.H. - 4

Site	Borehole	Depth m	Conductivity W/mK	Method	Lithology	Lith	Ambient	N69 48'27.5" Latitude N	W134 09'57.3" Longitude W	Uni
603	4	35.03	1.3930	T.P.A.	silt	sl	0.10	69.80764	134.16592	D
603	4	35.09	1.2336	N.P.	silt	sl	0.14	69.80764	134.16592	D
603	4	35.20	1.3294	N.P.	silt	sl	0.28	69.80764	134.16592	D
603	4	35.49	1.3499	N.P.	silt	sl	0.07	69.80764	134.16592	D
603	4	35.53	1.5870	T.P.A.	silty clay	slcl	-1.55	69.80764	134.16592	D
603	4	35.60	1.5240	N.P.	silty clay	slcl	-0.87	69.80764	134.16592	D
603	4	35.80	1.3345	N.P.	silty clay	slcl	0.79	69.80764	134.16592	D
603	4	35.98	1.6340	T.P.A.	silt	sl	-0.96	69.80764	134.16592	D
603	4	36.05	1.2902	N.P.	silt	sl	2.09	69.80764	134.16592	D
603	4	36.20	1.3945	N.P.	silt	sl	2.20	69.80764	134.16592	D
603	4	36.35	1.2991	N.P.	silt	sl	1.63	69.80764	134.16592	D
603	4	36.50	0.7813	N.P.	silt	sl	0.73	69.80764	134.16592	D
603	4	38.13	1.4710	T.P.A.	silt	sl	-1.86	69.80764	134.16592	D
603	4	38.17	1.3410	N.P.	silt-clay	slcl	-0.45	69.80764	134.16592	D
603	4	38.30	1.2360	N.P.	silt-clay	slcl	1.49	69.80764	134.16592	D
603	4	38.44	1.1849	N.P.	silt-clay	slcl	0.96	69.80764	134.16592	D
603	4	38.57	1.2985	N.P.	silt-clay	slcl	0.11	69.80764	134.16592	D
603	4	38.71	1.5380	T.P.A.	silty clay	slcl	-1.44	69.80764	134.16592	D
603	4	38.75	1.1790	N.P.	silty clay	slcl	0.35	69.80764	134.16592	D
603	4	38.95	1.1727	N.P.	silty clay	slcl	-0.33	69.80764	134.16592	D
603	4	39.09	1.5730	T.P.A.	silty clay	slcl	-1.45	69.80764	134.16592	D
603	4	39.15	1.3079	N.P.	silty clay	slcl	2.19	69.80764	134.16592	D
603	4	39.30	1.2545	N.P.	silty clay	slcl	1.87	69.80764	134.16592	D
603	4	39.45	1.2834	N.P.	silty clay	slcl	1.47	69.80764	134.16592	D
603	4	39.60	0.7449	N.P.	silty clay	slcl	0.79	69.80764	134.16592	D
603	4	39.65	1.6160	T.P.A.	silty clay	slcl	-0.57	69.80764	134.16592	D
603	4	39.70	1.3178	N.P.	silty clay	slcl	1.99	69.80764	134.16592	D

MEGATRANSECT 1990 603 B.H. - 4

Site	Borehole	Depth m	Conductivity W/mK	Method	Lithology	Lith	Ambient	N69 48'27.5" Latitude N	W134 09'57.3" Longitude W	Uni
603	4	39.90	1.4263	N.P.	silty clay	slcl	1.91	69.80764	134.16592	D
603	4	40.13	1.1710	N.P.	silty clay	slcl	2.16	69.80764	134.16592	D
603	4	40.31	1.0979	N.P.	silty clay	slcl	2.53	69.80764	134.16592	D
603	4	40.47	0.9919	N.P.	silty clay	slcl	1.83	69.80764	134.16592	D
603	4	40.60	1.3325	N.P.	silty clay	slcl	0.42	69.80764	134.16592	D
603	4	40.64	1.6760	T.P.A.	silty clay	slcl	-1.42	69.80764	134.16592	D
603	4	40.65	1.7300	T.P.A.	silty clay	slcl	-0.65	69.80764	134.16592	D
603	4	40.80	1.2758	N.P.	silty clay	slcl	2.17	69.80764	134.16592	D
603	4	41.00	1.2372	N.P.	silty clay	slcl	1.62	69.80764	134.16592	D
603	4	41.18	1.5700	T.P.A.	silty clay	slcl	-0.77	69.80764	134.16592	D
603	4	41.20	1.2905	N.P.	silty clay	slcl	2.99	69.80764	134.16592	D
603	4	41.35	1.4698	N.P.	silty clay	slcl	2.98	69.80764	134.16592	D
603	4	41.50	1.3030	N.P.	silty clay	slcl	2.51	69.80764	134.16592	D
603	4	41.65	1.3544	N.P.	silty clay	slcl	1.92	69.80764	134.16592	D
603	4	41.75	1.4110	N.P.	silty clay	slcl	0.97	69.80764	134.16592	D
603	4	41.83	1.5760	T.P.A.	silty clay	slcl	-1.94	69.80764	134.16592	D
603	4	41.88	1.4047	N.P.	silty clay	slcl	-0.53	69.80764	134.16592	D
603	4	42.08	1.2596	N.P.	silty clay	slcl	1.70	69.80764	134.16592	D
603	4	42.27	1.2333	N.P.	silty clay	slcl	1.52	69.80764	134.16592	D
603	4	42.50	1.2920	N.P.	silty clay	slcl	0.60	69.80764	134.16592	D
603	4	42.70	1.4890	T.P.A.	silty clay	slcl	-0.98	69.80764	134.16592	D
603	4	42.80	1.0999	N.P.	silty clay	slcl	2.19	69.80764	134.16592	D
603	4	42.92	1.3915	N.P.	silty clay	slcl	2.24	69.80764	134.16592	D
603	4	43.10	1.3412	N.P.	silty clay	slcl	1.47	69.80764	134.16592	D
603	4	43.35	1.2490	N.P.	silty clay	slcl	-0.29	69.80764	134.16592	D
603	4	43.55	1.2765	N.P.	silty clay	slcl	-0.54	69.80764	134.16592	D
603	4	43.75	1.3309	N.P.	silty clay	slcl	-1.11	69.80764	134.16592	D

MEGATRANSECT 1990 603 B.H. - 4

Site	Borehole	Depth m	Conductivity W/mK	Method	Lithology	Lith	Ambient	N69 48'27.5" Latitude N	W134 09'57.3" Longitude W	Uni
603	4	43.77	1.5940	T.P.A.	silty clay	slcl	-0.64	69.80764	134.16592	D
603	4	43.90	1.3256	N.P.	silty clay	slcl	0.94	69.80764	134.16592	D
603	4	44.10	1.5121	N.P.	silty clay	slcl	-0.79	69.80764	134.16592	D
603	4	44.17	1.4080	T.P.A.	silty clay	slcl	-1.36	69.80764	134.16592	D
603	4	44.30	1.2697	N.P.	silty clay	slcl	2.36	69.80764	134.16592	D
603	4	44.50	1.2603	N.P.	silty clay	slcl	2.19	69.80764	134.16592	D
603	4	44.87	1.7440	T.P.A.	silty clay	slcl	-0.71	69.80764	134.16592	E
603	4	44.90	1.2354	N.P.	silty clay	slcl	0.74	69.80764	134.16592	E
603	4	45.00	1.4796	N.P.	silty clay	slcl	2.90	69.80764	134.16592	E
603	4	45.15	1.6979	N.P.	silty clay	slcl	2.59	69.80764	134.16592	E
603	4	45.30	1.5782	N.P.	silty clay	slcl	2.10	69.80764	134.16592	E
603	4	45.45	1.6057	N.P.	silty clay	slcl	1.64	69.80764	134.16592	E
603	4	45.60	1.1595	N.P.	clayey silt	clsl	1.27	69.80764	134.16592	E
603	4	45.62	1.4790	T.P.A.	clayey silt	clsl	-1.02	69.80764	134.16592	E
603	4	46.03	1.6253	N.P.	silty clay	slcl	-0.51	69.80764	134.16592	E
603	4	46.17	1.5696	N.P.	silty clay	slcl	1.61	69.80764	134.16592	E
603	4	46.30	1.5046	N.P.	silty clay	slcl	1.30	69.80764	134.16592	E
603	4	46.43	1.4511	N.P.	sandy silt	sdsl	0.78	69.80764	134.16592	E
603	4	46.54	1.4440	T.P.A.	sandy clay	sdcl	-1.29	69.80764	134.16592	E
603	4	47.92	1.5192	N.P.	silty clay	slcl	0.99	69.80764	134.16592	E
603	4	48.07	1.9670	T.P.A.	silty sand	slsd	-0.20	69.80764	134.16592	E
603	4	48.10	1.3542	N.P.	silty clay	slcl	1.67	69.80764	134.16592	E
603	4	48.25	1.2950	N.P.	silty clay	slcl	1.93	69.80764	134.16592	E
603	4	48.40	1.3376	N.P.	silty clay	slcl	1.31	69.80764	134.16592	E
603	4	48.54	0.9992	N.P.	silty clay	slcl	-0.25	69.80764	134.16592	E
603	4	49.03	1.9630	T.P.A.	silty clay	slcl	-0.78	69.80764	134.16592	E
603	4	49.05	1.6695	N.P.	silt	sl	2.66	69.80764	134.16592	E

MEGATRANSECT 1990 603 B.H. - 4

Site	Borehole	Depth m	Conductivity W/mK	Method	Lithology	Lith	Ambient	N69 48'27.5" Latitude N	W134 09'57.3" Longitude W	Uni
603	4	49.25	1.6600	N.P.	silty clay	slcl	2.11	69.80764	134.16592	E
603	4	49.45	1.3725	N.P.	silty clay	slcl	1.37	69.80764	134.16592	E
603	4	49.65	1.3717	N.P.	silty clay	slcl	0.66	69.80764	134.16592	E
603	4	49.96	1.3310	N.P.	silty clay	slcl	2.39	69.80764	134.16592	E
603	4	50.00	1.2113	N.P.	silty clay	slcl	1.95	69.80764	134.16592	E
603	4	50.15	1.2947	N.P.	silty clay	slcl	1.41	69.80764	134.16592	E
603	4	50.26	1.7140	T.P.A.	silty clay	slcl	-0.59	69.80764	134.16592	E
603	4	50.43	1.6660	T.P.A.	silty clay	slcl	-0.85	69.80764	134.16592	E
603	4	50.53	1.2930	N.P.	silty clay	slcl	2.35	69.80764	134.16592	E
603	4	50.75	1.2670	N.P.	sandy silt	sdsl	1.20	69.80764	134.16592	E
603	4	50.89	1.7400	T.P.A.	silty sand	slsd	0.50	69.80764	134.16592	E
603	4	50.92	1.1422	N.P.	silty clay	slcl	0.39	69.80764	134.16592	E
603	4	51.20	1.1759	N.P.	silty clay	slcl	-0.03	69.80764	134.16592	E
603	4	51.46	1.1340	N.P.	silty clay	slcl	5.23	69.80764	134.16592	E
603	4	51.69	1.1613	N.P.	silty clay	slcl	-0.23	69.80764	134.16592	E
603	4	51.78	1.3250	T.P.A.	silty clay	slcl	-0.39	69.80764	134.16592	E
603	4	51.97	1.6820	T.P.A.	silty clay	slcl	-0.44	69.80764	134.16592	E
603	4	52.04	1.2425	N.P.	silty clay	slcl	0.95	69.80764	134.16592	E
603	4	52.17	1.3509	N.P.	silty clay	slcl	0.66	69.80764	134.16592	E
603	4	52.29	1.2992	N.P.	silty clay	slcl	0.42	69.80764	134.16592	E
603	4	52.41	1.0409	N.P.	silty clay	slcl	0.32	69.80764	134.16592	E
603	4	52.50	1.5180	T.P.A.	silty clay	slcl	-0.06	69.80764	134.16592	E
603	4	52.55	1.2964	N.P.	silty clay	slcl	1.65	69.80764	134.16592	E
603	4	52.70	1.4469	N.P.	sandy clay	sdcl	1.02	69.80764	134.16592	E
603	4	52.85	1.4446	N.P.	sandy silt	sdsl	1.33	69.80764	134.16592	E
603	4	53.00	1.2530	N.P.	silty clay	slcl	0.65	69.80764	134.16592	E
603	4	53.08	1.4760	T.P.A.	silty clay	slcl	0.32	69.80764	134.16592	E

MEGATRANSECT 1990 603 B.H. - 4

Site	Borehole	Depth m	Conductivity W/mK	Method	Lithology	Lith	Ambient	N69 48'27.5" Latitude N	W134 09'57.3" Longitude W	Uni
603	4	53.10	1.5291	N.P.	silty clay	slcl	-0.12	69.80764	134.16592	E
603	4	53.41	1.5730	T.P.A.	silty clay	slcl	-0.11	69.80764	134.16592	E
603	4	53.45	0.9145	N.P.	silty clay	slcl	-1.61	69.80764	134.16592	E
603	4	53.65	1.2217	N.P.	clayey silt	clsl	0.63	69.80764	134.16592	E
603	4	53.85	1.7375	N.P.	clayey silt	clsl	0.34	69.80764	134.16592	E
603	4	54.05	1.5160	N.P.	clayey silt	clsl	-0.72	69.80764	134.16592	E
603	4	54.16	1.7920	T.P.A.	silt	sl	0.18	69.80764	134.16592	E
603	4	54.20	1.3705	N.P.	silty clay	slcl	2.62	69.80764	134.16592	E
603	4	54.30	1.6630	N.P.	silty clay	slcl	2.46	69.80764	134.16592	E
603	4	54.40	2.0359	N.P.	sand	sd	2.29	69.80764	134.16592	E
603	4	54.50	2.0511	N.P.	sand	sd	2.24	69.80764	134.16592	E
603	4	54.60	1.5592	N.P.	mud	m	1.94	69.80764	134.16592	E
603	4	54.70	1.4394	N.P.	mud	m	1.69	69.80764	134.16592	E
603	4	54.80	1.0698	N.P.	mud	m	1.07	69.80764	134.16592	E
603	4	54.89	0.9080	T.P.A.	mud	m	-1.08	69.80764	134.16592	E
603	4	54.94	0.6973	N.P.	mud-lignite	ml	1.29	69.80764	134.16592	E
603	4	55.14	0.5591	N.P.	mud-lignite	ml	2.11	69.80764	134.16592	E
603	4	55.57	1.7633	N.P.	sand	sd	0.29	69.80764	134.16592	E
603	4	56.35	1.9989	N.P.	f. sand	sd	3.40	69.80764	134.16592	E
603	4	56.37	1.4750	T.P.A.	f. sand	sd	-1.96	69.80764	134.16592	E
603	4	56.50	1.8408	N.P.	f. sand	sd	2.77	69.80764	134.16592	E
603	4	56.65	1.9957	N.P.	f. sand	sd	2.18	69.80764	134.16592	E
603	4	90.88	1.2592	N.P.	f. sand	sd	1.96	69.80764	134.16592	E

MEGATRANSECT 1990 603 B.H. - 5

Site	Borehole	Depth m	Conductivity W/mK	Method	Lithology	Lith	Ambient	N69 52'34.4" Latitude N	W134 03'19.2" Longitude W	Unit
603	5	9.95	2.3840	T.P.A.	f. sand	sd	-2.66	69.87622	134.05533	C
603	5	9.95	2.2679	N.P.	f. sand	sd	-1.17	69.87622	134.05533	C
603	5	10.14	2.5616	N.P.	f. sand	sd	-1.39	69.87622	134.05533	C
603	5	10.27	2.4609	N.P.	f. sand	sd	-1.14	69.87622	134.05533	C
603	5	10.97	2.9815	N.P.	f. sand	sd	-1.25	69.87622	134.05533	C
603	5	11.93	2.2446	N.P.	silty sand	slsd	-1.76	69.87622	134.05533	C
603	5	12.01	1.9942	N.P.	silty sand	slsd	-1.61	69.87622	134.05533	C
603	5	12.19	2.5165	N.P.	silty sand	slsd	-1.35	69.87622	134.05533	C
603	5	12.33	2.7470	N.P.	silty sand	slsd	-1.32	69.87622	134.05533	C
603	5	12.47	2.9010	T.P.A.	silty sand	slsd	-1.17	69.87622	134.05533	C
603	5	12.47	2.7261	N.P.	silty sand	slsd	-1.42	69.87622	134.05533	C
603	5	13.33	2.4061	N.P.	silty sand	slsd	-0.26	69.87622	134.05533	C
603	5	13.46	2.2996	N.P.	m. sand	sd	0.03	69.87622	134.05533	C
603	5	13.64	2.0524	N.P.	m. sand	sd	0.04	69.87622	134.05533	C
603	5	13.79	1.9704	N.P.	silty sand	slsd	-0.58	69.87622	134.05533	C
603	5	13.90	2.3125	N.P.	silty sand	slsd	-1.26	69.87622	134.05533	C
603	5	14.03	3.0700	T.P.A.	silty sand	slsd	-1.82	69.87622	134.05533	C
603	5	15.50	2.3480	T.P.A.	f. sand	sd	-2.15	69.87622	134.05533	C
603	5	15.50	3.3360	N.P.	f. sand	sd	-2.25	69.87622	134.05533	C
603	5	15.57	3.5005	N.P.	silty sand	slsd	-1.40	69.87622	134.05533	C
603	5	15.71	1.7257	N.P.	silty sand	slsd	-0.99	69.87622	134.05533	C
603	5	15.98	1.5317	N.P.	silty sand	slsd	-1.03	69.87622	134.05533	C
603	5	16.24	2.1970	T.P.A.	silty sand	slsd	-3.48	69.87622	134.05533	C
603	5	16.28	2.4282	N.P.	silty sand	slsd	-1.68	69.87622	134.05533	C
603	5	16.33	2.7222	N.P.	f. sand	sd	-1.95	69.87622	134.05533	C
603	5	16.54	2.7175	N.P.	silty sand	slsd	-1.64	69.87622	134.05533	C
603	5	16.70	2.5055	N.P.	silty sand	slsd	-1.69	69.87622	134.05533	C

MEGATRANSECT 1990 603 B.H. - 5

Site	Borehole	Depth m	Conductivity W/mK	Method	Lithology	Lith	Ambient	N69 52'34.4" Latitude N	W134 03'19.2" Longitude W	Unit
603	5	16.97	2.6630	T.P.A.	silty sand	slsd	-2.54	69.87622	134.05533	C
603	5	16.97	2.9164	N.P.	silty sand	slsd	-1.19	69.87622	134.05533	C
603	5	17.18	3.1100	T.P.A.	f. sand	sd	-2.70	69.87622	134.05533	C
603	5	17.37	4.2122	N.P.	f. sand	sd	-2.42	69.87622	134.05533	C
603	5	17.91	2.0700	T.P.A.	m. sand	sd	-2.30	69.87622	134.05533	C
603	5	18.28	1.3914	N.P.	m. sand	sd	-1.08	69.87622	134.05533	C
603	5	18.63	1.2221	N.P.	f. sand	sd	-1.09	69.87622	134.05533	C
603	5	18.89	2.9166	N.P.	f. sand	sd	-1.17	69.87622	134.05533	C
603	5	18.95	1.6850	T.P.A.	sand-ice	sdi	-2.95	69.87622	134.05533	C
603	5	18.95	0.9090	N.P.	ice + sand	isd	-0.62	69.87622	134.05533	C
603	5	19.14	2.0134	N.P.	f. sand	sd	-0.80	69.87622	134.05533	C
603	5	19.37	2.3626	N.P.	f. sand	sd	-1.02	69.87622	134.05533	C
603	5	19.57	4.0808	N.P.	f. sand	sd	-1.52	69.87622	134.05533	C
603	5	19.69	1.7035	N.P.	silty sand	slsd	-1.02	69.87622	134.05533	C
603	5	19.75	1.8797	N.P.	f. sand	sd	-0.68	69.87622	134.05533	C
603	5	19.75	1.4260	T.P.A.	f. sand	sd	-1.95	69.87622	134.05533	C
603	5	20.00	2.5711	N.P.	f. sand	sd	-1.12	69.87622	134.05533	C
603	5	20.07	1.2704	N.P.	f. sand	sd	-0.69	69.87622	134.05533	C
603	5	20.13	2.5180	T.P.A.	silty sand	slsd	-2.45	69.87622	134.05533	C
603	5	20.13	2.4757	N.P.	f. silty sand	slsd	-0.89	69.87622	134.05533	C
603	5	20.26	1.5631	N.P.	f. silty sand	slsd	-0.77	69.87622	134.05533	C
603	5	20.37	1.6463	N.P.	f. silty sand	slsd	-0.96	69.87622	134.05533	C
603	5	20.43	1.3868	N.P.	f. sand	sd	-0.69	69.87622	134.05533	C
603	5	20.43	1.5660	T.P.A.	f. sand	sd	-2.46	69.87622	134.05533	C
603	5	20.60	1.2448	N.P.	f. sand	sd	-0.58	69.87622	134.05533	C
603	5	20.79	2.6191	N.P.	f. sand	sd	-0.56	69.87622	134.05533	C
603	5	20.94	2.3688	N.P.	f. sand	sd	-0.56	69.87622	134.05533	C

MEGATRANSECT 1990 603 B.H. - 5

Site	Borehole	Depth m	Conductivity W/mK	Method	Lithology	Lith	Ambient	N69 52'34.4" Latitude N	W134 03'19.2" Longitude W	Unit
603	5	21.00	2.6636	N.P.	f. sand	sd	-0.91	69.87622	134.05533	C
603	5	21.00	1.6040	T.P.A.	f. sand	sd	-1.93	69.87622	134.05533	C
603	5	21.18	2.6571	N.P.	f. sand	sd	-0.95	69.87622	134.05533	C
603	5	21.36	1.9415	N.P.	f. sand	sd	-0.88	69.87622	134.05533	C
603	5	21.53	1.9557	N.P.	f. sand	sd	-1.16	69.87622	134.05533	C
603	5	21.69	2.7475	N.P.	f. sand	sd	-1.32	69.87622	134.05533	C
603	5	21.71	2.0967	N.P.	silty sand	slsd	-1.46	69.87622	134.05533	C
603	5	21.87	3.0917	N.P.	m. sand	sd	-0.33	69.87622	134.05533	C
603	5	22.29	2.4976	N.P.	silty sand	slsd	-0.22	69.87622	134.05533	C
603	5	22.44	3.8366	N.P.	m. sand	sd	-0.22	69.87622	134.05533	C
603	5	22.56	3.3574	N.P.	m. sand	sd	-0.34	69.87622	134.05533	C
603	5	22.99	2.1392	N.P.	m. sand	sd	-1.35	69.87622	134.05533	C
603	5	23.17	4.1192	N.P.	m. sand	sd	-0.30	69.87622	134.05533	C
603	5	23.17	4.6410	T.P.A.	m. sand	sd	-2.30	69.87622	134.05533	C
603	5	23.23	2.6804	N.P.	f. sand	sd	-6.49	69.87622	134.05533	C
603	5	23.36	2.9666	N.P.	f. sand	sd	6.53	69.87622	134.05533	C
603	5	23.53	2.4735	N.P.	f. sand	sd	-6.47	69.87622	134.05533	C
603	5	23.73	1.4950	T.P.A.	m. sand	sd	-4.19	69.87622	134.05533	C
603	5	23.73	2.2020	T.P.A.	m. sand	sd	-4.96	69.87622	134.05533	C
603	5	23.73	1.5092	N.P.	m.c. sand	sd	-2.04	69.87622	134.05533	C
603	5	23.85	1.4673	N.P.	m.c. sand	sd	-1.75	69.87622	134.05533	C
603	5	23.91	2.0948	N.P.	m. sand	sd	-0.71	69.87622	134.05533	C
603	5	24.05	2.1894	N.P.	c. sand	sd	-0.79	69.87622	134.05533	C
603	5	24.20	3.5992	N.P.	m. sand	sd	-0.54	69.87622	134.05533	C
603	5	24.40	2.6437	N.P.	m. sand	sd	-0.46	69.87622	134.05533	C
603	5	24.60	1.9446	N.P.	m. sand	sd	-0.44	69.87622	134.05533	C
603	5	24.60	5.2460	T.P.A.	m. sand	sd	-3.56	69.87622	134.05533	C

MEGATRANSECT 1990 603 B.H. - 5

Site	Borehole	Depth m	Conductivity W/mK	Method	Lithology	Lith	Ambient	N69 52'34.4" Latitude N	W134 03'19.2" Longitude W	Unit
603	5	24.91	1.7216	N.P.	f. sand	sd	-6.79	69.87622	134.05533	C
603	5	25.11	1.9297	N.P.	f. sand	sd	-6.19	69.87622	134.05533	C
603	5	25.30	2.2451	N.P.	f. sand	sd	-6.51	69.87622	134.05533	C
603	5	25.49	2.1067	N.P.	f. sand	sd	-7.79	69.87622	134.05533	C
603	5	25.55	2.9799	N.P.	f. sand	sd	-7.09	69.87622	134.05533	C
603	5	25.73	2.9972	N.P.	f. sand	sd	-7.54	69.87622	134.05533	C
603	5	25.95	2.6201	N.P.	f. sand	sd	-7.84	69.87622	134.05533	C
603	5	26.17	2.2491	N.P.	f. sand	sd	-7.40	69.87622	134.05533	C
603	5	26.39	3.2777	N.P.	f. sand	sd	-6.41	69.87622	134.05533	C
603	5	26.45	3.1197	N.P.	f. sand	sd	-3.97	69.87622	134.05533	C
603	5	26.98	3.2593	N.P.	f. sand	sd	-2.81	69.87622	134.05533	C
603	5	27.20	1.9465	N.P.	f. sand	sd	-6.28	69.87622	134.05533	C
603	5	27.37	2.4047	N.P.	f. sand	sd	-6.35	69.87622	134.05533	C
603	5	27.60	2.1279	N.P.	f. sand	sd	-6.58	69.87622	134.05533	C
603	5	27.73	1.4565	N.P.	f. sand	sd	-7.06	69.87622	134.05533	C
603	5	28.80	2.1023	N.P.	f. sand	sd	-2.91	69.87622	134.05533	C
603	5	28.80	2.4820	T.P.A.	f. sand	sd	-5.22	69.87622	134.05533	C
603	5	29.05	2.5113	N.P.	f. sand	sd	-2.24	69.87622	134.05533	C
603	5	29.27	2.3930	N.P.	f. sand	sd	-2.22	69.87622	134.05533	C
603	5	29.33	1.9326	N.P.	m. sand	sd	-0.84	69.87622	134.05533	C
603	5	29.59	1.2351	N.P.	m. sand	sd	-0.45	69.87622	134.05533	C
603	5	29.76	0.6700	T.P.A.	m. sand	sd	-2.47	69.87622	134.05533	C
603	5	29.82	2.5798	N.P.	m. sand	sd	-7.13	69.87622	134.05533	C
603	5	30.10	2.5563	N.P.	m. sand	sd	-7.12	69.87622	134.05533	C
603	5	30.26	3.9570	T.P.A.	m. sand	sd	-3.03	69.87622	134.05533	C
603	5	30.55	2.6194	N.P.	m. sand	sd	-7.11	69.87622	134.05533	C
603	5	30.73	1.7918	N.P.	m. sand	sd	-7.09	69.87622	134.05533	C

MEGATRANSECT 1990 603 B.H. - 5

Site	Borehole	Depth m	Conductivity W/mK	Method	Lithology	Lith	Ambient	N69 52'34.4" Latitude N	W134 03'19.2" Longitude W	Unit
603	5	30.89	2.2919	N.P.	m. sand	sd	-6.95	69.87622	134.05533	C
603	5	31.04	2.0659	N.P.	m. sand	sd	-6.53	69.87622	134.05533	C
603	5	31.25	2.2872	N.P.	m. sand	sd	-6.58	69.87622	134.05533	C
603	5	31.38	1.2990	N.P.	m. sand	sd	-4.96	69.87622	134.05533	C
603	5	31.38	3.5770	T.P.A.	m. sand	sd	-3.02	69.87622	134.05533	C
603	5	31.52	2.8017	N.P.	m. sand	sd	-4.90	69.87622	134.05533	C
603	5	31.91	2.5203	N.P.	m. sand	sd	-6.39	69.87622	134.05533	C
603	5	32.32	2.1054	N.P.	m. sand	sd	-7.43	69.87622	134.05533	C
603	5	32.52	2.1143	N.P.	c. sand	sd	-5.95	69.87622	134.05533	C
603	5	33.12	3.0080	T.P.A.	f. sand	sd	-3.25	69.87622	134.05533	C
603	5	33.50	2.2479	N.P.	f. sand	sd	-7.88	69.87622	134.05533	C
603	5	33.83	1.1900	T.P.A.	f. sand	sd	-4.37	69.87622	134.05533	C
603	5	34.02	2.1046	N.P.	f. sand	sd	-6.10	69.87622	134.05533	C
603	5	34.33	2.6060	T.P.A.	f. sand	sd	-3.81	69.87622	134.05533	C
603	5	34.94	2.2724	N.P.	f. sand	sd	-7.25	69.87622	134.05533	C
603	5	35.38	3.8430	T.P.A.	f. sand	sd	-8.88	69.87622	134.05533	C
603	5	35.68	2.1659	N.P.	f. sand	sd	-8.22	69.87622	134.05533	C
603	5	35.90	5.9970	T.P.A.	m. sand	sd	-8.34	69.87622	134.05533	C
603	5	36.19	2.1740	N.P.	m. sand	sd	-5.60	69.87622	134.05533	C
603	5	36.43	4.4700	T.P.A.	m. sand	sd	-8.69	69.87622	134.05533	C
603	5	36.51	2.8832	N.P.	m. sand	sd	-2.83	69.87622	134.05533	C
603	5	36.86	3.3380	T.P.A.	f. sand	sd	-6.79	69.87622	134.05533	C
603	5	36.93	2.2043	N.P.	f. sand	sd	-3.63	69.87622	134.05533	C
603	5	37.19	2.1491	N.P.	f. sand	sd	-8.19	69.87622	134.05533	C
603	5	37.63	4.1810	T.P.A.	f. sand	sd	-8.34	69.87622	134.05533	C
603	5	37.76	2.3974	N.P.	f. sand	sd	-6.25	69.87622	134.05533	C
603	5	38.19	2.6643	N.P.	f. sand	sd	-4.90	69.87622	134.05533	C

MEGATRANSECT 1990 603 B.H. - 5

Site	Borehole	Depth m	Conductivity W/mK	Method	Lithology	Lith	Ambient	N69 52'34.4" Latitude N	W134 03'19.2" Longitude W	Unit
603	5	38.73	1.4365	N.P.	silt	sl	-1.71	69.87622	134.05533	D
603	5	38.87	0.9808	N.P.	silt	sl	-1.57	69.87622	134.05533	D
603	5	39.01	1.2085	N.P.	silt	sl	-1.81	69.87622	134.05533	D
603	5	39.06	1.8899	N.P.	silt	sl	-1.59	69.87622	134.05533	D
603	5	39.12	1.4933	N.P.	clay	cl	-1.49	69.87622	134.05533	D
603	5	39.13	2.1200	T.P.A.	clay-silt	clsl	-2.32	69.87622	134.05533	D
603	5	39.25	1.4053	N.P.	silty clay	slcl	-1.39	69.87622	134.05533	D
603	5	39.39	1.7850	T.P.A.	silty clay	slcl	-3.99	69.87622	134.05533	D
603	5	39.40	1.5592	N.P.	silty clay	slcl	-1.47	69.87622	134.05533	D
603	5	39.45	1.5916	N.P.	silty clay	slcl	-1.56	69.87622	134.05533	D
603	5	39.60	1.4408	N.P.	silty clay	slcl	-1.55	69.87622	134.05533	D
603	5	39.80	1.3396	N.P.	silty clay	slcl	-1.68	69.87622	134.05533	D
603	5	39.89	1.9800	T.P.A.	silty clay	slcl	-3.29	69.87622	134.05533	D
603	5	39.91	1.6142	N.P.	silty clay	slcl	-1.53	69.87622	134.05533	D
603	5	40.39	1.5283	N.P.	silty clay	slcl	-2.00	69.87622	134.05533	D
603	5	40.52	1.4774	N.P.	clay	cl	-1.80	69.87622	134.05533	D
603	5	40.69	1.4769	N.P.	clay	cl	-1.82	69.87622	134.05533	D
603	5	40.85	2.0570	T.P.A.	silty clay	slcl	-3.31	69.87622	134.05533	D
603	5	40.85	1.3936	N.P.	silty clay	slcl	-2.22	69.87622	134.05533	D
603	5	40.91	1.5084	N.P.	silty clay	slcl	-1.78	69.87622	134.05533	D
603	5	40.99	1.2979	N.P.	silty clay	slcl	-1.52	69.87622	134.05533	D
603	5	41.09	1.6699	N.P.	silty clay	slcl	-1.69	69.87622	134.05533	D
603	5	41.27	1.2919	N.P.	silty clay	slcl	-1.84	69.87622	134.05533	D
603	5	41.38	1.4650	T.P.A.	clayey silt	clsl	-2.85	69.87622	134.05533	D
603	5	41.38	1.7668	N.P.	silty clay	slcl	-1.40	69.87622	134.05533	D
603	5	41.42	1.4580	N.P.	silt-clay	slcl	-2.24	69.87622	134.05533	D
603	5	41.42	1.8340	T.P.A.	silty clay	slcl	-3.74	69.87622	134.05533	D

MEGATRANSECT 1990 603 B.H. - 5

Site	Borehole	Depth m	Conductivity W/mK	Method	Lithology	Lith	Ambient	N69 52'34.4" Latitude N	W134 03'19.2" Longitude W	Unit
603	5	41.54	1.7209	N.P.	clay + silt	clsl	-1.37	69.87622	134.05533	D
603	5	41.69	1.5327	N.P.	clay + silt	clsl	-1.42	69.87622	134.05533	D
603	5	42.80	1.5470	T.P.A.	silt	sl	-2.85	69.87622	134.05533	D
603	5	42.80	1.9238	N.P.	silt	sl	-4.82	69.87622	134.05533	D
603	5	42.97	0.9050	N.P.	clay-silt	clsl	-4.23	69.87622	134.05533	D
603	5	75.87	2.7843	N.P.	f. sand	sd	-2.30	69.87622	134.05533	E
603	5	75.87	2.3120	T.P.A.	f. sand	sd	-4.11	69.87622	134.05533	E
603	5	76.15	5.3514	N.P.	f. sand	sd	-3.69	69.87622	134.05533	E
603	5	76.23	2.8740	T.P.A.	f. sand	sd	-3.46	69.87622	134.05533	E
603	5	76.23	3.2220	N.P.	f. sand	sd	-2.16	69.87622	134.05533	E
603	5	76.54	3.1249	N.P.	f. sand	sd	-5.47	69.87622	134.05533	E
603	5	76.56	3.3363	N.P.	f. sand	sd	-5.01	69.87622	134.05533	E
603	5	76.92	3.4382	N.P.	f. sand	sd	-3.91	69.87622	134.05533	E
603	5	77.27	3.2230	T.P.A.	f. sand	sd	-4.22	69.87622	134.05533	E
603	5	77.27	1.9138	N.P.	f. sand	sd	-6.45	69.87622	134.05533	E
603	5	77.33	3.0101	N.P.	f. sand	sd	-3.70	69.87622	134.05533	E
603	5	77.77	2.4901	N.P.	f. sand	sd	-4.02	69.87622	134.05533	E
603	5	77.96	2.3870	T.P.A.	f. sand	sd	-3.55	69.87622	134.05533	E
603	5	77.96	2.1723	N.P.	f. sand	sd	-1.64	69.87622	134.05533	E
603	5	78.49	3.1049	N.P.	f. sand	sd	-2.12	69.87622	134.05533	E
603	5	78.64	3.4637	N.P.	f. sand	sd	-2.01	69.87622	134.05533	E
603	5	78.69	2.6190	T.P.A.	f. sand	sd	-3.44	69.87622	134.05533	E
603	5	78.91	3.0630	N.P.	f. sand	sd	-4.20	69.87622	134.05533	E
603	5	79.14	3.0705	N.P.	f. sand	sd	-4.28	69.87622	134.05533	E
603	5	79.21	3.4304	N.P.	f. sand	sd	-1.77	69.87622	134.05533	E
603	5	79.37	3.7527	N.P.	f. sand	sd	-4.32	69.87622	134.05533	E
603	5	79.43	3.3928	N.P.	f. sand	sd	-1.19	69.87622	134.05533	E

MEGATRANSECT 1990 603 B.H. - 5

Site	Borehole	Depth m	Conductivity W/mK	Method	Lithology	Lith	Ambient	N69 52'34.4" Latitude N	W134 03'19.2" Longitude W	Unit
603	5	79.64	3.5297	N.P.	f. sand	sd	-1.43	69.87622	134.05533	E
603	5	79.96	2.5101	N.P.	f. sand	sd	-1.69	69.87622	134.05533	E
603	5	80.09	1.7050	T.P.A.	f. sand	sd	-3.80	69.87622	134.05533	E
603	5	80.11	2.7896	N.P.	f. sand	sd	-2.15	69.87622	134.05533	E
603	5	80.17	3.0109	N.P.	f. sand	sd	-7.33	69.87622	134.05533	E
603	5	80.51	2.1944	N.P.	f. sand	sd	-6.62	69.87622	134.05533	E
603	5	80.77	1.9541	N.P.	f. sand	sd	-7.09	69.87622	134.05533	E
603	5	80.79	1.6110	T.P.A.	f. sand	sd	-3.72	69.87622	134.05533	E
603	5	80.96	2.6249	N.P.	silty sand	slsd	-3.91	69.87622	134.05533	E
603	5	80.96	2.2990	T.P.A.	silty sand	slsd	-3.50	69.87622	134.05533	E
603	5	81.36	2.7399	N.P.	f. sand	sd	-2.38	69.87622	134.05533	E
603	5	81.62	2.5609	N.P.	f. sand	sd	-3.32	69.87622	134.05533	E
603	5	81.69	3.3369	N.P.	f. sand	sd	-1.84	69.87622	134.05533	E
603	5	81.69	1.7700	T.P.A.	f. sand	sd	-3.18	69.87622	134.05533	E
603	5	81.95	2.7390	N.P.	f. sand	sd	-1.69	69.87622	134.05533	E
603	5	82.22	3.0389	N.P.	f. sand	sd	-1.73	69.87622	134.05533	E
603	5	82.43	3.2302	N.P.	f. sand	sd	-2.69	69.87622	134.05533	E
603	5	82.56	2.7535	N.P.	f. sand	sd	-4.05	69.87622	134.05533	E
603	5	82.72	2.6970	N.P.	f. sand	sd	-3.97	69.87622	134.05533	E
603	5	82.97	2.5509	N.P.	f. sand	sd	-4.12	69.87622	134.05533	E
603	5	83.24	2.6021	N.P.	f. sand	sd	-4.54	69.87622	134.05533	E
603	5	83.25	1.9310	T.P.A.	f. sand	sd	-4.02	69.87622	134.05533	E
603	5	83.31	2.7604	N.P.	f. sand	sd	-4.55	69.87622	134.05533	E
603	5	83.31	2.0520	T.P.A.	f. sand	sd	-4.58	69.87622	134.05533	E
603	5	83.57	2.9260	N.P.	f. sand	sd	-4.19	69.87622	134.05533	E
603	5	83.78	2.8827	N.P.	f. sand	sd	-4.23	69.87622	134.05533	E
603	5	83.97	2.9643	N.P.	f. sand	sd	-4.70	69.87622	134.05533	E

MEGATRANSECT 1990 603 B.H. - 5

Site	Borehole	Depth m	Conductivity W/mK	Method	Lithology	Lith	Ambient	N69 52'34.4" Latitude N	W134 03'19.2" Longitude W	Unit
603	5	84.03	3.1528	N.P.	f. sand	sd	-5.16	69.87622	134.05533	E
603	5	84.03	2.4040	T.P.A.	f. sand	sd	-3.89	69.87622	134.05533	E
603	5	84.24	2.4706	N.P.	f. sand	sd	-4.59	69.87622	134.05533	E
603	5	84.48	2.7962	N.P.	f. sand	sd	-4.91	69.87622	134.05533	E
603	5	84.70	4.0206	N.P.	f. sand	sd	-5.45	69.87622	134.05533	E
603	5	84.75	2.0600	T.P.A.	f. sand	sd	-4.35	69.87622	134.05533	E
603	5	85.00	3.1191	N.P.	f. sand	sd	-2.54	69.87622	134.05533	E
603	5	85.28	2.9365	N.P.	f. sand	sd	-2.90	69.87622	134.05533	E
603	5	85.47	3.3141	N.P.	f. sand	sd	-4.46	69.87622	134.05533	E
603	5	85.53	2.5370	T.P.A.	f. sand	sd	-3.66	69.87622	134.05533	E
603	5	85.71	2.9325	N.P.	f. sand	sd	-5.01	69.87622	134.05533	E
603	5	86.11	3.0264	N.P.	f. sand	sd	-4.52	69.87622	134.05533	E
603	5	86.39	3.1407	N.P.	f. sand	sd	-6.72	69.87622	134.05533	E
603	5	86.72	2.6187	N.P.	f. sand	sd	-6.22	69.87622	134.05533	E
603	5	86.97	1.9580	T.P.A.	f. sand	sd	-4.00	69.87622	134.05533	E
603	5	86.99	2.4525	N.P.	f. sand	sd	-6.87	69.87622	134.05533	E
603	5	87.11	2.3370	T.P.A.	f. sand	sd	-3.16	69.87622	134.05533	E
603	5	87.11	2.2269	N.P.	f. sand	sd	-3.35	69.87622	134.05533	E
603	5	87.44	2.9983	N.P.	f. sand	sd	-2.22	69.87622	134.05533	E
603	5	87.75	2.4992	N.P.	f. sand	sd	-3.31	69.87622	134.05533	E
603	5	87.81	2.3430	T.P.A.	f. sand	sd	-3.61	69.87622	134.05533	E
603	5	87.89	2.2959	N.P.	f. sand	sd	-3.65	69.87622	134.05533	E
603	5	88.25	2.6597	N.P.	f. sand	sd	-2.33	69.87622	134.05533	E
603	5	88.47	3.2405	N.P.	f. sand	sd	-5.34	69.87622	134.05533	E
603	5	94.75	2.8697	N.P.	f. sand	sd	-3.70	69.87622	134.05533	E

APPENDIX D

Physical property test data spreadsheets

Borehole BH1					
Total Density		Water Content		Salinity	
depth (m)	g/cu cm	depth (m)	(g/g, %)	depth (m)	PPT
-1.15	1.451	-1.05	94.98	-1.05	0
-2.12	1.671	-1.99	30.14	-1.99	4
-3.20	1.648	-3.09	33.75	-3.09	0
-4.72	1.488	-3.36	37.82	-3.36	1
-5.38	1.698	-5.06	59.59	-5.06	1
-6.42	1.744	-5.51	67.96	-5.51	2
-8.12	1.714	-6.56	43.21	-6.56	2
-9.35	1.715	-8.27	48.60	-8.27	1
-10.38	1.746	-8.74	44.44	-8.75	1
-12.33	1.808	-10.54	42.38	-10.52	1
-14.20	1.803	-11.04	40.21	-11.04	2
-14.72	1.816	-12.64	45.15	-12.64	1
-16.36	1.840	-12.81	36.40	-14.33	2
-18.12	1.842	-14.33	39.68	-15.66	2
-19.14	1.699	-15.66	26.33	-16.81	2
-20.34	1.119	-16.81	40.74	-17.69	2
-21.31	0.978	-17.69	33.50	-18.90	1
-22.11	0.976	-18.85	39.38	-20.04	0
-23.48	1.168	-20.04	198.43	-23.34	1
-24.78	1.151	-21.18	362.96	-23.79	1
-25.14	0.973	-22.52	477.78	-24.91	1
-26.38	1.152	-23.34	157.46	-25.29	1
-27.26	1.345	-23.81	81.03	-26.24	1
-28.42	1.908	-24.91	278.16	-26.94	0
		-25.29	288.89	-28.60	0
		-26.24	123.89		
		-28.60	27.04		

Borehole BH1		
Acoustical Properties		
depth (m)	VP (m/s)	VS (m/s)
-1.15	2307.7	1343.3
-2.12	3086.4	1714.3
-3.20	2907.0	1388.9
-4.72	3333.3	1602.6
-5.38	2427.2	1369.9
-6.42	2907.0	1404.5
-8.12	3086.4	1748.3
-9.35	2967.2	1388.9
-10.38	3205.1	1524.4
-12.33	3125.0	1488.1
-14.20	3571.4	1736.1
-14.72	2941.2	1470.6
-16.36	3086.4	1515.2
-18.12	3164.6	1506.0
-19.14	2941.2	1497.0
-20.34	2564.1	1396.6
-21.31	3048.8	1470.6
-22.11	2525.3	1470.6
-23.48	3164.6	1572.3
-24.78	2381.0	1497.0
-25.14	3086.4	1552.8
-26.38	3378.4	1677.9
-27.26	2993.0	1622.1
-28.42	3906.3	1879.7

Borehole BH1			
Grain Size Analysis			
depth (m)	<2.000 mm	<0.063 mm	<0.002 mm
-6.3	100	59	25
-8.8	100	55	22
-25.6	100	43	19
-28.6	100	8	4

Borehole BH1		
Atterberg Limits		
depth (m)	Plastic limit	Liquid limit
-3.3	14	26
-9.0	12	23
-19.0	15	21

Borehole BH1A			
Water Content		Salinity	
depth (m)	g/g, %	depth (m)	PPT
-0.07	373.80	-0.07	0.27
-0.68	187.39	-0.68	0.08
-1.25	44.16	-1.25	0.28
-1.87	25.57	-1.87	1.12
-2.72	23.08	-2.72	1.29
-4.84	20.41	-4.84	2.40
-6.15	21.62	-6.15	1.60
-6.72	25.19	-6.72	0.81
-7.27	20.98	-7.27	1.86
-8.65	21.04	-8.65	2.78
-9.21	18.76	-9.21	2.24
-10.76	21.33	-10.76	2.09
-11.36	12.88	-11.36	2.96
-12.17	35.32	-12.17	0.70
-12.40	26.29	-12.40	1.55
-14.43	32.69	-14.43	0.52
-16.10	28.00	-16.10	0.52
-16.91	28.68	-16.91	0.79
-18.36	28.00	-18.36	1.08
-20.49	30.58	-20.49	1.69
-22.47	30.31	-22.47	3.07
-24.47	20.41	-24.47	4.63
-25.37	30.16	-25.37	2.35
-25.67	24.24	-25.67	4.80
-26	24.29	-26	5.32
-27.68	30.59	-27.68	2.16
-28.19	46.20	-28.19	1.19
-28.72	28.07	-28.72	0.92
-29.38	47.91	-29.38	0.97
-29.79	40.01	-29.79	0.58
-30.75	17.16	-30.75	0.53
-32.16	20.44	-32.16	1.21
-33.33	28.10	-33.33	2.85
-33.58	17.52	-33.58	4.15
-34.44	17.50	-34.44	11.29
-35.51	35.97	-35.51	12.57
-35.80	25.32	-35.80	20.80

Borehole BH1A			
Water Content		Salinity	
depth (m)	g/g, %	depth (m)	PPT
-36.35	29.86	-36.35	14.10
-37.43	36.72	-37.43	19.38
-37.85	33.15	-37.85	21.89
-38.76	31.37	-38.76	28.33
-39.28	33.56	-39.28	28.85
-40.02	30.75	-40.02	17.69
-40.15	26.94	-40.15	20.27
-40.28	19.24	-40.28	5.80
-40.39	18.00	-40.39	27.05
-40.50	17.05	-40.50	22.59
-40.63	23.34	-40.63	35.40
-40.78	19.77	-40.78	4.72
-40.91	21.20	-40.91	5.10

Borehole BH1A			
Grain Size Analysis			
depth m	<2.000 mm	<0.063mm	<0.002mm
-4.8	100.0	2.5	0.0
-8.6	100.0	2.5	0.0
-14.4	100.0	50.0	4.5
-24.5	100.0	2.0	0.0
-27.7	100.0	22.0	0.0
-33.3	100.0	2.0	0.0
-35.5	100.0	100.0	15.0
-39.3	100.0	100.0	24.0
-40.4	100.0	100.0	28.0

Borehole BH1A		
Atterberg Limits		
depth m	Plastic limit	Liquid limit
-36.7	29	45
-39.7	30	50

Borehole BH2			
Water Content		Salinity	
depth m	g/g, %	depth m	PPT
-1.72	22.22	-1.74	28
-2.36	26.97	-2.40	26
-3.12	32.32	-3.16	23
-3.92	35.98	-3.96	20
-4.68	32.68	-4.72	18
-5.53	36.84	-5.75	20
-6.52	35.60	-6.56	19
-7.02	34.44	-7.05	18
-7.70	35.62	-7.74	19
-8.37	31.23	-8.41	16
-9.46	34.47	-9.46	18
-9.98	38.55	-10.02	17
-11.02	39.61	-11.04	17
-11.48	47.09	-11.52	17
-12.85	47.83	-12.80	13
-13.19	48.59	-13.23	13
-13.92	47.42	-13.95	15
-14.61	45.13	-14.63	17
-15.36	17.88	-15.33	20
-31.82	30.69	-15.40	31
-34.02	27.64	-16.58	50
-34.45	30.89	-16.78	37
-35.32	33.45	-31.86	25
-35.92	31.15	-31.93	30
-36.41	32.74	-34.03	41
-37.51	31.80	-34.06	
-38.18	33.11	-34.48	34
-38.94	34.39	-35.35	23
-39.72	36.70	-35.96	22
-40.52	36.59	-36.65	18
-41.32	32.55	-37.55	18
-41.89	32.14	-38.21	18
-42.92	31.15	-38.96	18
-43.52	28.74	-39.75	25
-44.27	16.04	-40.35	17

Borehole BH2			
Water Content		Salinity	
depth m	g/g, %	depth m	PPT
-44.95	19.84	-40.56	16
-45.02	25.22	-41.92	27
-45.93	31.90	-42.76	18
-50.72	22.68	-43.53	12
-99.52	30.59	-44.23	18
		-44.99	22
		-45.06	22
		-45.73	10
		-45.97	12
		-47.33	54
		-47.65	62
		-50.76	62
		-99.48	50
		-99.54	55

Borehole BH2			
Grain Size Analysis			
depth m	<2.000 mm	<0.063mm	<0.002mm
-1.80	100	10.5	3
-3.30	100	100	25
-7.20	100	95	24
-10.90	100	100	41
-14.80	100	11	7
-32.00	100	9	3
-36.10	100	100	32
-41.50	100	100	40
-44.40	100	8	3
-47.50	100	9	4
-50.40	100	9	5
-99.40	100	11	7

Borehole BH2		
Atterberg Limits		
depth m	Plastic limit	Liquid limit
-4.50	22	45
-9.00	21	43
-37.80	29	46
-41.70	29	47

Borehole BH3			
Water Content		Salinity	
depth m	g/g, %	depth m	PPT
-0.60	41.71	-0.32	17.0
-1.09	32.97	-0.93	15.0
-1.79	29.97	-1.75	14.0
-4.10	33.25	-3.56	12.0
-4.60	34.06	-4.53	12.0
-3.52	30.98	-4.71	12.0
-5.52	29.82	-5.56	12.0
-6.08	31.12	-6.13	12.0
-7.52	26.28	-7.48	10.0
-8.52	25.82	-8.56	14.0
-8.78	25.07	-8.82	15.0
-9.52	28.78	-9.58	14.0
-10.55	37.13	-10.48	17.0
-11.43	32.96	-11.38	15.0
-12.06	39.05	-11.99	15.0
-12.92	28.50	-12.83	14.4
-13.43	23.09	-13.38	17.0
-14.52	26.37	-14.56	16.0
-15.43	44.89	-15.14	17.0
-15.85	89.76	-15.78	18.0
-16.59	18.74	-16.33	18.0
-17.06	19.45	-17.11	12.0
-18.49	17.72	-18.44	22.0
-18.92	17.06	-18.96	21.0
-19.50	17.60	-19.53	20.0
-20.18	17.55	-20.14	18.0
-20.80	17.75	-20.77	20.0
-21.63	17.96	-21.68	18.0
-22.39	17.11	-22.43	20.0
-24.11	17.02	-24.08	20.0
-28.82	26.27	-28.86	21.0
-30.62	19.05	-30.66	33.8
-33.60	17.52	-32.05	28.1

Borehole BH3			
Water Content		**Salinity**	
depth m	g/g, %	depth m	PPT
-35.55	32.10	-33.58	15.5
-35.82	36.92	-35.59	17.0
-36.42	31.39	-35.86	23.0
-37.22	27.87	-36.46	27.0
-38.02	27.68	-37.26	24.1
-38.98	25.35	-38.06	28.9
-39.58	28.07	-39.03	26.1
-40.55	22.50	-39.63	25.7
-40.47	31.67	-40.43	31.8
-41.14	30.98	-41.18	25.4
-42.07	31.01	-42.11	19.0
-42.40	33.44	-42.43	20.0
-44.26	29.07	-44.26	24.0
-45.75	26.56	-45.73	20.4

Borehole BH3			
Grain Size Analysis			
depth m	<2.000 mm	<0.063mm	<0.002mm
-4.8	100	96	18
-9.0	100	79	13
-14.9	100	42	21
-19.0	100	52	21
-21.8	100	41	18
-28.9	100	6	3
-38.0	100	100	32
-39.8	100	100	31
-40.2	100	100	33

Borehole BH3		
Atterberg Limits		
depth m	Plastic limit	Liquid limit
-4.8	18	28
-9.0	19	26
-12.2	23	42
-15.0	17	28
-19.1	14	24
-21.8	14	20
-39.8	26	45
-40.2	28	47
-37.9	26	43
-42.7	29	45

Borehole BH4			
Water Content		**Salinity**	
depth m	g/g, %	depth m	PPT
-34.87	32.98	-34.91	14
-35.16	34.15	-35.12	14
-35.70	33.18	-35.73	25
-36.12	34.11	-36.16	23
-38.22	33.22	-38.26	31
-38.82	32.82	-38.86	25
-39.34	27.90	-39.38	24
-39.82	32.23	-39.86	22
-40.12	30.69	-40.16	27
-40.92	33.61	-40.95	25
-41.52	35.16	-41.55	18
-42.18	33.23	-42.22	25
-42.82	37.50	-42.86	15
-43.52	31.54	-43.55	22
-44.00	33.33	-44.03	21
-44.57	32.54	-44.61	20
-45.25	27.97	-45.28	28
-46.22	34.41	-46.25	14
-47.07	20.60	-47.11	48
-47.82	31.01	-47.86	22
-48.22	35.74	-48.26	19
-49.28	31.22	-49.32	22
-50.05	33.25	-50.08	16
-50.68	35.78	-50.72	21
-51.10	34.48	-51.13	22
-51.52	37.50	-51.56	19

Borehole BH4			
Water Content		Salinity	
depth m	g/g, %	depth m	PPT
-52.22	39.93	-52.24	18
-52.78	38.21	-52.81	16
-53.22	40.25	-53.26	14
-53.82	28.64	-53.85	19
-54.22	37.79	-55.15	17
-55.17	71.14	-56.26	46
-56.22	20.60		

Borehole BH4			
Grain Size Analysis			
depth m	<2mm	<0.063mm	<0.002mm
-35.3	100	100	26
-39.2	100	100	38
-45.3	100	81	37
-52.1	100	97	37
-56.3	100	8	4

Borehole BH4		
Atterberg Limits		
depth m	Plastic limit	Liquid limit
-40.0	27	47
-46.0	24	43
-51.3	29	47

Borehole BH5					
Density		**Water Content**		**Salinity**	
depth m	g/cu cm	depth m	g/g, %	depth m	PPT
-17.34	1.847	-10.26	19.17	-10.26	30
-18.34	1.151	-12.15	15.04	-12.18	25
-18.84	1.016	-13.62	15.17	-13.68	40
-19.88	1.926	-16.52	23.44	-16.52	10
-20.33	1.787	-17.42	27.74	-17.27	0
-22.14	1.927	-18.42	228.81	-18.28	1
-22.49	1.950	-18.76	814.81	-18.79	5
-25.22	1.823	-19.30	20.80	-18.93	1
-27.35	2.011	-19.93	26.65	-19.93	2
-29.66	1.969	-20.30	34.70	-20.34	4
-30.14	2.014	-20.50	38.13	-20.52	2
-30.64	1.932	-21.41	32.88	-21.42	5
-32.57	1.914	-22.02	27.93	-22.08	5
-34.98	2.054	-22.75	25.56	-22.68	0
-35.63	1.901	-23.72	27.40	-23.47	2
-36.14	1.908	-24.21	21.96	-24.14	0
-36.74	1.980	-25.43	27.56	-25.45	5
-37.25	1.925	-25.88	24.46	-25.78	2
-38.11	2.136	-26.38	30.71	-26.38	13
-76.43	1.864	-26.93	24.22	-26.90	5
-76.64	1.913	-27.28	21.96	-27.26	3
-77.72	1.911	-29.14	20.17	-29.12	2
-78.85	1.961	-29.62	22.48	-29.64	0
-80.06	1.924	-30.06	22.93	-30.04	2
-81.93	1.926	-30.57	26.10	-30.55	1
-83.02	2.057	-31.16	27.92	-31.19	5
-83.86	2.073	-31.25	27.97	-31.47	2

Borehole BH5					
Density		**Water Content**		**Salinity**	
depth m	g/cu cm	depth m	g/g, %	depth m	PPT
-84.52	2.006	-32.12	21.26	-32.12	0
-85.29	1.985	-32.63	25.16	-32.67	0
-85.76	2.066	-33.64	24.66	-33.62	5
-86.74	2.006	-34.07	28.31	-34.10	8
-87.16	1.945	-34.89	20.61	-34.89	2
-88.32	2.019	-35.86	24.56	-35.82	3
		-36.26	28.22	-36.26	1
		-36.52	26.28	-36.49	5
		-37.46	26.16	-37.51	5
		-37.84	22.88	-37.82	5
		-38.32	25.22	-38.29	5
		-38.85	32.06	-38.93	26
		-39.24	35.71	-39.28	21
		-39.55	33.33	-39.59	32
		-40.62	36.07	-40.68	32
		-41.12	32.38	-41.18	28
		-41.56	31.76	-41.60	38
		-42.88	34.08	-42.85	12
		-75.97	25.29	-75.99	30
		-76.35	28.64	-76.33	12
		-76.78	25.45	-76.82	10
		-77.69	22.04	-77.67	16
		-78.29	23.00	-78.27	10
		-79.12	26.55	-79.14	12
		-79.99	25.80	-79.98	13
		-80.22	25.55	-80.22	14
		-81.22	23.40	-81.21	10

Borehole BH5					
Density		**Water Content**		**Salinity**	
depth m	g/cu cm	depth m	g/g, %	depth m	PPT
		-82.08	25.90	-82.09	6
		-82.67	22.49	-82.92	14
		-83.76	20.16	-83.74	22
		-84.45	22.78	-84.44	19
		-84.89	22.07	-84.92	19
		-85.66	22.97	-85.66	18
		-86.67	21.65	-87.43	20
		-87.43	22.16	-88.26	15
		-88.24	21.67		

Borehole BH5		
Acoustical Properties		
depth m	VP m/s	VS m/s
-17.34	3342.4	1830.4
-18.34	3388.9	1859.8
-18.84	15625	1644.7
-19.88	2652.2	1270.8
-20.33	2772.7	1326.1
-22.14	3112.2	1452.4
-22.49	3028.8	1750
-25.22	3910.3	2440
-27.35	3812.5	1955.1
-29.66	3910.3	2675.4
-30.14	3719.5	2440
-30.64	3719.5	2259.3

Borehole BH5		
Acoustical Properties		
depth m	VP m/s	VS m/s
-32.57	4046.1	2196.4
-34.98	3910.3	2006.6
-35.63	3942.3	2165.5
-36.14	3812.5	2178.6
-36.74	3720.2	2083.3
-37.25	3910.3	2033.3
-38.11	3546.5	1955.1
-76.43	2847.2	1464.3
-76.64	2824.1	924.2
-77.72	2103.4	622.4
-78.85	2382.8	953.1
-80.06	2629.3	871.4
-81.93	3014.7	1147.4
-83.02	3719.5	2440
-83.86	2699.1	1129.6
-84.52	2629.3	635.4
-85.29	2672.4	911.8
-85.76	2584.7	1105.1
-86.74	2541.7	1089.3
-87.16	2500	1033.9
-88.32	2346.2	491.6

Borehole BH5			
Grain Size Analysis			
depth m	<2.000 mm	<0.063mm	<0.002mm
-12.30	100	26	9
-16.40	100	26	8
-19.90	100	51	9
-21.80	100	2	1
-24.30	100	2	1
-27.00	100	2	1
-29.50	100	1	1
-32.80	100	3	1
-35.50	100	2	1
-38.30	100	3	1
-40.80	100	100	35
-76.90	100	7	3
-77.50	100	6	2
-79.40	100	3	2
-79.80	100	10	4
-82.10	100	7	3
-85.00	100	18	7
-86.50	100	17	7
-88.10	100	15	6

Borehole BH5		
Atterberg Limits		
depth m	Plastic limit	Liquid limit
-40.75	24	41